Petrology of the Crystal Lake Gabbro and the Mount Mollie Dyke, Midcontinent Rift, Northwest Ontario

Sean O'Brien

A thesis submitted in partial fulfillment of the requirements
for the Degree Master of Science

Department of Geology

Lakehead University

June 2018

ABSTRACT

The Crystal Lake Gabbro (CLG) is a Y-shaped, up to 750 m wide, layered mafic intrusion with a 5 km long northern limb and a 2.75 km long southern limb, with localized Cu-Ni and Cr mineralization. The Mount Mollie Dyke (MMD) is an arcuate, 60 to 350 m wide, macrodyke that lies on trend east of the CLG and extends for 35 km toward Lake Superior. Both intrusions are part of the 1.1 Ga Midcontinent Rift (MCR) and were emplaced into the Paleoproterozoic Rove Formation of the Logan Basin, approximately 50 km south of Thunder Bay. Current U-Pb age determination implies a ~10 m.y. age difference with CLG being formed at ~1100 Ma and the MMD being formed at ~1109 Ma. However, this age difference is at odds with both intrusions being normally polarized (an attribute of MCR rocks younger than 1102 Ma) and their being on trend with each other. This study seeks to determine whether the two intrusions may be petrogenetically linked by evaluating the petrography, geochemistry, mineral composition, and sulphur isotopes of samples collected from drill core.

The CLG profiled in a drill core from its southern limb can be broadly divided into Upper, Main, and Lower Zones with further subdivisions of the Main and Lower Zones based largely on geochemistry. The Lower Zone occurs between two xenoliths of an early MCR (~1115 Ma) plagioclase porphyritic Logan Sill diabase. The Lower Zone consists of subophitic to ophitic troctolite, augite troctolite, and olivine gabbro and can be subdivided into an upper and basal marginal subzone as well as an interior subzone. Both marginal subzones host disseminated sulphides with the basal margin also containing Cr-spinel seams. An overall bottom-up-directed fractional crystallization of the Lower Zone is suggested by the progressive decrease in Fo content of olivine, Mg# of clinopyroxene, and whole-rock MgO upsection. Above the upper Logan Sill xenolith, the Main Zone similarly consists of subophitic to ophitic troctolite, augite troctolite, olivine gabbro, and gabbro. Petrography, lithogeochemistry, and mineral composition was used to subdivide the Main Zone into five subzones: a basal marginal subzone, upper margin subzone, and three interior cycles that display cryptic variations indicative of fractional crystallization and magma recharge events. Like the margins of the Lower Zone, the Upper Zone as well and the basal marginal subzone of the Main Zone contain disseminated sulphides and Cr-spinel, and are characterized by relatively high Fo content olivine and low incompatible trace element concentrations. These mineralized zones are interpreted to have crystallized from the same initial pulse of magma into the CLG, which was sulfide- and Cr-spinel-saturated. Cyclical cryptic variations in the internal subzone of the Main Zone are interpreted to indicate upward directed fractional crystallization, interrupted by emplacement of additional magma pulses into the core of the intrusion. All rocks of the Main Zone are olivine and plagioclase orthocumulates indicating that fractional crystallization was not particularly efficient (i.e., did not experience a strong segregation of cumulus minerals from the parental magma). The lack of Cr-spinel in the interior and upper marginal subzones of the Main Zone further indicates that subsequent magma pulses either were more evolved than the original parental magma or were volumetrically subordinate to the evolved

magmas that resided in the chamber. Throughout the evolution of the CLG, the differentiation of the magma was limited as it did not result in clinopyroxene and Fe-Ti oxide becoming cumulus phases. This was likely due to magmatic recharge and inefficient fractional crystallization.

Texturally and geochemically, the MMD can be broadly divided into an Upper and Main Zones, with a subdivision of the Main Zone into an upper and lower sequence and a pegmatitic segregation subzone. The Upper Zone consists of ferrodiorite and likely represents the end product of extensive fractionation. The Main Zone is characterized by troctolite, augite troctolite, olivine gabbro, and gabbro with MgO, CaO, Al_2O_3, and Ni concentrations decreasing upwards and SiO_2, TiO_2, K_2O, Na_2O, P_2O_5, and incompatible trace element concentrations increasing, consistent with bottom-up fractional crystallization. Strong differentiation of the MMD magma is indicated by the habit change of clinopyroxene from ophitic (intercumulus) to granular (cumulus), which is the basis for the subdivision of the lower and upper sequences. The lower sequence of the Main Zone also hosts a 24 m thick interval containing 1 to 2 m wide gabbroic pegmatite layers. These pegmatites are interpreted to be the result of localized enrichment of magmatic volatiles.

The presence of an evolved core in the MMD surface expression, coupled with the mineral composition of olivine, plagioclase, and clinopyroxene, remaining at relatively constant Fo, An, and Mg# values, respectively, below the pegmatitic layers suggests that there was some degree of lateral crystal fractionation as well as bottom up fractionation. The well-defined fractionation sequence as well as an absence of abrupt geochemical changes suggests that the MMD fractionally crystallized from a single pulse.

Liberation of external sulphur from the surrounding Rove Formation, is suggested by the greater than mantle S/Se values as well as $\delta^{34}S$ values between +4.0 and +21.0‰ of the sulphides within the CLG. The addition of external sulphur evidently resulted in sulphur saturation during initial emplacement of the CLG magmas. Primitive mantle normalized multi-element diagrams and trace element ratios provide supporting evidence for a localized shallow level of crustal contamination, as well as a deeper more widespread contamination component of both the CLG and MMD magmas.

The estimated parental magma compositions and average primitive mantle normalized trace element concentrations of the CLG and MMD suggest that they shared similar, if not the same, magma source. The CLG parental magma was slightly more evolved than the MMD suggesting that the magmas were sourced from a fractionating staging chamber. The estimated parental magma compositions of the CLG and MMD closely resemble those of the Layered Series intrusions of the Duluth Complex, supporting previous speculation that the CLG may be a satellite intrusion of the Duluth Complex. Despite current geochronology data to the contrary, the results of this study strongly suggest that the CLG and the MMD are petrogenetically linked, if not parts of the same intrusive system.

ACKNOWLEDGEMENTS

Thank you to my supervisors, Pete Hollings and Jim Miller, for the opportunity and guidance. Special thanks to Pete for partially funding this project from your personal research fund.

Many other individuals assisted in this research, through: sample preparation, mineral composition analysis, sulphur isotope analysis, field assistance, discussions and insights, and access to samples. Including: Dean Rossell, Anne Hammond, Kristi Tavener, Vittoria Smith, Rob Cundari, Mark Puumala, Mike D'Angelo, Mingjian Cao, Ed Ripley, and Bob Chataway. I thank you all.

Thank you, Rio Tinto for providing access to samples as well as analytical funding, Bending Lake Iron Group for providing access to samples, and the Ontario Geological Survey for providing geochemistry analysis.

I appreciate the funding from Lakehead University (Ontario Graduate Scholarship and Northern Lake Superior Graduate Award), Society of Economic Geologists Canada Foundation (Graduate Student Fellowship), and Memorial University of Newfoundland (Hugh Lilly Memorial Scholarship).

Thank you, to family and friends for your support.

TABLE OF CONTENTS

LIST OF FIGURES

LIST OF TABLES

LIST OF ABBREVIATIONS

AFM – Alkali FeO MgO

CLG – Crystal Lake Gabbro

CPX - Clinopyroxene

Fo - Forsterite

HAOT – High Alumina Olivine Tholeiite

HREE – Heavy Rare Earth Elements

ICP-MS - Inductively coupled plasma mass spectrometry

ICP-OES - Inductively coupled plasma optical emission spectrometry

iss - Intermediate solid solution

LREE – Light Rare Earth Elements

MMD – Mount Mollie Dyke

mss – Monosulphide solid solution

MREE – Middle Rare Earth Elements

OIB – Ocean Island Basalt

Ol – Olivine

PGE – Platinum Group Elements

Plag - Plagioclase

QFM – Quartz-Fayalite-Magnetite

REE – Rare Earth Elements

SCLM – Subcontinental Lithospheric Mantle

SEM-EDS - Scanning Electron Microscopy - Energy Dispersive Spectroscopy

TAS – Total Alkali vs. Silica

XRF – X-Ray Fluorescence

1 INTRODUCTION

The ~2500 km long, 1.1 Ga Midcontinent Rift (MCR) is a well-preserved failed rift comprised of volcanic and intrusive rocks exposed around Lake Superior. A series of dykes, sills, and intrusive bodies were emplaced during the igneous activity of the MCR, as well as coeval continental flood basalts and minor andesites and rhyolites (Nicholson et al., 1997). Compositionally the intrusive dykes, sills, and intrusions range from ultramafic-mafic, alkaline, mafic, to granophyric.

The MCR formed from ~1115 to 1084 Ma, with the majority of the igneous activity occurring in two pulses from ~1115 to 1105 Ma and ~1100 to 1094 Ma (Heaman et al., 2007; Vervoort et al., 2007). A magnetic polarity reversal was recognized by Davis and Green (1997) in MCR related volcanic and intrusive rocks during the gap between the main pulses, with rocks >1105 Ma having a R-polarity and those <1102 Ma having a N-polarity.

In this study two MCR related intrusive bodies, the Crystal Lake Gabbro (CLG) and the Mount Mollie Dyke (MMD), have been investigated using petrography, geochemistry, sulphur isotopes, and mineral composition. The spatial relationship, similar trend and rock types led to the belief that they were co-genetic and/or contemporaneous with the two sharing the same magma reservoir (Smith and Sutcliffe, 1987). However, recent age determination has revealed that the CLG formed at 1099.6 ± 1.2 Ma and the MMD formed at 1109.3 ± 6.3 Ma (Heaman et al., 2007; Hollings et al., 2010). There are still unresolved issues with this age gap, most notably that both have the same paleomagnetic N-polarity, where one would expect a R-polarity for MCR related rocks that are > 1105 Ma (Davis and Green, 1997).

Due to the large amounts of igneous activity during the formation of the MCR, the present-day exposure, and ease of access there has been on-going exploration in Ontario, Minnesota, and Wisconsin for magmatic Ni-Cu-PGE (platinum group elements) deposits. Broadly the mineralization can be classified into two styles. The early stages of the rift are associated with small and discrete ultramafic-mafic intrusions with high-grade disseminated to massive textured ore that formed in a magma conduit (e.g., Eagle and Tamarack; Ripley, 2014). These intrusions are sub-vertical dyke-like bodies, with host rocks of olivine-rich feldspathic peridotite, melatroctolite, and melagabbro with primarily pyrrhotite, chalcopyrite, cubanite, and pentlandite sulphides (Ripley, 2014). The mineralization is typically Ni-rich with Ni/Cu greater than 1 (Ripley, 2014). The second style of mineralization was formed later in the evolution of the rift and is found in sheet-like troctolitic to gabbroic intrusions of the Duluth Complex (Ripley, 2014). The mineralization associated with this second type is in the form of disseminated ore and is primarily low-grade and Cu-rich and Ni-poor and primarily found in the basal zones of the intrusions (Ripley, 2014; Benkó et al., 2015).

Mineralization within the CLG is of the second style. Previous exploration of the CLG defined a basal ore zone with disseminated and blebs of pyrrhotite, chalcopyrite, cubanite, and pentlandite with an indicated resource of 41.4 million tonnes grading 0.334% Cu, 0.183% Ni, 0.69 g/t Pd, 0.21 g/t Pt, 0.01 g/t Rh,0.07 g/t Au, and 2.06 g/t Ag (Smith and Sutcliffe, 1989). This orebody is located at the western tip the northern limb and is known as the Great Lakes Nickel deposit. The most extensive exploration took place in the 1960s and 1970s, but more recently Rio Tinto has acquired the claims on the CLG property and has developed a drilling program as well as re-logging and assaying of historic drill cores (Goldner, 2015). If the CLG and the MMD intrusions are part of the same magmatic system, this could have important implications for the mineralization potential of the MMD.

1.1 LOCATION AND ACCESS

The CLG and MMD are located approximately 50 km south of Thunder Bay towards the U.S.A border in Neebing Township (Fig. 1.1). The area can be accessed by traveling south from Thunder Bay on Highway 61. The CLG is located on the west side of the highway and the MMD extends to the east towards and into Lake Superior where it is exposed on a series of islands. Access to the CLG is restricted as it is situated on private property whereas the MMD lies within Crown Land. Access to the drill core from the CLG was provided by Rio Tinto and access to the MMD core was provided by Bending Lake Iron Group. Drilling of the CLG core (14CL0003), took place in July of 2014, with the collar located at 306239 E 5326523 N, to a depth of 828m at an azimuth of 180 and a dip of -85. This was part of an ongoing exploration project by Rio Tinto. The MMD (S88-1) drilling took place between December 1988 and January 1989, by Platinum Exploration Canada Inc., with the collar located at 311913 E 5326170 N, to a depth of 1095 m with a sub-vertical orientation.

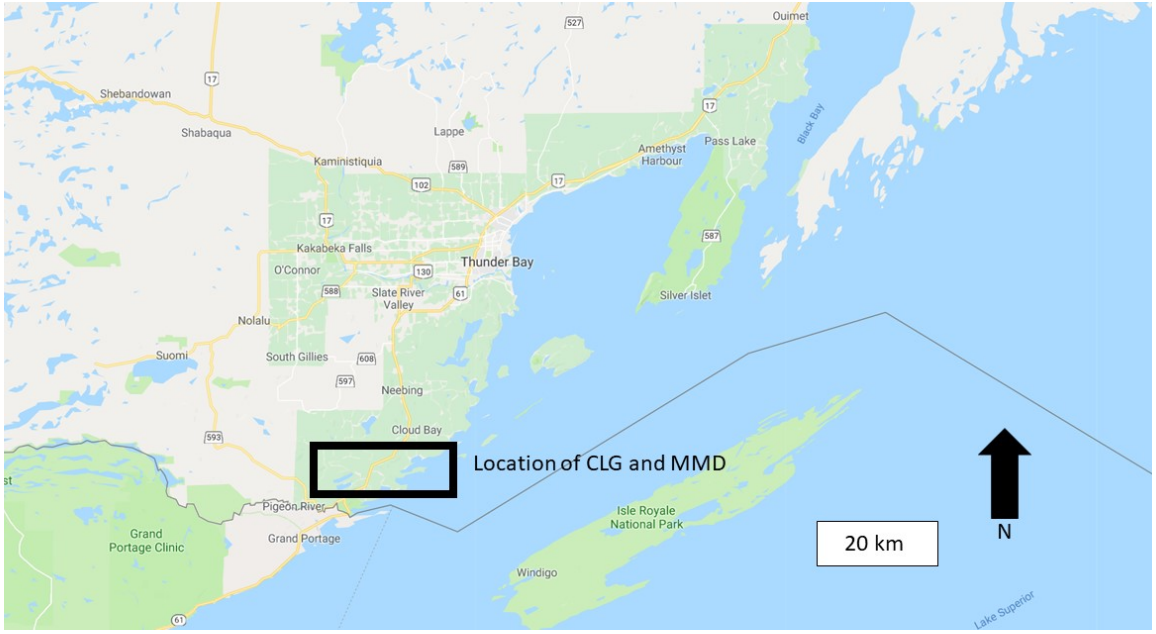

Figure 1.1. Location of the CLG and MMD. Modified from Google Maps (2018).

1.2 Objectives

The main objective of this study is to characterize the litho- and chemostratigraphy through the CLG and MMD by evaluating the mineralogy, textures, whole rock geochemistry, and mineral composition in long drill cores profiling each intrusion. This has been undertaken with the goal of evaluating whether these two spatially associated MCR related intrusive bodies are petrogenetically related.

Specific questions addressed include:

- What role did fractionation play in the overall development of the litho- and chemostratigraphy of the CLG and MMD?
- What role, if any, did crustal contamination play in the development of the CLG and MMD, particularly in regard to sulphide mineralization found within the CLG?
- Were the MMD and CLG formed by a single pulse or multiple pulses of magma?

- What was the parental magma compositions of the CLG and MMD?
- How do the estimated parental magmas of the MMD and CLG compare to other MCR-related intrusive systems?

2 REGIONAL GEOLOGY

The western Lake Superior region has had a long geological history recorded in a variety of rock types. These include Archean granites, greenstones, and gneisses of the Superior Province, Paleoproterozoic sedimentary rocks of the Animikie Basin, Mesoproterozoic redbed sedimentary rocks of the Sibley Group, younger Mesoproterozoic sedimentary, volcanic, and intrusive rocks of the MCR, and Quaternary glacial deposits. The key geologic terranes specifically related to the CLG and MMD are the Superior Province, the Animikie Basin, and the Midcontinent Rift. The main geological attributes of these terranes in the western Lake Superior area are described below.

2.1 SUPERIOR PROVINCE

The underlying crust of the MCR is largely the Archean basement of the Superior Province (Fig. 2.1). The Superior Province was developed by the amalgamation of distinct protocontinental and oceanic terranes, that ranged in age between 3.7 and 2.65 Ga, during the accretionary Kenoran Orogeny occurring between 2.72 to 2.68 Ga (Card and Ciesielski, 1986; Percival et al., 2006). The Superior Province is comprised of a series of east-trending belts that are composed of granite-greenstone, metasedimentary, plutonic, and high-grade gneisses and that have been metamorphosed to greenschist-granulite facies (Card and Ciesielski, 1986; Card, 1990). The belts have been subdivided into multiple subprovinces or terranes based on their lithologic, metamorphic, geochemical, isotopic, geochronologic and geophysical characteristics (Card and Ciesielski, 1986; Stott et al., 2010).

The Wawa subprovince underlies the section of the MCR that hosts the CLG and MMD. The Wawa subprovince is the western portion of the Wawa-Abitibi terrane with the Abitibi subprovince comprising the eastern portion, separated by the Kapuskasing structural zone (Stott et al., 2010). The Wawa subprovince is dominantly comprised of large masses of granitoid plutons with isolated arcuate to linear greenstone belts comprising 20 to 30% of the subprovince (Williams et al., 1990).

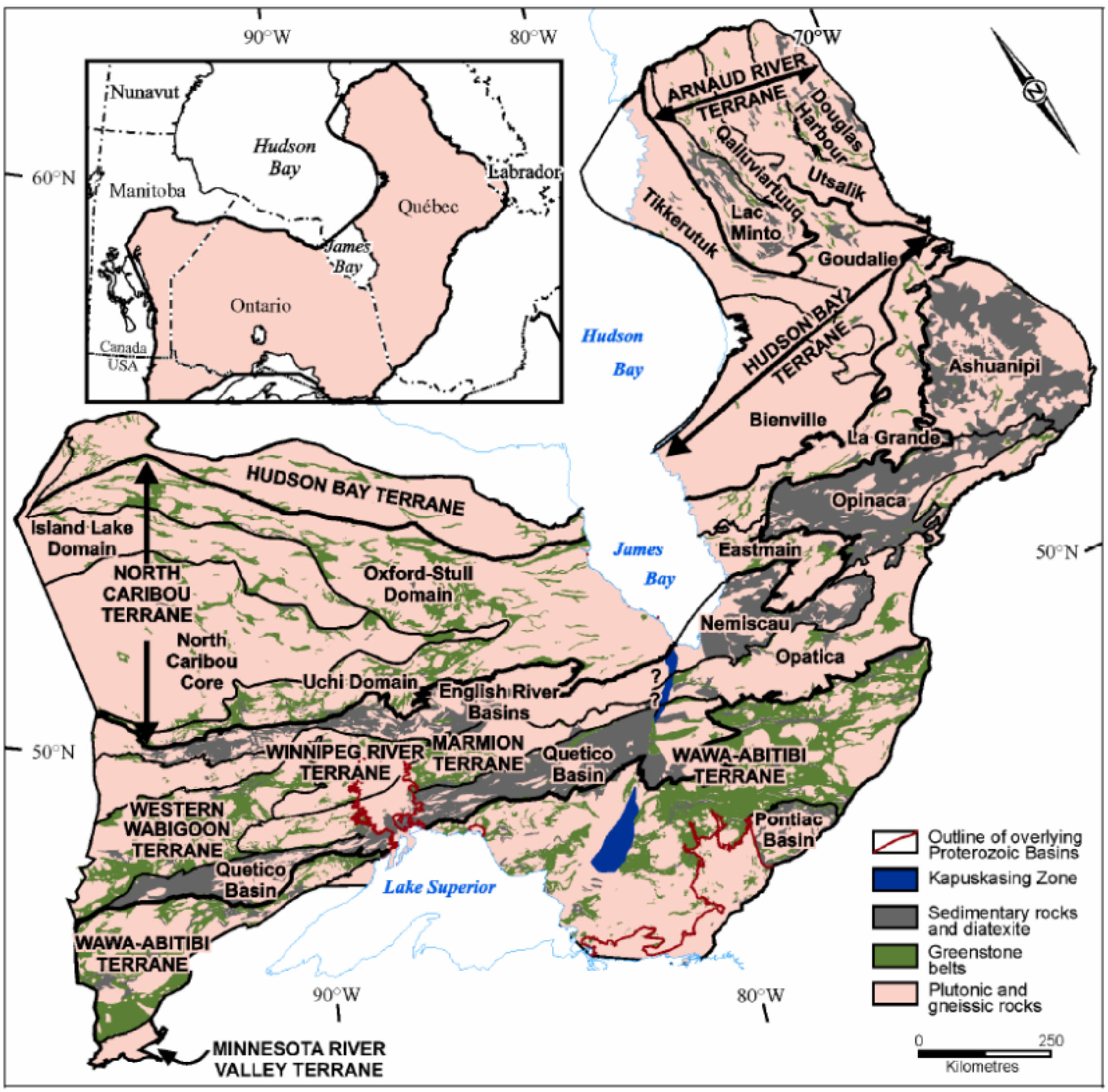

Figure 2.1. Map of the Archean Superior Province. From Stott et al. (2010).

2.2 ANIMIKIE BASIN

Paleoproterozoic sedimentary rocks of the Animikie Group, which extends through Ontario, Minnesota, Wisconsin, and Michigan, were deposited on Archean crust in a continental shelf/back arc basin about 1.85 Ga (Fig. 2.2; Johnston et al., 2006). The area of the Animikie Basin intruded by the CLG and MMD is termed the Logan Basin. The Animikie Group contains three conformable sedimentary formations: a basal conglomerate/quartzite unit, a chemically precipitated iron formation, and a shale/greywacke formation (Hemming et al., 1995; Fralick et al., 2002; Johnston et al., 2006). The MCR separated the basin into two segments located in Ontario-Minnesota and Wisconsin-Michigan. Local naming of the stratigraphy has occurred over a century of research, although each segment shares similar characteristics and can to be correlated with each other; the basal conglomerate/quartzite is known as the Mahnomen, Pokegama, and Kakabeka Formations, the iron formation is known as Trommald, Biwabik and Gunflint Formations, and the shale/grainstone is known as Thompson, Virginia, and Rove Formation (Hemming et al., 1995: Ojakangas et al., 2001). For simplicity Kakabeka, Gunflint, and Rove will be used for the remainder of this document as these are the names most widely used in the study area.

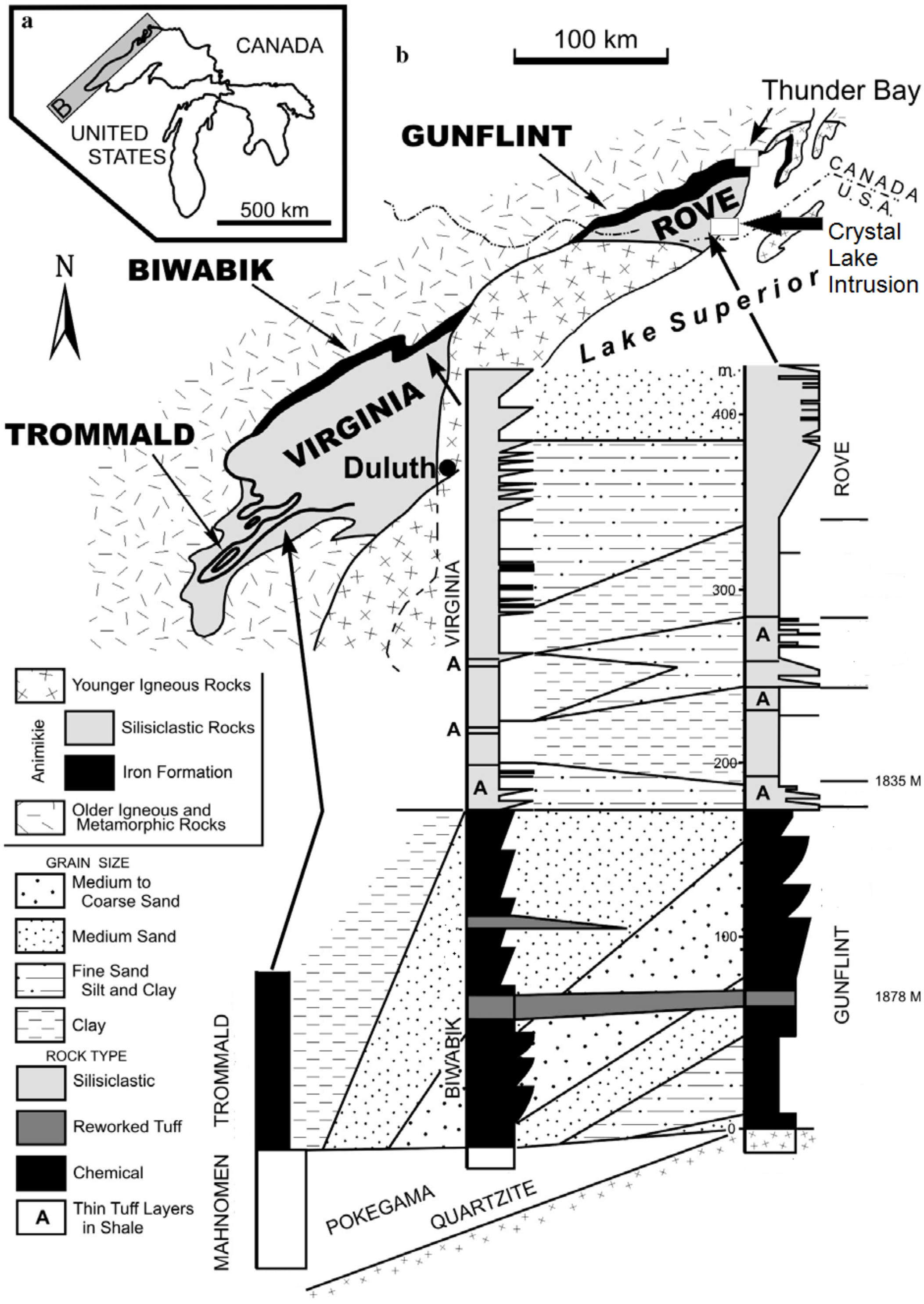

Figure 2.2. Location, geology, and generalized stratigraphy of the Animikie Group. Modified from Johnston et al. (2006).

Development of a passive margin between two land masses on the present southern edge of the Superior Province, was associated with rift development at ~2450 Ma (Johnston et al., 2006). The formation of the passive margin is thought to have occurred in three stages, an intrarift stage, a rift stage, and a post breakup stage (Southwick and Morey, 1991; Ojakangas et al., 2001). Two models have been proposed to explain how the Animikie Basin was formed, depicted schematically in Figure 2.3. One model, outlined in Hoffman (1987), Morey and Southwick (1995), and Ojakangas et al. (2001) suggested that, after initial continental rifting, further development led to the creation of a sea-floor which eventually closed as a result of northward subduction and creation of an island arc. This was followed by southward subduction and creation of a volcanic arc, known as the Wisconsin Magmatic Terrane. Eventually complete closure of the ocean occurred with an arc-continent collision.

Due to the collision, a foredeep was created in response to the loading during the Penokean Orogeny, in which the Animikie Group was deposited (Ojakangas et al., 2001). During the evolution of the foredeep there were changes in water depth creating the three formations of the Animikie group; a tidal flat environment where quartzite of the Kakabeka group formed, a shallow water environment where the Gunflint iron formation precipitated and finally to deep-water environment where the turbidities of the Rove Formation formed. The second model, outlined in Bond et al. (1988) for the Cenozoic Aleutian Basin formation and later expanded upon by Pufahl and Fralick (1995), Hemming et al. (1995) and Pufahl et al. (2000), suggests that the Animikie Basin evolved in a back-arc basin which formed as a result of extension created by a northward subduction zone during the sea-floor closure. The back-arc basin was subsequently destroyed by initiation of a fold and thrust belt being formed due to a change in the direction of plate convergence.

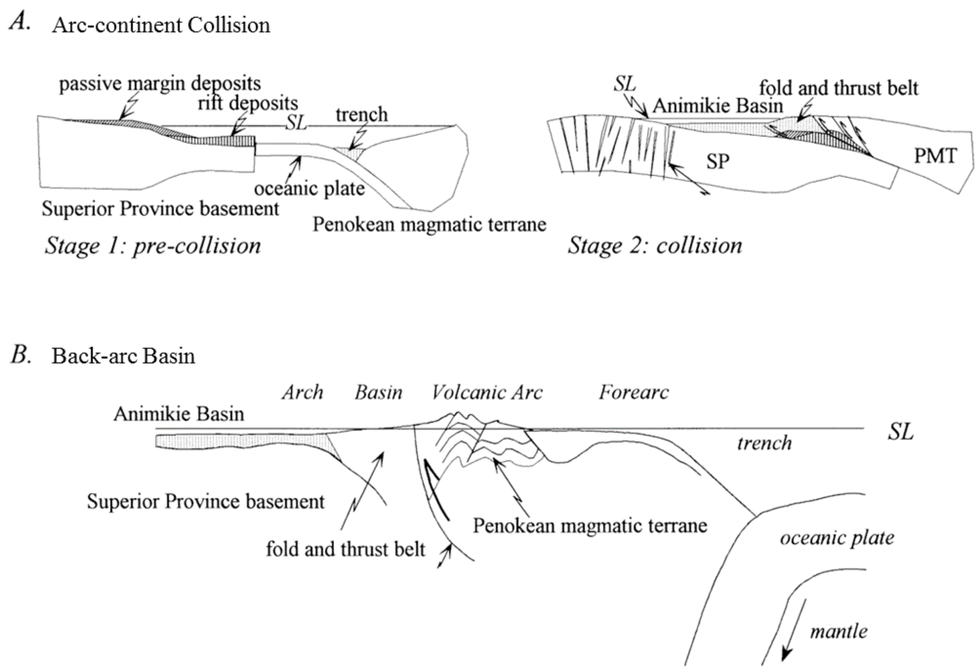

Figure 2.3. Proposed tectonic models for the development and depositional environment of the Animikie Basin. (A) Foredeep succession. (B) Back-arc basin. From Hemming et al. (1995).

2.2.1 Animikie Group in the Logan Basin

2.2.1.1 Kakabeka Formation

The Ontario portion of the Animikie Group, contains a sporadically discontinuous basal conglomerate <1.5 m thick (Pufahl, 1996) whereas, portions in the U.S.A have a <50 m thick Pokegama quartzite at the base. In locations where the conglomerate/quartzite is not present, the overlying Gunflint Formation lies unconformably on top of the Archean basement rock (Simonson and Hassler, 1996). The conglomerate represents an iron-poor shallow water deposit that contains stromatolitic cherts and coarse-grained clastic fragments. This formation is thought to have been deposited due to a transgression of the sea-level in shallow water (Simonson and Hassler, 1996). The depositional environment is suggested to have been near shoreline influenced by tides, with the sediments/clastics sourced from Archean basement rocks to the North (Hoffman, 1987; Ojakangas et al., 2001).

2.2.1.2 Gunflint Formation

The Gunflint Formation hosts one of the most diverse Precambrian fossil communities in the world, including stromatolites with cellular level preservation (Fralick et al., 2002). This formation is 120 to 185 m thick and dips 5^{o} to the south (Goodwin, 1956). Fining and coarsening upward successions found in the formation suggests that there were transgressive and regressive events during deposition (Fralick and Barrett, 1995). The environment during formation was an open and wave dominated shelf where water depth did not exceed 10 m (Pufahl and Fralick, 2004). The chemically precipitated rocks are thought to have formed by the introduction of iron-rich anoxic bottoms to the oxygenated shelf waters (Pufahl and Fralick, 2004). The Gunflint Formation has been divided into a lower member comprised of stromatolite bioherms, chert-carbonate, grainstones and chemical mud layers and a similar upper member that also contains shales and volcanic ash layers (Fralick et al., 2002). One of the ash layers has an age determined to be 1878 ± 1.3 Ma, which is believed to be the age of deposition (Fralick et al., 2002). The upper most portion of the Gunflint Formation contains agate and pyrite veins and vugs, which suggests that after deposition, during the Penokean Orogen (1860 to 1835 Ma) it was subareally exposed and altered (Johnston et al., 2006). Also, during this hiatus in deposition, an ejecta layer was deposited from the Sudbury Impact which took place 1850 ± 1 Ma (Krogh et al., 1984).

2.2.1.3 Rove Formation

Overlying the Gunflint, a sharp contact defines the bottom of the Rove Formation. The basal section of the Rove Formation consists of black carbonaceous shale with interbedded siltstone and very fine-grained sandstone, with friable tuffaceous layers (Maric and Fralick, 2005). Starting at around 5 m above the basal contact the siltstone and sandstone interlayers become less abundant and are followed by 100 to 150 m of black fissile shale (Maric and Fralick, 2005). This is overlain by a gradational contact to a sequence of over 100 stacked coarsening upward parasequences of a sandstone-shale unit of up to 350 m thickness (Maric and Fralick, 2005). The water depth for these successions is estimated to have been 100 to 200 m (Johnston et al., 2006). The uppermost unit consists of a black shale with wave and current rippled sandstones (Maric and Fralick, 2005). This unit also contains fine-grained and finely dispersed pyrite, suggesting formation in anoxic bottom waters with persistent sulphidic conditions and unrestricted access to open ocean waters (Poulton et al., 2004). The age of deposition was determined by zircons found in the basal and upper units of the Rove Formation that yielded ages of 1835 Ma and 1780 Ma (Heaman, 2005; Addison et al., 2005).

2.3 MIDCONTINENT RIFT

The MCR extends approximately 2,500 km from the Grenville front through northwestern Ontario to Kansas (Davis and Green, 1997). It is estimated to contain

1,300,000 km^3 of volcanic and intrusive rocks, although it is difficult to determine an accurate estimate due to loss to erosion, sills, dykes, intrusions still at depth, and magma that has been underplated (Hutchinson et al., 1990; Heaman et al., 2007). The evolution of the MCR started with a broad depression that has a correlated fluvial sequence ~100 m thick at the base of the supracrustal sequence (Ojakangas and Dickas, 2002). Extensive volcanism began around 1100 Ma over a broad area, but was ultimately focused into a central graben with approximately 25 km of basalt and lesser rhyolite fill (Cannon, 1992). Around 1086 Ma, extension and volcanism waned and the rift transitioned into a protracted period of subsidence and creation of a sedimentary basin, which was filled by ~8 km of post-rift sediments (Heaman et al., 2007).

The MCR formed from ~1115 to 1084 Ma, with the majority of the igneous activity occurring in two pulses from ~1115 to 1105 Ma and ~1100 to 1094 Ma (Heaman et al., 2007; Vervoort et al., 2007). A plume model has been suggested and is generally regarded as the most likely scenario for causing the rift, due to the amount and volume of magmatic activity, as well as the isotopic and chemical character of the associated rocks (Hutchinson et al., 1990; Nicholson and Shirey, 1990; Shirey et al.,1994; Nicholson et al., 1997; Shirey, 1997). There are also suggestions that there are some inconsistencies when comparing the MCR to other large igneous provinces (LIPs), largely due to the longer than normal time span of magmatism and lack of an associated radiating dyke swarm (Hollings and Heggie, 2014).

Along the length of the MCR there are a variety of pre-rift rocks into which the intrusions were emplaced. These crustal rocks range in age from 3.6 to 1.5 Ga, with the most voluminous intrusions in Ontario emplaced in the 2.7 Ga crust of the late Archean (Van Schmus, 1992). Hypabyssal rocks dominate the Ontario portion of the MCR related intrusions (Hollings et al., 2010). These intrusions, dykes, and sills are found from the Lake Nipigon area to the Ontario-Minnesota border (Fig. 2.4). These rocks are part of the proposed Logan Igneous Suite and subdivided into two informal groups; the Logan sills south of Thunder Bay and Nipigon sills north of Thunder Bay (Hollings et al., 2007a). Logan sills and Nipigon sills have a uniform paleomagnetic signature but are geochemically distinct from each other (Hollings et al., 2010 and references therein).

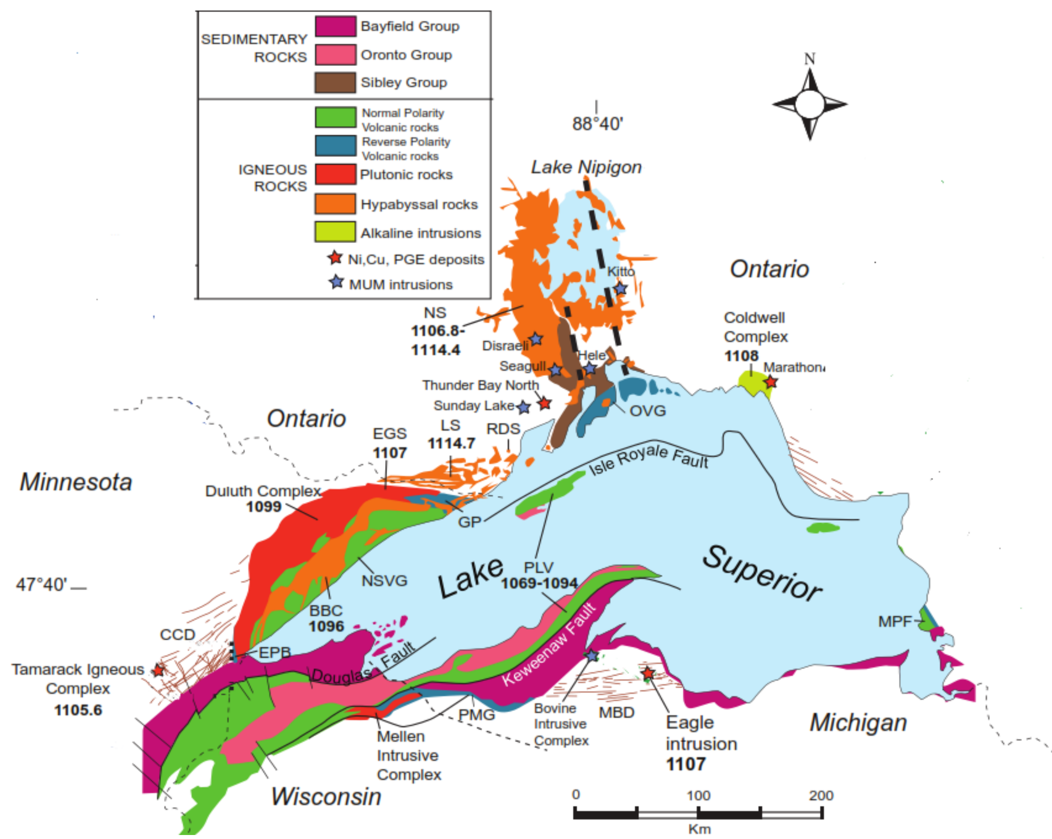

Figure 2.4. Generalized map of the MCR related rocks. Modified from Paces and Miller (1993) and Miller (pers. comm.). Abbreviations: EGS- Early Gabbro Series; BBC-Beaver Bay Complex; NSVG-North Shore Volcanic Group; GP-Grand Portage volcanics; EPB-Ely's Peak basalts; CCD-Carlton County dykes; LS-Logan sills; RDS-Riverdale sill; NS-Nipigon sills; OVG-Osler Group; MPF- Mamainse Point Formation; MBD-Marquette-Baraga dykes; PLV- Portage Lake Volcanics; PMG-Powder Mill Group.

2.3.1 MCR Intrusions in the Lake Nipigon Area

MCR rocks in the area surrounding Lake Nipigon are underlain primarily by Archean age greenstone belt rocks (2950 to 2700 Ma) of the English River, Wabigoon, and Quetico subprovinces of the Superior Province (Hart and MacDonald, 2007). There are four sill-like mafic to ultramafic intrusions in the area; Disraeli, Seagull, and Hele on the southern side of Lake Nipigon and Kitto on the eastern side (Fig. 2.4). The intrusions are sill-like and are comprised of equal amounts of ultramafic (lherzolite, websterite, and dunite) and mafic (olivine gabbro and gabbro) rocks, except Seagull where the ultramafic rocks are more abundant than mafic (Hart and MacDonald, 2007). Also in the area are a number of laterally extensive diabase sills including the Shillabeer, Inspiration, Jackfish sills. The sills are mostly massive, medium- to coarse-grained gabbronorite to gabbro (Hart and MacDonald, 2007). The Nipigon Embayment and associated intrusions and sills are among the oldest rocks of the MCR (Heaman et al., 2007). The lack of known extrusive rocks related to the intrusive rocks, and the absences of dykes in the area has led to the belief that the Nipigon Embayment was formed during a weakly extensional or compressional environment (Hollings et al., 2007a).

2.3.1.1 Seagull

The Seagull intrusion is comprised mainly of ultramafic (~650 m) and mafic (<100 m) rocks. The lower ultramafic unit consists mainly of peridotites with dominant cumulus olivine and post cumulus poikilitic pyroxenes, and the upper mafic units are comprised of feldspar-pyroxenites, olivine gabbros, and gabbros (Heggie, 2005). Ni-Cu-PGE mineralization was discovered near the base of this intrusion in 1998-2001 during a drilling program (Heggie, 2005). Heaman et al. (2007) determined a U-Pb baddeleyite age of 1112.8 ± 1.4 Ma.

2.3.1.2 Kitto

The Kitto intrusion, located on the Eastern side of Lake Nipigon, is a peridotitic to gabbroic intrusion with five main rock types; lherzolite, olivine websterite, vari-textured pyroxenite, pyroxenite, and melagabbro (Laarman, 2007). This intrusion is thought to have formed from two magma pulses and have been contaminated by Archean crust (Laarman, 2007). The Kitto Intrusion is geochemically distinct from the other ultramafic intrusions, which is thought to be because the others are hosted in either the Sibley or Quetico subprovinces whereas the Kitto is hosted in rocks of the Wabigoon subprovince (Hart and MacDonald, 2007). Heaman et al. (2007) determined a U-Pb baddeleyite age of 1117.5 ± 3.7 Ma.

2.3.1.3 Disraeli and Hele

The Disraeli and Hele intrusions are compositionally similar and are composed of roughly equal parts mafic and ultramafic rocks. The rock types present in both are ophitic lherzolite and olivine websterite with minor kaersutite and phlogopite in the ultramafics and olivine gabbro, olivine hypersthene gabbro, and gabbro for the mafics. Disraeli differs from Hele in that the olivine gabbro is interlayered with lherzolite and websterite (Hollings et al., 2007a and references therein). The Hele and Disraeli intrusions are among the least contaminated MCR related intrusions (Hollings et al., 2007a). Heaman et al. (2007) determined a U-Pb baddeleyite age of 1109.9 ± 1.5 Ma and 1106.6 ± 1.5 Ma for Disraeli and Hele, respectively.

2.3.1.4 Nipigon Sills

Nipigon sills are widespread in the Lake Nipigon area and range in thickness from 150 to 250 m and are estimated to have been emplaced at depths less than 1.5 km (Zieg, 2014, and references therein). These sills are hosted in the English River, Wabigoon, and Quetico subprovinces of the Archean Superior Province as well as Proterozoic rocks of; the English Bay Complex, Sibley Group, and other mafic and ultramafic intrusions (Heaman et al., 2007). These sills are mostly gabbro to gabbronorite and are generally medium- to coarse-grained (Hollings et al., 2007a). Complex cooling histories or multiple injections of magma are thought to have occurred during emplacement of the sills, as suggested by crude layering and a lack of internal chill zones (Hart, 2005; Hollings et al., 2007a). Heaman et al. (2007) determined U-Pb zircon ages of 1110.1 ± 2.1 Ma and 1106.8 ± 1.9 Ma for separate sills.

2.3.2 MCR Intrusions in the Logan Basin

The 70 km x 30 km area of the rugged terrane of mesas and ridges towering above flat lying valleys, between Thunder Bay and the Ontario-Minnesota border (Fig. 2.5), was termed the Logan Basin by North (2000). The first published geological map and rock descriptions of the area is that of T. L. Tanton (1931, 1935, and 1936). Further mapping and descriptions of the area was undertaken by Pye and Fenwick (1965), Geul (1970, 1973), and Smith and Sutcliffe (1987, 1989). Whereas the Nipigon sills and intrusions are underlain by the English River, Wabigoon, and Quetico subprovinces of the Superior Province, the Logan Basin is underlain by the Wawa subprovince.

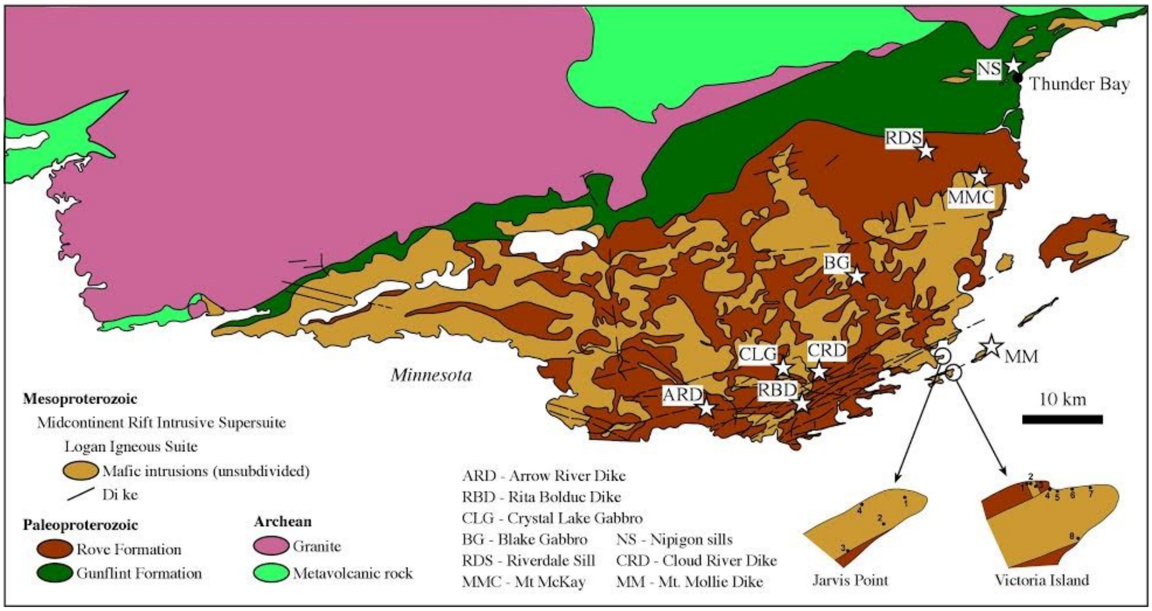

Figure 2.5. Geological map of the Logan Basin area. From Hollings et al (2010) and modified from Pye and Fenwick (1965).

2.3.2.1 Logan Sills

Logan sills were originally classified with the Nipigon Sills based on a similar paleomagnetic signature, but more recently a geochemical difference between the sills north and south of Thunder Bay, has resulted in them being subdivided into two populations (Hollings et al., 2010 and references therein). Sills in the Logan Basin area have higher TiO_2 and more depleted heavy rare earth elements (HREE) than the Nipigon Sills (Hollings et al., 2007a). The sills are mainly composed of equigranular tholeiitic diabase with chill zones at the contact with the sedimentary rocks of the Animikie Group. From the contact the sills grade upward to fine-grained ophitic diabase, medium-grained megacrystic plagioclase phyric diabase, and an iron-rich diabase which is usually found at surface (Smith and Sutcliffe, 1987). Bulk compositions of the sills are equivalent to an iron-rich quartz tholeiite basalt (Hollings et al., 2010). Thicker sills in the area may contain coarse-grained gabbro with granophyre in the interior of the sills (Hollings et al., 2010). The flat lying Rove Formation, into which most of the sills are emplaced, is the main control on the thickness and morphology, often capping mesas and cuestas in the area (Cundari, 2012). Heaman et al. (2007) determined a U-Pb baddeleyite age of 1114.7 ± 1.1 Ma for a Logan Sill within the basin.

2.3.2.2 Crystal Lake Gabbro

The CLG is Y-shaped in plan view with a 5 km long northern limb trending east and a 2.75 km long southern arm trending east northeast (Fig. 2.6). Based upon layering, foliation, and surface geometry it is thought to be a tilted canoe shaped body which plunges 15 to 20^{o}, opening of the western end of the intrusion (Smith and Sutcliffe, 1989; Cogulu, 1993a).

Based on field observations of the western portion of the northern limb of the CLG, the intrusion has been subdivided into four zones: Basal, Lower, Middle, and Upper. The base of the intrusion consists of a <7 m thick chilled zone of aphanitic to fine-grained gabbro, with partial assimilated xenoliths of the Rove Formation and oval inclusions of Pigeon River Dyke (Smith and Sutcliffe, 1989). The Lower Zone reaches a maximum thickness of 50 m. The lower part of the zone consists of medium- to coarse-grained gabbro with patches and blocks of pegmatitic gabbro and leucotrocolite as well as disseminated sulphides (Smith and Sutcliffe, 1989). The upper portion of the Lower Zone consists of coarse-grained to pegmatitic leucogabbro and leucotroctolite with elliptical-shaped segregations rich in disseminated chromite that elongate parallel to layering (Smith and

Sutcliffe, 1989). The Middle Zone is 30 m thick and defined by distinct phase layering of anorthosite, olivine leucogabbro, chromite rich anorthosite and melanocratic olivine gabbro. The Upper Zone is 80 m thick, defined by the disappearance of chromite rich layers and consists of coarse-grained olivine gabbro with an overlying medium-grained troctolite (Smith and Sutcliffe, 1989).

Cogulu (1993a) reported a great diversity in the chrome spinels in regard to composition, reflecting a complex history of crystallization and reequilibration during post cumulus reactions. Observed textures suggest that the chrome spinels were the first mineral to crystallize, as a result of magma mixing during influxes of new magma (Cogulu, 1993a). Cogulu (1993b) describes two sulphide populations, both consisting of pyrrhotite, chalcopyrite, cubanite, and pentlandite. The first sulphide population forms massive and disseminated ore and is found in the Basal and Lower Zones and the second population is found in the Middle Zone and forms low grade disseminated sulphides (Cogulu, 1993b). The Se/S ratios and sulphur isotopes suggest that assimilation and devolatilization of the sulphidic Rove Formation was the principal source of Cu-Ni mineralization, which was generated from a segregation of a Fe-Ni rich monosulphide solid solution (mss) and later, through fractional crystallization, a Cu rich intermediate solid solution (iss; Cogulu, 1993b; Thomas, 2015).

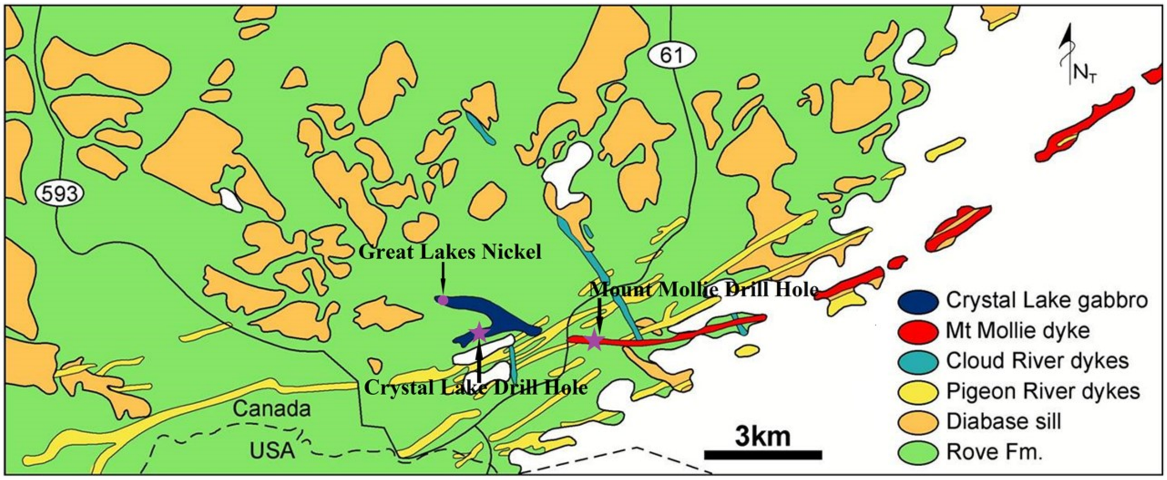

Figure 2.6. Generalized geology map of CLG, MMD and surrounding rocks. Modified from Cundari et al. (2013a).

2.3.2.3 Logan Basin Dykes

Three dyke suites have been recognised in the Logan basin; the Pigeon River dykes, Cloud River dykes, and the MMD, they are classified mainly by their orientation and age (Fig. 2.6; Cundari, 2012).

Pigeon River dykes trend east-northeast to northeast, dip steeply to the southeast, and are the most abundant in the area. These dykes are thought to have followed pre-existing normal faults, as suggested by warping of the Rove Formation on the southern sides of the dykes and slickensides on some contacts that suggests further reactivation of the faults (Smith and Sutcliffe, 1989). The observed contacts of the dykes and Rove Formation are either < 5 cm aphanitic to fine-grained diabase chill zones or 0.5 m to 1 m thick gradational contacts of fine- to medium-grained diorite containing xenoliths of Rove Formation (Smith and Sutcliffe, 1989). Most commonly the rocks are fine- to medium-grained ophitic diabase with oikocrystic clinopyroxene and glomoporphyritic plagioclase, with a typical mineral assemblage of 60% plagioclase, 20% augite ± hypersthene, up to 15% olivine and up to 5% magnetite, and trace ilmeno-magnetite and sulphides (Geul 1973; Smith and Sutcliffe, 1989). The Pigeon River dykes range in thickness from an average of 50 m to 70 m and up to 150 m, and extend for up to 15 km. Two U-Pb baddeleyite ages have been determined for the Pigeon River dykes 1141 ± 20 Ma and 1078 ± 4 Ma (Heaman et al., 2007). Generally, the Pigeon River dykes display a N polarity, however two dykes display a R polarity (Pesonen, 1978; Halls and Pesonen, 1982; Hollings et al., 2010).

Cloud River dykes trend northwest and consist mainly of plagioclase-phyric quartz diabase with a U-Pb baddeleyite age of 1109.3 ± 4.2 Ma (Hollings et al., 2010). Inconsistent and contradicting paleomagnetic signatures have also been reported for the Cloud River dykes with Piispa et al. (2011) reporting a N polarity and Hollings et al. (2010) reporting a R polarity, where the N polarity is more likely due to a higher sample size.

Extending east from the CLG lies the 35 km long 60 to 350 m wide MMD which dips between near vertically to 35° north (Geul, 1973). The MMD extends into a series of islands in Lake Superior where it shows a northeast trend compared to the east trend on the mainland (Fig. 2.6). The MMD is a composite dyke with a variety of rock types and textures. Variations in modal mineralogy result in rock types ranging from olivine gabbro to gabbro to hornblende diorite to granophyre. Grain size within the dyke varies from fine- to coarse-grained to locally pegmatitic patches. Though typically massive, locally the gabbros display foliation and modal layering (Smith and Sutcliffe, 1989). With increasing quartz and hornblende in the core of the dyke, the gabbro grades into a fine- to coarse-grained diorite with either gradational or sharp contacts with a fine-to medium-grained granophyre (Smith and Sutcliffe, 1989). Smith and Sutcliffe (1989) also note textural evidence for magma mixing of mafic and felsic magmas as noted by apophyses and net veining of granophyre within the diorite and gabbro.

Geul (1970, 1973) and Cundari (2012) have mapped this area to determine relationships between the dyke sets. Based on the cross-cutting relationships as well as textural similarities found in outcrop, Cundari (2012) proposed that the emplacement sequence of the dykes was likely Pigeon River followed by Cloud River and lastly Mount Mollie. Recent geochronological, geochemical, and paleomagnetic studies have attempted to understand the evolution of the dyke sets (Hollings et al., 2007a, 2010, 2012; Heaman et al., 2007; Piispa et al., 2011), though contradictions in geochronology and paleomagnetism still exist. It is generally accepted that MCR rocks >1105 Ma display a R polarity and rocks <1102 Ma have a N Polarity (Davis and Green, 1997), which is not consistent with some of the age determinations of Heaman et al. (2007). The most significant inconsistency for this study is that Piispa (2011), Robertson and Fahrig (1971), and Pesonen (1978) reports a N polarity for the MMD and Hollings et al. (2010) reports a 1109.3 ± 6.3 Ma age. Smith and Sutcliffe (1989) noted that the CLG post dates all sills and dykes in the area based on cross-cutting relationships. Table 2.1 summarizes the paleomagnetism and U-Pb age determination of the Logan Basin rocks.

Table 2.1. Polarity and age of Logan Basin Rocks.

Unit	Polarity	Age
Crystal Lake Gabbro	N[1]	1099.6 ± 1.2 Ma[5]
Mount Mollie Dyke	N[1,2]	1109.3 ± 6.3 Ma[2]
Cloud River Dykes	N[1], R[2,3]	1109.2 ± 4.2 Ma[2]
Pigeon River Dykes	N[1], N/R[2,3,4]	1141 ± 20 Ma[5]
		1078 ± 3 Ma[5]
Logan Sills	N[1], R[4]	1114.7 ± 1.1 Ma[5]

Data obtained from 1-Piispa et al. (2011) 2-Hollings et al. (2010) 3-Robertson and Fahrig (1971) 4-Pesonen (1978) 5-Heaman et al. (2007).

2.3.3 Duluth Complex

The CLG, due to its proximity, troctolite to olivine gabbro composition, and age, has been suggested to be a satellite intrusion of the Duluth Complex (Eckstrand, 1996). The Duluth Complex covers an area over 5000 km^2, is located in Minnesota and is comprised of many individual discrete intrusions (Miller et al., 2002). It the second largest gabbroic complex in the world behind South Africa's Bushveld Complex. Age, lithology, internal structure, and structural position within the complex have been used to classify four series of intrusive rocks (Miller et al., 2002). The Felsic Series and the Early Gabbro Series were emplaced during the early magmatic stage of the MCR (~1108 Ma). The Early Gabbro Series is comprised of semi continuous intrusions along the central roof zone and northeastern contact (Miller et al., 2002). The Early Gabbro Series also occurs along the northeastern basal contact and is comprised of gabbroic cumulates (Miller et al., 2002). The Anorthositic Series and Layered Series were emplaced about 1099 Ma during the second stage of MCR magmatism. The slightly older Anorthositic Series is comprised of plagioclase rich, unlayered, foliated cumulates and the Layered Series includes 11 troctolitic-ferrogabbroic cumulate intrusions at the base of the Duluth complex (Miller et al., 2002).

2.3.4 Exploration History of the Crystal Lake Gabbro

Interest in the area around the CLG and MMD (i.e., Logan Basin) began in the late 1800's with the discovery of silver bearing veins (Parks, 1925). At the turn of the 20th century Cu-Ni±PGE mineralization was discovered and explored for fairly extensively in many of the sills, dykes, and intrusions of the area, most notably the CLG (Geul, 1970). Many companies and individuals have explored and/or had claims/drilled in the area including J. A. McCuaig, United States Smelting and Refining Company, Frobisher Exploration Company Limited, Falconbridge Nickel Mines Limited, Anaconda American Brass Limited, Bordum Mining Corporation Limited, Bretton Mines Limited, Copperville Mining Corporation Limited, Grasset Lake Mines Limited, Noranda Mines Limited, Norpoint Explorations Limited, Pine River Mines Limited, Romex Mines and Explorations Limited, Seemar Mines Limited, Denison Mines Limited, Phelps Dodge Corporation of Canada Limited, Platinum Exploration Canada Inc., and Falconbridge Limited (Geul, 1970; Wells, 1998). The most extensive work was done by Great Lakes Nickel Corporation Limited and Boliden Aktiebolag of Sweden in the 1960s and 1970s. The two companies defined a potential orebody on the tip of the northern arm of the CLG containing proven and indicated reserves of 41.4 million tonnes grading 0.334% Cu, 0.183% Ni, 0.69 g/t Pd, 0.21 g/t Pt, 0.01 g/t Rh,0.07 g/t Au, and 2.06 g/t Ag (Smith and Sutcliffe, 1989). During their work, two adits of 37 m and 1052 m were excavated as well as 58,674 m and 25,268 m of surface and underground diamond drilling, respectively (Smith and Sutcliffe, 1989). Most recently Rio Tinto has acquired the claims on the CLG property and has developed a drilling program as well as re-logging and assaying of historic drill cores (Goldner, 2015).

3 METHODS

3.1 PETROGRAPHIC STUDY

Polished thin sections (forty-five from the CLG drill core and thirty-seven from the MMD drill core) were prepared at Lakehead University's lapidary facility. These thin sections were used for petrography and scanning electron microscopy - energy dispersive spectroscopy (SEM-EDS) mineral composition analysis. Full descriptions of thin sections can be found in Appendix A. Photomicrographs were taken using an Olympus Bx51 microscope with attached Olympus DP-70 camera. Microsoft Research Computational Photography Group's Image Composite Editor was used for photo stitching.

3.2 WHOLE-ROCK GEOCHEMISTRY

3.2.1 Crystal Lake Gabbro

The CLG analyses were provided by Rio Tinto and carried out by ALS Limited Geochemistry, Thunder Bay using their "complete characterization package" (CCP-PKG03) with additional nickel-copper (OG-62) and platinum group metals (PGM-ICP27) assay add-ons. A total of 323 samples were obtained from the CLG core from half-core samples taken over sample intervals of 1.5 to 3 m (data available in Goldner, 2015). Samples were crushed to 70% passing 2mm fraction size and then a representative 1kg split was taken from the crushed allotment. This subsample was then pulverized to 85% passing 75 microns in size. Major elements were analyzed using fused disk x-ray fluorescence (XRF). To achieve a full suite of trace elements including rare earth elements (REEs), samples were analyzed by three methods; a lithium borate fusion with inductively coupled plasma mass spectrometry (ICP-MS) analysis, a four-acid digestion and inductively coupled plasma optical emission spectrometry (ICP-OES) analysis, and an aqua regia digestion with ICP-MS analysis. Samples that contained "ore-grade values" of Cu, Ni, and/or PGE were analyzed using fire assay and an ICP-OES analysis. Further information regarding detection limits can be found in Goldner (2015). Concentrations of elements in this study have been recalculated based on a 100% volatile-free values.

3.2.2 Mount Mollie Dyke

The MMD analyses were completed at the Geoscience Laboratory (GeoLabs) of the Ontario Geological Survey in Sudbury, Ontario. A total of seventy-six samples were obtained from core and twenty-one field samples were collected. Samples were pulverized in a 99.8% pure aluminum oxide planetary ball mill and passed through a 90-micron mesh size. Samples were then analyzed for loss on ignition (105ºC in nitrogen atmosphere, 1000ºC in oxygen atmosphere) and then fused into a disk with a borate flux and analyzed using a XRF-PANalytical instrument for major elements. To achieve a full suite of trace elements including REE's, samples were analyzed using three methods; a pressed powder pellet XRF using a XRF-PANalytical instrument, a closed vessel multi-acid digestion (HCl, HF, and HNO_3) with both ICP-MS (PerkinElmer Elan 9000) and ICP-OES analyses. Further analyses were required for carbon and sulfur concentrations, with values obtained by infrared absorption after the sample was combusted in an oxygen rich environment. PGE concentrations were determined by ICP-MS after samples underwent a nickel sulphide fire assay. To ensure the accuracy of the analysis both in house and international standards (i.e., MRB-29, AGV-2, GSP-2, and BHVO-2) as well as blanks and duplicates were analysed alongside the samples. Further information regarding detection limits can be found in Appendix B, alongside data. Concentrations of elements have been recalculated based on 100% volatile-free values.

3.3 MINERAL COMPOSITION

Mineral composition was undertaken on twenty-two (eleven CLG and eleven MMD) carbon coated polished thin sections, at the Lakehead Instrumentation Laboratory using a JEOL 5900 SEM equipped with an Oxford EDS with a resoltion of 139eV using a backscatter electron detector. EDS spectra were obtained over 45 seconds (live time), using an accelerating voltage of 20 kV and a beam current of 0.30 nA. The spectras obtained were processed using the LINK ISIS SEMQUANT software, to determine elemental concentrations, using the sigma % output from the EDS detector (data available in Appendix C). Elements (Ca, Na, Fe, Mg, Al, Si, K, Mn, Ni) were standardized using materials from the Lakehead Instrumentation Laboratory standards library. The elements and standards codes used are the following; Na (Lu-JAD), Mg (LU-PER), Al (LU-COR), Ca (LU-WOLL), K (LU-ORTH), Si (LU-GARN), Fe (MN-HORT GI20), Ni (OL-NI), Mn (LU-MNSIO3). Standardization occurred at the beginning of each session and standards were periodically analysed throughout each session to assure good data quality. Three to six analyses per grain and two to six grains per sample were completed for each mineral species.

3.4 SULPHUR ISOTOPES

Sulphur isotope analyses were undertaken at the Indiana University Stable Isotope Research Facility following the procedure of Studley et al. (2002). Sulphide powders were obtained by drilling out visible sulphide minerals in rock samples, using a 0.3 mm tungsten carbide drill bit. The sample powder (0.1 to 0.2 mg) and V_2O_5 powder (1 to 2 mg) were added to tin cups and then combusted in an elemental analyzer to form SO_2, which was subsequently analyzed in a Finnigan Delta V stable isotope ratio mass spectrometer, with results repoted in ‰ delta notation relative to Vienna-Canyon Diablo Troilite (data available in Appendix D). International standards; NBS-127 (20.3‰), IAEA S-1 (-0.3‰), IAEA S-2 (21.7‰) and IAEA S-3 (-31.3‰) were used as reference standards. Sample reproducibility determined by multiple analyses was ± 0.3 ‰; instrumental measurement uncertainty is less than 0.05 ‰.

4 RESULTS

4.1 PETROGRAPHY

4.1.1 Introduction

Petrographic data for the CLG and MMD were collected from polished thin sections, prepared at Lakehead University Lapidary Laboratory. Transmitted and reflected light microscopy were utilized in this study and modal percentages were based on visual estimation. Grain sizes are reported as very fine-grained (<0.2 mm), fine-grained (<1 mm), medium-grained (1 to 5 mm), coarse-grained (5 to 20 mm), and very coarse-grained/pegmatitic (>20 mm). Detailed descriptions of each sample are present in Appendix A.

4.1.2 Crystal Lake Gabbro

Five lithologic units were identified by drill core observations and petrographic analysis of CLG thin sections; CLG-Upper Zone, CLG-Main Zone, CLG-Lower Zone, Logan Sill, and Rove Formation sedimentary rocks. Rocks of the Upper, Main, and Lower Zones of the CLG are defined by the modal abundances of the three most abundant mineral phases; plagioclase, clinopyroxene, and olivine, normalized to 100% and plotted on a ternary diagram developed by Miller et al. (2002; Fig. 4.1). Downhole modal abundances of the three minerals are presented in Figure 4.2.

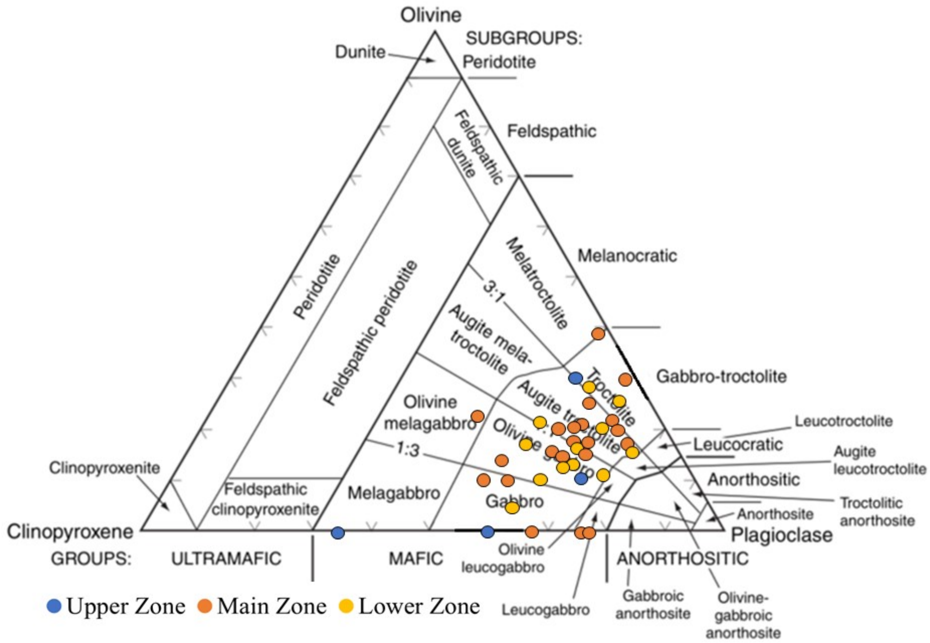

Figure 4.1. Ternary diagram of plagioclase, olivine, and clinopyroxene normalized modal abundances plotted for rock type for the CLG drill core samples. Fields after Miller et al. (2002).

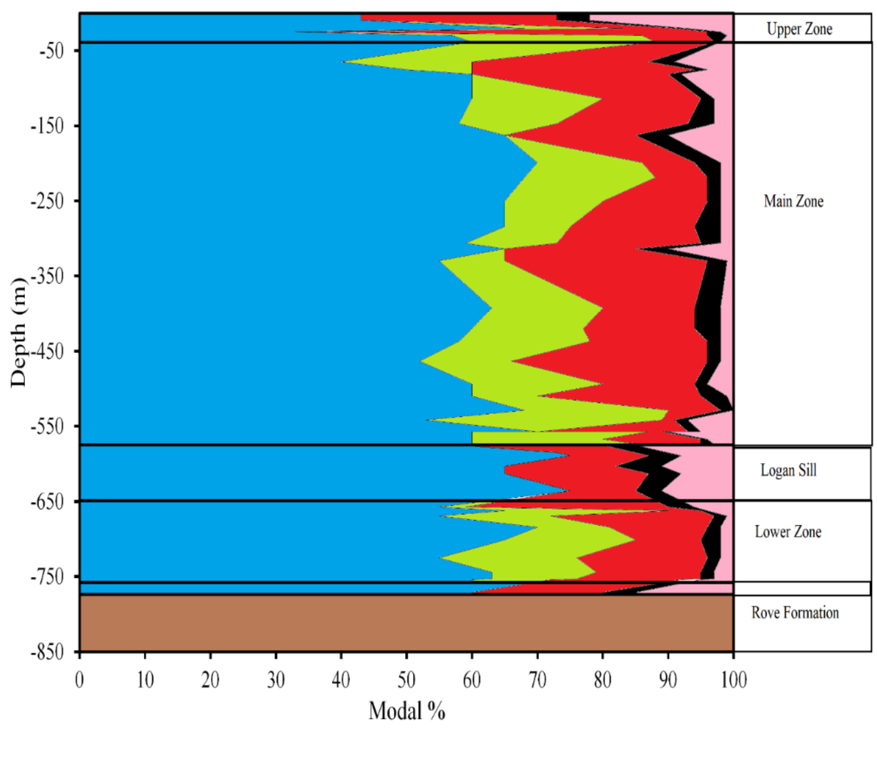

Figure 4.2. Downhole mineral modal abundance variations for the CLG drill core samples. Blue=plagioclase, green=olivine, red=clinopyroxene, black=Fe-Ti oxide, pink=accessory minerals.

4.1.2.1 Upper Zone

The rocks of the uppermost portion of the CLG drill core (0 to 38 m depth) represent the Upper Zone, consisting of gabbro and augite troctolite. The rocks in this zone are generally moderately to strongly altered with decreasing alteration with depth. This Upper Zone can be subdivided into an upper and lower portion. The upper portion of the Upper Zone contains fine- to medium-grained seriate, sub-equant (non-lath shaped), anhedral to subhedral plagioclase grains (Fig. 4.3A). Sericite alteration occurs in patches within plagioclase grains with variable amounts of replacement from 20% to complete pseudomorphing, with an average of 40% replacement. Cumulus olivine exists up to 18% and has been completely pseudomorphed by serpentine and minor talc (Fig. 4.3B). Material interstitial to the plagioclase is comprised of granophyre, free quartz (i.e., quartz not intergrown with K-feldspar), intergrown actinolite, chlorite, and biotite, Fe-Ti oxides, and sulphides (Fig. 4.3C). Granophyre and free quartz are found in roughly equal proportions and combined represents modally up to 20%. The actinolite and biotite present potentially could be either primary accessory phases (Fig. 4.3D), or could be alteration products of clinopyroxene which has been completely pseudomorphed (Fig. 4.4A). Fe-Ti oxides occur interstitially as irregular shaped amoeboidal and subpoikilitic, skeletal, or blade shaped grains (Fig. 4.4B).

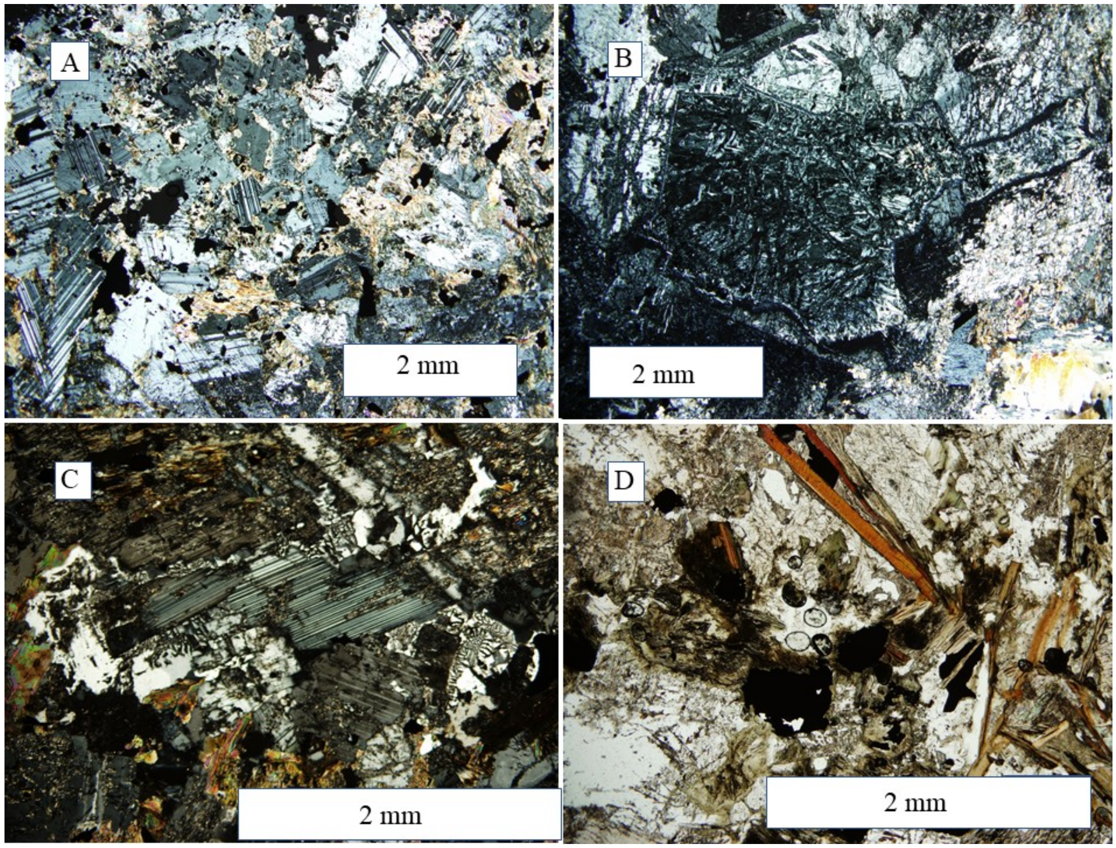

Figure 4.3. CLG-Upper Zone photomicrographs (A) Non-lath shaped, anhedral plagioclase laths. Interstitial to plagioclase are strongly altered pyroxene (Transmitted light; XPL; CLG-1). (B) Olivine that has been pseudomorphed by serpentine and Fe-oxide (Transmitted light; XPL; CLG-2). (C) Quartz and K-feldspar granophyric texture surrounding plagioclase lath (Transmitted light; XPL; CLG-1). (D) Possible primary biotite laths (Transmitted light; PPL; CLG-1).

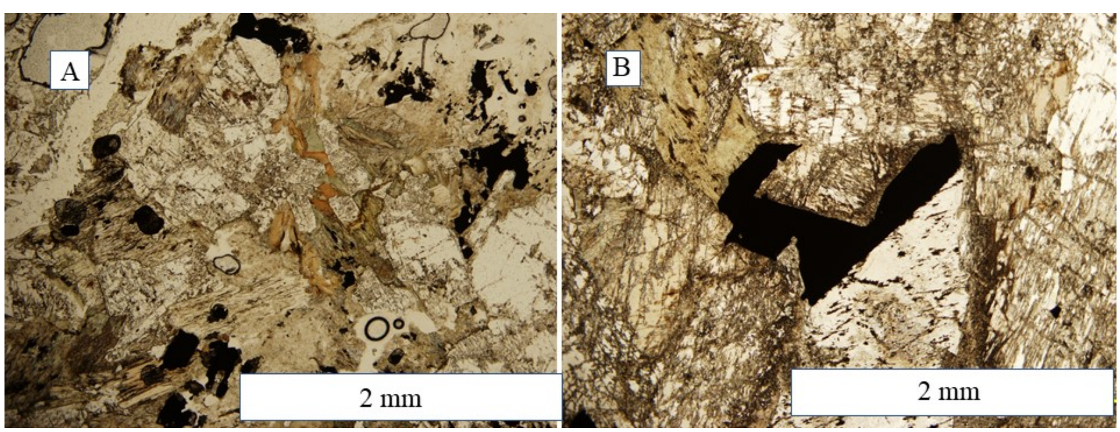

Figure 4.4. CLG-Upper Zone photomicrographs (A) Alteration assemblage of actinolite, biotite, and chlorite (Transmitted light; PPL; CLG-1). (B) Subpoikilitic Fe-Ti oxide (Transmitted light; PPL; CLG-2).

Chromite appears sporadically in interstitial pockets as fine, euhedral, and equant shaped grains (Fig. 4.5A). Sulphides comprise up to 3% of the rock, mostly pyrrhotite and minor chalcopyrite (Fig. 4.5B). The sulphides range in size from 0.5 to 6 mm and occur interstitial to plagioclase as well as disseminated blebs. Alteration is vey strong surrounding the blebs with locally occurring fibrous zeolites directly adjacent to one large (6 mm) bleb (Fig. 4.5C). This portion also contains rare sedimentary xenoliths (Fig. 4.5D).

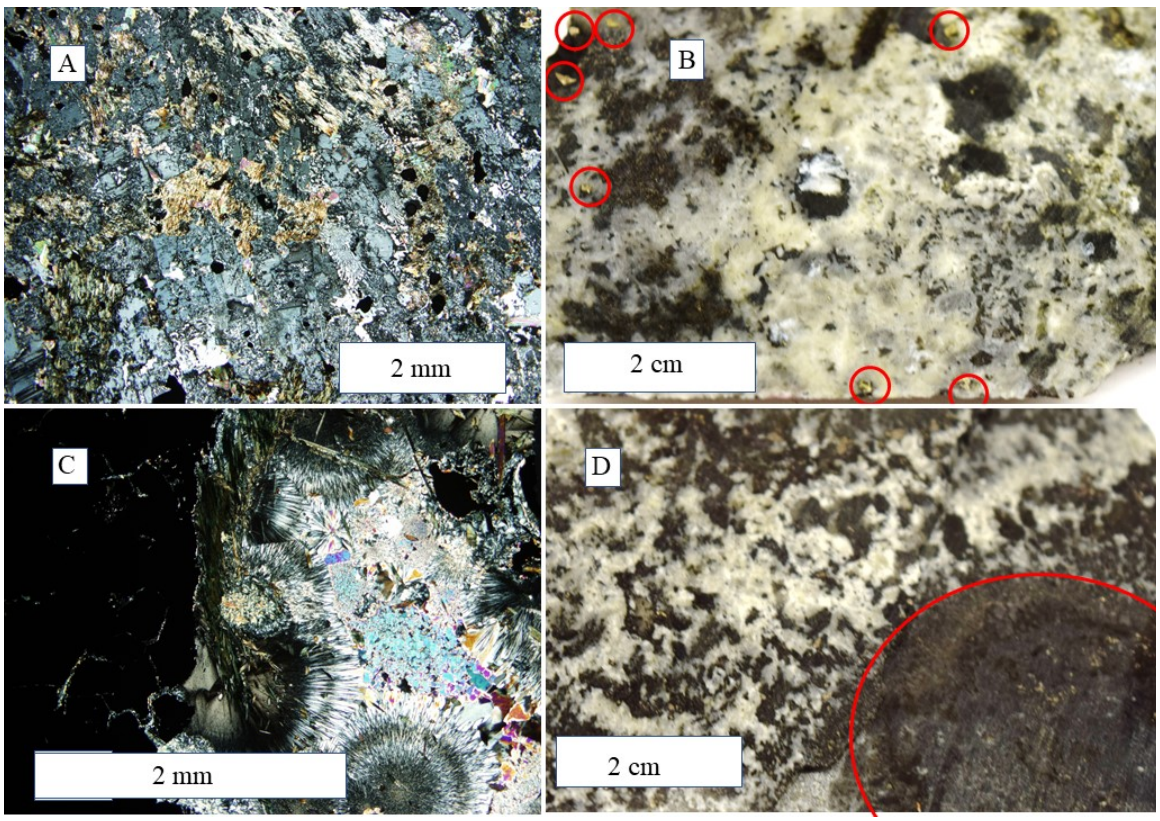

Figure 4.5. CLG-Upper Zone photomicrographs and photos (A) Fine-grained opaque minerals are sporadic equant Cr-spinel (Transmitted light; XPL; CLG-1). (B) Drill core sample containing fine-grained disseminated sulphides, circled in red (CLG-1). (C) Zeolites displaying radial extinction (Transmitted light; XPL; CLG-2). (D) Drill core sample with sulphidic sedimentary xenolith, circled in red (CLG-2).

The lower portion of the Upper Zone displays distinct modal and textural layering. The transition is sharp and distinct between coarse-grained melagabbro and augite troctolite (Figs. 4.1 and 4.6A). The melagabbro layer has large <2 cm oikocrysts of unaltered, ophitic clinopyroxene and (0.5 mm to 3 mm) plagioclase, which is moderately to strongly sericite altered. The augite troctolite layer contains subophitic clinopyroxene, which is optically continuous for up to 1 cm, patchy weakly sericite altered fine-grained (0.1 to 0.5 mm) plagioclase, and highly variable (5 to 100%) iddingsite/talc altered fine-grained (<0.5 mm) olivine (Fig. 4.6B). Modally the gabbro contains 33% plagioclase and 65% clinopyroxene whereas the troctolite contains 57% plagioclase, 30% olivine, and 10% clinopyroxene.

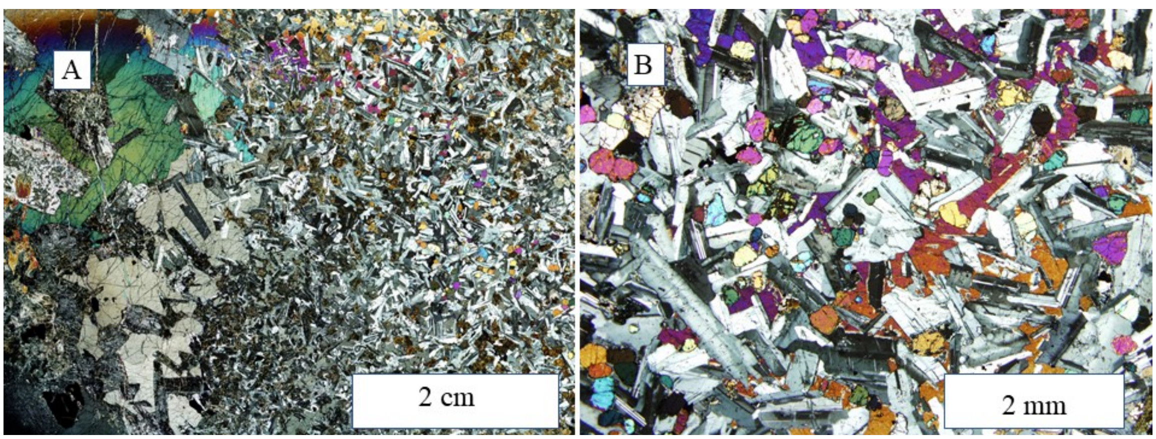

Figure 4.6. CLG-Upper Zone photomicrographs (A) Composite photomicrographs showing sharp contact of coarse grained gabbro and fine-grained troctolite (Transmitted light; XPL; CLG-3). (B) Photomicrograph of augite troctolite displaying subophitic clinopyroxene, fine-grained subhedral plagioclase, and fine-grained equant olivine (Transmitted light; XPL; CLG-3).

4.1.2.2 Main Zone

The rocks of the Main Zone (38 to 574 m depth) represent the most volumetrically significant portion of the CLG drill core. The Main Zone is comprised of various modal proportions of plagioclase, olivine, and clinopyroxene (Figs. 4.1 and 4.2). Plagioclase is present in all the rocks and constitutes between 40% and 70% modally, although between 60% and 68% is most common. Generally, the plagioclase is randomly orientated (Fig. 4.7B), but does display local alignment of laths to define a poorly to moderately developed foliation (Fig. 4.7A). Grain size varies considerably on both thin section scale as well as throughout the Main Zone. Most Main Zone sections display a seriate size distribution of fine- to medium-grains. The habit of plagioclase is generally subhedral laths with aspect ratios ranging from equigranular to highly elongated, almost acicular (Fig. 4.7C). Smooth zoning within plagioclase grains is a common occurrence throughout the Main Zone (Fig. 4.7D). Alteration in the Main Zone is variable in intensity, but is generally weak. Sericitation of plagioclase is present to some degree in every thin section, between 5% and 70% replacement, although 10 to 15% is most common. The sericite alteration occurs as patches, along grain fractures, and as core replacements. Overgrowths of K-feldspar on the rims of plagioclase can be found locally on some grains in the upper portion of the Main Zone.

Olivine modally comprises between 0 and 36% of the Main Zone rocks with grain sizes generally 1 to 5 mm but locally up to 20 mm. Olivine distribution is somewhat intermittent as there are localized areas in the interior of the Main Zone where it is absent, notably around 165 and 306 m depth (Fig. 4.2). Olivine occurs in three main textures; irregular amoeboidal (Fig. 4.8A), equant anhedral/subhedral (Fig. 4.8B), and marginally subpoikilitic grains (Fig. 4.8C). The subpoikilitic texture is rare, as only one section contained the texture. Primarily olivine takes the form of equant shaped grains. Plagioclase enclosed in olivine are common throughout the Main Zone resulting from plagioclase intergrown with olivine (Fig. 4.8D).

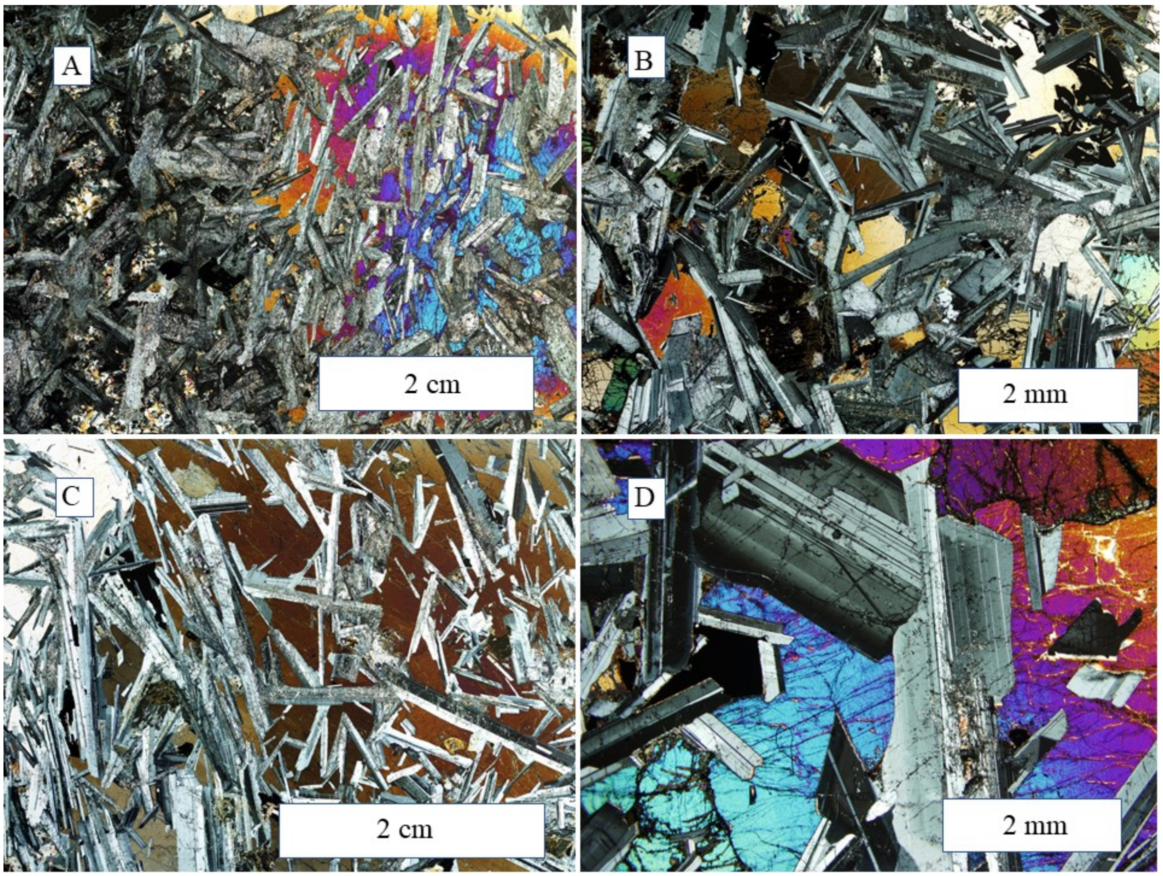

Figure 4.7. CLG-Main Zone photomicrographs (A) Composite photomicrographs displaying plagioclase with a moderate foliation enclosed in a clinopyroxene ophitic oikocryst (Transmitted light; XPL; CLG-10). (B) Randomly orientated plagioclase, subophitic clinopyroxene, and equant olivine (Transmitted light; XPL; CLG-8). (C) Composite photomicrograph showing plagioclase laths with a very high length:width ratio enclosed in a clinopyroxene ophitic oikocryst (Transmitted light; XPL; CLG-17). (D) Two plagioclase grains displaying smooth zoning (Transmitted light; XPL; CLG-9).

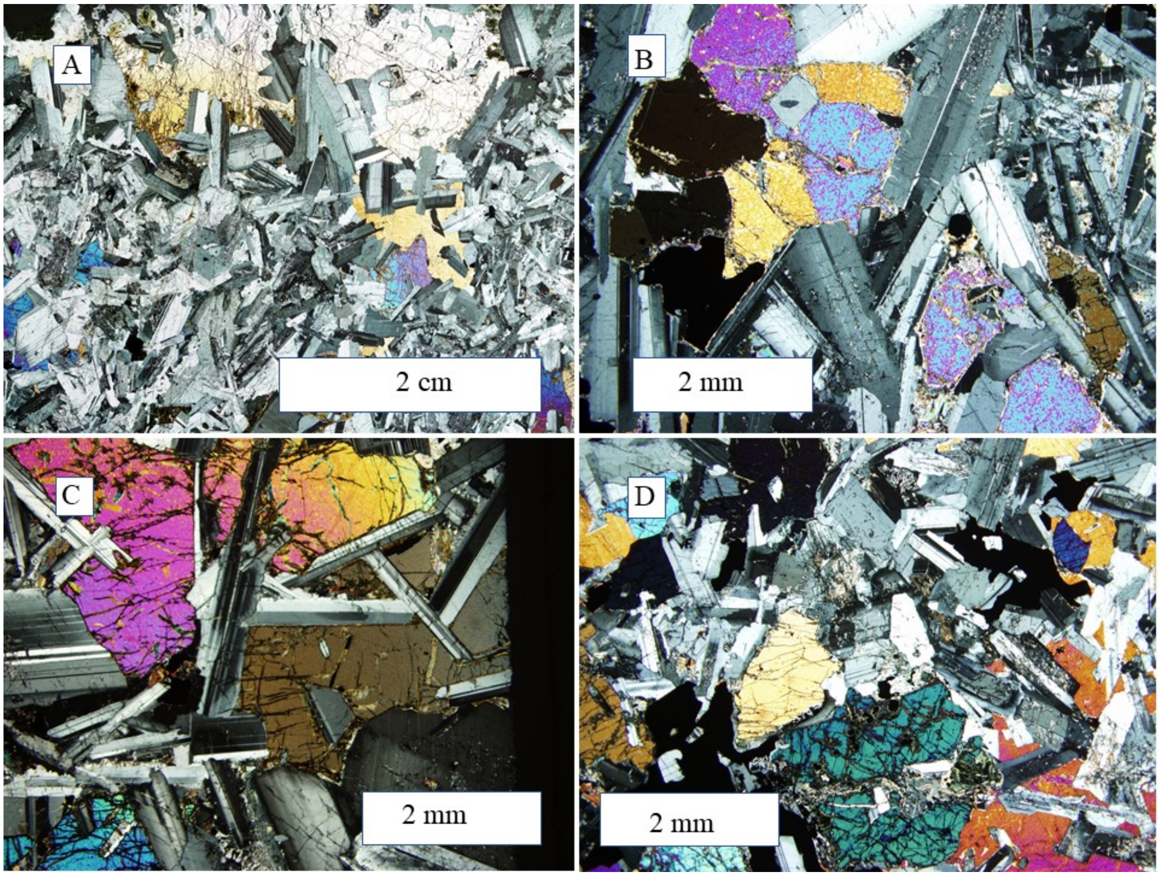

Figure 4.8. CLG-Main Zone photomicrographs (A) Composite photomicrographs showing irregular amoeboidal shaped olivine grains at the top of the photo (Transmitted light; XPL; CLG-4). (B) Equant shaped olivine grains (Transmitted light; XPL; CLG-18). (C) Subpoikilitic olivine, partially enclosing plagioclase grains (Transmitted light; XPL; CLG-27). (D) Olivine enclosing fine-grained plagioclase, bottom of photo (Transmitted light; XPL; CLG-21).

The alteration of olivine occurs throughout the Main Zone, with varying degrees of intensity and alteration products. The most frequent alteration products are iddingsite (Fig. 4.9A) and serpentine/Fe oxide (Fig. 4.9B) occurring in fractures and grain boundaries, but also as a complete pseudomorphs. Talc is common along grain boundaries but in some thin sections completely pseudomorphs olivine (Fig. 4.9C). Peritectic orthopyroxene overgrowth rims on olivine are locally present (Fig. 4.9D).

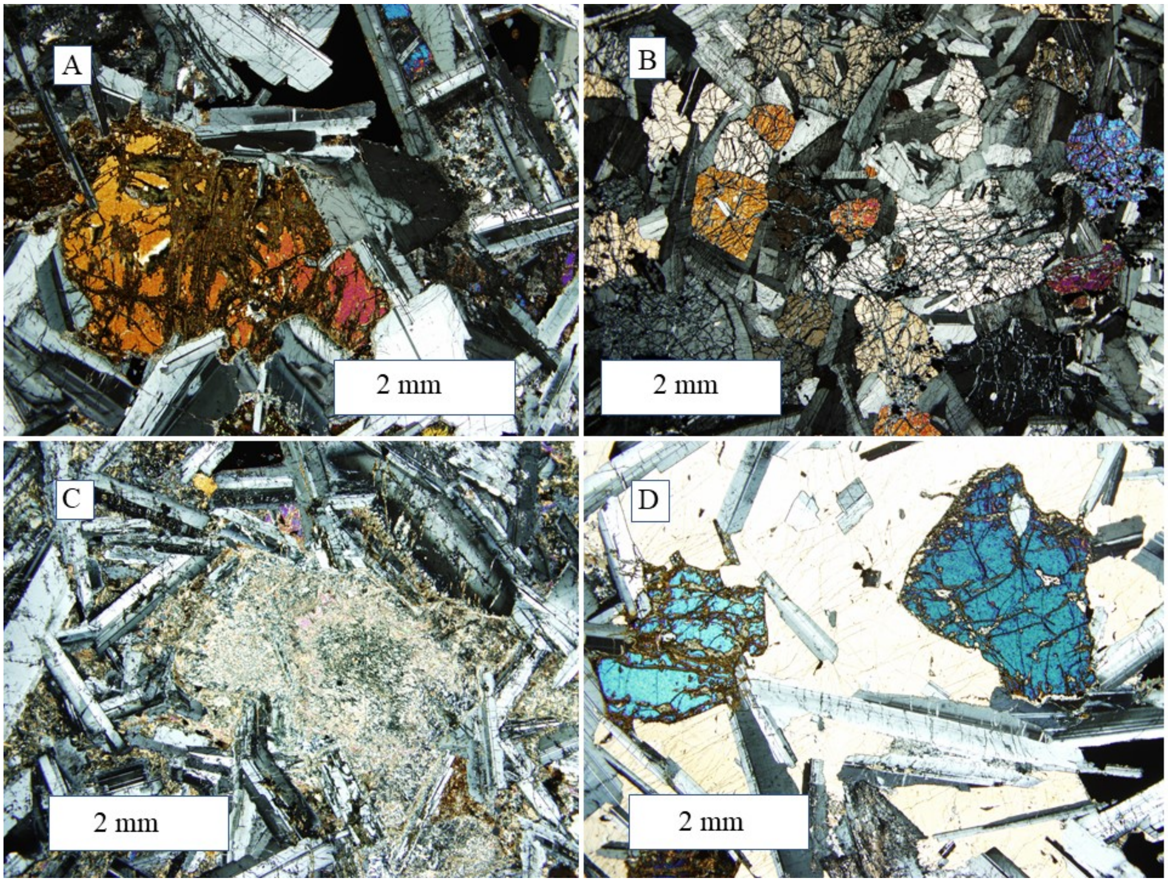

Figure 4.9. CLG-Main Zone photomicrographs (A) Iddingsite altered olivine grain (Transmitted light; XPL; CLG-9). (B) Olivine grains altered to serpentine and Fe-oxides in fractures (Transmitted light; XPL; CLG-25). (C) Olivine pseudomorphed by talc (Transmitted light; XPL; CLG-12). (D) Olivine rimmed by orthopyroxene, right side of photo (Transmitted light; XPL; CLG-17).

Clinopyroxene modally comprises between 2 and 34% of the Main Zone rocks with a general increase uphole (Fig. 4.2). The basal ~ 55 m has the lowest modal percentage of clinopyroxene (Fig. 4.2) and is texturally subophitic. Texturally throughout the Main Zone, it almost exclusively occurs as coarse- to very coarse-grained, 10 to >25 mm, ophitic (Fig. 4.10A) and subophitic oikocrysts (Fig. 4.10B) with ophitic texture being the most common. Only one thin section displays granular cumulus clinopyroxene, but this section also displays subophitic textured clinopyroxene. Alteration is generally weaker in the clinopyroxene when compared to plagioclase and olivine in the same rock. The main alteration minerals are uralite, chlorite, and actinolite.

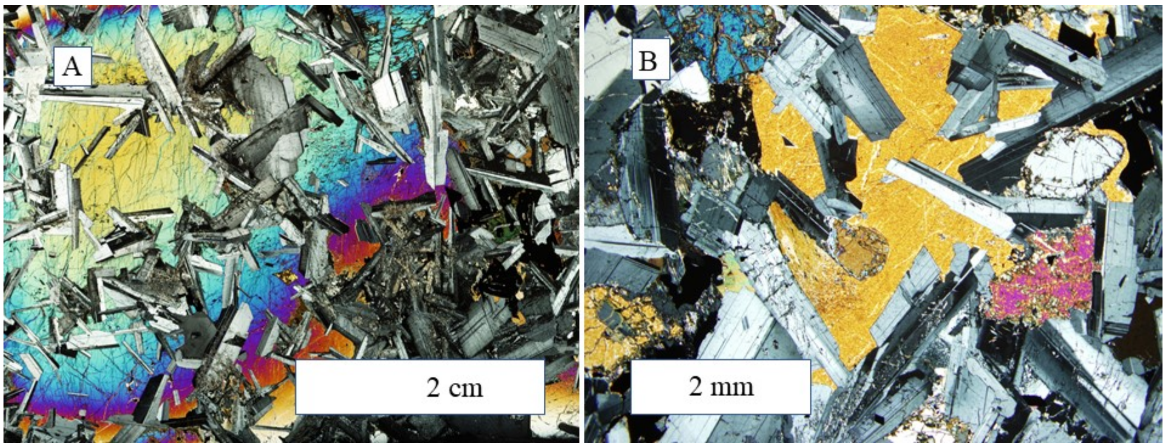

Figure 4.10. CLG-Main Zone photomicrographs (A) Composite photomicrographs displaying a coarse-grained ophitic clinopyroxene grain (Transmitted light; XPL; CLG-6). (B) Subophitic clinopyroxene partially enclosing plagioclase and olivine grains (Transmitted light; XPL; CLG-17).

Cr-spinels are present in <1 cm thick seams in the basal ~55 m of the Main Zone (Fig. 4.2). The Cr-spinels are euhedral, equigranular, and fine-grained. In an individual seam, the Cr-spinel modally comprises 10% of the rock. Where present, they were the first mineral to crystallize as they occur as chadacrysts inclusions in all other minerals. They are largely randomly distributed in the seam and are found wholly enclosed in plagioclase, olivine and clinopyroxene, as well as along grain boundaries. They are not evenly distributed in the seam as they are found in clusters (Fig. 4.11A), as well as being sparse (Fig. 4.11B).

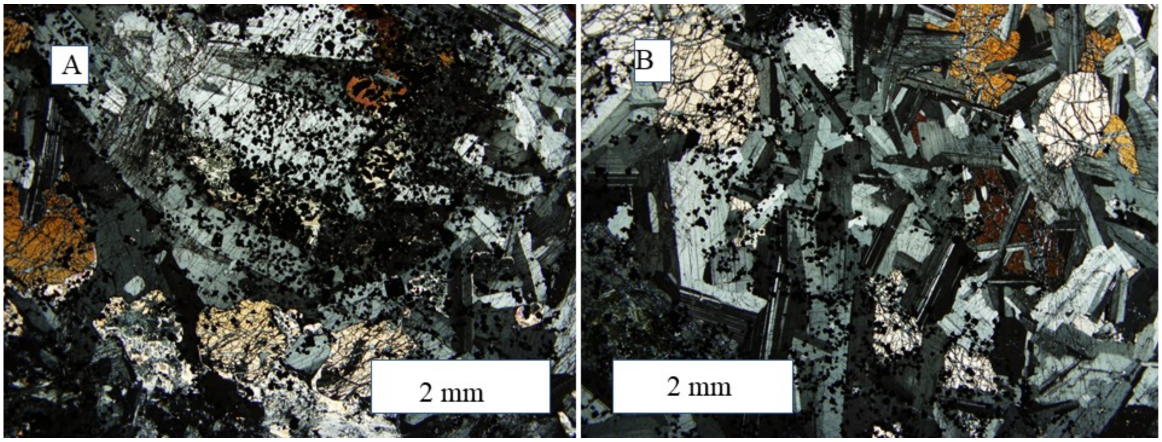

Figure 4.11. CLG-Main Zone photomicrographs (A) Clustered fine-grained opaque mineral are Cr-spinels wholly enclosed in olivine and plagioclase (Transmitted light; XPL; CLG-25). (B) Sparse distribution of opaque Cr-spinel grains (Transmitted light; XPL; CLG-25).

In addition to the main rock forming minerals, there are a variety of accessory and/or alteration intercumulus minerals that combined only account for <10% of the modal percentage of the rocks (Fig. 4.2). These include Fe-Ti oxides (magnetite and ilmenite), apatite, biotite, zeolite, sulphides (pyrrhotite/chalcopyrite/pentlandite), actinolite, chlorite, quartz, and K-feldspar. The Fe-Ti oxides are fine- to medium-grained and occur as anhedral, amoeboidal, and subpoikilitic grains; rare bladed and skeletal grains are also present. Apatite appears as euhedral, long, and slender prisms as well as equant hexagonal grains. It occurs in interstitial pockets along with other accessory minerals throughout the Main Zone rocks, but their abundance generally increases uphole. Biotite displays variable textures and abundances. It occurs as anhedral, elongate to equigranular grains, irregular shaped grains interstitial to early formed minerals, and as rims on Fe-Ti oxides. Biotite is commonly intergrown with (or altered by) secondary chlorite and actinolite. These textures of biotite suggest that it may be both a late primary and secondary (alteration) mineral phase. In two sections exhibiting moderate to heavy alteration, zeolites showing radial extinction dominate the interstitial pockets (Fig. 4.12A). The basal ~30 m of the Main Zone, contains disseminated blebs (Fig. 4.12B) and interstitial sulphides (Fig. 4.12C). In the uppermost ~100 m of the Main Zone rocks contains K-feldspar and quartz occurring as separate phases, as well as in granophyric mesostasis with the overall abundance decreasing with depth (Fig. 4.12D).

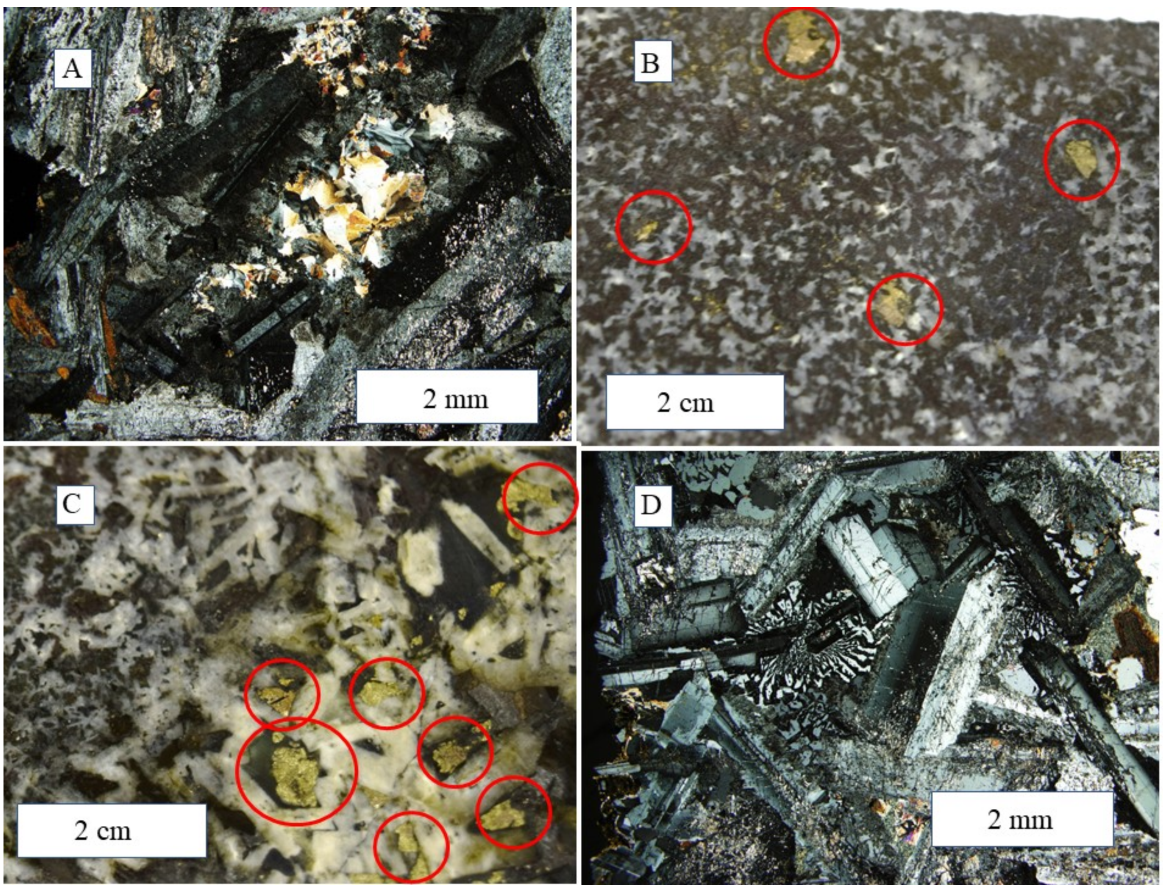

Figure 4.12. CLG-Main Zone photomicrographs and photos (A) Zeolites displaying radial extinction filling interstitial pockets between plagioclase grains (Transmitted light; XPL; CLG-10). (B) Drill core sample with disseminated blebs of sulphide (CLG-25). (C) Drill core sample with sulphides interstitial to plagioclase grains (CLG-27). (D) Quartz and K-feldspar with granophyric texture, surrounding a plagioclase grain in an interstitial pocket between plagioclase grains (Transmitted light; XPL; CLG-5).

4.1.2.3 Lower Zone

The Lower Zone of the CLG (649 to 759 m) is mineralogically and texturally similar to the Main Zone consisting of troctolite, augite troctolite, and olivine gabbro (Fig. 4.1). It is dominated by plagioclase, olivine and clinopyroxene (Fig. 4.2). Modally plagioclase comprises between 60 and 75% of the rocks, with an average of 65%. In each thin section the plagioclase has a seriate size distribution with the maximum grain size generally decreasing with depth. The plagioclase in the Lower Zone is always randomly orientated with no foliation present (Fig. 4.13A). The habit is subhedral lath shaped grains. Smooth zoning within plagioclase grains is common in all thin sections. Sericite alteration of plagioclase is bimodal with most samples displaying weak patchy alteration of 5 to 10% and one sample displaying strong alteration with 95% of plagioclase being replaced (Fig. 4.13B). Within the strongly altered sample, olivine and clinopyroxene displays only weak alteration.

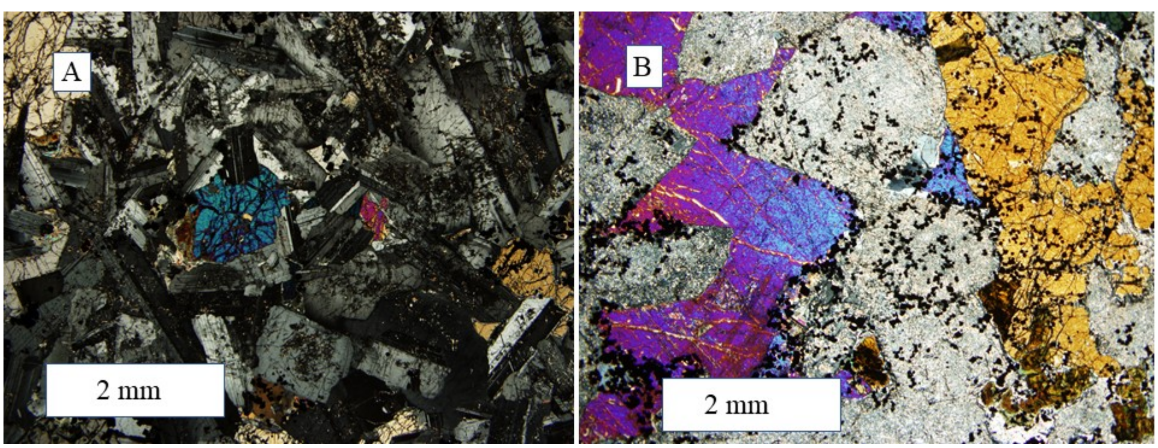

Figure 4.13. CLG-Lower Zone photomicrographs (A) Non-foliated plagioclase and olivine (Transmitted light; XPL; CLG-41). (B) Strongly sericitized plagioclase grains with weakly altered clinopyroxene and olivine (Transmitted light; XPL; CLG-43).

Olivine modally comprises between 11 to 25% of the Lower Zone (Fig.4.2) and is generally medium-grained (1 to 5 mm). The habit is mostly anhedral, subrounded and equant. One thin section displays irregular-shaped marginally subpoikilitic and ameboidal grains (Fig. 4.14A). Minor amounts of grains partially enclose plagioclase laths. Fracture-filling serpentine±Fe oxide alteration (Fig. 4.14B) is the primary alteration of olivine in the Lower Zone. Minor amounts of orthopyroxene and replacement talc are found locally on the rims of some grains.

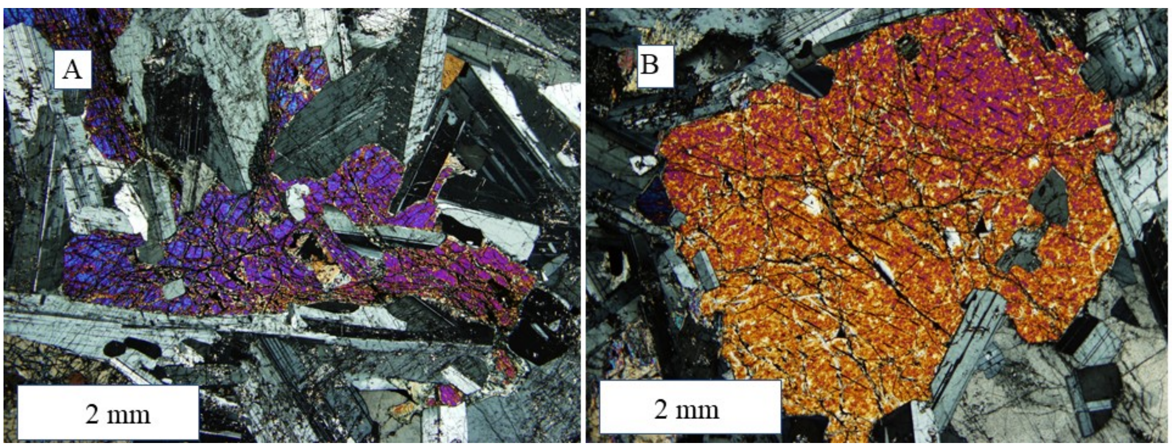

Figure 4.14. CLG-Lower Zone photomicrographs (A) Subpoikilitic olivine grain both wholly and partially enclosing plagioclase grains (Transmitted light; XPL; CLG-37). (B) Olivine grain with serpentine and Fe-oxide alteration (Transmitted light; XPL; CLG-40).

Clinopyroxene modally comprises between 5 to 20% (Fig. 4.2) and is medium- to coarse-grained (<20 mm). Texturally, it occurs as subophitic (Fig. 4.15A) to ophitic oikocrysts (Fig. 4.15B). Alteration is primarily to uralite with minor chlorite and actinolite, and is generally weak. The modal abundance of clinopyroxene is typically less than in the Main Zone (Fig. 4.2).

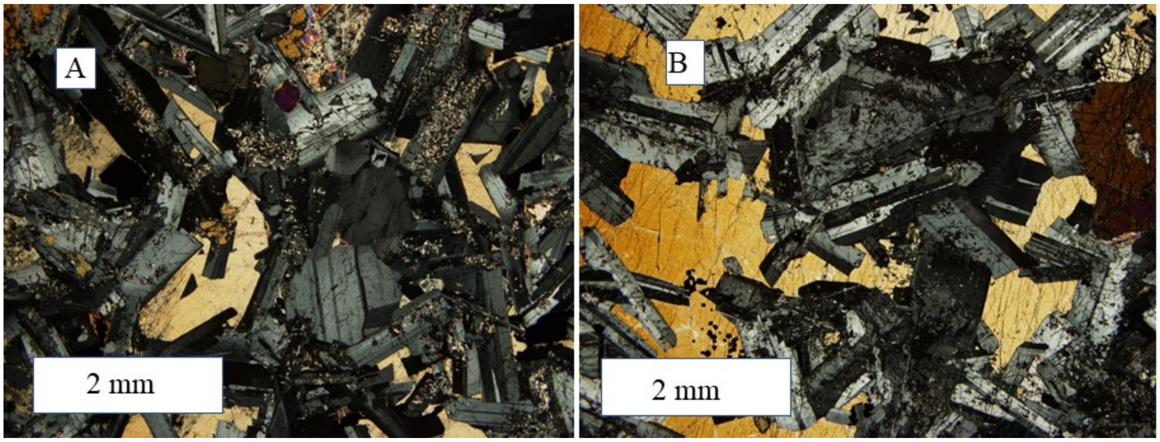

Figure 4.15. CLG-Lower Zone photomicrographs (A) Subophitic clinopyroxene partially enclosing plagioclase grains (Transmitted light; XPL; CLG-42). (B) Coarse-grained, optically continuous ophitic clinopyroxene grain (Transmitted light; XPL; CLG-39).

Cr-spinels are present in < 1cm thick seams appearing ~15 m from the basal contact of the Lower Zone, as well as being finely disseminated between seams. In both textures the Cr-spinels are euhedral, equigranular, and fine-grained. In an individual seam the Cr-spinel modally comprises up to 15% of the rock (Fig. 4.16A). They occur as chadacryst inclusions in all other minerals. They are generally randomly distributed in the seam and are found wholly enclosed in plagioclase, olivine and clinopyroxene, as well as along grain boundaries. They are not evenly distributed in the seam as they are found in clusters as well as being sparse (Fig. 4.16B). In the disseminated texture they are relatively evenly distributed and comprise 5% modally of the rock.

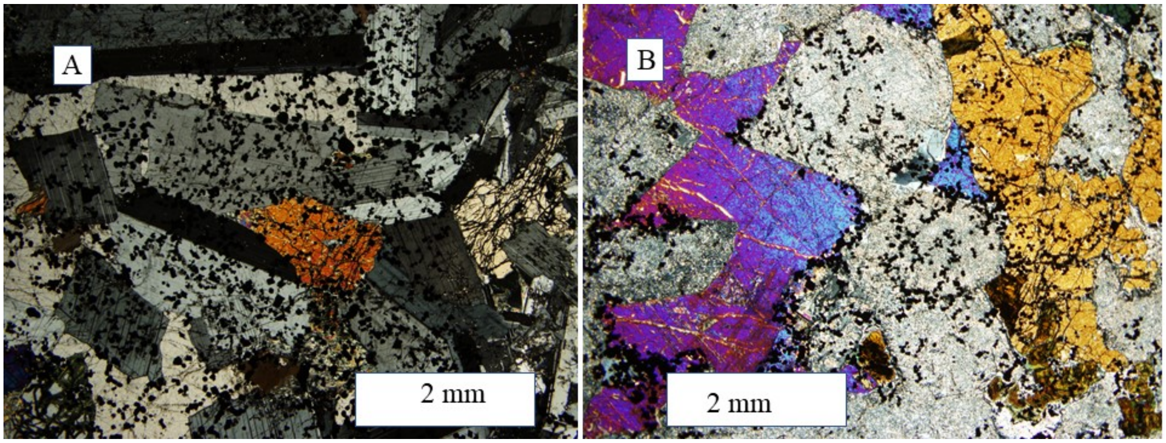

Figure 4.16. CLG-Lower Zone photomicrographs (A) Opaque fine-grained Cr-spinel grains in a seam wholly enclosed in plagioclase, olivine, and clinopyroxene (Transmitted light; XPL; CLG-42). (B) Sparsely disseminated opaque Cr-Spinel grains, wholly enclosed in strongly altered plagioclase and weakly altered olivine but absent within clinopyroxene (Transmitted light; XPL; CLG-43).

Intercumulus accessory and alteration minerals are less abundant in the Lower Zone, only comprising of <5% of the modal percentage (Fig. 4.2). Like the Main Zone, these minerals include Fe-Ti oxides (ilmenite and magnetite), apatite, biotite, sulphides (pyrrhotite/chalcopyrite/pentlandite), actinolite, and chlorite. In the Lower Zone granophyre, quartz, and zeolites are not present. Fe-Ti oxides, like the Main Zone, occurs as anhedral, amoeboidal, and subpoikilitic grains as well as rare bladed and skeletal grains. Biotite commonly rims the Fe-Ti oxides (Fig. 4.17A). Biotite is anhedral to subpoikilitic and locally intergrown with (altered by) chlorite and actinolite (Fig. 4.17B). The Lower Zone has two areas where sulphides are present; the top 15 m and the bottom 15 m. The sulphides are primarily subpoikilitic interstitial (Fig. 4.17C) grains with some disseminated blebs (Fig. 4.17D).

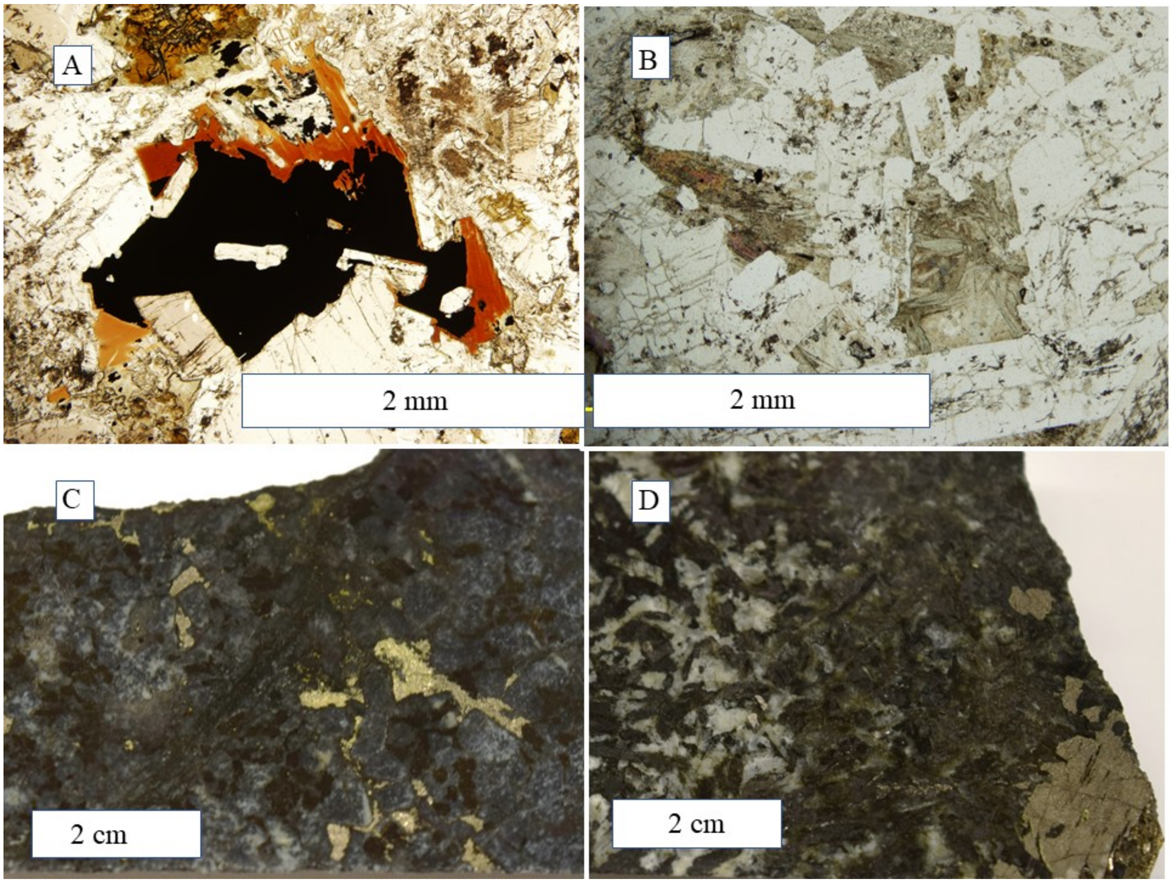

Figure 4.17. CLG-Lower Zone photomicrographs and photos (A) Fe-Ti-oxide rimmed by biotite (Transmitted light; PPL; CLG-37). (B) Alteration assemblage of actinolite, biotite and chlorite (Transmitted light; PPL; CLG-39). (C) Interstitial sulphide in a strongly altered drill core sample (CLG-43). (D) Bleb of sulphide, bottom-right of photo, in drill core sample (CLG-36).

4.1.2.4 Logan Sill

Separating the Main and Lower Zones of the CLG is a 75 m thick interval of plagioclase-porphyritic intergranular gabbro that is interpreted to be a large xenolith of Logan Sill. A distinctive sharp contact with the Main Zone is present (Fig. 4.18A). The Main Zone portion of the contact has a <1 cm fine-grained sulphidic gabbro that irregularly grades to a very fine- to fine-grained sulphide barren gabbro. The sulphidic gabbro contains strongly sericitized plagioclase, strongly uralitized subophitic clinopyroxene, and evenly distributed blebby and interstitial pyrrhotite. The barren gabbro consists mostly of moderately sericitizied plagioclase and equant, granular, largely unaltered clinopyroxene (Fig. 4.18B).

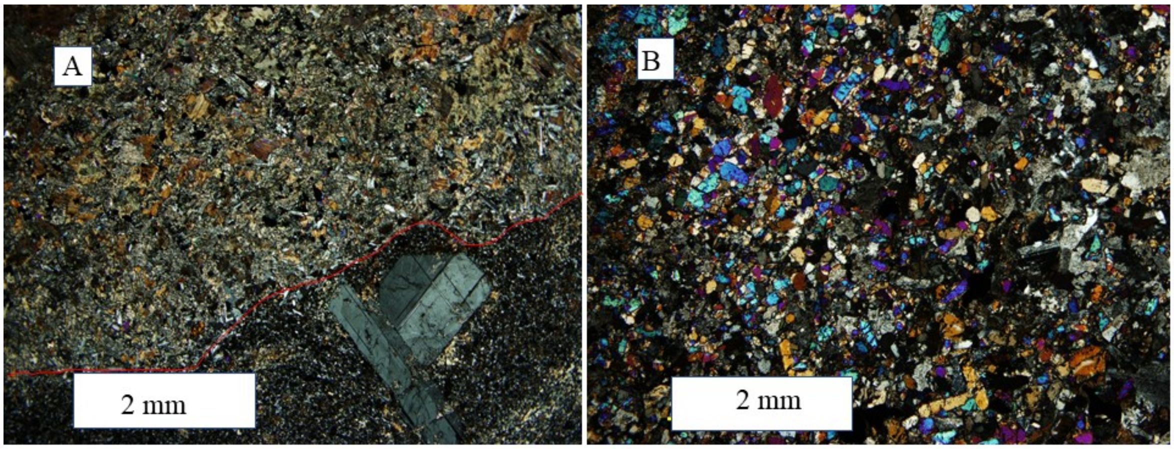

Figure 4.18. Logan Sill photomicrographs (A) Sharp contact between CLG sulphidic gabbro and plagioclase-phyric Logan sill (Transmitted light; XPL; CLG-29). (B) Fine-grained gabbro with granular clinopyroxene and plagioclase (Transmitted light; XPL; CLG-29).

The rocks of the Logan Sill have a variety of textures. The top 8 m of the sill is comprised of plagioclase-phyric diabase with very fine- to fine-grained matrix (Fig. 4.19A). The plagioclase in the matrix modally comprises of 50% of the rock. The matrix plagioclase is anhedral to subhedral, equigranular to elongate laths that define a moderate foliation. Very fine- to fine-grained granular clinopyroxene comprise 22% of the rock with minor elongated grains that also follow the defined foliation. The plagioclase phenocrysts are weakly altered subhedral tabular shaped laths that are up to 5 mm long and comprises 8% of the rock. The remaining minerals are secondary amphibole, biotite, actinolite, and chlorite as well as ameboidal Fe-Ti oxides.

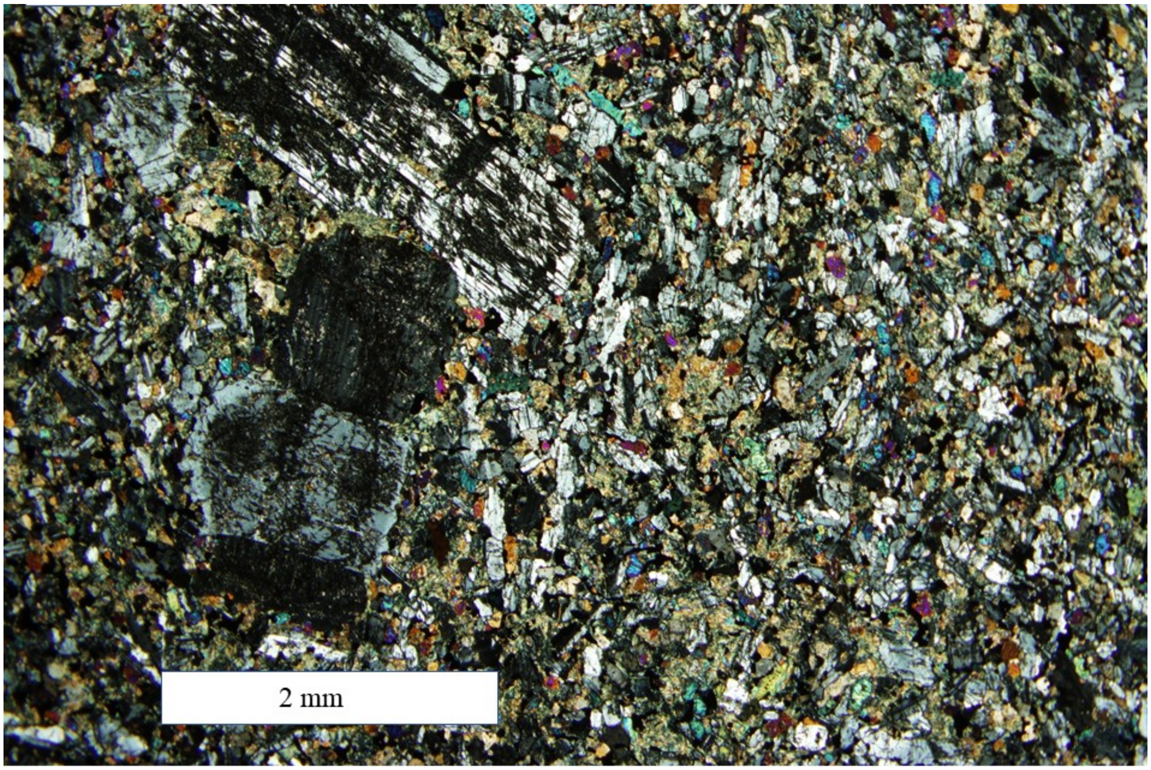

Figure 4.19. Logan Sill photomicrograph. Plagioclase phenocrysts in a fine-grained matrix comprised mainly of clinopyroxene, amphibole, and plagioclase (Transmitted light; XPL; CLG-30).

In the remainder of the sill, plagioclase phenocrysts are the modally dominant phase comprising between 65 to 75% of the rocks. Four of the five thin sections have grains that are >10 mm, and are distinctly porphyritic, with the fifth section, although modally similar, being aphyric. Fine-grained matrix/intergranular plagioclase are absent or only comprise <8% of the rocks. The phenocrysts are anhedral to subhedral and equigranular to lath shaped grains. The grain size of the phenocrysts range in size from 2 to >20 mm (Fig. 4.20A). Alteration of plagioclase to sericite is variable between samples from weak to heavy. Local alignment of plagioclase defines a poor foliation, although they are largely randomly orientated. Clinopyroxene is the second most modally abundant mineral in the sill. The clinopyroxene varies texturally between samples, from very fine- to fine-grained equant (Fig. 4.20B) to slightly elongated grains to subprismatic/prismatic simple twinned grains up to 4 mm long (Fig. 4.20C). Uralite, chlorite, biotite, and actinolite alteration of the clinopyroxene is moderate to heavy. Some of the amphibole and biotite could also have been a primary accessory phase based on subhedral grain texture.

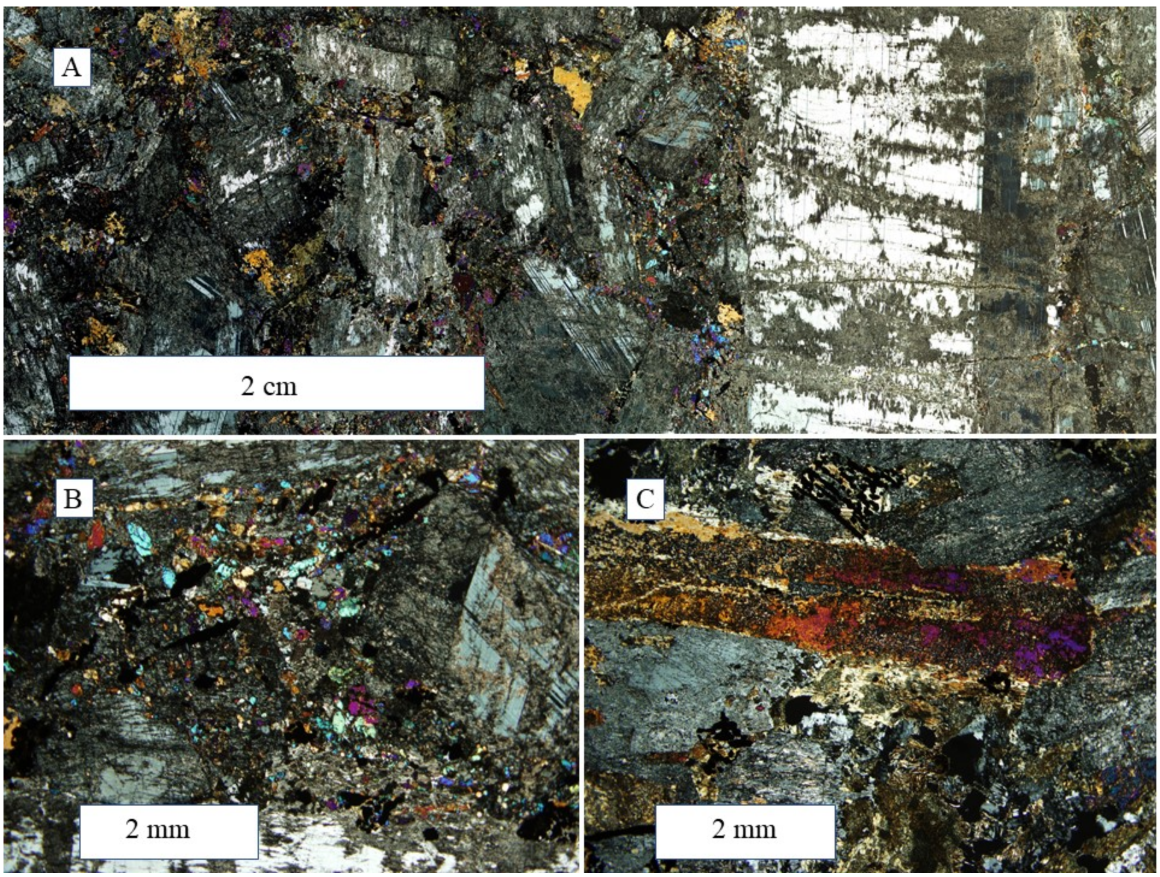

Figure 4.20. Logan Sill photomicrographs (A) Composite photomicrographs with highly variable grain sizes, up to > 20 mm, of plagioclase (Transmitted light; XPL; CLG-31). (B) Fine-grained granular clinopyroxene (Transmitted light; XPL; CLG-31). (C) Prismatic clinopyroxene (Transmitted light; XPL; CLG-32).

Iron-Ti oxides are primarily bladed or skeletal grains (Fig. 4.21A; Fig. 4.21B). Quartz and K-feldspar are fine- to medium-grained and are present as individual anhedral grains (Fig. 4.21C), as well as graphically intergrown mesostasis. Quartz is more abundant than K-feldspar, with one sample containing 6% quartz. Apatite is present in all thin sections and occurs as long slender prisms and equant hexagons.

The lower contact of the Logan Sill xenolith (i.e., contact with the Lower Zone) at ~649 m depth is more diffuse than the upper contact (i.e., contact with the Main Zone). There is a ~6 cm contact zone with interlayered fine-grained, perhaps re-melted, Logan Sill rocks and fine-grained CLG rocks (Fig. 4.21E). The CLG rocks have fairly high modal abundances of orthopyroxene, quartz, and sulphide within this contact zone suggesting the magma was locally silica and sulphide-rich (Fig. 4.21E). Between 759 and 776 m depth of the drill core, directly below the Lower Zone, there is a diabase unit that is modally and texturally similar to the rocks found in the sill (Fig. 4.21D).

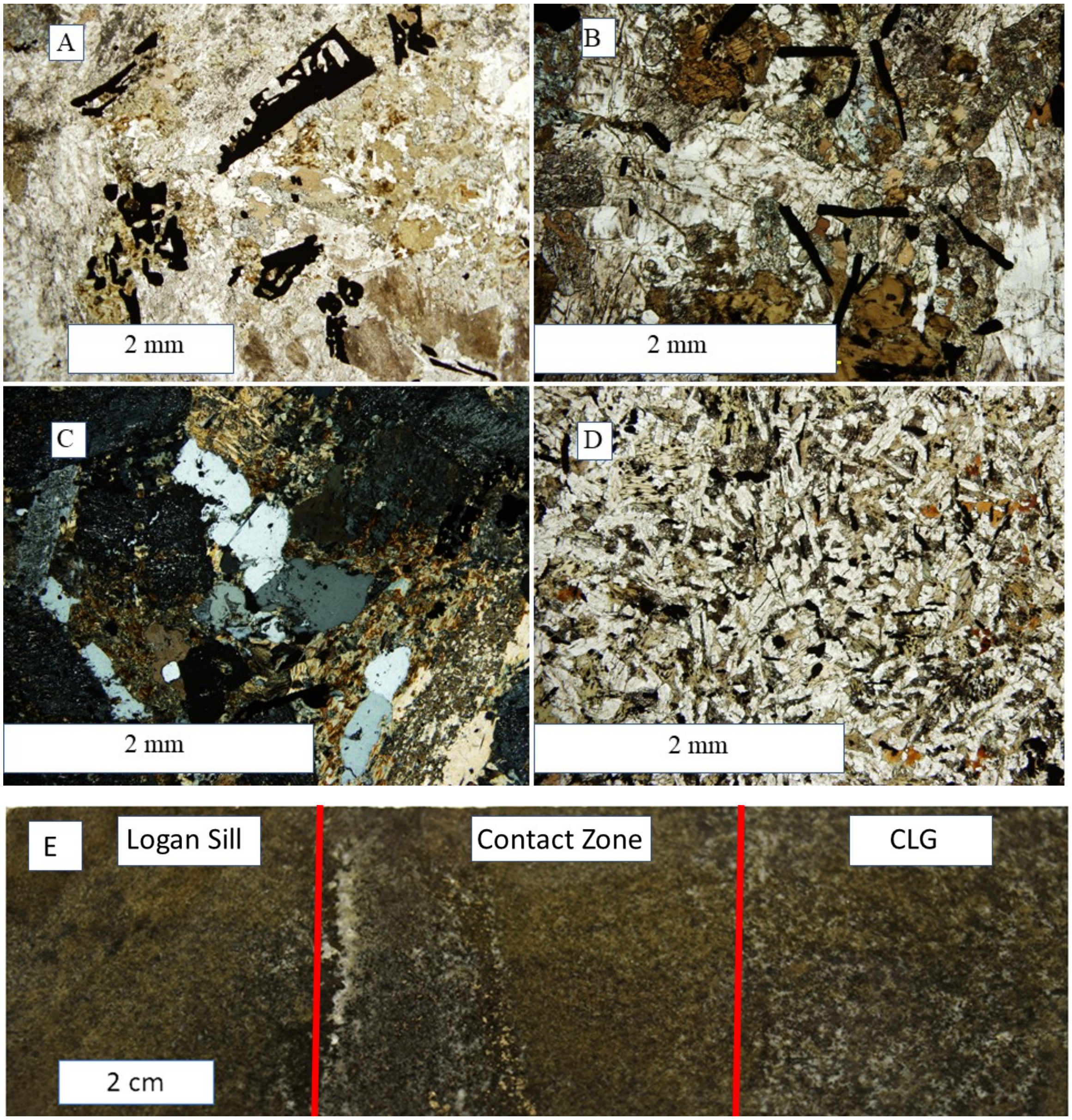

Figure 4.21. Logan Sill photomicrographs and photo (A) Opaque skeletal Fe-Ti oxides (Transmitted light; PPL; CLG-31). (B) Opaque bladed Fe-Ti oxides (Transmitted light; PPL; CLG-33). (C) Free-quartz interstitial to plagioclase phenocrysts (Transmitted light; XPL; CLG-34). (D) Logan Sill underlying the Lower Zone of the CLG (Transmitted light; XPL; CLG-45). (E) Contact Zone between Logan Sill and Lower Zone (CLG-35)

4.1.3 Mount Mollie Dyke

Petrographic analysis of the MMD distinguished four lithologic units in the S88-1 drill core: Upper Zone, Upper Main Zone, Lower Main Zone, and pegmatitic rocks. As with the CLG, rock types of the Main Zone, including the pegmatitic segregations, have been classified based upon the modal abundances of the three most abundant mineral phases; plagioclase, clinopyroxene, and olivine, normalized to 100% and plotted on a ternary diagram developed by Miller et al. (2002; Fig. 4.22). Upper Zone rocks are more intermediate than mafic such that an Ol-Plag-Cpx classification scheme does not apply. These rocks are classified as ferrodiorite. Downhole modal abundances of the three minerals as well as Fe-Ti oxide and accessory minerals are presented in Figure 4.23.

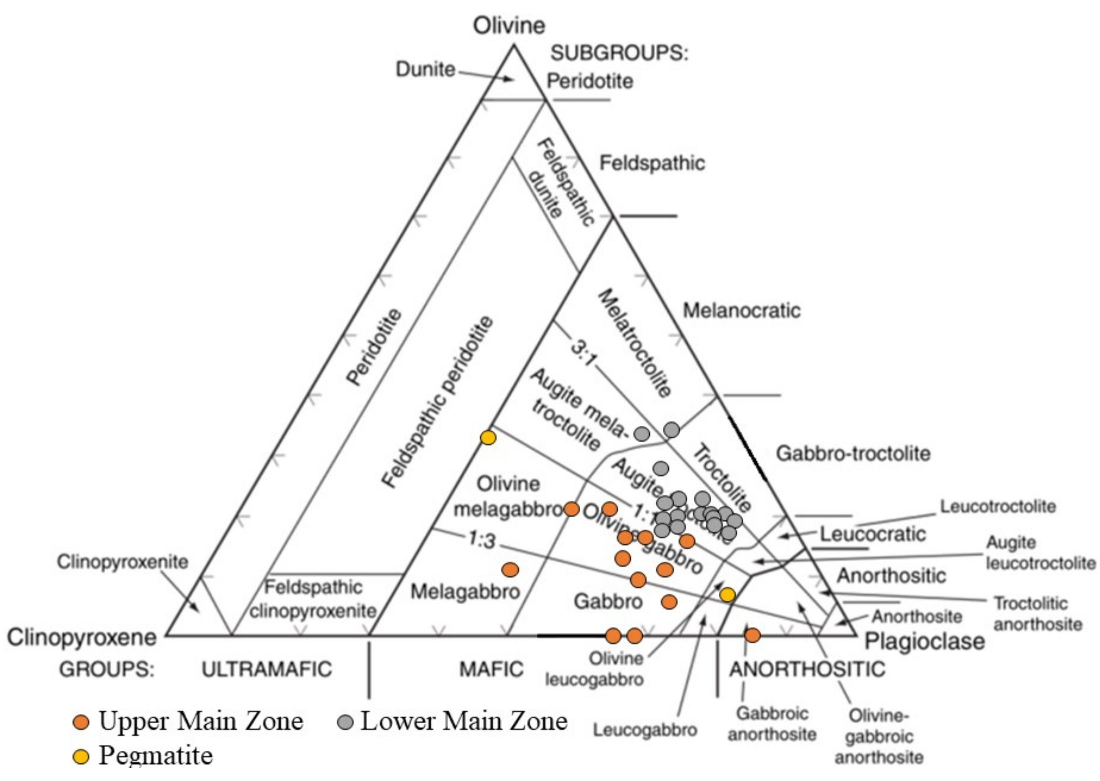

Figure 4.22. Ternary diagram of plagioclase, olivine, and clinopyroxene normalized modal abundances plotted for rock type for the MMD drill core samples. Fields after Miller et al. (2002).

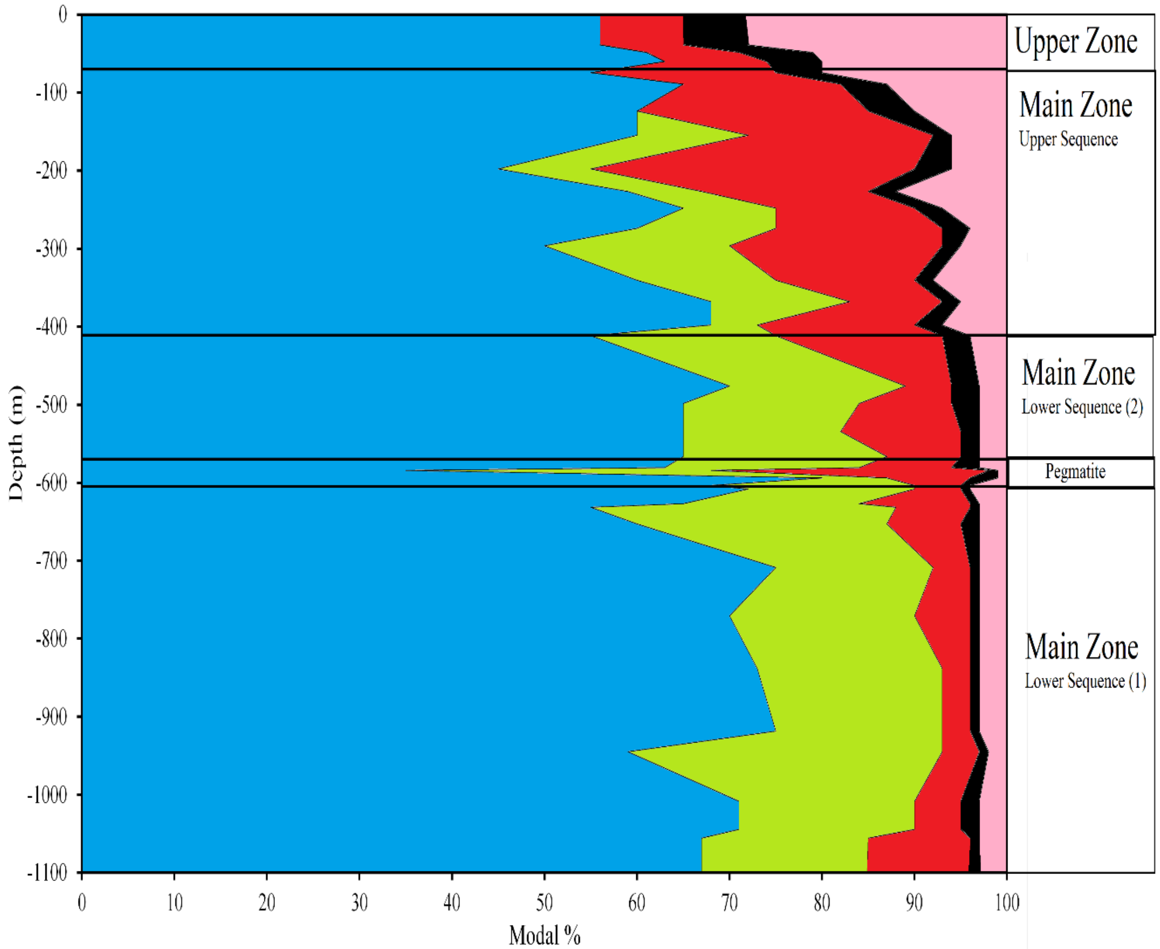

Figure 4.23. Downhole mineral modal abundance variations for the MMD drill core samples. Blue=plagioclase, green=olivine, red=clinopyroxene, black=Fe-Ti oxide, pink=accessory minerals.

4.1.3.1 Upper Zone

The Upper Zone of the MMD drill core (0 to 70 m) is characterized by a highly evolved quartz ferrodiorite as well as sedimentary xenoliths. The ferrodiorite consists of plagioclase, clinopyroxene, orthopyroxene, and quartz as the essential rock-forming minerals. Plagioclase in the ferrodiorite is fine-grained and accounts for 65% of the rocks. Plagioclase occurs as randomly orientated, tabular-shaped laths and are largely subhedral with weak patchy sericite alteration. Clinopyroxene is more modally abundant than orthopyroxene, roughly 2:1. Both pyroxenes occur as granular to intergranular, equant to slightly elongated grains (Figs. 4.24A and B). The clinopyroxene commonly displays simple single twins. Moderate alteration of the pyroxenes is generally to uralite. Quartz occurs interstitially as subpoikilitic anhedral, granular grains or as graphic intergrowths with K-feldspar to form a granophyric mesostasis (Fig. 4.24C). Iron-Ti oxides are present as bladed, skeletal, subequant, and subpoikilitic grains (Fig. 4.24D).

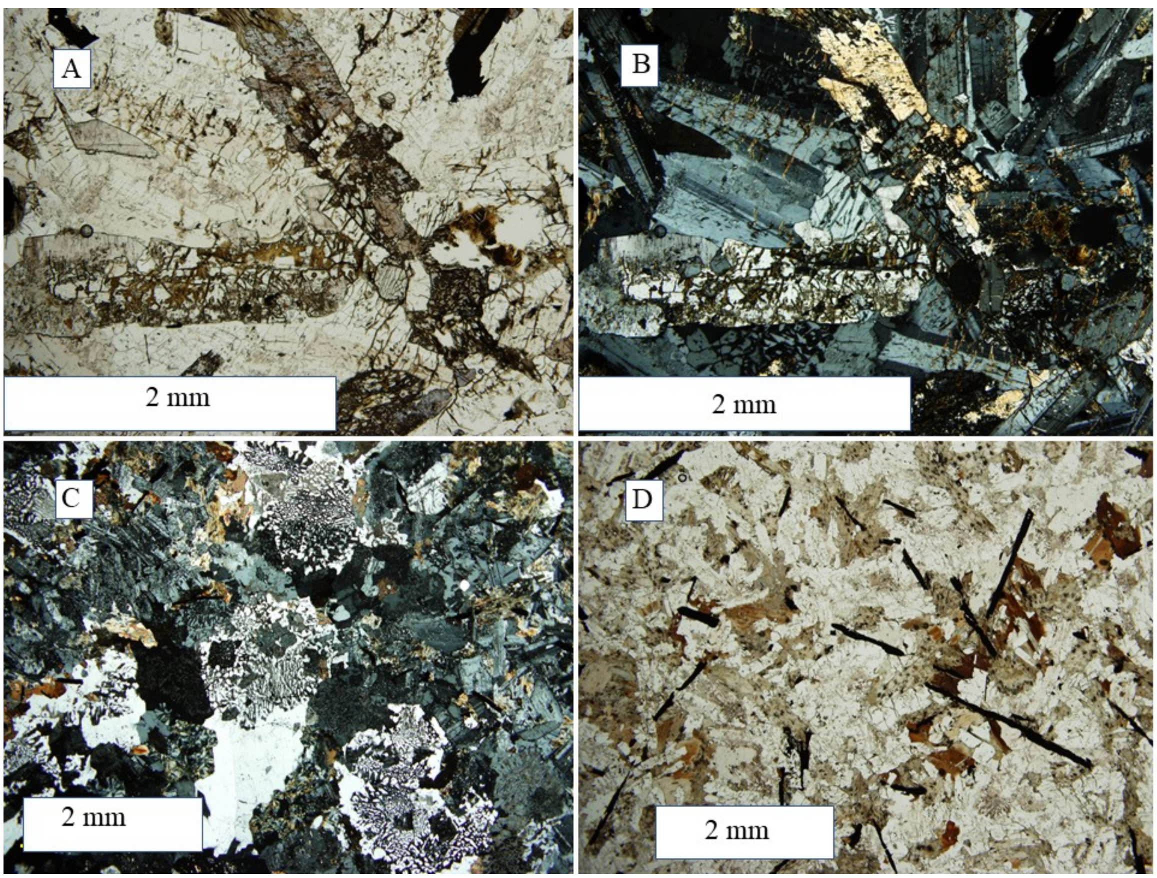

Figure 4.24. MMD-Upper Zone photomicrographs (A; B) Granular orthopyroxene and clinopyroxene (Transmitted light; PPL; XPL; MMD-5). (C) Quartz and K-feldspar with granophyric texture, free quartz is also present (Transmitted light; XPL; MMD-3). (D) Bladed Fe-Ti oxide grains (Transmitted light; PPL; MMD-3).

Apatite, amphibole, biotite, and chlorite are accessory phases in the interstitial pockets (Fig. 4.25A). Biotite and amphibole occur as both primary and secondary phases based on texture. From 15 to 37 m depth of the drill core there is a xenolith of massive fine-grained greywacke with sporadic minor thin (<1 mm) veins of calcite (Fig. 4.25B).

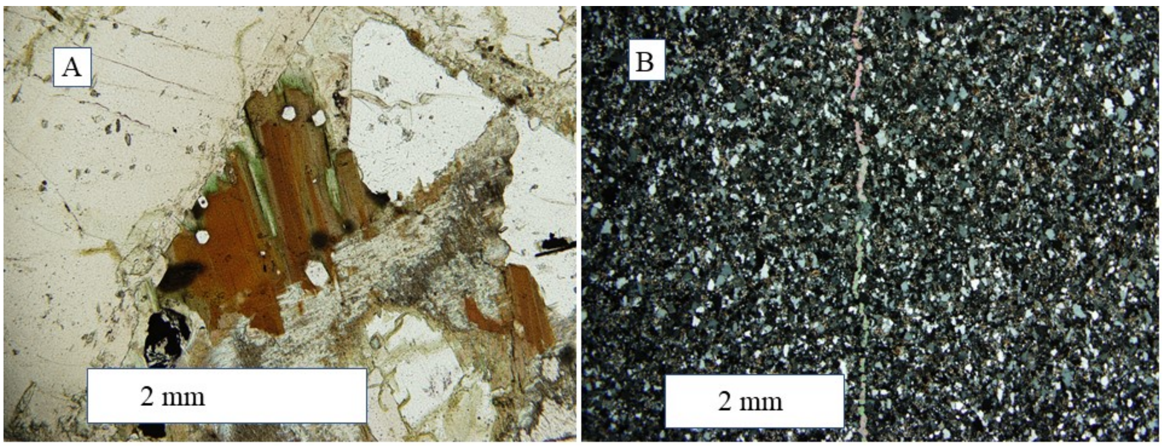

Figure 4.25. MMD- Upper Zone photomicrographs (A) Hexagonal apatite grains enclosed in intergrown biotite and chlorite (Transmitted light; PPL; MMD-3). (B) Greywacke with thin calcite vein (Transmitted light; XPL; MMD-2).

4.1.3.2 Main Zone

The remainder of the drill core can be considered as one unit, the "Main Zone", with a fairly well-developed differentiation sequence. Upsection, the Main Zone lithologies progress from largely troctolite and augite troctolite in the lower sequence to olivine gabbro, gabbro, and granophyric gabbro in the upper sequence (Figs. 4.22 and 4.23). Plagioclase, olivine, and clinopyroxene are the main rock-forming minerals in the drill core (Fig. 4.22).

Plagioclase grains throughout the Main Zone are texturally fairly consistent. They occur as subhedral to euhedral tabular to elongated laths. Grain size is most commonly medium with only some sections containing fine-grained laths. A seriate size distribution is common throughout. Modally there is a crude decrease of plagioclase abundance from an average of 70% in the bottom half to an average of 60% in the top half of the drill core. A poorly (Fig. 4.26B) to very well-developed (Fig. 4.26A) foliation of plagioclase grains is locally present as well as randomly orientated grains. There is not a systematic distribution of the foliation. Smooth zoning within plagioclase grains is a common occurrence of plagioclase. All of the thin sections display a weak patchy sericite alteration of generally around 15%.

Olivine in the Main Zone is present in rocks below 89 m depth in modal concentrations between 5 to 34%, with 15 to 20% being the most common (Fig 4.23). Grain size is consistently medium-grained (1 to 5 mm) with only one thin section having coarse grains. The habit is generally anhedral to subhedral, equant, and subrounded. Where a plagioclase foliation is well-developed some olivine grains show slight elongation in the direction of the foliation (Fig. 4.27A). Ameboidal and subpoikilitic textures are rarely present. Overall, olivine is weakly altered to iddingsite (Fig. 27D), Fe oxide/serpentine (Fig. 4.27C), and talc (Fig. 4.27B) and is most prevalent in fractures and along grain boundaries. One section displays a strong alteration with 80% of olivine being pseudomorphically replaced by iddingsite. Peritectic rims of orthopyroxene are locally present on grain boundaries. Some anhedral olivine grains are partially intergrown with plagioclase laths.

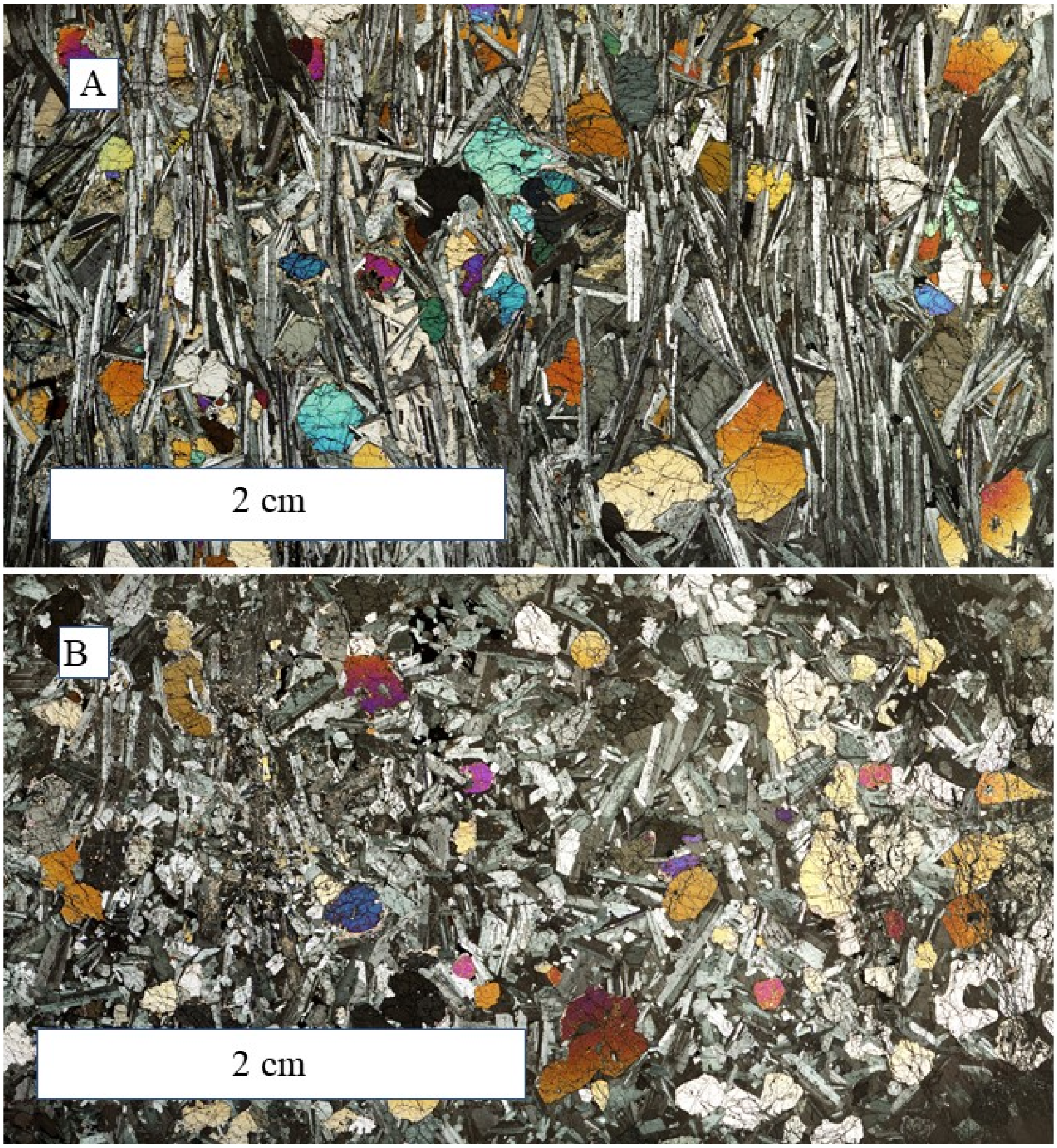

Figure 4.26. MMD-Main Zone photomicrographs (A) Composite photomicrographs displaying a very-well foliated troctolite (Transmitted light; XPL; MMD-39). (B) Composite photomicrographs displaying randomly orientated troctolite (Transmitted light; XPL; MMD-64).

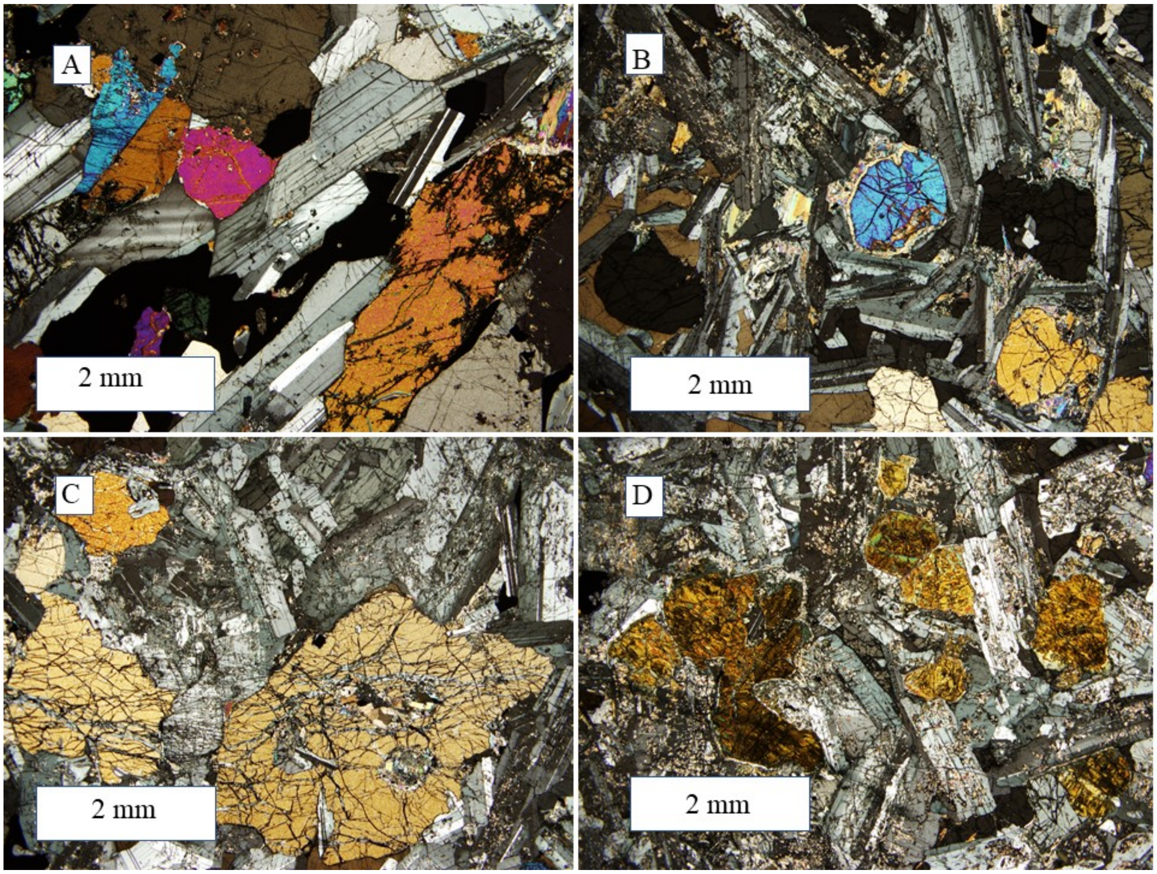

Figure 4.27. MMD-Main Zone photomicrographs (A) Elongated olivine grain following the same orientation as plagioclase (Transmitted light; XPL; MMD-18). (B) Talc altering the rim of an olivine grain (Transmitted light; XPL; MMD-32). (C) Serpentine and Fe-oxide alteration along fractures in olivine (Transmitted light; XPL; MMD-75). (D) Iddingsite pseudomorphed olivine grains (Transmitted light; XPL; MMD-77).

Clinopyroxene occurs in all rocks of the MMD drill core. The modal percentage decreases with depth with rocks below 593 m depth containing between 3 and 12% and those above containing between 5 and 35%. At 411 m depth there is a change in texture of clinopyroxene below this horizon, clinopyroxene occurs as subophitic to ophitic (intercumulus) oikocrysts (Fig. 4.28A) whereas above, it occurs as subhedral granular (cumulus) grains (Fig. 4.28B). This fundamental change in the cumulus status of clinopyroxene defines the transition between the lower and upper sequences of the MMD Main Zone. The cumulus clinopyroxene in the Upper Main Zone are fine- to medium-grained, anhedral to subhedral, and often contain simple twins. Uralite is the most common alteration mineral but chlorite and actinolite alteration is also present. One thin section from the Upper Main Zone, at 154 m depth, has ophitic instead of granular clinopyroxene, suggesting a slight regression in its cumulus status. Orthopyroxene is present between 226 and 411 m depth as an accessory mineral modally comprising of <5% of the rocks.

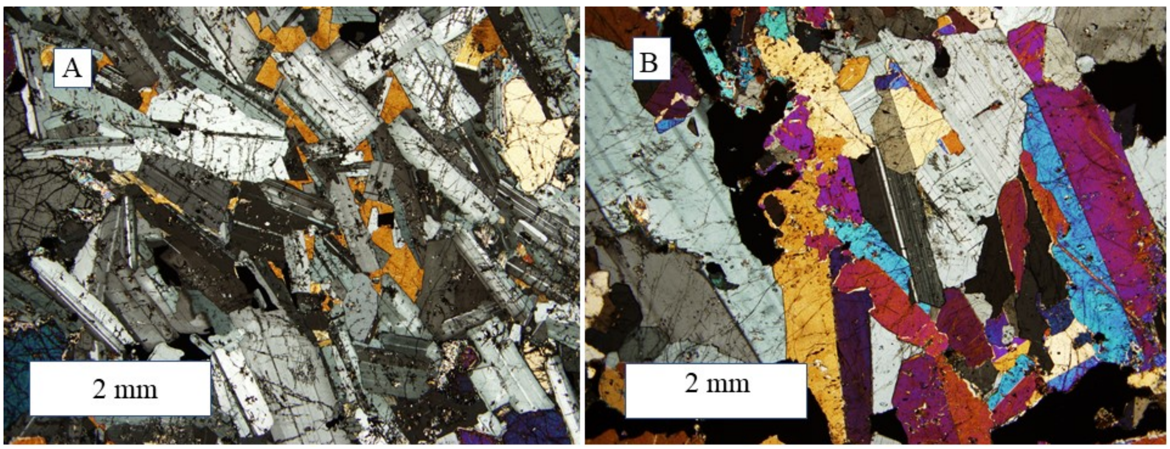

Figure 4.28. MMD-Main Zone photomicrographs (A) Subophitic clinopyroxene interstitial to plagioclase grains from the lower sequence (Transmitted light; XPL; MMD-49). (B) Granular clinopyroxene with simple twins from the upper sequence (Transmitted light; XPL; MMD-11).

The accessory and alteration mineral assemblage of the MMD rocks consists of Fe-Ti oxides (magnetite and ilmenite), apatite, biotite, actinolite, chlorite, quartz, and K-feldspar, all of which are found in the interstitial pockets between cumulus minerals. All of these minerals decrease modally with depth. One thin section at 197.5 m depth has a high modal abundance of (8%) Fe-Ti oxides, which may suggest that it briefly reached cumulus status.

4.1.3.3 Pegmatitic Segregations in the Main Zone

Between 578 and 602 m depth in the drill core is an interval containing several ~1 to 2 m wide pegmatitic layers. These pegmatites are generally leucocratic containing up to 80% plagioclase (Fig. 4.29A), although some segments are plagioclase poor with as little as 35% plagioclase (Fig. 4.29B). Plagioclase in the pegmatitic segregations are coarse-grained (<2cm), subhedral to euhedral, lath-shaped grains. They exhibit moderate sericite alteration in fractures and in patches. Olivine is also coarse-grained and ranges between 7% in the anorthositic rocks and up to 33% in the plagioclase-poor segments. It occurs as anhedral amoeboidal or skeletal grains. Iron oxides and serpentine are the only olivine alteration minerals present and occur in fractures. Clinopyroxene is subophitic to ophitic as grains are observed to partially and wholly encloses plagioclase and olivine grains. Clinopyroxene mode ranges between 9% in the leucocratic rocks and up to 30% in segments poor in plagioclase. Clinopyroxene is weakly altered to chlorite and actinolite. Subpoikilitic and amoeboidal Fe-Ti oxides are present along with biotite, chlorite, quartz, and apatite as accessory minerals.

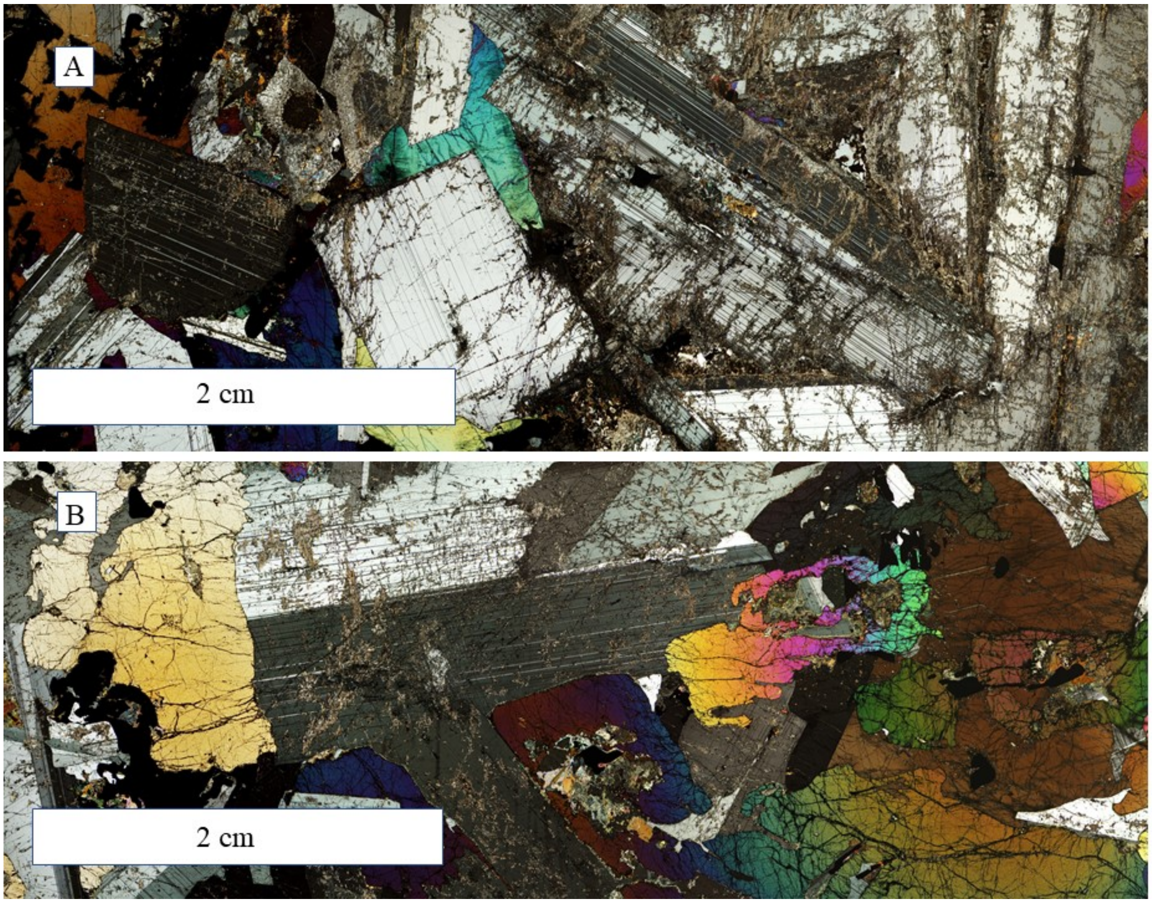

Figure 4.29. MMD-Main Zone photomicrographs (A) Composite photomicrographs of plagioclase-rich pegmatite (Transmitted light; XPL; MMD-38). (B) Composite photomicrographs of plagioclase-poor pegmatite (Transmitted light; XPL; MMD-39).

4.2 GEOCHEMISTRY

The geochemical characteristics of the CLG and MMD rocks were determined using the major and trace element concentrations. The full data set for the whole rock geochemical data used in this study are presented in Appendix B and Goldner (2015).

4.2.1 Crystal Lake Gabbro

A total of 323 samples collected from the CLG drill core were analyzed for whole rock geochemical compositions. The samples are grouped into the units determined by petrographic observations. These units include; Upper Zone (n=24), Main Zone (n=192), Lower Zone (n=50), Logan Sill (n=39), and Rove Formation (n=18).

4.2.1.1 Major Elements

The stratigraphic variations of major elements within and between units of the CLG are presented in downhole geochemical diagrams in Figure 4.30. The Lower Zone rocks contain concentrations of 43 to 52 wt% SiO_2, 0.8 to 1.9 wt% TiO_2, 15 to 20 wt% Al_2O_3, 9 to 25 wt% Fe_2O_3, 7 to 11 wt% MgO, 6 to 11 wt% CaO, 1.4 to 2.6 wt% Na_2O, 0.4 to 3.5 wt% K_2O, and 0.08 to 0.24 wt% P_2O_5. The margins of the Lower Zone, i.e. the top 10 m and bottom 13 m, display the largest variations of concentrations. The basal 13 m is marked by lower concentrations of SiO_2, K_2O, and CaO, as well as higher concentrations of Al_2O_3, Fe_2O_3 when compared to the interior. The upper 10 m margin is marked by an increase of SiO_2, Fe_2O_3, and Na_2O as well as a decrease of Al_2O_3, CaO, and K_2O when compared to the interior (Fig. 4.30). MgO displays several increasing and decreasing trends throughout the Lower Zone (Fig. 30). The interior contains one sample that has anomalous high SiO_2 and low Al_2O_3, Fe_2O_3, and TiO_2 at 690 m depth.

The Main Zone rocks contain concentrations of 39 to 54 wt% SiO_2, 0.7 to 3.6 wt% TiO_2, 14 to 22 wt% Al_2O_3, 10 to 19 wt% Fe_2O_3, 4 to 11 wt% MgO, 8 to 12 wt% CaO, 1.8 to 3.3 wt% Na_2O, 0.3 to 0.8 wt% K_2O, and 0.08 to 0.34 wt% P_2O_5. The trends of the major elements are different in the interior of the unit than at the margins. The interior has trends, moving uphole, of gradually increasing SiO_2, TiO_2, Fe_2O_3, K_2O, Na_2O, and P_2O_5 with Al_2O_3 and MgO decreasing and CaO remaining relatively constant (Fig. 4.30). These trends are generally smooth and unidirectional, however, MgO, TiO_2, Al_2O_3, Fe_2O_3, P_2O_5, and

CaO display localized subtle deviations of the trends all occurring at 165 and 306 m depth (Fig. 4.30). The most notable of these trend deviations are displayed in the downhole profiles of MgO where there are abrupt increases and TiO_2 where there are abrupt decreases in concentrations. These trend variations define three separate cycles.

The top 50 m of the Main Zone is defined by an inflection point of some of the major elements where there is a noticeable reversal of the major element oxide trends. In contrast to the interior of the Main Zone; TiO_2, K_2O, Na_2O, Fe_2O_3 and P_2O_5 all exhibit decreasing concentrations while MgO and Al_2O_3 exhibit increasing concentrations moving uphole (Fig. 4.30). The basal margin of the Main Zone, i.e. the bottom 55 m, displays the largest variation of concentrations. The upper border of this margin is defined by an abrupt increase of TiO_2, Fe_2O_3, K_2O, Na_2O, and P_2O_5 and decrease of Al_2O_3 and CaO. The basal marginal zone exhibits consistently lower concentrations of SiO_2, TiO_2, K_2O, CaO, MgO, and P_2O_5 as well as higher concentrations of Al_2O_3 when compared to the interior (Fig. 4.30). Fe_2O_3 and Na_2O have some samples that have higher concentrations than the interior as well as some samples that have lower concentrations (Fig. 4.30). Within this marginal zone there is a 10 m interval starting 12 m above the basal contact which has low SiO_2 concentrations (<44 wt%) and high Al_2O_3 and Fe_2O_3 concentrations, up to 20 and 19 wt% respectively. SiO_2 concentrations after this interval increase uphole and do not display a sudden change in trend or concentration at the defined marginal border. The Al_2O_3 after this spike increases uphole until, at the marginal border, there is a sudden decrease in concentration. The Fe_2O_3 after this spike decreases uphole until, at the marginal border, there is a sudden increase in concentration. CaO, MgO, and K_2O have an increasing trend where TiO_2 and Na_2O have a decreasing concentration trend throughout the marginal zone (Fig. 4.30).

The Upper Zone rocks have concentrations of 46 to 58 wt% SiO_2, 0.7 to 4.2 wt% TiO_2, 14 to 23 wt% Al_2O_3, 9 to 14 wt% Fe_2O_3, 4 to 10 wt% MgO, 5 to 11 wt% CaO, 1.9 to 4.0 wt% K_2O, 0.3 to 1.3 wt% Na_2O, and 0.06 to 0.50 wt% P_2O_5. There are no observable trends for any of the major element oxides in the Upper Zone. There are samples in this unit that display anomalously high or low values resulting in large variations in concentration. The top 5 m and two samples within the bottom 5 m of the Upper Zone have high SiO_2, TiO_2 K_2O, Na_2O, and P_2O_5 and lower Al_2O_3, MgO, and CaO concentrations. Whereas other samples in the Upper Zone show low concentrations of SiO_2, TiO_2, Fe_2O_3, K_2O, Na_2O, and P_2O_5 as well as high Al_2O_3, MgO, and CaO concentrations (Fig. 4.30).

The Logan Sill samples have concentrations of 47 to 54 wt% SiO_2, 0.8 to 0.9 wt% TiO_2, 11 to 19 wt% Al_2O_3, 9 to 18 wt% Fe_2O_3, 2 to 6 wt% MgO, 6 to 9 wt% CaO, 2.8 to 4.0 wt% K_2O, 1.0 to 3.5 wt% Na_2O, and 0.06 to 0.78 wt% P_2O_5. When compared to the adjacent Main and Lower Zones of the CLG, the Logan Sill displays distinct compositions of the major elements. The Logan Sill has higher concentrations SiO_2, TiO_2, K_2O, Na_2O, and P_2O_5 as well as lower concentrations of Al_2O_3 and MgO although the Fe_2O_3 concentrations are similar to the CLG (Fig. 4.30).

The Rove Formation at the bottom of the drill core have concentrations of 58 to 64 wt% SiO_2, 1.3 to 5.0 wt% TiO_2, 17 to 19 wt% Al_2O_3, 8 to 13 wt% Fe_2O_3, 2.9 to 3.5 wt% MgO, 0.3 to 0.7 wt% CaO, 1.3 to 2.1 wt% K_2O, 3.5 to 4.4 wt% Na_2O, and 0.10 to 0.13 wt% P_2O_5 (Fig. 4.30).

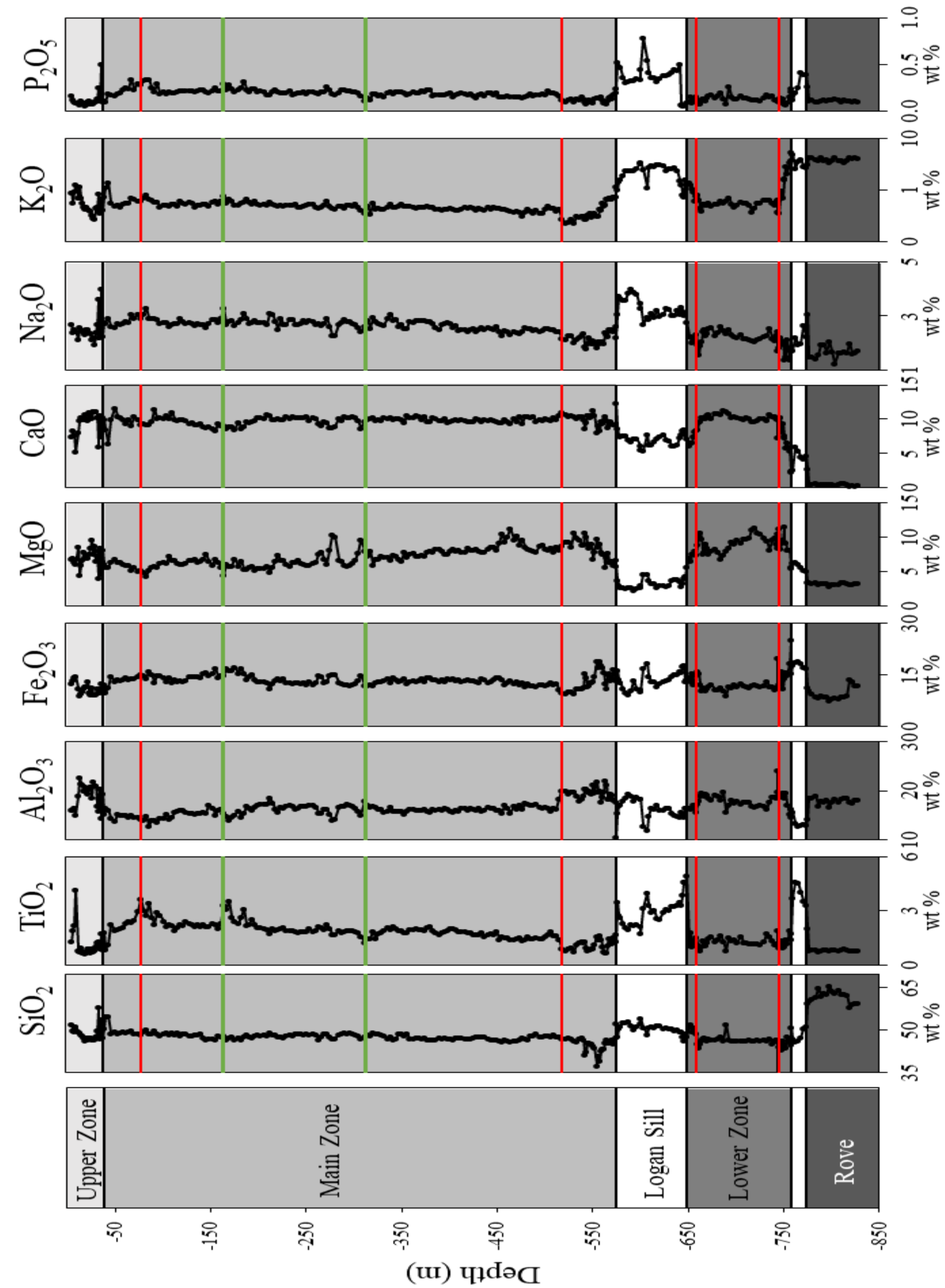

Figure 4.30. Downhole geochemical variation diagram of major element oxides in wt% for the CLG. Red lines represent marginal borders, green lines represent location of trend variations.

4.2.1.2 Major Element Classifications

The geochemical classification of rocks can be made using select major elements. The total alkali vs. silica (TAS) diagram of Cox et al. (1979) and adapted for plutonic rocks by Wilson (1989), is shown in Figure 4.31. On the diagram the rocks of the Upper, Main, and Lower zones all plot within the gabbro field with the vast majority being subalkaline. The rocks of the Logan Sill however, plot in the gabbro and syeno-diorite fields and are of alkaline affinity. To further classify the Upper, Main, and Lower Zone rocks, the AFM (FeO total, Na_2O+K_2O, MgO) ternary diagram with the boundary lines of Kuno (1968) and Irvine and Baragar (1971) is shown in Figure 4.32. In the diagram the rocks of the CLG follow a tholeiitic trend of iron enrichment.

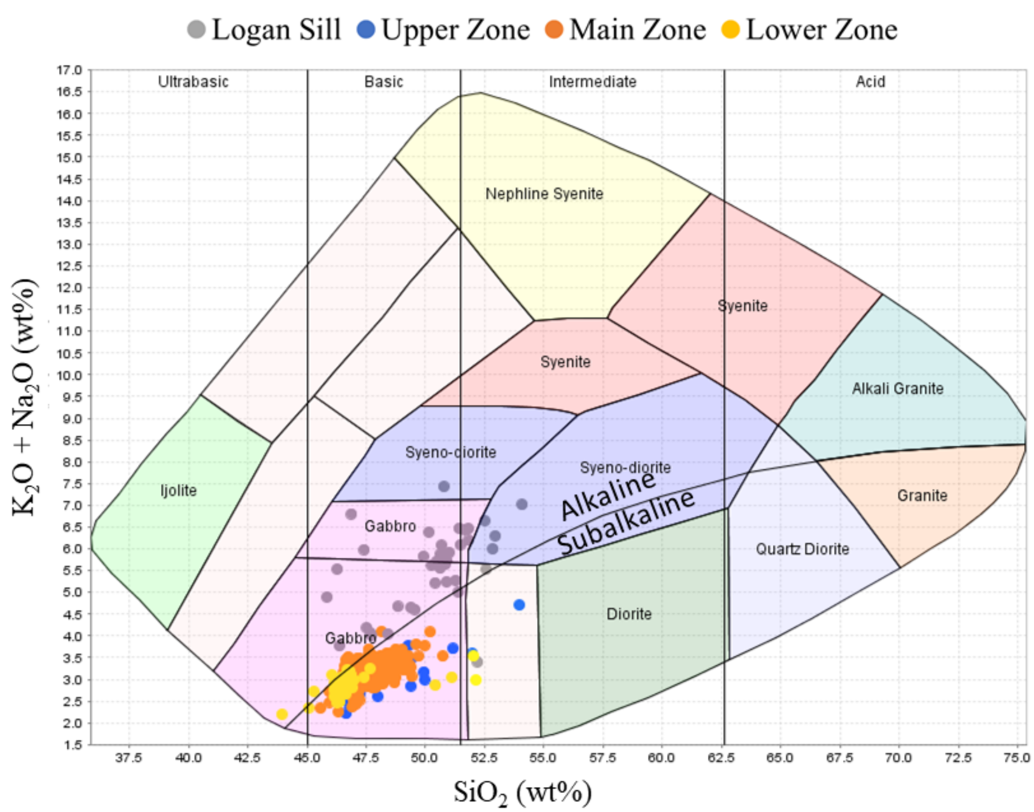

Figure 4.31. Total alkali vs. silica (TAS) diagram for the CLG. Adapted from Cox et al. (1979) and Wilson (1989).

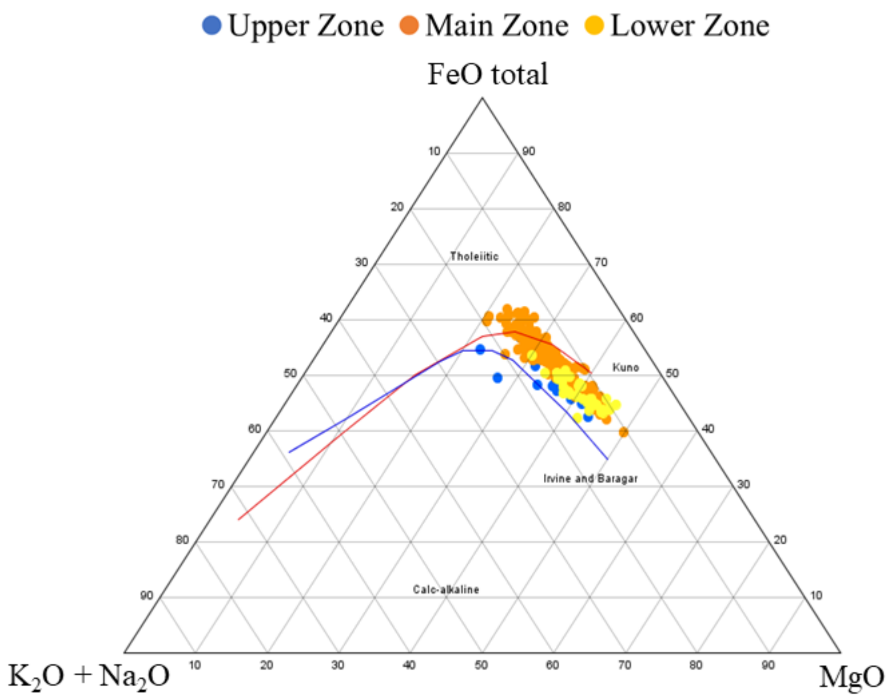

Figure 4.32. AFM (FeO total, Na_2O+K_2O, MgO) ternary diagram for the CLG. After Kuno (1968) and Irvine and Baragar (1971).

4.2.1.3 Trace Elements

As major elements reflect the cumulus mineral processes, trace elements, in particular incompatible trace elements, largely reflect the interstitial trapped liquid processes. To illustrate trace element variations in the CLG drill core, concentrations of selected compatible and incompatible trace elements have been plotted against depth (Fig. 4.33). The compatible trace element Ni has high concentrations in the upper and lower margins of the Lower Zone, the lower margin of the Main Zone, and the Upper Zone. This is consistent with the chalcophile nature of Ni and the petrographic observations of visible sulphides in these areas. High concentrations of Ni in olivine may also contribute to the high concentrations. The interiors of the Lower and Main Zones show a general decreasing Ni concentration moving up hole.

Scandium and vanadium have very similar downhole profiles to each other, displaying low concentrations in the upper and lower marginal zones of the Lower Zone, the lower marginal zone of the Main Zone, and many samples of the Upper Zone. Scandium displays a decreasing trend moving uphole in the interior of the Lower Zone while V increases in concentration. Both Sc and V have a general increasing trend in the interior of the Main Zone that is very similar to the TiO_2 profile in that there are three separate cycles. As with TiO_2, these cycles also appear at 165 and 306 m depth (Fig. 4.33).

The incompatible trace elements (e.g., Zr, Th, Y, Nb, and Ba) all share similar, almost parallel, downhole profiles, with low concentrations in the upper and lower marginal subzones of the Lower Zone, the lower marginal subzone of the Main Zone, and many samples of the Upper Zone as well as general increasing concentration moving uphole in both the Lower and Main Zones. Subtle jogs in the concentrations are also present at 165 and 306 m depth. In the upper marginal subzone of the Main Zone there are decreasing concentration trends moving uphole (Fig. 4.33).

REE chondrite normalized ratios of La/Sm_n and Gd/Yb_n do not display much variation in the CLG. La/Sm_n remains relatively constant between 1.74 to 2.40 in the Main and Lower Zones but increases to 3.01 in the Upper Zone with the Lower Zone having two samples with values of 2.85 in the upper margin. The Logan Sill has values between 1.75 and 2.45 and the Rove Formation has values between 2.99 and 3.61. Gd/Yb_n ranges from 1.42 to 1.99 in the entirety of the CLG where the Logan Sill has values between 1.80 to 2.55 (Fig. 4.33).

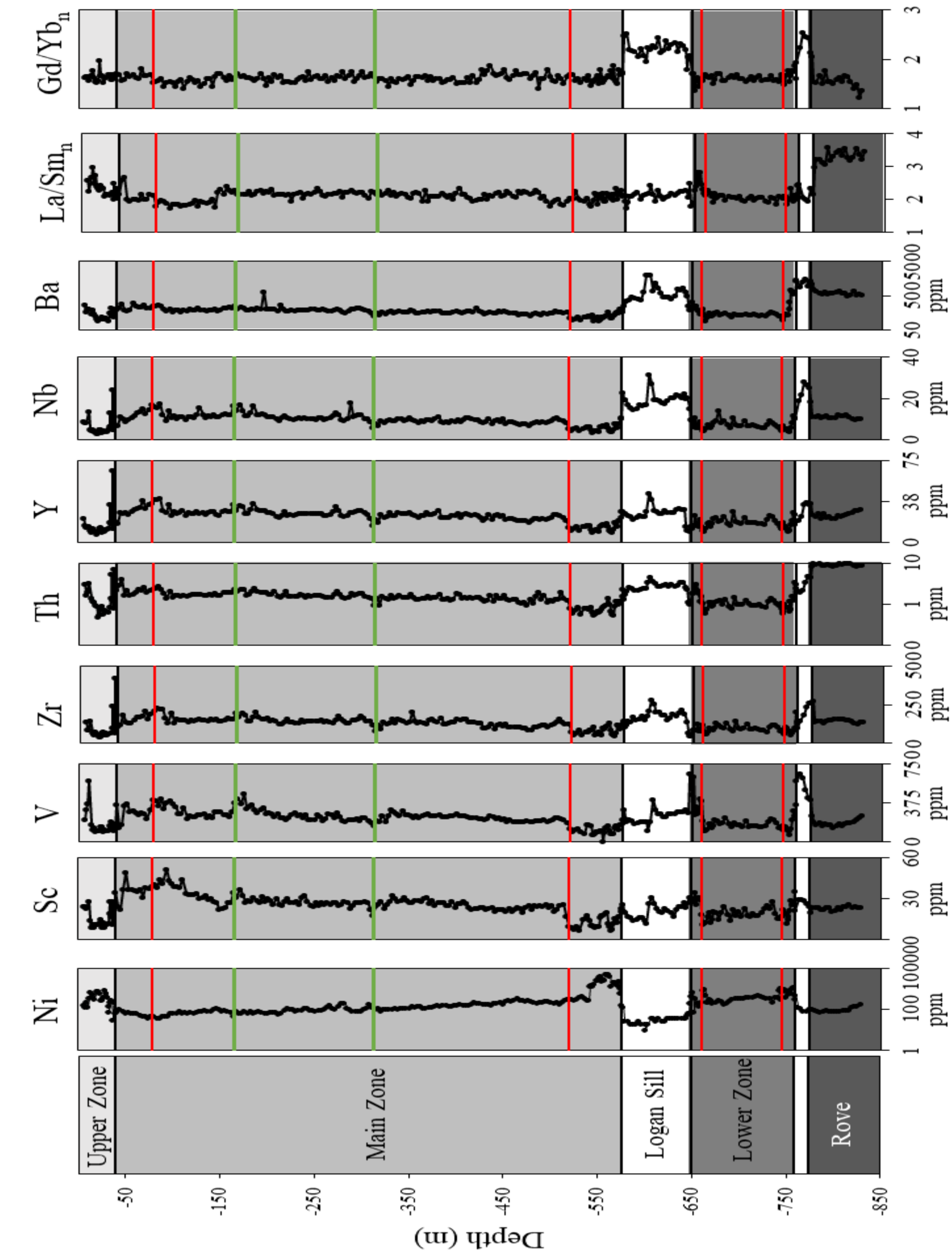

Figure 4.33. Downhole variation diagram for select trace elements for the CLG. Red lines represent marginal borders, green lines represent location of trend variations.

To get a broader sense of the trace element behavior, primitive mantle normalized multi-element diagrams of representative samples from each unit are presented in Figure 4.34. There is a general increase in trace element concentrations moving uphole, but the shape of the multi-element diagrams remain roughly parallel (Fig. 4.34). An enrichment of light rare earth elements (LREE) over middle rare earth elements (MREE) as well as MREE enrichment over HREE is common to all units. Anomalies of HFSE/HFSE* were calculated using the logarithmic method outlined in McCuaig et al. (1994), with Gd used in place of Eu for Hf/Hf* and Zr/Zr*. Common to all samples of the CLG are negative Nb anomalies with Nb/Nb* ranging from 0.33 to 0.69 in the Upper Zone, 0.43 to 0.77 in the Main Zone, and 0.33 to 0.86 in the Lower Zone (Fig. 4.34). The vast majority of the Logan Sill samples also display a negative Nb anomaly with Nb/Nb* as low as 0.33 but there are four samples that display positive anomalies as high as Nb/Nb* of 2.26. Generally, the CLG units do not display Zr-Hf anomalies whereas the Logan Sill consistently displays negative anomalies of Zr/Zr* ranging from 0.47 to 0.97 and Hf/Hf* ranging from 0.47 to 0.92. Ti/Ti* is variable throughout the drill core with both positive and negative anomalies occurring in all the units. The Upper Zone has generally negative Ti anomalies, but three samples, found in the uppermost 11 m of the drill core, display positive anomalies as high as Ti/Ti*=3.13. A few samples have slightly positive and negative Ti anomalies in the Main and Lower Zones rocks but generally the rocks do not display a Ti anomaly. The Logan Sill has the highest variability of Ti anomalies with Ti/Ti* ranging from 0.54 to 4.48. Europium anomalies, both positive and negative, also occur throughout all units in the CLG drill core (Fig. 4.34). Eu/Eu* was calculated using $2*Eu_{cn}/(Sm_{cn}+Gd_{cn})$. The majority of rocks in the Upper Zone display a positive Eu anomaly with Eu/Eu* as high as 1.76, however four samples display weak negative anomalies. The Main Zone has Eu/Eu* ranging from 0.76 to 1.53, with mostly positive anomalies occurring within the basal margin and mostly slightly negative anomalies occurring in the top 100 m. The interior of the Main Zone does not display Eu anomalies. The Lower Zone has Eu/Eu* ranging from 0.85 to 1.68 with the positive anomalies occurring within the upper margin. The Logan Sill rocks have Eu/Eu* ranging from 0.76 to 1.95, however, the vast majority do not display an anomaly.

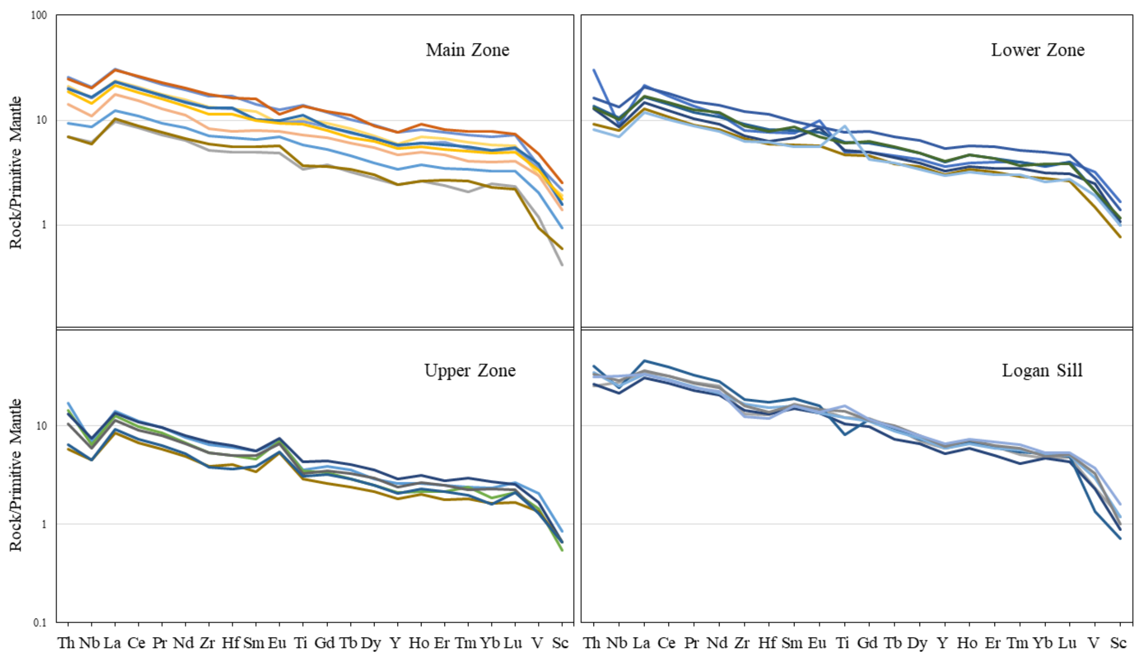

Figure 4.34. Primitive mantle normalized diagrams of representative samples of the CLG. Normalizing values from Sun and McDonough (1989).

4.2.2 Mount Mollie Dyke

A total of seventy-six samples collected from the MMD drill core were analyzed for whole rock geochemical compositions. The samples are grouped into the units determined by petrographic observations. These units include: Upper Zone (n=4), Upper

Main Zone (n=14), Lower Main Zone (n=53), and Lower Main Zone Pegmatitic Segregations (n=3).

4.2.2.1 Major Elements

The stratigraphic variations of major elements within and between units of the MMD are presented in downhole geochemical diagrams (Fig. 4.35). The Lower Main Zone rocks contain concentrations of 45 to 48 wt% SiO_2, 0.6 to 2.5 wt% TiO_2, 14 to 22 wt% Al_2O_3, 8 to 16 wt% Fe_2O_3, 7 to 15 wt% MgO, 8 to 12 wt% CaO, 0.2 to 1.0 wt% K_2O, 1.6 to 2.9 wt% Na_2O, and 0.07 to 0.19 wt% P_2O_5. Gradual increases of concentrations moving uphole and relatively smooth trends are present for SiO_2, TiO_2, K_2O, Na_2O, and P_2O_5. Whereas the Al_2O_3, Fe_2O_3, MgO, and CaO on the other hand, have more of a sawtooth pattern (Fig. 4.35). There are general trends of increasing Fe_2O_3 and decreasing MgO, CaO, and Al_2O_3 concentrations moving uphole. There is a correlation between these four oxides as samples that have increased CaO and Al_2O_3 have decreased Fe_2O_3 and MgO and vice versa (Fig. 4.35).

Pegmatitic Segregation in the Lower Main Zone contain concentrations of 45 to 49 wt% SiO_2, 1.5 to 3.0 wt% TiO_2, 13 to 20 wt% Al_2O_3, 10 to 19 wt% Fe_2O_3, 5 to 8 wt% MgO, 8 to 9 wt% CaO, 0.7 to 1.5 wt% K_2O, 2.4 to 3.3 wt% Na_2O, and 0.14 to 0.22 wt% P_2O_5. There are differences between samples within the unit as well as compared to the Lower Main Zone. One sample has relatively high SiO_2, Al_2O_3, K_2O, and Na_2O concentrations which corresponds with a high modal abundance of plagioclase from at 594 m depth. MgO concentrations are consistently lower in all three samples than the adjacent Lower Main Zone rocks, despite one sample having a high modal abundance of olivine. TiO_2 and Fe_2O_3

concentrations are consistently high in the three samples, suggesting that the pegmatite was enriched in Fe-Ti oxide minerals. There is also a slight increase in P_2O_5 concentrations in the three samples compared to the Main Zone Lower sequence

The Upper Main Zone, which is defined by clinopyroxene becoming a cumulus mineral, is characterized by concentrations of 46 to 52 wt% SiO_2, 1.5 to 3.4 wt% TiO_2, 13 to 18 wt% Al_2O_3, 11 to 18 wt% Fe_2O_3, 4 to 8 wt% MgO, 7 to 11 wt% CaO, 0.4 to 2.5 wt% K_2O, 2.3 to 2.8 wt% Na_2O, and 0.14 to 0.35 wt% P_2O_5. The largest variations of concentrations occur in SiO_2, TiO_2, Al_2O_3, and Fe_2O_3 (Fig. 4.35). These variations are directly related to each other as where TiO_2 and Fe_2O_3 increase, Al_2O_3 and SiO_2 decrease. The K_2O content remains relatively constant throughout the zone with only one sample showing a spiked increase, likely due to a large modal abundance of granophyre, at 123 m depth. MgO and CaO display a relatively smooth decrease of concentration moving uphole while P_2O_5 gradually increases. Na_2O displays little change throughout the zone (Fig. 4.35).

The Upper Zone rocks contain concentrations of 51 to 53 wt% SiO_2, 1.6 to 2.8 wt% TiO_2, 14 to 18 wt% Al_2O_3, 11 to 16 wt% Fe_2O_3, 4.9 to 5.3 wt% MgO, 4 to 7 wt% CaO, 1.4 to 3.8 wt% K_2O, 2.5 to 2.8 wt% Na_2O, and 0.19 to 0.41 wt% P_2O_5. Variations in SiO_2, TiO_2, Al_2O_3, Fe_2O_3, and P_2O_5 appear to be related to each other as low concentrations of TiO_2, Fe_2O_3, and P_2O_5 are associated with high concentrations of Al_2O_3 and SiO_2. A spiked increase in K_2O in the upper most sample is likely due to a large modal abundance of granophyre.

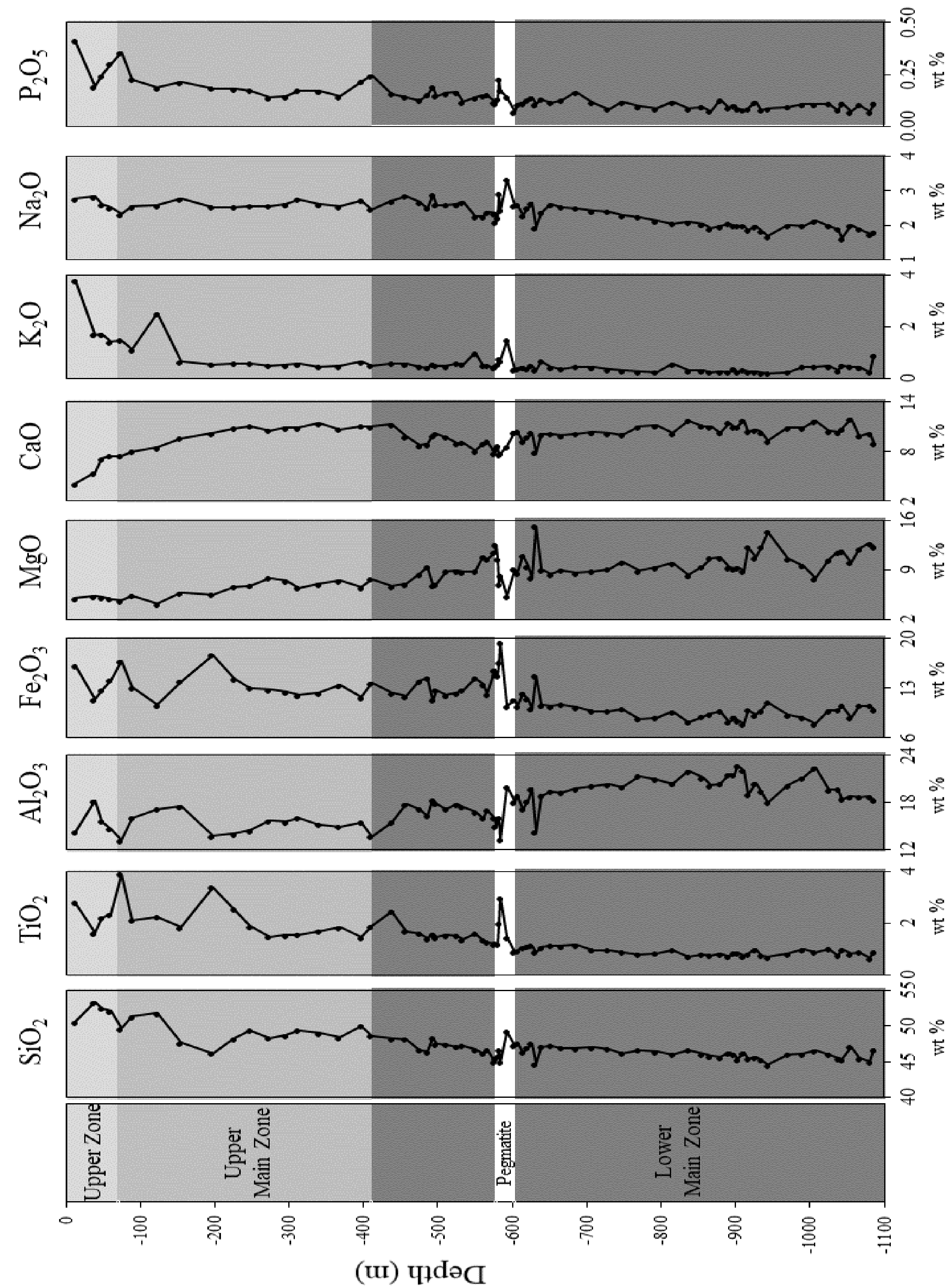

Figure 4.35. Downhole geochemical variation diagram of major element oxides in wt% for the MMD.

4.2.2.2 Major Element Classifications

On the TAS diagram the rocks of the Upper and Main Zones all plot within the gabbro field with the vast majority being subalkaline (Fig. 4.36). The pegmatitic rocks are of alkaline affinity. To further classify the rocks of the MMD, the AFM ternary diagram with the boundary lines of is shown in Figure 4.37. In the diagram the rocks of the MMD follow a tholeiitic trend of iron enrichment.

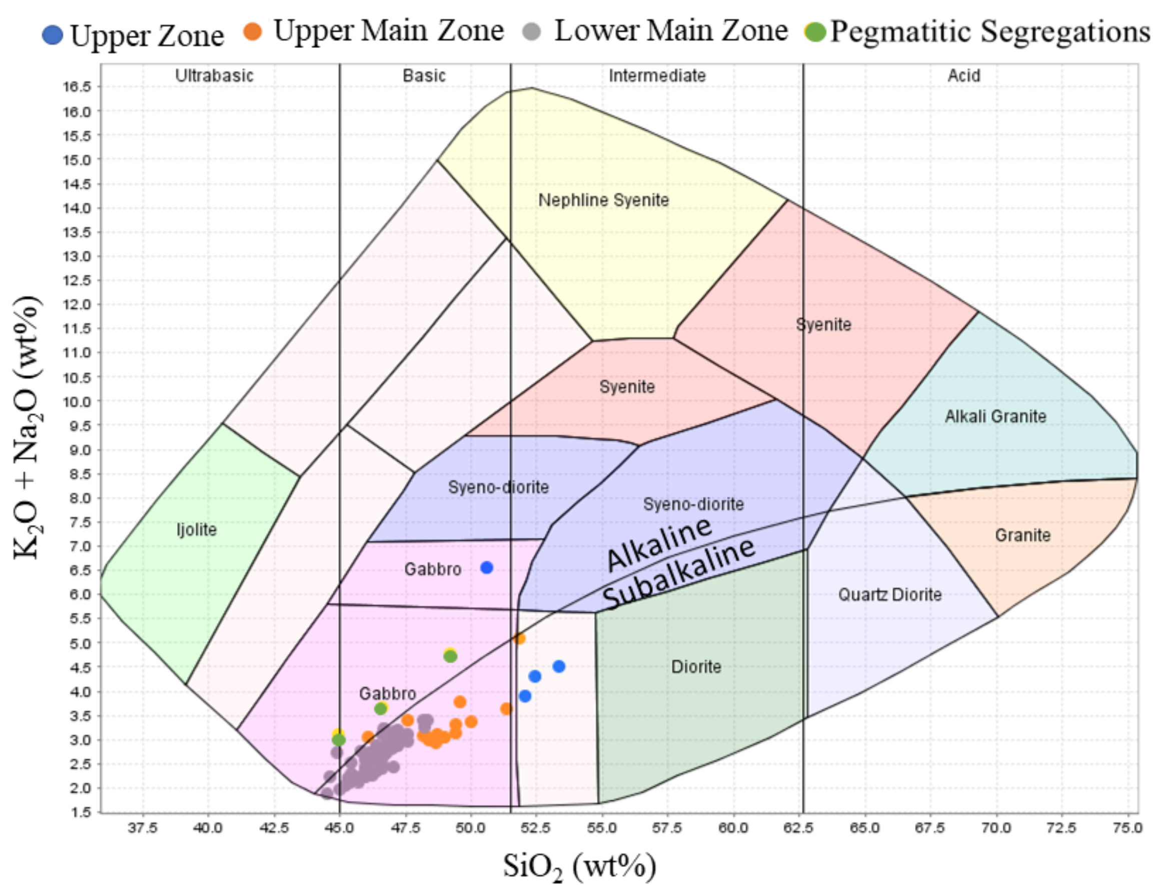

Figure 4.36. Total alkali vs. silica (TAS) diagram for the MMD. Adapted from Cox et al. (1979) and Wilson (1989).

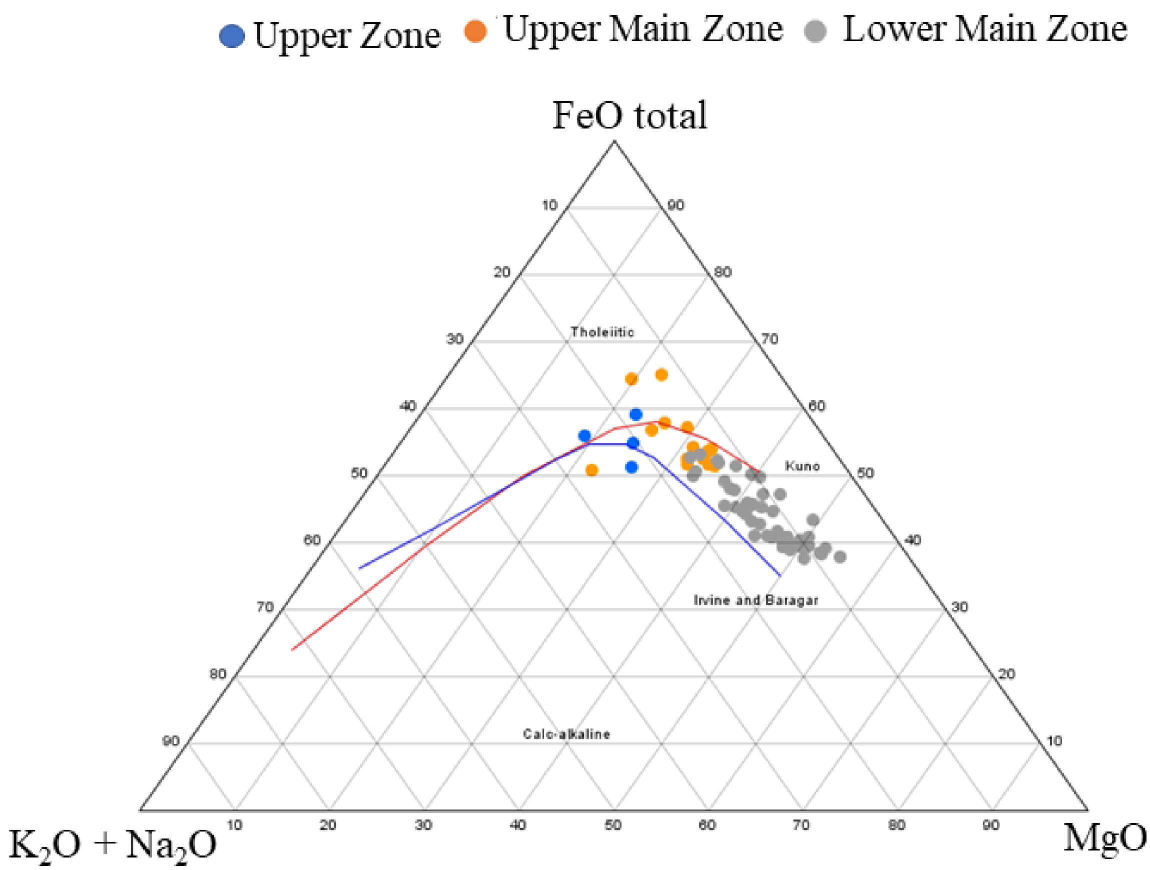

Figure 4.37. AFM (FeO total, Na_2O+K_2O, MgO) ternary diagram for the MMD. After Kuno (1968) and Irvine and Baragar (1971).

4.2.2.3 Trace Elements

To illustrate trace element variations in the MMD drill core, concentrations of selected compatible and incompatible trace elements have been plotted against depth in (Fig. 4.38). Unlike the CLG geochemical downhole profile, Ni concentrations in the MMD do not exceed 700 ppm. Concentrations of Ni generally decrease throughout the Lower Main Zone, albeit with a degree of variation giving rise to a sawtooth pattern. Nickel concentrations in the Upper Main Zone and Upper Zone remain low with a range of 8 to 125 ppm. Scandium and vanadium concentrations exhibit a gradual and smooth increases uphole in the Lower sequence. The boundary between the Lower and Upper Main Zone is coincident with an abrupt uphole increase of Sc concentration. Both Sc and V are variable throughout the Upper Main Zone which makes determining a trend difficult. The incompatible trace elements (e.g., Zr, Th, Y, Nb, and Ba) all generally increase downhole. The profiles of Zr, Y, and Nb are roughly parallel to one another with similar peaks and troughs, however Ba and Th do not follow the same pattern. Thorium concentrations increase uphole from the bottom of the drill hole at a gradual and steady rate until at 123 m depth there is a change to a steeper increasing rate. The downhole profile of Ba resembles the K_2O profile, however the spiked increases are more exaggerated.

Chondrite normalized ratios of La/Sm_n and Gd/Yb_n do not display much variation in the MMD (Fig. 4.38). La/Sm_n remains relatively constant between 1.86 to 2.20 for much of the downhole profile. Beginning at 123 m depth however, there is a slight increase to as much as 2.66 for the uppermost samples. Gd/Yb_n ranges from 1.53 to 1.81 throughout the MMD (Fig. 4.38).

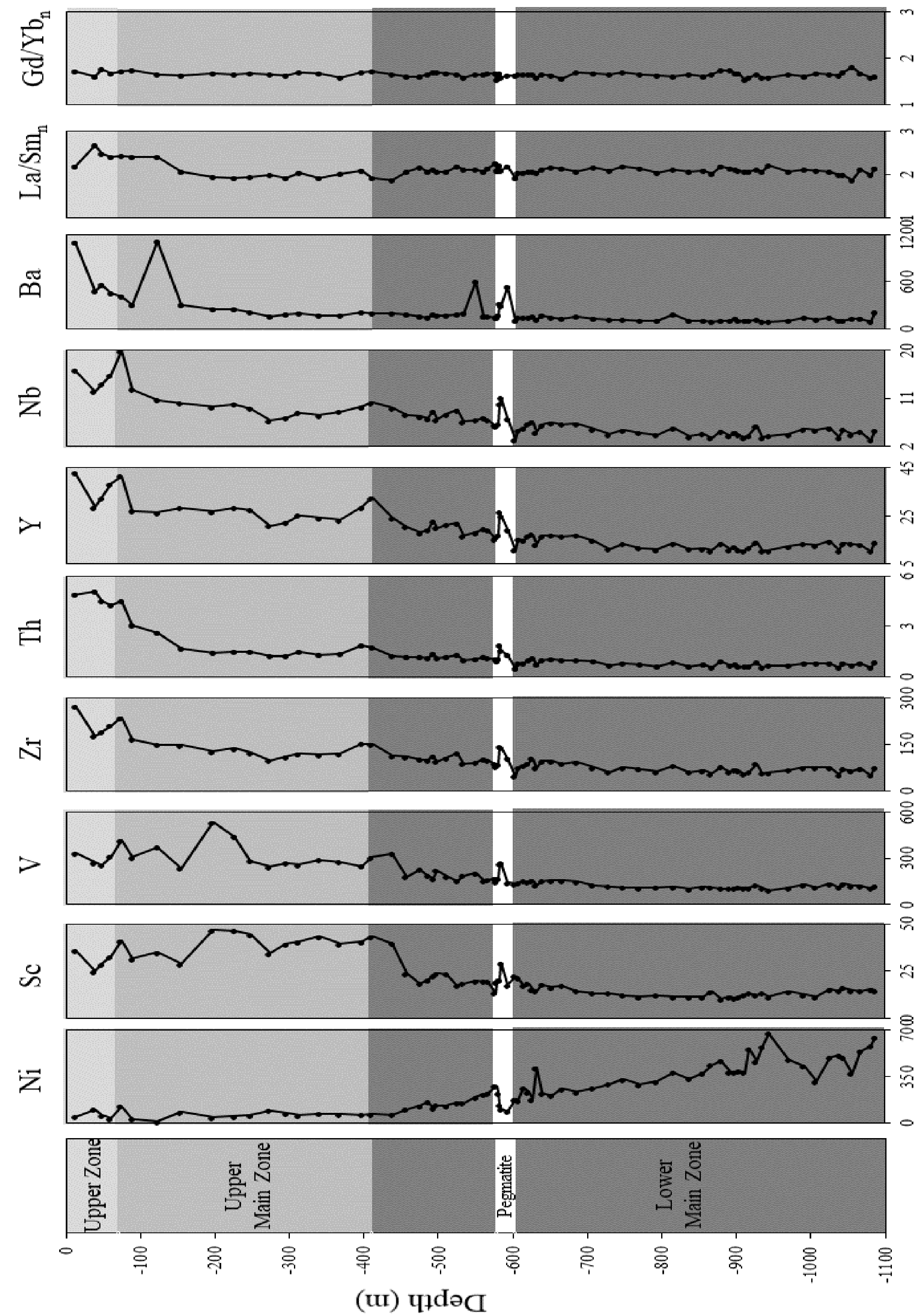

Figure 4.38. Downhole variation diagram for select trace elements for the MMD.

Primitive mantle normalized multi-element diagrams of representative samples from each unit of MMD are presented in Figure 4.39. Similar to the CLG, samples the MMD rock display an enrichment of LREE over MREE as well as MREE over HREE in all units. Consistent negative Nb anomalies are present in all units of the MMD with Nb/Nb* ranging from 0.42 to 0.65. Zr-Hf anomalies are either weak or not present. Ti/Ti* is variable throughout the drill core ranging from 0.66 to 1.67. The samples of the Upper Zone have consistently negative Ti anomalies. The Upper Zone has consistent weak negative europium anomalies (Eu/Eu* ranging from 0.80 to 0.89) while the remaining MMD samples generally have weakly positive or non-existent anomalies, with Eu/Eu* ranging from 0.90 to 1.52.

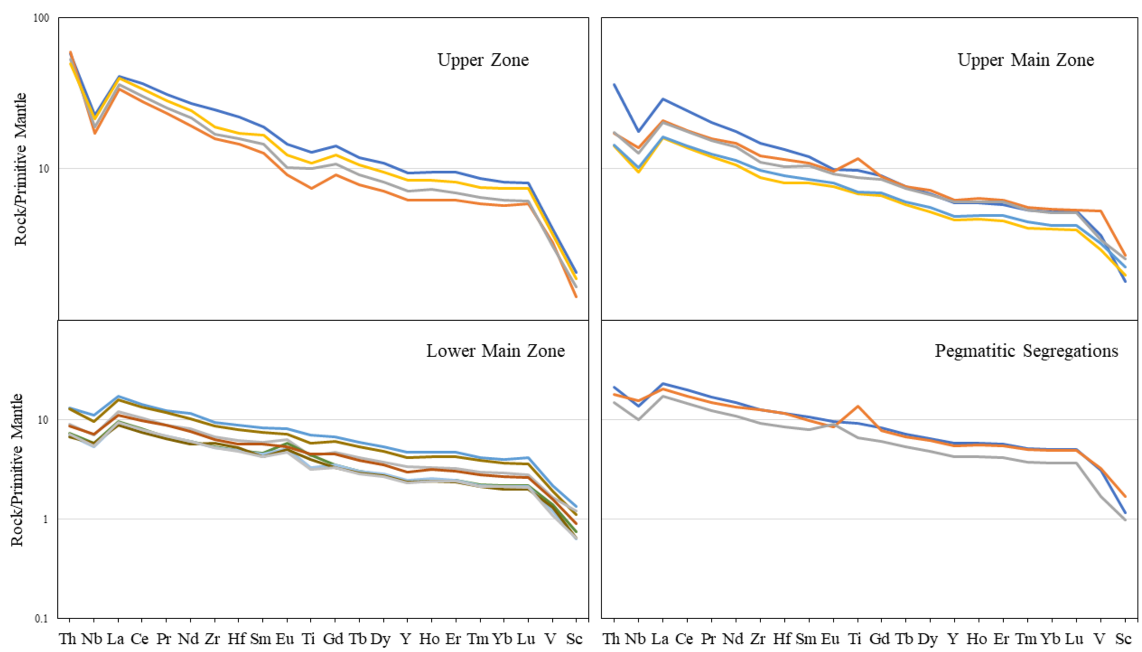

Figure 4.39. Primitive mantle normalized diagrams of representative samples of the MMD. Normalizing values from Sun and McDonough (1989).

4.2.3 Mount Mollie Dyke Surface Samples

Twenty-one surface samples of the MMD were analyzed for this study. Samples were collected from two portions of the MMD. Sample codes starting with "WM" were collected from a portion in the vicinity from the drill core of this study, whereas sample codes starting with "EM" were collected in a portion located to the east (Fig. 4.40).

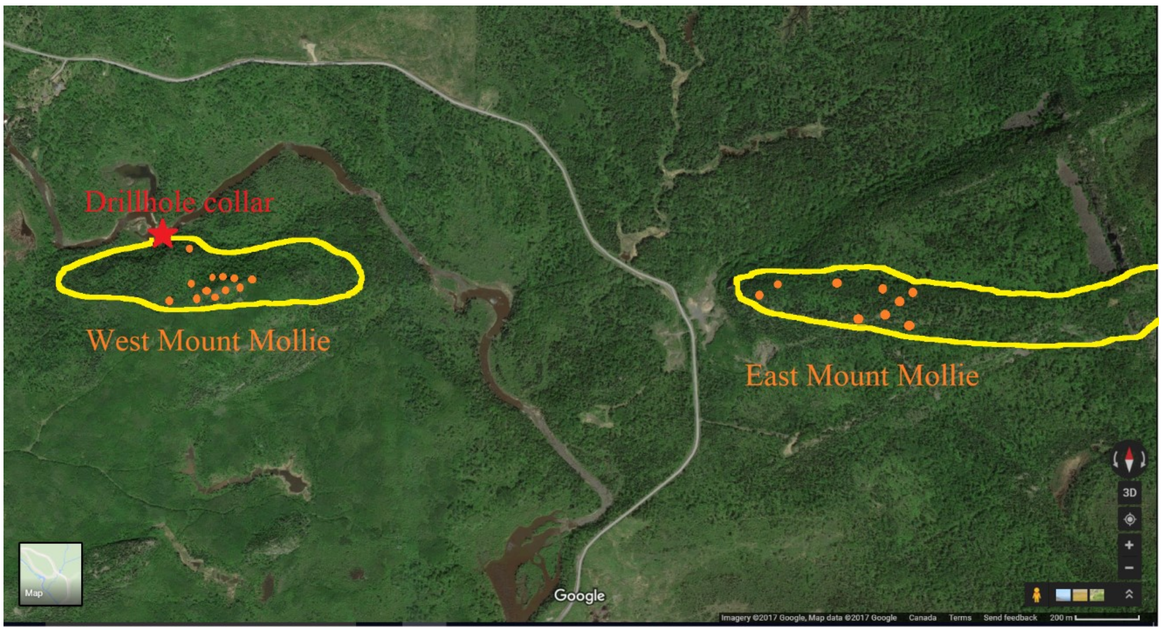

Figure 4.40. Location of surface samples collected in this study. Surface expression of the MMD outlined in yellow and sample locations denoted by orange circles. Modified from Google Earth (2017).

The samples ranged from olivine gabbro to granophyre. Full geochemical analyses, rock type, and location for each sample are presented in Appendix B. These samples have major element concentrations of 47 to 58 wt% SiO_2, 0.9 to 2.9 wt%, TiO_2, 16 to 22 wt% Al_2O_3, 9 to 15 wt% Fe_2O_3, 1 to 8 wt% MgO, 5 to 14 wt% CaO, 2.8 to 2.2 wt% Na_2O, 0.4 to 3.6 wt% K_2O, and 0.1 to 0.6 wt% P_2O_5. Using MgO concentrations as a proxy for comparison, the field samples all fall in the range of drill core samples from the Upper and Upper Main Zones.

Trace element concentrations of the field samples are broadly similar to those of the drill hole samples (Figs. 4.38 and 4.41), with an enrichment of LREE over MREE as well as MREE enrichment over HREE. Common to all samples are negative Nb anomalies with Nb/Nb* ranging from 0.39 to 0.62. Europium anomalies are generally weak or absent. La/Sm_n values range from 1.66 to 2.52 and Gd/Yb_n from 1.61 to 1.85. One sample of granophyre (EM-SOB-7), has noticeably higher trace element concentrations than other MMD samples. This sample has the highest La/Sm_n, highest negative Nb anomaly, a pronounced negative Ti and V anomaly (Ti/Ti*= 0.30), and is also high in SiO_2 (58%).

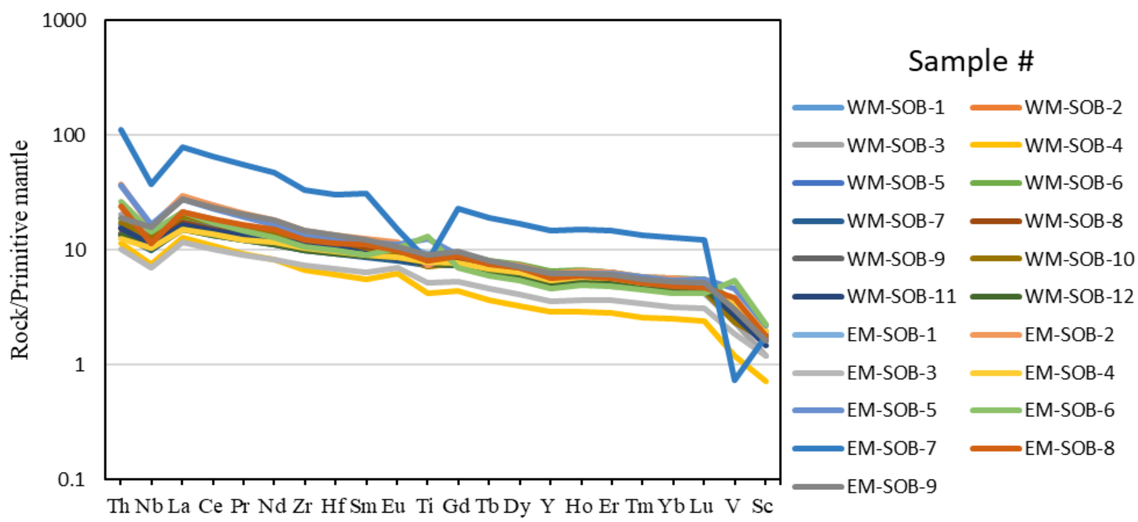

Figure 4.41. Primitive mantle normalized multi-element diagram for MMD surface samples. Normalizing values from Sun and McDonough (1989).

4.2.4 Sulphur Isotopes

Twelve samples containing visible disseminated sulphides were collected from four different areas of the CLG drill core: Upper Zone (n=2), basal margin of Main Zone (n=5), upper margin of Lower Zone (n=3), and basal margin of Lower Zone (n=2). These samples were analyzed for $\delta^{34}S$ to aid in the investigation of the role crustal sulphur had in the sulphur saturation history of the CLG. Overall the $\delta^{34}S$ values fall within a fairly large range of +4.0‰ to +21.0‰. Figure 4.42 presents the $\delta^{34}S$ values obtained for each sample and the corresponding depth. The Upper Zone samples have values of +11.6‰ and +13.2‰, the basal margin of the Main Zone samples range from +4.0‰ to +12.6‰, the upper margin of the Lower Zone range from +11.1‰ to +21.0‰, and the lower margin of the Lower Zone have values of +9.6‰ and +15.6‰.

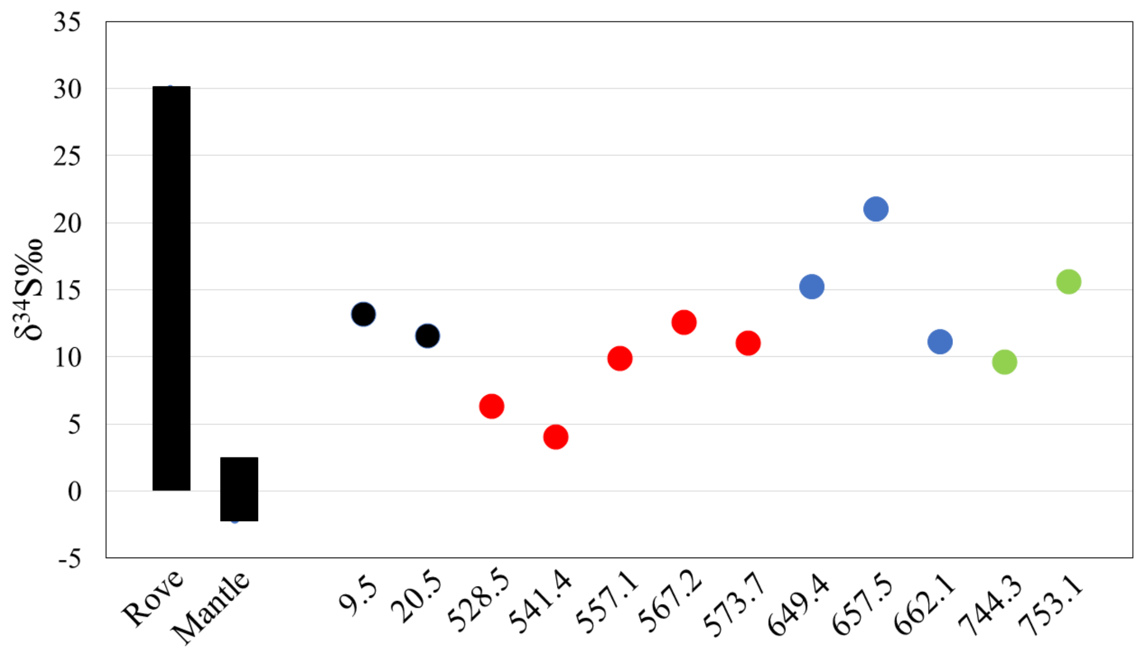

Figure 4.42. $\delta^{34}S$ values for samples of the CLG drill core. Black=Upper Zone, Red=Basal margin of Main Zone, Blue=Upper Margin of Lower Zone, Green=Lower Margin of Lower Zone.

4.3 Mineral Composition

4.3.1 Crystal Lake Gabbro

Mineral composition was determined by SEM-EDS analysis of olivine, plagioclase, and clinopyroxene for eleven samples from the CLG. Samples were taken from the Upper

Zone (n=1), Main Zone (n= 7), and Lower Zone (n=3). As alteration was variable in the CLG, samples were chosen that displayed overall weak alteration with the grains selected for analysis displaying weak to no alteration. Four to six analyses per grain and two to six grains per sample were analyzed for each mineral species. Compositions plotted on the following diagrams are the result of averaging the four to six analyses on individual grains. A complete compilation of the analyses is given in Appendix C.

4.3.1.1 Olivine Composition

Olivine, with the general mineral formula $(Mg,Fe)_2SiO_4$, has a complete solid solution between two endmembers Mg_2SiO_4 (forsterite) and Fe_2SiO_4 (fayalite). Forsterite mole percent, Fo=100*([Mg]/([Mg]+[Fe])), contents of olivine of the CLG vs. stratigraphic height are presented in Figure 4.43. The Upper Zone sample has a narrow range of Fo contents ($Fo_{61.8}$ to $Fo_{61.9}$). At the lower contact of the Main Zone, the Fo content of the olivine within 1 m of the contact ranges from $Fo_{53.8}$ to $Fo_{56.3}$, while ~30 m away from the contact the Fo content increases to $Fo_{74.7}$ to $Fo_{75.4}$. The remainder of the Main Zone displays a relatively constant Fo content in the olivine, ranging from $Fo_{49.1}$ to $Fo_{57.0}$, with a slight decreasing trend moving uphole. The Lower Zone has a decreasing trend of Fo content moving uphole with $Fo_{(71.4\text{ to }72.2)}$ near the lower contact and $Fo_{(60.3\text{ to }62.4)}$ near the upper contact.

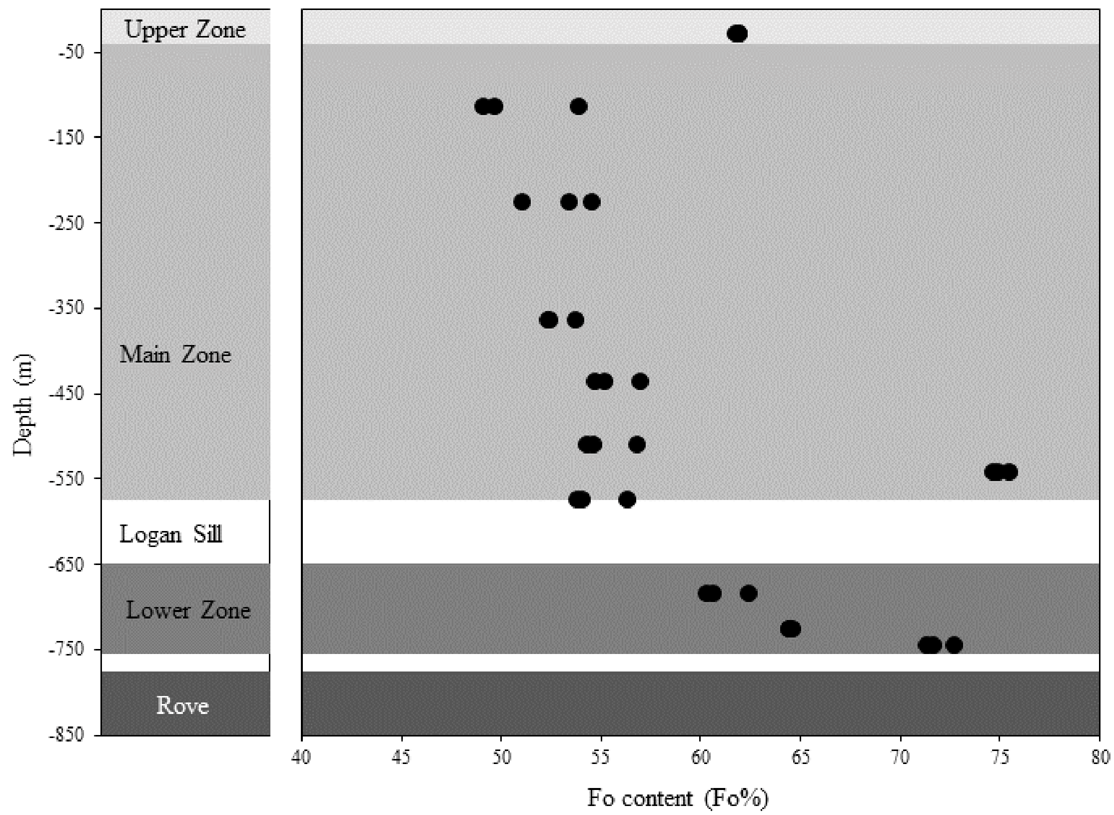

Figure 4.43. Stratigraphic variation of Fo content of olivine in the CLG.

4.3.1.2 Pyroxene Composition

In general pyroxene occurs as both orthorhombic (orthopyroxene) and monoclinic (clinopyroxene) minerals. Orthopyroxene varies between the Mg-end member enstatite ($Mg_2Si_2O_6$) and Fe-end member ferrosilite ($Fe_2Si_2O_6$). Clinopyroxene has a diverse range of mineral compositions, but in the Ca-Fe-Mg system it ranges between the Mg-end member diopside ($CaMgSi_2O$) and Fe-end member hedenbergite ($CaFeSi_2O_6$). Only clinopyroxenes were analyzed in this study as orthopyroxene is much less abundant and only locally present within the CLG samples. Clinopyroxene analyses all plot within the augite field of the pyroxene quadrilateral (Fig. 4.44).

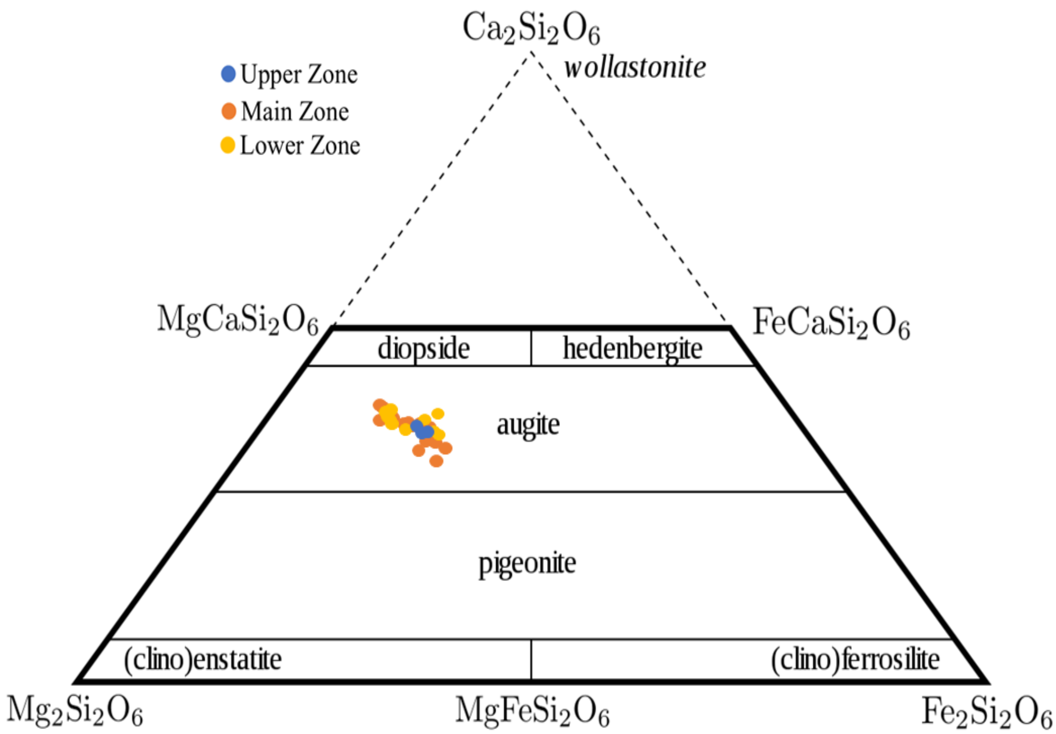

Figure 4.44. Pyroxene quadrilateral showing the composition of CLG clinopyroxene, fields from Deer et al. (1992).

The Mg# (=100*([Mg]/([Mg]+[Fe]))) of clinopyroxene has a somewhat erratic distribution with some samples having a wide range of values between individual grains (Fig. 4.45). The Upper Zone sample has Mg# ranging from 69.7 to 78.6. At the lower contact of the Main Zone, the Mg# of the clinopyroxene within 1 m of the contact has a narrow range of 67.5 to 68.2, while ~30 m away from the contact the Mg# increased to as high as 79.6 and also has a narrow range. The remainder of the Main Zone has an overall erratic distribution with Mg# ranging from 65.2 to 74.1. In an individual sample the widest variation of Mg# between grains is 7.0. The Lower Zone clinopyroxene has a decreasing trend of Mg# moving uphole with values of 77.4 to 78.0 near the lower contact and 70.3 to 70.6 near the upper contact.

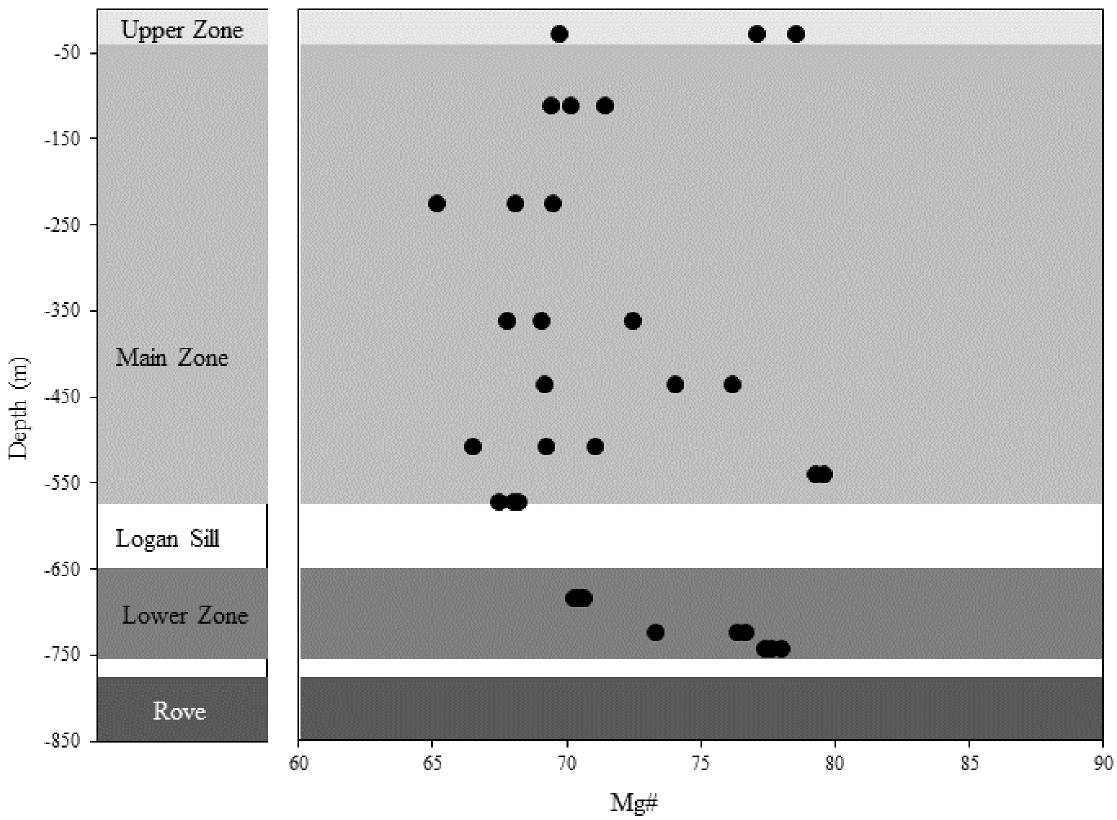

Figure 4.45. Stratigraphic variation of Mg# of clinopyroxene in the CLG.

4.3.1.3 Plagioclase Composition

Plagioclase is a member of the feldspar group of minerals and has a complete solid solution between two endmembers $CaAl_2Si_2O_8$ (anorthite) and $NaAlSi_3O_8$ (albite) which requires a coupled substitution of Na^+ and Si^{4+} for Ca^{2+} and Al^{3+} to maintain charge balance. Minor amounts of a third endmember (Orthoclase; $KAlSi_3O_8$) of the feldspar group is commonly present in the composition of plagioclase (Deer et al., 1992). Compositionally the plagioclase of the CLG plot within the labradorite and bytownite field of the orthoclase-albite-anorthite ternary diagram (Fig. 4.46).

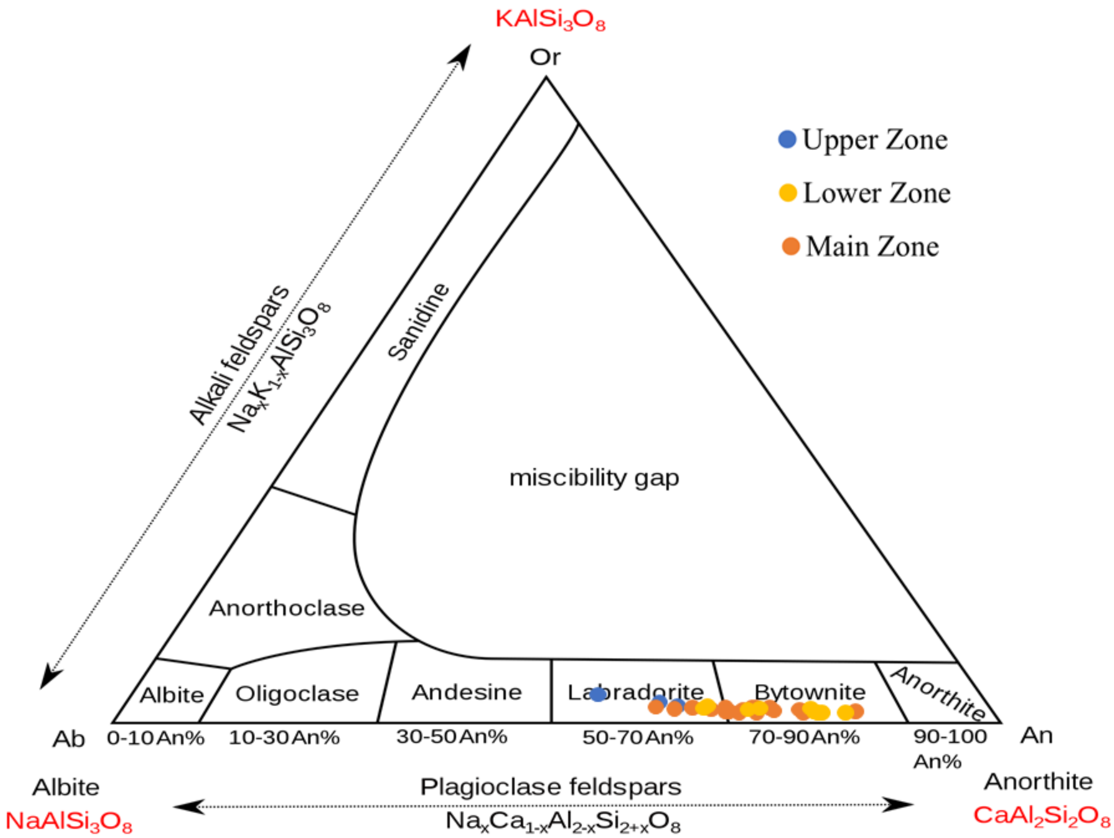

Figure 4.46. Orthoclase-albite-anorthite ternary diagram showing compositions of CLG plagioclase, fields from Deer et al. (1992).

Stratigraphic distribution of the An (=100*([Ca]/([Ca]+[Na]+[K]))) content is presented in Figure 4.47. An attempt was made to analyse the composition of the cores of the plagioclase grains for a good representation of primary composition, however as mentioned in the petrography section zoning was quite common and thus some of the analyses may not be from the true core. The Upper Zone sample has a wide range of An contents ($An_{52.8}$ to $An_{62.5}$). At the lower contact of the Main Zone, the An content of the plagioclase within 1 m of the contact ranged from $An_{68.6}$ to $An_{71.4}$, while ~30 m away from the contact the An content increases to $An_{73.3}$ to $An_{83.2}$. The remainder of the Main Zone displays a range of An content in the plagioclase, from $An_{60.2}$ to $An_{77.3}$, with a decreasing trend moving uphole. The Lower Zone has an erratic distribution of An content with an overall range of $An_{65.7}$ to $An_{82.2}$.

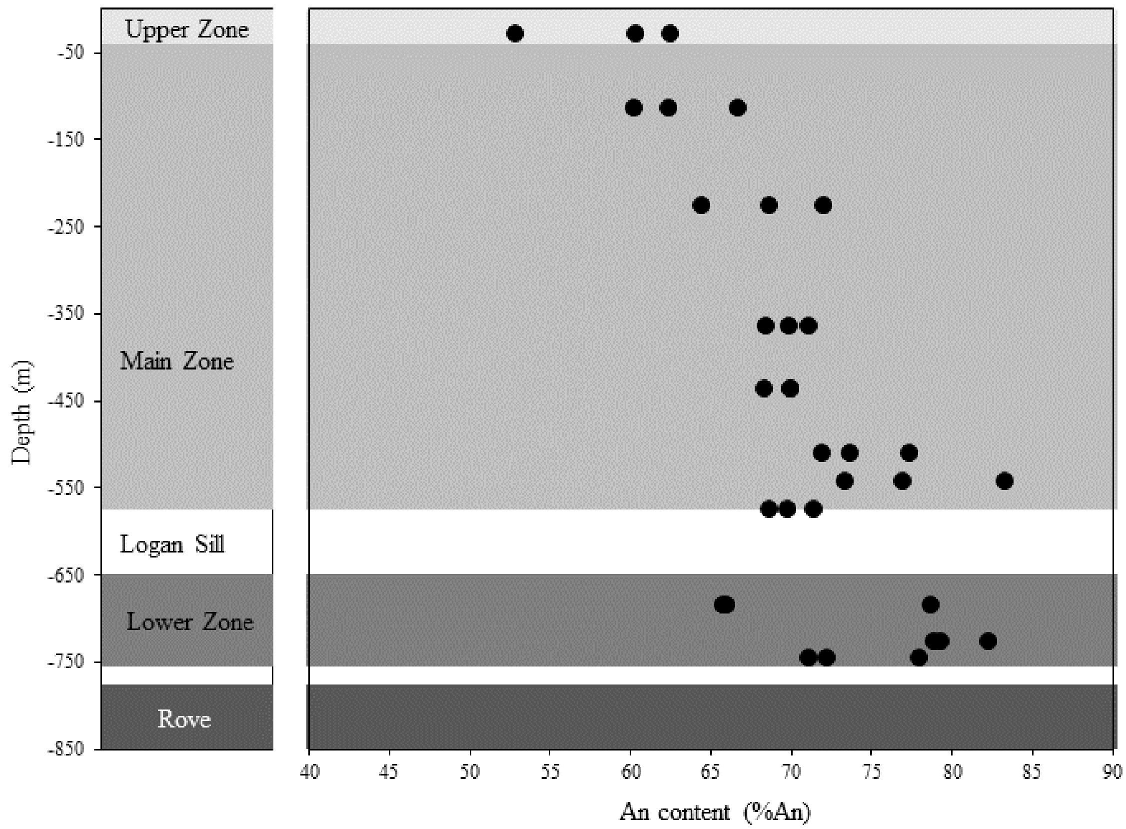

Figure 4.47. Stratigraphic variation of An content of plagioclase in the CLG.

4.3.1.4 Spinel Composition

The mineral composition of Cr-spinel grains from the basal margins of the Main Zone (n=3) and Lower Zone (n=5) are presented in Tables 4.1 and 4.2. Cr-spinel grains were present in four samples collected from the CLG drill core, whereas no samples collected from the MMD contained Cr-spinel grains. Of the four samples from the CLG, one was located in the Upper Zone, one was located in the Main Zone, and two were located in the Lower Zone. The sample from the Upper Zone and one sample from the Lower Zone were moderate to strongly altered, so mineral composition analysis was deemed inappropriate. With a general spinel formula containing four oxygens and assuming perfect stoichiometry and charge balance, the Fe^{2+} and Fe^{3+} contents were estimated using the method of Droop (1987).

Table 4.1. Mineral composition of spinel from the CLG, sample CLG-25, located in the basal margin of the Main Zone.

Sample CLG-25		Spinel 1 Average	Spinel 2 Average	Spinel 3 Average
Na_2O	Oxide wt%	0.23 ± 0.07	0.12 ± 0.08	0.08 ± 0.09
MgO		5.03 ± 0.10	7.62 ± 0.19	7.55 ± 0.21
Al_2O_3		9.18 ± 0.17	13.16 ± 0.04	12.60 ± 0.20
SiO_2		0.33 ± 0.08	0.35 ± 0.03	0.16 ± 0.18
CaO		0.13 ± 0.03	0.06 ± 0.05	0.06 ± 0.05
TiO_2		6.64 ± 0.05	7.09 ± 0.04	7.43 ± 0.12
V_2O_5		0.65 ± 0.08	0.60 ± 0.07	0.59 ± 0.03
Cr_2O_3		33.35 ± 0.28	29.77 ± 0.15	29.52 ± 0.09
FeO		31.77 ± 0.32	29.56 ± 0.41	29.77 ± 0.81
Fe_2O_3		12.83 ± 0.33	12.57 ± 0.67	12.90 ± 0.77
NiO		0.28 ± 0.06	0.33 ± 0.12	0.28 ± 0.11
Total		100.41 ± 0.22	101.22 ± 0.26	100.93 ± 0.34
Na	Cations	0.02	0.01	0.00
Mg	Normalized to	0.26	0.37	0.37
Al	4 oxygens	0.37	0.51	0.49
Si		0.01	0.01	0.01
Ca		0.00	0.00	0.00
Ti		0.17	0.18	0.19
V		0.01	0.01	0.01
Cr		0.90	0.77	0.77
Fe^{2+}		0.91	0.81	0.82
Fe^{3+}		0.33	0.31	0.32
Ni		0.01	0.01	0.01
Total		3.00	3.00	3.00

Table 4.2. Mineral composition of spinel from the CLG, sample CLG-42, located in the basal margin of the Lower Zone.

Sample CLG-42		Spinel 1 Average	Spinel 2 Average	Spinel 3 Average	Spinel 4 Average	Spinel 5 Average
MgO	Oxide wt%	4.87 ± 0.07	3.82 ± 0.10	3.10 ± 0.12	3.64 ± 0.11	10.50 ±0.15
Al_2O_3		9.19 ± 0.10	7.43 ± 0.12	6.42 ± 0.06	6.92 ± 0.11	25.64 ±0.09
SiO_2		0.26 ± 0.05	0.20 ± 0.05	0.25 ± 0.07	0.24 ± 0.10	0.34 ± 0.06
TiO_2		8.41 ± 0.07	9.27 ± 0.09	9.17 ± 0.12	10.40 ±0.12	2.70 ± 0.07
V_2O_5		0.85 ± 0.09	0.96 ± 0.05	0.89 ± 0.09	0.99 ± 0.14	0.46 ± 0.06
Cr_2O_3		29.27 ±0.34	25.85 ±0.22	23.67 ±0.31	24.03 ±0.15	27.60 ±0.13
FeO		34.97 ±0.15	37.25 ±0.21	38.23 ±0.31	39.12 ±0.31	23.67 ±0.24
Fe_2O_3		12.95 ±0.37	16.47 ±0.30	19.91 ±0.48	16.39 ±0.41	9.59 ± 0.28
MnO		0.57 ± 0.08	0.61 ± 0.02	0.46 ± 0.24		
Total		101.34 ± 0.31	101.86 ± 0.30	102.10 ± 0.44	101.72 ± 0.23	100.49 ± 0.38
Mg	Cations Normalized	0.25	0.20	0.17	0.19	0.47
Al	to	0.37	0.30	0.26	0.28	0.93
Si	4 oxygens	0.01	0.01	0.01	0.01	0.01
Ti		0.22	0.24	0.24	0.27	0.06
V		0.02	0.02	0.02	0.02	0.01
Cr		0.79	0.71	0.65	0.66	0.67
Fe^{2+}		1.00	1.08	1.12	1.14	0.61
Fe^{3+}		0.33	0.43	0.52	0.43	0.22
Mn		0.02	0.02	0.01	0.00	0.00
Total		3.00	3.00	3.00	3.00	2.99

Compositionally the spinels display various proportions of major elements. All three grains from the basal margin of the Main Zone and four out of the five grains from the basal margin of the Lower Zone share broadly similar major element concentrations of 3.1 to 7.6 wt% MgO, 6.4 to 13.2 wt% Al_2O_3, 6.6 to 10.4 wt%, TiO_2, 23.7 to 33.4 wt% Cr_2O_3. Whereas the fifth spinel from the lower zone has higher MgO (10.5 wt%) and Al_2O_3 (25.6 wt%) as well as lower TiO_2 (2.7 wt%). Grains from the Main Zone contain variable amounts of NiO, CaO and Na_2O but the Lower Zone samples do not, whereas grains from the Lower Zone contained variable amounts of MnO and the Main Zone grains do not. However, all of these elements are only found in trace amounts.

4.3.2 Mount Mollie Dyke

Mineral compositions were determined by SEM-EDS analysis of olivine, plagioclase, and clinopyroxene for eleven drill core samples from the MMD. All samples were taken from the Main Zone: Upper sequence (n=2), Lower sequence (n= 8), and Pegmatitic Segregation (n=1). As alteration was variable in the MMD, samples were chosen that displayed overall weak alteration with grains selected for analysis that displayed weak to no alteration. Four to six analyses per grain and two to six grains per sample were analyzed for each mineral species. Compositions plotted on various diagrams are the result of averaging the four to six analyses on individual grains. A complete compilation of the analyses is given in Appendix C.

4.3.2.1 Olivine Composition

Overall the downhole profile has a general decreasing trend with Fo content as high as ($Fo_{73.4}$ to $Fo_{73.6}$) the sample at 944.6 m depth and as low as ($Fo_{43.6}$ to $Fo_{44.3}$) in the uppermost analyzed sample at 226.9 m depth (Fig. 4.48). There are notable exceptions to the decreasing trend. The lowermost sample that was analyzed has a slightly lower Fo content than the sample stratigraphically above it. Between 837.9 and 631.5 m depth there is no change in the Fo content. The pegmatite sample at 584.3 m depth has a slightly lower Fo content than the samples stratigraphically directly above and below.

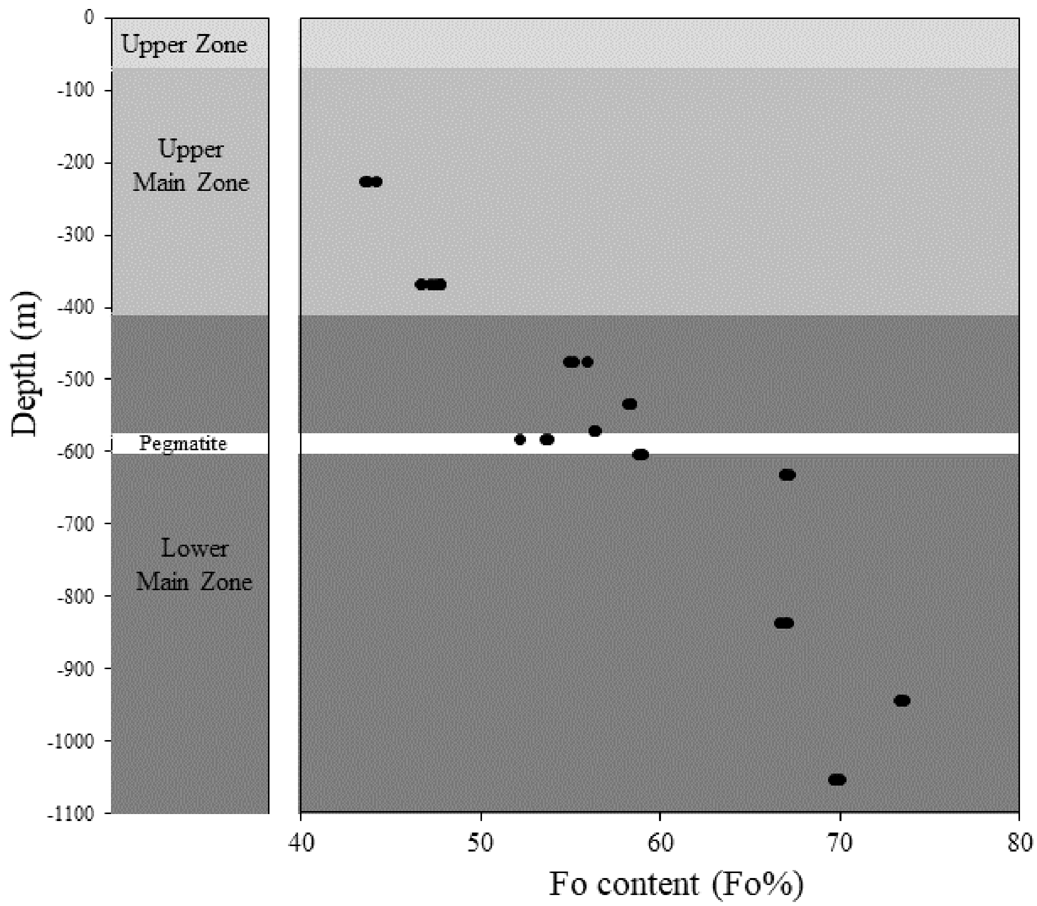

Figure 4.48. Stratigraphic variation of Fo content of olivine in the MMD.

4.3.2.2 Clinopyroxene Composition

Compositionally the clinopyroxene of the MMD drill hole all plot within the augite field on the pyroxene quadrilateral (Fig. 4.49). There is a general decreasing but erratic Mg# trend moving uphole of the clinopyroxene in the MMD (Fig. 4.50). Within individual samples there are a range of Mg# with the largest range occurring in the sample taken at 367.9 m depth (Mg# 65.4 to 71.5). The pegmatite has on average a lower Mg# (64.7 to 67.0) than the samples directly above (68.5 to 70.8) and below (70.2 to 73.3).

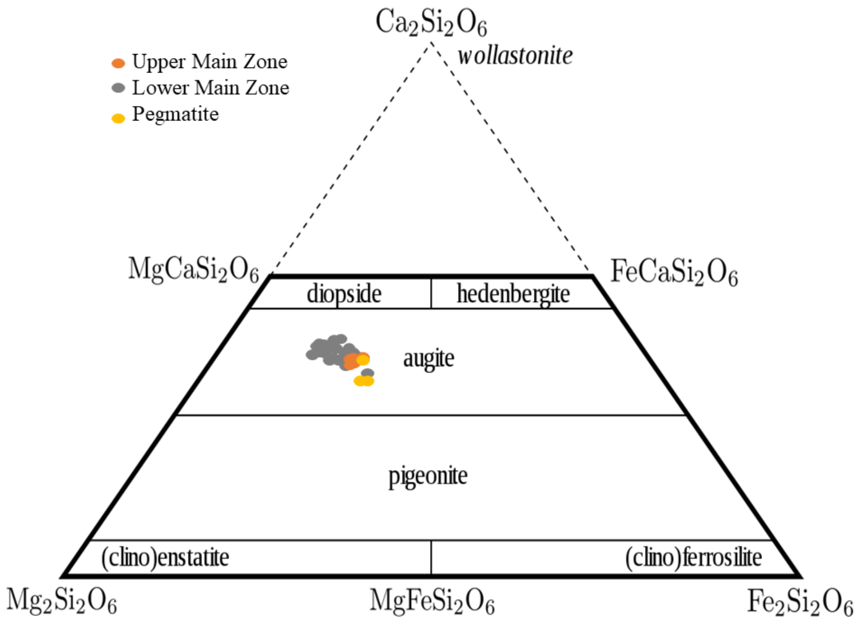

Figure 4.49. Pyroxene quadrilateral showing the composition of MMD clinopyroxene, fields from Deer et al. (1992).

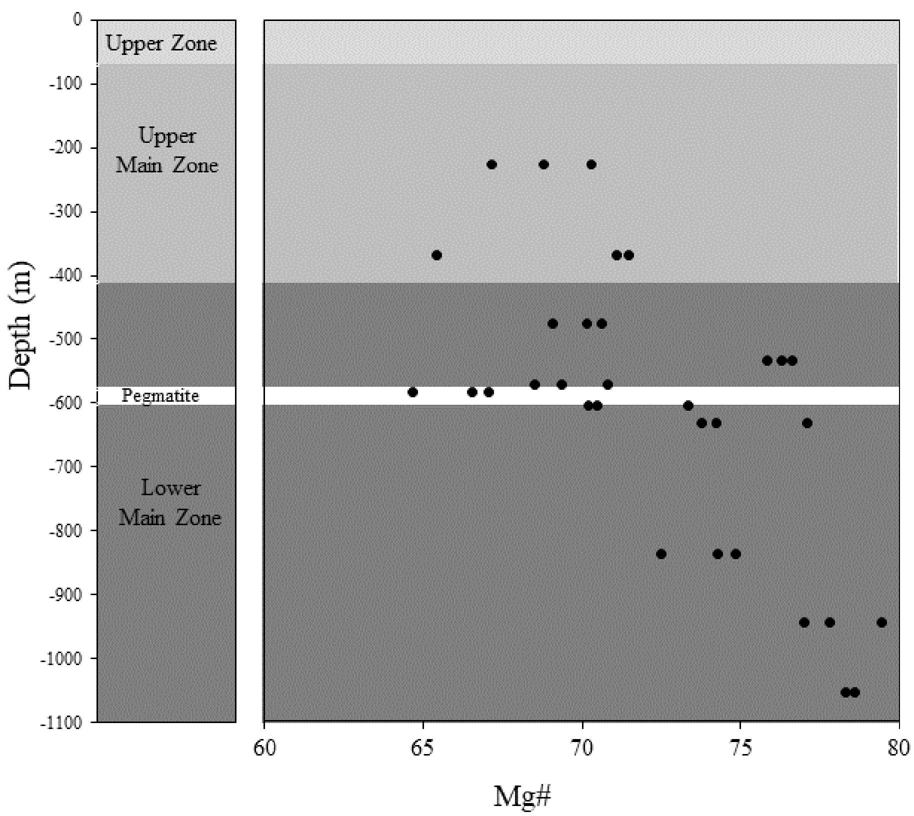

Figure 4.50. Stratigraphic variation of Mg# of clinopyroxene in the MMD.

4.3.2.3 Plagioclase Composition

The composition of the plagioclase from the MMD drill core plot within the labradorite and bytownite field on the orthoclase-albite-anorthite ternary diagram (Fig. 4.51). Overall the An content of the MMD plagioclase has a bimodal distribution of high An contents below the pegmatitic segregation zone and low An contents above (Fig. 4.52). Similar to the CLG, individual samples have a wide range of An content, with the lowermost sample having a range of $An_{64.7}$ to $An_{82.36}$. This is most likely the result of zoning where some of the analyses do not represent the true core composition. On average the pegmatite sample has a lower An content ($An_{53.5}$ to $An_{53.9}$) than the samples directly below ($An_{53.12}$ to $An_{78.41}$) and above ($An_{54.2}$ to $An_{58.7}$).

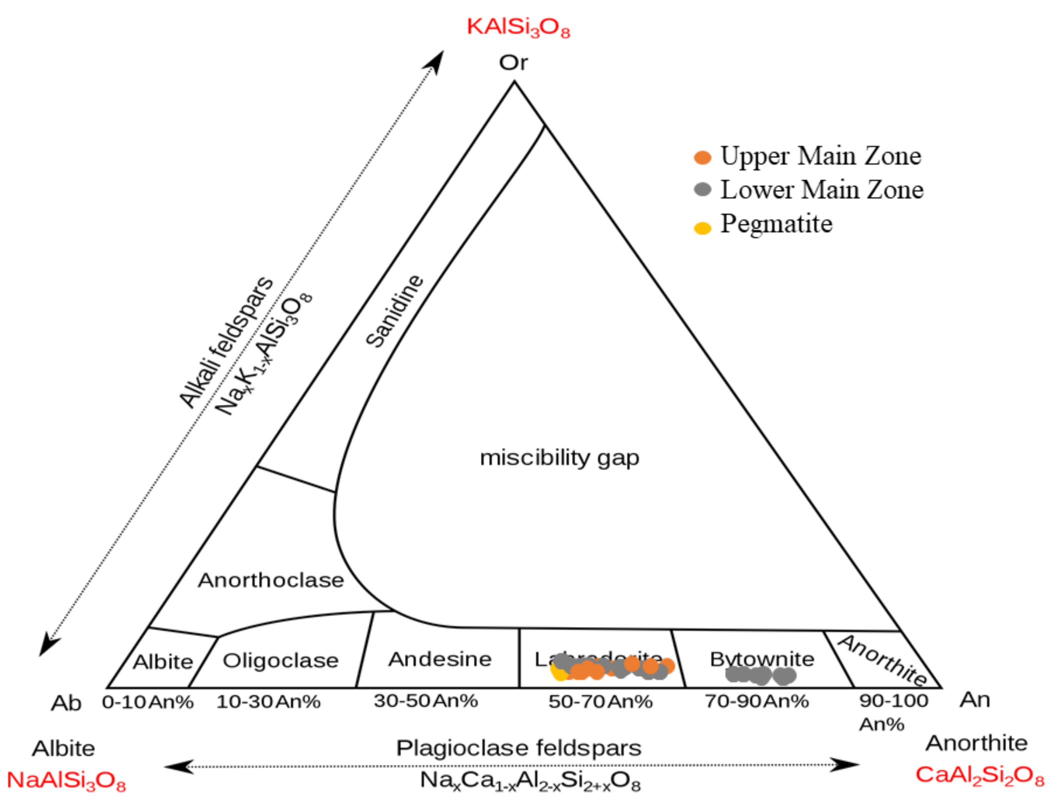

Figure 4.51. Orthoclase-albite-anorthite ternary diagram showing compositions of MMD plagioclase, fields from Deer et al. (1992).

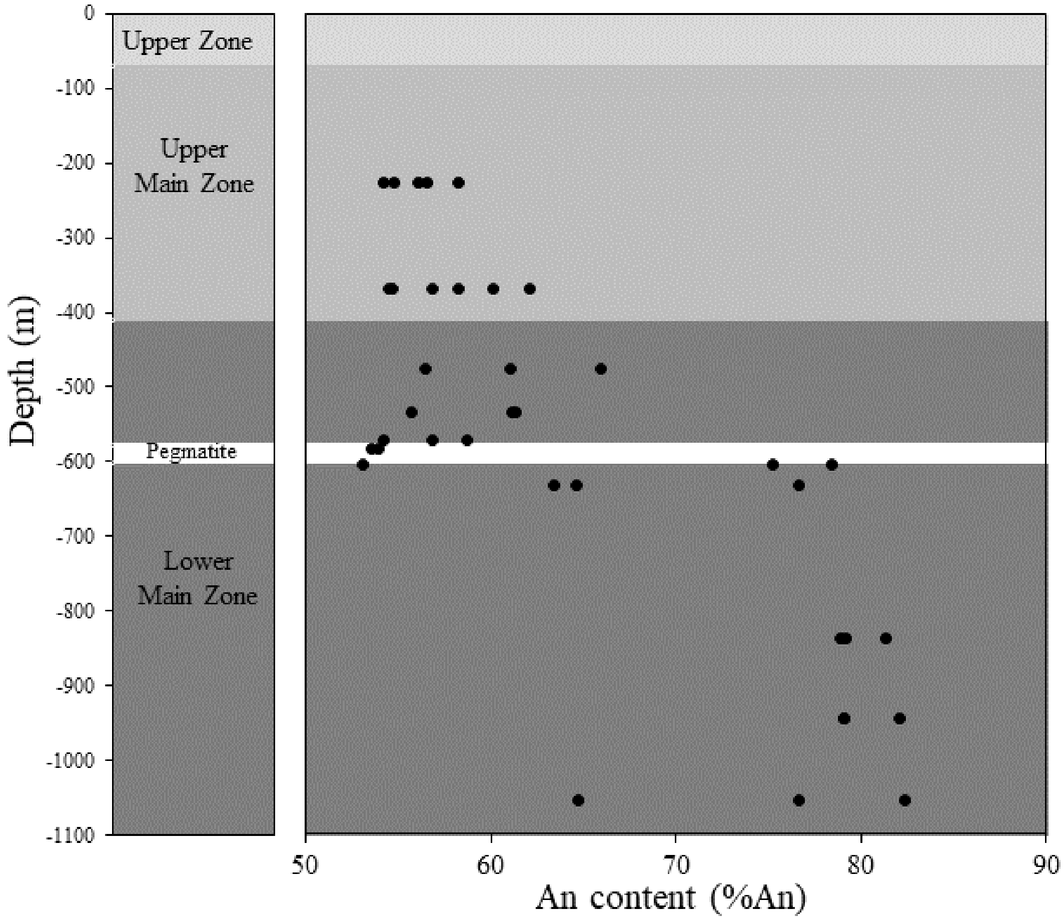

Figure 4.52. Stratigraphic variation of An content of plagioclase in the MMD.

5 DISCUSSION

5.1 INTRODUCTION

The data gathered in this study, as well as other studies, will be used to interpret and constrain the petrogenesis of the CLG and MMD and relate it to the MCR as a whole. Both intrusive bodies are located within the Logan Basin which is comprised of a series of dykes and sills, hosted in the Rove Formation. The CLG is unique in that it is the only known layered intrusion located within the Logan Basin while the MMD is unique in that it is the only arcuate dyke. This chapter discusses the lithostratigraphy, the role of crustal contamination, the parental magma composition, the overall context of both the CLG and MMD to the MCR, and proposes an emplacement model.

5.2 LITHOSTRATIGRAPHY

5.2.1 Crystal Lake Gabbro

The CLG is comprised of varying proportions of plagioclase, olivine, and clinopyroxene; resulting in a range of rock types, including troctolite, augite troctolite, olivine gabbro, and gabbro. Broadly the CLG can be divided in to three zones; Upper Zone, Main Zone, and Lower Zone. Detailed petrography as well as whole-rock geochemistry and mineral composition reveal that each of the zones can be further subdivided into subzones.

Two Logan sill units bound the Lower Zone, a ~75 m thick upper unit and a ~17 m thick lower unit. Texturally and geochemically the Logan Sill units are very similar. It is possible that the lower Logan Sill unit is a delaminated portion of the upper Logan Sill unit, or vice versa, that was displaced during the emplacement of the CLG. Alternatively, they could represent two distinct sills. With only a single drill hole it is difficult to distinguish these two options.

The Lower Zone is ~108 m thick and composed of medium-grained, non-foliated, subophitic to ophitic troctolite, augite troctolite, and olivine gabbro. This unit is subdivided into three subzones; upper marginal subzone, basal marginal subzone, and interior subzone. The upper marginal subzone is characterized by a fine-grained contact with the overlying Logan Sill. This subzone is sulphide bearing with S contents up to 1.8 wt%. Since sulphides are typically thought to settle to the bottom of intrusions, the presence of sulphides in the upper marginal subzone may suggest that the magma was sulphur saturated at the time of emplacement (this is discussed further in a following subsection). The basal marginal subzone coarsens upward from the contact with the underlying Logan Sill. This subzone contains abundant Cr-spinel seams which could have accumulated as a result of gravitational settling of grains shortly after emplacement of the magma, in a process similar to that suggested by Eales and Costin (2012) of the Bushveld Complex. The magma was either saturated in Cr-spinel or was emplaced with suspended grains as detailed petrography shows that Cr-spinel was the first mineral to crystallize.

The fractionation of the Lower Zone magma can only be recognized cryptically. During fractional crystallization of a mafic magma in a closed system, olivine initially crystallizes as Mg-rich and progressively becomes Fe-rich as the magma becomes more evolved (e.g., Morse, 1996). Whereas in an open system magma chamber, the mineral composition of olivine does not change in a systematic fashion, as it can be affected by replenishment of either more evolved or primitive magma (e.g., Pang et al., 2009; Namur et al., 2010, Wiebe and Snyder, 1993; White, 2007; Gao and Zhou, 2013). Subsolidous reequilibration with interstitial magma may also affect the composition of olivine, known as the trapped liquid shift, which can occur in both open or closed systems (Barnes, 1986). Much like olivine, clinopyroxene compositions have an evolutionary trend of decreasing Mg concentration with fractionation of a mafic magma (Wager and Deer, 1939; Brown and Vincent, 1963). The combined effects of these two minerals cause an overall Mg-depletion and Fe-enrichment during fractional crystallization of a tholeiitic magma. An overall bottom-up-directed fraction crystallization of the Lower Zone interior subzone is suggested by the progressive decreasing Fo content of the olivine grains, Mg# of the clinopyroxene, and whole-rock MgO concentrations moving uphole (Figs. 4.30, 4.43, and 4.45). With Cr-spinel, olivine, and plagioclase being the only cumulus minerals present in the Lower Zone, the magma crystallized before a modal or textual differentiation sequence could occur. Petrographic analysis reveals the cumulus stratigraphy of the Lower Zone is Spinel → Spinel + Plagioclase + Olivine → Plagioclase + Olivine. The incompatible trace element concentrations of the Lower Zone are lower than the majority of the Main Zone, suggesting that the Lower Zone formed from a slightly more primitive magma.

The Main Zone overlies the ~75 m thick upper Logan Sill unit. A sharp fine-grained contact is present between the Main Zone and the Logan Sill (Fig. 4.18A). Away from this contact there is an upward coarsening of the rocks. Petrographic, geochemical, and mineral composition can be used to subdivide the Main Zone into five subzones; a basal marginal subzone, upper margin subzone, and interior cycles 1, 2, and 3. The basal margin subzone

(575 to 519 m depth) is characterized by the presence of abundant Cr-spinel seams and disseminated sulphides. Samples within this subzone have concentrations as high as 3.1 wt% S and 1.0 wt% Cr. The lowermost 30 m of this subzone consistently has S concentrations >1 wt%, whereas Cr contents appear cyclically in three intervals with concentrations >0.5 wt%; 559 to 554 m, 544 to 542 m, and 534 m. Both sulphides and Cr-spinel grains likely accumulated in the basal subzone, due to gravitational settling. Based on their textures Cr-spinel likely settled as crystalized grains, whereas sulphides settled as liquid droplets (i.e. poikilitic vs. interstitial; Figs. 4.11 and 4.12). The Cr-spinel grains were likely mechanically sorted by the settling into the observed seams in by a process similar to that outlined in Eales and Costin (2012). Liquid sulphide droplets could have moved downward in between grains in a crystal mush, until they ultimately crystallized in interstitial pockets in a process similar to that outlined in Chung and Mungall (2009). High Al_2O_3 concentrations in this subzone can be attributed to the high modal abundance of Cr-spinel, which mineral composition analysis revealed that Al_2O_3 concentrations are as high as 25.6 wt%. Clinopyroxene is consistently subophitic and is less abundant in this subzone than in the overlying interior subzones of the Main Zone; the rocks in the basal marginal subzone are classified as mesocumulates, with cumulus spinel, plagioclase, and olivine consisting comprising between 75 and 93 modal % of the rocks (Irvine, 1982). Geochemically this subzone is characterized by low incompatible trace element and TiO_2 concentrations, likely due to the high proportion of cumulate minerals and low amounts of intercumulus material (Fig. 5.1). MgO concentrations show a progressive increase uphole as do the An content of plagioclase, Fo content of olivine and the Mg# of clinopyroxene, which is the opposite of what would be expected in a fractionating magma (Fig. 5.1; Wager

and Deer, 1939). Similar geochemical basal reversals have been observed globally in almost all mafic sills and intrusions, which has been attributed to a combination of processes including; the magma progressively becoming more primitive during emplacement, minerals crystalizing from progressively more undercooled magma closer to the country rock contact, and increasing effectiveness of adcumulus mineral growth (Latypov, 2015). The exact extent to which each of these processes is responsible for the observed reversal can not be determined. Petrographic analysis reveals the cumulus stratigraphy of this subzone is Spinel → Spinel + Plagioclase + Olivine → Plagioclase + Olivine.

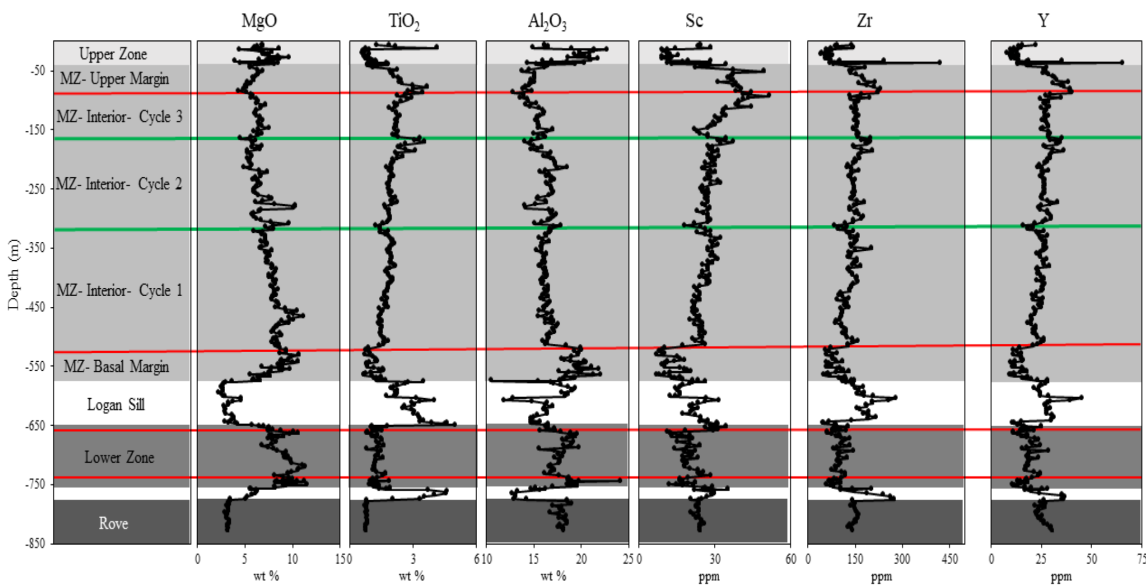

Figure 5.1. Downhole geochemical profiles for the CLG. Red lines represent marginal borders, green lines represent interior subzone boarders.

Moving up in the stratigraphy of the CLG, three interior subzones of the Main Zone are recognized. These subzones differ from the basal margin geochemically as well as texturally. The border between the basal margin and the interior is marked by an abrupt increase in incompatible trace element and TiO_2 concentrations, decrease of Al_2O_3 and an inflection point of the increasing trend of MgO concentrations (Fig. 5.1). Texturally the border is marked by the disappearance of Cr-spinel seams and a modal increase of clinopyroxene as well as a change of habit from subophitic to largely ophitic. This abrupt change could be due to a recharge event of a compositionally more evolved magma. Mineral composition of olivine and clinopyroxene support this hypothesis as they both display a significant change in composition across the boundary. The Fo contents decrease from $Fo_{74.7 \text{ to } 75.4}$ in the basal margin subzone (sample at 541 m depth) to $Fo_{54.3 \text{ to } 57.0}$ in the interior (sample at 509 m depth) as well as Mg# decreasing from (79.3 to 79.6) to (66.5 to 71.1). It does not seem likely that fractional crystallization alone of a magma would cause such a drastic decrease of olivine Fo content and clinopyroxene Mg# over a 32 m interval. Similar arguments have been made based on abrupt changes in geochemistry and mineral composition to suggest a new pulse of a more evolved magma (e.g., Wiebe and Snyder, 1993; Seat et al, 2007; White, 2007; Gao and Zhou, 2013; Luolavirta et al. in press)

The interior of the Main Zone can be subdivided into three subzones, cycles 1, 2, and 3. Texturally and geochemically these three units are very similar to each other. They all consist of augite troctolite, olivine gabbro, and gabbro. Clinopyroxene almost exclusively occurs as ophitic grains and together with the other interstitial minerals generally comprise between 25 and 50% of the rocks making them orthocumulates (Irvine, 1982). The basis for the subdivision between the three cycles is the intermittent appearance of olivine and increases in the accessory minerals which coincides with subtle but abrupt changes in the concentrations of major and trace elements, occurring at 306 and 165 m depth (Figs. 5.1

and 5.2). The three cycles may represent crystallization of separate magma pulses as previous studies of other intrusions suggest that similar textural and geochemical changes may represent of recharge of compositionally similar magma (e.g., Cawthorn, 1983; Chalokwu et al., 1995; Emeleus et al. 1996; Talusani et al., 2005; Leuthold et al., 2014).

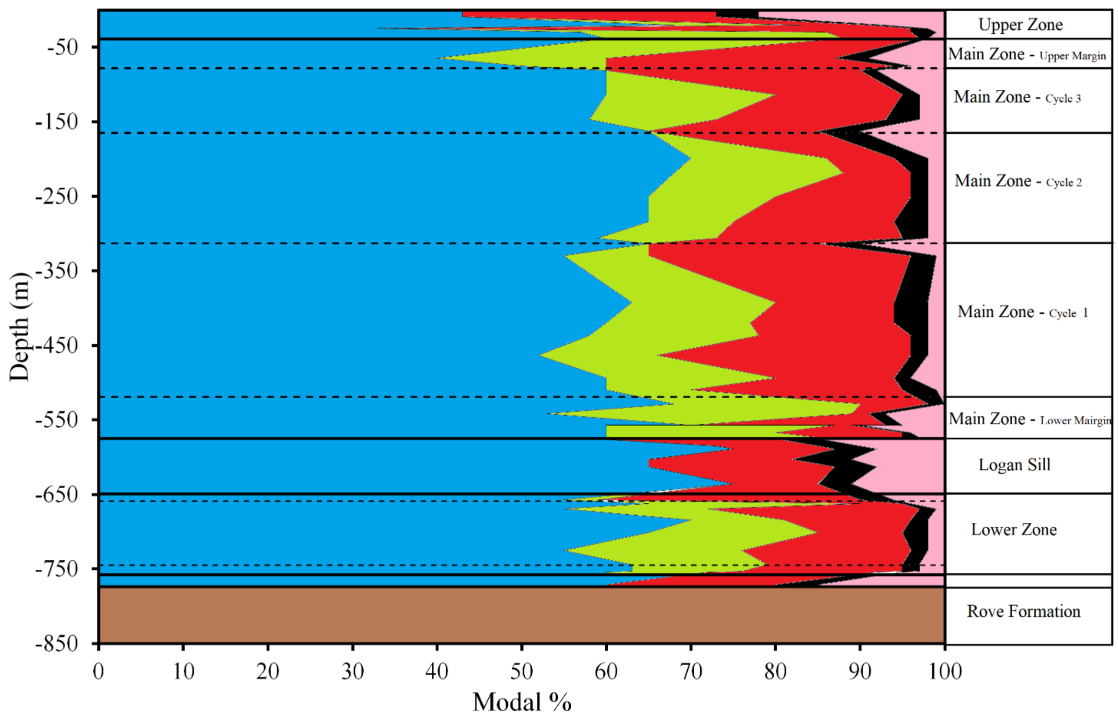

Figure 5.2. Downhole mineral modal abundance variations for the CLG drill core samples. Blue=plagioclase, green=olivine, red=clinopyroxene, black=Fe-Ti oxide, pink=accessory minerals, dashed lines represent subzone boundaries.

Each individual cycle displays a bottom-up fractionation, which is suggested by an upward increase of incompatible trace element, TiO_2, Na_2O, and K_2O concentrations and decrease of MgO and Al_2O_3 (Figs. 4.30 and 4.33). Compared to each other, the cycles are also progressively more texturally and geochemically evolved, with decreasing depth. The uppermost cycle has the highest abundance of quartz and K-feldspar as well as the highest concentration of incompatible trace elements (Fig. 4.33). This suggests that the individual magma pulses could have been of slightly different compositions upon emplacement or there was some interaction between the cycles, such as evolved magma migrating upward from the underlying cycle.

The petrographic, geochemical, and mineral composition data suggests that fractionation of the magmas was somewhat limited, in that, Fe_2O_3 and CaO concentrations remain fairly constant, olivine Fo contents have a narrow range from $Fo_{49.1}$ to $Fo_{57.0}$ (although they do decrease upward), and clinopyroxene and Fe-Ti oxides not being cumulus minerals, throughout the interior (Fig. 5.3). The lack of extensive differentiation of the magma could suggest that the magma chamber was an open system and underwent magma replenishment combined with a rapid rate of cooling after each successive magma pulse. Differentiated magma could have also been expelled from the magma chamber.

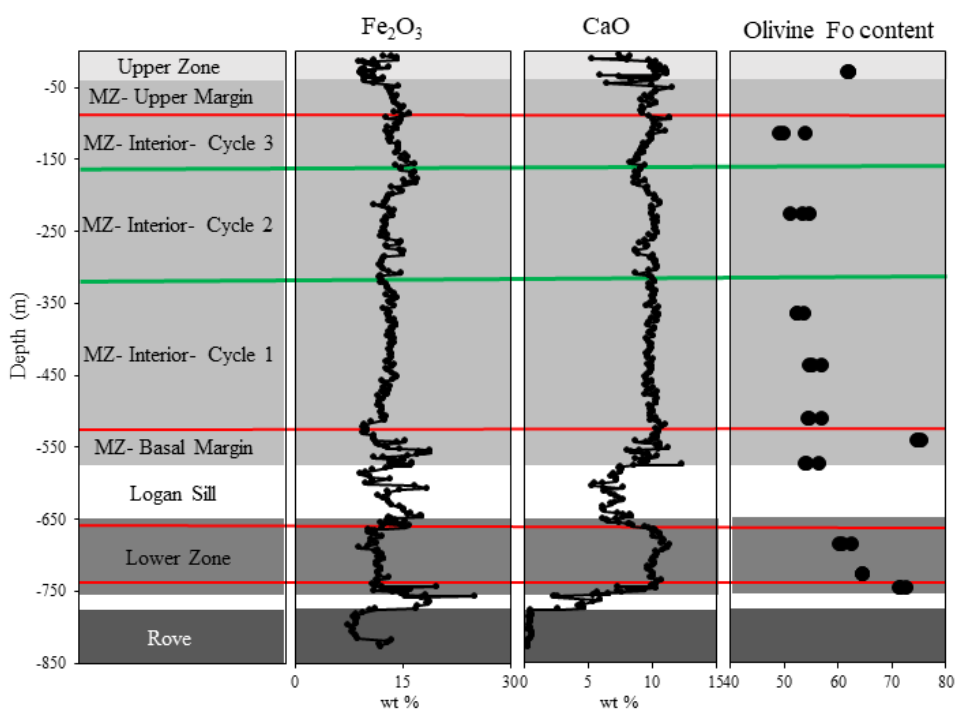

Figure 5.3. Downhole variation of Fe_2O_3, CaO and olivine Fo content for the CLG. Red lines represent marginal borders, green lines represent interior subzone borders.

A geochemical reversal of trends marks the lower border of the upper margin subzone which occurs at 78 m depth. Geochemical and petrographic data suggests that this subzone has an overall top to bottom fractionation sequence. Concentrations of the incompatible trace elements, TiO_2, Fe_2O_3, Na_2O, and P_2O_5 decrease uphole whereas the concentrations of MgO increases (Figs. 4.30 and 4.33). Petrographically there is no difference between this subzone and the underlying interior subzones with clinopyroxene occurring as an intercumulus mineral and plagioclase and olivine as cumulus minerals. Within this subzone the clinopyroxene modal percent decreases upward while olivine increases, resulting in an upward transition from gabbro to troctolite (Fig. 5.2).

An abrupt increase of Al_2O_3, MgO, and Ni, and a decrease of incompatible trace elements as well as the presence of Cr-spinel, sulphide, and sedimentary xenolith bearing rocks marks the border between the Main Zone and Upper Zone. Modal and textual layering within this zone suggests that this zone experienced thermal fluctuation during crystallization, with abrupt changes in grain size and modal percentages of minerals, perhaps as a result of localized re-melting of the rocks within the zone (Huppert and Sparks, 1989). The Upper Zone may have crystallized from a more primitive magma than that of the interior of the Main Zone as suggested by the olivine Fo content as well as higher clinopyroxene Mg# in the Upper Zone than the underlying Main Zone (Fig. 4.43; Fig. 4.45). The geochemical similarity to the basal margin subzone of the Main Zone (i.e. largely low incompatible trace element concentrations and high Al_2O_3 and Ni concentrations) suggests that they are related to each other. As previously mentioned, the basal margin subzone likely crystallized from a more primitive, Cr-spinel saturated magma than the interior of the Main Zone. It is likely that early on in the emplacement of the CLG, the basal margin of the Main Zone and the Upper Zone were connected to each other and that the successive magma pulses of the more evolved composition separated them through a process of inflation, similar to the intrusions described by Miller et al. (2011) and Owen-Smith and Ashwal (2015). There are several notable differences between the Main Zone basal margin and the Upper Zone which can be attributed largely to contamination and assimilation of the Rove Formation (discussed separately in a following subsection).

Overall the geochemistry and petrography suggest that CLG formed in an open system that had frequent replenishment of magma pulses as well as possible removal of differentiated magma. An overall bottom up directed fractionation of the magma is observed texturally as well geochemically in the Lower Zone and Main Zone, however the top 78 m of the Main Zone fractionated top to bottom. Fractionation did not result in significant magma differentiation as plagioclase ± olivine ± Cr-spinel are the only cumulus minerals, supporting the open-system model.

5.2.2 Mount Mollie Dyke

The MMD is comprised of varying proportions of plagioclase, olivine, and clinopyroxene; forming a range of rock types, including troctolite, augite troctolite, olivine gabbro, and gabbro (Fig. 4.22). The MMD can be divided in to two zones; Upper Zone and Main Zone. The Main Zone can be subdivided into an upper and lower sequence based on geochemical and petrographic observations. The lower sequence of the Main Zone also hosts a 24 m interval containing several 1 to 2 m wide pegmatitic layers (Fig. 5.4).

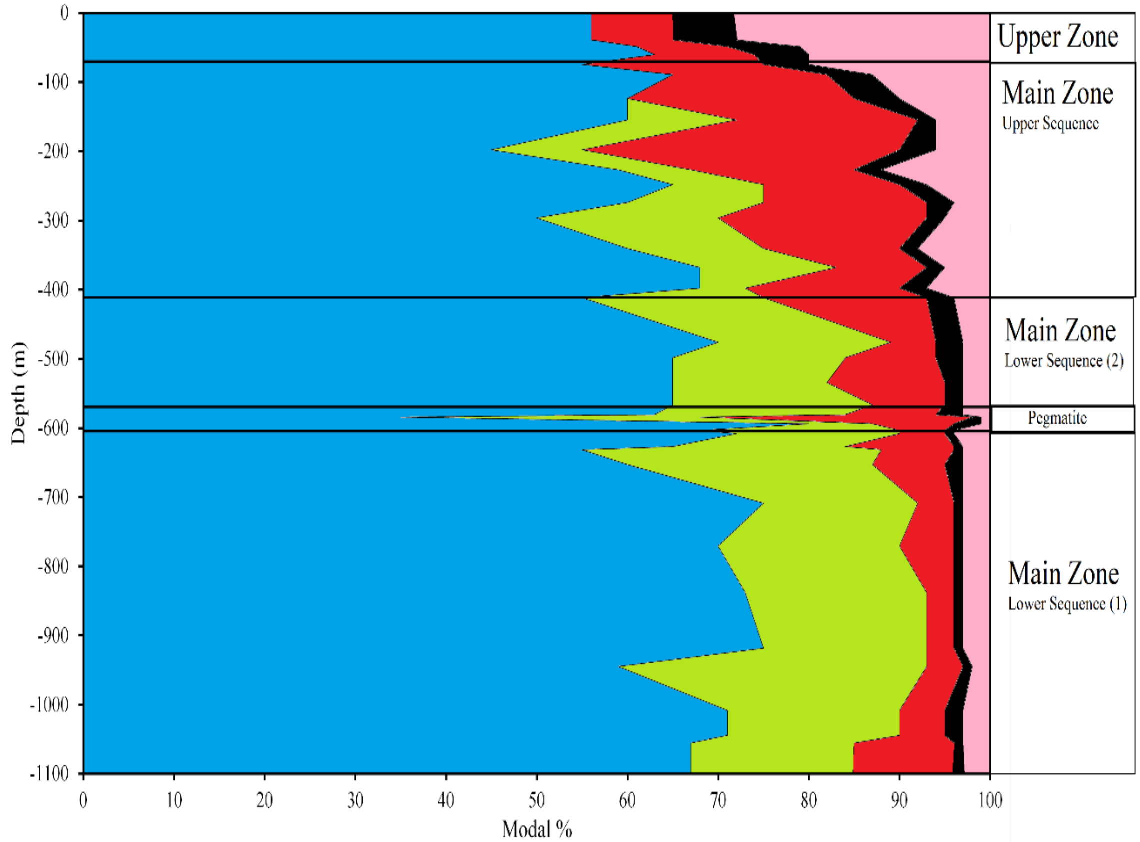

Figure 5.4. Downhole mineral modal abundance variations for the MMD drill core samples. Blue=plagioclase, green=olivine, red=clinopyroxene, black=Fe-Ti oxide, pink=accessory minerals.

The vertical thickness of the MMD as well as its relation to the footwall is unknown because of the lack of a lower contact in the drill core. The lack of extensive drilling or geophysical data means that the geometry of the MMD at depth is unclear. Regardless, the study of the ~1095 m long drill core from this study has revealed several features typical of a fractionating intrusive body.

The lower sequence of the Main Zone is predominantly augite troctolite (Fig. 4.22). The plagioclase and olivine are cumulus minerals and using the nomenclature of Irvine

(1982) are mesocumulates. Clinopyroxene primarily has a subophitic habit but locally develops a coarse-grained optically continuous ophitic habit. The variability of the modal proportions of plagioclase and olivine are the likely result of localized redistribution by way of crystal settling/floatation or perhaps convective currents (Chalokwu et al., 1993; Chalokwu et al., 1996; Monjoie et al., 2005; Hoshide et al., 2006; Fazlnia et al. 2013). This variability is seen not only in the petrography but also geochemically in the downhole profiles of MgO, Fe_2O_3, Al_2O_3, and CaO concentrations (Fig. 5.5). Samples that have high modal proportions of olivine have higher concentrations of MgO and Fe_2O_3 and lower concentrations of Al_2O_3 and CaO (Figs. 5.4 and 5.5). The result of this mineral redistribution is a sawtooth pattern moving uphole for major elements.

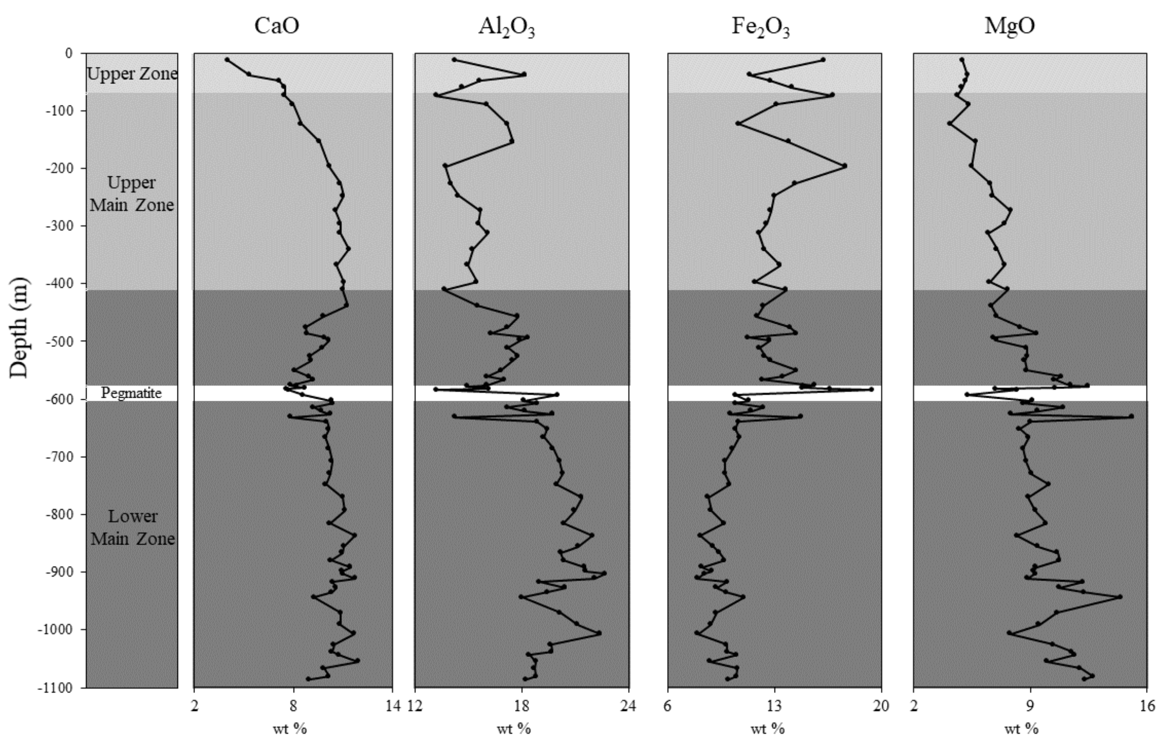

Figure 5.5. Downhole geochemical profiles for the MMD.

An overall bottom up directed fractionation of the magma is suggested by the upward increase in SiO_2, TiO_2, Fe_2O_3, Na_2O, P_2O_5, and incompatible trace element concentrations and a decrease in the Al_2O_3, MgO, CaO, and Ni concentrations (Figs. 4.35 and 4.39). Mineral composition is also an indicator of fractionation as olivine Fo content, clinopyroxene Mg#, and plagioclase An content all decrease during fractionation (Deer et al., 1992). The mineral composition downhole profiles of olivine, clinopyroxene, and plagioclase do not show progressive fractionation for the MMD. Forsterite contents of olivine, Mg# of clinopyroxene, and An content of plagioclase are broadly constant below the pegmatite segregations (Fig. 5.6).

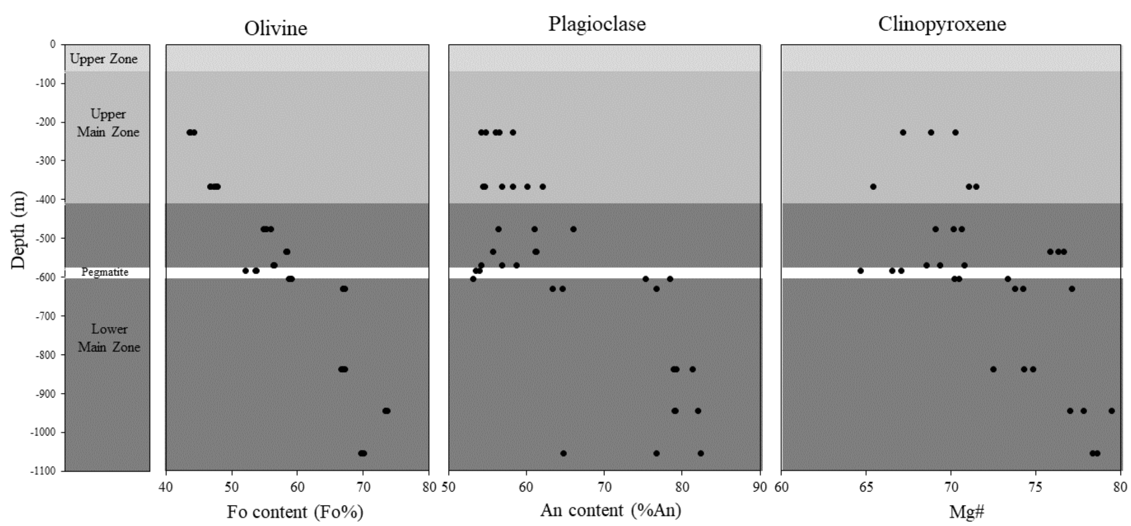

Figure 5.6. Downhole mineral composition profiles for the MMD.

Around the pegmatitic interval there is a decrease in olivine Fo content, clinopyroxene Mg#, and plagioclase An content which then remains somewhat constant for the remainder of the subzone. One sample had anomalously high clinopyroxene Mg# above the pegmatite, suggesting that clinopyroxene fractionated at a different rate than olivine and plagioclase. This could be due to clinopyroxene being an intercumulus mineral in the lower sequence, whereas olivine and plagioclase are cumulus, resulting in a slightly different differentiation process. This somewhat bimodal distribution of high Fo content, Mg#, and An content below the pegmatite and mostly lower values above within the same subzone suggests that there were two-stages of crystallization. It also suggests that the primary direction of cooling was not bottom up. It is possible that cooling was more laterally directed from the walls of the dyke, which would explain the observed surface expression of the MMD with a highly evolved granophyric and dioritic core of the dyke and gabbro and olivine gabbro along the edges (Fig. 5.7; Geul, 1973; Smith and Sutcliffe, 1989).

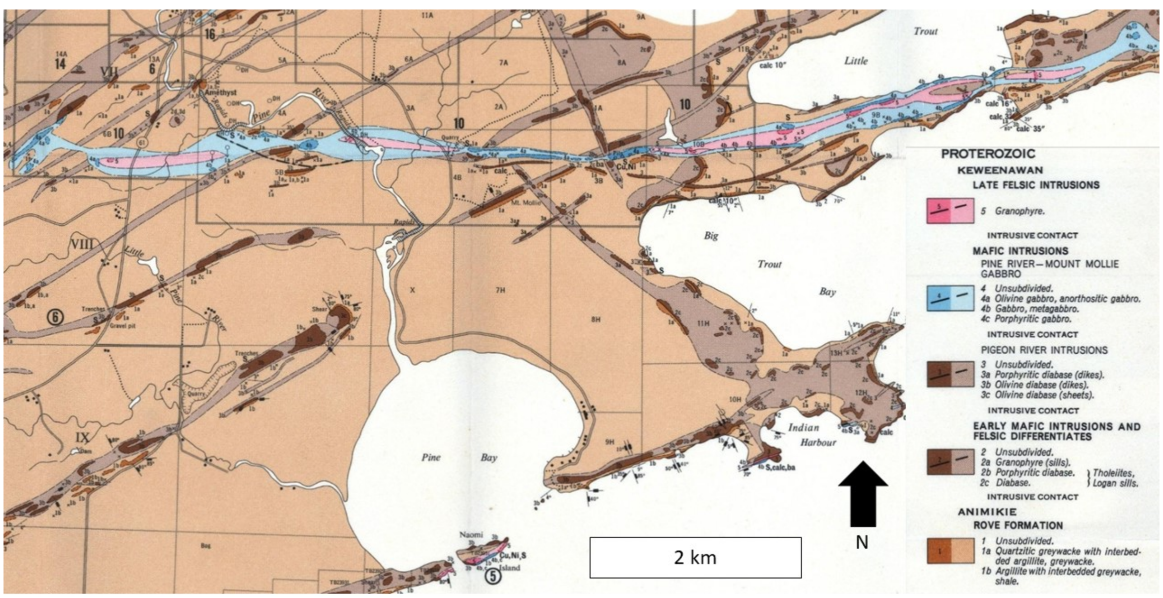

Figure 5.7. Geological map of a MMD segment, displaying compositional zoning, modified from (Geul, 1973).

Without knowing the extent of the MMD at depth, it is impossible to determine if the pegmatitic segregations are podiform or in the form of sheets, both of which are found in other layered intrusions, such as Skaergaard (Larsen and Brooks, 1994). Geochemistry and mineral composition reveal that the pegmatite is more evolved than the Lower Main Zone that it is bounded by. Olivine Fo content, clinopyroxene Mg#, and plagioclase An contents are all lower in the pegmatite sample than in the samples directly above and below (Fig.5.6). The concentrations of TiO_2, Fe_2O_3, K_2O, Na_2O, and P_2O_5, and incompatible trace elements are higher in the pegmatitic samples (Figs. 4.35 and 4.39). These pegmatites were likely formed as a result of localized areas rich in volatiles (Sonnenthal, 1992). The volatiles were likely of magmatic origin rather than of the country rock, as there are no geochemical indicators of contamination (i.e., Th enrichment, increased La/Sm_n, etc…).

The Upper Main Zone (411 to 74 m depth) is characterized by an abrupt increase in Sc concentration and decrease in Al_2O_3 compared to the lower sequence (Figs. 4.35 and 4.39). The modal percentage of clinopyroxene not only increases but also change to a granular habit with anhedral to subhedral grains. This suggests that the that the magma reached clinopyroxene saturation to produce a plagioclase + olivine + clinopyroxene cumulate. While the clinopyroxene Mg# and An content of the plagioclase remain constant in the two samples analysed, the Fo content of the olivine decreases upward, implying an overall bottom up fractionation of the magma. This bottom up fractionation is also suggested by the upward decreasing concentrations of MgO, CaO, and Al_2O_3 and increasing concentrations of P_2O_5 and incompatible trace elements (Figs. 4.35 and 4.39). A localized spiked increase, at 197 m depth, of TiO_2, Fe_2O_3, and V concentrations could imply that Fe-Ti oxides locally becomes a cumulate phase (Fig. 4.35; Fig 4.39). Olivine is no longer present in the mineral assemblage above 89 m depth, shortly after the arrival of cumulus Fe-Ti oxides. The disappearance of olivine after the arrival of cumulus Fe-Ti oxides has also been observed in the Skaergaard intrusion (Naslund, 1983).

The Upper Zone of the MMD is characterized by an evolved assemblage of quartz ferrodiorite with high modal abundance of accessory minerals (i.e., quartz, K-feldspar, biotite, amphibole, chlorite, apatite, orthopyroxene). The end-product of extensive fractionation of the MMD magma resulted in the crystallization of the rocks of the Upper Zone.

The geochemical and mineralogical features of the MMD can be explained by having formed in a closed system with only one pulse of magma, that subsequently underwent extensive fractionation and differentiation. Although there was a likely a significant laterally directed crystallization component, overall there is a bottom up directed fractionation trend with high olivine Fo content, plagioclase An content, clinopyroxene Mg#, MgO and Al_2O_3 concentrations at the bottom of the drill core and lower values at the top. Texturally the rocks become more evolved with a cumulate sequence of olivine + plagioclase → olivine + plagioclase + clinopyroxene → olivine + plagioclase + clinopyroxene + Fe-Ti oxide → plagioclase + clinopyroxene + Fe-Ti oxide with the Upper Zone representing a final highly evolved quartz rich magma. Geochemistry and mineral composition of drill core samples suggest the fractionation is not progressive implying that cooling was likely more laterally driven than vertically driven.

5.3 CONTAMINATION

The geochemical characteristics of the MMD and CLG can be used to evaluate the role of crustal contamination during emplacement. During the ascent of the magma that ultimately formed the CLG and MMD, there was potential for contamination from Archean crust, Paleoprotozoic crust, and subcontinental lithospheric mantle (SCLM). The Archean crust was likely from the Wawa subprovince, whereas the Paleoproterozoic crust was comprised largely of the Gunflint and Rove Formations. Continental crust is typically enriched in highly incompatible trace elements (e.g., Th and LREE) relative to moderately incompatible trace elements (e.g., Zr, Hf, MREE) but depleted in Nb relative to Th (Lesher et al., 2001). Both the Rove Formation and the granitoid rocks of the Wawa Subprovince have these geochemical features (Fig. 5.8). The composition of the SCLM at the time of the MCR is unknown as no xenoliths have been reported from any MCR related rocks, but previous studies have suggested that it has a high MgO concentration, is LREE enriched, and has a negative Nb anomaly (Shirey et al., 1994; Hollings et al., 2007a). Plots of La/Sm_n against Th/Yb and Nb/Nb* for samples from the CLG and MMD drill cores and surface samples suggest that there was both localized and widespread contamination (Fig. 5.9).

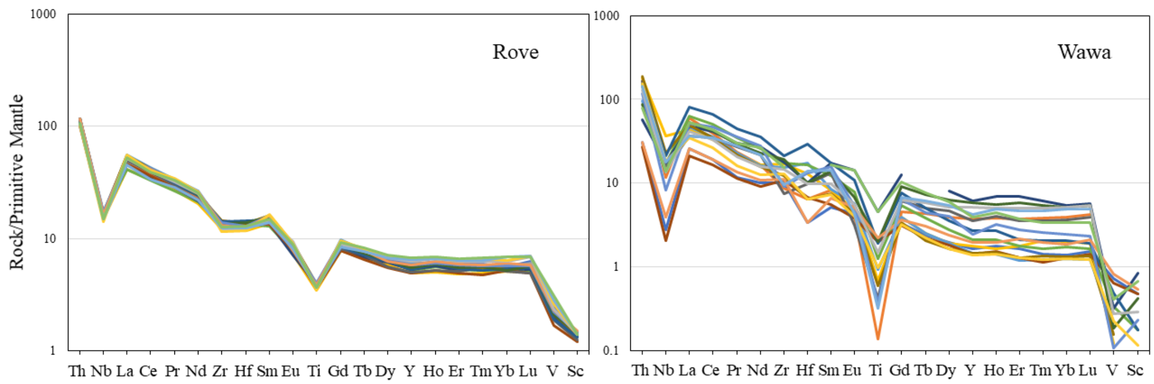

Figure 5.8. Primitive mantle normalized diagram of the Rove Formation, data from the CLG drill core, and Wawa Subprovince granitoid rocks. Data from Sage et al. (1996). Normalizing values from Sun and McDonough (1989).

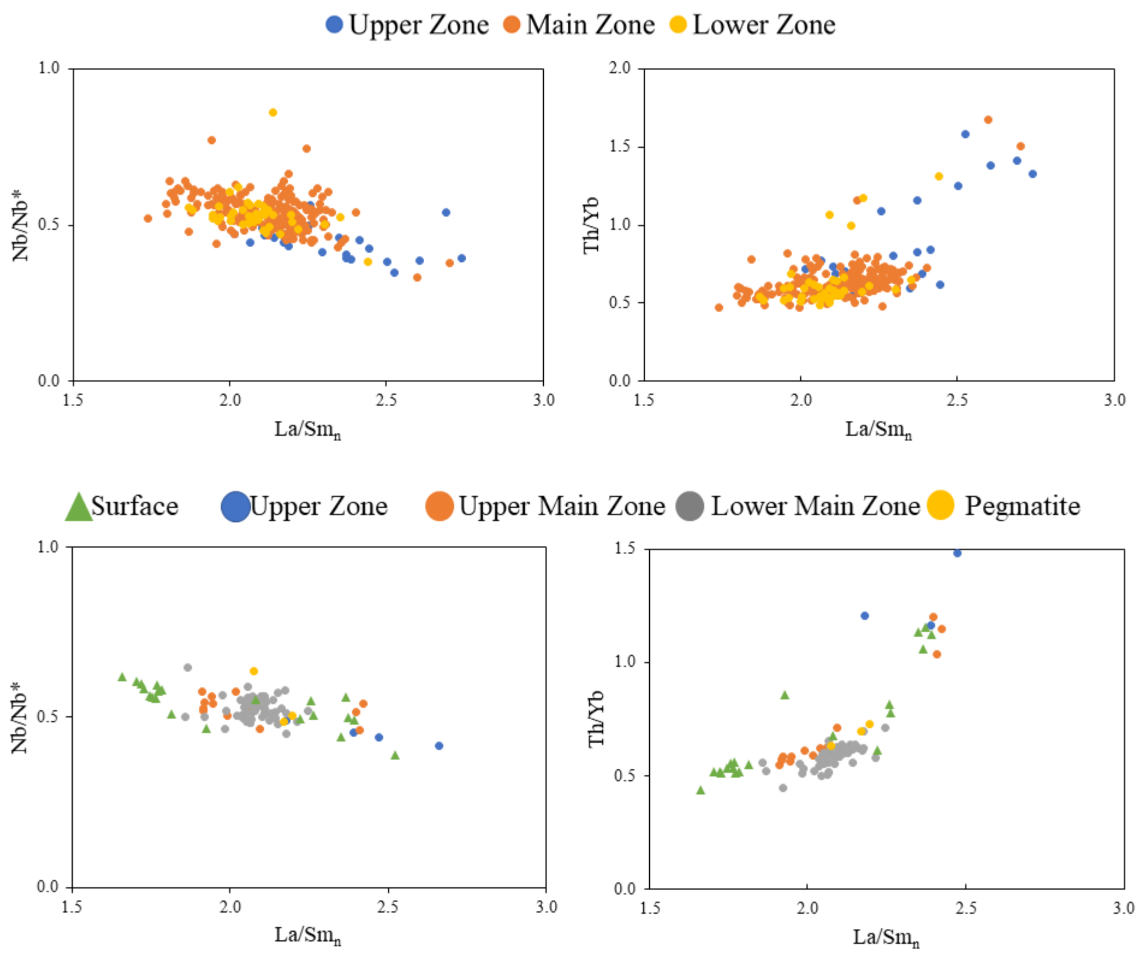

Figure 5.9. La/Sm$_n$ values vs Nb/Nb* and Th/Yb for the CLG (top) and MMD (bottom).

Localized contamination is suggested by the fact that only a limited number of samples in both the CLG and MMD having elevated La/Sm_n and Th/Yb values. Within the CLG these samples are primarily from the Upper Zone. As previously mentioned sedimentary xenoliths, likely of Rove Formation origin, were found in the Upper Zone, suggesting partial assimilation of the country rock. The two samples from the Main Zone that also have crustal contamination signatures are located within 10 m of the Upper Zone contact. The Lower Zone sample with the highest La/Sm_n and Th/Yb values is located near the upper contact with the Logan Sill. Since the Logan Sill does not have elevated La/Sm_n and Th/Yb values, contamination of the magma must have occurred during ascent of the magma rather than during emplacement. The likely source of this localized contamination is the Rove Formation as suggested by the $\delta^{34}S$ values obtained from sulphides in this area, (discussed further in a following subsection). Since this contamination signature is not widespread, only the leading edge of the magma was likely contaminated by the Rove Formation during ascent. The MMD has similar localized contamination signatures. Three out of the four samples from the Upper Zone of the MMD display noticeably increased La/Sm_n and Th/Yb values compared to most samples elsewhere in the drill hole (Fig. 5.9). Three samples from the Upper Main Zone have the same contamination signatures. These samples are the stratigraphically highest samples of the subzone. As previously mentioned there was likely an inward and upward directed crystallization front in the MMD, so the uppermost samples likely remained molten longer which would result in more interaction with the country rock, thus more opportunity for country rock assimilation.

The surface samples of the MMD display a wide range of La/Sm_n and Th/Yb values. Some samples have clear crustal contamination signatures whereas there is a cluster of samples that have lower La/Sm_n values than the drill core samples. This implies one of two scenarios. The first scenario is that these samples have experienced less contamination than the drill core samples which have slightly higher values due to widespread contamination. The second scenario is that the surface samples are from a completely different source with a slightly lower La/Sm_n.

The granophyre field sample with high trace element concentrations, the highest La/Sm_n, the highest negative Nb anomaly, pronounced negative Ti and V anomalies, and high SiO_2, likely crystallized from a highly crustally contaminated sample. These characteristics are consistent with a large degree of melting and assimilating silica-rich country rock, most likely from the Rove Formation.

A plume model has generally been accepted as the cause for the MCR related magmatism (Hutchinson et al., 1990; Nicholson and Shirey, 1990; Hollings et al., 2007a; Hollings et al., 2012). The consistent presence of a negative Nb anomaly is not expected for the rocks of the CLG and MMD, as plume generated igneous rocks would closely resemble an ocean island basalt (OIB) composition (Nicholson et al., 1997; Hollings et al., 2007a). This suggests widespread crustal contamination of the CLG and MMD magmas. Since the three possible sources of contamination (i.e., Paleoproterozoic crust, Archean crust, and SCLM) all have negative Nb anomalies, determining what was the cause of the Nb anomaly in the CLG and MMD rocks is challenging. Previous studies have attempted to differentiate the extent of deep contamination and shallow contamination of MCR rocks using radiogenic and stable isotopes (i.e. Re-Os, Sm-Nd, Rb-Sr, Pb-Pb, O, and S) and found that contamination is often complex and can occur at various depths (e.g., Shirey et al., 1994; Hollings et al. 2007b; Hollings et al., 2012; Ding et al., 2012). Hollings et al. (2012) in a study of the sills and dykes in the Logan Basin region, suggested pervasive interaction with the SCLM as well as further contamination during emplacement by both Archean and Protozoic rocks. Further study of the CLG and MMD using isotopes analysis is necessary to characterize the crustal contamination history of the magmas.

5.4 SULPHUR HISTORY

The addition of externally derived sulphur is often cited as being an important process in the formation of Ni-Cu-PGE deposits (Naldrett, 2010; Robertson et al., 2015; and references therein). To form a Ni-Cu-PGE deposit the sulphur content must exceed the point of saturation required to form an immiscible sulphide liquid into which the Ni, Cu, and PGE may partition into. Sulphur saturation in a magma can be reached by fractionation, depressurization, and/or magma mixing; however, significant addition of sulphur from surrounding crustal rocks either during ascent or emplacement is thought to be the most efficient (Holwell et al., 2014; and references therein). Analysis of sulphur isotopes is typically the most widely used method to determine whether crustal derived sulphur was incorporated into the magma chamber (Hughes et al., 2015), and if the sulphur isotope signature of the country rocks is dissimilar to that of mantle-derived sulphur ($\delta^{34}S = 0 \pm 2‰$; Ripley and Li, 2003). Previous studies of the sulphur isotope characteristics of the Rove Formation have found a range of $\delta^{34}S$ values from ~0 to 30‰ likely due to extensive bacterial sulphate reduction at the time of deposition (Ripley and Al-Jassar, 1987; Arcuri et al., 1998; Poulton et al., 2010; Pufahl et al., 2010).

$\delta^{34}S$ values of sulphides (i.e. +4.0 to +21.0‰) from the CLG strongly suggest that sulphur derived from the Rove Formation was assimilated into the magma, as the values are consistently above mantle values (Fig. 4.42). Ripley and Li (2003) proposed a two-component mixing model to quantify the amount of sulphur that was externally derived in an intrusion; however, due to the large variation of $\delta^{34}S$ values in the Rove Formation this is not a feasible approach for the CLG. The highly variable $\delta^{34}S$ obtained in this study is likely due to the magma incorporating crustal sulphur that was also highly variable. To put it simply, the same $\delta^{34}S$ value can either be obtained by a low degree of contamination by a high $\delta^{34}S$ value contaminant or a high degree of contamination by a low $\delta^{34}S$ value contaminant. Having said that, the highest $\delta^{34}S$ obtained in this study has a value of +21.0‰, which strongly suggests that the CLG interacted extensively with the Rove Formation. The two methods by which sulphur can be liberated from the surrounding country rock are; (1) a diffusive and advective transport of sulphurous fluids by thermal breakdown of sulphide or sulphate-bearing minerals during devolatilization or (2) assimilating and melting of country rock xenoliths (Robertson et al., 2015). Both processes have been suggested to account for the addition of sulphur in other MCR mineralized intrusions (e.g. Ripley et al., 2007; Robertson et al., 2015). The presence of localized xenoliths suggest assimilation occurred during the evolution of the CLG, whereas the role of devolatilization can not be assessed because no direct evidence is present, however, it is plausible that combination of the two processes took place during the ascent of the CLG magma.

Sulphur/Se ratios can be utilized as an additional line of evidence for the addition of externally derived sulphur. The S/Se ratio of the mantle has been estimated to be between 2850 and 4350 (Eckstrand and Hulbert, 1987). Consequently S/Se ratios that are greater than mantle values are interpreted to reflect the addition of sulphur to the magma and conversely lower values suggest a loss of sulphur (Maier and Barnes, 2010). Samples from the basal and upper margins of the Lower Zone have S/Se values above mantle values as well as a few samples from the Upper Zone (Fig. 5.10). This suggests that sulphur has been added to the magma. Interestingly the sulphide mineral bearing rocks of the basal margin subzone of the Main Zone have S/Se values that are within mantle range. This seemingly contradicts the $\delta^{34}S$ values that were obtained from sulphides in this subzone that strongly suggested a significant amount of sulphur was derived from the Rove Formation. Queffurus and Barnes (2015) have suggested that the interaction and equilibration of sulphide melt with silicate melt will increase the Se content of the sulphides (i.e. lowering the S/Se value) and dilute the contamination signature. Taking into consideration the higher than mantle $\delta^{34}S$ values for sulphides in the basal margin of the Main Zone, the sulphides in the basal margin likely originally also had higher than mantle S/Se values. Subsequently upon emplacement the sulphides likely achieved equilibrium with a large amount of silicate melt, whereas sulphides in the Upper and Lower Zone did not. Considering the much lower than mantle S/Se values found in the interior subzones (suggesting sulphur loss), it is possible that the sulphides present in the basal margin were derived via gravitational settling of immiscible sulphide droplets that originated in the interior of the CLG and scavenged Se from the surrounding silicate melt during descent.

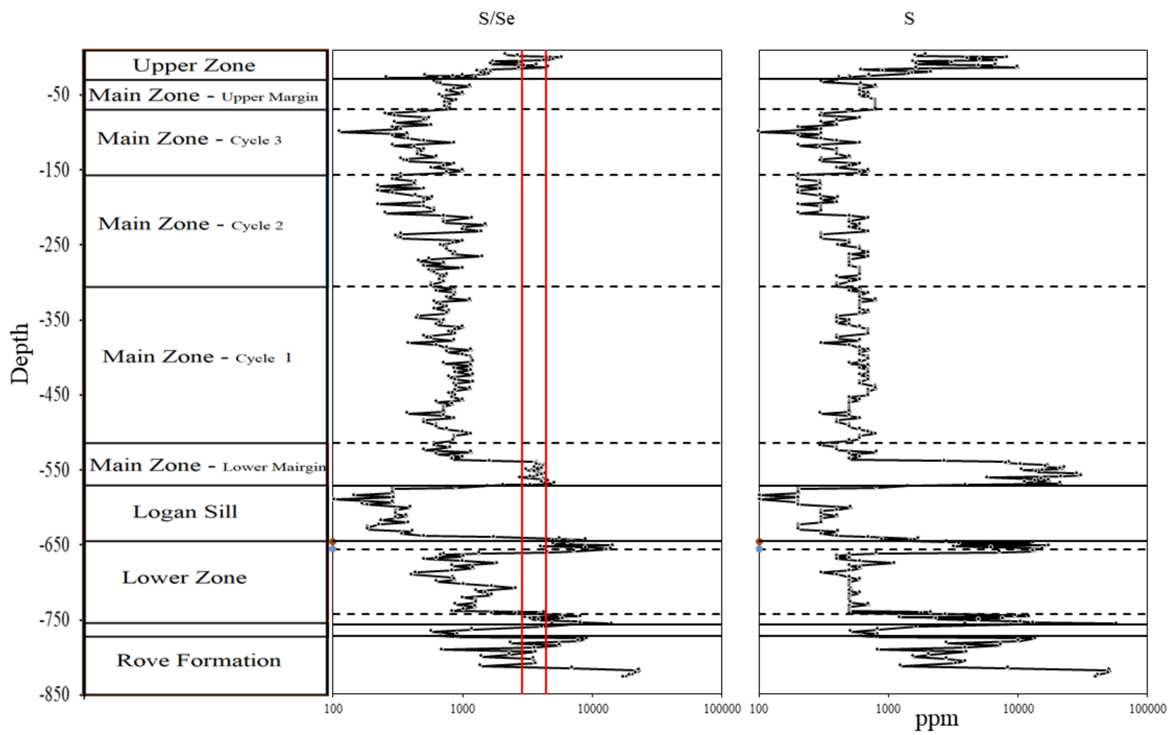

Figure 5.10. Downhole profile of S/Se values and S concentrations from the CLG, red lines represent mantle value range, values from Eckstrand and Hulbert (1987). Solid black lines represent Zone boundaries, dashed lines represent subzone boundaries.

If the basal margin subzone of the Main Zone sulphides equilibrated with a larger amount of silicate liquid to generate mantle like S/Se values, the concentration of chalcophile elements should also be enriched. The sulphides in the basal margin subzone of the Main Zone are enriched in the chalcophile elements, likely due to equilibration at a relatively higher silicate to sulfide mass ratios (i.e., R factor; Campbell and Naldrett, 1979; Fig. 5.11). Samples from the Lower Zone do not display an enrichment of the chalcophile elements, as the highest sulphur concentration in the CLG is located in the Lower Zone but has significantly lower concentrations of the chalcophile elements compared to the Main Zone.

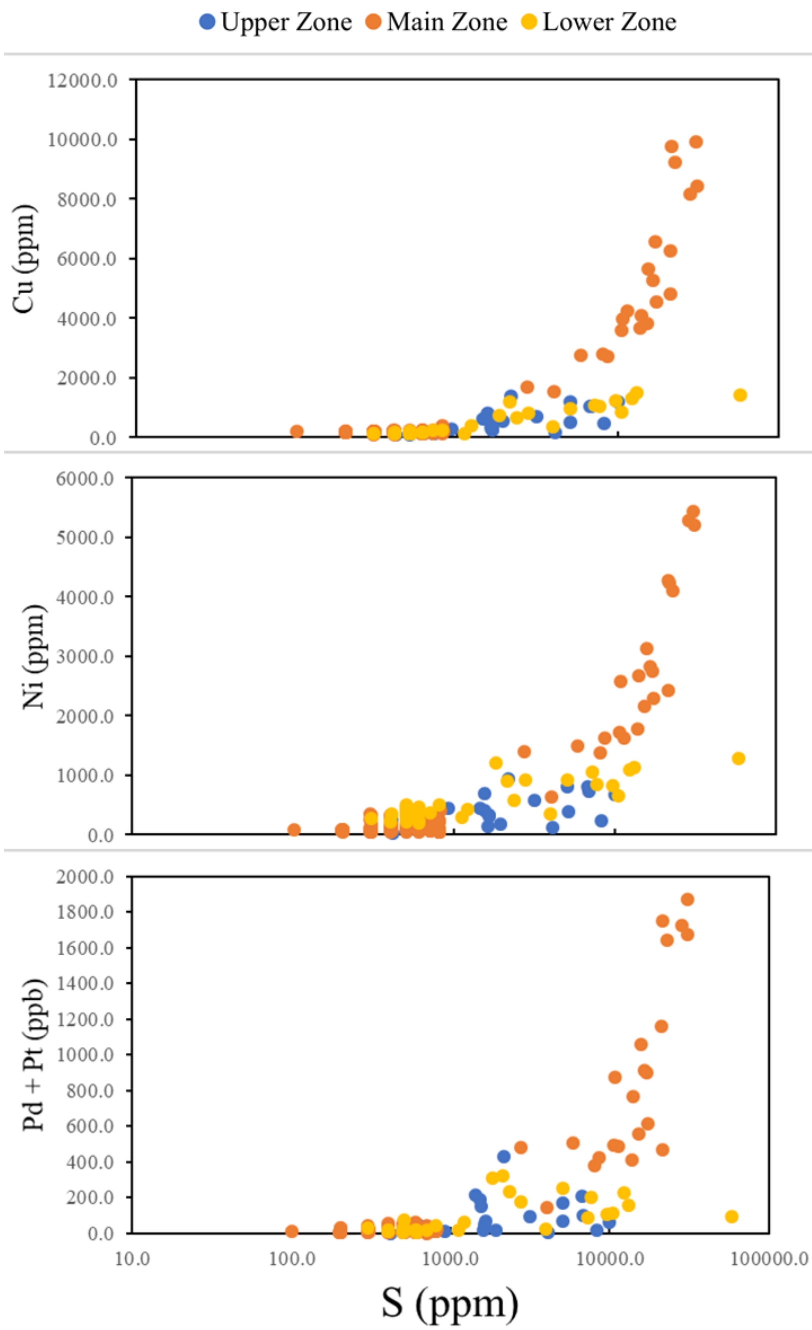

Figure 5.11. Sulphur concentrations vs. chalcophile element concentrations from samples of the CLG.

An early saturation of sulphur is thought to be needed to generate a Ni-Cu-PGE deposit because olivine is one of, if not the first mineral to crystallize and will sequester a significant proportion of the Ni in the magma (Ripley and Li, 2013). Sulphur saturation prior to the emplacement of the CLG magma is suggested by the presence of visible sulphides and S concentrations up to 1.7 wt% in the upper margin of the Lower Zone. Since the Logan Sill is sulphur barren, the sulphide present in the upper margin was not sourced locally, and since sulphide is generally thought to sink due to gravitational segregation accumulation after emplacement is highly unlikely for the upper margin, so the high sulphur content must have been in the magma at the time of emplacement. The high $\delta^{34}S$ and S/Se values supports the premise that sulphur was liberated from the Rove Formation during the ascent of the magma and saturation was reached early in the crystallization of the magma.

The addition of sulphur from surrounding county rocks is not unique to the CLG as previous studies have shown that it also occurred in other MCR related intrusions. It is suggested that the Bovine Igneous Complex and the Eagle deposit had sulphur added from both Archean and Proterozoic country rocks (Ding et al., 2012; Donoghue et al., 2014). Similarly, Proterozoic crust has been proposed as the primary source of externally derived sulphur for intrusions in the Duluth Complex that are host to Cu-Ni-PGE mineralization (e.g. South Kawishiwi and Partridge River intrusions; Ripley, 2014). The Seagull intrusion in the Nipigon embayment and the Marathon deposit in the Coldwell Complex likely derived sulphur from Archean rocks (Kissin et al., 2007; Shahabi Far, 2016).

5.5 Parental Magma Compositions

As previously discussed, the CLG likely formed in an open system with multiple magma replenishment events. A more primitive magma likely formed the Upper Zone, Lower Zone, and the basal margin of the Main Zone, whereas a slightly more evolved magma likely formed the interior subzone of the Main Zone. Primitive mantle normalized multi-element diagrams can be used to evaluate whether these two magmas types were sourced from different fractions of the same parental magma or two separate parental magmas. Because fractionation does not effect the shape of the multi-element diagrams, only abundances; parallel patterns across all the subzones of the CLG suggest that all the magma pulses were sourced from a common parental magma (Fig. 5.12).

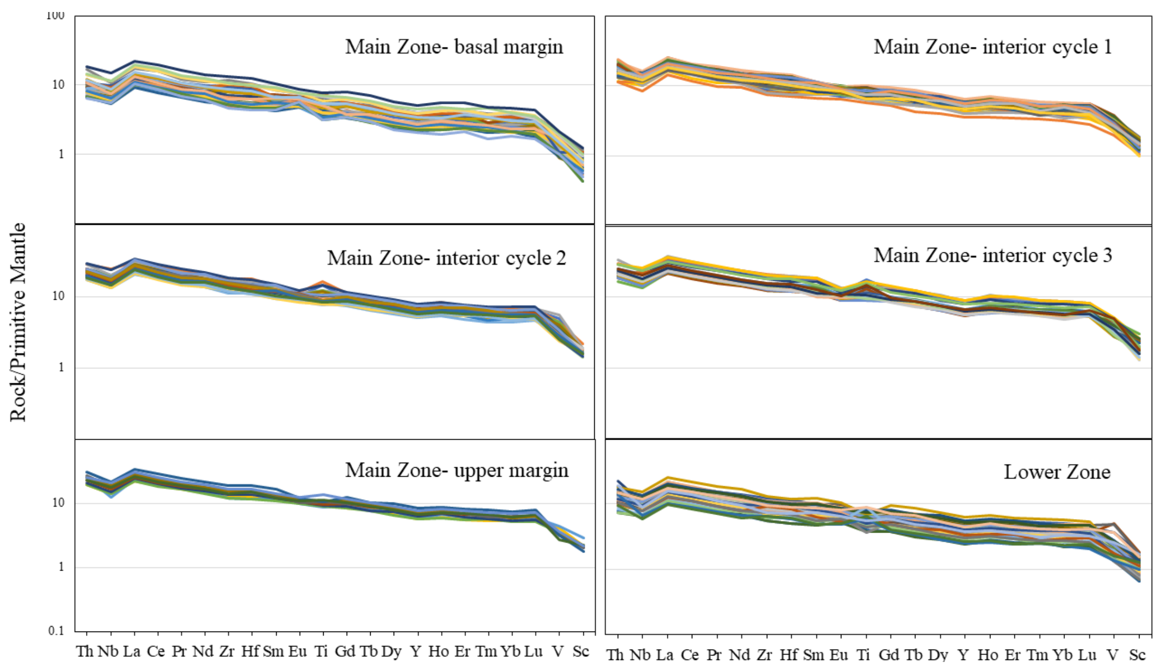

Figure 5.12. Primitive mantle normalized diagrams of representative samples of the CLG. Normalizing values from Sun and McDonough (1989).

Estimating the parental magma composition of layered intrusions is often difficult due to fractionation and cumulate effects that can substantially change the composition of the magma over time. Previous studies have used a variety of methods to overcome this challenge, including; (1) seeking samples that display a quenched texture indicating rapid cooling, located at chilled margins or spatially associated sills, dykes, or volcanic rocks (Godel et al., 2011; and references therein), (2) using mineral composition of cumulus minerals and back-calculating the composition of the parental magma, using mineral/melt partition coefficients (Godel et al., 2011; and references therein), (3) analysis of melt inclusions in primary Cr-Spinel grains (Spandler et al., 2000), or (4) calculating the bulk composition of the intrusion by the summation of whole-rock compositions throughout the stratigraphy (Wager, 1960; Wager and Brown, 1967; Morse, 1981; Nielsen, 2004). Each method has draw backs and limitations, for example; chilled margins may have been contaminated by the wall rocks or the chill zone may not be representative of the magma; cumulus minerals may re-equilibrate after crystallization affecting their mineral composition, or melt inclusions may not be preserved. Latypov (2015) recognized the shortcomings of the bulk composition method (i.e., incomplete sections, multiple magma pulses, presence of phenocrysts) and still concluded that it is the “best” approach for determining a parental magma composition.

The bulk composition was calculated by assuming each sample throughout the stratigraphy of both the CLG and MMD represented the composition half-way between the sample above and below and then dividing by the total stratigraphic height, similar to the methods used by Morse (1981), Naslund (1989), and Tegner (1997). The proposed parental magma compositions for the CLG and MMD are presented in Table 5.1.

Table 5.1. Estimated parental magma compositions of the CLG and MMD.

	SiO_2	TiO_2	Al_2O_3	Fe_2O_3	MnO	MgO	CaO	Na_2O	K_2O	P_2O_5	Mg#
CLG	47.55	1.77	16.78	13.07	0.17	7.53	9.84	2.57	0.54	0.19	0.56
MMD	47.58	1.49	17.77	11.69	0.16	8.21	9.95	2.38	0.63	0.15	0.60

The compositions are broadly similar, although the estimated parental magma for the CLG is slightly more evolved with higher concentrations of TiO_2, Fe_2O_3, Na_2O, and P_2O_5 and lower Al_2O_3, MgO, CaO, and Mg#. To test the estimated parental magma compositions, the concentrations were applied to the PELE program developed by Boudreau (1999), which is an adaptation of the MELTS thermodynamic phase equilibrium algorithm developed by Ghiorso and Sack (1995). Fractional crystallization models were run with; the quartz-fayalite-magnetite (QFM) and QFM -2 oxygen fugacity buffers; 1 wt% H_2O, and a pressure of 2 kbars, which has been suggested as reasonable for MCR related intrusions (Ripley and Li, 2013). Three out of the four fractional crystallization models produced a mineral paragenetic sequence of olivine → plagioclase → clinopyroxene → ilmenite → apatite → biotite → K-feldspar, with the fourth model reversing the order of arrival of biotite and K-feldspar (Figs. 5.13 and 5.14). This matches the observed cumulate stratigraphy of the MMD and CLG, however the CLG likely cooled and crystallized before the cumulus arrival of clinopyroxene. PELE also calculates the Fo content of olivine that was in equilibrium with the parental magma, which is consistently higher than the analysed Fo content in both the CLG and MMD (Table. 5.2). This suggests that either there was reequilibration due to a trapped liquid shift and/or this study failed to analyse the most primitive olivine in either the CLG or MMD (Barnes, 1986).

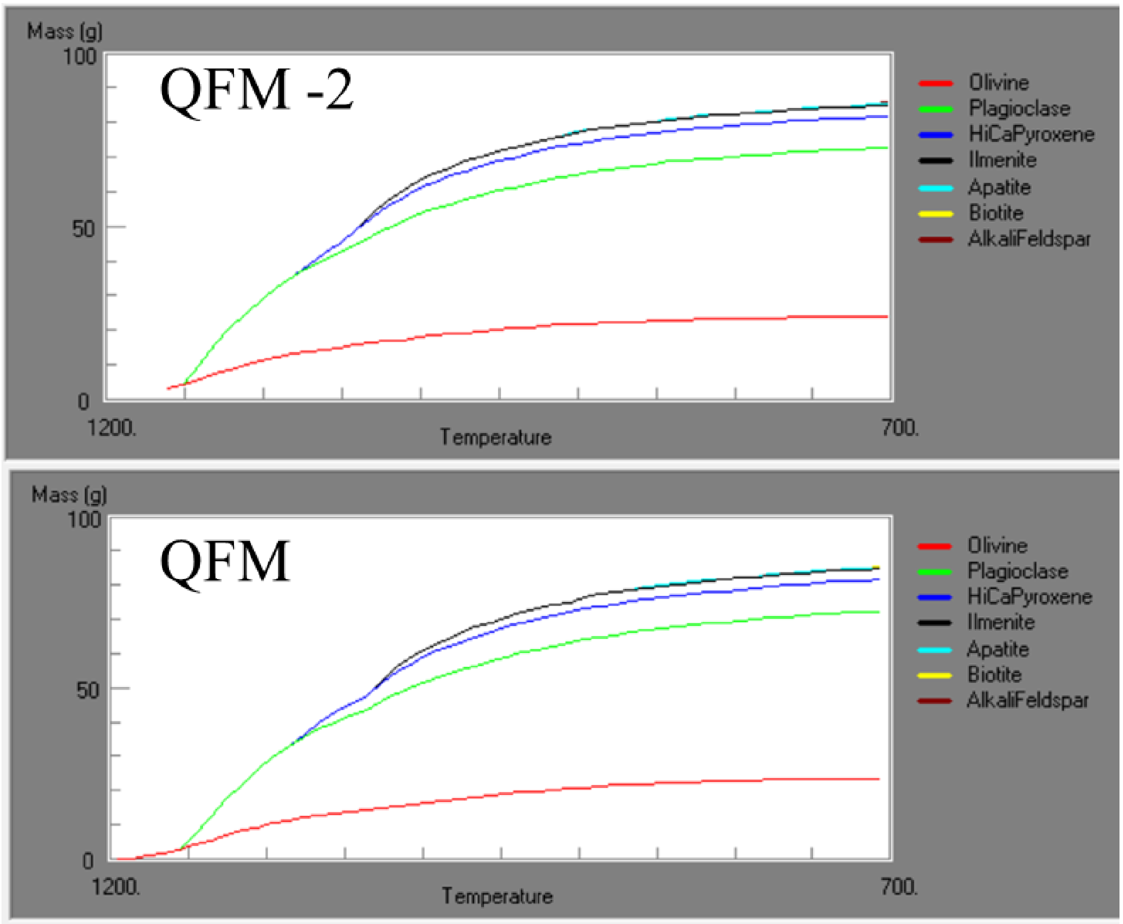

Figure 5.13. Modeled fractional crystallization mineral paragenesis of the estimated CLG parental magma with oxygen fugacities buffered at QFM and QFM -2. Modeling completed using the Pele program of Boudreau (1999).

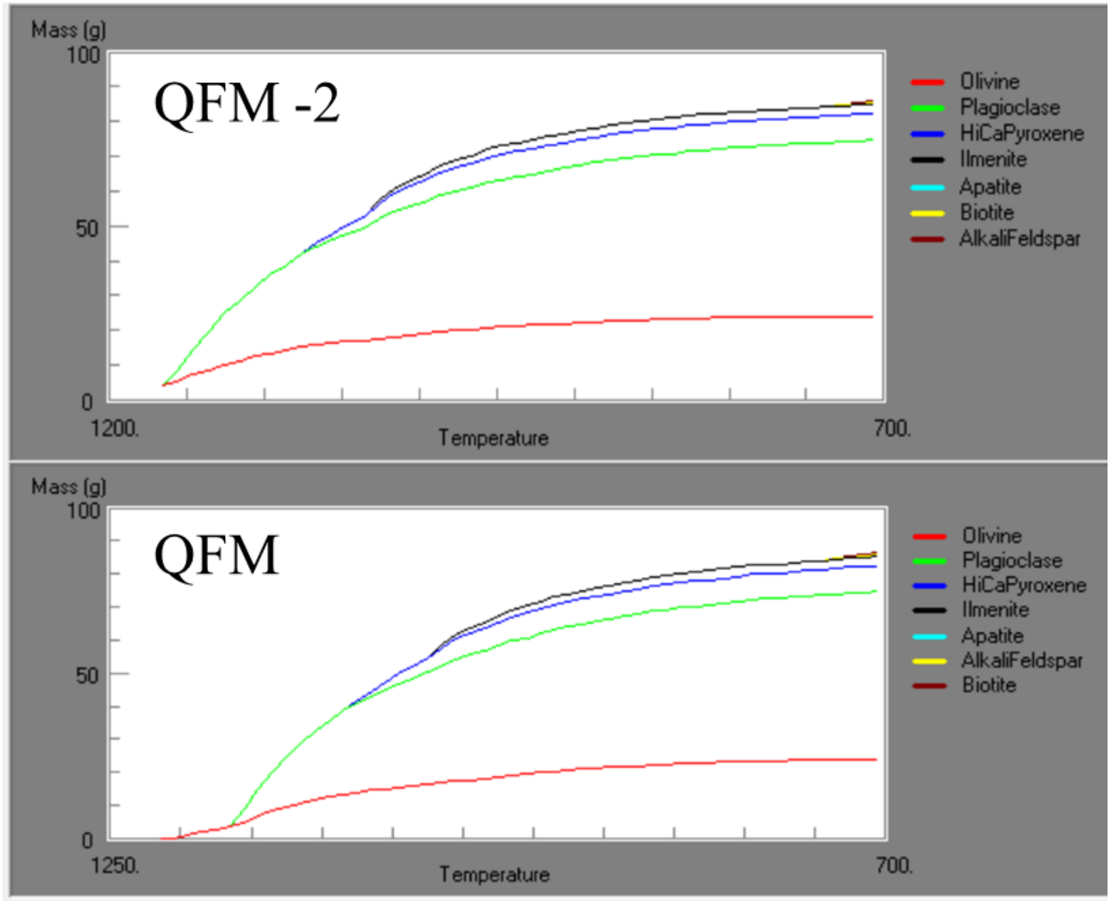

Figure 5.14. Modeled fractional crystallization mineral paragenesis of the estimated MMD parental magma with oxygen fugacities buffered at QFM and QFM -2. Modeling completed using the Pele program of Boudreau (1999).

Table 5.2. Analysed and predicted Fo content of olivine for the CLG and MMD.

Fo Content	CLG	MMD
Highest measured value	75.4	73.6
Modelled QFM -2 value	78.3	82.6
Modelled QFM value	81.2	84.1

5.6 CLG and MMD Comparison

Previous studies by Geul (1970, 1973) and Smith and Sutcliffe (1989) suggested the CLG and MMD are coeval based on their spatial relationship, similar orientation, and rock types. A shared N paleomagnetic polarity determined by Piispa et al. (2011) may also suggest a contemporaneous relationship. This hypothesis was called into question by the U-Pb age determination by Hollings et al. (2010) who determined an emplacement age of 1109 ± 6.3 Ma for the MMD and Heaman et al. (2007) who determined an emplacement age of 1099.6 ± 1.2 Ma for the CLG.

The detailed petrography of this study confirms that there are textural similarities between the CLG and MMD. Both bodies largely consist of plagioclase + olivine cumulates with interstitial clinopyroxene. However, the CLG rocks, especially in the interior subzones of the Main Zone, contain very coarse-grained optically continuous ophitic clinopyroxene whereas the MMD rarely has ophitic clinopyroxene, instead is largely comprised of subophitic or granular clinopyroxene. The presence of granular clinopyroxene implies that the magma differentiated to the point of clinopyroxene saturation whereas the lack of granular clinopyroxene in the CLG implies that crystallization occurred prior to clinopyroxene saturation (Irvine, 1982). This suggests that the cooling histories of the MMD and CLG were different, perhaps due to different cooling rates and/or that the CLG could have formed in an open system whereas the MMD formed in a closed system.

Another difference between the drill holes is that the CLG contains disseminated sulphides and Cr-spinel seams at various stratigraphic horizons whereas the MMD does not. The absence of evidence is not evidence of absence, as a basal contact was not found in the MMD drill core and the majority of the sulphides and Cr-spinel seams present in the CLG were located in the vicinity of a basal contact. The MMD drill hole may not have been deep enough to intersect the basal contact which may or may not be present and may or may not contain a sulphides and Cr-spinel bearing horizon. Since the geometry of the MMD is unknown at depth, and it could very well be a vertical body, there may not have been a structure for which settling Cr-spinel grains or liquid sulphide droplets could collect. The Logan Sills present in the CLG core are likely laterally extensive flat lying bodies, which could have provided a horizontal barrier that allowed for the collection of Cr-spinel grains and liquid sulphide droplets.

Both the CLG and MMD have Upper Zones that show geochemical evidence of contamination by the Rove Formation. Localized increased La/Sm_n and Th/Yb values and the presence of sedimentary xenolith bearing rocks suggest that there was partial assimilation of the country rock in both the MMD and CLG. The Upper Zone in the CLG has sulphides with high $\delta^{34}S$ values which also suggests assimilation of country rock. The Upper Zone in the MMD has an absence of sulphides which could be due to the lack of sulphides present in the observed greywacke xenoliths, whereas the CLG xenoliths are a sulphide bearing shale. The Upper Zone of the CLG is characterized by low concentrations of incompatible trace elements and high Al_2O_3 and MgO concentrations as well as a presence of olivine and Cr-spinel. The Upper Zone of the MMD is characterized by an evolved assemblage of quartz ferrodiorite with high modal abundance of accessory minerals as well as high incompatible trace element concentrations with an absence of olivine and Cr-spinel. This suggests that the CLG Upper Zone was formed from a primitive magma whereas the MMD Upper Zone was formed from a highly evolved magma. This could be due to the CLG magma inwardly crystallizing and differentiation from the roof while the highly evolved assemblage of the Upper Zone in the MMD implies that there was not a significant downward crystallization and differentiation component.

Despite these few differences, the CLG and MMD display geochemical similarities that may suggest that they had the same magma source. The average trace element concentrations for the MMD and CLG on a primitive mantle normalized multi-element diagram plot as near perfect parallel lines (Fig. 5.15), with similar incompatible trace element ratios (Table. 5.3). The main difference between the two patterns on the multi element diagrams is that the CLG has higher concentrations than the MMD. This suggests that the CLG is on average slightly more evolved than the MMD.

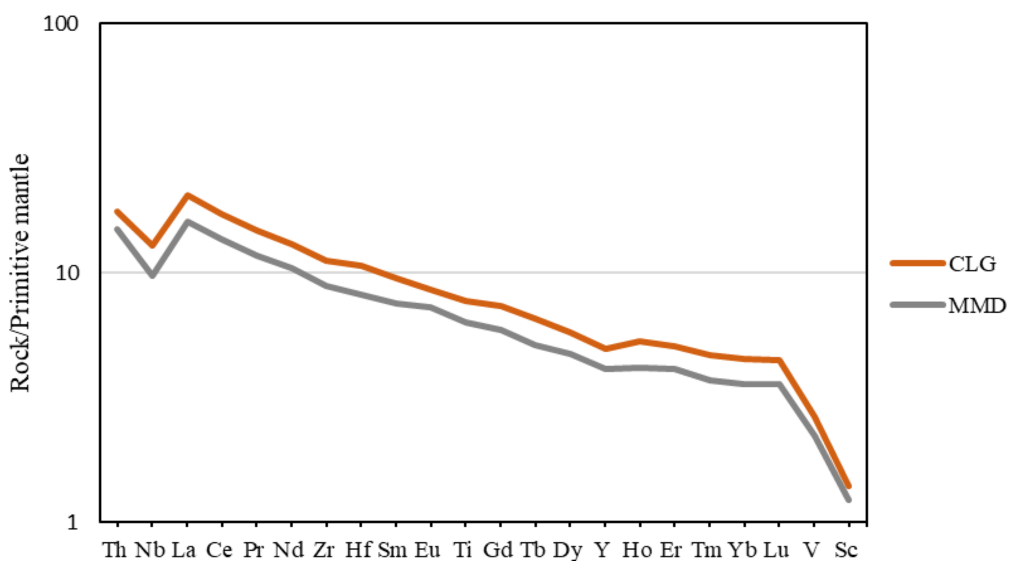

Figure 5.15. Primitive mantle normalized diagrams of average concentration of trace elements from all the CLG and MMD samples. Normalizing values from Sun and McDonough (1989).

Table 5.3. Average incompatible trace element ratios for the CLG and MMD.

	MM (n=67)		CLG (n=237)	
	Av	StD	Av	StD
(La/Sm)n	2.07	0.08	2.12	0.15
(Gd/Yb)n	1.64	0.05	1.63	0.08
Zr/Hf	39.28	0.69	38.34	1.60
Nb/Ta	16.01	0.45	18.02	4.22
Nb/Th	6.47	0.47	6.59	0.90
Y/Ce	0.80	0.05	0.75	0.05
Nd/Lu	52.28	2.75	53.25	3.60
Nb/Nb*	0.53	0.04	0.54	0.06
Ti/Ti*	0.94	0.17	0.94	0.13

The major element concentrations of the estimated parental magmas of the MMD and CLG also show similarities as they both yielded nearly identical modelled fractionation sequences (Figs. 5.13 and 5.14). On a normalized multi-element diagram of the major elements, where the MMD estimated parental magma composition is normalized to the CLG estimated parental magma composition, the ratios for each element are very close to 1 (Fig. 5.16). The estimated parental magma composition of the CLG is slightly more evolved than the MMD parental magma with higher concentrations of TiO_2, Fe_2O_3, Na_2O, and P_2O_5 and lower Al_2O_3, MgO, CaO, and Mg# (Table. 5.1).

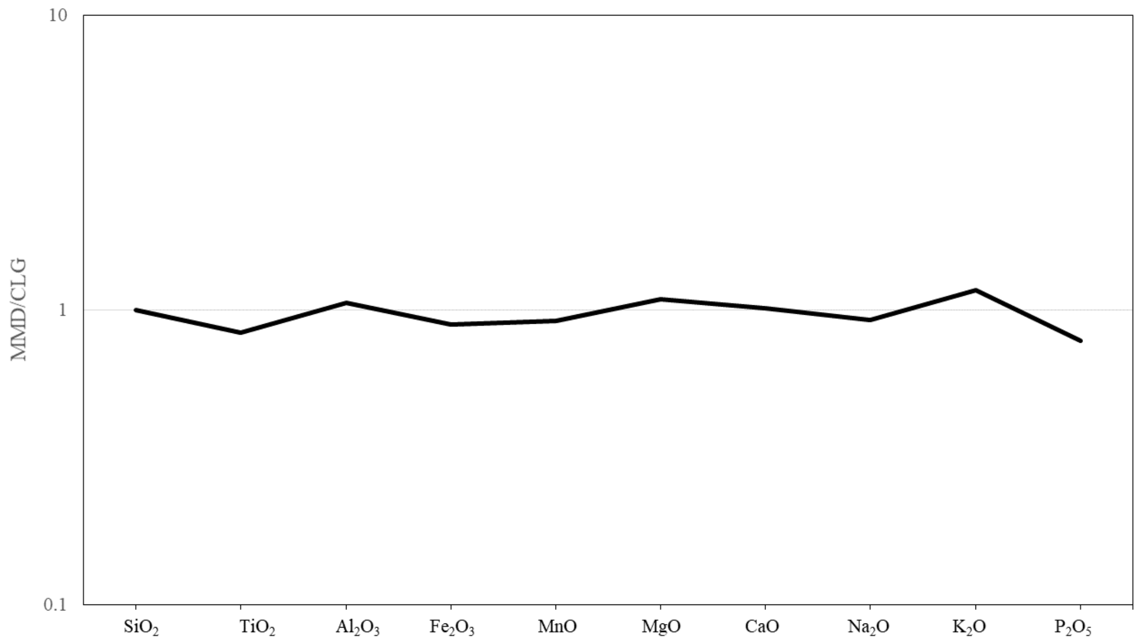

Figure 5.16. Ratio of parental magma composition of MMD normalized to CLG.

The textural differences between the CLG and MMD can be attributed to emplacement/post-emplacement processes whereas the geochemical similarities suggest that the MMD and CLG shared a magma source. Both the major element and trace element compositions suggest that the CLG is slightly more evolved than the MMD which could be the result of the magma source fractionating at depth, perhaps in a staging chamber.

What remains unresolved is the timespan between emplacement suggested by the U-Pb ages. It is extremely unlikely for the CLG and MMD to have the same magma source and have been emplaced 9.7 ± 7.5 million years apart, as this is a very long period of time for a magma chamber to remain active. For example, the largest layered intrusion in the world, the Bushveld Complex, formed from multiple magma pulses that were injected over 75,000 years and crystallized over 200,000 years (Cawthorn and Walraven, 1998). It also seems unlikely that two separate magma sources 9.7 ± 7.5 million years apart, in an evolving rift system, produced two geochemically nearly identical magmas that were emplaced with a close spatial relationship and similar orientation with the same N polarity. Further investigation is warranted to resolve the inconsistencies, perhaps another U-Pb age determination analysis for both the CLG and MMD to confirm that the published ages of emplacement are accurate representations.

5.7 REGIONAL CONTEXT

The CLG and MMD are located within the Logan Basin portion of the MCR, which is comprised of a number of sills and dyke sets (Fig. 5.17). The CLG is unique to the Logan Basin in that it is the only known layered intrusion, while the MMD is unique in that it is the only dyke with an arcuate trend.

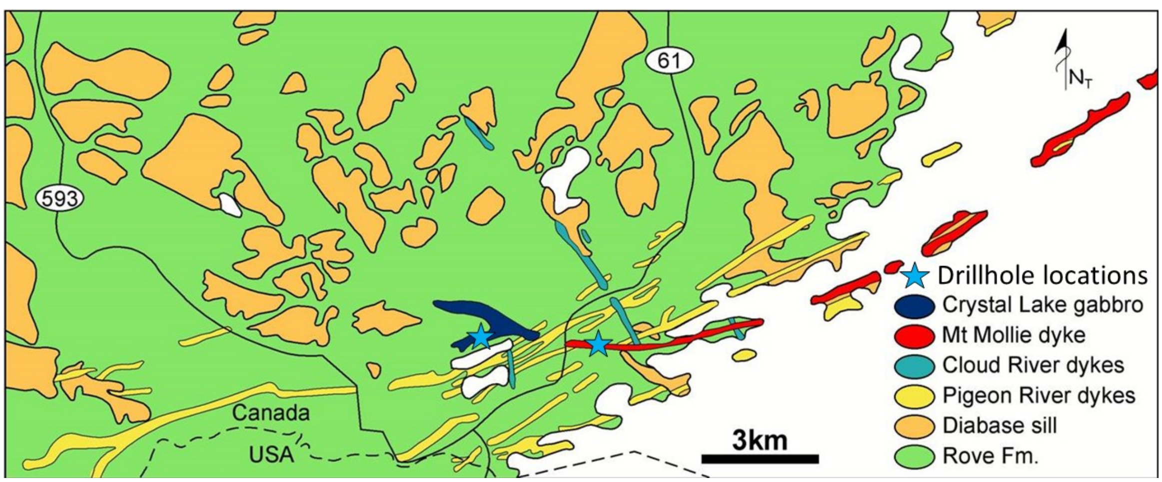

Figure 5.17. Generalized geology map of CLG, MMD, and surrounding rocks. Modified from Cundari et al. (2013a).

The current understanding of the Logan Basin rocks is unclear as there are inconsistencies between the geochronology, paleomagnetism, and field relationships. The cross-cutting relationships observed in the field suggest that the Logan Sills were emplaced earlier than the dyke sets as the Pigeon River dykes cross-cut the sills (Cundari, 2012). Cundari (2012) showed that the dyke sets have an emplacement sequence of Pigeon River dykes → Cloud River dykes → MMD, with Cloud River dykes cross-cutting the Pigeon River dykes and the MMD cross-cutting both the Pigeon River and Cloud River dykes. Geul (1970) recognised that the CLG cross-cut the Pigeon River dykes.

Two emplacement ages have been reported for the Pigeon River dykes, neither of which align with the cross-cutting relationships. Based on the cross-cutting relationships the Pigeon River dykes should fall between the 1114.7 ± 1.1 Ma Logan Sill age and the 1109.2 ± 4.2 Ma and 1109.3 ± 6.3 Ma ages for the Cloud River and MMD, respectively. One age for the Pigeon River dyke is too old at 1141 ± 20 Ma while the other age is too young at 1078 ± 3 Ma (Heaman et al., 2007). The paleomagnetic data of the Pigeon River dykes does not help to resolve this issue as both N and R polarities have been reported (Robertson and Fahrig, 1971; Pesonen, 1978). Davis and Green (1997) recognised that MCR associated rocks older than 1105 Ma have a R-polarity whereas those younger than 1102 Ma have a N-polarity. In a comprehensive paleomagnetic study of the Logan Basin rocks, Piispa (2011) determined that the MMD with a N-polarity and a 1109.3 ± 6.3 Ma age, Cloud River with a N-polarity and a 1109.2 ± 4.2 Ma age, Logan sill with an N-polarity and a 1114.7 ± 1.1 Ma age are not consistent with the Davis and Green (1997) observations. Piispa (2011) explained the N-polarity of a Logan sill as being due to the close emplacement of a later N-polarity dyke that thermally overprinted the original R-polarity reported by Pesonen (1978). The CLG with an age of 1099.6 ± 1.2 Ma and a N-polarity agrees with Davis and Green (1997)'s observation. This conflicting data suggests that the Davis and Green (1997) observation may not apply to all MCR related rocks and/or that some of the published ages are not accurate representations.

Cundari (2012) proposed that the three dyke sets in the Logan Basin (i.e., Pigeon River, Cloud River, and Mount Mollie) shared a similar source based on the geochemical similarities. The results from this study suggest a similar, if not the same, source for the CLG and MMD. Therefore, the CLG should also be geochemically similar to the Pigeon River and Cloud River dykes. The MCR discrimination diagrams proposed by Hollings et al. (2007a) shows that there are similarities (Fig. 5.18). On the La/Sm_n vs. Gd/Yb_n diagram the CLG, MMD, Pigeon River dykes, and Cloud River dykes plot as a cluster with similar values to the Nipigon Sill samples, although the Nipigon sill samples extend to lower values of both Gd/Yb_n and La/Sm_n (Fig. 5.18). On the Mg# vs. TiO_2 diagram the CLG, MMD, and Pigeon River dyke samples plot in a previously unrecognized intermediate TiO_2 field, whereas the Cloud River dyke samples plot within the Nipigon Sill field (Fig. 5.18). The MMD and Pigeon River dyke samples a similar trend whereas, the CLG has, on average, a slightly higher TiO_2 concentration at a given Mg#. The MMD extends to higher Mg#'s than the Pigeon River dykes suggesting it is more primitive. Samples from the Basal Margin subzone, Upper Zone, and Lower Zone of the CLG are not on the same trend as the interior of the Main Zone and extend into the Nipigon sill field, which further suggests that these zones are compositionally distinct but related to each other (Fig. 5.19).

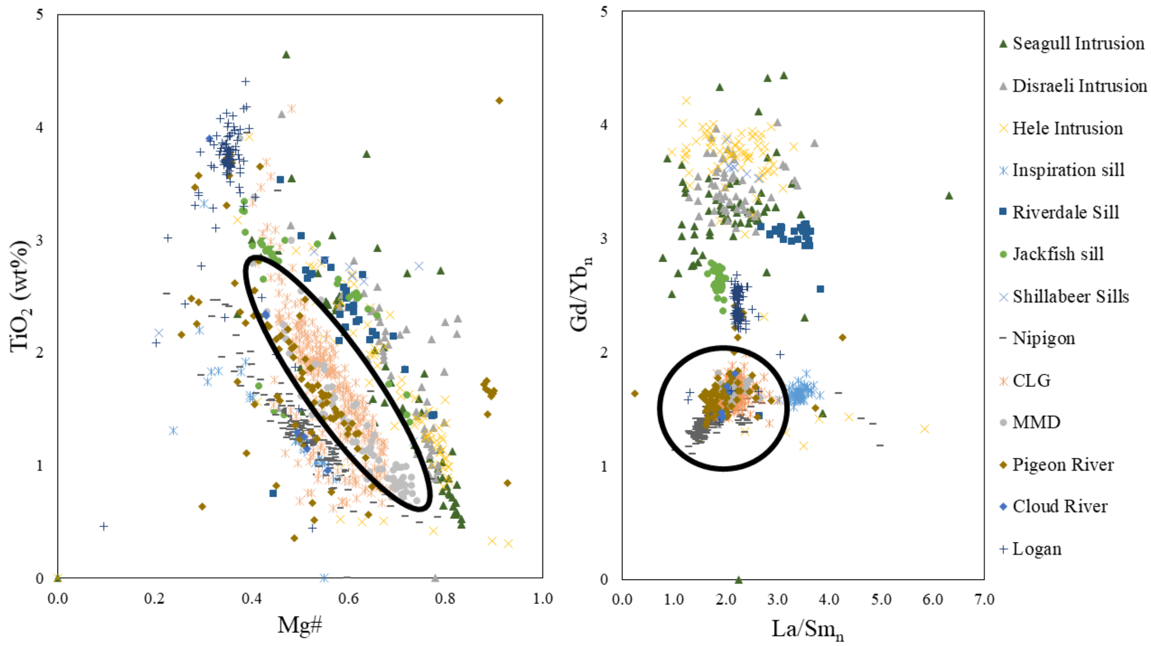

Figure 5.18. Diagram showing the variation of Mg# vs. TiO_2 and La/Sm_n vs Gd/Yb_n for the CLG and MMD as well as other MCR rocks. Circles represent area where vast majority of CLG and MMD plot. Data from Cundari et al. (2013b). Normalizing values from Sun and McDonough (1989).

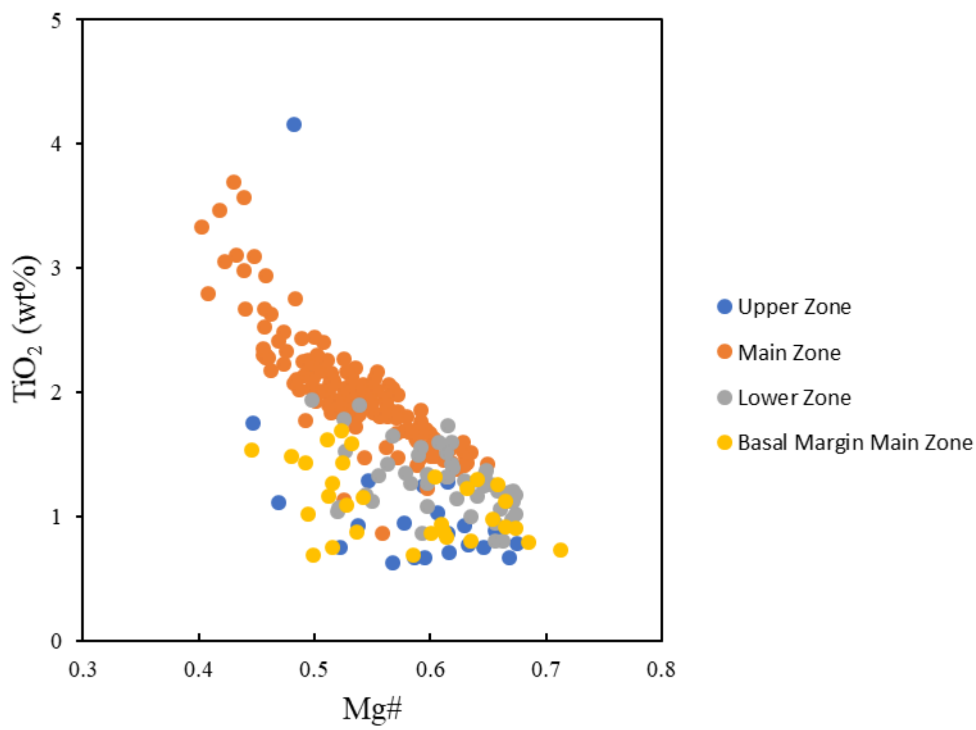

Figure 5.19. Variation of Mg# vs. TiO_2 for the CLG samples.

Comparisons have been made of the CLG to the Duluth Complex's Layered Series (e.g., Eckstrand, 1996; Thomas, 2015). The Layered Series of the Duluth Complex is comprised of several discrete intrusions that are characterised by thick (3 to 7 km) sheet like troctolite to gabbro bodies (Miller et al., 2002). The CLG, at least in the studied drill core, is also largely comprised of troctolite and gabbro but is not as thick. Cu-Ni-PGE mineralization is found in some (e.g., South Kawishiwi and Partridge River intrusions) but not all (e.g., Duluth Layered Series) intrusions of the Duluth Complex, which is primarily in the form of disseminated sulphides likely as a result of extensive assimilation of country rock sulphides (Miller and Ripley, 1996; Ripley, 2014). Mineralization in the South Kawishiwi and Partridge River intrusions is generally restricted to the basal 100 to 300 m and has higher sulphide tenors of Cu than of Ni, with Cu/Ni ranging from 3 to 8 (Ripley et al., 2015). The majority of the mineralization present in the CLG is also located in the basal 30 m and the whole-rock Cu/Ni ratios of samples containing >1 wt% S range from 1.2 to 2.6, with olivine also present in the rocks the Cu/Ni ratios of the sulphides are likely greater.

The parental magmas of the Duluth Complex are informally classified as high-alumina olivine tholeiite (HAOT; Lee and Ripley, 1996; Ripley et al., 2007). The estimated parental magma composition of the CLG and MMD bears a striking resemblance to the proposed HAOT parental magma of the South Kawishiwi intrusion (Fig. 5.20), suggesting that the CLG and MMD can also be classified as HAOT intrusions. Finally, the similar reported ages for the CLG and the Layer Series intrusions of the Duluth Complex of 1099.6 ± 1.2 Ma (Heaman et al., 2007) and 1099.0 ± 0.5 Ma (Paces and Miller, 1993), respectively further support the theory that the CLG is a satellite intrusion of the Duluth Complex.

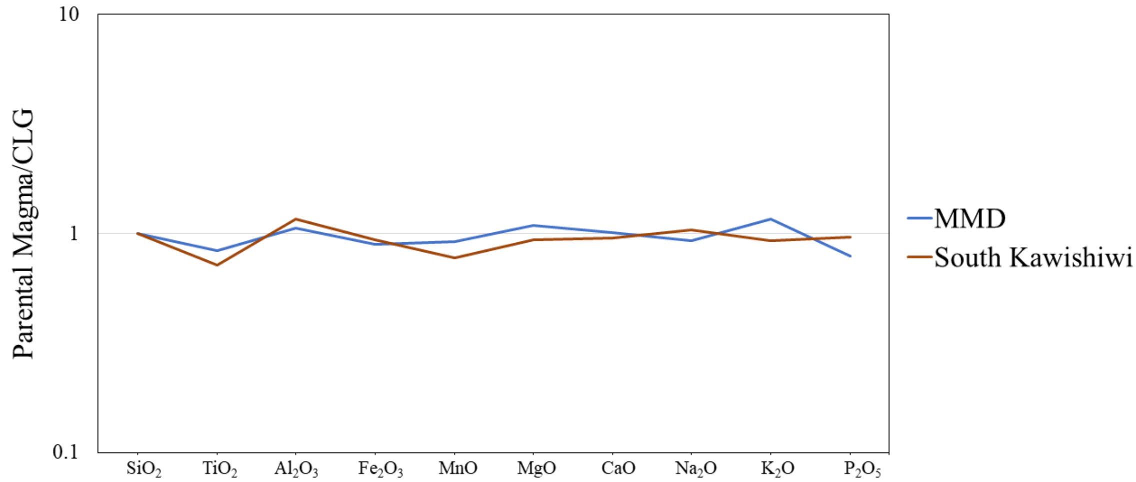

Figure 5.20. Ratios of parental magma composition of the South Kawishiwi intrusion and MMD normalized to CLG, values from Lee and Ripley (1996).

When compared to the early ultramafic intrusions of the MCR, the HAOT parental magma composition differs mainly by having higher Al_2O_3 and lower MgO concentrations (Fig. 5.21). The ultramafic intrusion of the MCR are characterised by massive, semi-massive, net-textured, and disseminated sulphide mineralization that is Ni-rich with Cu/Ni <1 (Ripley, 2014).

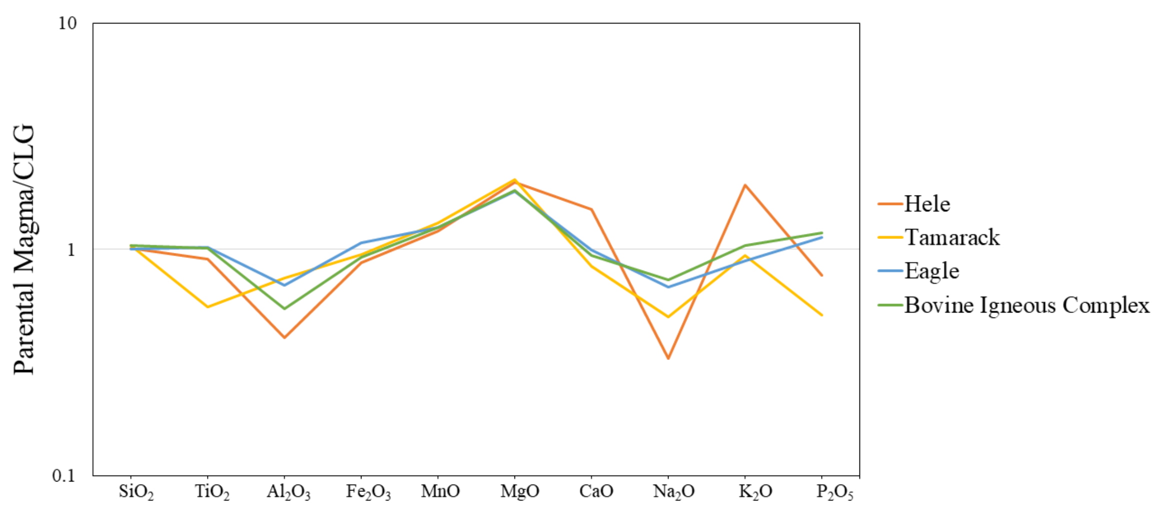

Figure 5.21. Parental magma composition of the Hele, Tamarack, Bovine Igneous Complex, and Eagle intrusions normalized to CLG, values from (Hollings, pers. comm., 2017; Berg and Klewin, 1988; Taranovic et al., 2015; Foley, 2011).

This study adds complexity to an area that was already not fully understood and has conflicting geochronological, paleomagnetic, and field observational results. A comprehensive study of the relationship of the rocks of the Logan Basin is warranted to gain a better perspective on the timing of emplacement as well as the compositional similarities apparently spanning 9.7 ± 7.5 million years. With the largely N-polarity and geochemical similarities of the CLG, MMD, Pigeon River dykes, and Cloud River dykes as well as the geochemical and textural similarities to the Layered Series of the Duluth Complex, the 1109.3 ± 6.3 Ma MMD age, the 1109.2 ± 4.2 Ma Cloud River dyke age, and the 1141 ± 20 Ma/1078 ± 3 Ma Pigeon River dyke ages do not conform to the current understanding of the MCR. Additional geochronology is required to resolve the apparent discrepancies.

5.8 Emplacement Model

An emplacement model for the CLG and MMD can be developed by integrating the results and interpretations of the petrological, geochemical, mineral composition, and isotopic data presented in this study. Since the proposed emplacement model is primarily based on the observations and interpretations from only one drill hole from each of the two bodies (i.e. the MMD and the CLG) it is preliminary and further work is needed to determine the lateral extent of the observed units.

The first stage in the evolution of the CLG and MMD involves mantle derived magma ascending through the continental crust where it collects in a staging chamber potentially situated in lower crust comprised of Archean aged rocks. The presence of a staging chamber has been suggested for other HAOT intrusions of the MCR (e.g., Lee and Ripley, 1996;

Ripley et al., 2007; Ripley, 2014). It has been suggested that HAOT magmas can be generated by fractional crystallization of an originally picritic magma, a process that could potentially occur in a staging chamber (Ripley and Li, 2013; Ripley et al., 2015). It has also been suggested that staging chamber dynamics are responsible for the high Cu/Ni ratios of the sulphides, where crystallization of olivine and/or the retention of a Ni-rich monosulphide solid solution within the staging chamber depletes the residual magma of Ni (Ripley, 2014 and refences therein). The similar composition of the parental magmas of the MMD and CLG to that of the HAOT intrusions of the Duluth Complex, coupled with the similar high Cu/Ni ratios for the CLG sulphides, suggests that they may have undergone a similar evolution involving a staging chamber. The widespread presence of a negative Nb-anomaly in all of the sampled rocks of the MMD and CLG suggests a pervasive crustal contamination that could have occurred in a lower crustal staging chamber or during ascent through the Archean crust rather than during emplacement in the Rove Formation. Or as previous studies have suggested the negative Nb-anomaly may also suggest extensive interaction with the SCLM (e.g., Shirey et al., 1994; Hollings et al., 2007a; Hollings et al., 2010).

The residual CLG and MMD HAOT magmas were then expelled from the staging chamber and ascended to be emplaced into the Proterozoic upper crust of the Rove Formation (Fig. 5.22). The geometry of the CLG and MMD suggest that the two took separate paths, one which formed the MMD and the other which formed the CLG (Fig. 5.22). Higher than mantle values of $\delta^{34}S$ and S/Se values in the CLG, suggests that during the ascent of the magma through the Rove Formation, there likely occurred assimilation as well as devolatilization of sulphides from the wall rocks (Fig. 5.22). This may or may not have also occurred in the MMD, but no evidence was found to support or deny a similar claim. Assimilation of sulphur during ascent of the CLG magma through the Rove Formation likely caused the magma to become at least locally sulphur saturated resulting in immiscible liquid sulphide droplets (Fig. 5.22). Assimilation and an early sulphur saturation during ascent is suggested by the crustal contamination geochemical signature and the presence of disseminated sulphide in the upper margin of the Lower Zone in the CLG (Fig. 5.22). Assimilation during ascent rather than during emplacement is suggested by the fact that the Logan Sill is neither sulphur bearing nor has the whole-rock geochemical signature of increased Th concentrations and La/Sm_n values which would suggest contamination. The Rove Formation being the source of at least some, if not most, of the sulphur in the CLG is suggested by the higher than mantle $\delta^{34}S$ and S/Se values of the sulphides and whole-rock geochemistry (Hughes et al., 2015; Queffurus and Barnes, 2015). The crustally contaminated and sulphur saturated magma retained its geochemical signature when it chilled against the Logan Sill. Cr-spinel grains were an early crystallizing mineral as they are wholly enclosed in plagioclase, olivine, and clinopyroxene. It is possible they formed in the staging chamber and were carried by the magma during ascension and emplacement or crystallized shortly after emplacement (Fig. 5.22). Most of the Cr-spinel grains and liquid sulphide droplets began to settle to the bottom of the Lower and Main Zones in the CLG due to gravitational segregation, because they would be heavier than the magma (Fig. 5.22). There is no evidence to support an argument for or against the same assimilation, addition of external sulphur, or Cr-spinel crystallization processes occurring in the MMD during ascent of the magma, as the drill core did not intersect sulphide, crustal xenoliths, or Cr-spinel bearing rocks at depth. There is however, evidence for crustal contamination of the Rove Formation after emplacement in the CLG and MMD as the Upper Zones of both bodies have localized crustal contamination signatures and presence of crustal xenoliths. The CLG Upper Zone is sulphide bearing whereas the MMD Upper Zone is barren of sulphide. This is likely due to the xenoliths in the CLG being sulphide bearing shale whereas the xenoliths in the MMD were sulphide barren greywacke.

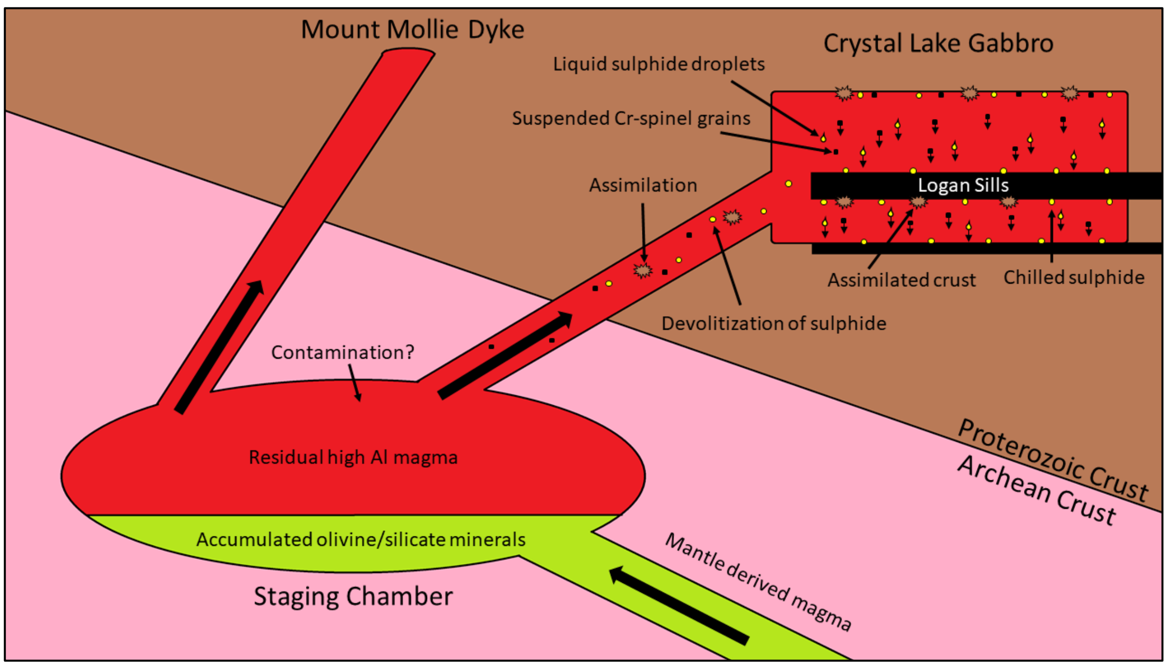

Figure 5.22. Cartoon illustration depicting the first stage of the CLG and MMD emplacement model.

After the emplacement of likely a single pulse of magma that formed the MMD, it began to crystallize. The crystallization resulted in an overall observed fractionation trend of the drill hole of a bottom to top cumulate sequence of plagioclase + olivine → plagioclase + olivine + clinopyroxene → plagioclase + clinopyroxene ± olivine ± Fe-Ti oxide, with the upper most samples containing a high modal abundance of quartz and K-feldspar. The fractional crystallization models, run with PELE, of the proposed parental magma composition also generated a sequence consistent with the observed mineralogy. Although there is a general bottom to top fractionation sequence of the drill hole samples, two features of the MMD can not be explained by solely bottom to top directed crystallization. Mineral composition analysis shows that the olivine Fo content, plagioclase An content, and clinopyroxene Mg# remaining fairly constant at depths >600 m. These values would steadily decrease upward if there was only an upward crystallization front (Wager and Brown, 1968; Tegner, 1997; Tegner et al., 2006). Secondly, the surface expression of the MMD has a highly evolved core composed of granophyre and diorite and the edges being composed of olivine gabbro and gabbro (Fig. 5.7; Geul, 1973; Smith and Sutcliffe, 1989). Both of these features can be explained if there was a laterally directed crystallization front directed inward from the walls, which is consistent with the relatively narrow nature of the MMD. Clearly there must be both a lateral and vertical component to the crystallization front to explain all of the features of the MMD. Inward and upward differentiation has also been recognized, using similar criteria as in this study, in the Great Dyke in Zimbabwe and the Jimberlana dyke in Australia (Campbell, 1987; Wilson, 1991). Figure 5.23 is a schematic depiction of a possible cross-section of the MMD that would result from an inward and upward crystallization/differentiation direction. This cross-section resembles the proposed cross-sections of the Great and Jimberlana dykes (Campbell, 1987; Wilson, 1991). In this model, the more differentiated the rock is, the longer the magma would have remained molten and thus interacted with the country rock, resulting in a higher crustal contamination geochemical signature. Not depicted in Figure 5.23 are two processes that also possibly occurred during the crystallization of the MMD. The first being the localized convection currents or sinking/floating of olivine and plagioclase that would explain the varying proportions of the minerals found mostly in the Lower Main Zone as well as the saw-toothed appearance in the major element downhole geochemical profiles (Fig. 5.5). The second being the localized accumulation of magmatic volatile fluids that resulted in the crystallization of a pegmatitic segregation zone, found in the Lower Main Zone (~600 m depth; Fig. 5.4).

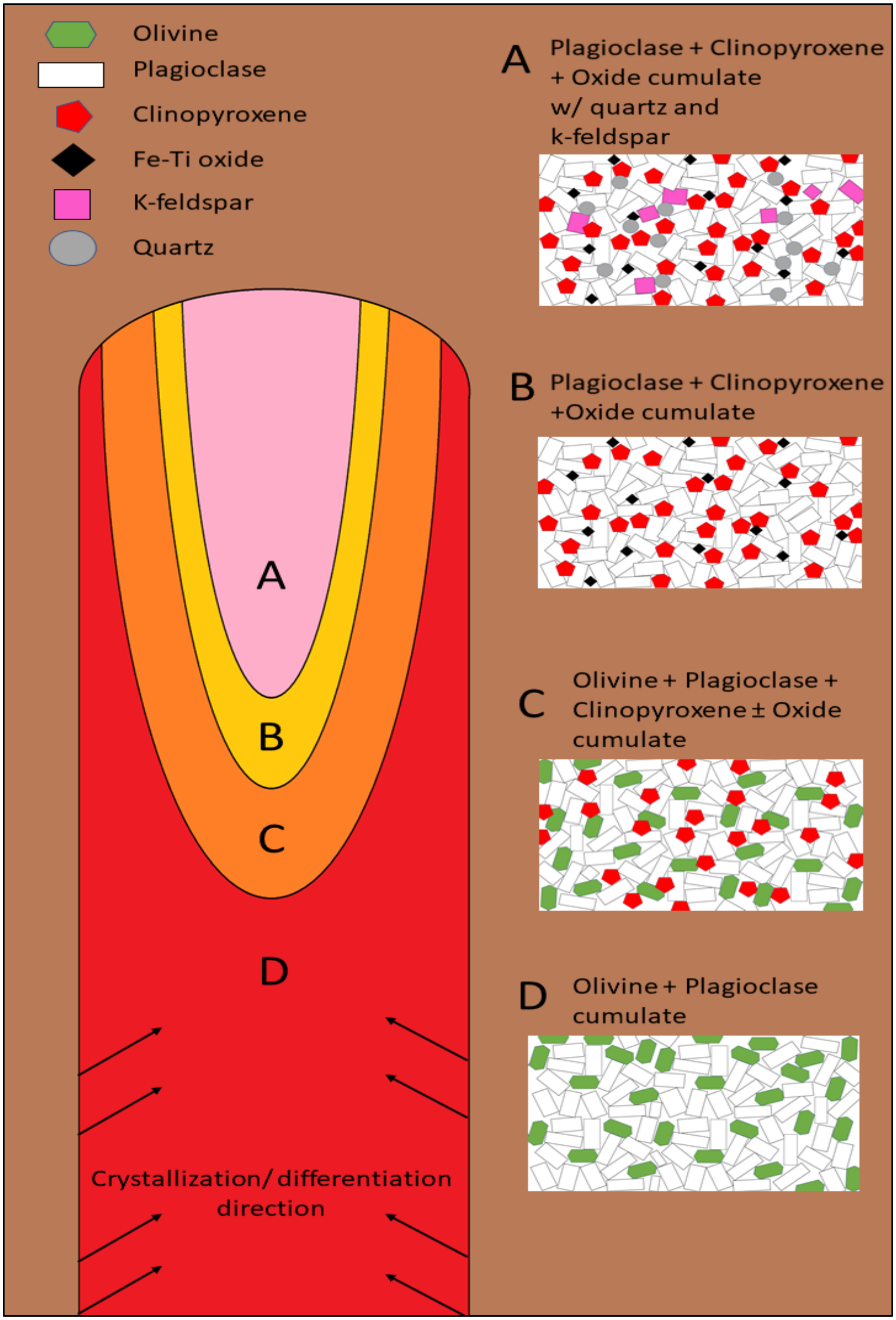

Figure 5.23. Schematic cartoon showing the evolution of the MMD.

During a hiatus of magmatism, the first pulse of magma that formed the CLG would have been crystallizing as well as the magma within the staging chamber. Further fractional crystallization within the staging chamber would lead to a more evolved residual magma, with higher concentrations of incompatible trace elements, TiO_2, Fe_2O_3, K_2O, Na_2O, and P_2O_5, and a lower MgO concentration, which in turn would result in lower Fo content of olivine and Mg# of clinopyroxene that would crystallize from the magma. The evolved magma in the staging chamber ascended through the crust, where it was injected into the portion of the CLG above the Logan Sills perhaps as three separate pulses forming the interior subzones of the Main Zone (Figs. 5.24 and 5.25). At the time of emplacement of these pulses of magma, the CLG was likely a crystal mush of olivine, plagioclase, and interstitial liquid magma as well as Cr-spinel grains that were mechanically sorted into seams by gravitational segregation. The geochemical similarities of the Main Zone basal marginal subzone and Upper Zone suggests that these later pulses were injected into the middle of the chamber separating the Upper Zone and Main Zone basal marginal subzone (Figs. 5.24 and 5.25). A similar placement of magma in the middle of a magma chamber was proposed for the Doros layered intrusion and the Shiant Isles Main Sill (Owen-Smith and Ashwal, 2015; Holness et al., 2017). Some of the Cr-spinel grains did not settle prior to the emplacement of the subsequent pulses and remained in the Upper Zone as randomly distributed grains, possibly due to rapid chilling or the magma was turbulent enough to prevent the settling of some grains (Spandler et al., 2005). During ascent of the evolved magma pulses, perhaps in a feeder conduit, devolatilization of sulphides and assimilation of the Rove Formation could have also occurred. There is no direct evidence for assimilation as no crustal xenoliths were observed in the interior subzones, so if assimilation did occur, there must have been complete melting of the crustal material. Also, it is possible that since this study only looked at one drill hole, there may be xenoliths elsewhere.

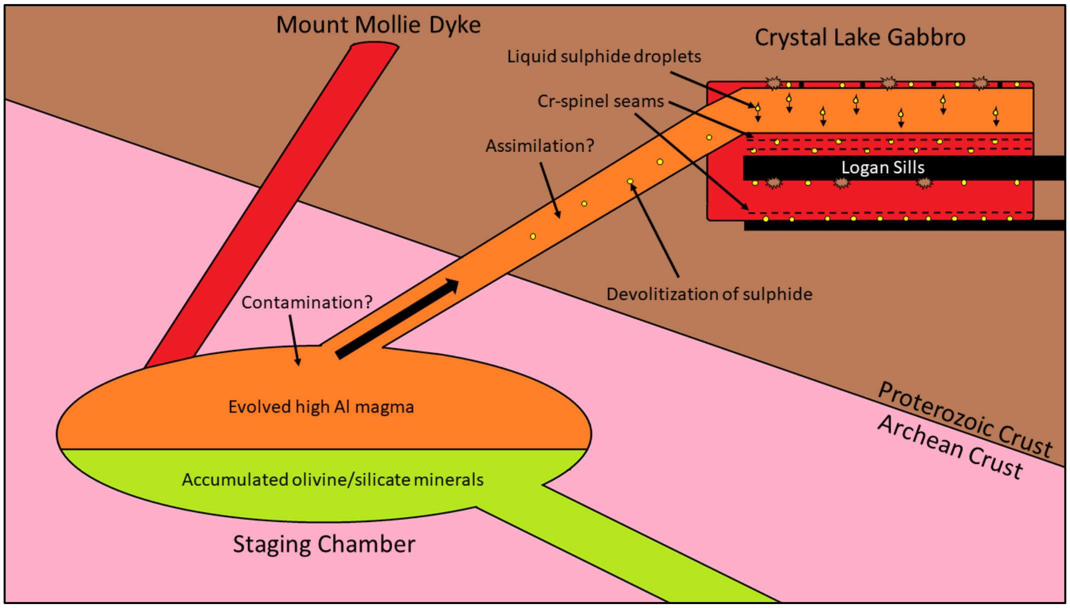

Figure 5.24. Cartoon illustration of an evolving staging chamber as well as subsequent pulses of magma into the CLG chamber.

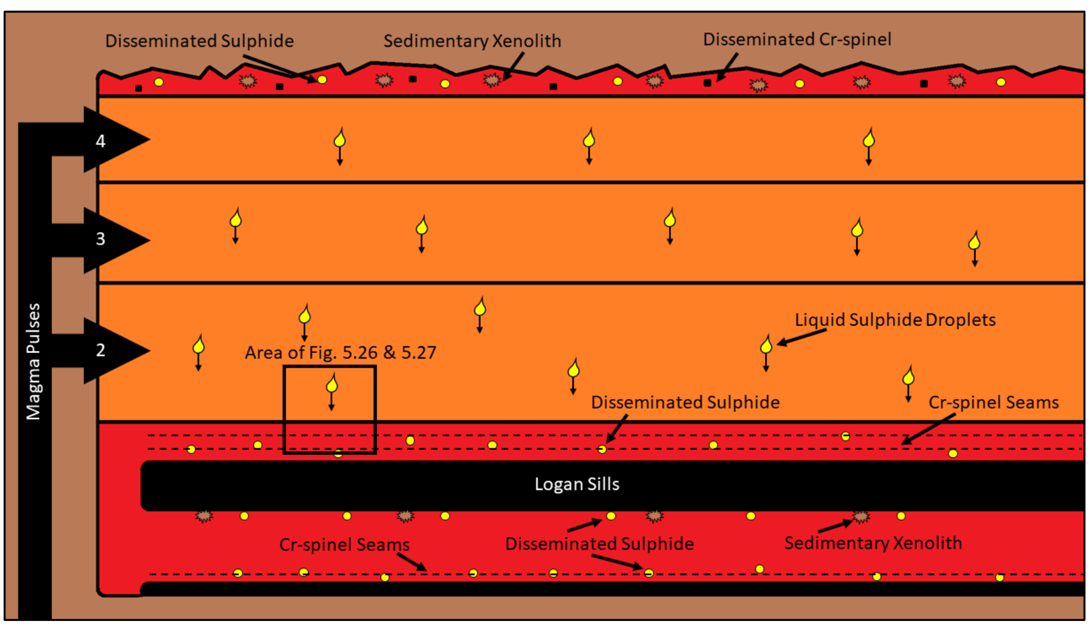

Figure 5.25. Cartoon illustration of the CLG shortly after the emplacement of the evolved magma pulses.

Sulphur added to the magma pulses through devolatilization and/or assimilation and melting did not remain in the interior subzones, instead immiscible liquid sulphide droplets settled and were able to navigate into and through the crustal mush of the basal marginal subzone (Figs. 5.25 and 5.26). During the downward movement of the sulphide droplets, they would have interacted and scavenged chalcophile elements (e.g. Cu, Ni, Pd, Se) from the silicate magma. The new pulses of magma could have also increased the pressure in the CLG magma chamber and thus result in compaction of the basal margin crystal mush, in a process similar to that outlined by Zieg and Marsh (2012) for the Bushveld Complex. This compaction effect would have expelled the interstitial magma from the crystal mush pile (Fig. 5.27). Evidence for this occurring is found texturally and geochemically as less interstitial magma in the basal marginal subzone would result in the mesocumulate texture of the rocks as well as a depletion of incompatible trace elements producing the abrupt geochemical difference between the basal marginal subzone and the interior subzones.

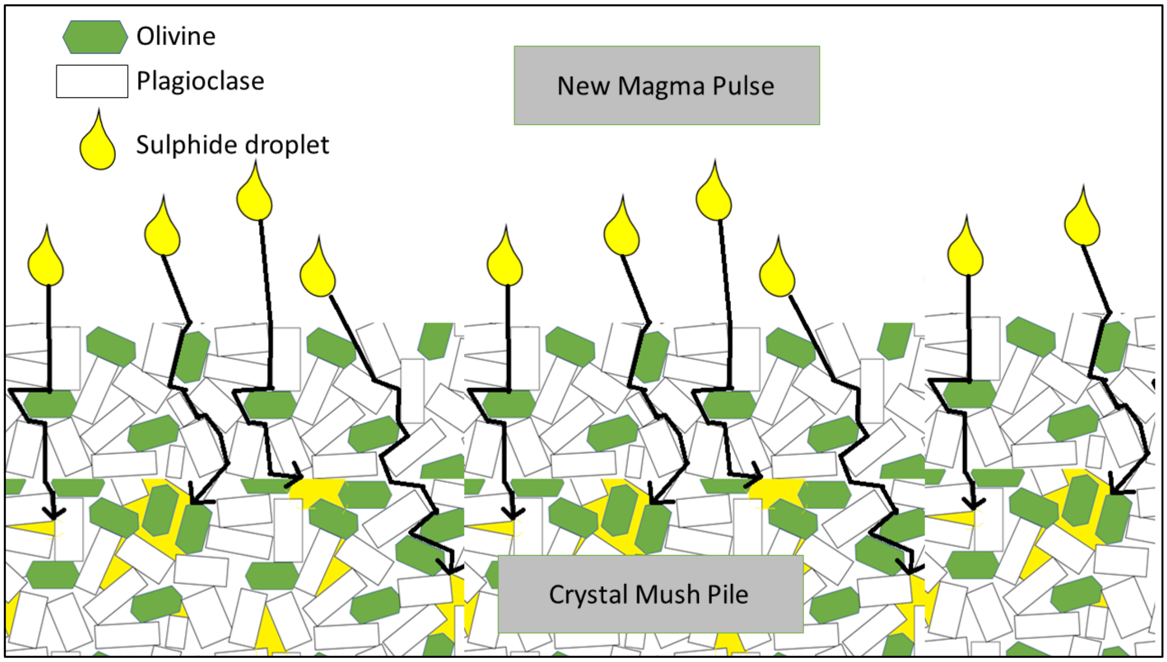

Figure 5.26. Cartoon illustration of the settling and movement of liquid sulphide droplets through the new magma pulse and the pre-existing crystal mush.

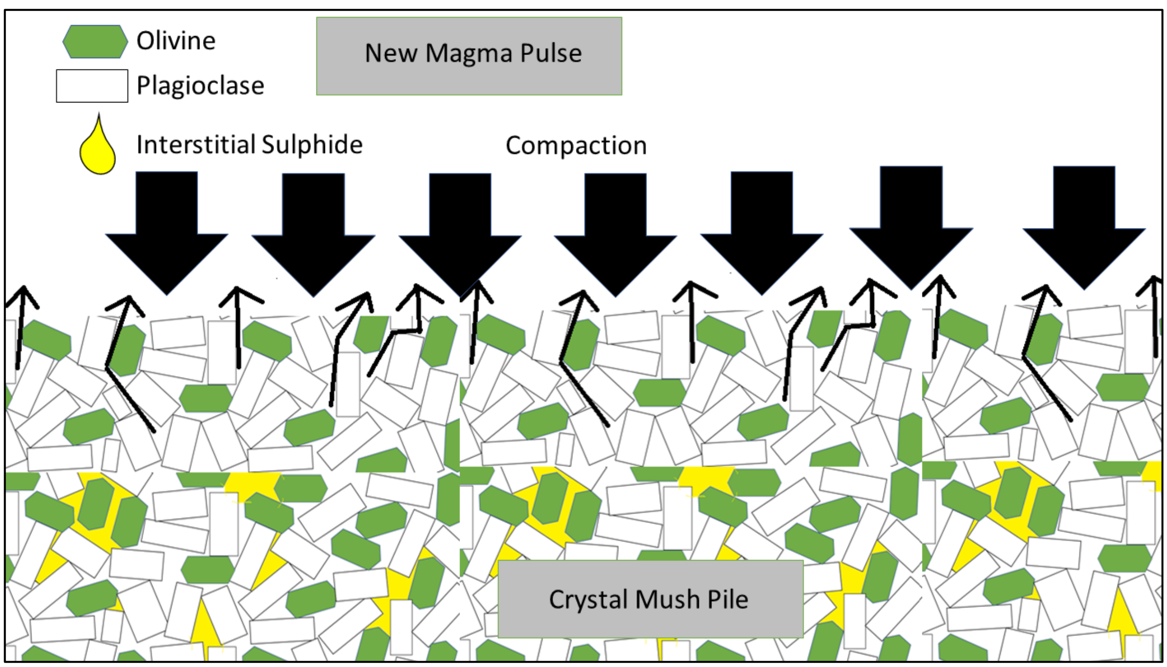

Figure 5.27. Cartoon illustration of the compaction effect expelling interstitial magma from the pre-existing crystal mush.

The level of interaction between the three pulses of magma that formed the interior of the Main Zone is difficult to determine. The cyclical nature of the stratigraphy (i.e. disappearance/appearance of olivine) suggests that they remained at least partially segregated during crystallization. But as a whole, the interior subzones are progressively more texturally and geochemically evolved (i.e., increasing quartz/granophyre and incompatible trace element concentrations) with decreasing depth, which may suggest that they, in some way, behaved as a single unit. Or that each pulse was, initially upon emplacement, progressively more evolved than the last. Crystallization/differentiation in the CLG could have also had a lateral component from the walls of the intrusion, similar to the MMD, but since only one drill hole was studied and previous studies/mapping do not mention an evolved core, the extent of laterally directed crystallization can not be determined. The downhole geochemical profiles suggest that the overall net crystallization/differentiation front was mainly bottom to top directed with a minor top to bottom front from the roof (i.e. the Upper Zone and upper margins of the Main and Lower Zones; Fig. 5.28).

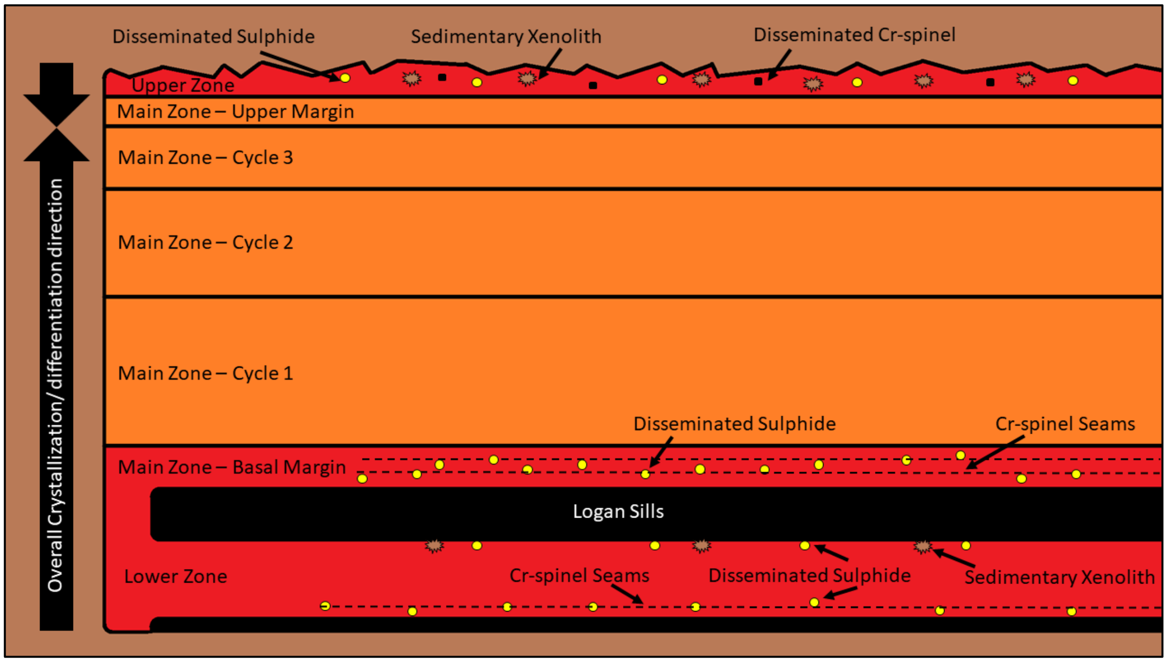

Figure 5.28. Cartoon illustration of a hypothetical model of the CLG.

The largest unresolved uncertainty is the relationship of the Lower Zone and the Main Zone. It is not clear whether the magma circumvented or breached the Logan Sill in one or multiple pulses (i.e. contemporaneous or sequential emplacement). This could be investigated by examining addition drill holes throughout the intrusion but was beyond the scope of this thesis.

6 CONCLUSIONS

The CLG and MMD mafic intrusions share similar petrographical and geochemical characteristics. Both are largely comprised of troctolite, augite troctolite, olivine gabbro and gabbro. The estimated parental magma compositions suggest that the CLG and the MMD shared a similar, if not the same, magma source. The parental magmas are geochemically very similar to the Layered Series intrusions of the Duluth Complex and can be classified as a high alumina olivine tholeiitic (HAOT) magmas. It is possible that the shared CLG and MMD magma source was a staging chamber situated in the lower to middle crust. Before entering the staging chamber, the magma was likely derived from a plume-related mantle source with OIB-like trace element patterns. The magma within the staging chamber underwent a moderate degree of fractionation prior to the emplacement at shallow levels. Fractionation of a mantle-derived picritic magma potentially can generate the HAOT magmas and high sulphide Cu/Ni ratios that were found in this study (Ripley and Li, 2013; Ripley et al., 2015).

The data from this study is consistent with an open-system style of formation for the CLG. Abrupt changes in the major and trace element concentrations coinciding with the intermittent appearance of olivine suggest that multiple pulses of magma formed the CLG. The geochemical data suggest that there was likely a first pulse of primitive Cr-spinel bearing magma and later pulses of slightly more evolved magma. The CLG magmas crystallized before the point of clinopyroxene saturation and display a predominantly bottom up fractionation with a minor top down fractionation from the now eroded roof of the intrusion. In contrast, the MMD was a closed system and likely formed from a single pulse of magma, with textural and geochemical attributes that are consistent with uninterrupted progressive fractionation. The MMD is characterised by a fractionation sequence where clinopyroxene and Fe-Ti oxide became saturated and crystallized as cumulus grains with the most evolved samples containing high abundances of quartz and K-feldspar. Geochemistry and mineral composition data from this study as well as the surface expression of the MMD which shows a central core of more evolved rocks, suggest that there was both inward as well bottom up fractionation of the magma.

The consistent presence of a negative Nb anomaly in both intrusions suggests that there was a pervasive contamination of both magmas at depth by either Archean crust or SCLM. In addition, localized contamination by the Rove Formation either during or after emplacement is suggested by the geochemical signatures of increased La/Sm_n and Th/Yb primarily in the Upper Zones of each intrusion. Crustal contamination, as a result of assimilation and/or devolatilization of the sulphide bearing Rove Formation suggested by the higher than mantle $\delta^{34}S$ and S/Se values of the sulphides of the CLG resulted in the intrusion becoming sulphur saturated early during the emplacement of the magma. The MMD drill core did not contain sulphide mineralization at depth, but with the absence of a lower contact the possibility of a hidden mineralized zone exists.

The relationship between the CLG/MMD and the MCR needs further study as uncertainties and discrepancies still remain. The emplacement ages determined by Heaman et al. (2007) and Hollings et al. (2010) of 1099.6 ± 1.2 Ma and 1109.3 ± 6.3 Ma for the CLG and MMD respectively, are not consistent with the data gathered in this study. Given that the CLG and MMD are proposed, in this study, to have been derived from the same source and staging chamber, it is unlikely that this source was active for 9.7 ± 7.5 million years suggested by the geochronology, as this is a very long period of time for a magma chamber to remain active (Cawthorn and Walraven, 1998). It also seems unlikely that two separate magma sources 9.7 ± 7.5 million years apart, in an evolving rift system, produced two geochemically nearly identical magmas that were emplaced with a close spatial relationship and similar orientation with the same N polarity. Because some surface samples had slightly lower La/Sm_n values than drill core samples, it is possible that the age for the MMD does not reflect the true age of the main intrusion, which could be tested with additional geochronology analysis.

Previous studies have suggested that the CLG is related to the Layered Series intrusions of the Duluth Complex (e.g., Cogulu, 1993a,b; Eckstrand, 1996; Thomas, 2015) which was emplaced ~ 1099.0 ± 0.5. In contrast, Cundari (2012) suggested that the MMD shared the same magma source as the Pigeon and Cloud River dykes, which have emplacement ages of 1141 ± 20 Ma/1078 ± 3 Ma and 1109.2 ± 4.2 Ma, respectively. Hollings et al. (2010) questioned the reliability of the Pigeon River dyke age as the analysis that determined 1141 ± 20 Ma was discordant (4 to 12%) and the 1078 ± 3 Ma age was based on a single analysis. Davis and Green (1997) observed that MCR related rocks older than 1105 Ma have a R polarity, which is not consistent with the N polarities of the Cloud River dykes and MMD. The geochemical similarities of the CLG and MMD to the Layered Series intrusions of the Duluth Complex and the Pigeon River and Cloud River dykes as well as apparent discrepancies of the cross-cutting relationships, paleomagnetism, and geochronology of the

Logan Basin rocks including the CLG and MMD, leave uncertainties remaining on their relation to the MCR.

Additional work, including radiogenic and stable isotope analyses may provide insight into the extent and sources of contamination of the two intrusions. This could be combined with further study of recent and/or re-analysing historic core in order to fully investigate the lateral extent of the horizons identified in the CLG. Additional geochronological analysis of the Logan Basin dyke sets and the CLG is required to resolve the apparent discrepancies found in this and other studies.

REFERENCES

Addison, W.D., Brumpton, G.R., Vallini, D.A., McNaughton, N.J., Davis, D.W., Kissin, S.A., Fralick, P.W. and Hammond, A.L. (2005) Discovery of distal ejecta from the 1850 Ma Sudbury impact event. Geology 33, 193-196.

Arcuri, T., Ripley, E.M. and Hauck, S.A. (1998) Sulfur and oxygen isotope studies of the interaction between pelitic xenoliths and basaltic magma at the Babbitt and Serpentine Cu-Ni deposits, Duluth Complex, Minnesota. Economic Geology 93, 1063-1075.

Barnes, S.J. (1986) The effect of trapped liquid crystallization on cumulus mineral compositions in layered intrusions. Contributions to Mineralogy and Petrology 93, 524-531.

Benkó, Z., Mogessie, A., Molnár, F., Severson, M.J., Hauck, S.A. and Raič, S. (2015) Partial Melting Processes and Cu-Ni-PGE Mineralization in the Footwall of the South Kawishiwi Intrusion at the Spruce Road Deposit, Duluth Complex, Minnesota. Economic Geology 110, 1269-1293.

Berg, J.H. and Klewin, K.W. (1988) High-MgO lavas from the Keweenawan midcontinent rift near Mamainse Point, Ontario. Geology 16, 1003-1006.

Bond, G. C., Lewis, S. D., Taber, J., Steckler, M. S. and Kominz, M. A. (1988) Evidence for formation of a flexural backarc basin by compression and crustal thickening in the central Alaska Peninsula. Geology 16, 1147-1150.

Boudreau, A.E. (1999) PELE—a version of the MELTS software program for the PC platform. Computers & Geosciences 25, 201-203.

Brown, G. and Vincent, E. (1963) Pyroxenes from the late stages of fractionation of the Skaergaard intrusion, East Greenland. Journal of Petrology 4, 175-197.

Campbell, I. (1987) Distribution of orthocumulate textures in the Jimberlana Intrusion. The Journal of Geology 95, 35-53.

Campbell, I. and Naldrett, A. (1979) The influence of silicate: sulfide ratios on the geochemistry of magmatic sulfides. Economic Geology 74, 1503-1506.

Cannon, W.F. (1992) The Midcontinent rift in the Lake Superior region with emphasis on its geodynamic evolution. Tectonophysics 213, 41-48.

Card, K. (1990) A review of the Superior Province of the Canadian Shield, a product of Archean accretion. Precambrian Research 48, 99-156.

Card, K. and Ciesielski, A. (1986) Subdivisions of the Superior Province of the Canadian shield. Geoscience Canada 13, 5-13.

Cawthorn, R.G. (1983) Magma addition and possible decoupling of major-and trace-element behaviour in the Bushveld Complex, South Africa. Chemical Geology 39, 335-345.

Cawthorn, R.G. and Walraven, F. (1998) Emplacement and crystallization time for the Bushveld Complex. Journal of Petrology 39, 1669-1687.

Chalokwu, C.I., Ariskin, A.A. and Koptev-Dvornikov, E.V. (1996) Magma dynamics at the base of an evolving mafic magma chamber: Incompatible element evidence from the Partridge River intrusion, Duluth Complex, Minnesota, USA. Geochimica et cosmochimica acta 60, 4997-5011.

Chalokwu, C.I., Armitage, A.E., Seney, P.J., Wurie, C.A. and Bersch, M. (1995) Petrology of the Freetown Layered Complex, Sierra Leone: Part I. Stratigraphy and Mineral-Chemical Evidence for Multiple Magma Injection. International Geology Review 37, 230-253.

Chalokwu, C.I., Grant, N.K., Ariskin, A.A. and Barmina, G.S. (1993) Simulation of primary phase relations and mineral compositions in the Partridge River intrusion, Duluth Complex, Minnesota: implications for the parent magma composition. Contributions to Mineralogy and Petrology 114, 539-549.

Chung, H.-Y. and Mungall, J.E. (2009) Physical constraints on the migration of immiscible fluids through partially molten silicates, with special reference to magmatic sulfide ores. Earth and Planetary Science Letters 286, 14-22.

Cogulu, E. (1993a) Factors controlling postcumulus compositional changes of chrome-spinels in the Crystal Lake intrusion, Thunder Bay, Ontario. Geological Survey of Canada, Open File 2748, 28.

Cogulu, E. (1993b) Mineralogy and chemical variations of sulphides from the Crystal Lake intrusion, Thunder Bay, Ontario. Geological Survey of Canada, Open File 2749, 21.

Cox, K., Bell, J. and Pankhurst, R. (1979) The interpretation of igneous rocks. Allen and Unwin, London. p. 528.

Cundari, R. (2012) Geology and geochemistry of Midcontinent Rift-related igneous rocks; unpublished M. Sc thesis, Lakehead University, Thunder Bay, Ontario, 153p.

Cundari, R.M., Smyk, M.C., Campbell, D.A. and Puumala, M.A. (2013a) Geology, geochemistry and Cu-Ni-PGE mineralization of the Crystal Lake gabbro; presentation in Copper-nickel-platinum group element deposits of the Lake Superior region, University of Minnesota–Duluth, Precambrian Research Center, 6th Annual Professional Workshop, Duluth, Minnesota.

Cundari, R., Carl, C., Hollings, P. and Smyk, M. (2013b) New and compiled whole-rock geochemical and isotope data of Midcontinent Rift-related rocks. Thunder Bay area: Ontario Geological Survey, Miscellaneous Release Data 308.

Davis, D. and Green, J. (1997) Geochronology of the North American Midcontinent rift in western Lake Superior and implications for its geodynamic evolution. Canadian Journal of Earth Sciences 34, 476-488.

Deer, W.A., Howie, R.A. and Zussman, J. (1992) An introduction to the rock-forming minerals. Longman Scientific & Technical, Hong Kong. p. 680.

Ding, X., Ripley, E.M., Shirey, S.B. and Li, C. (2012) Os, Nd, O and S isotope constraints on country rock contamination in the conduit-related Eagle Cu–Ni–(PGE) deposit, Midcontinent Rift System, Upper Michigan. Geochimica et Cosmochimica Acta 89, 10-30.

Donoghue, K.A., Ripley, E.M. and Li, C. (2014) Sulfur isotope and mineralogical studies of Ni-Cu sulfide mineralization in the Bovine Igneous Complex intrusion, Baraga Basin, Northern Michigan. Economic Geology 109, 325-341.

Droop, G. (1987) A general equation for estimating Fe3+ concentrations in ferromagnesian silicates and oxides from microprobe analyses, using stoichiometric criteria. Mineralogical Magazine 51, 431-435.

Eales, H. and Costin, G. (2012) Crustally contaminated komatiite: primary source of the chromitites and Marginal, Lower, and Critical Zone magmas in a staging chamber beneath the Bushveld Complex. Economic Geology 107, 645-665.

Eckstrand, O. (1996) Magmatic nickel-copper-platinum group elements. Geology of Canadian Mineral Deposit Types, Geology of Canada, 583-614.

Eckstrand, O. and Hulbert, L. (1987) Selenium and the source of sulfur in magmatic nickel and platinum deposits [abs.], Geological Association of Canada-Mineralogical Association Canada Program with Abstracts, p. 40.

Emeleus, C., Cheadle, M., Hunter, R., Upton, B. and Wadsworth, W. (1996) The Rum layered suite, Developments in Petrology. Elsevier. 403-439.

Fazlnia, A., Schenk, V., Appel, P. and Alizade, A. (2013) Petrology, geochemistry, and geochronology of the Chah-Bazargan gabbroic intrusions in the south Sanandaj–Sirjan zone, Neyriz, Iran. International Journal of Earth Sciences 102, 1403-1426.

Foley, D.J. (2011) Petrology and Cu-Ni-PGE mineralization of the Bovine Igneous Complex, Baraga County, Northern Michigan, Unpublished M.Sc. thesis. University of Minnesota Duluth, p. 83.

Fralick, P.W. and Barrett, T.J. (1995). Depositional controls on iron formtion association in Canada. Sedimentary facies analysis. International Association of Sedimentologists, Special Publication No. 22, 35-39.

Fralick, P., Davis, D.W. and Kissin, S.A. (2002) The age of the Gunflint Formation, Ontario, Canada: single zircon U–Pb age determinations from reworked volcanic ash. Canadian Journal of Earth Sciences 39, 1085-1091.

Gao, J.-F. and Zhou, M.-F. (2013) Generation and evolution of siliceous high magnesium basaltic magmas in the formation of the Permian Huangshandong intrusion (Xinjiang, NW China). Lithos 162, 128-139.

Geul, J. (1970) Devon and Pardee townships and the Stuart location. Ontario Deptartment of Mines. Geological Report 87, 31-36.

Geul, J. (1973) Geology of Crooks Township, Jarvis and Prince Locations, and Off-shore Islands, District of Thunder Bay. Ontario Department of Mines Geological Report 102, 46.

Ghiorso, M.S. and Sack, R.O. (1995) Chemical mass transfer in magmatic processes IV. A revised and internally consistent thermodynamic model for the interpolation and extrapolation of liquid-solid equilibria in magmatic systems at elevated temperatures and pressures. Contributions to Mineralogy and Petrology 119, 197-212.

Godel, B., Seat, Z., Maier, W.D. and Barnes, S.-J. (2011) The Nebo-Babel Ni-Cu-PGE sulfide deposit (West Musgrave Block, Australia): Pt. 2. Constraints on parental magma and processes, with implications for mineral exploration. Economic Geology 106, 557-584.

Goldner (2015) Rio Tinto Exploration Canada Inc. Assessment Report On the Cu-Ni-PGE Crystal Lake Project; Pardee, Devon, and Crooks Townships. Thunder Bay Resident Geologist's Office, p. 48.

Goodwin, A.M. (1956) Facies relations in the Gunflint iron formation [Ontario]. Economic Geology 51, 565-595.

Halls, H. and Pesonen, L. (1982) Paleomagnetism of Keweenawan rocks. Geology and tectonics of the Lake Superior Basin. Geological Society of America, Memoir 156, 165-171.

Hart, T. (2005) Precambrian geology of the southern Black Sturgeon River and Seagull Lake area, Nipigon Embayment, northwestern Ontario. Ontario Geological Survey.

Hart, T.R. and MacDonald, C.A. (2007) Proterozoic and Archean geology of the Nipigon Embayment: implications for emplacement of the Mesoproterozoic Nipigon diabase sills and mafic to ultramafic intrusions. Canadian Journal of Earth Sciences 44, 1021-1040.

Heaman, L., Easton, R., Hart, T., Hollings, P., MacDonald, C. and Smyk, M. (2007) Further refinement to the timing of Mesoproterozoic magmatism, Lake Nipigon region, Ontario. Canadian Journal of Earth Sciences 44, 1055-1086.

Heaman, L., Easton, R., Hart, T., MacDonald, C., Fralick, P. and Hollings, P. (2005) Proterozoic history of the Lake Nipigon area, Ontario: constraints from U–Pb zircon and baddeleyite dating, Ontario Exploration and Geoscience Symposium, Abstract

Volume. Ontario Prospectors Association and Northern Ontario Heritage Fund, Toronto, 12-14.

Heggie, G. (2005) Whole rock geochemistry, mineral chemistry, petrology and Pt, Pd mineralization of the Seagull intrusion, northwestern Ontario, Unpublished M.Sc. thesis. Lakehead University. p. 156.

Hemming, S., McLennan, S. and Hanson, G. (1995) Geochemical and Nd/Pb isotopic evidence for the provenance of the Early Proterozoic Virginia Formation, Minnesota. Implications for the tectonic setting of the Animikie Basin. The Journal of Geology 103, 147-168.

Hoffman, P.F. (1987) Early Proterozoic Foredeeps, Foredeep Magmatism, and Superior-Type Iron-Formations of the Canadian Shield. Proterozic Lithospheric Evolution, 85-98.

Hollings, P., Hart, T., Richardson, A. and MacDonald, C.A. (2007a) Geochemistry of the Mesoproterozoic intrusive rocks of the Nipigon Embayment, northwestern Ontario: evaluating the earliest phases of rift development. Canadian Journal of Earth Sciences 44, 1087-1110.

Hollings, P. and Heggie, G. (2014) Rethinking the Midcontinent Rift–puncturing the “plume paradigm”. Proceedings, Institute on Lake Superior Geology, 60th, Part 1, 57.

Hollings, P., Richardson, A., Creaser, R.A. and Franklin, J.M. (2007b) Radiogenic isotope characteristics of the Mesoproterozoic intrusive rocks of the Nipigon embayment, northwestern Ontario. Canadian Journal of Earth Sciences 44, 1111-1129.

Hollings, P., Smyk, M. and Cousens, B. (2012) The radiogenic isotope characteristics of dikes and sills associated with the Mesoproterozoic Midcontinent Rift near Thunder Bay, Ontario, Canada. Precambrian Research 214, 269-279.

Hollings, P., Smyk, M., Heaman, L.M. and Halls, H. (2010) The geochemistry, geochronology and paleomagnetism of dikes and sills associated with the Mesoproterozoic Midcontinent Rift near Thunder Bay, Ontario, Canada. Precambrian Research 183, 553-571.

Holness, M.B., Farr, R. and Neufeld, J.A. (2017) Crystal settling and convection in the Shiant Isles Main Sill. Contributions to Mineralogy and Petrology 172, 7.

Holwell, D.A., Keays, R.R., Firth, E.A. and Findlay, J. (2014) Geochemistry and mineralogy of platinum group element mineralization in the river valley intrusion, Ontario, Canada: a model for early-stage sulfur saturation and multistage emplacement and the implications for “Contact-Type” Ni-Cu-PGE sulfide mineralization. Economic Geology 109, 689-712.

Hoshide, T., Obata, M. and Akatsuka, T. (2006) Crystal settling and crystal growth of olivine in magmatic differentiation− the Murotomisaki Gabbroic Complex, Shikoku, Japan. Journal of Mineralogical and Petrological Sciences 101, 223-239.

Hughes, H.S., Boyce, A.J., McDonald, I., Davidheiser-Kroll, B., Holwell, D.A., McDonald, A. and Oldroyd, A. (2015) Contrasting mechanisms for crustal sulphur contamination of mafic magma: evidence from dyke and sill complexes from the British Palaeogene Igneous Province. Journal of the Geological Society 172, 443-458.

Huppert, H.E. and Sparks, R.S.J. (1989) Chilled margins in igneous rocks. Earth and Planetary Science Letters 92, 397-405.

Hutchinson, D., White, R., Cannon, W. and Schulz, K. (1990) Keweenaw hot spot: geophysical evidence for a 1.1 Ga mantle plume beneath the Midcontinent Rift System. Journal of Geophysical Research: Solid Earth 95, 10869-10884.

Irvine, T. (1982) Terminology for layered intrusions. Journal of Petrology 23, 127-162.

Irvine, T. and Baragar, W. (1971) A guide to the chemical classification of the common volcanic rocks. Canadian journal of earth sciences 8, 523-548.

Johnston, D.T., Poulton, S.W., Fralick, P.W., Wing, B.A., Canfield, D.E. and Farquhar, J. (2006) Evolution of the oceanic sulfur cycle at the end of the Paleoproterozoic. Geochimica et Cosmochimica Acta 70, 5723-5739.

Kissin, S.A., Heggie, G.J., Franklin, J.M. and Somarin, A.K. (2007) Sulfide saturation mechanisms in gabbroic intrusions in the Nipigon Embayment. Canadian Journal of Earth Sciences 44, 1203-1214.

Krogh, T., Davis, D. and Corfu, F. (1984) Precise U-Pb zircon and baddeleyite ages for the Sudbury area, The geology and ore deposits of the Sudbury structure. Ontario: Ontario Geological Survey, pp. 431-446.

Kuno, H. (1968) Origin of andesite and its bearing on the island arc structure. Bulletin Volcanologique 32, 141-176.

Laarman, J.E. (2007) Geochemistry and PGE mineralization of the Kitto intrusion: a product of Mesoproterozoic plume magmatism through fault bounded archean crust, East Nipigon Embayment, Northern Ontario. Unpublished M.Sc. thesis, Lakehead University. p. 213.

Larsen, R. and Brooks, C. (1994) Origin and Evolution of Gabbroic Pegmatites in the Skaergaard Intrusion, East Greenland. Journal of Petrology 35, 1651-1679.

Latypov, R. (2015) Basal reversals in mafic sills and layered intrusions, Layered Intrusions. Springer, pp. 259-293.

Lee, I. and Ripley, E.M. (1996) Mineralogic and Oxygen Isotopic Studies of Open System Magmatie Processes in the South Kawishiwi Intrusion, Spruce Road Area, Duluth Complex, Minnesota. Journal of Petrology 37, 1437-1461.

Lesher, C.M., Burnham, O.M., Keays, R.R., Barnes, S.J. and Hulbert, L. (2001) Trace-element geochemistry and petrogenesis of barren and ore-associated komatiites. The Canadian Mineralogist 39, 673-696.

Leuthold, J., Blundy, J., Holness, M. and Sides, R. (2014) Successive episodes of reactive liquid flow through a layered intrusion (Unit 9, Rum Eastern Layered Intrusion, Scotland). Contributions to Mineralogy and Petrology 168, 1021.

Luolavirta, K., Hanski, E., Maier, W. and Santaguida, F. Characterization and origin of dunitic rocks in the Ni-Cu-(PGE) sulfide ore-bearing Kevitsa intrusion, northern Finland: whole-rock and mineral chemical constraints.

Maier, W.D., Barnes, S.-J., Sarkar, A., Ripley, E., Li, C. and Livesey, T. (2010) The Kabanga Ni sulfide deposit, Tanzania: I. Geology, petrography, silicate rock geochemistry, and sulfur and oxygen isotopes. Mineralium Deposita 45, 419-441.

Maric, M. and Fralick, P. (2005) Sedimentology of the Rove and Virginia Formations and their tectonic significance. Institute of Lake Superior Geology 51, 41-42.

McCuaig, T. C., Kerrich, R., & Xie, Q. (1994). Phosphorus and high field strength element anomalies in Archean high-magnesian magmas as possible indicators of source mineralogy and depth. Earth and Planetary Science Letters 124, 221-239.

Miller, C.F., Furbish, D.J., Walker, B.A., Claiborne, L.L., Koteas, G.C., Bleick, H.A. and Miller, J.S. (2011) Growth of plutons by incremental emplacement of sheets in crystal-rich host: Evidence from Miocene intrusions of the Colorado River region, Nevada, USA. Tectonophysics 500, 65-77.

Miller Jr, J., Green, J., Severson, M., Chandler, V., Hauck, S., Peterson, D. and Wahl, T. (2002) Geology and mineral potential of the Duluth Complex and related rocks of northeastern Minnesota: Minnesota Geological Survey. Report of Investigations 58, 207.

Miller Jr, J. and Ripley, E. (1996) Layered intrusions of the Duluth complex, Minnesota, USA, Developments in Petrology. Elsevier, pp. 257-301.

Monjoie, P., Bussy, F., Lapierre, H. and Pfeifer, H.-R. (2005) Modeling of in-situ crystallization processes in the Permian mafic layered intrusion of Mont Collon (Dent Blanche nappe, western Alps). Lithos 83, 317-346.

Morey, G. and Southwick, D. (1995) Allostratigraphic relationships of Early Proterozoic Iron-formations in the Lake Superior region. Economic Geology 90, 1983-1993.

Morse, S. (1981) Kiglapait geochemistry IV: the major elements. Geochimica et Cosmochimica Acta 45, 461-479.

Morse, S. (1996) Kiglapait mineralogy III: olivine compositions and Rayleigh fractionation models. Journal of Petrology 37, 1037-1061.

Naldrett, A. J. (2010). Secular variation of magmatic sulfide deposits and their source magmas. Economic Geology 105, 669-688.

Namur, O., Charlier, B., Toplis, M.J., Higgins, M.D., Liégeois, J.-P. and Vander Auwera, J. (2010) Crystallization sequence and magma chamber processes in the ferrobasaltic Sept Iles layered intrusion, Canada. Journal of Petrology 51, 1203-1236.

Naslund, H. (1983) Petrology of the Upper Border Series of the Skaergaard intrusion. Journal of Petrology 25, 185-212.

Nicholson, S.W., Schulz, K.J., Shirey, S.B. and Green, J.C. (1997) Rift-wide correlation of 1.1 Ga Midcontinent rift system basalts: implications for multiple mantle sources during rift development. Canadian Journal of Earth Sciences 34, 504-520.

Nicholson, S.W. and Shirey, S.B. (1990) Midcontinent rift volcanism in the Lake Superior region: Sr, Nd, and Pb isotopic evidence for a mantle plume origin. Journal of Geophysical Research: Solid Earth 95, 10851-10868.

Nielsen, T.F. (2004) The shape and volume of the Skaergaard intrusion, Greenland: implications for mass balance and bulk composition. Journal of Petrology 45, 507-530.

North, J. (2000) Nature and distribution of Logan diabase sills and gabbro channels in the Keweenawan rift near Thunder Bay, Ontario. Brief comparison to Noril'sk. Abstract, 46th Institute on Lake Superior Geology, Annual Meeting, Proceedings, pp. 43-44.

Ojakangas, R., Morey, G. and Southwick, D. (2001) Paleoproterozoic basin development and sedimentation in the Lake Superior region, North America. Sedimentary Geology 141, 319-341.

Ojakangas, R.W. and Dickas, A.B. (2002) The 1.1-Ga Midcontinent Rift System, central North America: sedimentology of two deep boreholes, Lake Superior region. Sedimentary Geology 147, 13-36.

Owen-Smith, T. and Ashwal, L. (2015) Evidence for multiple pulses of crystal-bearing magma during emplacement of the Doros layered intrusion, Namibia. Lithos 238, 120-139.

Paces, J.B. and Miller, J.D. (1993) Precise U-Pb ages of Duluth complex and related mafic intrusions, northeastern Minnesota: Geochronological insights to physical, petrogenetic, paleomagnetic, and tectonomagmatic processes associated with the 1.1 Ga midcontinent rift system. Journal of Geophysical Research: Solid Earth 98, 13997-14013.

Pang, K.-N., Li, C., Zhou, M.-F. and Ripley, E.M. (2009) Mineral compositional constraints on petrogenesis and oxide ore genesis of the late Permian Panzhihua layered gabbroic intrusion, SW China. Lithos 110, 199-214.

Parks, W. A. (1925) The Mineral Resources of Northern Ontario. Journal of the Royal Society of Arts, 73, 898-917.

Percival, J., Sanborn-Barrie, M., Skulski, T., Stott, G., Helmstaedt, H. and White, D. (2006) Tectonic evolution of the western Superior Province from NATMAP and Lithoprobe studies. Canadian Journal of Earth Sciences 43, 1085-1117.

Pesonen, L. (1978) Paleomagnetic, paleointensity and paleosecular variation studies on Keweenawan igneous and baked contact rocks. Unpublished Ph.D. thesis. University of Toronto, p.346.

Piispa, E., Smirnov, A. and Pesonen, L. (2011) Paleomagnetism of Midcontinent Rift rocks from the northern shore of Lake Superior (Ontario Canada): Preliminary results, Institute on Lake Superior Geology Proceedings, 57th Annual Meeting, Ashland, WI, p. 65.

Poulton, S.W., Fralick, P.W. and Canfield, D.E. (2004) The transition to a sulphidic ocean ∼ 1.84 billion years ago. Nature 431, 173.

Poulton, S.W., Fralick, P.W. and Canfield, D.E. (2010) Spatial variability in oceanic redox structure 1.8 billion years ago. Nature Geoscience 3, 486.

Pufahl, P. and Fralick, P. (1995) Paleogeographic reconstruction of the Gunflint–Mesabi–Cuyuna depositional system: a basin analysis approach. Proc. Ins. Lake Super. Geol 41, 59-60.

Pufahl, P., Fralick, P. and Scott, J. (2000) Depositional environments of the Paleoproterozoic Gunflint Formation;46th Institute on Lake Superior Geology, v. 46, pt.2, Proceedings with abstracts.

Pufahl, P.K. (1996) Stratigraphic architecture of a Paleoproterozoic iron formation depositional system: the Gunflint, Mesabi and Cuyuna iron ranges. Unpublished M.Sc. thesis. Lakehead University, p. 152.

Pufahl, P.K. and Fralick, P.W. (2004) Depositional controls on Palaeoproterozoic iron formation accumulation, Gogebic Range, Lake Superior region, USA. Sedimentology 51, 791-808.

Pufahl, P.K., Hiatt, E.E. and Kyser, T.K. (2010) Does the Paleoproterozoic Animikie Basin record the sulfidic ocean transition? Geology 38, 659-662.

Pye, E. and Fenwick, K. (1965) Atikokan-Lakehead Sheet, Kenora, Rainy River and Thunder Bay Districts. Ontario Department of Mines. Geological Compilation Series, Map 2065, scale 1 inch = 4 miles.

Queffurus, M. and Barnes, S.-J. (2015) A review of sulfur to selenium ratios in magmatic nickel–copper and platinum-group element deposits. Ore Geology Reviews 69, 301-324.

Ripley, E.M. (2014) Ni-Cu-PGE mineralization in the Partridge River, South Kawishiwi, and Eagle intrusions: A review of contrasting styles of sulfide-rich occurrences in the Midcontinent rift system. Economic Geology 109, 309-324.

Ripley, E.M. and Al-Jassar, T.J. (1987) Sulfur and oxygen isotope studies of melt-country rock interaction, Babbitt Cu-Ni deposit, Duluth Complex, Minnesota. Economic Geology 82, 87-107.

Ripley, E.M., Dong, S., Li, C. and Wasylenki, L.E. (2015) Cu isotope variations between conduit and sheet-style Ni–Cu–PGE sulfide mineralization in the Midcontinent Rift System, North America. Chemical Geology 414, 59-68.

Ripley, E. M., & Li, C. (2003). Sulfur isotope exchange and metal enrichment in the formation of magmatic Cu-Ni-(PGE) deposits. Economic Geology 98, 635-641.

Ripley, E.M. and Li, C. (2013) Sulfide saturation in mafic magmas: is external sulfur required for magmatic Ni-Cu-(PGE) ore genesis? Economic Geology 108, 45-58.

Ripley, E.M., Taib, N.I., Li, C. and Moore, C.H. (2007) Chemical and mineralogical heterogeneity in the basal zone of the Partridge River Intrusion: implications for the origin of Cu–Ni sulfide mineralization in the Duluth Complex, midcontinent rift system. Contributions to Mineralogy and Petrology 154, 35.

Robertson, J., Ripley, E.M., Barnes, S.J. and Li, C. (2015) Sulfur liberation from country rocks and incorporation in mafic magmas. Economic Geology 110, 1111-1123.

Robertson, W. and Fahrig, W. (1971) The great Logan paleomagnetic loop—the polar wandering path from Canadian Shield rocks during the Neohelikian Era. Canadian Journal of Earth Sciences 8, 1355-1372.

Sage, R. P., Lightfoot, P. C., & Doherty, W. (1996). Geochemical characteristics of granitoid rocks from within the Archean Michipicoten Greenstone Belt, Wawa Subprovince, Superior Province, Canada: implications for source regions and tectonic evolution. Precambrian Research 76, 155-190.

Seat, Z., Beresford, S.W., Grguric, B.A., Waugh, R.S., Hronsky, J.M., Gee, M.M., Groves, D.I. and Mathison, C.I. (2007) Architecture and emplacement of the Nebo–Babel gabbronorite-hosted magmatic Ni–Cu–PGE sulphide deposit, West Musgrave, Western Australia. Mineralium Deposita 42, 551.

Shahabi Far, M. (2016) The magmatic and volatile evolution of gabbros hosting the Marathon PGE-Cu deposit: evolution of a conduit system, Earth and Environmental Sciences. Unpublished Ph.D. Thesis, University of Windsor, p. 198.

Shirey, S.B. (1997) Re-Os isotopic compositions of Midcontinent rift system picrites: implications for plume–lithosphere interaction and enriched mantle sources. Canadian Journal of Earth Sciences 34, 489-503.

Shirey, S.B., Berg, J.H. and Carlson, R.W. (1994) Temporal changes in the sources of flood basalts: isotopic and trace element evidence from the 1100 Ma old Keweenawan Mamainse Point Formation, Ontario, Canada. Geochimica et Cosmochimica Acta 58, 4475-4490.

Simonson, B.M. and Hassler, S.W. (1996) Was the deposition of large Precambrian iron formations linked to major marine transgressions? The Journal of Geology 104, 665-676.

Smith, A. and Sutcliffe, R. (1987) Keweenawan intrusive rocks of the Thunder Bay area. Summary of field work, 248-255.

Smith, A. and Sutcliffe, R. (1989) Precambrian Geology, Keweenawan Intrusive Rocks in the Crystal Lake-Pigeon River Area. Ontario Geological Survey. Map 3139, scale 1:50 000.

Sonnenthal, E.L. (1992) Geochemistry of dendritic anorthosites and associated pegmatites in the Skaergaard Intrusion, East Greenland: Evidence for metasomatism by a chlorine-rich fluid. Journal of Volcanology and Geothermal Research 52, 209-230.

Southwick, D.L., Morey, G.B. and Holst, T.B. (1991) Tectonic imbrication and foredeep development in the Penokean Orogen, east-central Minnesota: an interpretation based on regional geophysics and the results of test-drilling. US Geological Survey, p. 17.

Spandler, C. J., Eggins, S. M., Arculus, R. J., & Mavrogenes, J. A. (2000). Using melt inclusions to determine parent-magma compositions of layered intrusions: Application to the Greenhills Complex (New Zealand), a platinum group minerals–bearing, island-arc intrusion. Geology 28, 991-994.

Spandler, C., Mavrogenes, J. and Arculus, R. (2005) Origin of chromitites in layered intrusions: Evidence from chromite-hosted melt inclusions from the Stillwater Complex. Geology 33, 893-896.

Stott, G., Corkery, M., Percival, J., Simard, M. and Goutier, J. (2010) A revised terrane subdivision of the Superior Province. Ontario Geological Survey, Open File Report 6260, 20-21.

Studley, S., Ripley, E., Elswick, E., Dorais, M., Fong, J., Finkelstein, D. and Pratt, L. (2002) Analysis of sulfides in whole rock matrices by elemental analyzer–continuous flow isotope ratio mass spectrometry. Chemical Geology 192, 141-148.

Sun, S. and McDonough, W. (1989) Chemical and isotopic systematics of oceanic basalts: implications for mantle composition and processes. Geological Society, London, Special Publications 42, 313-345.

Talusani, R.V., Sivell, W.J. and Ashley, P.M. (2005) Mineral chemistry, petrogenesis, and tectonic setting of the Wateranga layered intrusion, southeast Queensland, Australia. Canadian Journal of Earth Sciences 42, 1967-1985.

Tanton, T.L. (1931) Fort William and Port Arthur, and Thunder cape map-areas: Thunder bay district, Ontario. Map 354A, scale 1:63360.

Tanton, T.L. (1935) Pigeon River area, Thunder Bay District. Geological Survey of Canada, Sheet 1. Map 354A, scale 1:63360.

Tanton, T.L. (1936) Pigeon River area, Thunder Bay District. Geological Survey of Canada, Sheet 2. Map 355A, scale 1:63360.

Taranovic, V., Ripley, E.M., Li, C. and Rossell, D. (2015) Petrogenesis of the Ni–Cu–PGE sulfide-bearing Tamarack Intrusive Complex, Midcontinent Rift System, Minnesota. Lithos 212, 16-31.

Tegner, C. (1997) Iron in plagioclase as a monitor of the differentiation of the Skaergaard intrusion. Contributions to Mineralogy and Petrology 128, 45-51.

Tegner, C., Cawthorn, R.G. and Kruger, F.J. (2006) Cyclicity in the Main and Upper Zones of the Bushveld Complex, South Africa: crystallization from a zoned magma sheet. Journal of Petrology 47, 2257-2279.

Thomas, B. (2015) Geochemistry, sulfur isotopes, and petrography of the Cu-Ni-PGE mineralized Crystal Lake Intrusion, Thunder Bay, Ontario. Unpublished M.Sc. Thesis, Indiana University, p. 49.

Van Schmus, W. (1992) Tectonic setting of the Midcontinent Rift system. Tectonophysics 213, 1-15.

Vervoort, J.D., Wirth, K., Kennedy, B., Sandland, T. and Harpp, K.S. (2007) The magmatic evolution of the Midcontinent rift: New geochronologic and geochemical evidence from felsic magmatism. Precambrian Research 157, 235-268.

Wager, L.R. (1960) The major element variation of the layered series of the Skaergaard intrusion and a re-estimation of the average composition of the hidden layered series and of the successive residual magmas. Journal of Petrology 1, 364-398.

Wager, L.R. and Brown, G.M. (1967) Layered igneous rocks. Oliver and Boyd, Edinburgh, p. 588.

Wager, L.R. and Deer, W.A. (1939) Geological investigations in East Greenland, Part III. The petrology of the Skaergaard Intrusion, Kangerdlugssuaq, East Greenland. Meddr. Gronland 105, p. 352.

Wells, K. (1998) Assessment Report on the 1998 Linecutting and Ground Magnetic Survey: Pigeon River Area, Crooks Townships, Thunder Bay Mining District. Thunder Bay Resident Geologist's Office File 52A04SE2002, 9.

White, C.M. (2007) The Graveyard Point Intrusion: An example of extreme differentiation of Snake River Plain Basalt in a shallow crustal pluton. Journal of Petrology 48, 303-325.

Wiebe, R. and Snyder, D. (1993) Slow, dense replenishments of a basic magma chamber: the layered series of the Newark Island layered intrusion, Nain, Labrador. Contributions to Mineralogy and Petrology 113, 59-72.

Williams, H., Stott, G., Heather, K., Muir, T. and Sage, R. (1990) Wawa subprovince. Geology of Ontario, Ontario Geological Survey, Special Volume 4, 485-541.

Wilson, A.H. (1991) The geology of the Great Dyke, Zimbabwe: Crystallization, layering, and cumulate formation in the P1 Pyroxenite of cyclic unit 1 of the Darwendale Subchamber. Journal of Petrology 33, 611-663.

Wilson M. (1989) Igneous Petrogenesis. A Global Tectonic Approach. Harper Collins Academic. London, p. 466.

Zieg, M. and Marsh, B. (2012) Multiple reinjections and crystal-mush compaction in the Beacon Sill, McMurdo Dry Valleys, Antarctica. Journal of Petrology 53, 2567-2591.

Zieg, M.J. (2014) Petrologic evolution of a Nipigon diabase sill, Ontario, Canada: insights from compositional and textural profiles. Economic Geology 109, 1383-1401.

APPENDIX A – THIN SECTION DESCRIPTIONS

CRYSTAL LAKE GABBRO THIN SECTION DESCRIPTIONS

Sample: CLG-1	**Depth: 9.5 m**	**Rock Type: Gabbro**		
Mineral	Abundance	Habit	Grain Size	Comments
Plagioclase	43	Anhedral-subhedral	Fine to medium W=.5-2 mm L=<2 mm	Generally anhedral, although local subhedral grains exist. Majority are equidimensional (i.e. L=W). Minor zoning present. Moderate sericite alteration (~40%).
Pyroxene	30	?	?	Complete alteration by interlayered medium grained sheafs of amphibole-uralite-biotite-chlorite. Biotite and amphibole could also be primary accessory phases in some cases (1/3 of total).
Quartz/ Granophyre	10/10	Anhedral	Fine to Medium	Both free quartz and granophyre occurs interstitially to plagioclase. Quartz locally forms aggregates of fine sized grains also locally is found in thin <0.5 mm veins.
Fe-Ti oxides	5	Anhedral-subhedral	Fine	Occurs as equant round grains (Cr-spinel) as well as bladed and irregular shaped amoeboidal and subpoikilitic grains, found interstitially to plagioclase.
Sulphides	2	Anhedral	Fine	Evenly distributed disseminated blebs throughout, also included in plagioclase. Pyrrhotite dominant, trace chalcopyrite.
General Comments: This sample is largely equigranular, non-foliated, and is moderately to strongly altered overall. The habit of pyroxene can not be determined (i.e. granular, subophitic, ophitic) due to the complete alteration. Sericite alteration of the plagioclase is not uniform, some grains have as low as 10% alteration where other grains are completely altered to sericite. The presence of sulphides and quartz/granophyre as well				

as the strong alteration suggests, that this rock contains assimilated and recrystalized material from the surrounding Rove Formation sedimentary country rocks.				
Sample: CLG-2	**Depth: 20.5 m**	**Rock Type: Augite troctolite**		
Mineral	Abundance	Habit	Grain Size	Comments
Plagioclase	70	Subhedral	Fine to medium W=0.5-1.5mm L= <5 mm	Cumulus grains. Generally subhedral, although some anhedral grains exist. Seriate distribution of grain size. Strong sericite alteration (~75%)
Olivine	15	Anhedral?	Medium (2-5 mm)	Cumulus grains. Complete alteration by serpentine + oxide. Individual relict grain boundaries can not be determined in some areas.
Pyroxene	8	Subophitic ?	Fine to medium?	Complete alteration by chlorite-uralite-actinolite.
Fe-Ti Oxides	2	Anhedral	Fine	Bladed and irregular shaped amoeboidal and subpoikilitic grains, found interstitially to plagioclase.
Sulphides	5	Anhedral	Fine to medium (<0.5-5mm)	One large bleb of fractured pyrrhotite (5 mm). The remaining sulphides are fine grained blebs and irregular shaped amoeboidal and subpoikilitic pyrrhotite and minor chalcopyrite found interstitially to plagioclase.
General Comments: This sample is medium grained, seriate, sulphidic, non-foliated, and is strongly altered overall. Although the pyroxene has been completely altered to chlorite-uralite-actinolite, the texture does resemble being subophitic. Sericite alteration of the plagioclase is not uniform, some grains have as low as 10% alteration where other grains are completely altered to sericite. Several types of fibrous and non-fibrous zeolites present directly adjacent to the large sulphide bleb. Very strong alteration within a ~1cm radius of the bleb.				
Sample: CLG-3	**Depth: 28.0 m**	**Rock Type: Layered melagabbro and troctolite**		
Mineral	Abundance	Habit	Grain Size	Comments
Top				

Plagioclase	33	Subhedral	Medium to coarse W=0.5-3 mm L= <10 mm	Cumulus grains. Randomly orientated, patchy variable, overall moderate, sericite alteration (50%). Local patches of zeolite alteration. Tabular shaped grains.
Clinopyroxene	65	Ophitic	Coarse (<20 mm)	Two large ophitic oikocrysts wholly enclose plagioclase grains. Fracturing is present, high birefringent material fills wider (0.1 mm) fractures. Largely unaltered (~5% uralite-chlorite-actinolite).
Fe-Ti Oxide	2	Anhedral	Fine to medium	Irregular shaped amoeboidal and subpoikilitic grains.
Bottom				
Plagioclase	57	Subhedral	Fine W=0.1-0.5 mm L=<1.5 mm	Cumulus grains. Randomly orientated, largely unaltered in most of slide (~5% sericite), moderately altered close to contact (40%). Zoning is common. Elongated lath shaped grains.
Olivine	30	Subhedral	Fine (0.2-0.5 mm)	Cumulus grains. Highly variable alteration, patches where grains are completely pseudomorphed by either iddingsite (most common) or talc+chlorite (less common). Other areas have grains that are unaltered. 60% of grains altered (strong alteration close to contact), 40% unaltered.
Clinopyroxene	10	Subophitic	Coarse (<10 mm)	Optically continuous subophitic, largely unaltered (~5%)
Fe-Ti oxide	3	Anhedral	Fine	Irregular shaped amoeboidal and subpoikilitic grains interstitial to plagioclase.
General Comments: This sample contains a distinct abrupt contact between two layers with regards to plagioclase grainsize reduction and sudden presence/absence of olivine,				

however clinopyroxene does remain optically continuous on either side of the contact. Alteration is stronger closer to contact but overall weak to moderate.				
Sample: CLG-4	**Depth: 38.4 m**	**Rock Type: Troctolite**		
Mineral	Abundance	Habit	Grain Size	Comments
Plagioclase	60	Subhedral	Fine to medium W=0.2-1.5 mm L=<4mm	Cumulus grains. Randomly orientated, seriate size distribution. Largely unaltered (~5% sericite). Zoning fairly common. Mostly tabular shaped grains.
Olivine	28	Anhedral	Medium to coarse (5-20mm)	Cumulus grains. Highly irregular shaped amoeboidal grains. Contains intergrown grains of plagioclase. Weak iddingsite alteration (~15%), in the form of fracture filling and strongest at grain boundaries.
Clinopyroxene	9	Subophitic	Medium (<5mm)	Occurs as discrete interstitial subophitic grains. Unaltered
Granophyre/ Free Quartz	2	Anhedral	Fine	Irregular shaped interstitial to plagioclase.
Fe-Ti Oxide	1	Anhedral	Fine	Irregular shaped amoeboidal and subpoikilitic grains interstitial to plagioclase.
General Comments: This sample is non-foliated, medium to coarse grained, seriate size distributed, and is very weakly altered				
Sample: CLG-5	**Depth: 64.5 m**	**Rock Type: Olivine melagabbro**		
Mineral	Abundance	Habit	Grain Size	Comments
Plagioclase	40	Subhedral	Fine to medium W=0.1-1.5 mm L=<3.5 mm	Cumulus grains. Randomly orientated, seriate size distribution. Weakly altered (~10% sericite). Zoning fairly common. Mostly elongated lath shaped grains, minor tabular.
Clinopyroxene	27	Ophitic	Coarse (<20 mm)	Large optically continuous ophitic oikocrysts. Weak uralite alteration (~5%).

Olivine	20	Anhedral	Medium to coarse (1-7 mm)	Cumulus grains. Weak iddingsite alteration (~15%), in the form of fracture filling.
Granophyre/ Free Quartz	6	Anhedral	Fine to medium	Irregular shaped interstitial to plagioclase.
Fe-Ti oxides	4	Anhedral	Fine to medium	Irregular shaped amoeboidal and subpoikilitic grains interstitial to plagioclase.
Accessory/ Alteration Assemblage	3	Anhedral	Fine	Patches of biotite + amphibole + chlorite + apatite + actinolite found interstitially to the plagioclase.
General Comments: This sample is non-foliated, medium to coarse grained, seriate size distributed, and is weakly altered.				
Sample: CLG-6	**Depth: 75.2 m**	**Rock Type: Gabbro**		
Mineral	Abundance	Habit	Grain Size	Comments
Plagioclase	50	Subhedral	Fine to medium W=0.2-2 mm L=<5 mm	Cumulus grains. Randomly orientated, seriate size distribution. Weakly altered (~10% sericite). Zoning fairly common. Mostly elongated lath shaped grains, minor tabular.
Clinopyroxene	34	Ophitic	Coarse (>20 mm)	Large optically continuous ophitic oikocrysts. Weak uralite alteration (~5%).
Olivine	10	Anhedral-Subhedral	Medium to coarse (2-7 mm)	Cumulus grains. Weak iddingsite alteration (~15%), in the form of fracture filling. Some are highly irregular shaped amoeboidal grains.
Fe-Ti Oxides	2	Anhedral	Fine	Irregular shaped amoeboidal and subpoikilitic grains interstitial to plagioclase.
Granophyre/ Free Quartz	1	Anhedral	Fine	Irregular shaped interstitial to plagioclase.
Accessory/ Alteration Assemblage	3	Anhedral	Fine	Patches of biotite + amphibole + chlorite + apatite + actinolite found interstitially to the plagioclase.

General Comments: This sample is non-foliated, medium to coarse grained, seriate size distributed, and is weakly altered.				
Sample: CLG-7	**Depth: 81.3 m**	**Rock Type: Gabbro**		
Mineral	Abundance	Habit	Grain Size	Comments
Plagioclase	60	Subhedral	Fine to coarse W=0.2-4 mm L=<10 mm	Cumulus grains. Poorly foliated, seriate size distribution. Moderate altered (~35% sericite). Zoning fairly common. Mostly elongated lath shaped grains, minor tabular.
Clinopyroxene	30	Anhedral-Subophitic	Medium to coarse (4-13mm)	Occurs as both subophitic grains as well as individual anhedral grains. There is a weak dusting? of uralite alteration.
Fe-Ti Oxides	2	Anhedral	Fine	Irregular shaped amoeboidal and subpoikilitic grains interstitial to plagioclase.
Accessory/ Alteration Assemblage	8	Anhedral	Fine	Patches of biotite + amphibole + chlorite + apatite + actinolite found interstitially to the plagioclase.
General Comments: This sample is poorly foliated, medium to coarse grained, seriate size distributed, and is moderately altered.				
Sample: CLG-8	**Depth: 113.4 m**	**Rock Type: Augite troctolite**		
Mineral	Abundance	Habit	Grain Size	Comments
Plagioclase	60	Subhedral	Fine to medium W=0.2-2 mm L=<6 mm	Cumulus grains. Randomly orientated, seriate size distribution. Weakly altered (~10% sericite). Zoning fairly common. Mostly elongated lath shaped grains, minor tabular.
Olivine	20	Anhedral	Medium to coarse (1-5 mm)	Cumulus grains. Weak iddingsite alteration (~15%), in the form of fracture filling.

Clinopyroxene	15	Subophitic Anhedral	Medium to coarse (2-8mm)	Clots of subophitic clinopyroxene, not optically continuous with one another weak uralite alteration (~10%). There are minor amounts of intergranular anhedral grains.
Fe-Ti Oxides	2	Anhedral	Fine	Irregular shaped amoeboidal and subpoikilitic grains interstitial to plagioclase.
Accessory/ Alteration Assemblage	3	Anhedral	Fine	Patches of biotite + amphibole + chlorite + apatite + actinolite + quartz found interstitially to the plagioclase. Trace granophyre also present.
General Comments: This sample is non-foliated, medium to coarse grained, seriate size distributed, and is weakly altered.				
Sample: CLG-9	**Depth: 146.8 m**	**Rock Type: Olivine gabbro**		
Mineral	Abundance	Habit	Grain Size	Comments
Plagioclase	58	Subhedral	Fine to medium W=0.2-2 mm L=<5 mm	Cumulus grains. Randomly orientated, seriate size distribution. Weakly altered (~15% sericite). Zoning fairly common. Mostly elongated lath shaped grains, very minor tabular.
Olivine	15	Anhedral-subhedral	Medium (1-3 mm)	Cumulus grains. Weak iddingsite alteration (~20%), in the form of fracture filling. Talc alteration on rims are fairly common.
Clinopyroxene	20	Ophitic	Coarse (>30 mm)	Large optically continuous ophitic oikocryst. Weak uralite alteration (~10%).
Fe-Ti Oxides	4	Anhedral	Fine	Irregular shaped amoeboidal and subpoikilitic grains interstitial to plagioclase.
Accessory/ Alteration Assemblage	3	Anhedral	Fine	Patches of biotite + amphibole + chlorite + apatite + actinolite found

				interstitially to the plagioclase.
General Comments: This sample is non-foliated, medium to coarse grained, seriate size distributed, and is weakly altered. Note quartz and granophyre are not present in this sample. Intensity of sericite alteration is variable with patches of moderate alteration (~60%).				
Sample: CLG-10	**Depth: 162.6 m**	**Rock Type: Gabbro**		
Mineral	Abundance	Habit	Grain Size	Comments
Plagioclase	65	Subhedral	Fine to medium W=0.1-1.5 mm L=<5 mm	Cumulus grains. Randomly orientated, seriate size distribution. moderately altered (~50/30% sericite). Zoning fairly common. Mostly elongated lath shaped grains, minor tabular.
Clinopyroxene	20	Ophitic	Coarse (>20 mm)	Large optically continuous ophitic oikocrysts. Weak uralite alteration (~5%).
Zeolite	7	Anhedral	Fine	Irregular shaped interstitial to plagioclase. Consists of aggregates of radially extincting grains with low to moderate birefringence
Fe-Ti oxides	5	Anhedral	Fine to medium	Irregular shaped amoeboidal and subpoikilitic grains interstitial to plagioclase. There is one coarse grain in the section.
Accessory/ Alteration Assemblage	3	Anhedral	Fine	Patches of biotite + amphibole + chlorite + apatite + actinolite found interstitially to the plagioclase.
General Comments: This sample is non/moderately foliated, medium to coarse grained, seriate size distributed, and is weak-moderately altered. This sample has two distinct areas, one being where ophitic clinopyroxene dominates and the other where clinopyroxene is largely absent. In the latter area, interstitial to the plagioclase grains is the same assemblage of accessory/alteration minerals but also contains an abundance of zeolites. Also in that area, the plagioclase grains are non-foliated and sericite alteration is moderate in in general (50%), replacing up to 100% in some patches. The clinopyroxene dominated area the plagioclase grains are moderately foliated and weakly altered (30%).				

Sample: CLG-11	**Depth: 198.8 m**	**Rock Type: Augite troctolite**		
Mineral	Abundance	Habit	Grain Size	Comments
Plagioclase	70	Subhedral	Fine to medium W=0.2-1.5 mm L=<4 mm	Cumulus grains. Poorly foliated, seriate size distribution. Weakly altered (~10% sericite). Zoning fairly common. Mostly elongated lath shaped grains, minor tabular.
Olivine	16	Anhedral Subhedral	Medium (1-4 mm)	Cumulus grains. Weak talc/iddingsite alteration (~25%), in the form of fracture filling.
Clinopyroxene	8	Subophitic	Medium to coarse (4-10mm)	Clots of subophitic clinopyroxene, optically continuous weak uralite alteration (~10%).
Fe-Ti Oxides	4	Anhedral	Fine	Irregular shaped amoeboidal and subpoikilitic grains interstitial to plagioclase.
Accessory/ Alteration Assemblage	2	Anhedral	Fine	Patches of biotite + amphibole + chlorite + apatite + actinolite + quartz found interstitially to the plagioclase.
General Comments: This sample is poorly foliated, medium grained, seriate size distributed, and is weakly altered.				
Sample: CLG-12	**Depth: 218.6 m**	**Rock Type: Olivine gabbro**		
Mineral	Abundance	Habit	Grain Size	Comments
Plagioclase	68	Subhedral	Fine to medium W=0.2-1.5 mm L=<4 mm	Cumulus grains. Randomly orientated, seriate size distribution. Weakly altered (~15% sericite). Zoning fairly common. Elongated lath shaped grains.
Olivine	20	Anhedral	Medium (1-3 mm)?	Cumulus grains. Complete alteration by 90% talc and 10% iddingsite.
Clinopyroxene	8	Subophitic	Medium to coarse	Clots of subophitic clinopyroxene, optically

			(<10mm)	continuous weak uralite alteration (~10%).
Fe-Ti Oxides	2	Anhedral	Fine	Irregular shaped amoeboidal and subpoikilitic grains interstitial to plagioclase.
Accessory/ Alteration Assemblage	2	Anhedral	Fine	Patches of biotite + amphibole + chlorite + apatite + actinolite found interstitially to the plagioclase.
General Comments: This sample is non-foliated, medium grained, seriate size distributed, and is overall moderately altered.				
Sample: CLG-13	**Depth: 250.4 m**	**Rock Type: Olivine gabbro**		
Mineral	Abundance	Habit	Grain Size	Comments
Plagioclase	65	Subhedral	Fine to medium W=0.2-1.5 mm L=<4 mm	Cumulus grains. Poorly foliated, seriate size distribution. Weakly altered (~10% sericite). Zoning fairly common. Elongated lath shaped grains, minor tabular.
Olivine	15	Anhedral	Medium (1-4 mm)	Cumulus grains. Moderate iddingsite alteration in the form of fracture filling (25%). Talc alteration also present found mostly on rims of grains.
Clinopyroxene	16	Ophitic	Coarse (<20mm)	Large optically continuous ophitic oikocryst. Weak uralite alteration (~15%).
Fe-Ti Oxides	2	Anhedral	Fine	Irregular shaped amoeboidal and subpoikilitic grains interstitial to plagioclase.
Accessory/ Alteration Assemblage	2	Anhedral	Fine	Patches of biotite + amphibole + chlorite + apatite + actinolite found interstitially to the plagioclase.
General Comments: This sample is poorly foliated, medium grained, seriate size distributed, and is overall weakly altered.				

Sample: CLG-14	**Depth: 284.4 m**	**Rock Type: Olivine gabbro**		
Mineral	Abundance	Habit	Grain Size	Comments
Plagioclase	65	Subhedral	Fine to medium W=0.2-1 mm L=<3 mm	Cumulus grains. Poorly foliated, seriate size distribution. Weakly altered (~10% sericite). Zoning fairly common. Elongated lath shaped grains.
Olivine	10	Anhedral	Medium (1-4 mm)	Cumulus grains. Moderate iddingsite alteration in the form of fracture filling (25%). Talc alteration also present found mostly on rims of grains.
Clinopyroxene	19	Ophitic	Coarse (>20mm)	Large optically continuous ophitic oikocrysts. Weak uralite alteration (~15%).
Fe-Ti Oxides	4	Anhedral	Fine	Irregular shaped amoeboidal and subpoikilitic grains interstitial to plagioclase.
Accessory/ Alteration Assemblage	2	Anhedral	Fine	Patches of biotite + amphibole + chlorite + apatite + actinolite found interstitially to the plagioclase.
General Comments: This sample is poorly foliated, medium grained, seriate size distributed, and is overall weakly altered.				
Sample: CLG-15	**Depth: 306.0 m**	**Rock Type: Olivine gabbro**		
Mineral	Abundance	Habit	Grain Size	Comments
Plagioclase	59	Subhedral	Fine to medium W=0.1-0.7 mm L=<2.5 mm	Cumulus grains. Poorly foliated, seriate size distribution. Weakly altered (~10% sericite). Zoning fairly common. Elongated lath shaped grains.
Olivine	14	Subhedral	Medium (1-3.5 mm)	Cumulus grains. Moderate iddingsite alteration in the form of fracture filling (15%). Talc alteration also

				present found mostly on rims of grains.
Clinopyroxene/ Orthopyroxene	19/3	Ophitic	Coarse (<15mm)	Large optically continuous ophitic oikocrysts. Weak uralite alteration (~15%). One subophitic grain (6 mm) of orthopyroxene.
Fe-Ti Oxides	3	Anhedral	Fine	Irregular shaped amoeboidal and subpoikilitic grains interstitial to plagioclase.
Accessory/ Alteration Assemblage	1	Anhedral	Fine	Patches of biotite + amphibole + chlorite + apatite + actinolite found interstitially to the plagioclase.
General Comments: This sample is poorly foliated, medium to coarse grained, seriate size distributed, and is overall weakly altered.				
Sample: CLG-16	**Depth: 313.4 m**	**Rock Type: Leucogabbro**		
Mineral	Abundance	Habit	Grain Size	Comments
Plagioclase	65	Anhedral Subhedral	Fine to medium W=0.1-1.5 mm L=<4 mm	Cumulus grains. Randomly orientated, seriate size distribution. moderately altered (~70/30% sericite). Zoning fairly common. Mostly elongated lath shaped grains, minor tabular.
Clinopyroxene	20	Ophitic	Coarse (<15 mm)	Large optically continuous ophitic oikocrysts. Moderate uralite alteration (~40%).
Zeolite	9	Anhedral	Fine	Irregular shaped interstitial to plagioclase. Consists of aggregates of radially extincting grains with low to moderate birefringence
Fe-Ti oxides	5	Anhedral	Fine to medium	Irregular shaped amoeboidal and subpoikilitic grains interstitial to plagioclase. There is one coarse grain in the section.
Accessory/ Alteration Assemblage	1	Anhedral	Fine	Patches of biotite + amphibole + chlorite + apatite + actinolite found

				interstitially to the plagioclase.
General Comments: This sample is non-foliated, medium to coarse grained, seriate size distributed, and is moderate to heavily altered. This sample has two distinct areas, one being where ophitic clinopyroxene dominates and the other where clinopyroxene is largely absent. In the latter area, alteration is heavy, interstitial to the plagioclase grains is dominated by zeolites. The zeolites alteration also propagates into plagioclase grains, which are also heavily sericitized. The clinopyroxene dominated area displays moderate alteration of both the plagioclase and clinopyroxene.				
Sample: CLG-17	**Depth: 329.6 m**	**Rock Type: Gabbro**		
Mineral	Abundance	Habit	Grain Size	Comments
Plagioclase	55	Anhedral Subhedral	Fine to medium W=0.1-1.5 mm L=<9 mm	Cumulus grains. Moderately foliated, seriate size distribution. Weakly altered (~15 sericite). Zoning fairly common. Mostly elongated lath shaped grains.
Clinopyroxene	31	Ophitic	Coarse (<25 mm)	Large optically continuous ophitic oikocrysts. Weak uralite alteration (~10%).
Olivine	10	Anhedral	Medium (1-3 mm)	Cumulus grains. Moderate iddingsite alteration in the form of fracture filling (25%).
Fe-Ti oxides	3	Anhedral	Fine to medium	Irregular shaped amoeboidal and subpoikilitic grains interstitial to plagioclase.
Accessory/ Alteration Assemblage	1	Anhedral	Fine	Patches of biotite + amphibole + chlorite + apatite + actinolite found interstitially to the plagioclase.
General Comments: This sample is moderately foliated, medium to coarse grained, seriate size distributed, and is overall weakly altered.				
Sample: CLG-18	**Depth: 392.5 m**	**Rock Type: Augite troctolite**		
Mineral	Abundance	Habit	Grain Size	Comments
Plagioclase	63	Anhedral Subhedral	Fine to medium	Cumulus grains. Randomly orientated, seriate size distribution. Weakly altered

			W=0.1-1.5 mm L=<3 mm	(~15 sericite). Zoning fairly common. Mostly elongated lath shaped grains.
Clinopyroxene	14	Subophitic	Medium to Coarse (<10 mm)	Discrete interstitial pockets of subophitic grains. Weak uralite alteration (~10%). Also present is minor serpentine alteration.
Olivine	17	Subhedral Anhedral	Medium (1-2.5 mm)	Cumulus grains. Moderate iddingsite alteration in the form of fracture filling (15%). Also present is minor serpentine alteration.
Fe-Ti oxides	4	Anhedral	Fine to medium	Irregular shaped amoeboidal and subpoikilitic grains interstitial to plagioclase.
Accessory/ Alteration Assemblage	2	Anhedral	Fine	Patches of biotite + amphibole + chlorite + apatite + actinolite found interstitially to the plagioclase.
General Comments: This sample is non-foliated, medium to coarse grained, seriate size distributed, and is overall weakly altered.				
Sample: CLG-19	**Depth: 419.8 m**	**Rock Type: Augite troctolite**		
Mineral	Abundance	Habit	Grain Size	Comments
Plagioclase	60	Anhedral Subhedral	Fine to medium W=0.1-1.5 mm L=<3 mm	Cumulus grains. Poorly foliated, seriate size distribution. Weakly altered (~20 sericite). Zoning fairly common. Elongated lath shaped grains.
Clinopyroxene/ Orthopyroxene	16/1	Ophitic	Medium to Coarse (<15 mm)	Discrete interstitial pockets of subophitic grains. Also one oikocryst of ophitic orthopyroxene. Weak uralite alteration (~10%).
Olivine	17	Subhedral Anhedral	Medium (1-3 mm)	Cumulus grains. Moderate iddingsite alteration in the form of fracture filling (15%). Also talc alteration is found locally on rims of grains.

Fe-Ti oxides	4	Anhedral	Fine to medium	Irregular shaped amoeboidal and subpoikilitic grains interstitial to plagioclase.
Accessory/ Alteration Assemblage	2	Anhedral	Fine	Patches of biotite + amphibole + chlorite + apatite + actinolite found interstitially to the plagioclase.
General Comments: This sample is poorly foliated, medium to coarse grained, seriate size distributed, and is overall weakly altered.				
Sample: CLG-20	**Depth: 436.8 m**	**Rock Type: Augite troctolite**		
Mineral	Abundance	Habit	Grain Size	Comments
Plagioclase	58	Anhedral Subhedral	Fine to medium W=0.1-1.2 mm L=<3 mm	Cumulus grains. Randomly orientated, seriate size distribution. Weakly altered (~15 sericite). Zoning fairly common. Elongated lath shaped grains.
Clinopyroxene	18	Ophitic	Medium to Coarse (<15 mm)	Discrete interstitial pockets of subophitic grains. Also one large oikocryst of ophitic clinopyroxene. Weak uralite alteration (~10%).
Olivine	20	Subhedral Anhedral	Medium (1-2.5 mm)	Cumulus grains. Moderate iddingsite alteration in the form of fracture filling (10%). Also talc and serpentine alteration is found locally on rims of grains.
Fe-Ti oxides	2	Anhedral	Fine to medium	Irregular shaped amoeboidal and subpoikilitic grains interstitial to plagioclase.
Accessory/ Alteration Assemblage	2	Anhedral	Fine	Patches of biotite + amphibole + chlorite + apatite + actinolite found interstitially to the plagioclase.
General Comments: This sample is non-foliated, medium to coarse grained, seriate size distributed, and is overall weakly altered.				

Sample: CLG-21	**Depth: 463.3 m**	**Rock Type: Olivine gabbro**		
Mineral	Abundance	Habit	Grain Size	Comments
Plagioclase	52	Anhedral Subhedral	Fine to medium W=0.1-1.2 mm L=<3 mm	Cumulus grains. Randomly orientated, seriate size distribution. Weakly altered (~15 sericite). Zoning fairly common. Elongated lath shaped grains.
Clinopyroxene	30	Ophitic	Medium to Coarse (<25 mm)	Large oikocrysts of ophitic clinopyroxene. Weak uralite alteration (~10%).
Olivine	14	Subhedral Anhedral	Medium (1-3 mm)	Cumulus grains. Moderate iddingsite alteration in the form of fracture filling (15%). Also talc and serpentine alteration is found locally on rims of grains.
Fe-Ti oxides	2	Anhedral	Fine to medium	Irregular shaped amoeboidal and subpoikilitic grains interstitial to plagioclase.
Accessory/ Alteration Assemblage	2	Anhedral	Fine	Patches of biotite + amphibole + chlorite + apatite + actinolite found interstitially to the plagioclase.
General Comments: This sample is non-foliated, medium to coarse grained, seriate size distributed, and is overall weakly altered.				
Sample: CLG-22	**Depth: 493.7 m**	**Rock Type: Olivine gabbro**		
Mineral	Abundance	Habit	Grain Size	Comments
Plagioclase	60	Anhedral Subhedral	Fine to medium W=0.1-1.2 mm L=<3 mm	Cumulus grains. Randomly orientated, seriate size distribution. Weakly altered (~25 sericite). Zoning fairly common. Elongated lath shaped grains.
Clinopyroxene	20	Ophitic	Medium to Coarse (<20 mm)	Large oikocrysts of ophitic clinopyroxene as well as discrete pockets of subophitic. Weak uralite alteration (~15%).

Olivine	14	Subhedral Anhedral	Medium (1-4 mm)	Cumulus grains. Moderate iddingsite alteration in the form of fracture filling (30%). Also talc alteration is found locally on rims of grains.
Fe-Ti oxides	2	Anhedral	Fine to medium	Irregular shaped amoeboidal and subpoikilitic grains interstitial to plagioclase.
Accessory/ Alteration Assemblage	4	Anhedral	Fine	Patches of biotite + amphibole + chlorite + apatite + actinolite found interstitially to the plagioclase.
General Comments: This sample is non-foliated, medium to coarse grained, seriate size distributed, and is overall weakly altered.				
Sample: CLG-23	**Depth: 509.5 m**	**Rock Type: Olivine gabbro**		
Mineral	Abundance	Habit	Grain Size	Comments
Plagioclase	60	Anhedral Subhedral	Fine to medium W=0.1-2.0 mm L=<5 mm	Cumulus grains. Randomly orientated, seriate size distribution. Weakly altered (~15 sericite). Zoning fairly common. Elongated lath shaped grains.
Clinopyroxene	25	Ophitic	Medium to Coarse (<20 mm)	Large oikocrysts of ophitic clinopyroxene. Weak uralite alteration (~15%).
Olivine	10	Subhedral Anhedral	Medium (1-3 mm)	Cumulus grains. Moderate serpentine/oxide alteration in the form of fracture filling (20%). Also talc alteration is found locally on rims of grains.
Fe-Ti oxides	4	Anhedral	Fine to medium	Irregular shaped amoeboidal and subpoikilitic grains interstitial to plagioclase.
Accessory/ Alteration Assemblage	1	Anhedral	Fine	Patches of biotite + amphibole + chlorite + apatite + actinolite found interstitially to the plagioclase.

General Comments: This sample is non-foliated, medium to coarse grained, seriate size distributed, and is overall weakly altered.				
Sample: CLG-24	**Depth: 528.5 m**	**Rock Type: Augite troctolite**		
Mineral	Abundance	Habit	Grain Size	Comments
Plagioclase	68	Anhedral Subhedral	Fine to medium W=0.1-1.0 mm L=<2.5 mm	Cumulus grains. Randomly orientated, seriate size distribution. Weakly altered (~15 sericite). Zoning fairly common. Elongated lath shaped grains. Fractured grains present adjacent to olivine grains, fractures propagate from olivine serpentine veins.
Clinopyroxene	8	Subophitic	Medium (<5 mm)	Discrete subophitic clinopyroxene pockets. Weak uralite alteration (~10%).
Olivine	22	Subhedral Anhedral	Medium (1-4 mm)	Cumulus grains. Weak serpentine/oxide alteration in the form of fracture filling (20%). Orthopyroxene found on some grain rims.
Fe-Ti oxides	2	Anhedral	Fine to medium	Irregular shaped amoeboidal and subpoikilitic grains interstitial to plagioclase.
Accessory/ Alteration Assemblage	Tr	Anhedral	Fine	Patches of biotite + amphibole + chlorite + apatite + actinolite found interstitially to the plagioclase.
General Comments: This sample is non-foliated, medium grained, seriate size distributed, and is overall weakly altered.				
Sample: CLG-25	**Depth: 541.4 m**	**Rock Type: Melatroctolite**		
Mineral	Abundance	Habit	Grain Size	Comments
Plagioclase	53	Anhedral Subhedral	Fine to medium W=0.1-1.0 mm	Cumulus grains. Randomly orientated, seriate size distribution. Weakly altered (~10% sericite). Zoning fairly common. Elongated

			L=<1.5 mm	lath shaped grains. Fractured grains present adjacent to olivine grains, fractures propagate from olivine serpentine veins.
Clinopyroxene	2	Subophitic	Medium (<4 mm)	Discrete subophitic clinopyroxene pockets. Weak uralite alteration (~10%).
Olivine	36	Subhedral Anhedral	Medium (1-2.5 mm)	Cumulus grains. Weak serpentine/oxide alteration in the form of fracture filling (25%). Orthopyroxene found on some grain rims.
Cr-Spinel	5	Subhedral Euhedral	Fine (<1 mm)	1 cm wide layer of a high concentration of Cr-spinel chadacrysts, equant in shape. These spinels are randomly "peppered" in this layer and are included in both plagioclase and olivine.
Fe-Ti oxides	2	Anhedral	Fine to medium	Irregular shaped amoeboidal and subpoikilitic grains interstitial to plagioclase.
Sulphides	2	Anhedral	Fine to medium	<3mm blebs of disseminated pyrrhotite+chalcopyrite.
Accessory/ Alteration Assemblage	Tr	Anhedral	Fine	Patches of biotite + amphibole + chlorite + apatite + actinolite found interstitially to the plagioclase.
General Comments: This sample is non-foliated, fine-medium grained, seriate size distributed, and is overall weakly altered.				
Sample: CLG-26	**Depth: 557.1 m**	**Rock Type: Layered gabbro and troctolite**		
Mineral	Abundance	Habit	Grain Size	Comments
Top				
Plagioclase	70	Subhedral	Medium W=0.5-3 mm L= <6 mm	Cumulus grains. Randomly orientated, patchy variable, overall moderate sericite alteration (50%). Local patches of intense muscovite and zeolite? alteration.

				Elongated lath shaped grains, minor tabular.
Clinopyroxene	23	Subophitic	Coarse (<15 mm?)	Completely pseudomorphed by uralite-chlorite-biotite
Sulphides	5	Anhedral	Fine to medium	Irregular shaped disseminated interstitial blebs of chalcopyrite+pyrrhotite.
Fe-Ti oxides	2	Anhedral	Fine	Irregular shaped amoeboidal and subpoikilitic grains interstitial to plagioclase.
Bottom				
Plagioclase	60	Subhedral	Fine to medium W=0.1-1.0 mm L=<1.5 mm	Cumulus grains. Randomly orientated, largely weakly altered (~15% sericite). Zoning is fairly common. Elongated lath shaped grains.
Olivine	27	Subhedral	Fine to medium (0.5-2 mm)	Cumulus grains. Overall weakly altered mainly in the form of oxide/serpentine fracture filling. Local pseudomorphs of iddingsite.
Clinopyroxene	2	Subophitic	Coarse (<5 mm)	Discrete grains of subophitic clinopyroxene. Moderately altered to uralite (50%).
Fe-Ti oxide	1	Anhedral	Fine	Irregular shaped amoeboidal and subpoikilitic grains interstitial to plagioclase.
General Comments: This sample contains a distinct abrupt contact between two layers with regards to plagioclase grainsize reduction, sudden presence/absence of olivine, and intensity of alteration.				
Sample: CLG-27	**Depth: 567.2 m**	**Rock Type: Augite troctolite**		
Mineral	Abundance	Habit	Grain Size	Comments
Plagioclase	60	Anhedral Subhedral	Fine to medium W=0.1-0.8 mm L=<2 mm	Cumulus grains. Overall randomly orientated, locally poorly foliated, seriate size distribution. Weakly altered (~20 sericite). Zoning fairly common. Elongated lath shaped grains.

Clinopyroxene	15	Subophitic	Medium (<8 mm)	Discrete subophitic clinopyroxene pockets. Weak uralite alteration (~10%).
Olivine	20	Anhedral	Medium (1-5 mm)	Interstitial, 'subophitic' like grains. Weak serpentine/oxide alteration in the form of fracture filling (20%). Orthopyroxene found on some grain rims.
Fe-Ti oxides	1	Anhedral	Fine to medium	Irregular shaped amoeboidal and subpoikilitic grains interstitial to plagioclase.
Sulphides	3	Anhedral	Fine to medium	Interstitial disseminated pyrrhotite+chalcopyrite.
Accessory/ Alteration Assemblage	1	Anhedral	Fine	Patches of biotite + amphibole + chlorite + apatite + actinolite found interstitially to the plagioclase.
General Comments: This sample is non-foliated, fine-medium grained, seriate size distributed, and is overall weakly altered.				

Sample: CLG-28	**Depth: 573.7 m**	**Rock Type: Augite troctolite**		
Mineral	Abundance	Habit	Grain Size	Comments
Plagioclase	60	Anhedral Subhedral	Fine W=0.1-0.5 mm L=<1 mm	Cumulus grains. Poorly foliated, equigranular size distribution. Weakly altered (~20 sericite). Zoning fairly common. Elongated lath shaped grains.
Clinopyroxene	10	Subophitic	Fine to medium (<2 mm)	Discrete subophitic clinopyroxene pockets. Weak uralite alteration (~10%).
Olivine	25	Anhedral	Fine (0.5-1 mm)	Cumulus grains. Weak serpentine/oxide alteration in the form of fracture filling (10%). Orthopyroxene found on some grain rims.
Fe-Ti oxides	2	Anhedral	Fine	Irregular shaped amoeboidal and subpoikilitic grains interstitial to plagioclase.

Sulphides	1	Anhedral	Fine	Interstitial disseminated pyrrhotite+chalcopyrite.
Accessory/ Alteration Assemblage	1	Anhedral	Fine	Patches of biotite + amphibole + chlorite + apatite + actinolite found interstitially to the plagioclase.
General Comments: This sample is non-foliated, fine grained, seriate size distributed, and is overall weakly altered.				
Sample: CLG-29	**Depth: 574.4 m**	**Rock Type: Contact Plagioclase phyric-diabase/sulphidic gabbro/gabbro**		
Mineral	Abundance	Habit	Grain Size	Comments
Top				
Plagioclase	65	Subhedral	Fine W=<0.2-mm L= <.5 mm	Cumulus grains. Randomly orientated, patchy variable, overall moderate sericite alteration (50%). Elongated lath shaped grains. Equigranular
Clinopyroxene	27	Anhedral	Fine (<0.5 mm)	Cumulus equant roundish grains. Weakly uralite altered (5%). Equigranular. At/near contact modal percentage is (80%) gradually grading to (10%).
Fe-Ti Oxide	1	Anhedral	Fine	Irregular shaped amoeboidal and subpoikilitic grains interstitial to plagioclase.
Accessory/ Alteration Assemblage	7	Anhedral	Fine	Patches of biotite + amphibole + apatite + chlorite + actinolite found interstitially to the plagioclase. Amphibole dominant
Middle				
Plagioclase	56	Anhedral Subhedral	Fine	Randomly orientated, heavy (95%) sericite altered.
Clinopyroxene	20	Subophitic ? Anhedral	Fine	Difficult to determine habit as uralite alteration is heavy (95%), most likely subophitic, one patch appears to be mass of intergranular relict grains.

Sulphides	8	Anhedral	Fine	Irregular shaped blebs of pyrrhotite, evenly distributed.
Accessory/ Alteration Assemblage	15	Anhedral	Fine	Patches of biotite + amphibole + chlorite + apatite + actinolite found interstitially to the plagioclase. Amphibole dominant.
Fe-Ti oxide	1	Anhedral	Fine	Irregular shaped amoeboidal and subpoikilitic grains interstitial to plagioclase.
Bottom				
Plagioclase Phenocrysts	8	Subhedral	Medium W=0.5-2 mm L=<5 mm	Tabular shaped laths. Moderate sericite alteration (35%).
Plagioclase Matrix	67	Anhedral	Very fine to fine	Elongated lath shaped grains define a moderate foliation. Weak sericite alteration (10%).
Clinopyroxene	10	Anhedral	Very fine to fine	Intergranular. Slightly elongated grains, also following plagioclase foliation. Most are equant in shape. Moderate uralite alteration (40%).
Fe-Ti oxides	10	Anhedral	Fine	Irregular shaped amoeboidal and subpoikilitic interstitial to plagioclase as well as bladed grains.
Accessory/ Alteration Assemblage	5	Anhedral	Fine	Patches of biotite + amphibole + apatite + chlorite + actinolite found interstitially to the plagioclase. Amphibole dominated
General Comments: This sample contains two abrupt contacts between three layers. The top and middle of the slide is marked by a somewhat diffuse contact zone with a very high modal abundance of clinopyroxene grains separating the two modally and texturally distinctive layers. Above the contact clinopyroxene gradually becomes less modally abundant. Below the contact the clinopyroxene grains are sparsely present in the middle layer rock for 3 mm. The contact between the middle and bottom rocks is very abrupt. The bottom rock is the same texturally to sample taken at 574.8 m.				

Sample: CLG-30	**Depth: 574.8 m**	**Rock Type: Plagioclase-phyric diabase**		
Mineral	Abundance	Habit	Grain Size	Comments
Plagioclase Phenocrysts	8	Subhedral	Medium W=0.5-2 mm L=<5 mm	Tabular shaped laths. Weakly sericite alteration (25%).
Plagioclase Matrix	50	Anhedral	Very fine to fine	Slightly elongated grains define a moderate foliation. Weak sericite alteration (10%). Equigranular
Clinopyroxene	22	Anhedral	Very fine to fine	Granular. Slightly elongated grains, also following plagioclase foliation. Most are equant in shape. Moderate uralite alteration (40%).
Fe-Ti oxides	5	Anhedral	Fine	Irregular shaped amoeboidal and subpoikilitic grains interstitial to plagioclase.
Accessory/ Alteration Assemblage	15	Anhedral	Fine	Patches of biotite + amphibole + chlorite + actinolite found interstitially to the plagioclase. Amphibole dominated
General Comments: This sample is moderately foliated, very fine to fine grained, equigranular, plagioclase-phyric, and is overall moderately altered.				
Sample: CLG-31	**Depth: 585.0 m**	**Rock Type: Plagioclase-phyric diabase**		
Mineral	Abundance	Habit	Grain Size	Comments
Plagioclase Phenocrysts	65	Subhedral	Coarse to very Coarse W=3-12 mm L=<20 mm	Tabular shaped laths. Moderate sericite alteration (50%).
Plagioclase Matrix	8	Anhedral	Very fine to fine	Complete sericite pseudomorphed.

Clinopyroxene	12	Anhedral	Very fine to fine	Occurs mostly of clusters of very fine to fine grained equant shaped granular grains. Minor amounts of sub ophitic clots. Moderate uralite alteration (40%).
Fe-Ti oxides	5	Anhedral	Fine	Bladed and skeletal grains
Accessory/ Alteration Assemblage	10	Anhedral	Fine	Patches of biotite + amphibole + chlorite + apatite + actinolite + quartz found interstitially to the plagioclase. Amphibole dominated
General Comments: This sample is non-foliated, very fine to fine grained, plagioclase-phyric, and is overall moderately altered.				
Sample: CLG-32	**Depth: 589.0 m**	**Rock Type: Plagioclase-phyric diabase**		
Mineral	Abundance	Habit	Grain Size	Comments
Plagioclase Phenocrysts	70	Subhedral	Coarse to very Coarse W=2-10 mm L=<12 mm	Tabular shaped laths. Moderate sericite alteration (30%).
Plagioclase Matrix	5	Anhedral	Very fine to fine	Complete sericite pseudomorphed.
Clinopyroxene	12	Anhedral	Fine to Medium	Heavy uralite alteration (80%). Grain boundaries can not be determined for the most part, but appears to have been interstitial (subophitic). One 8mm long elongated intergranular grain observed
Fe-Ti oxides	5	Anhedral	Fine	Bladed and skeletal grains
Accessory/ Alteration Assemblage	10	Anhedral	Fine	Patches of biotite + amphibole + chlorite + actinolite + quartz + apatite found interstitially to the plagioclase. Amphibole dominated

General Comments: This sample is non-foliated, very fine to fine grained, plagioclase-phyric, and is overall moderately altered.				
Sample: CLG-32	**Depth: 603.0 m**	**Rock Type: Quartz ferrodiabase**		
Mineral	Abundance	Habit	Grain Size	Comments
Plagioclase	65	Anhedral	Fine to Medium W=0.2-1.0 mm L=<2 mm	Tabular shaped lath. Seriate size distribution. Moderate sericite alteration (40%).
Clinopyroxene	17	Anhedral	Fine to Medium	Subprismatic, intergranular, heavy uralite alteration (80%).
Fe-Ti oxides	7	Anhedral	Fine	Bladed and skeletal grains
Accessory/ Alteration Assemblage	11	Anhedral	Fine to medium	Patches of biotite + amphibole + chlorite + apatite + actinolite + quartz found interstitially to the plagioclase. Amphibole and quartz dominated
General Comments: This sample is non-foliated, fine to medium grained, and is overall moderately altered.				
Sample: CLG-33	**Depth: 613.0 m**	**Rock Type: Plagioclase-phyric diabase**		
Mineral	Abundance	Habit	Grain Size	Comments
Plagioclase Phenocrysts	65	Anhedral to subhedral	Medium to coarse W=0.5-4.0 mm L=<10 mm	Tabular shaped lath. Seriate size distribution. Moderate sericite alteration (40%). Poorly foliated
Clinopyroxene	22	Anhedral	Fine to Medium	Subprismatic, intergranular, commonly twinned, moderate to heavy uralite alteration (60%).
Fe-Ti oxides	5	Anhedral	Fine	Bladed and skeletal grains
Accessory/ Alteration Assemblage	8	Anhedral	Fine to medium	Patches of biotite + amphibole + chlorite + actinolite + quartz + apatite found interstitially to the

				plagioclase. Amphibole dominated
General Comments: This sample is poorly foliated, fine to medium grained, plagioclase phyric, and is overall moderately altered.				
Sample: CLG-34	**Depth: 636.1 m**	**Rock Type: Plagioclase-phyric diabase**		
Mineral	Abundance	Habit	Grain Size	Comments
Plagioclase Phenocrysts	75	Anhedral to subhedral	Medium to coarse W=0.5-3.5 mm L=<8 mm	Tabular shaped lath. Seriate size distribution. Moderate sericite alteration (50%). Randomly orientated.
Clinopyroxene	10	Anhedral Subophitic	Fine to Medium	Subprismatic, intergranular, minor relic twins present, heavy uralite alteration (85%). Minor subophitic grains.
Fe-Ti oxides	4	Anhedral	Fine	Bladed and skeletal grains
Accessory/ Alteration Assemblage	6	Anhedral	Fine to medium	Patches of biotite + amphibole + chlorite + apatite + actinolite + quartz found interstitially to the plagioclase. Amphibole dominated
General Comments: This sample is non-foliated, fine to medium grained, plagioclase phyric, and is overall moderately to heavily altered.				
Sample: CLG-35	**Depth: 649.4 m**	**Rock Type: Noritic diabase/Sulphidic Norite**		
Mineral	Abundance	Habit	Grain Size	Comments
Top				
Plagioclase	67	Subhedral	Fine W=<0.2-mm L= <.5 mm	Randomly orientated, patchy variable, overall weakly, sericite alteration (50%). Elongated lath shaped grains. Equigranular
Orthopyroxene	30	Anhedral	Fine (<0.2 mm)	Intergranular. Weakly altered to chlorite+actinolite. Equigranular.
Fe-Ti Oxide	1	Anhedral	Fine	Irregular shaped amoeboidal and subpoikilitic grains

				interstitial to plagioclase, minor bladed grains.
Accessory/ Alteration Assemblage	2	Anhedral	Fine	Patches of biotite + amphibole + chlorite + apatite + actinolite found interstitially to the plagioclase.
Bottom				
Plagioclase	59	Anhedral Subhedral	Fine to medium W=0.1-1.3 mm L=<3 mm	Randomly orientated, largely fine grains but have patches of medium sized grains. Moderate (60%) sericite altered.
Orthopyroxene	15	Anhedral	Fine (0.2-0.5 mm)	Intergranular. Moderate chlorite + actinolite alteration (50%). At contact, grains are medium sized.
Sulphides	4	Anhedral	Fine	Irregular shaped blebs of pyrrhotite. Highest concentration at or near contact
Granophyre	5	Anhedral	Fine	Present throughout however high concentration directly below contact. Both irregular shaped interstitial to plagioclase and equant grains.
Accessory/ Alteration Assemblage	15	Anhedral	Fine	Patches of biotite + amphibole + chlorite + apatite + actinolite + quartz + k-feldspar found interstitially to the plagioclase.
Fe-Ti oxide	2	Anhedral	Fine	Irregular shaped amoeboidal and subpoikilitic grains interstitial to plagioclase.
General Comments: This sample contains a distinct abrupt contact between two layers with regards to plagioclase grainsize reduction and sudden presence/absence of sulphide, granophyre, quartz, and K-feldspar. The top section is weakly altered where the bottom section is moderately altered.				
Sample: CLG-36	**Depth: 657.5 m**	**Rock Type: Gabbro**		
Mineral	Abundance	Habit	Grain Size	Comments

Plagioclase	55	Anhedral Subhedral	Medium W=0.3-4 mm L=<6 mm	Cumulus grains. Non-foliated, seriate size distribution. Weakly altered (~25 sericite). Zoning fairly common. Elongated lath shaped grains, minor tabular.
Clinopyroxene	31	Anhedral Subophitic	Coarse (<10 mm)	Largely intergranular anhedral prismatic grains as well as discrete subophitic clinopyroxene pockets. Strong uralite alteration (~80%).
Olivine	4	Anhedral	Medium (< 5 mm)	Cumulus grains. Complete pseudomorphing by serpentine/oxide alteration.
Fe-Ti oxides	4	Anhedral	Fine	Irregular shaped amoeboidal and subpoikilitic grains interstitial to plagioclase, skeletal grains also present.
Sulphides	1	Anhedral	Fine	Interstitial of disseminated pyrrhotite. Large (1.5 cm pyrrhotite bleb in hand sample)
Granophyre	1	Anhedral	Fine	Interstitial to plagioclase.
Accessory/ Alteration Assemblage	4	Anhedral	Fine	Patches of biotite + amphibole + chlorite + apatite + actinolite + quartz found interstitially to the plagioclase.
General Comments: This sample is non-foliated, medium grained, seriate size distributed, and is overall moderately altered.				
Sample: CLG-37	**Depth: 662.1 m**	**Rock Type: Troctolite**		
Mineral	Abundance	Habit	Grain Size	Comments
Plagioclase	65	Anhedral Subhedral	Medium W=0.5-2 mm L=<6 mm	Cumulus grains. Non-foliated, seriate size distribution. Weakly altered (~15 sericite). Zoning fairly common. Elongated lath shaped grains, minor tabular.
Clinopyroxene	5	Subophitic	Coarse (<10 mm)	Discrete subophitic clinopyroxene pockets. Weak uralite alteration (~15%).

Olivine	25	Anhedral	Medium to coarse (< 8 mm)	Interstitial to plagioclase grains, Fracture filling by serpentine/oxide alteration (20%). Minor talc/orthopyroxene alteration on rims of some grains.
Fe-Ti oxides	1	Anhedral	Fine	Irregular shaped amoeboidal and subpoikilitic grains interstitial to plagioclase.
Sulphides	3	Anhedral	Fine to medium	Interstitial grains of disseminated pyrrhotite+chalcopyrite.
Accessory/ Alteration Assemblage	1	Anhedral	Fine	Patches of biotite + amphibole + chlorite + apatite + actinolite found interstitially to the plagioclase.
General Comments: This sample is non-foliated, medium to coarse grained, seriate size distributed, and is overall weakly altered.				
Sample: CLG-38	**Depth: 669.3 m**	**Rock Type: Olivine gabbro**		
Mineral	Abundance	Habit	Grain Size	Comments
Plagioclase	55	Anhedral Subhedral	Medium W=0.3-1.8 mm L=<5 mm	Cumulus grains. Non-foliated, seriate size distribution. Weakly altered (~15 sericite). Zoning fairly common. Elongated lath shaped grains, minor tabular.
Clinopyroxene	25	Ophitic	Coarse (~20 mm)	Large 2 cm oikocryst of ophitic clinopyroxene. The gain is not optically continuous, and is composed of several smaller (5-10 mm) grains.
Olivine	17	Anhedral	Medium to coarse (< 8 mm)	Cumulus grains. Fracture filling by serpentine/oxide alteration (35%). Minor talc/orthopyroxene alteration on rims of some grains.
Fe-Ti oxides	2	Anhedral	Fine	Irregular shaped amoeboidal and subpoikilitic grains interstitial to plagioclase.

				Some grains also included in clinopyroxene.
Accessory/ Alteration Assemblage	1	Anhedral	Fine	Patches of biotite + amphibole + chlorite + apatite + actinolite found interstitially to the plagioclase.
General Comments: This sample is non-foliated, medium to coarse grained, seriate size distributed, and is overall weakly altered.				
Sample: CLG-39	**Depth: 684.3 m**	**Rock Type: Olivine gabbro**		
Mineral	Abundance	Habit	Grain Size	Comments
Plagioclase	70	Anhedral Subhedral	Fine to medium W=0.2-1.3 mm L=<2 mm	Cumulus grains. Non-foliated, seriate size distribution. Weakly altered (~15 sericite). Zoning fairly common. Elongated lath shaped grains.
Clinopyroxene	15	Subophitic	Coarse (<15 mm)	Optically continuous series of subophitc pockets, interstitial to plagioclase. Weak uralite alteration (10%)
Olivine	11	Anhedral	Medium (<5 mm)	Cumulus grains. Fracture filling by serpentine/oxide alteration (15%). Minor talc/orthopyroxene alteration on rims of some grains.
Fe-Ti oxides	2	Anhedral	Fine	Irregular shaped amoeboidal and subpoikilitic grains interstitial to plagioclase. Some grains also included in clinopyroxene, commonly bladed.
Accessory/ Alteration Assemblage	2	Anhedral	Fine	Patches of biotite + amphibole + chlorite + apatite + actinolite found interstitially to the plagioclase.
General Comments: This sample is non-foliated, medium to coarse grained, seriate size distributed, and is overall weakly altered.				
Sample: CLG-40	**Depth: 701.1 m**	**Rock Type: Augite troctolite**		

Mineral	Abundance	Habit	Grain Size	Comments
Plagioclase	65	Anhedral Subhedral	Fine to medium W=0.2-1.3 mm L=<2 mm	Cumulus grains. Non-foliated, seriate size distribution. Weakly altered (~15 sericite). Zoning fairly common. Elongated lath shaped grains.
Clinopyroxene	10	Subophitic	Medium (<5 mm)	Discrete subophitc pockets, interstitial to plagioclase. Weak uralite alteration (10%)
Olivine	20	Anhedral	Medium (<3 mm)	Cumulus grains. Fracture filling by serpentine/oxide alteration (10%). Minor talc/orthopyroxene alteration on rims of some grains.
Fe-Ti oxides	3	Anhedral	Fine to medium	Irregular shaped amoeboidal and subpoikilitic grains interstitial to plagioclase.
Accessory/ Alteration Assemblage	2	Anhedral	Fine	Patches of biotite + amphibole + chlorite + apatite + actinolite found interstitially to the plagioclase.
General Comments: This sample is non-foliated, medium grained, seriate size distributed, and is overall weakly altered.				
Sample: CLG-41	**Depth: 725.1 m**	**Rock Type: Augite troctolite**		
Mineral	Abundance	Habit	Grain Size	Comments
Plagioclase	55	Anhedral Subhedral	Fine to medium W=0.2-1.2 mm L=<2.5 mm	Cumulus grains. Non-foliated, seriate size distribution. Weakly altered (~15 sericite). Zoning fairly common. Elongated lath shaped grains.
Clinopyroxene	20	Ophitic	Coarse (<15 mm)	Several large oikocrysts. Weak uralite alteration (10%)
Olivine	21	Anhedral	Medium (<4 mm)	Cumulus grains. Fracture filling by serpentine/oxide alteration (10%). Minor talc/orthopyroxene alteration on rims of some grains.

Fe-Ti oxides	2	Anhedral	Fine to medium	Irregular shaped amoeboidal and subpoikilitic grains interstitial to plagioclase.
Accessory/ Alteration Assemblage	2	Anhedral	Fine	Patches of biotite + amphibole + chlorite + apatite + actinolite found interstitially to the plagioclase.
General Comments: This sample is non-foliated, medium to coarse grained, seriate size distributed, and is overall weakly altered.				
Sample: CLG-42	**Depth: 744.3 m**	**Rock Type: Augite troctolite**		
Mineral	Abundance	Habit	Grain Size	Comments
Plagioclase	60	Anhedral Subhedral	Fine to medium W=0.2-1.4 mm L=<3 mm	Cumulus grains. Non-foliated, seriate size distribution. Weakly altered (~15 sericite). Zoning fairly common. Elongated lath shaped grains.
Clinopyroxene	14	Ophitic	Coarse (<20 mm)	Large oikocrysts present in between Cr-spinel layers. Weak uralite alteration (10%)
Olivine	16	Anhedral	Medium (<3 mm)	Cumulus grains. Fracture filling by serpentine/oxide alteration (15%). Minor talc/orthopyroxene alteration on rims of some grains.
Cr-spinel	5	Euhedral	Fine	Two 1 cm wide layers of a high concentration of Cr-spinel chadacrysts, equant in shape. These spinels are randomly "peppered" in this layer and are included in both plagioclase, clinopyroxene, and olivine.
Fe-Ti oxides	2	Anhedral	Fine to medium	Irregular shaped amoeboidal and subpoikilitic grains interstitial to plagioclase.
Sulphides	1	Anhedral	Fine	Disseminated blebs of chalcopyrite+pyrrhotite.
Accessory/ Alteration Assemblage	2	Anhedral	Fine	Patches of biotite + amphibole + chlorite + apatite + actinolite found

				interstitially to the plagioclase.
General Comments: This sample is non-foliated, medium to coarse grained, seriate size distributed, and is overall weakly altered.				
Sample: CLG-43	**Depth: 753.3 m**	**Rock Type: Olivine gabbro**		
Mineral	Abundance	Habit	Grain Size	Comments
Plagioclase	60	Anhedral Subhedral	Fine to medium	Non-foliated? seriate size distribution? Very strongly altered (~95 sericite). Individual grains can not be distinguished. Only some grains have rims that are unaltered.
Clinopyroxene	18	Ophitic	Coarse (<15 mm)	Large oikocrysts. Weak uralite alteration (10%) for half but some oikocrysts have strong (75%) uralite alteration.
Olivine	12	Anhedral	Medium (<3 mm)	Marginally subpoikilitic (intergrown with plagioclase). One skeletal grain. Fracture filling by serpentine/oxide alteration (15%). Somewhat minor talc/orthopyroxene alteration on rims of some grains (10%).
Cr-spinel	5	Euhedral	Fine	Entire sample has Cr-spinel chadacrysts, equant in shape. These spinels are randomly "peppered" throughout and are included in both plagioclase, clinopyroxene, and olivine.
Fe-Ti oxides	2	Anhedral	Fine to medium	Irregular shaped interstitial to plagioclase.
Sulphides	<1	Anhedral	Fine	Disseminated blebs of chalcopyrite+pyrrhotite. Hand sample contains coarse and medium grained interstitial blebs (~5%).

Accessory/ Alteration Assemblage	2	Anhedral	Fine	Patches of biotite + amphibole + chlorite + apatite + actinolite found interstitially to the plagioclase.
General Comments: This sample is non-foliated, medium to coarse grained, seriate size distributed, and is overall strongly altered. It is cut by a 3 mm vein of fine grained plagioclase, biotite, chlorite, and actinolite.				
Sample: CLG-44	**Depth: 754.0 m**	**Rock Type: Olivine gabbro**		
Mineral	Abundance	Habit	Grain Size	Comments
Plagioclase	60	Subhedral	Fine W=0.1-0.5 mm L=<1.5	Non-foliated. equigranular size distribution. Weakly altered (20%) sericite.
Clinopyroxene	20	Ophitic Subophitic	Coarse (<12 mm)	Three larger ophitic oikocrysts, with the remaining being subophitic. Weak uralite alteration (15%) on ophitic grains, moderate (50%) on subophitic grains
Olivine	12	Anhedral	Fine (<1.5 mm)	Marginally subpoikilitic (intergrown with plagioclase). Complete talc/serpentine psuedomorphing
Fe-Ti oxides	3	Anhedral	Fine	Irregular shaped amoeboidal and subpoikilitic grains interstitial to plagioclase. Also bladed and skeletal grains.
Accessory/ Alteration Assemblage	5	Anhedral	Fine	Patches of biotite + amphibole + chlorite + apatite + actinolite found interstitially to the plagioclase.
General Comments: This sample is non-foliated, fine grained, equigranular, and is overall weak to moderately altered.				
Sample: CLG-45	**Depth: 771.7 m**	**Rock Type: Diabase**		
Mineral	Abundance	Habit	Grain Size	Comments

Plagioclase	60	Anhedral Subhedral	Fine W=0.1-0.5 mm L=<1.5 mm	Non-foliated. equigranular size distribution. moderately altered (35%) sericite.
Clinopyroxene	20	Subophitic	Medium	Heavily altered to uralite (80%) only small patches of unaltered material.
Fe-Ti oxides	5	Anhedral	Fine	Irregular shaped amoeboidal and subpoikilitic grains interstitial to plagioclase. Also bladed and skeletal grains.
Accessory/ Alteration Assemblage	15	Anhedral	Fine	Patches of biotite + amphibole + chlorite + apatite + actinolite + quartz found interstitially to the plagioclase.
General Comments: This sample is non-foliated, fine grained, equigranular, and is overall moderate to heavily altered.				

MOUNT MOLLIE DYKE THIN SECTION DESCRIPTIONS

Sample: MM-3	**Depth: 38.9 m**	**Rock Type: Quartz ferrodiorite**		
Mineral	Abundance	Habit	Grain Size	Comments
Plagioclase	54	Anhedral-Subhedral	Fine W=0.1-0.4 mm L=<1 mm	Non-foliated, bimodal size distribution. Moderate altered (~35% sericite). Zoning rare. Mostly lath shaped grains.
Orthopyroxene-Clinopyroxene	7	Anhedral-subhedral	Fine to medium (<1.5 mm)	Granular/intergranular, relict simple twins, heavy uralite/chlorite/actinolite alteration (85%)
Free quartz/ Granophyre	10	Anhedral	Fine to medium	Irregular shaped interstitial to plagioclase.
Fe-Ti Oxides	7	Anhedral	Fine to medium	Equal amounts bladed grains and skeletal grains. 1cm^2 area of high concentration of equant grains. Dendritic grains surrounds the cluster.
Accessory/ Alteration Assemblage	12	Anhedral	Fine to medium	Patches of biotite + amphibole + chlorite + apatite + actinolite found interstitially to the plagioclase.
General Comments: This sample is non-foliated, fine to medium grained, is overall moderately altered.				
Sample: MM-4	**Depth: 48.3 m**	**Rock Type: Ferrodiorite**		
Mineral	Abundance	Habit	Grain Size	Comments
Plagioclase	61	Anhedral-Subhedral	Fine W=0.1-0.4 mm L=<1 mm	Non-foliated, bimodal size distribution. Moderate altered (~35% sericite). Zoning rare. Mostly lath shaped grains.
Orthopyroxene-Clinopyroxene	10	Anhedral-subhedral	Fine to medium (<1.5 mm)	Granular/intergranular, relict simple twins, heavy uralite/chlorite/actinolite alteration (85%)
Free Quartz/ Granophyre	5	Anhedral	Fine to medium	Irregular shaped, interstitial to plagioclase.
Fe-Ti Oxides	6	Anhedral	Fine to medium	Irregular shaped amoeboidal and subpoikilitic interstitial grains, minor bladed and skeletal grains

Accessory/ Alteration Assemblage	8	Anhedral	Fine to medium	Patches of biotite + amphibole + chlorite + apatite + actinolite found interstitially to the plagioclase.
General Comments: This sample is non-foliated, fine to medium grained, is overall moderately altered.				
Sample: MM-5	**Depth: 59.9 m**	**Rock Type: Ferrodiorite**		
Mineral	Abundance	Habit	Grain Size	Comments
Plagioclase	61	Anhedral-Subhedral	Fine to medium W=0.1-0.4 mm L=<1.5 mm	Non-foliated, bimodal size distribution. Weakly altered (~20% sericite). Zoning rare. Mostly lath shaped grains.
Orthopyroxene-Clinopyroxene	10	Anhedral-subhedral	Fine (<1 mm)	Cumulate grains, relict simple twins, heavy uralite/chlorite/actinolite alteration (85%)
Free Quartz/ Granophyre	4	Anhedral	Fine to medium	Irregular shaped, interstitial to plagioclase.
Fe-Ti Oxides	7	Anhedral	Fine to medium	Irregular shaped amoeboidal and subpoikilitic grains interstitial to plagioclase., minor bladed and skeletal grains
Accessory/ Alteration Assemblage	8	Anhedral	Fine to medium	Patches of biotite + amphibole + chlorite + apatite + actinolite found interstitially to the plagioclase.
General Comments: This sample is non-foliated, fine to medium grained, is overall weak to moderately altered.				
Sample: MM-7	**Depth: 74.4 m**	**Rock Type: Gabbro**		
Mineral	Abundance	Habit	Grain Size	Comments
Plagioclase	55	Anhedral-Subhedral	Fine to medium W=0.1-1 mm L=<5 mm	Non-foliated, bimodal size distribution. Moderate altered (~35% sericite). Zoning rare. Mostly tabular shaped grains.

				Pericline twinning in some grains.
Clinopyroxene	20	Anhedral-subhedral	Fine to medium (<3 mm)	Cumulate grains, bimodal size distributed, relict simple twins, heavy uralite alteration (85%)
Free Quartz/ Granophyre	5	Anhedral	Fine to medium	Irregular shaped interstitial to plagioclase/clinopyroxene
Fe-Ti Oxides	5	Anhedral	Fine to medium	Mostly bladed grains minor skeletal grains.
Accessory/ Alteration Assemblage	10	Anhedral	Fine to medium	Patches of biotite + amphibole + chlorite + apatite + apatite + actinolite found interstitially to the plagioclase.
General Comments: This sample is non-foliated, fine to medium grained, bimodal size distributed, and is overall moderately altered. This sample has two distinct areas, a medium grained area and a fine grained area.				
Sample: MM-8	**Depth: 89.3 m**	**Rock Type: Gabbroic anorthosite**		
Mineral	Abundance	Habit	Grain Size	Comments
Plagioclase	65	Anhedral-Subhedral	Fine to medium W=0.1-0.5 mm L=<2 mm	Non-foliated,. Weakly altered (~15% sericite). Zoning rare. Mostly tabular shaped grains.
Clinopyroxene	10	Anhedral-subhedral	Fine to medium (<3 mm)	Cumulate grains, heavy uralite/chlorite alteration (85%)
Orthopyroxene	7	Anhedral-subhedral	Fine to medium (<2 mm)	Cumulate grains, moderate uralite/chlorite alteration (65%).
Free Quartz/ Granophyre	4	Anhedral	Fine to medium	Irregular shaped interstitial to plagioclase/clinopyroxene
Fe-Ti Oxides	6	Anhedral	Fine to medium	Irregular shaped amoeboidal and subpoikilitic grains interstitial to plagioclase. and skeletal grains.
Accessory/ Alteration Assemblage	8	Anhedral	Fine to medium	Patches of biotite + amphibole + chlorite + apatite + actinolite found interstitially to the plagioclase.

General Comments: This sample is non-foliated, fine to medium grained, and is overall weak to moderately altered.				
Sample: MM-9	**Depth: 123.4 m**	**Rock Type: Gabbro**		
Mineral	Abundance	Habit	Grain Size	Comments
Plagioclase	60	Anhedral-Subhedral	Fine to medium W=0.2-0.7 mm L=<4 mm	Cumulate grains. Non-foliated, weakly altered (~15% sericite). Zoning rare. Mostly lath shaped grains some minor tabular.
Clinopyroxene	25	Anhedral-subhedral	Fine to medium (<5 mm)	Cumulate grains, heavy uralite/chlorite alteration (85%). Relic simple twins can be observed.
Free Quartz/ Granophyre	3	Anhedral	Fine to medium	Irregular shaped interstitial to plagioclase/clinopyroxene
Fe-Ti Oxides	5	Anhedral	Fine to medium	Irregular shaped amoeboidal and subpoikilitic grains interstitial to plagioclase. and skeletal grains.
Accessory/ Alteration Assemblage	7	Anhedral	Fine to medium	Patches of biotite + amphibole + chlorite + apatite + actinolite found interstitially to the plagioclase.
General Comments: This sample is non-foliated, fine to medium grained, and is overall weak to moderately altered.				
Sample: MM-10	**Depth: 154.5 m**	**Rock Type: Olivine gabbro**		
Mineral	Abundance	Habit	Grain Size	Comments
Plagioclase	60	Anhedral-Subhedral	Fine to medium W=0.2-0.6 mm L=<4 mm	Cumulate grains. Poorly foliated, weakly altered (~15% sericite). Zoning common. Lath and elongated lath shaped grains.
Clinopyroxene	20	Ophitic	Coarse (<20 mm)	Ophitic grains, weak uralite/chlorite alteration (10%). Relic simple twins can be observed.
Olivine	12	Subhedral	Medium (<3mm)	Cumulate grains, moderately altered primarily by iddingsite and minor talc.

				Oikocryst to plagioclase grains.
Free quartz/ Granophyre	1	Anhedral	Fine to medium	Irregular shaped interstitial to plagioclase/clinopyroxene
Fe-Ti Oxides	2	Anhedral	Fine to medium	Irregular shaped amoeboidal and subpoikilitic grains interstitial to plagioclase.
Accessory/ Alteration Assemblage	5	Anhedral	Fine to medium	Patches of biotite + amphibole + chlorite + apatite + actinolite found interstitially to the plagioclase.
General Comments: This sample is poorly foliated, fine to medium grained, and is overall weak to moderately altered.				
Sample: MM-11	**Depth: 197.5 m**	**Rock Type: Gabbro**		
Mineral	Abundance	Habit	Grain Size	Comments
Plagioclase	45	Anhedral-Subhedral	Fine to medium W=0.2-1.4 mm L=<4 mm	Cumulate grains. Non-foliated, weakly altered (~15% sericite). Zoning minor. Tabular shaped grains.
Clinopyroxene	31	Anhedral-subhedral	Fine to medium (<4 mm)	Cumulate grains, weak uralite/chlorite alteration (10%). Simple twins very common. Seriate size distribution
Olivine	10	Subhedral	Medium (<3mm)	Cumulate grains, strongly altered to iddingsite and minor talc along some grain boundaries. Oikocryst to plagioclase grains.
Free Quartz/ Granophyre	1	Anhedral	Fine to medium	Irregular shaped interstitial to plagioclase/clinopyroxene
Fe-Ti Oxides	8	Anhedral	Fine to medium	Irregular shaped amoeboidal and subpoikilitic grains interstitial to plagioclase. and skeletal grains.
Accessory/ Alteration Assemblage	5	Anhedral	Fine to medium	Patches of biotite + amphibole + chlorite + apatite + actinolite found interstitially to the plagioclase.

General Comments: This sample is non-foliated, fine to medium grained, and is overall weak to moderately altered.				
Sample: MM-12	**Depth: 226.9 m**	**Rock Type: Olivine gabbro**		
Mineral	Abundance	Habit	Grain Size	Comments
Plagioclase	59	Anhedral-Subhedral	Fine to medium W=0.2-1.1 mm L=<3 mm	Cumulate grains. Non-foliated, weakly altered (~15% sericite). Zoning minor. Tabular and lath shaped grains.
Clinopyroxene	18	Anhedral-subhedral	Fine to medium (<2 mm)	Cumulate grains, weak uralite/chlorite alteration (10%). Simple twins very common.
Orthopyroxene	5	Anhedral-subhedral	Fine to medium (<2 mm)	Cumulate grains, weak uralite/chlorite alteration (10%).
Olivine	8	Subhedral	Fine to medium (<1.5mm)	Cumulate equant shaped grains, weak to moderately altered to iddingsite and minor talc along some grain boundaries.
Free Quartz/ Granophyre	1	Anhedral	Fine to medium	Irregular shaped interstitial to plagioclase/clinopyroxene
Fe-Ti Oxides	3	Anhedral	Fine to medium	Irregular shaped amoeboidal and subpoikilitic grains interstitial to plagioclase. and skeletal grains.
Accessory/ Alteration Assemblage	6	Anhedral	Fine to medium	Patches of biotite + amphibole + chlorite + apatite + actinolite found interstitially to the plagioclase.
General Comments: This sample is non-foliated, fine to medium grained, and is overall weak to moderately altered.				
Sample: MM-13	**Depth: 247.8 m**	**Rock Type: Olivine gabbro**		
Mineral	Abundance	Habit	Grain Size	Comments
Plagioclase	65	Anhedral-Subhedral	Fine to medium W=0.2-1.1 mm	Cumulate grains. Poorly foliated, weakly altered (~15% sericite). Zoning

			L=<3 mm	minor. Tabular and lath shaped grains.
Clinopyroxene	15	Anhedral-subhedral	Fine to medium (<1.5 mm)	Cumulate grains, weak uralite/chlorite alteration (10%). Simple twins very common.
Orthopyroxene	3	Anhedral-subhedral	Fine to medium (<1 mm)	Cumulate grains, weak uralite/chlorite alteration (10%).
Olivine	10	Subhedral	Fine to medium (<2 mm)	Cumulate equant shaped grains, weak to moderately altered to iddingsite and minor talc along some grain boundaries.
Free Quatz/ Granophyre	tr	Anhedral	Fine to medium	Irregular shaped interstitial to plagioclase/clinopyroxene
Fe-Ti Oxides	3	Anhedral	Fine to medium	Irregular shaped amoeboidal and subpoikilitic grains interstitial to plagioclase. and skeletal grains.
Accessory/ Alteration Assemblage	4	Anhedral	Fine to medium	Patches of biotite + amphibole + chlorite + apatite + actinolite found interstitially to the plagioclase.
General Comments: This sample is poorly foliated, fine to medium grained, and is overall weak to moderately altered.				
Sample: MM-14	**Depth: 273.7 m**	**Rock Type: Olivine gabbro**		
Mineral	Abundance	Habit	Grain Size	Comments
Plagioclase	65	Anhedral-Subhedral	Fine to medium W=0.2-1.1 mm L=<3 mm	Cumulate grains. Moderately foliated, weakly altered (~15% sericite). Zoning minor. Tabular and lath shaped grains.
Clinopyroxene	20	Anhedral-subhedral	Fine to medium (<2 mm)	Cumulate grains, weak uralite/chlorite alteration (10%). Simple twins very common.
Orthopyroxene	1	Anhedral-subhedral	Fine to medium (<1 mm)	Cumulate grains, weak uralite/chlorite alteration (10%).

Olivine	17	Subhedral	Fine to medium (<2 mm)	Cumulate equant shaped grains, weak to moderately altered to iddingsite and minor talc along some grain boundaries.
Fe-Ti Oxides	3	Anhedral	Fine to medium	Irregular shaped amoeboidal and subpoikilitic grains interstitial to plagioclase. and skeletal grains.
Accessory/ Alteration Assemblage	4	Anhedral	Fine to medium	Patches of biotite + amphibole + chlorite + apatite + actinolite + quartz found interstitially to the plagioclase.
General Comments: This sample is moderately foliated, fine to medium grained, and is overall weak to moderately altered.				
Sample: MM-15	**Depth: 296.3 m**	**Rock Type: Olivine gabbro**		
Mineral	Abundance	Habit	Grain Size	Comments
Plagioclase	50	Anhedral-Subhedral	Fine to medium W=0.2-1.1 mm L=<3 mm	Cumulate grains. Well foliated, weakly altered (~15% sericite). Zoning minor. Tabular and lath shaped grains.
Clinopyroxene	23	Anhedral-subhedral	Fine to medium (<2 mm)	Cumulate grains, weak uralite/chlorite alteration (10%). Simple twins very common.
Orthopyroxene	1	Anhedral-subhedral	Fine (<1 mm)	Cumulate grains, weak uralite/chlorite alteration (10%).
Olivine	20	Subhedral	Fine to medium (<2 mm)	Cumulate equant shaped grains, weakly altered to iddingsite and minor talc along some grain boundaries.
Fe-Ti Oxides	2	Anhedral	Fine to medium	Irregular shaped amoeboidal and subpoikilitic grains interstitial to plagioclase.
Accessory/ Alteration Assemblage	4	Anhedral	Fine to medium	Patches of biotite + amphibole + chlorite + apatite + actinolite + quartz found interstitially to the plagioclase.

General Comments: This sample is well foliated, fine to medium grained, and is overall weak to moderately altered.				
Sample: MM-17	**Depth: 340.5 m**	**Rock Type: Augite troctolite**		
Mineral	Abundance	Habit	Grain Size	Comments
Plagioclase	60	Anhedral-Subhedral	Fine to medium W=0.2-1.3 mm L=<4 mm	Cumulate grains. Moderately foliated, weakly altered (~15% sericite). Zoning minor. Tabular and lath shaped grains.
Clinopyroxene	15	Anhedral-subhedral	Fine to medium (<2 mm)	Cumulate grains, weak uralite/chlorite alteration (10%). Simple twins common.
Orthopyroxene	4	Anhedral-subhedral	Fine to medium (<2 mm)	Cumulate grains, weak uralite/chlorite alteration (10%).
Olivine	15	Subhedral	Fine to medium (<2 mm)	Cumulate equant shaped grains, weakly altered to iddingsite and minor talc along some grain boundaries.
Fe-Ti Oxides	2	Anhedral	Fine to medium	Irregular shaped amoeboidal and subpoikilitic grains interstitial to plagioclase.
Accessory/ Alteration Assemblage	4	Anhedral	Fine to medium	Patches of biotite + amphibole + chlorite + apatite + actinolite + quartz found interstitially to the plagioclase.
General Comments: This sample is moderately foliated, fine to medium grained, and is overall weak to moderately altered.				
Sample: MM-18	**Depth: 367.9 m**	**Rock Type: Augite troctolite**		
Mineral	Abundance	Habit	Grain Size	Comments
Plagioclase	68	Anhedral-Subhedral	Fine to medium W=0.2-1.3 mm L=<4 mm	Cumulate grains. Well foliated, weakly altered (~15% sericite). Zoning minor. Lath shaped grains.
Clinopyroxene	10	Anhedral-subhedral	Fine to medium (<2 mm)	Cumulate grains, weak uralite/chlorite alteration

				(10%). Simple twins common.
Orthopyroxene	2	Anhedral-subhedral	Fine to medium (<2 mm)	Cumulate grains, weak uralite/chlorite alteration (10%).
Olivine	15	Subhedral	Fine to medium (<2.5 mm)	Cumulate equant shaped grains, some grains are elongated in same direction of foliation, weakly altered to iddingsite and minor talc along some grain boundaries.
Fe-Ti Oxides	2	Anhedral	Fine to medium	Irregular shaped amoeboidal and subpoikilitic grains interstitial to plagioclase.
Accessory/ Alteration Assemblage	3	Anhedral	Fine to medium	Patches of biotite + amphibole + chlorite + apatite + actinolite + quartz found interstitially to the plagioclase.
General Comments: This sample is well foliated, fine to medium grained, and is overall weakly moderately altered.				
Sample: MM-19	**Depth: 397.6 m**	**Rock Type: Leucogabbro**		
Mineral	Abundance	Habit	Grain Size	Comments
Plagioclase	68	Anhedral-Subhedral	Fine to medium W=0.2-1.2 mm L=<4 mm	Cumulate grains. Non-foliated, weakly altered (~15% sericite). Zoning minor. Tabular and lath shaped grains.
Clinopyroxene	17	Anhedral-subhedral	Fine to medium (<2 mm)	Cumulate grains, weak uralite/chlorite alteration (10%). Simple twins minor. Oikocryst to plagioclase grains.
Orthopyroxene	2	Anhedral-subhedral	Fine to medium (<2 mm)	Cumulate grains, weak uralite/chlorite alteration (10%).
Olivine	5	Subhedral	Fine to medium (<2 mm)	Cumulate equant shaped grains, moderately altered to iddingsite.
Fe-Ti Oxides	3	Anhedral	Fine to medium	Irregular shaped amoeboidal and subpoikilitic grains interstitial to plagioclase.

Accessory/ Alteration Assemblage	3	Anhedral	Fine	Patches of biotite + amphibole + chlorite + apatite + actinolite + quartz found interstitially to the plagioclase.
General Comments: This sample is non-foliated, fine to medium grained, and is overall weakly altered.				
Sample: MM-20	**Depth: 411.3 m**	**Rock Type: Augite troctolite**		
Mineral	Abundance	Habit	Grain Size	Comments
Plagioclase	55	Anhedral-Subhedral	Fine to medium W=0.2-1.2 mm L=<3 mm	Cumulate grains. Non-foliated, weakly altered (~15% sericite). Zoning minor. Tabular and lath shaped grains.
Clinopyroxene	18	Anhedral-subhedral	Fine to medium (<1.5 mm)	Cumulate grains, weak uralite/chlorite alteration (10%). Simple twins minor.
Orthopyroxene	1	Anhedral-subhedral	Fine to medium (<1.5 mm)	Cumulate grains, weak uralite/chlorite alteration (10%).
Olivine	20	Subhedral	Medium (<5 mm)	Cumulate equant shaped grains, weakly altered to iddingsite. Oikocryst to plagioclase grains.
Fe-Ti Oxides	3	Anhedral	Fine to medium	Irregular shaped amoeboidal and subpoikilitic grains interstitial to plagioclase.
Accessory/ Alteration Assemblage	3	Anhedral	Fine	Patches of biotite + amphibole + chlorite + apatite + actinolite + quartz found interstitially to the plagioclase.
General Comments: This sample is non-foliated, fine to medium grained, and is overall weakly altered.				
Sample: MM-23	**Depth: 476.1 m**	**Rock Type: Troctolite**		
Mineral	Abundance	Habit	Grain Size	Comments
Plagioclase	70	Anhedral-Subhedral	Fine to medium	Cumulate grains. Non-foliated, weakly altered

			W=0.2-0.8 mm L=<2.5 mm	(~15% sericite). Zoning minor. Lath shaped grains.
Clinopyroxene	5	Subophitic	Medium (<5 mm)	Optically continuous subophitic grains, weak uralite/chlorite alteration (10%).
Olivine	19	Subhedral	Medium (<2.5 mm)	Cumulate equant shaped grains, weakly altered to iddingsite, talc alteration on some grain boundaries. Oikocryst to plagioclase grains.
Fe-Ti Oxides	3	Anhedral	Fine to medium	Irregular shaped amoeboidal and subpoikilitic grains interstitial to plagioclase.
Accessory/ Alteration Assemblage	3	Anhedral	Fine	Patches of biotite + amphibole + chlorite + apatite + actinolite + quartz found interstitially to the plagioclase.
General Comments: This sample is non-foliated, fine to medium grained, and is overall weakly altered.				
Sample: MM-26	**Depth: 498.5 m**	**Rock Type: Augite troctolite**		
Mineral	Abundance	Habit	Grain Size	Comments
Plagioclase	65	Anhedral-Subhedral	Fine to medium W=0.2-0.8 mm L=<5 mm	Cumulate grains. Non-foliated, weakly altered (~20% sericite). Zoning minor. Lath shaped grains minor tabular.
Clinopyroxene	10	Subophitic	Medium (<15 mm)	Optically continuous subophitic grains, weak uralite/chlorite alteration (10%).
Olivine	19	Subhedral	Medium (<2.5 mm)	Cumulate equant shaped grains, weak to heavily altered to iddingsite, talc alteration on some grain boundaries. Oikocryst to plagioclase grains.

Fe-Ti Oxides	3	Anhedral	Fine to medium	Irregular shaped amoeboidal and subpoikilitic grains interstitial to plagioclase.
Accessory/ Alteration Assemblage	3	Anhedral	Fine	Patches of biotite + amphibole + chlorite + apatite + actinolite + quartz found interstitially to the plagioclase.
General Comments: This sample is non-foliated, fine to medium grained, and is overall weakly altered.				
Sample: MM-29	**Depth: 534.3 m**	**Rock Type: Augite troctolite**		
Mineral	Abundance	Habit	Grain Size	Comments
Plagioclase	65	Anhedral-Subhedral	Fine to medium W=0.2-0.7 mm L=<2 mm	Cumulate grains.Poorly foliated, weakly altered (~20% sericite). Zoning minor. Lath shaped grains minor tabular.
Clinopyroxene	13	Subophitic -ophitic	Coarse (<15 mm)	Optically continuous subophitic/ophitic grains, weak uralite/chlorite alteration (10%).
Olivine	17	Subhedral	Fine to medium (<1.5 mm)	Cumulate equant shaped grains, weak to heavily altered to iddingsite, talc alteration on some grain boundaries.
Fe-Ti Oxides	2	Anhedral	Fine to medium	Irregular shaped amoeboidal and subpoikilitic grains interstitial to plagioclase.
Accessory/ Alteration Assemblage	3	Anhedral	Fine	Patches of biotite + amphibole + chlorite + actinolite + quartz found interstitially to the plagioclase.
General Comments: This sample is poorly foliated, fine to medium grained, and is overall weakly altered.				
Sample: MM-32	**Depth: 566.6 m**	**Rock Type: Troctolite**		
Mineral	Abundance	Habit	Grain Size	Comments
Plagioclase	65	Anhedral-Subhedral	Fine to medium	Cumulate grains. Non-foliated, weakly altered

			W=0.2-0.6 mm L=<2.5 mm	(~20% sericite). Zoning minor. Lath and elongated lath shaped grains.
Clinopyroxene	8	Subophitic	Coarse (<10 mm)	Optically continuous subophitic grains, weak uralite/chlorite alteration (10%).
Olivine	22	Subhedral	Fine to medium (<2.5 mm)	Cumulate equant shaped grains, weakly altered to iddingsite, talc alteration on some grain boundaries. Oikocryst to plagioclase grains.
Fe-Ti Oxides	2	Anhedral	Fine to medium	Irregular shaped amoeboidal and subpoikilitic grains interstitial to plagioclase.
Accessory/ Alteration Assemblage	3	Anhedral	Fine	Patches of biotite + amphibole + chlorite + apatite + actinolite + quartz found interstitially to the plagioclase.
General Comments: This sample is non-foliated, fine to medium grained, and is overall weakly altered.				
Sample: MM-35	**Depth: 580.9 m**	**Rock Type: Augite troctolite**		
Mineral	Abundance	Habit	Grain Size	Comments
Plagioclase	63	Anhedral-Subhedral	Fine to medium W=0.1-0.5 mm L=<1.5 mm	Cumulate grains. Non-foliated, weakly altered (~25% sericite). Zoning minor. Lath and elongated lath shaped grains.
Clinopyroxene	10	Subophitic	Coarse (<13 mm)	Optically continuous subophitic grains, weak uralite/chlorite alteration (10%).
Olivine	21	Subhedral	Fine to medium (<2.5 mm)	Cumulate equant shaped grains, weakly altered to iddingsite, talc alteration on some grain boundaries. Oikocryst to plagioclase grains.

Fe-Ti Oxides	3	Anhedral	Fine to medium	Irregular shaped amoeboidal and subpoikilitic grains interstitial to plagioclase.
Accessory/ Alteration Assemblage	3	Anhedral	Fine	Patches of biotite + amphibole + chlorite + apatite + actinolite found interstitially to the plagioclase.
General Comments: This sample is non-foliated, fine to medium grained, and is overall weakly altered.				
Sample: MM-37	**Depth: 584.3 m**	**Rock Type: Augite melatroctolite**		
Mineral	Abundance	Habit	Grain Size	Comments
Plagioclase	35	Anhedral-Subhedral	Coarse to very coarse W=0.5-8 mm L=<20 mm	Cumulate grains. Non-foliated, weakly altered (~25% sericite). Zoning minor. Lath shaped grains.
Clinopyroxene	30	Subophitic ?	Coarse (<15 mm)	Optically continuous subophitic? grains, weak uralite/chlorite alteration (10%).
Olivine	33	Anhedral-Subhedral	Coarse to very coarse (<25 mm)	Cumulate equant shaped grains, one skeletal grain, weakly altered to iddingsite, Oikocryst to plagioclase grains.
Fe-Ti Oxides	1	Anhedral	Fine to medium	Blebs found enclosed in clinopyroxene grains.
Accessory/ Alteration Assemblage	1	Anhedral	Fine	Patches of biotite + amphibole + chlorite + apatite + actinolite.
General Comments: This sample is non-foliated, coarse to very coarse, and is overall weakly altered. Due to coarse grained nature, habit of clinopyroxene difficult to determine.				
Sample: MM-38	**Depth: 593.8 m**	**Rock Type: Olivine gabbroic anorthosite**		
Mineral	Abundance	Habit	Grain Size	Comments

Plagioclase	80	Subhedral	Coarse to very coarse W=0.5-8 mm L=<20 mm	Cumulate grains. Non-foliated, weakly altered (~30% sericite). Zoning minor. Lath and tabular shaped grains.
Clinopyroxene	9	Subophitic ?	Coarse (<15 mm)	Optically continuous subophitic? grains, weak uralite/chlorite alteration (10%).
Olivine	7	Anhedral	Coarse (<7 mm)	Cumulate irregular shaped, weakly altered to iddingsite,
Fe-Ti Oxides	3	Anhedral-subhedral	Fine to medium	Blebs found enclosed in clinopyroxene grains. Some skeletal grains.
Accessory/ Alteration Assemblage	1	Anhedral	Fine	Patches of biotite + amphibole + chlorite + apatite + actinolite.
General Comments: This sample is non-foliated, coarse to very coarse, and is overall weakly altered. Due to coarse grained nature, habit of clinopyroxene difficult to determine.				
Sample: MM-39	**Depth: 603.7 m**	**Rock Type: Troctolite**		
Mineral	Abundance	Habit	Grain Size	Comments
Plagioclase	68	Anhedral-Subhedral	Fine to medium W=0.1-0.5 mm L=<2.5 mm	Cumulate grains. Very well foliated, weakly altered (~15% sericite). Zoning minor. Elongated lath shaped grains.
Clinopyroxene	5	Subophitic	Medium (<5 mm)	Optically continuous subophitic grains, weak uralite/chlorite alteration (10%).
Olivine	22	Subhedral	Fine to medium (<2.5 mm)	Cumulate equant shaped grains, weakly altered to iddingsite, talc alteration on some grain boundaries. Some grains are oikocryst to plagioclase grains.

Fe-Ti Oxides	1	Anhedral	Fine to medium	Irregular shaped amoeboidal and subpoikilitic grains interstitial to plagioclase.
Accessory/ Alteration Assemblage	4	Anhedral	Fine	Patches of biotite + amphibole + chlorite + apatite + actinolite found interstitially to the plagioclase.
General Comments: This sample is very well foliated, fine to medium grained, and is overall weakly altered.				
Sample: MM-40	**Depth: 608.1 m**	**Rock Type: Troctolite**		
Mineral	Abundance	Habit	Grain Size	Comments
Plagioclase	72	Anhedral-Subhedral	Fine to medium W=0.1-0.5 mm L=<4 mm	Cumulate grains. Well foliated, weakly altered (~15% sericite). Zoning minor. Elongated lath shaped grains.
Clinopyroxene	5	Subophitic	Medium (<5 mm)	Optically continuous subophitic grains, weak uralite/chlorite alteration (10%).
Olivine	18	Subhedral	Fine to medium (<3 mm)	Cumulate equant shaped grains, weakly altered to iddingsite, talc alteration on some grain boundaries. Some grains are oikocryst to plagioclase grains. Some grains are slightly elongate in direction of foliation.
Fe-Ti Oxides	1	Anhedral	Fine to medium	Irregular shaped amoeboidal and subpoikilitic grains interstitial to plagioclase.
Accessory/ Alteration Assemblage	4	Anhedral	Fine	Patches of biotite + amphibole + chlorite + apatite + actinolite found interstitially to the plagioclase.
General Comments: This sample is very well foliated, fine to medium grained, and is overall weakly altered.				
Sample: MM-43	**Depth: 627.0 m**	**Rock Type: Augite troctolite**		

Mineral	Abundance	Habit	Grain Size	Comments
Plagioclase	65	Anhedral-Subhedral	Fine to medium W=0.1-0.5 mm L=<3.5 mm	Cumulate grains. Moderately foliated, weakly altered (~15% sericite). Zoning minor. Lath and elongated lath shaped grains.
Clinopyroxene	12	Subophitic	Coarse (<18 mm)	Optically continuous subophitic grains, weak uralite/chlorite alteration (10%).
Olivine	19	Subhedral	Fine to medium (<2.5 mm)	Cumulate equant shaped grains, weakly altered to iddingsite, talc alteration on some grain boundaries. Some grains are oikocryst to plagioclase grains.
Fe-Ti Oxides	1	Anhedral	Fine to medium	Irregular shaped amoeboidal and subpoikilitic grains interstitial to plagioclase.
Accessory/ Alteration Assemblage	3	Anhedral	Fine	Patches of biotite + amphibole + chlorite + apatite + actinolite found interstitially to the plagioclase.
General Comments: This sample is moderately foliated, fine to medium grained, and is overall weakly altered.				
Sample: MM-44	**Depth: 631.5 m**	**Rock Type: Troctolite**		
Mineral	Abundance	Habit	Grain Size	Comments
Plagioclase	55	Anhedral-Subhedral	Fine to medium W=0.1-0.5 mm L=<2.5 mm	Cumulate grains. well foliated, weakly altered (~15% sericite). Zoning minor. Lath and elongated lath shaped grains.
Clinopyroxene	8	Subophitic	Coarse (<10 mm)	Optically continuous subophitic grains, weak uralite/chlorite alteration (10%).
Olivine	33	Subhedral	Fine to medium (<2 mm)	Cumulate equant shaped grains, weakly altered to iddingsite, talc alteration on

				some grain boundaries. Some grains are oikocryst to plagioclase grains.
Fe-Ti Oxides	1	Anhedral	Fine to medium	Irregular shaped amoeboidal and subpoikilitic grains interstitial to plagioclase.
Accessory/ Alteration Assemblage	3	Anhedral	Fine	Patches of biotite + amphibole + chlorite + apatite + actinolite found interstitially to the plagioclase.
General Comments: This sample is well foliated, fine to medium grained, and is overall weakly altered.				
Sample: MM-46	**Depth: 652.9 m**	**Rock Type: Troctolite**		
Mineral	Abundance	Habit	Grain Size	Comments
Plagioclase	60	Anhedral-Subhedral	Fine to medium W=0.1-0.5 mm L=<3.5 mm	Cumulate grains. moderately foliated, weakly altered (~15% sericite). Zoning minor. Lath and elongated lath shaped grains.
Clinopyroxene	8	Subophitic	Coarse (<15 mm)	Optically continuous subophitic grains, weak uralite/chlorite alteration (10%).
Olivine	27	Subhedral	Fine to medium (<2.5 mm)	Cumulate equant shaped grains, weakly altered to iddingsite, talc alteration on some grain boundaries. Some grains are oikocryst to plagioclase grains.
Fe-Ti Oxides	2	Anhedral	Fine to medium	Irregular shaped amoeboidal and subpoikilitic grains interstitial to plagioclase.
Accessory/ Alteration Assemblage	3	Anhedral	Fine	Patches of biotite + amphibole + chlorite + apatite + actinolite found interstitially to the plagioclase.
General Comments: This sample is moderately foliated, fine to medium grained, and is overall weakly altered.				

Sample: MM-49	**Depth: 708.7 m**	**Rock Type: Troctolite**		
Mineral	Abundance	Habit	Grain Size	Comments
Plagioclase	75	Anhedral-Subhedral	Fine to medium W=0.1-0.4 mm L=<1.5 mm	Cumulate grains. well foliated, weakly altered (~15% sericite). Zoning minor. Lath and elongated lath shaped grains.
Clinopyroxene	4	Subophitic	Coarse (<15 mm)	Optically continuous subophitic grains, weak uralite/chlorite alteration (10%).
Olivine	17	Subhedral	Fine to medium (<2 mm)	Cumulate equant shaped grains, weakly altered to iddingsite, talc alteration on some grain boundaries. Some grains are oikocryst to plagioclase grains.
Fe-Ti Oxides	1	Anhedral	Fine to medium	Irregular shaped amoeboidal and subpoikilitic grains interstitial to plagioclase.
Accessory/ Alteration Assemblage	3	Anhedral	Fine	Patches of biotite + amphibole + chlorite + apatite + actinolite found interstitially to the plagioclase.
General Comments: This sample is well foliated, fine to medium grained, and is overall weakly altered.				

Sample: MM-52	**Depth: 770.7 m**	**Rock Type: Troctolite**		
Mineral	Abundance	Habit	Grain Size	Comments
Plagioclase	70	Anhedral-Subhedral	Fine to medium W=0.1-0.5 mm L=<2 mm	Cumulate grains. poorly foliated, weakly altered (~15% sericite). Zoning minor. Lath and elongated lath shaped grains.
Clinopyroxene	6	Subophitic	Coarse (<15 mm)	Optically continuous subophitic grains, weak uralite/chlorite alteration (10%).

Olivine	20	Subhedral	Fine to medium (<2.5 mm)	Cumulate equant shaped grains, weakly altered to iddingsite, talc alteration on some grain boundaries. Some grains are oikocryst to plagioclase grains.
Fe-Ti Oxides	1	Anhedral	Fine to medium	Irregular shaped amoeboidal and subpoikilitic grains interstitial to plagioclase.
Accessory/ Alteration Assemblage	3	Anhedral	Fine	Patches of biotite + amphibole + chlorite + apatite + actinolite found interstitially to the plagioclase.
General Comments: This sample is poorly foliated, fine to medium grained, and is overall weakly altered.				
Sample: MM-55	**Depth: 837.9 m**	**Rock Type: Troctolite**		
Mineral	Abundance	Habit	Grain Size	Comments
Plagioclase	73	Anhedral-Subhedral	Fine W=0.1-0.5 mm L=<1 mm	Cumulate grains. non-foliated, weakly altered (~20% sericite). Zoning minor. Lath and elongated lath shaped grains.
Clinopyroxene	3	Subophitic	Medium (<5 mm)	Optically continuous subophitic grains, weak uralite/chlorite alteration (10%).
Olivine	20	Subhedral	Fine to medium (<3 mm)	Cumulate equant shaped grains, weakly altered to iddingsite, talc alteration on some grain boundaries. Some grains are oikocryst to plagioclase grains.
Fe-Ti Oxides	1	Anhedral	Fine to medium	Irregular shaped amoeboidal and subpoikilitic grains interstitial to plagioclase.
Accessory/ Alteration Assemblage	3	Anhedral	Fine	Patches of biotite + amphibole + chlorite + apatite + actinolite found interstitially to the plagioclase.

General Comments: This sample is non-foliated, fine to medium grained, and is overall weakly altered.				
Sample: MM-64	**Depth: 918.2 m**	**Rock Type: Troctolite**		
Mineral	Abundance	Habit	Grain Size	Comments
Plagioclase	75	Anhedral-Subhedral	Fine to medium W=0.1-0.5 mm L=<1.5 mm	Cumulate grains. non-foliated, weakly altered (~20% sericite). Zoning minor. Lath and elongated lath shaped grains.
Clinopyroxene	3	Subophitic	Medium to coarse (<8 mm)	Optically continuous subophitic grains, weak uralite/chlorite alteration (10%).
Olivine	18	Anhedral-Subhedral	Fine to medium (<3 mm)	Cumulate equant shaped grains, weakly altered to iddingsite, talc alteration on some grain boundaries. Some grains are oikocryst to plagioclase grains.
Fe-Ti Oxides	1	Anhedral	Fine to medium	Irregular shaped amoeboidal and subpoikilitic grains interstitial to plagioclase.
Accessory/ Alteration Assemblage	2	Anhedral	Fine	Patches of biotite + amphibole + chlorite + apatite + actinolite found interstitially to the plagioclase.
General Comments: This sample is non-foliated, fine to medium grained, and is overall weakly altered.				
Sample: MM-67	**Depth: 944.6 m**	**Rock Type: Troctolite**		
Mineral	Abundance	Habit	Grain Size	Comments
Plagioclase	59	Anhedral-Subhedral	Fine to medium W=0.1-0.5 mm L=<1.5 mm	Cumulate grains. non-foliated, weakly altered (~20% sericite). Zoning minor. Lath and elongated lath shaped grains.

Clinopyroxene	4	Subophitic	Medium to coarse (<8 mm)	Optically continuous subophitic grains, weak uralite/chlorite alteration (10%).
Olivine	34	Anhedral-Subhedral	Medium (<5 mm)	Cumulate equant shaped grains, weakly altered to serpentine/FeOx in fractures, talc alteration on some grain boundaries. Some grains are oikocryst to plagioclase grains.
Fe-Ti Oxides	1	Anhedral	Fine to medium	Irregular shaped amoeboidal and subpoikilitic grains interstitial to plagioclase.
Accessory/ Alteration Assemblage	2	Anhedral	Fine	Patches of biotite + amphibole + chlorite + apatite + actinolite found interstitially to the plagioclase.
General Comments: This sample is non-foliated, fine to medium grained, and is overall weakly altered.				
Sample: MM-70	**Depth: 1008.1 m**	**Rock Type: Troctolite**		
Mineral	Abundance	Habit	Grain Size	Comments
Plagioclase	71	Anhedral-Subhedral	Fine to medium W=0.1-0.5 mm L=<1.5 mm	Cumulate grains. non-foliated, weakly to moderately altered (~15-40% sericite). Zoning minor. Lath and elongated lath shaped grains.
Clinopyroxene	5	Subophitic	Medium to coarse (<10 mm)	Optically continuous subophitic grains, weak uralite/chlorite alteration (10%).
Olivine	19	Anhedral-Subhedral	Medium (<5 mm)	Cumulate equant shaped grains, strongly altered to iddingsite on bottom 5/6th of the slide, weakly altered to serpentine/FeOx in fractures on top 1/6th of the slide, talc alteration on some grain boundaries. Some grains are

				oikocryst to plagioclase grains.
Fe-Ti Oxides	2	Anhedral	Fine to medium	Irregular shaped amoeboidal and subpoikilitic grains interstitial to plagioclase.
Accessory/ Alteration Assemblage	3	Anhedral	Fine	Patches of biotite + amphibole + chlorite + apatite + actinolite found interstitially to the plagioclase.
General Comments: This sample is non-foliated, fine to medium grained, and is overall strongly altered.				
Sample: MM-73	**Depth: 1044.1 m**	**Rock Type: Troctolite**		
Mineral	Abundance	Habit	Grain Size	Comments
Plagioclase	71	Anhedral-Subhedral	Fine to medium W=0.1-0.5 mm L=<1.5 mm	Cumulate grains. non-foliated, weakly to moderately altered (~15-40% sericite). Zoning minor. Lath and elongated lath shaped grains.
Clinopyroxene	5	Subophitic	Medium to coarse (<10 mm)	Optically continuous subophitic grains, weak uralite/chlorite alteration (10%).
Olivine	19	Anhedral-Subhedral	Medium (<5 mm)	Cumulate equant shaped grains, strongly altered to iddingsite on bottom 5/6th of the slide, weakly altered to serpentine/FeOx in fractures on top 1/6th of the slide, talc alteration on some grain boundaries. Some grains are oikocryst to plagioclase grains.
Fe-Ti Oxides	2	Anhedral	Fine to medium	Irregular shaped amoeboidal and subpoikilitic grains interstitial to plagioclase.
Accessory/ Alteration Assemblage	3	Anhedral	Fine	Patches of biotite + amphibole + chlorite + apatite + actinolite found interstitially to the plagioclase.

General Comments: This sample is non-foliated, fine to medium grained, and is overall strongly altered.				
Sample: MM-75	**Depth: 1055.7 m**	**Rock Type: Augite troctolite**		
Mineral	Abundance	Habit	Grain Size	Comments
Plagioclase	67	Anhedral-Subhedral	Fine to medium W=0.1-0.5 mm L=<1.5 mm	Cumulate grains. non-foliated, weakly (~20% sericite). Zoning minor. Lath and elongated lath shaped grains.
Clinopyroxene	11	Subophitic	Medium to coarse (<15 mm)	Optically continuous subophitic grains, weak uralite/chlorite alteration (10%).
Olivine	18	Anhedral-Subhedral	Medium (<3 mm)	Cumulate equant shaped grains, weakly altered to serpentine/FeOx in fractures, talc alteration on some grain boundaries. Some grains are oikocryst to plagioclase grains.
Fe-Ti Oxides	1	Anhedral	Fine to medium	Irregular shaped amoeboidal and subpoikilitic grains interstitial to plagioclase.
Accessory/ Alteration Assemblage	3	Anhedral	Fine	Patches of biotite + amphibole + chlorite + apatite + actinolite found interstitially to the plagioclase.
General Comments: This sample is non-foliated, fine to medium grained, and is overall weakly altered.				

APPENDIX B – WHOLE ROCK GEOCHEMISTRY

MOUNT MOLLIE DYKE GEOCHEMISTRY

Sample		Lower	MMD-1	MMD-2	MMD-3	MMD-4	MMD-5
Depth (m)		Detection	-12.6	-23.7	-38.9	-48.3	-59.9
Zone		Limit	U	Xeno	U	U	U
SiO_2	wt%	0.04	48.5	72.23	51.86	50.8	50.81
TiO_2		0.01	2.68	0.56	1.57	2.12	2.3
Al_2O_3		0.02	13.69	12.44	17.7	15.18	14.34
Fe_2O_3		0.01	15.55	5.15	11.09	12.32	13.8
MnO		0.002	0.2	0.041	0.12	0.154	0.188
MgO		0.01	4.74	1.71	5.1	4.97	4.78
CaO		0.006	3.857	0.599	5.196	6.911	7.283
Na_2O		0.02	2.65	2.91	2.75	2.52	2.44
K_2O		0.01	3.63	1.89	1.64	1.65	1.37
P_2O_5		0.002	0.394	0.112	0.185	0.236	0.291
LOI		0.05	2.64	1.93	2.5	2.26	1.71
Total			98.65	99.67	99.81	99.21	99.39
Ba	ppm	0.8	1064.1	635.2	469.2	540.9	443.9
Ce		0.12	63.38	36.34	48.24	52.27	58.61
Co		0.13	45.02	14.7	34.61	37.36	31.93
Cr		2	68	148	270	194	191
Cs		0.013	1.301	1.005	5.643	2.952	2.313
Cu		1.4	254.7	31.3	218.7	109.5	71.7
Dy		0.009	7.815	2.368	5.144	5.928	6.933
Er		0.007	4.422	1.391	2.926	3.266	3.878
Eu		0.0031	2.3978	0.7949	1.4938	1.6763	2.0384
Ga		0.04	22.4	12.73	23.72	21.8	22.19
Gd		0.009	8.221	2.501	5.319	6.32	7.262
Hf		0.14	6.59	4.9	4.39	4.78	5.21
Ho		0.0025	1.5229	0.4685	0.9914	1.1695	1.3504
In		0.0018	0.149	0.0393	0.0833	0.0943	0.0834
La		0.1	27.5	17.5	22.7	24.23	26.88
Lu		0.002	0.5803	0.224	0.4251	0.4427	0.5413
Nb		0.028	15.738	7.479	11.96	13.283	15.033
Nd		0.06	35.73	16.29	25.23	28.84	32.18
Ni		0.7	46.6	44	108.8	59.7	35.9
P		30	1654	448	735	981	1140
Pb		0.18	9.2	26.9	13	7	7.6
Pr		0.014	8.385	4.293	6.268	6.788	7.668
Rb		0.11	163.57	52.34	73.75	60.34	46.1
Sc		1.1	36	9.5	27.9	30.4	35.7
Sm		0.026	8.149	3.089	5.509	6.333	7.267
Sr		0.6	319.3	227.4	283.4	261.9	231.7
Ta		0.007	1.053	0.522	0.784	0.883	0.96
Tb		0.0023	1.2472	0.3811	0.8301	0.9627	1.1253
Th		0.018	4.761	6.568	4.957	4.417	4.179
Ti		7	16229	3199	9454	12636	13942
Tl		0.002	1.373	0.386	0.61	0.502	0.403
Tm		0.0019	0.6227	0.2107	0.4232	0.4708	0.5521
U		0.011	1.397	2.503	4.014	2.707	2.15
V		1	327	69	267	251	306
Y		0.05	41.73	12.91	27.76	31.75	37.67
Yb		0.009	3.95	1.402	2.761	2.98	3.587
Zn		1.8	216	93	164	150	175
Zr		1.8	267	191	164	179	207
Au	ppb	0.4	1.21	1.62	4.05	1.92	1.32
Ir		0.01	0.05	0.03	0.09	0.05	0.03
Pd		0.12	2.02	0.64	6.52	2.71	1.79
Pt		0.17	3.31	0.56	4.55	3.46	1.66
Rh		0.04	0.11	0.05	0.24	0.14	0.07
Ru		0.08			0.19	0.1	
S	wt%	0.003	0.048	0.03	0.289	0.098	0.032

Sample		MMD-6	MMD-7	MMD-8	MMD-9	MMD-10	MMD-11
Depth (m)		-66.9	-74.4	-89.3	-123.4	-154.5	-197.5
Zone		Xeno	M-US	M-US	M-US	M-US	M-US
SiO_2	wt%	61	47.97	50.42	50.35	46.09	45.41
TiO_2		0.86	3.77	2.08	2.18	1.78	3.33
Al_2O_3		15.84	12.8	15.74	16.72	16.95	13.52
Fe_2O_3		8.13	16.3	12.91	10.35	13.52	17.41
MnO		0.065	0.219	0.185	0.146	0.191	0.229
MgO		2.86	4.48	5.23	4.08	5.55	5.41
CaO		1.122	7.223	7.822	8.234	9.273	10.008
Na_2O		2.49	2.24	2.49	2.5	2.68	2.48
K_2O		3.45	1.41	1.09	2.44	0.61	0.53
P_2O_5		0.086	0.343	0.222	0.179	0.205	0.179
LOI		2.91	2.3	0.98	2.32	2.28	1.08
Total		98.93	99.11	99.23	99.64	99.18	99.64
Ba	ppm	786.1	402.7	291.5	1082.9	294.8	243.3
Ce		67.42	62.1	42.48	37.69	34.17	29.69
Co		22.74	44.08	32.32	27.87	53.1	56.36
Cr		185	140	214	146	152	198
Cs		3.357	2.167	1.969	2.42	3.592	1.686
Cu		75.9	137.4	52.7	40.1	256.4	345.3
Dy		3.578	7.53	5.017	4.768	5.137	4.912
Er		2.133	4.191	2.75	2.716	2.864	2.791
Eu		1.3853	2.1948	1.6444	1.7255	1.6178	1.6058
Ga		19.51	23.18	21.43	22.72	22.72	22.73
Gd		4.352	7.939	5.298	4.94	5.097	4.995
Hf		4.98	5.82	4.09	3.67	3.76	3.3
Ho		0.7086	1.4544	0.9728	0.9421	1.0002	0.9777
In		0.0752	0.1016	0.0685	0.064	0.0721	0.0939
La		33.7	28.91	19.63	17.76	15.37	13.55
Lu		0.3541	0.5844	0.384	0.3645	0.3873	0.3735
Nb		11.042	19.452	12.561	10.381	9.837	9.314
Nd		31.75	34.54	23.7	20.63	20.29	18.29
Ni		84.2	136.9	30	10.5	83.3	45.3
P		343	1346	879	723	854	727
Pb		16.9	6.9	5.5	4.9	2.3	2.8
Pr		8.144	8.12	5.566	4.86	4.568	4.086
Rb		78.31	46.58	35.19	82.89	17.49	15.38
Sc		17	44	35.2	37.7	29.5	50
Sm		5.571	7.709	5.288	4.76	4.814	4.503
Sr		204.1	217	249.8	428.8	263.6	225.6
Ta		0.709	1.253	0.822	0.695	0.643	0.607
Tb		0.6056	1.2286	0.8157	0.7545	0.81	0.7783
Th		7.412	4.388	3.034	2.563	1.621	1.397
Ti		5015	22473	12521	13248	10537	20143
Tl		0.72	0.635	0.27	0.445	1.51	0.168
Tm		0.3258	0.5921	0.3916	0.3837	0.3979	0.3904
U		3.109	2.336	1.351	1.126	0.429	0.406
V		141	407	304	365	230	>530
Y		19.27	40.59	26.84	25.8	27.62	26.49
Yb		2.223	3.827	2.525	2.471	2.587	2.464
Zn		141	195	141	119	118	148
Zr		202	226	154	138	135	119
Au	ppb	2.67	1.67	1.15	1.59	7.02	3.67
Ir		0.06	0.16	0.02	0.01	0.14	0.03
Pd		2.16	24.7	0.65	0.25	5.1	1.74
Pt		1.47	5.56	0.95	0.31	7.87	1.98
Rh		0.11	0.57	0.04		0.36	0.08
Ru		0.13	0.27			0.23	
S	wt%	0.024	0.102	0.131	0.048	0.042	0.101

Sample		MMD-12	MMD-13	MMD-14	MMD-15	MMD-16	MMD-17
Depth (m)		-226.9	-247.8	-273.7	-296.3	-313.2	-340.5
Zone		M-US	M-US	M-US	M-US	M-US	M-US
SiO_2	wt%	47.7	48.87	47.75	48.51	48.71	48.56
TiO_2		2.52	1.87	1.46	1.53	1.53	1.67
Al_2O_3		13.87	14.3	15.52	15.51	15.86	15.12
Fe_2O_3		14.24	12.87	12.62	12.46	11.84	12.21
MnO		0.194	0.187	0.17	0.172	0.165	0.174
MgO		6.53	6.67	7.74	7.42	6.38	6.95
CaO		10.699	10.898	10.406	10.785	10.663	11.26
Na_2O		2.5	2.53	2.53	2.59	2.71	2.58
K_2O		0.56	0.57	0.49	0.5	0.55	0.43
P_2O_5		0.177	0.17	0.135	0.141	0.168	0.168
LOI		0.32	0.49	0.86	0.26	0.55	0.32
Total		99.35	99.49	99.74	99.93	99.19	99.51
Ba	ppm	243	210.9	153.2	171.5	189.3	164.4
Ce		31.95	31.44	24.25	25.21	30.42	27.41
Co		48.57	45.79	53.08	51.01	44.85	46.32
Cr		178	241	320	305	284	349
Cs		1.539	1.777	2.546	1.709	1.694	1.692
Cu		277.6	242.2	206.2	234.9	220.3	248.7
Dy		5.29	4.985	3.801	4.073	4.583	4.458
Er		2.986	2.871	2.153	2.342	2.638	2.512
Eu		1.6073	1.5498	1.2736	1.3535	1.5291	1.4287
Ga		21.43	20.45	19.95	20.18	20.9	20.14
Gd		5.308	5.075	3.915	4.117	4.722	4.503
Hf		3.54	3.2	2.48	2.79	3.04	3.02
Ho		1.046	0.9862	0.7544	0.8	0.906	0.8893
In		0.0827	0.0814	0.0628	0.0651	0.0681	0.0688
La		14.25	13.96	11.01	11.22	13.6	12.28
Lu		0.3968	0.3773	0.29	0.3116	0.3407	0.3234
Nb		9.834	9.009	6.768	7.289	8.262	7.74
Nd		20.05	18.93	14.35	15.41	18.2	16.77
Ni		52.5	62.6	95.9	77.9	57.1	74.9
P		722	699	574	578	719	671
Pb		2.7	2.9	2.2	1.9	2.4	2.2
Pr		4.379	4.236	3.295	3.445	4.048	3.68
Rb		14.85	15.95	12.99	12.74	14.49	10.6
Sc		49.8	49.5	38.4	41.9	41.8	45.2
Sm		4.818	4.631	3.573	3.772	4.31	4.138
Sr		227.1	245.6	247.7	244.3	256.1	232.7
Ta		0.625	0.582	0.435	0.468	0.521	0.498
Tb		0.8185	0.804	0.6179	0.6549	0.7221	0.7029
Th		1.464	1.472	1.198	1.227	1.448	1.286
Ti		15047	11339	8756	9276	9251	10084
Tl		0.095	0.129	0.144	0.075	0.1	0.081
Tm		0.4102	0.3949	0.2991	0.3287	0.3625	0.3404
U		0.418	0.451	0.333	0.354	0.422	0.371
V		442	283	244	269	260	289
Y		28.21	27.23	20.61	22.11	25.15	24.01
Yb		2.679	2.512	1.957	2.089	2.314	2.243
Zn		118	112	107	99	99	97
Zr		132	116	94	100	116	105
Au	ppb	7.37	7.31	6.08	7.77	7.01	10.4
Ir		0.07	0.16	0.27	0.34	0.17	0.19
Pd		0.9	6	19.5	22.1	10.3	7.32
Pt		8.64	15	16.9	18.5	11.9	12.4
Rh		0.12	0.5	0.85	1.07	0.53	0.43
Ru			0.08	0.23	0.29		
S	wt%	0.089	0.097	0.036	0.054	0.052	0.076

Sample		MMD-18	MMD-19	MMD-20	MMD-21	MMD-22	MMD-23
Depth (m)		-367.9	-397.6	-411.3	-438.5	-457.2	-476.1
Zone		M-US	M-US	M-US	M-LS	M-LS	M-LS
SiO_2	wt%	47.73	49.1	47.94	47.35	47.17	46.34
TiO_2		1.82	1.42	1.86	2.42	1.66	1.6
Al_2O_3		14.78	15.22	13.47	15.24	17.41	17.11
Fe_2O_3		13.21	11.53	13.57	12.08	11.61	13.94
MnO		0.181	0.169	0.198	0.173	0.155	0.175
MgO		7.37	6.44	7.54	6.54	6.86	8.35
CaO		10.478	10.841	10.833	11.04	9.578	8.687
Na_2O		2.5	2.67	2.42	2.65	2.78	2.65
K_2O		0.46	0.63	0.48	0.56	0.54	0.45
P_2O_5		0.14	0.211	0.24	0.152	0.136	0.124
LOI		0.37	0.93	0.69	1.47	1.53	0.35
Total		99.1	99.24	99.33	99.76	99.5	99.85
Ba	ppm	165.3	209.8	187.8	190	177.9	157.2
Ce		27.18	35.94	37.08	26.06	24	23.62
Co		51.75	41.54	48.99	44.62	49.44	61.12
Cr		316	378	415	444	366	390
Cs		1.787	1.876	1.886	1.61	2.993	1.864
Cu		244.6	233.7	217.4	229.2	142.6	160.4
Dy		4.312	5.189	6.069	4.419	3.703	3.291
Er		2.444	2.949	3.338	2.508	2.092	1.936
Eu		1.3725	1.5868	1.7158	1.4668	1.3692	1.2298
Ga		19.82	20.81	20.05	20.7	20.95	20.22
Gd		4.265	5.291	6.121	4.444	3.721	3.367
Hf		3.07	3.87	3.8	2.87	2.74	2.52
Ho		0.8519	1.0174	1.1893	0.8666	0.7163	0.6571
In		0.0744	0.0713	0.0857	0.0819	0.0593	0.0536
La		12.17	16.37	16.45	11.65	10.86	10.76
Lu		0.3304	0.3745	0.4329	0.3311	0.2917	0.2633
Nb		8.412	9.306	10.139	9.037	7.796	7.533
Nd		16.02	21.11	23.25	16.17	14.21	13.52
Ni		73.9	65.6	71.2	67	109.9	143.2
P		552	878	963	608	544	485
Pb		2.2	2.9	2.6	1.8	1.9	1.9
Pr		3.622	4.753	5.104	3.618	3.201	3.064
Rb		12.14	16.3	13.24	15.49	15.13	11.34
Sc		43	43.1	47.1	45.2	25.7	20.5
Sm		3.897	5.052	5.542	4.03	3.411	3.232
Sr		225.3	239.2	205.5	296	274.8	247.1
Ta		0.53	0.593	0.638	0.586	0.513	0.47
Tb		0.6831	0.8296	0.9383	0.6965	0.5952	0.5172
Th		1.321	1.843	1.69	1.165	1.131	1.117
Ti		10888	8597	11257	14816	10155	9573
Tl		0.079	0.088	0.076	0.075	0.141	0.073
Tm		0.346	0.4141	0.4678	0.3487	0.2937	0.2697
U		0.389	0.565	0.49	0.312	0.339	0.308
V		275	248	307	326	179	229
Y		23.19	28.2	32.33	23.88	20.15	17.96
Yb		2.229	2.577	2.954	2.24	1.911	1.753
Zn		107	99	118	108	99	116
Zr		108	133	146	108	103	95
Au	ppb	3.65	6.34	3.91	10.6	3.72	2.2
Ir		0.31	0.07	0.02	0.03	1.56	0.16
Pd		24.7	18	1.22	0.32	29.8	12.4
Pt		16.9	5.67	1.47	3.08	101	8.17
Rh		1.07	0.29	0.06		3.2	0.37
Ru		0.31				1.12	0.23
S	wt%	0.078	0.093	0.069	0.033	0.031	0.051

Sample		MMD-24	MMD-25	MMD-26	MMD-27	MMD-28	MMD-29
Depth (m)		-486.3	-493.6	-498.5	-511.6	-525.5	-534.3
Zone		M-LS	M-LS	M-LS	M-LS	M-LS	M-LS
SiO_2	wt%	46.01	47.5	46.2	46.84	46.59	46.26
TiO_2		1.41	1.56	1.41	1.52	1.51	1.35
Al_2O_3		16.18	18.06	17.42	17.01	17.63	17.14
Fe_2O_3		14.34	11.11	12.37	11.89	12.25	12.51
MnO		0.184	0.149	0.161	0.159	0.159	0.157
MgO		9.34	6.69	6.79	8.67	8.74	8.49
CaO		8.745	9.722	9.853	9.611	8.9	8.864
Na_2O		2.47	2.82	2.51	2.55	2.57	2.61
K_2O		0.39	0.52	0.47	0.45	0.56	0.52
P_2O_5		0.148	0.185	0.142	0.157	0.162	0.113
LOI		0.32	0.86	1.76	0.73	0.91	1.29
Total		99.59	99.23	99.13	99.63	100.02	99.37
Ba	ppm	143.7	174.1	156.6	161.6	173.9	186.2
Ce		24.01	28.65	23.81	25.6	27.82	21.12
Co		66.73	46.39	51.77	56.24	58.42	60.46
Cr		269	234	207	202	119	364
Cs		1.998	2.348	2.312	2.029	1.746	3.721
Cu		148.1	137.8	178.4	118	133.8	157.8
Dy		3.495	4.186	3.564	3.948	3.993	3.131
Er		2.034	2.332	2.007	2.233	2.322	1.735
Eu		1.2105	1.4267	1.3777	1.3641	1.3561	1.2288
Ga		19.29	21.48	20.77	19.8	19.88	20.4
Gd		3.605	4.258	3.703	3.995	4.084	3.053
Hf		2.45	2.77	2.34	2.7	2.96	2.18
Ho		0.6918	0.8098	0.7105	0.7776	0.7854	0.6089
In		0.0549	0.0586	0.0527	0.0581	0.0581	0.0539
La		10.86	13.17	10.86	11.78	12.49	9.55
Lu		0.2767	0.309	0.271	0.3053	0.3091	0.2405
Nb		7.165	8.54	6.838	7.884	8.734	6.496
Nd		13.99	17.17	14.36	15.62	15.85	12.17
Ni		177.4	121.4	136	142.5	164.1	163.5
P		584	743	639	628	655	459
Pb		1.7	2	2.2	1.7	3.2	2.2
Pr		3.177	3.907	3.207	3.437	3.645	2.754
Rb		10.12	13.78	12.75	11.88	15.62	15.36
Sc		22.6	23.8	25.5	25.8	19.7	21.3
Sm		3.403	4.034	3.426	3.697	3.71	2.939
Sr		234	267.5	269.3	244.7	263.7	268.6
Ta		0.459	0.537	0.424	0.5	0.553	0.415
Tb		0.5612	0.6718	0.5751	0.6365	0.6413	0.4858
Th		1.08	1.329	1.057	1.106	1.258	0.964
Ti		8515	9274	8506	8965	9093	8232
Tl		0.07	0.084	0.388	0.066	0.074	0.113
Tm		0.2722	0.3283	0.2787	0.3074	0.3252	0.2431
U		0.291	0.366	0.296	0.279	0.335	0.242
V		187	169	217	181	153	184
Y		19.1	22.65	19.67	21.21	21.83	16.55
Yb		1.824	2.076	1.805	1.977	2.055	1.602
Zn		114	93	106	94	101	108
Zr		96	107	89	100	119	85
Au	ppb	2.24	2.1	4.5	3.71	2.33	6.3
Ir		0.38	0.13	0.13	0.2	0.11	2.54
Pd		13.4	9.48	3.34	12.3	9.04	241
Pt		14.9	8.52	4.85	11	4.06	141
Rh		1.4	0.37	0.26	0.52	0.31	11.9
Ru		0.39	0.32	0.19	0.32	0.24	4.76
S	wt%	0.053	0.042	0.051	0.019	0.047	0.025

Sample		MMD-30	MMD-31	MMD-32	MMD-33	MMD-34	MMD-35
Depth (m)		-550.5	-561.1	-566.6	-576.4	-578.5	-580.9
Zone		M-LS	M-LS	M-LS	M-LS	M-LS	M-LS
SiO_2	wt%	44.68	45.61	45.97	44.7	45.26	45.18
TiO_2		1.53	1.33	1.25	1.2	1.21	1.19
Al_2O_3		16.12	15.89	16.76	15.97	14.92	15.69
Fe_2O_3		13.83	13.39	12.02	15.54	14.83	14.66
MnO		0.192	0.175	0.162	0.191	0.195	0.188
MgO		8.4	10.76	10.3	11.35	12.45	10.36
CaO		7.722	8.821	9.059	7.758	8.193	8.554
Na_2O		2.16	2.23	2.34	2.33	2.06	2.19
K_2O		0.94	0.48	0.47	0.4	0.45	0.54
P_2O_5		0.132	0.147	0.149	0.116	0.108	0.129
LOI		3.46	0.77	1.12	0.23	0.57	0.94
Total		99.25	99.66	99.64	99.84	100.3	99.67
Ba	ppm	575.8	153.5	156.6	137.9	143.5	164.7
Ce		21.81	25.08	23.76	20.31	18.86	21.32
Co		70.87	69.63	65.15	81.14	86.99	69.48
Cr		248	254	281	244	242	253
Cs		2.962	1.872	3.099	2.815	1.945	2.203
Cu		193	124.8	104.1	164.7	114.4	191.5
Dy		3.141	3.601	3.523	2.797	2.928	3.141
Er		1.791	2.052	2.022	1.603	1.653	1.791
Eu		1.1596	1.2126	1.191	1.0446	1.1927	1.122
Ga		19.63	17.98	18.37	18.1	17.28	18.39
Gd		3.291	3.692	3.61	2.835	2.903	3.149
Hf		2.23	2.62	2.45	2.17	2	2.16
Ho		0.6331	0.7123	0.6968	0.5367	0.577	0.6287
In		0.059	0.0551	0.0495	0.0464	0.0577	0.0495
La		9.84	11.34	10.86	9.29	8.68	9.7
Lu		0.2531	0.272	0.2646	0.2149	0.2425	0.2377
Nb		6.681	7.289	6.839	5.901	5.752	6.082
Nd		12.88	14.45	13.9	11.53	11.11	12.65
Ni		216.7	236.2	227.5	309.3	308.9	244.1
P		525	595	623	468	433	530
Pb		2.7	4	6.3	3	4.6	5.5
Pr		2.917	3.332	3.221	2.662	2.546	2.829
Rb		33.19	13.05	12.59	9.93	12.23	16.41
Sc		21.6	21.8	20.8	14.9	21.8	21.7
Sm		3.02	3.539	3.296	2.673	2.687	3.025
Sr		302.1	237.8	252.4	226.3	221.6	259.6
Ta		0.43	0.461	0.43	0.373	0.376	0.392
Tb		0.5124	0.5956	0.5741	0.4434	0.4608	0.5151
Th		1.008	1.131	1.078	1.012	0.867	1.01
Ti		9163	7874	7308	7158	7386	7061
Tl		1.72	0.074	0.087	0.064	0.093	0.134
Tm		0.2534	0.287	0.2845	0.2229	0.2312	0.2515
U		0.253	0.282	0.284	0.283	0.254	0.277
V		197	157	158	169	148	170
Y		17.42	19.32	18.89	15.29	15.84	16.81
Yb		1.659	1.846	1.797	1.414	1.562	1.598
Zn		126	116	117	127	>9100	3534
Zr		84	103	97	83	73	81
Au	ppb	3.82	1.24	0.9	3.04	0.88	0.53
Ir		0.38	0.03	0.04	0.09	0.14	0.02
Pd		3.97	1.32	0.72	1.31	2.81	0.76
Pt		12.4	0.85	0.77	4.84	5.09	
Rh		0.92	0.05	0.06	0.15	0.19	
Ru		0.81	0.21	0.29	0.4	0.46	0.19
S	wt%	0.048	0.051	0.041	0.029	0.056	0.07

Sample		MMD-36	MMD-37	MMD-38	MMD-39	MMD-40	MMD-41
Depth (m)		-582.8	-584.3	-593.8	-603.7	-608.1	-614.8
Zone		P	P	P	M-LS	M-LS	M-LS
SiO_2	wt%	45.84	44.45	47.96	46.91	47.23	45.72
TiO_2		1.96	2.96	1.41	0.87	0.93	1.03
Al_2O_3		15.89	13.1	19.5	18	18.74	16.98
Fe_2O_3		16.36	19.19	10.2	11.25	10.36	12.14
MnO		0.196	0.243	0.143	0.149	0.14	0.159
MgO		6.8	8.15	5.12	9.05	8.51	10.87
CaO		7.473	7.597	8.359	10.227	10.316	9.094
Na_2O		2.85	2.4	3.23	2.53	2.57	2.25
K_2O		0.76	0.67	1.42	0.32	0.37	0.42
P_2O_5		0.221	0.171	0.136	0.067	0.104	0.108
LOI		1.15	0.67	1.03	0.38	0.79	0.96
Total		99.55	99.65	98.57	99.8	100.1	99.77
Ba	ppm	313.3	283.6	527.3	102	131.9	133
Ce		35.12	30.61	25.62	11.56	18.56	18.46
Co		65.7	73.84	41.66	57.47	53.76	65.77
Cr		142	126	152	321	295	276
Cs		3.486	2.029	1.8	2.378	2.509	1.881
Cu		321	205.3	162.6	190.3	138	150.5
Dy		4.718	4.594	3.552	2.032	2.767	2.775
Er		2.691	2.628	1.995	1.145	1.558	1.534
Eu		1.613	1.43	1.5069	0.9447	1.0543	1.0149
Ga		22.39	18.57	22.52	18.37	19.26	17.37
Gd		4.936	4.665	3.561	2.026	2.819	2.757
Hf		3.56	3.57	2.61	1.26	1.91	2.01
Ho		0.9447	0.9033	0.6952	0.3998	0.5435	0.5419
In		0.0695	0.0809	0.0497	0.0393	0.0423	0.047
La		15.88	14.02	11.86	5.26	8.26	8.3
Lu		0.3712	0.3639	0.2715	0.1544	0.207	0.2115
Nb		9.742	10.962	7.171	3.208	4.981	5.294
Nd		20.19	18.03	14.52	7.13	10.87	10.83
Ni		151.7	116.4	93.3	201.3	183.6	265.4
P		857	691	562	258	422	469
Pb		4.9	3.8	3.4	2.3	2.2	2.5
Pr		4.632	4.12	3.419	1.573	2.435	2.471
Rb		23.92	20.21	49.01	6.09	8.44	10.48
Sc		22.8	32.2	19.3	24.4	23.3	18.9
Sm		4.67	4.367	3.529	1.769	2.618	2.622
Sr		298.7	235.1	431.6	244	261.1	236.4
Ta		0.626	0.738	0.461	0.207	0.312	0.324
Tb		0.7688	0.7328	0.5767	0.3166	0.4483	0.4355
Th		1.794	1.543	1.264	0.462	0.768	0.77
Ti		11836	17754	8143	5097	5721	6186
Tl		0.317	0.176	0.17	0.031	0.046	0.079
Tm		0.3785	0.369	0.2772	0.1598	0.2181	0.2171
U		0.495	0.47	0.362	0.132	0.198	0.204
V		259	270	142	136	139	151
Y		26.37	24.79	19.09	10.7	15.13	14.49
Yb		2.455	2.431	1.813	1.026	1.419	1.391
Zn		3992	4045	3875	1155	1118	94
Zr		137	133	102	43	70	73
Au	ppb	1.55	1.66	1.31	1.38	1.79	2.52
Ir		0.08	0.03	0.04	0.02	0.11	0.06
Pd		1.77	1.5	3.37	1.39	4.64	3.09
Pt		0.68	0.89	1.12	0.42	4.09	2.65
Rh		0.13	0.07	0.1	0.05	0.27	0.14
Ru		0.36	0.11	0.13	0.15	0.29	0.17
S	wt%	0.119	0.074	0.035	0.027	0.015	0.057

Sample		MMD-42	MMD-43	MMD-44	MMD-45	MMD-46	MMD-47
Depth (m)		-621.2	-627.0	-631.5	-640.1	-652.9	-666.6
Zone		M-LS	M-LS	M-LS	M-LS	M-LS	M-LS
SiO_2	wt%	46.52	46.88	44.09	45.78	46.71	46.23
TiO_2		1.11	1.11	0.87	1.05	1.12	1.09
Al_2O_3		18.05	19.48	14.08	18.34	19.23	18.95
Fe_2O_3		11.4	9.97	14.56	10.36	10.32	10.57
MnO		0.147	0.13	0.184	0.136	0.133	0.134
MgO		9.39	7.7	14.95	8.79	8.27	8.77
CaO		9.595	10.085	7.739	9.755	10.012	9.776
Na_2O		2.47	2.59	1.9	2.3	2.57	2.48
K_2O		0.35	0.48	0.31	0.63	0.42	0.35
P_2O_5		0.126	0.135	0.104	0.125	0.113	0.122
LOI		0.7	0.91	0.76	2.58	0.75	0.76
Total		99.9	99.53	99.62	99.91	99.7	99.28
Ba	ppm	131.4	152.3	108.2	163.8	139.8	129.9
Ce		21.1	22.09	16.93	21.29	21.92	21.42
Co		58.69	48.91	88.35	54.17	51.82	54.82
Cr		276	299	309	308	278	313
Cs		1.806	0.876	0.272	2.72	1.998	1.608
Cu		152.2	127.2	152.3	119.7	134	127.3
Dy		3.104	3.255	2.559	3.068	3.162	3.056
Er		1.754	1.891	1.498	1.763	1.828	1.737
Eu		1.1134	1.1562	0.9283	1.1637	1.1764	1.1406
Ga		18.37	20.07	14.81	18.49	19.56	18.97
Gd		3.133	3.245	2.554	3.109	3.163	3.105
Hf		2.27	2.61	1.84	2.36	2.42	2.22
Ho		0.6224	0.6519	0.5087	0.6122	0.631	0.5999
In		0.0431	0.0448	0.0447	0.044	0.0438	0.0464
La		9.41	9.94	7.61	9.64	9.92	9.65
Lu		0.2366	0.2418	0.2067	0.2336	0.2441	0.2335
Nb		6.138	6.539	4.584	5.874	6.335	6.022
Nd		12.44	13.05	10.04	12.45	12.71	12.39
Ni		233.7	187.8	419.9	227.1	210.9	246.6
P		546	564	447	534	481	567
Pb		2.5	1.9	1.5	1.9	1.6	1.6
Pr		2.834	2.962	2.295	2.859	2.963	2.901
Rb		7.95	12.02	7.27	15.67	10.44	8.73
Sc		19.7	18.2	16.2	18.5	17.9	17.4
Sm		2.967	3.108	2.406	2.964	2.962	2.909
Sr		244.3	272.7	191.9	270	266.9	256.5
Ta		0.382	0.395	0.286	0.359	0.388	0.373
Tb		0.4943	0.5186	0.4008	0.4747	0.4936	0.4872
Th		0.932	1.075	0.671	0.915	1.01	0.92
Ti		6744	6732	5256	6444	6796	6666
Tl		0.047	0.038	0.028	0.524	0.041	0.035
Tm		0.2447	0.2563	0.208	0.2428	0.2522	0.2469
U		0.238	0.277	0.178	0.244	0.248	0.231
V		147	154	126	149	157	155
Y		16.57	17.1	13.09	16.29	16.87	16.23
Yb		1.568	1.641	1.342	1.564	1.614	1.647
Zn		88	76	102	79	76	76
Zr		82	93	63	82	87	84
Au	ppb	2.17	0.64	3.67	1.53	1.62	2.11
Ir		0.11	0.12	0.12	0.05	0.05	0.06
Pd		3.88	2.68	7.35	1.68	0.94	1.28
Pt		4.07	2.77	7.47	1.59	0.59	1.54
Rh		0.2	0.18	0.27	0.12	0.12	0.1
Ru		0.26	0.35	0.29	0.22	0.26	0.23
S	wt%	0.047	0.037	0.054	0.039	0.052	0.039

Sample		MMD-48	MMD-49	MMD-50	MMD-51	MMD-52	MMD-53
Depth (m)		-686.7	-708.7	-730.3	-748.7	-770.7	-794.3
Zone		M-LS	M-LS	M-LS	M-LS	M-LS	M-LS
SiO_2	wt%	46.34	46.54	46.46	45.97	46.31	46.04
TiO_2		1.14	0.95	0.96	0.87	0.8	0.83
Al_2O_3		19.54	19.93	20.17	19.88	21.25	20.8
Fe_2O_3		10.18	9.68	9.71	10.04	8.62	8.79
MnO		0.129	0.122	0.123	0.124	0.11	0.113
MgO		8.47	8.66	8.99	10.07	8.82	9.22
CaO		10.019	10.234	10.134	9.919	10.914	11.018
Na_2O		2.46	2.38	2.38	2.27	2.22	2.11
K_2O		0.43	0.41	0.33	0.3	0.25	0.22
P_2O_5		0.162	0.112	0.08	0.114	0.095	0.083
LOI		1.22	0.71	0.58	0.63	0.52	0.54
Total		100.13	99.78	99.95	100.21	99.96	99.81
Ba	ppm	144.4	126.1	109.3	111.7	98	92.8
Ce		21.65	19.03	14.29	17.69	14.34	12.73
Co		52.26	52.38	53.85	59.61	51.58	53.54
Cr		292	299	271	239	256	267
Cs		2.937	0.879	1.143	1.064	0.426	0.157
Cu		137.3	119.2	100.4	114.1	125.1	138.2
Dy		3.17	2.74	2.07	2.439	2.143	2.028
Er		1.751	1.552	1.168	1.402	1.202	1.147
Eu		1.1202	1.0729	0.9719	0.9894	0.8374	0.8391
Ga		18.59	18.7	18.75	18.03	18.18	17.55
Gd		3.197	2.811	2.111	2.542	2.143	2.01
Hf		2.27	1.89	1.53	1.86	1.74	1.55
Ho		0.6261	0.5383	0.4067	0.4948	0.4179	0.3984
In		0.0435	0.0396	0.0379	0.031	0.0342	0.0326
La		9.84	8.73	6.54	8.05	6.59	5.95
Lu		0.2294	0.2055	0.1608	0.1902	0.1621	0.153
Nb		6.135	5.154	4.172	5.025	4.462	4.102
Nd		13.34	11.11	8.27	10.26	8.15	7.69
Ni		233.4	270.1	291.5	341.4	307.8	336.3
P		707	485	367	489	397	354
Pb		1.6	1.3	1.6	1.4	1.1	1.1
Pr		2.982	2.529	1.874	2.386	1.917	1.754
Rb		12.04	9.96	7.36	7.65	5.42	3.96
Sc		15.8	15.6	14.2	13.1	13.4	14.6
Sm		3.097	2.621	2.033	2.389	1.992	1.889
Sr		271.9	274.8	272.2	267.7	278.2	273.1
Ta		0.388	0.317	0.27	0.31	0.273	0.253
Tb		0.4921	0.436	0.3298	0.3962	0.3464	0.3156
Th		0.94	0.872	0.625	0.777	0.692	0.591
Ti		6911	5706	5969	5529	4951	5127
Tl		0.057	0.057	0.042	0.024	0.021	0.02
Tm		0.2412	0.2174	0.1646	0.1985	0.1696	0.1605
U		0.234	0.243	0.188	0.203	0.173	0.15
V		147	124	118	112	108	110
Y		16.67	14.53	11.02	13.35	11.45	10.9
Yb		1.562	1.386	1.061	1.249	1.083	1.024
Zn		75	69	77	70	61	63
Zr		82	71	53	69	65	56
Au	ppb	0.71	1.75	0.85	1.12	0.7	0.57
Ir		0.04	0.06	0.05	0.05	0.07	0.05
Pd		3.96	6.36	2.46	1.96	1.68	0.75
Pt		1.17	2.32	0.83	1.05	1.09	0.4
Rh		0.09	0.14	0.12	0.07	0.1	
Ru		0.2	0.23	0.2	0.28	0.25	0.17
S	wt%	0.053	0.03	0.047	0.016	0.03	0.039

Sample		MMD-54	MMD-55	MMD-56	MMD-57	MMD-59	MMD-60
Depth (m)		-816.3	-837.9	-856.8	-867.2	-880.9	-892.5
Zone		M-LS	M-LS	M-LS	M-LS	M-LS	M-LS
SiO_2	wt%	45.19	46.31	45.59	45.36	45.36	45.82
TiO_2		0.94	0.71	0.78	0.74	0.81	0.71
Al_2O_3		20.03	21.85	20.96	20.04	20.25	21.36
Fe_2O_3		9.55	8.13	8.93	9.34	9.7	8.18
MnO		0.12	0.105	0.112	0.117	0.12	0.103
MgO		9.8	8.16	9.37	10.56	10.7	9.25
CaO		10.032	11.663	10.925	10.874	10.219	11.354
Na_2O		2.01	2.08	2	1.88	1.96	2.03
K_2O		0.54	0.3	0.3	0.23	0.25	0.22
P_2O_5		0.115	0.084	0.09	0.069	0.125	0.086
LOI		1.18	0.54	0.64	0.44	0.59	0.54
Total		99.55	99.99	99.74	99.7	100.11	99.71
Ba	ppm	173.4	96.5	99.2	86.5	103	95.1
Ce		16.54	13.96	14.38	12.75	18.89	13.33
Co		56.86	46.97	52.74	59.3	61.55	51.18
Cr		210	309	242	293	132	252
Cs		1.562	0.805	0.948	0.601	0.538	0.266
Cu		130.7	105.5	103	109.3	126.1	92
Dy		2.405	2.116	2.173	1.967	2.516	2.035
Er		1.452	1.169	1.235	1.111	1.41	1.136
Eu		0.9271	0.8673	0.8434	0.8266	0.9159	0.8414
Ga		17.73	18.03	17.46	16.66	17.25	17.85
Gd		2.462	2.092	2.105	1.945	2.615	2.069
Hf		1.99	1.52	1.68	1.35	1.94	1.49
Ho		0.4805	0.422	0.4256	0.3849	0.4998	0.3975
In		0.0365	0.0329	0.0352	0.0336	0.0323	0.032
La		7.7	6.36	6.61	5.71	8.62	6.29
Lu		0.1884	0.1584	0.1621	0.1492	0.1891	0.1513
Nb		5.309	3.781	4.345	3.474	4.785	3.953
Nd		9.77	8.17	8.24	7.58	10.74	7.99
Ni		395.2	334.7	365	441	466	400.4
P		488	379	424	315	566	375
Pb		1.3	1.2	1.2	1.1	1.3	1.1
Pr		2.269	1.882	1.914	1.718	2.523	1.825
Rb		17.11	7.62	7.82	5.51	5.81	4.65
Sc		12.8	15.3	12.2	15.9	11.1	13.5
Sm		2.358	1.989	2.041	1.824	2.556	1.896
Sr		289.1	286.5	272.5	267.3	264.2	281
Ta		0.328	0.229	0.263	0.209	0.293	0.237
Tb		0.3836	0.326	0.337	0.3029	0.4035	0.3196
Th		0.793	0.593	0.681	0.512	0.871	0.606
Ti		5759	4375	4748	4604	4974	4426
Tl		0.154	0.035	0.083	0.03	0.024	0.016
Tm		0.1997	0.1617	0.1714	0.1531	0.1984	0.1594
U		0.194	0.15	0.165	0.117	0.208	0.144
V		114	102	113	110	56	105
Y		13.37	11.15	11.35	10.43	13.5	10.85
Yb		1.266	1.057	1.086	0.978	1.249	0.981
Zn		68	59	64	66	71	59
Zr		74	55	62	49	73	56
Au	ppb	4.6	1.28	1.81	1.61	2.48	1.5
Ir		0.11	0.14	0.21	0.17	0.2	0.21
Pd		3.54	21.1	16.1	7.21	10.8	10.2
Pt		4.25	4.94	5.66	3.62	3.84	3.5
Rh		0.11	0.22	0.43	0.26	0.24	0.22
Ru		0.19	0.28	0.45	0.45	0.46	0.45
S	wt%	0.041	0.04	0.035	0.028	0.013	0.02

Sample		MMD-61	MMD-62	MMD-63	MMD-64	MMD-65	MMD-66
Depth (m)		-899.2	-903.9	-911.7	-918.2	-927.5	-935.4
Zone		M-LS	M-LS	M-LS	M-LS	M-LS	M-LS
SiO_2	wt%	44.98	44.69	45.82	45.01	45.25	44.65
TiO_2		0.84	0.85	0.73	0.81	0.98	0.74
Al_2O_3		21.12	22.39	21.89	18.85	20.3	19.2
Fe_2O_3		8.72	8.33	7.91	9.84	9.13	9.72
MnO		0.108	0.105	0.102	0.124	0.112	0.121
MgO		9	9.19	8.74	12.07	10.63	12.04
CaO		10.694	10.836	11.608	10.277	10.504	10.205
Na_2O		1.93	1.95	1.96	1.84	1.95	1.81
K_2O		0.36	0.23	0.31	0.25	0.25	0.21
P_2O_5		0.098	0.082	0.075	0.082	0.116	0.075
LOI		1.46	0.71	0.64	0.67	0.77	0.67
Total		99.33	99.41	99.83	99.88	100.04	99.49
Ba	ppm	125.6	92.8	98	92.1	104.4	87.4
Ce		15.75	13.16	13.18	14.15	18.98	13.19
Co		52.56	51.32	48.64	65.05	59.11	65.69
Cr		148	184	243	263	172	245
Cs		1.898	0.937	0.857	0.663	0.101	0.461
Cu		98.6	85.4	91.6	86.8	81	102.4
Dy		2.213	2.007	1.981	2.177	2.661	1.961
Er		1.272	1.126	1.137	1.234	1.497	1.119
Eu		0.8843	0.8398	0.8335	0.8581	0.9357	0.8273
Ga		17.51	18.42	17.99	16.08	17.3	15.85
Gd		2.255	1.975	1.996	2.173	2.746	1.953
Hf		1.67	1.63	1.35	1.52	2.2	1.39
Ho		0.4391	0.3929	0.3934	0.4269	0.529	0.3935
In		0.033	0.0331	0.0317	0.0367	0.0318	0.032
La		7.19	6.05	6.01	6.58	8.53	6.09
Lu		0.1662	0.1482	0.1504	0.1653	0.1981	0.1512
Nb		4.515	4.093	3.621	3.982	5.773	3.655
Nd		9.16	7.7	7.84	8.54	10.92	7.72
Ni		393.7	394.4	376.4	548.8	476.9	561
P		407	365	346	384	506	350
Pb		1.3	1.2	1.7	1.1	1.3	1.1
Pr		2.09	1.787	1.795	1.976	2.582	1.803
Rb		12.19	5.4	9.46	5.98	5.28	4.44
Sc		11.9	12.6	13.9	15	13.1	14.1
Sm		2.199	1.874	1.878	2.059	2.611	1.905
Sr		293.7	277.3	303.2	248.9	262.6	253.9
Ta		0.278	0.248	0.225	0.243	0.353	0.221
Tb		0.3499	0.3144	0.3062	0.3381	0.4291	0.3095
Th		0.677	0.569	0.556	0.572	0.843	0.533
Ti		5156	5185	4504	4908	5979	4569
Tl		0.242	0.024	0.043	0.017	0.019	0.015
Tm		0.1798	0.1568	0.1568	0.1733	0.2097	0.1572
U		0.155	0.145	0.133	0.135	0.209	0.129
V		104	110	108	107	123	109
Y		11.85	10.64	10.54	11.54	13.91	10.43
Yb		1.117	0.983	1.08	1.133	1.378	1.029
Zn		63	57	59	68	64	66
Zr		61	58	51	53	81	50
Au	ppb	1.47	1.53	1.57	1.92	1.26	3.34
Ir		0.2	0.19	0.2	0.3	0.19	0.17
Pd		7.29	5.79	5.54	9.25	6.51	3
Pt		2.99	2.85	2.37	9.62	2.45	1.16
Rh		0.18	0.16	0.19	1.09	0.18	0.16
Ru		0.49	0.48	0.54	0.81	0.52	0.55
S	wt%	0.04	0.035	0.033	0.03	0.029	0.035

Sample		MMD-67	MMD-68	MMD-69	MMD-70	MMD-71	MMD-72
Depth (m)		-944.6	-971.1	-991.8	-1008.1	-1026.3	-1038.8
Zone		M-LS	M-LS	M-LS	M-LS	M-LS	M-LS
SiO_2	wt%	44.2	45.72	45.33	45.88	45.32	44.96
TiO_2		0.68	0.81	0.96	0.87	0.99	0.75
Al_2O_3		17.91	20.05	20.79	22.09	19.36	19.47
Fe_2O_3		10.95	9.14	8.7	7.89	9.72	9.79
MnO		0.135	0.117	0.109	0.097	0.121	0.123
MgO		14.31	10.53	9.36	7.68	10.24	11.36
CaO		9.188	10.778	10.645	11.502	10.298	10.204
Na_2O		1.67	1.98	1.94	2.09	1.95	1.87
K_2O		0.19	0.23	0.44	0.44	0.45	0.29
P_2O_5		0.084	0.092	0.104	0.105	0.106	0.075
LOI		0.6	0.4	1.5	0.9	0.95	0.73
Total		99.95	99.9	99.93	99.61	99.56	99.68
Ba	ppm	86.4	99.5	135.5	109	138.7	90.9
Ce		14.05	16.03	17.33	16.46	18.24	13.02
Co		76.73	57.26	52.11	44.7	59.21	62.91
Cr		159	265	280	484	279	271
Cs		0.196	0.325	2.153	1.392	1.292	1.349
Cu		99.1	95.4	98.4	119.8	129.2	101.8
Dy		1.968	2.337	2.536	2.439	2.702	1.954
Er		1.151	1.316	1.42	1.367	1.502	1.131
Eu		0.7846	0.9335	0.9627	0.9429	0.9848	0.8173
Ga		15.01	16.99	17.38	18.18	17.28	16.12
Gd		1.974	2.349	2.51	2.445	2.692	1.957
Hf		1.48	1.69	1.91	1.87	1.92	1.29
Ho		0.3954	0.4602	0.4919	0.4773	0.5361	0.3881
In		0.0303	0.0353	0.0353	0.0358	0.0384	0.033
La		6.45	7.19	7.81	7.37	8.12	5.76
Lu		0.1538	0.1735	0.1829	0.1783	0.2011	0.1479
Nb		3.866	4.229	5.141	4.97	5.398	3.558
Nd		8.14	9.32	9.97	9.49	10.76	7.81
Ni		698.4	480.7	419.7	318.2	510.3	501.9
P		365	413	463	460	438	353
Pb		1.1	1.3	1.4	1.6	1.7	1.1
Pr		1.903	2.18	2.294	2.202	2.467	1.783
Rb		4.09	5.12	15.33	16.79	15.47	8.53
Sc		11.6	15	13	12.6	16.3	14
Sm		1.882	2.264	2.385	2.296	2.549	1.871
Sr		238.3	266.6	287.7	299.5	272.8	258.2
Ta		0.235	0.255	0.318	0.303	0.335	0.219
Tb		0.3103	0.3697	0.3988	0.3815	0.4157	0.3075
Th		0.603	0.656	0.783	0.746	0.755	0.529
Ti		4155	4866	5796	5267	6055	4591
Tl		0.014	0.016	0.047	0.044	0.136	0.04
Tm		0.1577	0.1815	0.1988	0.1879	0.2131	0.1569
U		0.142	0.156	0.187	0.189	0.179	0.127
V		91	108	127	110	134	111
Y		10.54	12.28	13.24	12.65	14.35	10.34
Yb		1.038	1.179	1.298	1.21	1.355	0.991
Zn		77	67	61	56	69	68
Zr		53	58	70	67	73	49
Au	ppb	1.52	1.99	1.28	1.21	2.53	1.71
Ir		0.17	0.21	0.23	0.91	0.16	0.2
Pd		5.16	8.28	3.58	108	3.41	5.61
Pt		2.43	3.15	1.92	29.9	2.06	3.67
Rh		0.21	0.19	0.23	3.82	0.07	0.3
Ru		0.64	0.57	0.57	2.47	0.29	0.47
S	wt%	0.029	0.037	0.031	0.036	0.034	0.031

Sample		MMD-73	MMD-74	MMD-75	MMD-76	MMD-77
Depth (m)		-1044.1	-1055.7	-1067.3	-1081.7	-1087.5
Zone		M-LS	M-LS	M-LS	M-LS	M-LS
SiO_2	wt%	42.91	45.6	45	44.56	45
TiO_2		0.93	0.8	0.88	0.63	0.86
Al_2O_3		17.44	18.22	18.54	18.61	17.62
Fe_2O_3		9.98	8.53	10.48	10.42	9.66
MnO		0.134	0.127	0.131	0.131	0.145
MgO		11.05	9.7	11.88	12.62	11.83
CaO		10.146	11.55	9.718	10.048	8.638
Na_2O		1.53	1.93	1.86	1.72	1.72
K_2O		0.46	0.42	0.42	0.23	0.86
P_2O_5		0.104	0.066	0.101	0.067	0.104
LOI		4.92	2.74	1.13	0.83	3.11
Total		99.65	99.72	100.19	99.91	99.6
Ba	ppm	90.1	123.7	116.8	84.1	198.1
Ce		16.59	18.28	16.93	12.27	17.52
Co		61.76	45.28	67.43	68.3	71.76
Cr		264	229	250	335	244
Cs		1.641	1.792	1.434	0.825	3.501
Cu		113	61.6	114.8	102.1	72.4
Dy		2.48	2.487	2.455	1.908	2.546
Er		1.4	1.379	1.382	1.09	1.469
Eu		0.8642	0.8169	0.9389	0.7882	0.9364
Ga		14.06	15.49	16.4	15.73	16.39
Gd		2.565	2.537	2.462	1.909	2.51
Hf		1.67	1.54	1.79	1.24	1.86
Ho		0.4958	0.4806	0.4926	0.3739	0.5052
In		0.0367	0.0412	0.0369	0.0336	0.0398
La		7.31	7.44	7.58	5.53	7.97
Lu		0.184	0.1695	0.1838	0.1453	0.1939
Nb		4.886	4.069	4.685	3.114	4.785
Nd		9.85	11.01	9.86	7.44	10.2
Ni		476.1	368.7	544.8	592	642.3
P		467	294	451	305	455
Pb		1.3	1.3	1.4	1.1	2.9
Pr		2.331	2.578	2.265	1.677	2.411
Rb		19.06	17.04	16.01	5.96	40.76
Sc		15.5	14.3	15.3	15.8	15.3
Sm		2.39	2.585	2.321	1.801	2.424
Sr		222.8	253.2	254.9	243.9	286.7
Ta		0.299	0.235	0.285	0.188	0.297
Tb		0.4041	0.3969	0.389	0.2955	0.4075
Th		0.699	0.65	0.731	0.507	0.802
Ti		5690	4846	5287	3829	5267
Tl		0.973	0.058	0.11	0.06	1.42
Tm		0.1987	0.1886	0.1917	0.1509	0.2039
U		0.161	0.329	0.175	0.125	0.26
V		128	120	120	103	118
Y		13.01	12.92	12.75	10.1	13.54
Yb		1.26	1.158	1.222	0.995	1.302
Zn		67	57	75	73	79
Zr		65	59	65	45	68
Au	ppb	2.36	1.69	3.7	1.33	2.46
Ir		0.2	0.21	0.25	0.21	0.25
Pd		5.77	5.25	8.23	5.31	7.83
Pt		4.15	3.93	5.53	3.65	5.39
Rh		0.27	0.3	0.36	0.29	0.43
Ru		0.54	0.54	0.53	0.52	0.56
S	wt%	0.033	0.018	0.033	0.03	0.031

Sample		Lower	WM-SOB-1	WM-SOB-2	WM-SOB-3	WM-SOB-4	WM-SOB-5
Rock Type		Detection	Olivine Gabbro	Olivine Gabbro	Leucogabbro	Leuco-Ol-Gabbro	Olivine Gabbro
Easting		Limit	311893	311928	311943	311950	311938
Northing			5325924	5325967	5326089	5326113	5325933
SiO_2	wt%	0.04	48.26	48.37	45.09	47.51	48.29
TiO_2		0.01	1.77	1.61	1.72	0.92	1.85
Al_2O_3		0.02	15.72	16.31	20.02	22.14	16.31
Fe_2O_3		0.01	14.77	13.94	8.6	9.12	14.28
MnO		0.002	0.194	0.183	0.129	0.119	0.189
MgO		0.01	6.77	6.89	3.01	6.52	6.34
CaO		0.006	8.638	9.26	13.806	10.116	9.049
Na_2O		0.02	2.6	2.74	2.2	2.57	2.75
K_2O		0.01	0.97	0.59	1.05	0.6	0.68
P_2O_5		0.002	0.202	0.181	0.173	0.116	0.227
LOI		0.05	0.25	0.27	3.53	0.69	0.53
Total			100.18	100.37	99.4	100.46	100.53
Ba	ppm	8	298	157	573	179	351
Ce		0.12	29.05	26.08	31.86	19.09	30.21
Co		0.13	59.51	58.13	33.3	45.63	55.03
Cr		3	110	136	180	205	96
Cs		0.013	2.931	1.924	2.078	1.53	3.429
Cu		1.4	184.2	165.6	2180.7	97.2	174.4
Dy		0.009	5.003	4.612	4.188	2.396	5.277
Er		0.007	2.858	2.596	2.263	1.341	3.045
Eu		0.0031	1.5906	1.5141	1.6339	1.0488	1.6568
Ga		0.04	21.27	20.94	24.55	19.85	21.56
Gd		0.009	5.001	4.526	4.303	2.59	5.393
Hf		0.14	3.42	3.08	3.12	1.89	3.52
Ho		0.0025	0.9938	0.9274	0.8363	0.4746	1.0724
In		0.0018	0.075	0.0691	0.134	0.0409	0.0735
La		0.1	12.24	11.3	14.34	8.68	12.89
Lu		0.002	0.3862	0.3457	0.3014	0.1767	0.3994
Nb		0.028	8.287	7.635	9.493	5.347	8.633
Nd		0.06	17.93	16.21	17.94	10.98	18.95
Ni		0.7	135.6	138.8	838.1	191.2	123.1
P		30	847	787	791	498	999
Pb		0.18	2.5	2.6	4.2	2.1	4.9
Pr		0.014	3.967	3.616	4.137	2.556	4.172
Rb		0.8	33	19	45	20	25
Sb		0.04	0.07	0.06	0.54	0.13	0.07
Sc		1.1	31.8	30.1	19.9	12.4	31.1
Sm		0.026	4.593	4.089	4.104	2.479	4.822
Sn		0.16	1.27	1.18	1.73	0.8	1.37
Sr		0.6	337.3	284	245.2	361.1	264.6
Ta		0.007	0.538	0.478	0.607	0.334	0.559
Tb		0.0023	0.7917	0.7323	0.6689	0.3941	0.8433
Th		0.018	1.323	1.199	1.673	0.962	1.401
Ti		5	10213	9494	10675	5384	11364
Tl		0.002	0.236	0.175	0.449	0.462	0.18
Tm		0.0019	0.4007	0.3649	0.3272	0.1884	0.423
U		0.011	0.383	0.357	0.435	0.255	0.416
V		1	258	245	191	100	285
Y		0.05	26.64	24.65	22.21	12.58	28.37
Yb		0.009	2.543	2.298	2.044	1.237	2.714
Zn		1.8	106	99	78	69	105
Zr		6	130	118	124	74	135
Au	ppb	0.4	4.63	3.13	20.6	1.44	1.99
Ir		0.01	0.12	0.1	1.61	0.19	0.1
Pd		0.12	6.71	5.03	246	9.24	4.42
Pt		0.17	5.97	4.47	112	6.42	4.52
Rh		0.04	0.32	0.24	8.44	0.58	0.24
Ru		0.08	0.23	0.2	5.09	0.51	0.18
S	wt%	0.003	0.055	0.045	0.195	0.027	0.028

Sample		WM-SOB-6	WM-SOB-7	WM-SOB-8	WM-SOB-9	WM-SOB-10	WM-SOB-11
Rock Type		Gabbro	Olivine Gabbro	Olivine Gabbro	Olivine Gabbro	Olivine Gabbro	Olivine Gabbro
Easting		311972	311983	311985	312009	312002	312019
Northing		5325945	5325949	5325957	5325981	5325985	5325988
SiO_2	wt%	47.03	47.59	47.71	47.92	47.86	47.89
TiO_2		1.87	1.59	1.81	1.68	1.56	1.6
Al_2O_3		15.32	16.46	15.38	16.54	16.9	16.68
Fe_2O_3		14.69	13.8	14.32	13.17	13.04	13.45
MnO		0.194	0.178	0.189	0.173	0.174	0.176
MgO		6.53	7.66	6.63	6.69	7.65	6.86
CaO		7.864	9.106	9.174	9.211	9.494	8.844
Na_2O		2.3	2.53	2.63	2.56	2.73	2.62
K_2O		1.63	0.62	0.6	0.83	0.55	0.52
P_2O_5		0.219	0.174	0.19	0.175	0.187	0.17
LOI		1.92	0.78	0.43	1.22	0.18	1.5
Total		99.64	100.52	99.1	100.21	100.38	100.33
Ba	ppm	558	153	169	242	194	148
Ce		30.25	23.51	26.77	25.39	30.72	25.83
Co		57.17	62.44	57.94	55.07	56.18	54.47
Cr		117	103	124	103	292	66
Cs		2.989	2.092	2.013	1.887	2.178	1.857
Cu		204.3	147.4	173.8	166	166.7	156.7
Dy		5.412	4.237	4.82	4.418	4.375	4.584
Er		3.037	2.395	2.742	2.546	2.438	2.545
Eu		1.6315	1.332	1.5408	1.4554	1.5091	1.413
Ga		21.22	20.26	20.73	20.31	20.87	20.64
Gd		5.51	4.31	4.764	4.455	4.603	4.492
Hf		3.69	2.87	3.27	2.99	3.19	3.21
Ho		1.0658	0.8534	0.971	0.889	0.8631	0.9019
In		0.0794	0.0655	0.0752	0.0695	0.0634	0.0652
La		13.2	10.48	11.88	11.03	13.7	11.19
Lu		0.4029	0.3195	0.3658	0.3398	0.3255	0.3442
Nb		8.625	6.956	7.946	7.423	9.063	7.753
Nd		19.69	15.14	17.26	15.93	18.59	16.56
Ni		129.7	194.2	131.2	169.1	146.6	158.3
P		951	744	812	778	781	738
Pb		2.6	2.1	2.6	2.5	4.2	5
Pr		4.253	3.352	3.792	3.533	4.091	3.663
Rb		61	22	20	29	15	18
Sb		0.46	0.16	0.64	0.2	0.11	0.75
Sc		33.1	28.7	32.8	27.7	28.5	25.1
Sm		4.856	3.835	4.393	4.02	4.252	4.084
Sn		1.26	1.05	1.29	1.45	1.42	1.55
Sr		580.6	288.7	271.2	341.7	259.2	281
Ta		0.576	0.467	0.515	0.481	0.573	0.505
Tb		0.8557	0.6737	0.7691	0.6966	0.7088	0.7091
Th		1.546	1.157	1.312	1.154	1.485	1.285
Ti		11177	9520	10410	10416	9066	9382
Tl		0.289	0.234	0.186	0.369	0.147	0.149
Tm		0.4227	0.3426	0.3824	0.3594	0.34	0.3644
U		0.434	0.334	0.379	0.373	0.367	0.385
V		285	260	278	280	199	226
Y		28.67	22.98	25.65	23.25	23.35	23.87
Yb		2.769	2.149	2.451	2.248	2.181	2.289
Zn		104	95	104	225	102	96
Zr		139	111	122	115	127	123
Au	ppb	1.8	2.03	2.06	3.39	2.73	3.33
Ir		0.11	0.15	0.11	0.23	0.2	0.14
Pd		5.48	3.56	5.42	31.4	15.4	22.3
Pt		4.86	5.78	5.16	11.9	9.87	5.5
Rh		0.26	0.23	0.26	1.09	0.73	0.54
Ru		0.19	0.24	0.19	0.53	0.44	0.33
S	wt%	0.069	0.018	0.021	0.033	0.036	0.065

Sample		WM-SOB-12	EM-SOB-1	EM-SOB-2	EM-SOB-3	EM-SOB-4	EM-SOB-5
Rock Type		Olivine Gabbro	Gabbro	Gabbro	Leucogabbro	Olivine Gabbro	Ferrodiorite
Easting		312025	313946	313948	313886	313691	313753
Northing		5325973	5325911	5325841	5325809	5325855	5325893
SiO_2	wt%	48.18	52.15	52.66	48.57	48.05	51.71
TiO_2		1.67	1.99	1.57	1.1	1.71	2.73
Al_2O_3		15.76	16.77	17.4	20.04	16.41	16.12
Fe_2O_3		14.36	11.53	10.51	9.99	14.05	12.52
MnO		0.189	0.161	0.155	0.141	0.191	0.172
MgO		7.18	4.64	4.56	5.91	6.78	4.7
CaO		9.29	7.66	8.236	9.493	9.874	8.066
Na_2O		2.59	2.8	2.93	2.57	2.62	2.69
K_2O		0.58	1.5	1.41	0.92	0.43	1.2
P_2O_5		0.17	0.209	0.223	0.133	0.175	0.19
LOI		0.35	0.98	0.95	1.38	-0.07	0.44
Total		100.35	100.46	100.71	100.35	100.24	100.63
Ba	ppm	144	313	526	773	129	316
Ce		23.98	43	42.84	17.7	24.32	40.67
Co		58.75	27.03	26.97	45.31	56.08	26.15
Cr		135	293	331	124	128	234
Cs		2.141	1.848	1.757	3.832	1.441	2.156
Cu		154.4	26.8	34.9	128	186.1	16.8
Dy		4.353	5.235	5.339	3.003	4.685	5.199
Er		2.453	2.939	3.017	1.727	2.735	2.971
Eu		1.4356	1.91	1.9374	1.1513	1.4585	1.882
Ga		20.68	22.56	23.22	19.77	20.25	21.99
Gd		4.381	5.466	5.539	3.103	4.59	5.383
Hf		2.87	4.05	4.11	2.08	3	3.86
Ho		0.8742	1.0201	1.0528	0.5972	0.9534	1.0119
In		0.0637	0.0626	0.0729	0.0419	0.0734	0.0606
La		10.37	19.54	20.12	7.95	10.39	18.82
Lu		0.327	0.3944	0.4024	0.2276	0.3566	0.4055
Nb		7.283	11.703	11.197	4.888	7.371	11.712
Nd		15.04	23.95	24.26	11.14	15.77	22.53
Ni		140.1	12.2	11.3	154.8	126.6	8
P		774	865	912	556	792	775
Pb		2.8	5.4	5.5	2.4	2	5.9
Pr		3.379	5.609	5.729	2.477	3.394	5.32
Rb		20	52	48	35	12	42
Sb		0.07	0.4	0.31	0.15	0.04	0.47
Sc		31.8	31.9	30.1	20.5	33.9	38.1
Sm		3.933	5.274	5.527	2.828	4.04	5.123
Sn		1.17	1.7	1.7	0.68	1.17	1.47
Sr		263.1	348.7	322	386.7	227.4	255
Ta		0.462	0.768	0.723	0.319	0.471	0.811
Tb		0.7006	0.81	0.8382	0.4894	0.7333	0.8349
Th		1.141	3.069	3.135	0.856	1.073	3.114
Ti		10208	11528	9042	6272	10508	15718
Tl		0.101	0.325	0.285	0.838	0.116	0.36
Tm		0.3422	0.4186	0.4309	0.2465	0.3852	0.427
U		0.347	1.653	1.414	0.256	0.3	1.719
V		273	286	272	156	300	381
Y		23.38	28.06	28.95	16.51	25.34	27.64
Yb		2.189	2.725	2.758	1.548	2.445	2.693
Zn		100	124	107	70	99	136
Zr		110	156	162	81	116	145
Au	ppb	1.96	1.22	<0.4	1.74	2.57	0.53
Ir		0.11	0.02	0.02	2.37	0.1	0.02
Pd		4.61	0.22	0.28	6.91	5.43	0.23
Pt		4.55	0.55	0.38	4.86	5.11	0.48
Rh		0.23			0.5	0.22	
Ru		0.19			1.26	0.1	
S	wt%	0.032	0.016	0.044	0.054	0.045	0.11

Sample		EM-SOB-6	EM-SOB-7	EM-SOB-8	EM-SOB-9
Rock Type		Gabbro	Granophyre	Gabbro	Gabbro
Easting		313867	313992	313986	314015
Northing		5325916	5325886	5325815	5325900
SiO_2	wt%	50.89	56.92	49.54	47.49
TiO_2		2.87	1.73	1.75	1.95
Al_2O_3		16.11	13.29	15.05	15.82
Fe_2O_3		12.44	13.1	14.17	13.86
MnO		0.175	0.166	0.158	0.191
MgO		5.45	1.33	5.86	6.77
CaO		8.072	4.857	9.823	9.03
Na_2O		2.54	2.95	2.21	2.46
K_2O		1.24	3.29	0.76	0.47
P_2O_5		0.141	0.551	0.19	0.278
LOI		0.42	1.89	0.57	1.99
Total		100.44	100.17	100.15	100.35
Ba	ppm	450	956	531	215
Ce		30.67	113.03	33.13	41.24
Co		33.41	12.51	53.71	55.08
Cr		396	7	131	127
Cs		2.265	4.631	1.986	6.808
Cu		30.5	34.4	186.1	138.5
Dy		4.024	12.373	5.083	5.244
Er		2.309	6.936	2.736	2.902
Eu		1.7227	2.516	1.6614	1.759
Ga		21.39	27.04	21.37	21.11
Gd		4.117	13.574	5.285	5.653
Hf		3.04	9.14	3.55	4.08
Ho		0.7999	2.4386	0.9624	1.0141
In		0.0527	0.1482	0.0758	0.0726
La		14.5	53.18	14.61	18.55
Lu		0.3125	0.8968	0.3448	0.3723
Nb		10.284	26.248	8.094	11.075
Nd		17.38	62.38	20.25	24.08
Ni		12.9	2.2	123	154.4
P		616	2561	818	1260
Pb		4.2	18.5	2.2	4.5
Pr		4.009	14.963	4.524	5.467
Rb		44	117	27	19
Sb		0.29	0.45	0.36	0.81
Sc		38.8	30.2	30.5	27.6
Sm		3.96	13.616	4.897	5.392
Sn		1.19	4.51	0.81	1.18
Sr		326.5	194.5	403.2	280.3
Ta		0.694	1.619	0.523	0.688
Tb		0.635	2.0173	0.8129	0.8546
Th		2.208	9.394	2.024	1.574
Ti			10475	10280	12087
Tl		0.308	1.1	0.298	0.47
Tm		0.3292	0.9707	0.3774	0.4011
U		1.075	4.576	0.495	0.385
V		457	61	317	247
Y		21.83	66.62	26.33	27.68
Yb		2.077	6.19	2.36	2.56
Zn		121	214	85	128
Zr		119	362	135	163
Au	ppb	0.5	0.69	1.8	1.39
Ir		0.02	0.01	0.15	0.05
Pd		0.19		10.3	0.88
Pt		0.46		9	1.54
Rh				0.55	0.05
Ru				0.3	<0.08
S	wt%	0.037	0.019	0.035	0.041

APPENDIX C – MINERAL COMPOSITION

*note- although reported, some trace elements have very poor presision and accuracy due to instrument limitations including; Al_2O_3, NiO, and CaO in olivine, Cr_2O_3 and V_2O_5 in clinopyroxene, MgO and TiO_2 in plagioclase.

CRYSTAL LAKE GABBRO PLAGIOCLASE

CLG-3		Plag 1 Spec. 1	Plag 1 Spec. 2	Plag 1 Spec. 3	Plag 1 Spec. 4	Plag 1 Spec. 5	Plag 1 Spec. 6	Plag 1 Avg.
Na_2O	Oxide	4.58	4.51	4.16	4.32	4.29	4.39	4.38
MgO	wt%							
Al_2O_3		28.78	29.05	29.01	29.04	29.04	28.85	28.96
SiO_2		52.87	52.88	52.77	52.59	52.97	52.74	52.80
CaO		12.70	12.85	12.62	12.87	12.76	12.70	12.75
FeO		0.54	0.45	0.59	0.50	0.44	0.59	0.52
K_2O		0.37	0.41	0.42	0.34	0.44	0.38	0.39
TiO_2								
Total		99.85	100.14	99.58	99.66	99.94	99.65	
Na	Cations	0.41	0.40	0.37	0.38	0.38	0.39	0.39
Mg	Norm.							
Al	to	1.55	1.56	1.56	1.56	1.56	1.55	1.56
Si	8 oxygens	2.41	2.41	2.41	2.40	2.41	2.41	2.41
Ca		0.62	0.63	0.62	0.63	0.62	0.62	0.62
Fe		0.02	0.02	0.02	0.02	0.02	0.02	0.02
K		0.02	0.02	0.02	0.02	0.03	0.02	0.02
Ti								
Total		5.03	5.03	5.01	5.02	5.01	5.02	5.02
An		59.27	59.77	61.12	61.02	60.63	60.20	60.33
Ab		38.68	37.96	36.46	37.06	36.89	37.66	37.45
Or		2.06	2.27	2.42	1.92	2.49	2.14	2.22

CLG-3		Plag 2 Spec. 1	Plag 2 Spec. 2	Plag 2 Spec. 3	Plag 2 Spec. 4	Plag 2 Spec. 5	Plag 2 Spec. 6	Plag 2 Avg.
Na_2O	Oxide	4.13	4.18	4.12	4.12	4.27	4.18	4.17
MgO	wt%	0.10	0.11	0.07	0.15	0.12	0.05	0.10
Al_2O_3		28.95	28.96	29.03	29.23	28.82	29.32	29.05
SiO_2		52.44	52.55	52.29	52.01	52.17	52.31	52.30
CaO		13.04	13.26	13.18	13.22	13.08	13.12	13.15
FeO		0.45	0.37	0.43	0.41	0.46	0.49	0.44
K_2O		0.28	0.26	0.27	0.29	0.30	0.36	0.29
TiO_2								
Total		99.39	99.70	99.38	99.43	99.23	99.82	
Na	Cations	0.37	0.37	0.37	0.37	0.38	0.37	0.37
Mg	Norm.	0.01	0.01	0.00	0.01	0.01	0.00	0.01
Al	to	1.56	1.56	1.57	1.58	1.56	1.58	1.57
Si	8 oxygens	2.40	2.40	2.40	2.38	2.40	2.39	2.39
Ca		0.64	0.65	0.65	0.65	0.64	0.64	0.64
Fe		0.02	0.01	0.02	0.02	0.02	0.02	0.02
K		0.02	0.02	0.02	0.02	0.02	0.02	0.02
Ti								
Total		5.01	5.01	5.01	5.02	5.02	5.02	5.02

An		62.55	62.74	62.89	62.89	61.80	62.14	62.50
Ab		35.85	35.79	35.58	35.47	36.51	35.83	35.84
Or		1.60	1.46	1.53	1.64	1.69	2.03	1.66

CLG-3		Plag 3 Spec. 1	Plag 3 Spec. 2	Plag 3 Spec. 3	Plag 3 Spec. 4	Plag 3 Spec. 5	Plag 3 Spec. 6	Plag 3 Avg.
Na_2O	Oxide	5.16	5.10	5.10	5.07	4.97	5.19	5.10
MgO	wt%	0.06	0.13	0.03	0.13	0.09	0.07	0.09
Al_2O_3		27.55	27.66	27.78	27.82	27.49	27.78	27.68
SiO_2		54.69	54.59	54.91	54.75	54.42	54.49	54.64
CaO		11.19	11.11	11.34	11.26	11.06	11.14	11.18
FeO		0.44	0.55	0.39	0.51	0.42	0.38	0.45
K_2O		0.61	0.67	0.62	0.65	0.69	0.69	0.66
TiO_2								
Total		99.70	99.83	100.17	100.19	99.14	99.73	
Na	Cations	0.45	0.45	0.45	0.45	0.44	0.46	0.45
Mg	Norm.	0.00	0.01	0.00	0.01	0.01	0.00	0.01
Al	to	1.48	1.48	1.48	1.48	1.48	1.49	1.48
Si	8 oxygens	2.49	2.48	2.48	2.48	2.49	2.48	2.48
Ca		0.55	0.54	0.55	0.55	0.54	0.54	0.54
Fe		0.02	0.02	0.01	0.02	0.02	0.01	0.02
K		0.04	0.04	0.04	0.04	0.04	0.04	0.04
Ti								
Total		5.02	5.02	5.02	5.02	5.01	5.03	5.02
An		52.65	52.56	53.22	53.09	52.98	52.17	52.78
Ab		43.93	43.66	43.31	43.26	43.08	43.98	43.54
Or		3.42	3.77	3.46	3.65	3.94	3.85	3.68

CLG-8		Plag 1 Spec. 1	Plag 1 Spec. 2	Plag 1 Spec. 3	Plag 1 Spec. 4	Plag 1 Spec. 5	Plag 1 Avg.
Na_2O	Oxide	3.67	3.89	3.39	3.82	3.94	3.74
MgO	wt%						
Al_2O_3		30.20	30.29	30.27	29.78	29.88	30.08
SiO_2		51.28	50.97	50.86	51.57	50.95	51.13
CaO		13.99	14.05	14.51	13.92	13.93	14.08
FeO		0.42	0.47	0.48	0.46	0.56	0.48
K_2O		0.24	0.24	0.26	0.20	0.17	0.22
TiO_2							
Total		99.80	99.91	99.77	99.76	99.43	
Na	Cations	0.33	0.35	0.30	0.34	0.35	0.33
Mg	Norm.						
Al	to	1.63	1.63	1.63	1.61	1.62	1.62
Si	8 oxygens	2.34	2.33	2.33	2.36	2.34	2.34
Ca		0.69	0.69	0.71	0.68	0.69	0.69
Fe		0.02	0.02	0.02	0.02	0.02	0.02
K		0.01	0.01	0.02	0.01	0.01	0.01
Ti							
Total		5.01	5.03	5.01	5.01	5.03	5.02
An		66.88	65.73	69.25	66.06	65.52	66.69
Ab		31.75	32.93	29.28	32.81	33.53	32.06
Or		1.37	1.34	1.48	1.13	0.95	1.25

CLG-8		Plag 2	Plag 2	Plag 2	Plag 2	Plag 2	Plag 2

		Spec. 1	Spec. 2	Spec. 3	Spec. 4	Spec. 5	Avg.
Na_2O	Oxide	4.42	4.48	4.70	4.49	4.36	4.49
MgO	wt%						
Al_2O_3		29.04	29.24	28.34	29.02	28.90	28.91
SiO_2		52.50	52.64	52.63	52.92	52.77	52.69
CaO		13.04	13.08	12.53	12.79	12.62	12.81
FeO		0.49	0.52	0.40	0.54	0.56	0.50
K_2O		0.28	0.30	0.31	0.25	0.30	0.29
TiO_2							
Total		99.77	100.26	98.91	100.01	99.52	
Na	Cations	0.39	0.39	0.42	0.40	0.39	0.40
Mg	Norm.						
Al	to	1.56	1.57	1.54	1.56	1.56	1.56
Si	8 oxygens	2.40	2.39	2.42	2.41	2.41	2.41
Ca		0.64	0.64	0.62	0.62	0.62	0.63
Fe		0.02	0.02	0.02	0.02	0.02	0.02
K		0.02	0.02	0.02	0.01	0.02	0.02
Ti							
Total		5.02	5.03	5.03	5.02	5.01	5.02
An		61.01	60.71	58.54	60.29	60.48	60.21
Ab		37.43	37.63	39.74	38.30	37.81	38.18
Or		1.56	1.66	1.72	1.40	1.71	1.61

CLG-8		Plag 3 Spec. 1	Plag 3 Spec. 2	Plag 3 Spec. 3	Plag 3 Spec. 4	Plag 3 Spec. 5	Plag 3 Spec. 6	Plag 3 Avg.
Na_2O	Oxide	4.25	4.17	4.33	4.22	4.28	4.20	4.24
MgO	wt%							
Al_2O_3		29.58	29.13	29.43	29.38	29.38	29.53	29.41
SiO_2		52.32	52.28	52.24	52.20	52.10	52.04	52.20
CaO		13.30	13.23	13.11	13.16	13.20	12.95	13.16
FeO		0.48	0.44	0.58	0.55	0.58	0.46	0.52
K_2O		0.20	0.29	0.25	0.20	0.27	0.17	0.23
TiO_2								
Total		100.14	99.54	99.93	99.70	99.81	99.35	
Na	Cations	0.37	0.37	0.38	0.37	0.38	0.37	0.38
Mg	Norm.							
Al	to	1.59	1.57	1.58	1.58	1.58	1.59	1.58
Si	8 oxygens	2.38	2.39	2.38	2.38	2.38	2.38	2.38
Ca		0.65	0.65	0.64	0.64	0.65	0.64	0.64
Fe		0.02	0.02	0.02	0.02	0.02	0.02	0.02
K		0.01	0.02	0.01	0.01	0.02	0.01	0.01
Ti								
Total		5.02	5.02	5.02	5.02	5.03	5.01	5.02
An		62.65	62.64	61.71	62.56	62.07	62.40	62.34
Ab		36.23	35.73	36.89	36.30	36.42	36.62	36.36
Or		1.12	1.63	1.40	1.13	1.51	0.98	1.30

CLG-13		Plag 1 Spec. 1	Plag 1 Spec. 2	Plag 1 Spec. 3	Plag 1 Spec. 4	Plag 1 Avg.
Na_2O	Oxide	3.07	3.18	3.19	3.13	3.14
MgO	wt%					
Al_2O_3		30.54	30.59	30.63	30.67	30.61
SiO_2		49.97	49.38	49.50	49.66	49.63
CaO		15.11	15.00	15.25	15.09	15.11

FeO		0.52	0.59	0.51	0.60	0.56
K_2O		0.17	0.20	0.14	0.14	0.16
TiO_2		0.11	0.15	0.13	0.12	0.13
Total		99.48	99.09	99.35	99.40	
Na	Cations	0.27	0.29	0.29	0.28	0.28
Mg	Norm.					
Al	to	1.66	1.67	1.67	1.67	1.66
Si	8 oxygens	2.30	2.29	2.29	2.29	2.29
Ca		0.75	0.74	0.75	0.75	0.75
Fe		0.02	0.02	0.02	0.02	0.02
K		0.01	0.01	0.01	0.01	0.01
Ti		0.00	0.01	0.00	0.00	0.00
Total		5.01	5.02	5.02	5.02	5.02
An		72.41	71.45	71.97	72.13	71.99
Ab		26.62	27.41	27.24	27.07	27.09
Or		0.97	1.13	0.79	0.80	0.92

CLG-13		Plag 2 Spec. 1	Plag 2 Spec. 2	Plag 2 Spec. 3	Plag 2 Spec. 4	Plag 2 Avg.
Na_2O	Oxide	3.99	3.96	3.97	4.04	3.99
MgO	wt%					
Al_2O_3		29.65	29.62	29.41	29.75	29.61
SiO_2		51.53	51.65	51.85	51.61	51.66
CaO		13.62	13.80	13.64	13.54	13.65
FeO		0.51	0.54	0.50	0.50	0.51
K_2O		0.26	0.29	0.32	0.24	0.28
TiO_2		0.08	0.09	0.10		0.09
Total		99.63	99.96	99.79	99.68	
Na	Cations	0.35	0.35	0.35	0.36	0.35
Mg	Norm.					
Al	to	1.60	1.60	1.59	1.60	1.60
Si	8 oxygens	2.36	2.36	2.37	2.36	2.36
Ca		0.67	0.68	0.67	0.66	0.67
Fe		0.02	0.02	0.02	0.02	0.02
K		0.02	0.02	0.02	0.01	0.02
Ti		0.00	0.00	0.00		0.00
Total		5.02	5.02	5.02	5.02	5.02
An		64.40	64.75	64.32	64.06	64.38
Ab		34.14	33.63	33.88	34.59	34.06
Or		1.46	1.62	1.80	1.35	1.56

CLG-13		Plag 3 Spec. 1	Plag 3 Spec. 2	Plag 3 Spec. 3	Plag 3 Spec. 4	Plag 3 Avg.
Na_2O	Oxide	3.70	3.42	3.64	3.47	3.56
MgO	wt%					
Al_2O_3		30.46	30.63	30.56	30.75	30.60
SiO_2		50.92	50.44	50.73	50.68	50.69
CaO		14.45	14.72	14.84	14.68	14.67
FeO		0.53	0.45	0.62	0.49	0.52
K_2O		0.21	0.24	0.23	0.25	0.23
TiO_2		0.15				0.15
Total		100.41	99.89	100.61	100.32	
Na	Cations	0.33	0.30	0.32	0.31	0.31

Mg	Norm.					
Al	to	1.64	1.65	1.64	1.65	1.65
Si	8 oxygens	2.32	2.31	2.31	2.31	2.31
Ca		0.71	0.72	0.72	0.72	0.72
Fe		0.02	0.02	0.02	0.02	0.02
K		0.01	0.01	0.01	0.01	0.01
Ti		0.01				0.00
Total		5.03	5.02	5.04	5.02	5.03
An		67.54	69.45	68.38	69.06	68.61
Ab		31.29	29.20	30.35	29.54	30.10
Or		1.17	1.35	1.26	1.40	1.29

CLG-18		Plag 1 Spec. 1	Plag 1 Spec. 2	Plag 1 Spec. 3	Plag 1 Spec. 4	Plag 1 Avg.
Na_2O	Oxide	3.35	3.38	3.58	3.34	3.41
MgO	wt%					
Al_2O_3		30.76	30.52	30.72	30.74	30.69
SiO_2		50.60	50.78	50.66	50.29	50.58
CaO		14.75	14.75	14.86	14.99	14.84
FeO		0.47	0.56	0.61	0.58	0.56
K_2O		0.18	0.21	0.18	0.18	0.19
TiO_2		0.09		0.07	0.07	0.08
Total		100.20	100.20	100.69	100.20	
Na	Cations	0.30	0.30	0.32	0.30	0.30
Mg	Norm.					
Al	to	1.65	1.64	1.65	1.66	1.65
Si	8 oxygens	2.31	2.32	2.31	2.30	2.31
Ca		0.72	0.72	0.72	0.73	0.73
Fe		0.02	0.02	0.02	0.02	0.02
K		0.01	0.01	0.01	0.01	0.01
Ti		0.00		0.00	0.00	0.00
Total		5.01	5.02	5.03	5.02	5.02
An		70.15	69.85	68.95	70.55	69.87
Ab		28.83	28.97	30.06	28.44	29.08
Or		1.02	1.18	0.99	1.01	1.05

CLG-18		Plag 2 Spec. 1	Plag 2 Spec. 2	Plag 2 Spec. 3	Plag 2 Spec. 4	Plag 2 Avg.
Na_2O	Oxide	3.31	3.21	3.23	3.33	3.27
MgO	wt%					
Al_2O_3		30.88	31.14	30.92	30.81	30.94
SiO_2		50.77	50.27	50.53	50.36	50.48
CaO		15.08	15.35	15.02	15.01	15.12
FeO		0.42	0.54	0.40	0.37	0.43
K_2O		0.22	0.20	0.20	0.20	0.21
TiO_2		0.07		0.14		0.11
Total		100.76	100.70	100.45	100.07	
Na	Cations	0.29	0.28	0.29	0.30	0.29
Mg	Norm.					
Al	to	1.65	1.67	1.66	1.66	1.66
Si	8 oxygens	2.31	2.29	2.30	2.30	2.30
Ca		0.73	0.75	0.73	0.74	0.74
Fe		0.02	0.02	0.02	0.01	0.02
K		0.01	0.01	0.01	0.01	0.01

Ti		0.00		0.00		0.00
Total		5.02	5.02	5.01	5.02	5.02
An		70.69	71.74	71.17	70.56	71.04
Ab		28.08	27.15	27.70	28.33	27.81
Or		1.23	1.11	1.13	1.12	1.15

CLG-18		Plag 3 Spec. 1	Plag 3 Spec. 2	Plag 3 Spec. 3	Plag 3 Spec. 4	Plag 3 Avg.
Na_2O	Oxide	3.55	3.60	3.66	3.53	3.59
MgO	wt%					
Al_2O_3		30.53	30.49	30.67	30.65	30.59
SiO_2		51.02	50.96	50.76	50.84	50.90
CaO		14.61	14.47	14.70	14.47	14.56
FeO		0.56	0.45	0.50	0.51	0.51
K_2O		0.23	0.20	0.21	0.20	0.21
TiO_2		0.12	0.12	0.09	0.10	0.11
Total		100.62	100.29	100.58	100.31	
Na	Cations	0.31	0.32	0.32	0.31	0.32
Mg	Norm.					
Al	to	1.64	1.64	1.65	1.65	1.64
Si	8 oxygens	2.32	2.32	2.31	2.32	2.32
Ca		0.71	0.71	0.72	0.71	0.71
Fe		0.02	0.02	0.02	0.02	0.02
K		0.01	0.01	0.01	0.01	0.01
Ti		0.00	0.00	0.00	0.00	0.00
Total		5.02	5.02	5.03	5.02	5.02
An		68.57	68.18	68.14	68.59	68.37
Ab		30.15	30.70	30.70	30.28	30.46
Or		1.29	1.12	1.16	1.13	1.17

CLG-20		Plag 1 Spec. 1	Plag 1 Spec. 2	Plag 1 Spec. 3	Plag 1 Spec. 4	Plag 1 Avg.
Na_2O	Oxide	3.57	3.59	3.52	3.39	3.52
MgO	wt%					
Al_2O_3		30.01	30.22	30.53	30.33	30.27
SiO_2		50.78	50.75	50.80	50.48	50.70
CaO		14.19	14.39	14.37	14.47	14.36
FeO		0.43	0.49	0.50	0.45	0.47
K_2O		0.28	0.24	0.25	0.23	0.25
TiO_2		0.15	0.10	0.16	0.11	0.13
Total		99.41	99.77	100.14	99.45	
Na	Cations	0.32	0.32	0.31	0.30	0.31
Mg	Norm.					
Al	to	1.63	1.63	1.64	1.64	1.64
Si	8 oxygens	2.33	2.33	2.32	2.32	2.33
Ca		0.70	0.71	0.70	0.71	0.71
Fe		0.02	0.02	0.02	0.02	0.02
K		0.02	0.01	0.01	0.01	0.01
Ti		0.01	0.00	0.01	0.00	0.00
Total		5.02	5.02	5.02	5.01	5.02
An		67.62	67.97	68.31	69.31	68.30
Ab		30.79	30.68	30.28	29.38	30.28
Or		1.59	1.35	1.41	1.31	1.42

CLG-20		Plag 2 Spec. 1	Plag 2 Spec. 2	Plag 2 Spec. 3	Plag 2 Spec. 4	Plag 2 Avg.
Na_2O	Oxide	3.36	3.35	3.37	3.36	3.36
MgO	wt%					
Al_2O_3		30.78	30.30	30.31	30.31	30.43
SiO_2		50.15	50.01	50.19	50.05	50.10
CaO		14.92	14.69	14.71	14.75	14.77
FeO		0.45	0.46	0.40	0.47	0.45
K_2O		0.22	0.23	0.21	0.26	0.23
TiO_2						
Total		99.89	99.04	99.20	99.21	
Na	Cations	0.30	0.30	0.30	0.30	0.30
Mg	Norm.					
Al	to	1.66	1.65	1.65	1.65	1.65
Si	8 oxygens	2.30	2.31	2.31	2.31	2.31
Ca		0.73	0.73	0.73	0.73	0.73
Fe		0.02	0.02	0.02	0.02	0.02
K		0.01	0.01	0.01	0.02	0.01
Ti						
Total		5.02	5.02	5.02	5.02	5.02
An		70.17	69.87	69.85	69.77	69.92
Ab		28.60	28.83	28.96	28.76	28.79
Or		1.23	1.30	1.19	1.46	1.30

CLG-20		Plag 3 Spec. 1	Plag 3 Spec. 2	Plag 3 Spec. 3	Plag 3 Spec. 4	Plag 3 Avg.
Na_2O	Oxide	3.26	3.43	3.34	3.24	3.32
MgO	wt%					
Al_2O_3		30.34	30.21	30.10	30.03	30.17
SiO_2		50.31	50.21	50.32	50.15	50.25
CaO		14.47	14.50	14.66	14.71	14.59
FeO		0.50	0.59	0.60	0.57	0.57
K_2O		0.18	0.24	0.28	0.21	0.23
TiO_2		0.09	0.10		0.22	0.14
Total		99.15	99.28	99.29	99.13	
Na	Cations	0.29	0.31	0.30	0.29	0.30
Mg	Norm.					
Al	to	1.65	1.64	1.64	1.63	1.64
Si	8 oxygens	2.32	2.32	2.32	2.32	2.32
Ca		0.71	0.72	0.72	0.73	0.72
Fe		0.02	0.02	0.02	0.02	0.02
K		0.01	0.01	0.02	0.01	0.01
Ti		0.00	0.00		0.01	0.00
Total		5.01	5.02	5.02	5.01	5.01
An		70.30	69.07	69.69	70.64	69.92
Ab		28.66	29.57	28.73	28.16	28.78
Or		1.04	1.36	1.58	1.20	1.30

CLG-23		Plag 1 Spec. 1	Plag 1 Spec. 2	Plag 1 Spec. 3	Plag 1 Spec. 4	Plag 1 Avg.
Na_2O	Oxide	2.95	2.95	2.99	2.79	2.92
MgO	wt%					

Al_2O_3		31.55	31.36	31.32	31.31	31.39
SiO_2		49.99	49.70	49.75	49.04	49.62
CaO		15.47	15.27	15.54	15.61	15.47
FeO		0.54	0.42	0.40	0.50	0.47
K_2O		0.25	0.24	0.22	0.16	0.22
TiO_2		0.08	0.08		0.11	0.09
Total		100.84	100.02	100.22	99.51	
Na	Cations	0.26	0.26	0.27	0.25	0.26
Mg	Norm.					
Al	to	1.69	1.69	1.69	1.70	1.69
Si	8 oxygens	2.27	2.28	2.28	2.26	2.27
Ca		0.75	0.75	0.76	0.77	0.76
Fe		0.02	0.02	0.02	0.02	0.02
K		0.01	0.01	0.01	0.01	0.01
Ti		0.00	0.00		0.00	0.00
Total		5.02	5.01	5.02	5.01	5.02
An		73.30	73.08	73.26	74.87	73.63
Ab		25.29	25.55	25.51	24.22	25.14
Or		1.41	1.37	1.23	0.91	1.23

CLG-23		Plag 2 Spec. 1	Plag 2 Spec. 2	Plag 2 Spec. 3	Plag 2 Spec. 4	Plag 2 Avg.
Na_2O	Oxide	2.56	2.49	2.54	2.57	2.54
MgO	wt%					
Al_2O_3		32.20	32.02	32.23	32.03	32.12
SiO_2		48.44	48.25	48.93	48.40	48.51
CaO		16.44	16.18	16.34	16.42	16.35
FeO		0.42	0.42	0.46	0.39	0.42
K_2O		0.16	0.15	0.16	0.19	0.17
TiO_2						
Total		100.21	99.52	100.67	100.00	
Na	Cations	0.23	0.22	0.22	0.23	0.23
Mg	Norm.					
Al	to	1.74	1.74	1.73	1.74	1.74
Si	8 oxygens	2.22	2.23	2.23	2.23	2.23
Ca		0.81	0.80	0.80	0.81	0.80
Fe		0.02	0.02	0.02	0.02	0.02
K		0.01	0.01	0.01	0.01	0.01
Ti						
Total		5.03	5.02	5.02	5.03	5.02
An		77.32	77.55	77.34	77.10	77.33
Ab		21.79	21.60	21.76	21.84	21.74
Or		0.90	0.86	0.90	1.06	0.93

CLG-23		Plag 3 Spec. 1	Plag 3 Spec. 2	Plag 3 Spec. 3	Plag 3 Spec. 4	Plag 3 Avg.
Na_2O	Oxide	3.32	3.28	2.91	3.10	3.15
MgO	wt%					
Al_2O_3		31.11	30.81	31.38	31.31	31.15
SiO_2		50.52	50.45	49.31	49.63	49.98
CaO		14.99	15.06	15.80	15.41	15.32
FeO		0.39	0.59	0.37	0.49	0.46
K_2O		0.25	0.25	0.23	0.20	0.23
TiO_2		0.11		0.10	0.10	0.10

Total		100.70	100.45	100.11	100.25	
Na	Cations	0.29	0.29	0.26	0.28	0.28
Mg	Norm.					
Al	to	1.67	1.66	1.70	1.69	1.68
Si	8 oxygens	2.30	2.30	2.26	2.27	2.28
Ca		0.73	0.74	0.78	0.76	0.75
Fe		0.01	0.02	0.01	0.02	0.02
K		0.01	0.01	0.01	0.01	0.01
Ti		0.00		0.00	0.00	0.00
Total		5.02	5.02	5.02	5.02	5.02
An		70.39	70.73	74.04	72.49	71.91
Ab		28.21	27.88	24.68	26.39	26.79
Or		1.40	1.40	1.28	1.12	1.30

CLG-25		Plag 1 Spec. 1	Plag 1 Spec. 2	Plag 1 Spec. 3	Plag 1 Spec. 4	Plag 1 Avg.
Na_2O	Oxide	1.87	1.93	1.82	1.75	1.84
MgO	wt%					
Al_2O_3		32.83	32.51	32.72	32.36	32.61
SiO_2		46.98	46.78	46.80	47.03	46.90
CaO		17.31	17.30	17.38	17.56	17.39
FeO		0.40	0.42	0.45	0.40	0.42
K_2O		0.12	0.18	0.14	0.12	0.14
TiO_2		0.00		0.10		0.05
Total		99.52	99.11	99.42	99.22	
Na	Cations	0.17	0.17	0.16	0.16	0.17
Mg	Norm.					
Al	to	1.79	1.78	1.79	1.77	1.78
Si	8 oxygens	2.18	2.18	2.17	2.19	2.18
Ca		0.86	0.86	0.86	0.87	0.86
Fe		0.02	0.02	0.02	0.02	0.02
K		0.01	0.01	0.01	0.01	0.01
Ti		0.00		0.00		0.00
Total		5.02	5.02	5.02	5.01	5.02
An		83.07	82.35	83.40	84.14	83.24
Ab		16.24	16.63	15.80	15.17	15.96
Or		0.69	1.02	0.80	0.68	0.80

CLG-25		Plag 2 Spec. 1	Plag 2 Spec. 2	Plag 2 Spec. 3	Plag 2 Spec. 4	Plag 2 Avg.
Na_2O	Oxide	2.96	2.84	3.00	2.94	2.94
MgO	wt%	0.20	0.20	0.07	0.11	0.15
Al_2O_3		31.00	30.87	30.93	31.14	30.99
SiO_2		49.19	49.68	49.53	49.20	49.40
CaO		15.43	15.42	15.51	15.42	15.45
FeO		0.46	0.57	0.28	0.53	0.46
K_2O		0.28	0.25	0.28	0.27	0.27
TiO_2		0.13			0.08	0.11
Total		99.65	99.83	99.60	99.66	
Na	Cations	0.26	0.25	0.27	0.26	0.26
Mg	Norm.	0.01	0.01	0.00	0.01	0.01
Al	to	1.68	1.67	1.68	1.69	1.68
Si	8 oxygens	2.27	2.28	2.28	2.27	2.27

Ca		0.76	0.76	0.76	0.76	0.76
Fe		0.02	0.02	0.01	0.02	0.02
K		0.02	0.01	0.02	0.02	0.02
Ti		0.00			0.00	0.00
Total		5.03	5.02	5.02	5.03	5.02
An		73.06	73.93	72.91	73.21	73.28
Ab		25.36	24.64	25.52	25.26	25.20
Or		1.58	1.43	1.57	1.53	1.52

CLG-25		Plag 3 Spec. 1	Plag 3 Spec. 2	Plag 3 Spec. 3	Plag 3 Spec. 4	Plag 3 Avg.
Na_2O	Oxide	2.49	2.71	2.51	2.56	2.57
MgO	wt%	0.10				0.10
Al_2O_3		31.64	31.85	31.81	31.76	31.77
SiO_2		48.44	48.70	48.51	48.77	48.61
CaO		16.20	16.18	16.34	16.24	16.24
FeO		0.47	0.47	0.36	0.60	0.48
K_2O		0.23	0.14	0.12	0.24	0.18
TiO_2						
Total		99.58	100.05	99.65	100.16	
Na	Cations	0.22	0.24	0.22	0.23	0.23
Mg	Norm.	0.01				0.00
Al	to	1.72	1.72	1.73	1.72	1.72
Si	8 oxygens	2.24	2.24	2.24	2.24	2.24
Ca		0.80	0.80	0.81	0.80	0.80
Fe		0.02	0.02	0.01	0.02	0.02
K		0.01	0.01	0.01	0.01	0.01
Ti						
Total		5.02	5.03	5.02	5.02	5.02
An		77.22	76.14	77.72	76.75	76.96
Ab		21.48	23.08	21.60	21.89	22.01
Or		1.31	0.78	0.68	1.35	1.03

CLG-28		Plag 1 Spec. 1	Plag 1 Spec. 2	Plag 1 Spec. 3	Plag 1 Spec. 4	Plag 1 Avg.
Na_2O	Oxide	3.21	3.28	3.15	3.24	3.22
MgO	wt%					
Al_2O_3		31.13	31.25	30.95	31.43	31.19
SiO_2		50.19	50.47	50.21	50.11	50.25
CaO		15.28	15.22	15.12	15.07	15.17
FeO		0.32	0.31	0.40	0.33	0.34
K_2O		0.22	0.22	0.22	0.24	0.23
TiO_2		0.16	0.09	0.10	0.11	0.12
Total		100.51	100.84	100.16	100.53	
Na	Cations	0.28	0.29	0.28	0.29	0.28
Mg	Norm.					
Al	to	1.67	1.67	1.67	1.69	1.67
Si	8 oxygens	2.29	2.29	2.30	2.28	2.29
Ca		0.75	0.74	0.74	0.74	0.74
Fe		0.01	0.01	0.02	0.01	0.01
K		0.01	0.01	0.01	0.01	0.01
Ti		0.01	0.00	0.00	0.00	0.00
Total		5.02	5.02	5.01	5.02	5.02

An		71.57	71.06	71.72	71.02	71.34
Ab		27.21	27.71	27.04	27.63	27.40
Or		1.23	1.22	1.24	1.35	1.26

CLG-28		Plag 2 Spec. 1	Plag 2 Spec. 2	Plag 2 Spec. 3	Plag 2 Spec. 4	Plag 2 Avg.
Na_2O	Oxide	3.47	3.55	3.53	3.49	3.51
MgO	wt%					
Al_2O_3		30.69	30.75	30.50	30.55	30.62
SiO_2		51.31	50.67	50.75	50.90	50.91
CaO		14.64	14.49	14.69	14.50	14.58
FeO		0.35	0.32	0.42	0.41	0.38
K_2O		0.29	0.24	0.30	0.29	0.28
TiO_2		0.08	0.13	0.09	0.11	0.10
Total		100.83	100.15	100.29	100.25	
Na	Cations	0.30	0.31	0.31	0.31	0.31
Mg	Norm.					
Al	to	1.64	1.65	1.64	1.64	1.64
Si	8 oxygens	2.33	2.31	2.32	2.32	2.32
Ca		0.71	0.71	0.72	0.71	0.71
Fe		0.01	0.01	0.02	0.02	0.01
K		0.02	0.01	0.02	0.02	0.02
Ti		0.00	0.00	0.00	0.00	0.00
Total		5.01	5.02	5.02	5.02	5.02
An		68.85	68.35	68.53	68.52	68.56
Ab		29.53	30.30	29.80	29.85	29.87
Or		1.62	1.35	1.67	1.63	1.57

CLG-28		Plag 3 Spec. 1	Plag 3 Spec. 2	Plag 3 Spec. 3	Plag 3 Spec. 4	Plag 3 Avg.
Na_2O	Oxide	3.37	3.36	3.41	3.44	3.40
MgO	wt%					
Al_2O_3		30.89	31.07	31.27	31.05	31.07
SiO_2		50.71	51.10	50.59	50.92	50.83
CaO		14.77	14.68	14.77	14.87	14.77
FeO		0.27	0.41	0.31	0.32	0.33
K_2O		0.19	0.21	0.19	0.27	0.22
TiO_2		0.16	0.14	0.16	0.10	0.14
Total		100.37	100.97	100.70	100.96	
Na	Cations	0.30	0.29	0.30	0.30	0.30
Mg	Norm.					
Al	to	1.66	1.66	1.67	1.66	1.66
Si	8 oxygens	2.31	2.31	2.30	2.31	2.31
Ca		0.72	0.71	0.72	0.72	0.72
Fe		0.01	0.02	0.01	0.01	0.01
K		0.01	0.01	0.01	0.02	0.01
Ti		0.01	0.00	0.01	0.00	0.00
Total		5.01	5.01	5.02	5.02	5.01
An		70.02	69.87	69.78	69.43	69.77
Ab		28.91	28.94	29.15	29.07	29.02
Or		1.07	1.19	1.07	1.50	1.21

CLG-39		Plag 1	Plag 1	Plag 1	Plag 1	Plag 1

		Spec. 1	Spec. 2	Spec. 3	Spec. 4	Avg.
Na_2O	Oxide	3.79	4.00	3.73	3.86	3.85
MgO	wt%					
Al_2O_3		29.42	29.68	29.82	29.53	29.61
SiO_2		51.31	51.06	50.99	51.16	51.13
CaO		13.79	14.09	13.90	13.78	13.89
FeO		0.62	0.54	0.52	0.54	0.56
K_2O		0.28	0.29	0.22	0.21	0.25
TiO_2						
Total		99.20	99.67	99.19	99.08	
Na	Cations	0.34	0.36	0.33	0.34	0.34
Mg	Norm.					
Al	to	1.60	1.61	1.62	1.60	1.61
Si	8 oxygens	2.36	2.34	2.35	2.36	2.35
Ca		0.68	0.69	0.69	0.68	0.68
Fe		0.02	0.02	0.02	0.02	0.02
K		0.02	0.02	0.01	0.01	0.01
Ti						
Total		5.02	5.04	5.02	5.02	5.02
An		65.72	65.01	66.47	65.57	65.69
Ab		32.69	33.40	32.28	33.24	32.90
Or		1.59	1.59	1.25	1.19	1.41

CLG-39		Plag 2 Spec. 1	Plag 2 Spec. 2	Plag 2 Spec. 3	Plag 2 Spec. 4	Plag 2 Avg.
Na_2O	Oxide	3.80	3.82	3.71	3.76	3.77
MgO	wt%					
Al_2O_3		29.92	29.81	29.69	29.90	29.83
SiO_2		51.31	51.12	51.20	50.93	51.14
CaO		13.77	14.02	13.90	13.87	13.89
FeO		0.52	0.50	0.47	0.45	0.49
K_2O		0.30	0.27	0.27	0.34	0.30
TiO_2		0.15		0.12	0.13	0.13
Total		99.76	99.53	99.36	99.38	
Na	Cations	0.34	0.34	0.33	0.34	0.34
Mg	Norm.					
Al	to	1.61	1.61	1.61	1.62	1.61
Si	8 oxygens	2.35	2.35	2.35	2.34	2.35
Ca		0.68	0.69	0.68	0.68	0.68
Fe		0.02	0.02	0.02	0.02	0.02
K		0.02	0.02	0.02	0.02	0.02
Ti		0.01	0.00	0.00	0.00	0.00
Total		5.02	5.02	5.01	5.02	5.02
An		65.56	65.96	66.40	65.80	65.93
Ab		32.74	32.52	32.07	32.28	32.40
Or		1.70	1.51	1.54	1.92	1.67

CLG-39		Plag 3 Spec. 1	Plag 3 Spec. 2	Plag 3 Spec. 3	Plag 3 Spec. 4	Plag 3 Avg.
Na_2O	Oxide	2.37	2.43	2.34	2.42	2.39
MgO	wt%					
Al_2O_3		31.82	32.09	31.81	31.77	31.87
SiO_2		47.94	48.03	47.95	48.17	48.02
CaO		16.56	16.57	16.39	16.75	16.57

FeO		0.40	0.55	0.48	0.50	0.48
K_2O		0.16	0.12	0.14	0.14	0.14
TiO_2		0.07				0.07
Total		99.33	99.80	99.10	99.74	
Na	Cations	0.21	0.22	0.21	0.22	0.21
Mg	Norm.					
Al	to	1.74	1.74	1.74	1.73	1.74
Si	8 oxygens	2.22	2.22	2.22	2.22	2.22
Ca		0.82	0.82	0.81	0.83	0.82
Fe		0.02	0.02	0.02	0.02	0.02
K		0.01	0.01	0.01	0.01	0.01
Ti		0.00				0.00
Total		5.02	5.02	5.02	5.02	5.02
An		78.71	78.49	78.83	78.65	78.67
Ab		20.38	20.83	20.37	20.56	20.54
Or		0.91	0.68	0.80	0.78	0.79

CLG-41		Plag 1 Spec. 1	Plag 1 Spec. 2	Plag 1 Spec. 3	Plag 1 Spec. 4	Plag 1 Avg.
Na_2O	Oxide	2.29	2.21	2.57	2.26	2.33
MgO	wt%					
Al_2O_3		32.32	32.34	32.23	32.25	32.29
SiO_2		48.19	47.98	47.97	48.04	48.05
CaO		16.61	16.86	16.85	16.80	16.78
FeO		0.54	0.43	0.52	0.46	0.49
K_2O		0.14	0.12	0.14	0.13	0.13
TiO_2		0.13				0.13
Total		100.20	99.94	100.27	99.94	
Na	Cations	0.20	0.20	0.23	0.20	0.21
Mg	Norm.					
Al	to	1.75	1.75	1.75	1.75	1.75
Si	8 oxygens	2.21	2.21	2.21	2.21	2.21
Ca		0.82	0.83	0.83	0.83	0.83
Fe		0.02	0.02	0.02	0.02	0.02
K		0.01	0.01	0.01	0.01	0.01
Ti		0.00				0.00
Total		5.01	5.02	5.04	5.02	5.02
An		79.40	80.28	77.77	79.83	79.32
Ab		19.81	19.04	21.46	19.43	19.94
Or		0.80	0.68	0.77	0.74	0.75

CLG-41		Plag 2 Spec. 1	Plag 2 Spec. 2	Plag 2 Spec. 3	Plag 2 Spec. 4	Plag 2 Avg.
Na_2O	Oxide	2.32	2.33	2.38	2.47	2.38
MgO	wt%					
Al_2O_3		32.23	32.05	32.32	32.32	32.23
SiO_2		47.93	48.18	48.23	48.05	48.10
CaO		16.65	16.69	16.65	16.80	16.70
FeO		0.53	0.53	0.60	0.43	0.52
K_2O		0.15	0.13	0.12	0.18	0.15
TiO_2		0.10				0.10
Total		99.92	99.90	100.30	100.25	
Na	Cations	0.21	0.21	0.21	0.22	0.21

Mg	Norm.					
Al	to	1.75	1.74	1.75	1.75	1.75
Si	8 oxygens	2.21	2.22	2.21	2.21	2.21
Ca		0.82	0.82	0.82	0.83	0.82
Fe		0.02	0.02	0.02	0.02	0.02
K		0.01	0.01	0.01	0.01	0.01
Ti		0.00				0.00
Total		5.02	5.02	5.02	5.03	5.02
An		79.18	79.25	78.91	78.20	78.88
Ab		19.97	20.02	20.41	20.80	20.30
Or		0.85	0.73	0.68	1.00	0.81

CLG-41		Plag 3 Spec. 1	Plag 3 Spec. 2	Plag 3 Spec. 3	Plag 3 Spec. 4	Plag 3 Avg.
Na_2O	Oxide	1.97	2.00	2.01	2.03	2.00
MgO	wt%					
Al_2O_3		32.28	32.74	32.63	32.62	32.57
SiO_2		46.79	47.06	47.05	47.19	47.02
CaO		17.32	17.53	17.36	17.28	17.37
FeO		0.60	0.47	0.57	0.55	0.55
K_2O		0.06	0.10	0.10	0.18	0.11
TiO_2		0.08				0.08
Total		99.10	99.89	99.72	99.84	
Na	Cations	0.18	0.18	0.18	0.18	0.18
Mg	Norm.					
Al	to	1.77	1.78	1.78	1.78	1.78
Si	8 oxygens	2.18	2.17	2.18	2.18	2.18
Ca		0.86	0.87	0.86	0.86	0.86
Fe		0.02	0.02	0.02	0.02	0.02
K		0.00	0.01	0.01	0.01	0.01
Ti		0.00				0.00
Total		5.02	5.03	5.03	5.03	5.03
An		82.65	82.42	82.21	81.63	82.23
Ab		17.01	17.02	17.23	17.35	17.15
Or		0.34	0.56	0.56	1.01	0.62

CLG-42		Plag 1 Spec. 1	Plag 1 Spec. 2	Plag 1 Spec. 3	Plag 1 Spec. 4	Plag 1 Spec. 5	Plag 1 Spec. 6	Plag 1 Avg.
Na_2O	Oxide	2.27	2.37	2.46	2.46	2.47	2.46	2.42
MgO	wt%	0.31	0.16	0.17	0.04	0.10	0.11	0.15
Al_2O_3		31.57	31.84	31.58	31.81	31.80	31.45	31.68
SiO_2		48.07	48.15	48.62	48.54	48.81	48.85	48.51
CaO		16.35	16.49	16.41	16.29	16.22	16.44	16.37
FeO		0.55	0.44	0.42	0.44	0.57	0.53	0.49
K_2O		0.34	0.22	0.18	0.15	0.17	0.19	0.21
TiO_2								
Total		99.45	99.67	99.84	99.73	100.13	100.02	
Na	Cations	0.20	0.21	0.22	0.22	0.22	0.22	0.22
Mg	Norm.	0.02	0.01	0.01	0.00	0.01	0.01	0.01
Al	to	1.72	1.73	1.71	1.73	1.72	1.70	1.72
Si	8 oxygens	2.23	2.22	2.24	2.24	2.24	2.25	2.23
Ca		0.81	0.82	0.81	0.80	0.80	0.81	0.81
Fe		0.02	0.02	0.02	0.02	0.02	0.02	0.02
K		0.02	0.01	0.01	0.01	0.01	0.01	0.01

Ti								
Total		5.03	5.02	5.02	5.01	5.02	5.02	5.02
An		78.37	78.37	77.86	77.87	77.64	77.85	77.99
Ab		19.69	20.38	21.12	21.28	21.39	21.08	20.82
Or		1.94	1.24	1.02	0.85	0.97	1.07	1.18

CLG-42		Plag 2 Spec. 1	Plag 2 Spec. 2	Plag 2 Spec. 3	Plag 2 Spec. 4	Plag 2 Spec. 5	Plag 2 Spec. 6	Plag 2 Avg.
Na_2O	Oxide	3.10	3.00	3.03	3.03	3.19	3.17	3.09
MgO	wt%	0.13	0.17	0.07	0.13	0.15	0.09	0.12
Al_2O_3		30.36	30.29	31.02	30.80	30.57	30.72	30.63
SiO_2		49.77	49.87	49.51	49.73	49.48	49.81	49.70
CaO		15.05	15.08	15.19	15.11	15.23	15.11	15.13
FeO		0.48	0.47	0.47	0.46	0.57	0.41	0.48
K_2O		0.27	0.22	0.23	0.15	0.18	0.21	0.21
TiO_2								
Total		99.17	99.11	99.52	99.41	99.38	99.53	
Na	Cations	0.28	0.27	0.27	0.27	0.29	0.28	0.28
Mg	Norm.	0.01	0.01	0.00	0.01	0.01	0.01	0.01
Al	to	1.65	1.65	1.68	1.67	1.66	1.67	1.66
Si	8 oxygens	2.30	2.30	2.28	2.29	2.29	2.29	2.29
Ca		0.75	0.75	0.75	0.75	0.75	0.75	0.75
Fe		0.02	0.02	0.02	0.02	0.02	0.02	0.02
K		0.02	0.01	0.01	0.01	0.01	0.01	0.01
Ti								
Total		5.02	5.01	5.02	5.01	5.03	5.02	5.02
An		71.73	72.60	72.52	72.74	71.78	71.62	72.17
Ab		26.74	26.14	26.18	26.40	27.21	27.19	26.64
Or		1.53	1.26	1.31	0.86	1.01	1.19	1.19

CLG-42		Plag 3 Spec. 1	Plag 3 Spec. 2	Plag 3 Spec. 3	Plag 3 Spec. 4	Plag 3 Spec. 5	Plag 3 Avg.
Na_2O	Oxide	3.14	3.34	3.30	3.14	3.18	3.22
MgO	wt%	0.09	0.13	0.07	0.20	0.16	0.13
Al_2O_3		30.34	30.32	30.20	30.39	30.31	30.31
SiO_2		50.29	49.97	50.65	50.04	50.26	50.24
CaO		14.77	14.71	14.96	14.92	15.03	14.88
FeO		0.46	0.44	0.50	0.61	0.50	0.50
K_2O		0.23	0.16	0.20	0.17	0.20	0.19
TiO_2							
Total		99.33	99.07	99.88	99.47	99.64	
Na	Cations	0.28	0.30	0.29	0.28	0.28	0.29
Mg	Norm.	0.01	0.01	0.00	0.01	0.01	0.01
Al	to	1.65	1.65	1.63	1.65	1.64	1.64
Si	8 oxygens	2.32	2.31	2.32	2.30	2.31	2.31
Ca		0.73	0.73	0.73	0.74	0.74	0.73
Fe		0.02	0.02	0.02	0.02	0.02	0.02
K		0.01	0.01	0.01	0.01	0.01	0.01
Ti							
Total		5.01	5.02	5.02	5.02	5.02	5.02
An		71.26	70.23	70.67	71.71	71.49	71.07
Ab		27.42	28.86	28.21	27.31	27.37	27.83
Or		1.32	0.91	1.12	0.97	1.13	1.09

Crystal Lake Gabbro Clinopyroxene

CLG-3		CPX 1 Spec. 1	CPX 1 Spec. 2	CPX 1 Spec. 3	CPX 1 Spec. 4	CPX 1 Spec. 5	CPX 1 Spec. 6	CPX 1 Avg.
Na_2O	Oxide	0.30	0.36	0.43	0.47	0.37	0.34	0.38
MgO	wt%	16.23	16.22	16.21	16.29	16.21	16.34	16.25
Al_2O_3		2.14	2.00	2.14	2.03	2.11	2.08	2.08
SiO_2		51.61	51.74	51.85	51.35	51.87	51.71	51.69
CaO		20.26	20.37	20.26	20.05	20.31	20.41	20.28
TiO_2		1.01	0.95	0.85	1.00	1.03	0.84	0.95
V_2O_5		0.07	0.03	0.12		0.13	0.14	0.10
Cr_2O_3		0.53	0.59	0.52	0.66	0.56	0.55	0.57
MnO		0.14	0.21	0.19		0.10	0.16	0.16
FeO		7.89	7.98	8.02	7.72	8.04	7.81	7.91
Total		100.18	100.45	100.59	99.57	100.72	100.39	
Na	Cations	0.02	0.03	0.03	0.03	0.03	0.02	0.03
Mg	Norm,	0.90	0.89	0.89	0.90	0.89	0.90	0.90
Al	to	0.09	0.09	0.09	0.09	0.09	0.09	0.09
Si	6 oxygens	1.91	1.91	1.91	1.91	1.91	1.91	1.91
Ca		0.80	0.81	0.80	0.80	0.80	0.81	0.80
Ti		0.03	0.03	0.02	0.03	0.03	0.02	0.03
V		0.00	0.00	0.00	0.00	0.00	0.00	0.00
Cr		0.02	0.02	0.02	0.02	0.02	0.02	0.02
Mn		0.00	0.01	0.01	0.00	0.00	0.01	0.00
Fe		0.24	0.25	0.25	0.24	0.25	0.24	0.24
Total		4.02	4.02	4.02	4.02	4.02	4.02	
Mg#		78.57	78.37	78.28	79.00	78.23	78.86	78.55
%wo		41.34	41.43	41.28	41.13	41.33	41.45	41.33
%en		46.09	45.90	45.96	46.50	45.90	46.17	46.09
%fs		12.57	12.67	12.76	12.36	12.77	12.38	12.58

CLG-3		CPX 2 Spec. 1	CPX 2 Spec. 2	CPX 2 Spec. 3	CPX 2 Spec. 4	CPX 2 Spec. 5	CPX 2 Spec. 6	CPX 2 Avg.
Na_2O	Oxide	0.28	0.29	0.36	0.30	0.31	0.32	0.31
MgO	wt%	16.25	15.76	16.08	15.13	15.23	15.46	15.65
Al_2O_3		1.73	1.90	1.80	1.99	2.05	1.83	1.88
SiO_2		50.90	50.66	50.90	51.05	51.39	51.74	51.11
CaO		17.17	17.44	17.35	18.49	18.33	18.20	17.83
TiO_2		1.21	0.93	1.13	1.05	1.13	0.93	1.06
V_2O_5		0.09	0.12	0.22	0.19	0.18	0.14	0.16
Cr_2O_3		0.21	0.07	0.13	0.12	0.06	0.14	0.12
MnO		0.30	0.33	0.35	0.26	0.34	0.28	0.31
FeO		12.72	12.01	12.55	11.86	11.82	11.79	12.13
		100.88	99.53	100.86	100.43	100.84	100.85	
Na	Cations	0.02	0.02	0.03	0.02	0.02	0.02	0.02
Mg	Norm,	0.90	0.89	0.89	0.84	0.84	0.86	0.87
Al	to	0.08	0.08	0.08	0.09	0.09	0.08	0.08
Si	6 oxygens	1.90	1.91	1.90	1.91	1.91	1.92	1.91
Ca		0.69	0.70	0.69	0.74	0.73	0.72	0.71
Ti		0.03	0.03	0.03	0.03	0.03	0.03	0.03
V		0.00	0.00	0.01	0.00	0.00	0.00	0.00
Cr		0.01	0.00	0.00	0.00	0.00	0.00	0.00
Mn		0.01	0.01	0.01	0.01	0.01	0.01	0.01
Fe		0.40	0.38	0.39	0.37	0.37	0.37	0.38
Total		4.03	4.03	4.03	4.02	4.02	4.02	

Mg#		69.49	70.05	69.55	69.46	69.67	70.04	69.71
%wo		34.54	35.78	35.03	37.89	37.60	37.21	36.34
%en		45.49	44.99	45.18	43.14	43.47	43.98	44.38
%fs		19.97	19.23	19.78	18.97	18.93	18.81	19.28

CLG-3		CPX 3 Spec. 1	CPX 3 Spec. 2	CPX 3 Spec. 3	CPX 3 Spec. 4	CPX 3 Spec. 5	CPX 3 Spec. 6	CPX 3 Avg.
Na_2O	Oxide	0.29	0.36	0.39	0.40	0.37	0.27	0.35
MgO	wt%	15.61	15.62	15.73	15.72	15.39	15.45	15.59
Al_2O_3		3.11	3.21	3.13	3.13	3.27	3.31	3.19
SiO_2		50.44	50.55	50.56	50.35	50.70	50.60	50.53
CaO		20.56	20.34	20.26	20.16	20.31	20.30	20.32
TiO_2		1.19	1.14	1.13	1.36	1.32	1.18	1.22
V_2O_5		0.13	0.10	0.21	0.15	0.27	0.25	0.19
Cr_2O_3		0.79	0.79	0.86	0.74	0.75	0.84	0.80
MnO		0.21	0.08	0.22	0.12	0.21	0.17	0.17
FeO		8.01	8.25	8.33	8.21	8.33	8.41	8.26
		100.32	100.43	100.82	100.34	100.91	100.79	
Na	Cations	0.02	0.03	0.03	0.03	0.03	0.02	0.02
Mg	Norm,	0.86	0.86	0.87	0.87	0.85	0.85	0.86
Al	to	0.14	0.14	0.14	0.14	0.14	0.14	0.14
Si	6 oxygens	1.87	1.87	1.87	1.87	1.87	1.87	1.87
Ca		0.82	0.81	0.80	0.80	0.80	0.80	0.81
Ti		0.03	0.03	0.03	0.04	0.04	0.03	0.03
V		0.00	0.00	0.01	0.00	0.01	0.01	0.00
Cr		0.02	0.02	0.03	0.02	0.02	0.02	0.02
Mn		0.01	0.00	0.01	0.00	0.01	0.01	0.01
Fe		0.25	0.26	0.26	0.25	0.26	0.26	0.26
Total		4.02	4.02	4.03	4.02	4.02	4.01	
Mg#		77.65	77.14	77.10	77.34	76.71	76.61	77.09
%wo		42.36	41.92	41.64	41.61	42.11	41.97	41.94
%en		44.76	44.80	44.99	45.16	44.41	44.45	44.76
%fs		12.88	13.27	13.37	13.23	13.48	13.57	13.30

CLG-8		CPX 1 Spec. 1	CPX 1 Spec. 2	CPX 1 Spec. 3	CPX 1 Spec. 4	CPX 1 Spec. 5	CPX 1 Spec. 6	CPX 1 Avg.
Na_2O	Oxide	0.42	0.34	0.27	0.29	0.42	0.32	0.34
MgO	wt%	14.93	14.75	14.75	14.80	14.82	14.72	14.80
Al_2O_3		2.16	2.15	2.22	2.08	2.07	2.10	2.13
SiO_2		50.59	50.29	50.64	50.29	50.38	50.12	50.39
CaO		19.37	19.63	19.71	19.49	19.28	19.54	19.50
TiO_2		1.02	1.07	1.14	1.08	1.19	1.10	1.10
V_2O_5		0.06		0.19	0.05	0.10	0.11	0.10
Cr_2O_3		0.34	0.39	0.22	0.25	0.24	0.25	0.28
MnO		0.36	0.25	0.13	0.21	0.23	0.25	0.24
FeO		10.49	10.51	10.66	10.53	10.44	10.71	10.56
		99.76	99.38	99.95	99.07	99.17	99.23	
Na	Cations	0.03	0.02	0.02	0.02	0.03	0.02	0.03
Mg	Norm,	0.84	0.83	0.83	0.84	0.84	0.83	0.83
Al	to	0.10	0.10	0.10	0.09	0.09	0.09	0.09
Si	6 oxygens	1.90	1.90	1.90	1.90	1.90	1.90	1.90
Ca		0.78	0.79	0.79	0.79	0.78	0.79	0.79
Ti		0.03	0.03	0.03	0.03	0.03	0.03	0.03
V		0.00		0.00	0.00	0.00	0.00	0.00
Cr		0.01	0.01	0.01	0.01	0.01	0.01	0.01

Mn		0.01	0.01	0.00	0.01	0.01	0.01	0.01
Fe		0.33	0.33	0.33	0.33	0.33	0.34	0.33
Total		4.03	4.03	4.02	4.02	4.02	4.03	
Mg#		71.73	71.44	71.15	71.47	71.68	71.02	71.41
%wo		40.07	40.59	40.59	40.35	40.12	40.39	40.35
%en		42.98	42.44	42.27	42.64	42.92	42.34	42.60
%fs		16.94	16.97	17.14	17.02	16.96	17.28	17.05

CLG-8		CPX 2 Spec. 1	CPX 2 Spec. 2	CPX 2 Spec. 3	CPX 2 Spec. 4	CPX 2 Spec. 5	CPX 2 Spec. 6	CPX 2 Avg.
Na_2O	Oxide	0.26	0.25	0.36	0.38	0.38	0.40	0.34
MgO	wt%	14.88	14.99	14.63	14.67	14.66	14.92	14.79
Al_2O_3		2.04	2.05	2.05	1.97	2.00	1.89	2.00
SiO_2		51.10	50.82	50.67	50.79	50.99	50.95	50.89
CaO		19.26	19.35	19.30	19.37	19.48	19.37	19.36
TiO_2		1.19	1.39	1.24	1.30	1.31	1.22	1.28
V_2O_5		0.14			0.20	0.17		0.17
Cr_2O_3								
MnO		0.18	0.33	0.26	0.29	0.28	0.21	0.26
FeO		11.60	11.67	11.48	11.81	11.63	11.56	11.63
		100.64	100.84	99.99	100.78	100.91	100.52	
Na	Cations	0.02	0.02	0.03	0.03	0.03	0.03	0.02
Mg	Norm,	0.83	0.83	0.82	0.82	0.82	0.83	0.82
Al	to	0.09	0.09	0.09	0.09	0.09	0.08	0.09
Si	6 oxygens	1.91	1.90	1.91	1.90	1.90	1.91	1.90
Ca		0.77	0.77	0.78	0.78	0.78	0.78	0.78
Ti		0.03	0.04	0.04	0.04	0.04	0.03	0.04
V		0.00			0.00	0.00		0.00
Cr								0.00
Mn		0.01	0.01	0.01	0.01	0.01	0.01	0.01
Fe		0.36	0.36	0.36	0.37	0.36	0.36	0.36
Total		4.02	4.03	4.03	4.03	4.02	4.03	
Mg#		69.57	69.60	69.44	68.89	69.20	69.70	69.40
%wo		39.29	39.23	39.70	39.53	39.79	39.41	39.49
%en		42.24	42.29	41.87	41.66	41.67	42.24	42.00
%fs		18.47	18.47	18.43	18.81	18.54	18.36	18.51

CLG-8		CPX 3 Spec. 1	CPX 3 Spec. 2	CPX 3 Spec. 3	CPX 3 Spec. 4	CPX 3 Spec. 5	CPX 3 Avg.
Na_2O	Oxide	0.34	0.38	0.40	0.33	0.41	0.37
MgO	wt%	14.90	14.66	15.08	15.01	14.83	14.90
Al_2O_3		1.91	1.81	1.89	1.74	1.77	1.82
SiO_2		50.43	50.51	50.46	50.32	50.54	50.45
CaO		19.33	19.08	19.17	19.33	19.10	19.20
TiO_2		1.17	1.21	1.11	1.14	1.17	1.16
V_2O_5		0.13	0.06	0.06	0.03	0.12	0.08
Cr_2O_3		0.11	0.11	0.05	0.12	0.07	0.09
MnO		0.20	0.35	0.26	0.22	0.21	0.25
FeO		11.05	11.47	11.36	11.27	11.27	11.28
		99.56	99.64	99.82	99.51	99.47	
Na	Cations	0.02	0.03	0.03	0.02	0.03	0.03
Mg	Norm,	0.84	0.83	0.85	0.85	0.84	0.84
Al	to	0.08	0.08	0.08	0.08	0.08	0.08
Si	6 oxygens	1.90	1.91	1.90	1.90	1.91	1.91

Ca		0.78	0.77	0.77	0.78	0.77	0.78
Ti		0.03	0.03	0.03	0.03	0.03	0.03
V		0.00	0.00	0.00	0.00	0.00	0.00
Cr		0.00	0.00	0.00	0.00	0.00	0.00
Mn		0.01	0.01	0.01	0.01	0.01	0.01
Fe		0.35	0.36	0.36	0.36	0.36	0.36
Total		4.03	4.03	4.04	4.03	4.03	
Mg#		70.62	69.50	70.29	70.36	70.11	70.18
%wo		39.70	39.39	39.10	39.44	39.35	39.40
%en		42.58	42.12	42.81	42.61	42.52	42.53
%fs		17.72	18.49	18.09	17.95	18.13	18.07

CLG-13		CPX 1 Spec. 1	CPX 1 Spec. 2	CPX 1 Spec. 3	CPX 1 Spec. 4	CPX 1 Avg.
Na_2O	Oxide	0.33	0.39	0.38	0.42	0.38
MgO	wt%	14.32	14.35	14.75	14.28	14.43
Al_2O_3		1.35	1.31	1.31	1.52	1.37
SiO_2		51.16	51.11	51.41	51.12	51.20
CaO		18.09	17.96	17.97	18.00	18.01
TiO_2		0.76	0.83	0.84	0.72	0.79
V_2O_5		0.19			0.12	0.16
Cr_2O_3						
MnO		0.35	0.35	0.31	0.37	0.35
FeO		13.52	13.81	13.84	13.78	13.74
		100.07	100.12	100.82	100.34	
Na	Cations	0.02	0.03	0.03	0.03	0.03
Mg	Norm,	0.81	0.81	0.83	0.80	0.81
Al	to	0.06	0.06	0.06	0.07	0.06
Si	6 oxygens	1.93	1.93	1.93	1.93	1.93
Ca		0.73	0.73	0.72	0.73	0.73
Ti		0.02	0.02	0.02	0.02	0.02
V		0.00			0.00	0.00
Cr						
Mn		0.01	0.01	0.01	0.01	0.01
Fe		0.43	0.44	0.43	0.43	0.43
Total		4.02	4.03	4.03	4.03	
Mg#		65.38	64.94	65.52	64.88	65.18
%wo		37.24	36.87	36.45	37.02	36.90
%en		41.03	41.00	41.63	40.86	41.13
%fs		21.73	22.13	21.91	22.12	21.97

CLG-13		CPX 2 Spec. 1	CPX 2 Spec. 2	CPX 2 Spec. 3	CPX 2 Spec. 4	CPX 2 Avg.
Na_2O	Oxide	0.30	0.35	0.39	0.41	0.36
MgO	wt%	14.75	14.88	14.60	14.67	14.73
Al_2O_3		1.67	1.70	1.76	1.81	1.74
SiO_2		50.94	50.56	50.53	50.66	50.67
CaO		19.15	19.12	18.94	19.24	19.11
TiO_2		1.05	1.16	1.08	1.11	1.10
V_2O_5		0.11	0.21	0.09	0.19	0.15
Cr_2O_3						
MnO		0.41	0.30	0.29	0.36	0.34
FeO		11.54	11.35	11.87	11.42	11.55
		99.93	99.63	99.55	99.86	

Na	Cations	0.02	0.03	0.03	0.03	0.03
Mg	Norm,	0.83	0.84	0.82	0.82	0.83
Al	to	0.07	0.08	0.08	0.08	0.08
Si	6 oxygens	1.92	1.91	1.91	1.91	1.91
Ca		0.77	0.77	0.77	0.78	0.77
Ti		0.03	0.03	0.03	0.03	0.03
V		0.00	0.01	0.00	0.00	0.00
Cr						
Mn		0.01	0.01	0.01	0.01	0.01
Fe		0.36	0.36	0.38	0.36	0.36
Total		4.02	4.03	4.03	4.03	
Mg#		69.50	70.03	68.68	69.60	69.45
%wo		39.34	39.27	39.03	39.61	39.31
%en		42.16	42.53	41.87	42.03	42.15
%fs		18.50	18.20	19.10	18.35	18.54

CLG-13		CPX 3 Spec. 1	CPX 3 Spec. 2	CPX 3 Spec. 3	CPX 3 Spec. 4	CPX 3 Avg.
Na_2O	Oxide	0.40	0.31	0.45	0.42	0.40
MgO	wt%	14.63	14.88	14.55	14.64	14.68
Al_2O_3		1.89	1.89	2.04	1.89	1.93
SiO_2		50.43	50.55	50.48	50.28	50.44
CaO		18.76	18.54	18.65	18.58	18.63
TiO_2		1.20	1.15	1.18	1.18	1.18
V_2O_5		0.16	0.09	0.23	0.20	0.17
Cr_2O_3						
MnO		0.23	0.26	0.26	0.39	0.29
FeO		12.40	12.31	12.14	12.21	12.27
		100.10	99.99	99.96	99.78	
Na	Cations	0.03	0.02	0.03	0.03	0.03
Mg	Norm,	0.82	0.84	0.82	0.83	0.83
Al	to	0.08	0.08	0.09	0.08	0.09
Si	6 oxygens	1.90	1.91	1.90	1.90	1.90
Ca		0.76	0.75	0.75	0.75	0.75
Ti		0.03	0.03	0.03	0.03	0.03
V		0.00	0.00	0.01	0.00	0.00
Cr						
Mn		0.01	0.01	0.01	0.01	0.01
Fe		0.39	0.39	0.38	0.39	0.39
Total		4.03	4.03	4.03	4.03	
Mg#		67.78	68.30	68.12	68.13	68.08
%wo		38.44	37.95	38.55	38.32	38.32
%en		41.72	42.38	41.86	42.02	41.99
%fs		19.84	19.67	19.59	19.66	19.69

CLG-18		CPX 1 Spec. 1	CPX 1 Spec. 2	CPX 1 Spec. 3	CPX 1 Spec. 4	CPX 1 Avg.
Na_2O	Oxide	0.28	0.35	0.34	0.35	0.33
MgO	wt%	15.17	15.00	15.07	15.08	15.08
Al_2O_3		2.32	2.34	2.38	2.52	2.39
SiO_2		50.70	50.49	50.25	50.92	50.59
CaO		19.71	19.63	19.75	19.66	19.69
TiO_2		1.30	1.26	1.29	1.29	1.29
V_2O_5		0.20	0.10	0.11		0.14
Cr_2O_3		0.13	0.21	0.23	0.26	0.21

MnO		0.24	0.23	0.29	0.27	0.26
FeO		10.02	10.29	10.13	10.37	10.20
		100.07	99.91	99.82	100.73	
Na	Cations	0.02	0.03	0.02	0.03	0.02
Mg	Norm,	0.85	0.84	0.84	0.84	0.84
Al	to	0.10	0.10	0.11	0.11	0.11
Si	6 oxygens	1.90	1.89	1.89	1.89	1.89
Ca		0.79	0.79	0.79	0.78	0.79
Ti		0.04	0.04	0.04	0.04	0.04
V		0.00	0.00	0.00		0.00
Cr		0.00	0.01	0.01	0.01	0.01
Mn		0.01	0.01	0.01	0.01	0.01
Fe		0.31	0.32	0.32	0.32	0.32
Total		4.02	4.02	4.03	4.02	
Mg#		72.96	72.21	72.62	72.16	72.49
%wo		40.52	40.44	40.61	40.34	40.48
%en		43.40	43.01	43.12	43.05	43.15
%fs		16.08	16.55	16.26	16.61	16.38

CLG-18		CPX 2 Spec. 1	CPX 2 Spec. 2	CPX 2 Spec. 3	CPX 2 Spec. 4	CPX 2 Avg.
Na_2O	Oxide	0.34	0.38	0.36	0.42	0.38
MgO	wt%	14.97	14.90	14.76	14.83	14.87
Al_2O_3		2.19	2.09	2.17	2.15	2.15
SiO_2		50.41	50.56	50.54	50.74	50.56
CaO		19.12	19.04	19.01	19.12	19.07
TiO_2		1.29	1.29	1.30	1.29	1.29
V_2O_5		0.23	0.11			0.17
Cr_2O_3						
MnO		0.20	0.26	0.28	0.31	0.26
FeO		11.75	12.00	11.87	11.93	11.89
		100.50	100.63	100.29	100.80	
Na	Cations	0.02	0.03	0.03	0.03	0.03
Mg	Norm,	0.84	0.83	0.83	0.83	0.83
Al	to	0.10	0.09	0.10	0.09	0.09
Si	6 oxygens	1.89	1.89	1.90	1.90	1.89
Ca		0.77	0.76	0.76	0.77	0.77
Ti		0.04	0.04	0.04	0.04	0.04
V		0.01	0.00			0.00
Cr						
Mn		0.01	0.01	0.01	0.01	0.01
Fe		0.37	0.38	0.37	0.37	0.37
Total		4.03	4.03	4.03	4.03	
Mg#		69.43	68.88	68.91	68.91	69.03
%wo		38.92	38.75	38.94	38.96	38.89
%en		42.41	42.19	42.08	42.06	42.18
%fs		18.67	19.06	18.98	18.98	18.92

CLG-18		CPX 3 Spec. 1	CPX 3 Spec. 2	CPX 3 Spec. 3	CPX 3 Spec. 4	CPX 3 Avg.
Na_2O	Oxide	0.35	0.35	0.35	0.35	0.35
MgO	wt%	14.74	14.74	14.57	14.86	14.73
Al_2O_3		1.87	1.87	1.79	1.87	1.85
SiO_2		50.87	50.87	50.68	50.74	50.79

CaO		18.81	18.81	18.82	19.00	18.86
TiO_2		1.10	1.10	1.12	1.10	1.11
V_2O_5		0.25	0.25	0.00	0.21	0.18
Cr_2O_3						
MnO		0.24	0.24	0.32	0.23	0.26
FeO		12.66	12.66	12.37	12.27	12.49
		100.91	100.91	100.02	100.64	
Na	Cations	0.03	0.03	0.03	0.03	0.03
Mg	Norm,	0.82	0.82	0.82	0.83	0.82
Al	to	0.08	0.08	0.08	0.08	0.08
Si	6 oxygens	1.90	1.90	1.91	1.90	1.90
Ca		0.75	0.75	0.76	0.76	0.76
Ti		0.03	0.03	0.03	0.03	0.03
V		0.01	0.01	0.00	0.01	0.00
Cr						
Mn		0.01	0.01	0.01	0.01	0.01
Fe		0.40	0.40	0.39	0.38	0.39
Total		4.03	4.03	4.03	4.03	
Mg#		67.49	67.49	67.74	68.34	67.76
%wo		38.23	38.23	38.60	38.57	38.41
%en		41.69	41.69	41.59	41.98	41.74
%fs		20.09	20.09	19.81	19.45	19.86

CLG-20		CPX 1 Spec. 1	CPX 1 Spec. 2	CPX 1 Spec. 3	CPX 1 Spec. 4	CPX 1 Avg.
Na_2O	Oxide	0.40	0.35	0.34	0.41	0.38
MgO	wt%	15.00	14.82	14.86	14.80	14.87
Al_2O_3		2.45	2.48	2.33	2.45	2.43
SiO_2		49.85	50.31	49.88	49.82	49.97
CaO		17.96	18.61	18.08	18.25	18.23
TiO_2		1.37	1.28	1.32	1.28	1.31
V_2O_5		0.23		0.10		0.17
Cr_2O_3		0.10	0.15	0.10	0.17	0.13
MnO		0.38	0.20	0.29	0.29	0.29
FeO		11.73	11.72	12.16	11.70	11.83
		99.48	99.92	99.47	99.16	
Na	Cations	0.03	0.03	0.02	0.03	0.03
Mg	Norm,	0.85	0.83	0.84	0.84	0.84
Al	to	0.11	0.11	0.10	0.11	0.11
Si	6 oxygens	1.88	1.89	1.89	1.89	1.89
Ca		0.73	0.75	0.73	0.74	0.74
Ti		0.04	0.04	0.04	0.04	0.04
V		0.01		0.00		0.00
Cr		0.00	0.00	0.00	0.01	0.00
Mn		0.01	0.01	0.01	0.01	0.01
Fe		0.37	0.37	0.39	0.37	0.37
Total		4.03	4.03	4.03	4.03	
Mg#		69.51	69.27	68.54	69.28	69.15
%wo		37.42	38.46	37.47	38.04	37.85
%en		43.50	42.63	42.86	42.93	42.98
%fs		19.08	18.91	19.67	19.04	19.17

CLG-20		CPX 2 Spec. 1	CPX 2 Spec. 2	CPX 2 Spec. 3	CPX 2 Spec. 4	CPX 2 Avg.

Na_2O	Oxide	0.39	0.34	0.33	0.34	0.35
MgO	wt%	15.38	14.85	15.72	15.59	15.39
Al_2O_3		2.67	2.72	2.46	2.60	2.61
SiO_2		50.43	50.34	50.11	50.05	50.23
CaO		20.18	20.48	19.58	19.16	19.85
TiO_2		1.03	1.13	1.17	1.12	1.11
V_2O_5		0.18		0.22	0.18	0.19
Cr_2O_3		0.37	0.39	0.46	0.41	0.41
MnO		0.25	0.16	0.25	0.30	0.24
FeO		9.50	9.32	9.74	9.88	9.61
		100.38	99.72	100.06	99.62	
Na	Cations	0.03	0.02	0.02	0.02	0.03
Mg	Norm,	0.85	0.83	0.88	0.87	0.86
Al	to	0.12	0.12	0.11	0.12	0.12
Si	6 oxygens	1.88	1.89	1.88	1.88	1.88
Ca		0.81	0.82	0.79	0.77	0.80
Ti		0.03	0.03	0.03	0.03	0.03
V		0.00		0.01	0.00	0.00
Cr		0.01	0.01	0.01	0.01	0.01
Mn		0.01	0.01	0.01	0.01	0.01
Fe		0.30	0.29	0.30	0.31	0.30
Total		4.03	4.03	4.03	4.03	
Mg#		74.27	73.96	74.21	73.77	74.05
%wo		41.19	42.30	39.91	39.45	40.71
%en		43.68	42.68	44.59	44.67	43.90
%fs		15.14	15.03	15.50	15.88	15.38

CLG-20		CPX 3 Spec. 1	CPX 3 Spec. 2	CPX 3 Spec. 3	CPX 3 Spec. 4	CPX 3 Avg.
Na_2O	Oxide	0.32	0.39	0.41	0.39	0.38
MgO	wt%	15.36	15.50	15.58	15.51	15.49
Al_2O_3		2.78	2.73	2.75	2.88	2.79
SiO_2		50.31	50.07	50.33	50.07	50.20
CaO		20.12	19.98	20.08	20.07	20.06
TiO_2		1.23	1.08	1.19	1.15	1.16
V_2O_5		0.09		0.00	0.20	0.10
Cr_2O_3		0.58	0.69	0.58	0.69	0.64
MnO		0.20	0.21	0.12	0.27	0.20
FeO		8.80	8.60	8.49	8.67	8.64
		99.81	99.25	99.53	99.89	
Na	Cations	0.02	0.03	0.03	0.03	0.03
Mg	Norm,	0.86	0.87	0.87	0.86	0.86
Al	to	0.12	0.12	0.12	0.13	0.12
Si	6 oxygens	1.88	1.88	1.88	1.87	1.88
Ca		0.81	0.80	0.81	0.80	0.80
Ti		0.03	0.03	0.03	0.03	0.03
V		0.00		0.00	0.00	0.00
Cr		0.02	0.02	0.02	0.02	0.02
Mn		0.01	0.01	0.00	0.01	0.01
Fe		0.28	0.27	0.27	0.27	0.27
Total		4.02	4.03	4.03	4.03	
Mg#		75.68	76.26	76.59	76.13	76.16
%wo		41.60	41.40	41.50	41.45	41.49
%en		44.19	44.69	44.81	44.57	44.57
%fs		14.20	13.91	13.70	13.98	13.95

CLG-23		CPX 1 Spec. 1	CPX 1 Spec. 2	CPX 1 Spec. 3	CPX 1 Spec. 4	CPX 1 Avg.
Na_2O	Oxide	0.49	0.48	0.45	0.33	0.44
MgO	wt%	14.63	14.16	14.57	14.41	14.44
Al_2O_3		1.66	1.68	1.69	1.74	1.69
SiO_2		50.75	50.85	50.62	50.48	50.68
CaO		19.65	19.69	18.91	19.29	19.39
TiO_2		0.81	0.90	0.80	0.91	0.86
V_2O_5		0.17				0.09
Cr_2O_3		0.08				0.08
MnO		0.38	0.32	0.32	0.25	0.32
FeO		11.25	11.03	11.86	11.67	11.45
		99.86	99.09	99.23	99.08	
Na	Cations	0.04	0.04	0.03	0.02	0.03
Mg	Norm,	0.82	0.80	0.82	0.82	0.82
Al	to	0.07	0.08	0.08	0.08	0.08
Si	6 oxygens	1.91	1.93	1.92	1.92	1.92
Ca		0.79	0.80	0.77	0.79	0.79
Ti		0.02	0.03	0.02	0.03	0.02
V		0.00				0.00
Cr		0.00				0.00
Mn		0.01	0.01	0.01	0.01	0.01
Fe		0.35	0.35	0.38	0.37	0.36
Total		4.04	4.03	4.03	4.03	
Mg#		69.86	69.59	68.65	68.76	69.22
%wo		40.27	41.02	39.04	39.81	40.03
%en		41.73	41.05	41.85	41.39	41.50
%fs		18.00	17.94	19.11	18.80	18.46

CLG-23		CPX 2 Spec. 1	CPX 2 Spec. 2	CPX 2 Spec. 3	CPX 2 Spec. 4	CPX 2 Avg.
Na_2O	Oxide	0.45	0.34	0.43	0.49	0.43
MgO	wt%	14.46	14.85	15.08	14.62	14.75
Al_2O_3		1.97	1.87	1.98	1.96	1.95
SiO_2		50.35	50.38	50.15	50.33	50.30
CaO		20.11	19.14	19.82	19.51	19.65
TiO_2		1.09	1.12	1.03	1.10	1.09
V_2O_5		0.24	0.15	0.22	0.21	0.21
Cr_2O_3					0.07	0.07
MnO		0.31	0.31	0.27	0.31	0.30
FeO		10.41	11.18	10.69	10.59	10.72
		99.37	99.33	99.67	99.18	
Na	Cations	0.03	0.02	0.03	0.04	0.03
Mg	Norm,	0.81	0.84	0.85	0.83	0.83
Al	to	0.09	0.08	0.09	0.09	0.09
Si	6 oxygens	1.90	1.91	1.89	1.91	1.90
Ca		0.81	0.78	0.80	0.79	0.80
Ti		0.03	0.03	0.03	0.03	0.03
V		0.01	0.00	0.01	0.01	0.01
Cr					0.00	0.00
Mn		0.01	0.01	0.01	0.01	0.01
Fe		0.33	0.35	0.34	0.34	0.34
Total		4.03	4.03	4.04	4.03	

Mg#		71.23	70.31	71.55	71.11	71.05
%wo		41.59	39.44	40.33	40.54	40.47
%en		41.61	42.58	42.70	42.28	42.29
%fs		16.80	17.98	16.98	17.18	17.24

CLG-23		CPX 3 Spec. 1	CPX 3 Spec. 2	CPX 3 Spec. 3	CPX 3 Avg.
Na_2O	Oxide	0.30	0.34	0.25	0.30
MgO	wt%	15.18	14.95	15.25	15.13
Al_2O_3		1.54	1.53	1.52	1.53
SiO_2		50.43	50.29	50.43	50.38
CaO		17.29	16.99	16.60	16.96
TiO_2		0.82	0.88	0.83	0.84
V_2O_5		0.10	0.19	0.16	0.15
Cr_2O_3					
MnO		0.38	0.40	0.38	0.39
FeO		13.27	13.52	13.98	13.59
		99.31	99.08	99.41	
Na	Cations	0.02	0.03	0.02	0.02
Mg	Norm,	0.86	0.85	0.86	0.86
Al	to	0.07	0.07	0.07	0.07
Si	6 oxygens	1.92	1.92	1.92	1.92
Ca		0.70	0.69	0.68	0.69
Ti		0.02	0.03	0.02	0.02
V		0.00	0.00	0.00	0.00
Cr					
Mn		0.01	0.01	0.01	0.01
Fe		0.42	0.43	0.44	0.43
Total		4.03	4.03	4.03	
Mg#		67.10	66.34	66.04	66.49
%wo		35.45	35.14	34.06	34.88
%en		43.31	43.03	43.54	43.30
%fs		21.24	21.83	22.39	21.82

CLG-25		CPX 1 Spec. 1	CPX 1 Spec. 2	CPX 1 Spec. 3	CPX 1 Spec. 4	CPX 1 Avg.
Na_2O	Oxide	0.46	0.40	0.36	0.49	0.43
MgO	wt%	15.72	15.80	15.52	15.51	15.64
Al_2O_3		3.51	3.31	3.48	3.27	3.39
SiO_2		50.55	50.42	50.54	50.66	50.54
CaO		20.74	20.77	21.07	20.97	20.89
TiO_2		1.51	1.56	1.56	1.45	1.52
V_2O_5						
Cr_2O_3		0.82	0.80	0.82	0.73	0.79
MnO		0.17	0.20	0.19	0.16	0.18
FeO		7.30	7.36	7.19	7.27	7.28
		100.77	100.62	100.73	100.52	
Na	Cations	0.03	0.03	0.03	0.04	0.03
Mg	Norm,	0.86	0.87	0.85	0.85	0.86
Al	to	0.15	0.14	0.15	0.14	0.15
Si	6 oxygens	1.86	1.86	1.86	1.87	1.86
Ca		0.82	0.82	0.83	0.83	0.83
Ti		0.04	0.04	0.04	0.04	0.04
V						
Cr		0.02	0.02	0.02	0.02	0.02

Mn		0.01	0.01	0.01	0.01	0.01
Fe		0.22	0.23	0.22	0.22	0.22
Total		4.02	4.03	4.02	4.02	
Mg#		79.33	79.28	79.37	79.18	79.29
%wo		42.93	42.82	43.64	43.48	43.22
%en		45.28	45.33	44.73	44.75	45.02
%fs		11.79	11.85	11.63	11.77	11.76

CLG-25		CPX 2 Spec. 1	CPX 2 Spec. 2	CPX 2 Spec. 3	CPX 2 Spec. 4	CPX 2 Avg.
Na_2O	Oxide	0.42	0.51	0.50		0.48
MgO	wt%	15.63	16.03	15.65	15.13	15.61
Al_2O_3		3.20	3.09	3.13	3.25	3.17
SiO_2		50.33	50.61	50.26	50.25	50.36
CaO		20.95	20.31	20.66	21.34	20.82
TiO_2		1.56	1.53	1.63	1.55	1.57
V_2O_5		0.10			0.18	0.14
Cr_2O_3		0.96	0.94	0.92	0.89	0.93
MnO		0.26	0.20	0.21	0.23	0.23
FeO		7.20	7.44	7.14	6.80	7.15
		100.61	100.66	100.10	99.62	
Na	Cations	0.03	0.04	0.04		0.03
Mg	Norm,	0.86	0.88	0.87	0.84	0.86
Al	to	0.14	0.13	0.14	0.14	0.14
Si	6 oxygens	1.86	1.87	1.86	1.87	1.87
Ca		0.83	0.80	0.82	0.85	0.83
Ti		0.04	0.04	0.05	0.04	0.04
V		0.00			0.00	0.00
Cr		0.03	0.03	0.03	0.03	0.03
Mn		0.01	0.01	0.01	0.01	0.01
Fe		0.22	0.23	0.22	0.21	0.22
Total		4.02	4.03	4.03	4.00	
Mg#		79.47	79.34	79.62	79.86	79.57
%wo		43.36	41.94	43.03	44.74	43.27
%en		45.01	46.06	45.36	44.14	45.14
%fs		11.63	11.99	11.61	11.13	11.59

CLG-28		CPX 1 Spec. 1	CPX 1 Spec. 2	CPX 1 Spec. 3	CPX 1 Spec. 4	CPX 1 Avg.
Na_2O	Oxide	0.35	0.38	0.29	0.44	0.37
MgO	wt%	14.56	14.13	14.35	14.33	14.34
Al_2O_3		1.66	1.65	1.66	1.67	1.66
SiO_2		51.06	50.76	50.79	51.05	50.92
CaO		19.17	19.12	19.09	19.29	19.17
TiO_2		0.98	0.99	1.07	1.05	1.02
V_2O_5		0.12				0.12
Cr_2O_3		0.00	0.07	0.10		0.06
MnO		0.34	0.18	0.27	0.29	0.27
FeO		12.05	12.07	12.06	11.88	12.02
		100.30	99.34	99.67	99.99	
Na	Cations	0.03	0.03	0.02	0.03	0.03
Mg	Norm,	0.82	0.80	0.81	0.80	0.81
Al	to	0.07	0.07	0.07	0.07	0.07
Si	6 oxygens	1.92	1.93	1.92	1.92	1.92

Ca		0.77	0.78	0.77	0.78	0.78
Ti		0.03	0.03	0.03	0.03	0.03
V		0.00				0.00
Cr		0.00	0.00	0.00		0.00
Mn		0.01	0.01	0.01	0.01	0.01
Fe		0.38	0.38	0.38	0.37	0.38
Total		4.03	4.02	4.02	4.03	
Mg#		68.29	67.60	67.96	68.26	68.03
%wo		39.25	39.66	39.38	39.77	39.52
%en		41.49	40.79	41.20	41.11	41.15
%fs		19.26	19.55	19.42	19.12	19.34

CLG-28		CPX 2 Spec. 1	CPX 2 Spec. 2	CPX 2 Spec. 3	CPX 2 Spec. 4	CPX 2 Avg.
Na_2O	Oxide	0.43	0.40	0.43	0.43	0.42
MgO	wt%	13.39	13.31	13.52	13.12	13.34
Al_2O_3		3.48	3.82	3.68	3.79	3.69
SiO_2		48.76	48.53	48.77	48.99	48.76
CaO		20.19	20.03	19.33	20.21	19.94
TiO_2		2.21	2.13	2.17	2.23	2.19
V_2O_5						
Cr_2O_3						
MnO		0.19	0.23	0.32	0.35	0.27
FeO		10.92	10.84	11.40	11.13	11.07
		99.57	99.31	99.61	100.25	
Na	Cations	0.03	0.03	0.03	0.03	0.03
Mg	Norm,	0.76	0.75	0.76	0.74	0.75
Al	to	0.16	0.17	0.16	0.17	0.16
Si	6 oxygens	1.85	1.84	1.85	1.85	1.85
Ca		0.82	0.82	0.78	0.82	0.81
Ti		0.06	0.06	0.06	0.06	0.06
V						
Cr						
Mn		0.01	0.01	0.01	0.01	0.01
Fe		0.35	0.34	0.36	0.35	0.35
Total		4.03	4.03	4.02	4.02	
Mg#		68.61	68.64	67.89	67.76	68.22
%wo		42.64	42.60	41.09	42.86	42.30
%en		39.35	39.40	39.99	38.72	39.37
%fs		18.00	18.00	18.92	18.42	18.34

CLG-28		CPX 3 Spec. 1	CPX 3 Spec. 2	CPX 3 Spec. 3	CPX 3 Spec. 4	CPX 3 Avg.
Na_2O	Oxide	0.48	0.42	0.43	0.40	0.43
MgO	wt%	14.20	14.30	14.08	14.22	14.20
Al_2O_3		2.41	2.31	2.52	2.65	2.47
SiO_2		50.43	50.10	50.04	50.04	50.15
CaO		18.82	18.85	18.83	19.06	18.89
TiO_2		1.48	1.53	1.45	1.46	1.48
V_2O_5		0.13	0.14	0.18	0.20	0.16
Cr_2O_3						
MnO		0.31	0.21	0.23	0.34	0.27
FeO		12.29	12.27	12.07	12.16	12.20
		100.55	100.13	99.83	100.53	

Na	Cations	0.03	0.03	0.03	0.03	0.03
Mg	Norm,	0.79	0.80	0.79	0.80	0.80
Al	to	0.11	0.10	0.11	0.12	0.11
Si	6 oxygens	1.89	1.89	1.89	1.88	1.89
Ca		0.76	0.76	0.76	0.77	0.76
Ti		0.04	0.04	0.04	0.04	0.04
V		0.00	0.00	0.00	0.00	0.00
Cr						
Mn		0.01	0.01	0.01	0.01	0.01
Fe		0.39	0.39	0.38	0.38	0.38
Total		4.03	4.03	4.02	4.03	
Mg#		67.32	67.51	67.53	67.58	67.48
%wo		39.07	39.00	39.36	39.43	39.21
%en		41.02	41.18	40.95	40.93	41.02
%fs		19.91	19.82	19.69	19.64	19.77

CLG-39		CPX 1 Spec. 1	CPX 1 Spec. 2	CPX 1 Spec. 3	CPX 1 Spec. 4	CPX 1 Avg.
Na_2O	Oxide	0.34	0.48	0.52	0.47	0.45
MgO	wt%	14.76	14.79	14.65	14.75	14.74
Al_2O_3		2.64	2.77	2.75	2.64	2.70
SiO_2		49.63	49.89	49.69	49.77	49.75
CaO		18.84	19.14	19.22	19.35	19.14
TiO_2		1.61	1.69	1.66	1.74	1.68
V_2O_5				0.13	0.12	0.13
Cr_2O_3		0.11	0.00	0.13	0.12	0.09
MnO		0.30	0.29	0.34	0.20	0.28
FeO		10.97	10.92	11.07	10.77	10.93
		99.22	99.97	100.16	99.93	
Na	Cations	0.02	0.03	0.04	0.03	0.03
Mg	Norm,	0.83	0.83	0.82	0.83	0.83
Al	to	0.12	0.12	0.12	0.12	0.12
Si	6 oxygens	1.88	1.88	1.87	1.87	1.87
Ca		0.76	0.77	0.77	0.78	0.77
Ti		0.05	0.05	0.05	0.05	0.05
V				0.00	0.00	0.00
Cr		0.00	0.00	0.00	0.00	0.00
Mn		0.01	0.01	0.01	0.01	0.01
Fe		0.35	0.34	0.35	0.34	0.34
Total		4.03	4.03	4.04	4.03	
Mg#		70.58	70.71	70.23	70.94	70.61
%wo		39.30	39.67	39.84	40.08	39.72
%en		42.84	42.66	42.25	42.51	42.57
%fs		17.86	17.67	17.91	17.41	17.71

CLG-39		CPX 2 Spec. 1	CPX 2 Spec. 2	CPX 2 Spec. 3	CPX 2 Spec. 4	CPX 2 Avg.
Na_2O	Oxide	0.56	0.34	0.33	0.41	0.41
MgO	wt%	15.04	14.98	15.11	14.67	14.95
Al_2O_3		1.64	1.77	1.42	1.61	1.61
SiO_2		51.37	51.27	51.15	51.21	51.25
CaO		19.18	19.31	19.57	19.47	19.38
TiO_2		1.03	1.12	1.02	1.03	1.05
V_2O_5						
Cr_2O_3		0.10		0.10		0.10

MnO		0.30	0.29	0.28	0.34	0.30
FeO		11.13	11.31	11.17	11.08	11.17
		100.34	100.39	100.15	99.80	
Na	Cations	0.04	0.02	0.02	0.03	0.03
Mg	Norm,	0.84	0.84	0.85	0.82	0.84
Al	to	0.07	0.08	0.06	0.07	0.07
Si	6 oxygens	1.92	1.92	1.92	1.93	1.92
Ca		0.77	0.77	0.79	0.78	0.78
Ti		0.03	0.03	0.03	0.03	0.03
V						0.00
Cr		0.00		0.00		0.00
Mn		0.01	0.01	0.01	0.01	0.01
Fe		0.35	0.35	0.35	0.35	0.35
Total		4.03	4.02	4.03	4.02	
Mg#		70.66	70.25	70.69	70.24	70.46
%wo		39.31	39.42	39.68	40.12	39.63
%en		42.89	42.56	42.64	42.06	42.54
%fs		17.80	18.02	17.68	17.82	17.83

CLG-39		CPX 3 Spec. 1	CPX 3 Spec. 2	CPX 3 Spec. 3	CPX 3 Spec. 4	CPX 3 Avg.
Na_2O	Oxide	0.35	0.39	0.41	0.45	0.40
MgO	wt%	14.30	14.37	14.46	14.13	14.32
Al_2O_3		2.13	2.06	2.22	2.30	2.18
SiO_2		50.70	51.10	50.58	50.80	50.80
CaO		20.18	19.88	20.24	19.99	20.07
TiO_2		1.33	1.20	1.13	1.11	1.19
$V2O_5$		0.11	0.21	0.00	0.12	0.11
Cr_2O_3		0.09				0.09
MnO		0.37	0.32	0.40	0.32	0.35
FeO		10.83	10.87	10.78	10.68	10.79
		100.39	100.39	100.23	99.90	
Na	Cations	0.03	0.03	0.03	0.03	0.03
Mg	Norm,	0.80	0.80	0.81	0.79	0.80
Al	to	0.09	0.09	0.10	0.10	0.10
Si	6 oxygens	1.90	1.91	1.90	1.91	1.90
Ca		0.81	0.80	0.81	0.80	0.81
Ti		0.04	0.03	0.03	0.03	0.03
V		0.00	0.01	0.00	0.00	0.00
Cr		0.00				0.00
Mn		0.01	0.01	0.01	0.01	0.01
Fe		0.34	0.34	0.34	0.34	0.34
Total		4.02	4.02	4.03	4.02	
Mg#		70.18	70.21	70.51	70.22	70.28
%wo		41.58	41.11	41.49	41.65	41.46
%en		41.00	41.35	41.25	40.97	41.14
%fs		17.42	17.55	17.25	17.37	17.40

CLG-41		CPX 1 Spec. 1	CPX 1 Spec. 2	CPX 1 Spec. 3	CPX 1 Spec. 4	CPX 1 Avg.
Na_2O	Oxide	0.36	0.39	0.31	0.38	0.36
MgO	wt%	15.58	16.43	15.68	15.41	15.78
Al_2O_3		2.93	3.01	2.91	2.82	2.92
SiO_2		50.93	50.57	50.80	50.48	50.70

CaO		19.83	19.19	20.18	20.39	19.90
TiO_2		1.15	1.16	1.15	1.20	1.17
V_2O_5						
Cr_2O_3		0.47	0.32	0.43	0.47	0.42
MnO		0.09	0.23	0.30	0.18	0.20
FeO		8.50	9.31	8.79	8.31	8.73
		99.85	100.60	100.54	99.64	
Na	Cations	0.03	0.03	0.02	0.03	0.03
Mg	Norm,	0.86	0.91	0.87	0.86	0.87
Al	to	0.13	0.13	0.13	0.12	0.13
Si	6 oxygens	1.89	1.87	1.88	1.89	1.88
Ca		0.79	0.76	0.80	0.82	0.79
Ti		0.03	0.03	0.03	0.03	0.03
V						
Cr		0.01	0.01	0.01	0.01	0.01
Mn		0.00	0.01	0.01	0.01	0.01
Fe		0.26	0.29	0.27	0.26	0.27
Total		4.02	4.04	4.03	4.03	
Mg#		76.57	75.88	76.08	76.77	76.32
%wo		41.19	38.91	41.30	42.20	40.90
%en		45.03	46.36	44.66	44.38	45.11
%fs		13.78	14.74	14.04	13.42	14.00

CLG-41		CPX 2 Spec. 1	CPX 2 Spec. 2	CPX 2 Spec. 3	CPX 2 Spec. 4	CPX 2 Avg.
Na_2O	Oxide	0.38	0.38	0.45	0.42	0.41
MgO	wt%	15.52	15.68	15.41	15.41	15.51
Al_2O_3		2.73	2.63	2.68	2.67	2.68
SiO_2		50.36	50.76	50.53	50.77	50.61
CaO		19.33	19.64	19.63	19.84	19.61
TiO_2		1.56	1.52	1.60	1.68	1.59
V_2O_5				0.20		0.20
Cr_2O_3					0.00	0.00
MnO		0.25	0.21	0.11	0.19	0.19
FeO		9.92	10.14	10.20	9.98	10.06
		100.04	100.98	100.80	100.96	
Na	Cations	0.03	0.03	0.03	0.03	0.03
Mg	Norm,	0.86	0.87	0.85	0.85	0.86
Al	to	0.12	0.11	0.12	0.12	0.12
Si	6 oxygens	1.88	1.88	1.88	1.88	1.88
Ca		0.77	0.78	0.78	0.79	0.78
Ti		0.04	0.04	0.04	0.05	0.04
V				0.00		0.00
Cr				0.00	0.00	0.00
Mn		0.01	0.01		0.01	0.01
Fe		0.31	0.31	0.32	0.31	0.31
Total		4.03	4.03	4.03	4.03	
Mg#		73.61	73.38	72.92	73.35	73.32
%wo		39.72	39.78	40.03	40.43	39.99
%en		44.37	44.19	43.73	43.70	44.00
%fs		15.91	16.03	16.24	15.88	16.01

CLG-41		CPX 3 Spec. 1	CPX 3 Spec. 2	CPX 3 Spec. 3	CPX 3 Spec. 4	CPX 3 Avg.

Na_2O	Oxide	0.41	0.45	0.38	0.55	0.45
MgO	wt%	15.75	15.39	15.39	15.59	15.53
Al_2O_3		3.34	3.33	3.33	3.32	3.33
SiO_2		50.09	50.05	49.70	50.39	50.06
CaO		19.78	19.75	19.55	19.49	19.64
TiO_2		1.20	1.18	1.25	1.20	1.21
V_2O_5		0.17	0.11	0.14	0.23	0.16
Cr_2O_3		0.73	0.76	0.74	0.77	0.75
MnO		0.17	0.23	0.21	0.13	0.19
FeO		8.26	8.41	8.43	8.56	8.42
		99.91	99.65	99.12	100.22	
Na	Cations	0.03	0.03	0.03	0.04	0.03
Mg	Norm,	0.87	0.86	0.86	0.86	0.86
Al	to	0.15	0.15	0.15	0.15	0.15
Si	6 oxygens	1.86	1.87	1.87	1.87	1.87
Ca		0.79	0.79	0.79	0.77	0.79
Ti		0.03	0.03	0.04	0.03	0.03
V		0.00	0.00	0.00	0.01	0.00
Cr		0.02	0.02	0.02	0.02	0.02
Mn		0.01	0.01	0.01	0.00	0.01
Fe		0.26	0.26	0.26	0.27	0.26
Total		4.03	4.02	4.02	4.02	
Mg#		77.27	76.54	76.49	76.45	76.69
%wo		41.08	41.38	41.12	40.72	41.07
%en		45.52	44.87	45.04	45.32	45.19
%fs		13.39	13.75	13.84	13.96	13.74

CLG-42		CPX 1 Spec. 1	CPX 1 Spec. 2	CPX 1 Spec. 3	CPX 1 Spec. 4	CPX 1 Spec. 5	CPX 1 Spec. 6	CPX 1 Avg.
Na_2O	Oxide	0.33	0.32	0.36	0.42	0.36	0.25	0.34
MgO	wt%	15.35	15.21	15.35	15.96	15.20	16.64	15.62
Al_2O_3		2.92	2.98	2.78	2.96	2.88	2.66	2.86
SiO_2		50.77	50.62	50.61	50.82	50.47	51.12	50.74
CaO		20.48	20.79	20.62	19.71	20.46	19.41	20.25
TiO_2		1.20	1.05	1.11	1.16	1.07	1.08	1.11
$V2O_5$		0.10	0.07	0.07	0.11	0.14	0.11	0.10
$Cr2O_3$		0.60	0.72	0.64	0.69	0.63	0.66	0.66
MnO		0.19	0.27	0.20	0.18	0.17	0.20	0.20
FeO		7.98	7.94	7.96	8.34	7.91	8.67	8.13
		99.93	99.97	99.71	100.34	99.29	100.80	
Na	Cations	0.02	0.02	0.03	0.03	0.03	0.02	0.02
Mg	Norm,	0.85	0.84	0.85	0.88	0.85	0.91	0.87
Al	to	0.13	0.13	0.12	0.13	0.13	0.12	0.13
Si	6 oxygens	1.89	1.88	1.89	1.88	1.89	1.88	1.89
Ca		0.82	0.83	0.82	0.78	0.82	0.77	0.81
Ti		0.03	0.03	0.03	0.03	0.03	0.03	0.03
V		0.00	0.00	0.00	0.00	0.00	0.00	0.00
Cr		0.02	0.02	0.02	0.02	0.02	0.02	0.02
Mn		0.01	0.01	0.01	0.01	0.01	0.01	0.01
Fe		0.25	0.25	0.25	0.26	0.25	0.27	0.25
Total		4.01	4.02	4.02	4.02	4.02	4.02	
Mg#		77.42	77.35	77.47	77.33	77.40	77.38	77.39
%wo		42.60	43.17	42.79	40.70	42.82	39.34	41.90
%en		44.44	43.95	44.32	45.86	44.26	46.94	44.96
%fs		12.96	12.87	12.89	13.44	12.92	13.72	13.13

CLG-42		CPX 2 Spec. 1	CPX 2 Spec. 2	CPX 2 Spec. 3	CPX 2 Spec. 4	CPX 2 Spec. 5	CPX 2 Spec. 6	CPX 2 Avg.
Na_2O	Oxide	0.35	0.36	0.48	0.39	0.34	0.50	0.40
MgO	wt%	15.32	15.61	15.67	15.39	15.40	15.64	15.51
Al_2O_3		3.37	3.24	3.13	3.26	3.29	3.24	3.26
SiO_2		50.29	50.41	50.42	50.30	50.32	50.29	50.34
CaO		20.30	20.65	20.54	20.40	20.80	20.63	20.55
TiO_2		1.29	1.19	1.16	1.33	1.27	1.20	1.24
V_2O_5		0.17	0.13	0.10	0.21	0.13	0.09	0.14
Cr_2O_3		0.70	0.69	0.80	0.62	0.89	0.84	0.76
MnO		0.16	0.28	0.19	0.16	0.22	0.23	0.21
FeO		7.76	7.69	7.94	7.82	7.67	7.83	7.79
		99.71	100.23	100.44	99.86	100.32	100.50	
Na	Cations	0.03	0.03	0.03	0.03	0.02	0.04	0.03
Mg	Norm,	0.85	0.86	0.87	0.85	0.85	0.86	0.86
Al	to	0.15	0.14	0.14	0.14	0.14	0.14	0.14
Si	6 oxygens	1.87	1.87	1.87	1.87	1.87	1.86	1.87
Ca		0.81	0.82	0.82	0.81	0.83	0.82	0.82
Ti		0.04	0.03	0.03	0.04	0.04	0.03	0.03
V		0.00	0.00	0.00	0.01	0.00	0.00	0.00
Cr		0.02	0.02	0.02	0.02	0.03	0.02	0.02
Mn		0.01	0.01	0.01	0.01	0.01	0.01	0.01
Fe		0.24	0.24	0.25	0.24	0.24	0.24	0.24
Total		4.01	4.02	4.03	4.02	4.02	4.03	
Mg#		77.87	78.35	77.87	77.82	78.16	78.07	78.02
%wo		42.58	42.69	42.31	42.57	43.14	42.53	42.64
%en		44.72	44.90	44.92	44.69	44.44	44.87	44.76
%fs		12.71	12.41	12.77	12.74	12.42	12.60	12.61

CLG-42		CPX 3 Spec. 1	CPX 3 Spec. 2	CPX 3 Spec. 3	CPX 3 Spec. 4	CPX 3 Spec. 5	CPX 3 Spec. 6	CPX 3 Avg.
Na_2O	Oxide	0.44	0.43	0.41	0.37	0.45	0.37	0.41
MgO	wt%	15.20	15.34	15.44	15.24	15.25	15.12	15.27
Al_2O_3		3.49	3.53	3.51	3.45	3.61	3.50	3.52
SiO_2		49.83	50.31	50.37	50.30	50.04	50.58	50.24
CaO		20.50	20.69	20.44	20.60	20.31	20.66	20.53
TiO_2		1.38	1.28	1.34	1.31	1.28	1.39	1.33
V_2O_5		0.23	0.15	0.08	0.06	0.04	0.06	0.10
Cr_2O_3		0.82	0.92	0.81	0.83	0.85	0.95	0.86
MnO		0.15	0.15	0.23	0.25	0.08	0.24	0.18
FeO		7.71	7.83	7.97	7.82	7.92	7.81	7.84
		99.75	100.64	100.60	100.21	99.85	100.67	
Na	Cations	0.03	0.03	0.03	0.03	0.03	0.03	0.03
Mg	Norm,	0.85	0.85	0.85	0.84	0.85	0.83	0.84
Al	to	0.15	0.15	0.15	0.15	0.16	0.15	0.15
Si	6 oxygens	1.86	1.86	1.86	1.87	1.86	1.87	1.86
Ca		0.82	0.82	0.81	0.82	0.81	0.82	0.82
Ti		0.04	0.04	0.04	0.04	0.04	0.04	0.04
V		0.01	0.00	0.00	0.00	0.00	0.00	0.00
Cr		0.02	0.03	0.02	0.02	0.03	0.03	0.03
Mn		0.00	0.00	0.01	0.01	0.00	0.01	0.01
Fe		0.24	0.24	0.25	0.24	0.25	0.24	0.24
Total		4.02	4.02	4.02	4.02	4.02	4.01	

Mg#	77.85	77.74	77.55	77.65	77.44	77.53	77.63
%wo	43.00	42.97	42.45	43.00	42.57	43.22	42.87
%en	44.37	44.33	44.63	44.26	44.48	44.02	44.35
%fs	12.63	12.69	12.92	12.74	12.96	12.76	12.78

Crystal Lake Gabbro Olivine

CLG-3		Ol. 1 Spec. 1	Ol. 1 Spec. 2	Ol. 1 Spec. 3	Ol. 1 Spec. 4	Ol. 1 Spec. 5	Ol. 1 Spec. 6	Ol. 1 Avg.
MgO	Oxide	30.17	30.39	30.63	30.41	30.22	29.99	30.30
Al_2O_3	wt%	0.18		0.02	0.19	0.14	0.09	0.12
SiO_2		35.39	35.52	35.87	35.66	35.54	35.62	35.60
CaO		0.12	0.14	0.15	0.12	0.13	0.15	0.14
MnO		0.40	0.36	0.39	0.41	0.55	0.49	0.43
FeO		33.45	33.20	33.41	33.24	33.21	32.96	33.25
NiO								
Total		99.71	99.61	100.46	100.03	99.79	99.30	99.82
Mg	Cations	1.24	1.25	1.25	1.25	1.24	1.24	1.25
Al	Norm.	0.01		0.00	0.01	0.00	0.00	0.00
Si	to	0.98	0.98	0.98	0.98	0.98	0.99	0.98
Ca	4 oxygens	0.00	0.00	0.00	0.00	0.00	0.00	0.00
Mn		0.01	0.01	0.01	0.01	0.01	0.01	0.01
Fe		0.77	0.77	0.77	0.77	0.77	0.76	0.77
Ni								
Total		3.02	3.02	3.02	3.01	3.02	3.01	3.02
Fo		61.65	62.00	62.04	61.99	61.86	61.86	61.90

CLG-3		Ol. 2 Spec. 1	Ol. 2 Spec. 2	Ol. 2 Spec. 3	Ol. 2 Spec. 4	Ol. 2 Spec. 5	Ol. 2 Spec. 6	Ol. 2 Avg.
MgO	Oxide	30.05	30.64	29.99	30.18	30.37	30.25	30.25
Al_2O_3	wt%	0.18	0.11	0.10	0.22	0.19	0.04	0.14
SiO_2		35.49	35.44	35.02	35.49	35.10	35.05	35.27
CaO		0.15	0.07	0.16	0.16	0.13	0.17	0.14
MnO		0.53	0.41	0.54	0.48	0.46	0.55	0.50
FeO		33.41	33.41	33.30	33.12	32.90	33.08	33.20
NiO								
Total		99.81	100.07	99.10	99.66	99.16	99.13	99.49
Mg	Cations	1.24	1.26	1.25	1.24	1.26	1.26	1.25
Al	Norm.	0.01	0.00	0.00	0.01	0.01	0.00	0.00
Si	to	0.98	0.98	0.98	0.98	0.98	0.98	0.98
Ca	4 oxygens	0.00	0.00	0.00	0.00	0.00	0.01	0.00
Mn		0.01	0.01	0.01	0.01	0.01	0.01	0.01
Fe		0.77	0.77	0.78	0.77	0.77	0.77	0.77
Ni								
Total		3.02	3.02	3.02	3.01	3.02	3.02	3.02
Fo		61.59	62.05	61.62	61.90	62.20	61.98	61.89

CLG-3		Ol. 3 Spec. 1	Ol. 3 Spec. 2	Ol. 3 Spec. 3	Ol. 3 Spec. 4	Ol. 3 Spec. 5	Ol. 3 Spec. 6	Ol. 3 Avg.
MgO	Oxide	29.96	29.87	30.29	30.11	29.90	30.21	30.06
Al_2O_3	wt%	0.17	0.14	0.26	0.08	0.02	0.17	0.14
SiO_2		35.56	35.53	35.54	35.59	35.93	35.44	35.60
CaO		0.20	0.16	0.21	0.14	0.14	0.22	0.18
MnO		0.43	0.42	0.38	0.49		0.45	0.43
FeO		32.98	33.01	33.09	32.94	33.32	33.59	33.16
NiO								
Total		99.30	99.14	99.77	99.34	99.31	100.07	99.49
Mg	Cations	1.24	1.24	1.25	1.24	1.23	1.24	1.24

Al	Norm.	0.01	0.00	0.01	0.00	0.00	0.01	0.00
Si	to	0.99	0.99	0.98	0.99	0.99	0.98	0.99
Ca	4 oxygens	0.01	0.00	0.01	0.00	0.00	0.01	0.01
Mn		0.01	0.01	0.01	0.01		0.01	0.01
Fe		0.76	0.77	0.76	0.76	0.77	0.78	0.77
Ni								
Total		3.01	3.01	3.01	3.01	3.00	3.02	3.01
Fo		61.82	61.73	62.00	61.97	61.53	61.59	61.77

CLG-8		Ol. 1 Spec. 1	Ol. 1 Spec. 2	Ol. 1 Spec. 3	Ol. 1 Spec. 4	Ol. 1 Spec. 5	Ol. 1 Avg.
MgO	Oxide	22.91	22.84	22.81	22.97	22.73	22.85
Al_2O_3	wt%						
SiO_2		33.95	33.62	33.37	33.79	33.89	33.72
CaO		0.21	0.25	0.25	0.30	0.26	0.25
MnO		0.70	0.56	0.67	0.68	0.71	0.66
FeO		42.45	42.28	42.53	42.05	42.00	42.26
NiO							
Total		100.22	99.56	99.63	99.79	99.60	99.76
Mg	Cations	0.99	0.99	0.99	0.99	0.98	0.99
Al	Norm.						
Si	to	0.98	0.98	0.97	0.98	0.98	0.98
Ca	4 oxygens	0.01	0.01	0.01	0.01	0.01	0.01
Mn		0.02	0.01	0.02	0.02	0.02	0.02
Fe		1.03	1.03	1.04	1.02	1.02	1.03
Ni							
Total		3.02	3.02	3.03	3.02	3.02	3.02
Fo		49.03	49.06	48.88	49.34	49.10	49.08

CLG-8		Ol. 2 Spec. 1	Ol. 2 Spec. 2	Ol. 2 Spec. 3	Ol. 2 Spec. 4	Ol. 2 Spec. 5	Ol. 2 Spec. 6	Ol. 2 Avg.
MgO	Oxide	25.62	25.70	25.65	25.59	25.84	25.23	25.61
Al_2O_3	wt%							
SiO_2		34.55	34.65	34.68	34.72	34.82	34.92	34.72
CaO		0.37	0.30	0.29	0.24	0.30	0.37	0.31
MnO		0.57	0.47	0.55	0.61	0.50	0.61	0.55
FeO		39.18	39.17	39.08	39.16	39.13	38.96	39.11
NiO								
Total		100.29	100.29	100.25	100.33	100.59	100.10	100.31
Mg	Cations	1.08	1.09	1.08	1.08	1.09	1.07	1.08
Al	Norm.							
Si	to	0.98	0.98	0.98	0.98	0.98	0.99	0.98
Ca	4 oxygens	0.01	0.01	0.01	0.01	0.01	0.01	0.01
Mn		0.01	0.01	0.01	0.01	0.01	0.01	0.01
Fe		0.93	0.93	0.93	0.93	0.92	0.92	0.93
Ni								
Total		3.02	3.02	3.02	3.02	3.02	3.01	3.02
Fo		53.82	53.91	53.92	53.81	54.07	53.58	53.85

CLG-8		Ol. 3 Spec. 1	Ol. 3 Spec. 2	Ol. 3 Spec. 3	Ol. 3 Spec. 4	Ol. 3 Spec. 5	Ol. 3 Spec. 6	Ol. 3 Avg.
MgO	Oxide	23.12	23.34	23.11	22.93	23.05	23.34	23.15

Al_2O_3	wt%							
SiO_2		34.26	33.76	33.74	33.86	34.15	34.01	33.96
CaO		0.21	0.21	0.26	0.28	0.20	0.32	0.25
MnO		0.62	0.66	0.59	0.64	0.71	0.68	0.65
FeO		42.00	41.71	41.94	41.49	41.40	42.20	41.79
NiO								
Total		100.21	99.69	99.64	99.20	99.51	100.55	99.80
Mg	Cations	0.99	1.01	1.00	0.99	1.00	1.00	1.00
Al	Norm.							
Si	to	0.99	0.98	0.98	0.99	0.99	0.98	0.98
Ca	4 oxygens	0.01	0.01	0.01	0.01	0.01	0.01	0.01
Mn		0.02	0.02	0.01	0.02	0.02	0.02	0.02
Fe		1.01	1.01	1.02	1.01	1.00	1.02	1.01
Ni								
Total		3.01	3.02	3.02	3.01	3.01	3.02	3.02
Fo		49.53	49.94	49.55	49.63	49.81	49.65	49.68

CLG-13		Ol. 1 Spec. 1	Ol. 1 Spec. 2	Ol. 1 Spec. 3	Ol. 1 Spec. 4	Ol. 1 Avg.
MgO	Oxide	23.86	23.82	23.74	23.69	23.78
Al_2O_3	wt%		0.13			0.13
SiO_2		33.81	33.69	33.72	33.76	33.75
CaO		0.22	0.16	0.19	0.23	0.20
MnO		0.63	0.56	0.74	0.57	0.63
FeO		40.40	40.86	40.67	40.93	40.72
NiO		0.23				0.23
Total		99.16	99.22	99.06	99.17	99.15
Mg	Cations	1.03	1.03	1.03	1.03	1.03
Al	Norm.		0.00			0.00
Si	to	0.98	0.98	0.98	0.98	0.98
Ca	4 oxygens	0.01	0.00	0.01	0.01	0.01
Mn		0.02	0.01	0.02	0.01	0.02
Fe		0.98	0.99	0.99	0.99	0.99
Ni		0.01				0.00
Total		3.02	3.02	3.02	3.02	3.02
Fo		51.29	50.96	50.99	50.78	51.01

CLG-13		Ol. 2 Spec. 1	Ol. 2 Spec. 2	Ol. 2 Spec. 3	Ol. 2 Spec. 4	Ol. 2 Avg.
MgO	Oxide	25.32	25.23	25.27	25.15	25.24
Al_2O_3	wt%					
SiO_2		34.36	34.41	34.46	34.06	34.32
CaO		0.11	0.17	0.17	0.18	0.16
MnO		0.66	0.59	0.71	0.58	0.64
FeO		39.33	38.82	39.53	39.30	39.25
NiO		0.20	0.17			0.19
Total		99.99	99.40	100.15	99.28	99.71
Mg	Cations	1.08	1.08	1.07	1.08	1.08
Al	Norm.					
Si	to	0.98	0.99	0.98	0.98	0.98
Ca	4 oxygens	0.00	0.01	0.01	0.01	0.00
Mn		0.02	0.01	0.02	0.01	0.02
Fe		0.94	0.93	0.94	0.94	0.94

Ni		0.00	0.00			0.00
Total		3.02	3.01	3.02	3.02	3.02
Fo		53.44	53.67	53.26	53.29	53.41

CLG-13		Ol. 3 Spec. 1	Ol. 3 Spec. 2	Ol. 3 Spec. 3	Ol. 3 Spec. 4	Ol. 3 Avg.
MgO	Oxide	26.05	26.22	26.25	26.08	26.15
Al_2O_3	wt%					
SiO_2		34.63	34.79	34.73	34.63	34.70
CaO		0.19	0.27	0.15	0.20	0.20
MnO		0.51	0.50	0.57	0.58	0.54
FeO		39.13	38.84	38.73	38.57	38.82
NiO					0.18	0.18
Total		100.50	100.63	100.43	100.24	100.45
Mg	Cations	1.10	1.10	1.11	1.10	1.10
Al	Norm.					
Si	to	0.98	0.98	0.98	0.98	0.98
Ca	4 oxygens	0.01	0.01	0.00	0.01	0.01
Mn		0.01	0.01	0.01	0.01	0.01
Fe		0.93	0.92	0.91	0.91	0.92
Ni					0.00	0.00
Total		3.02	3.02	3.02	3.02	3.02
Fo		54.27	54.62	54.71	54.66	54.56

CLG-18		Ol. 1 Spec. 1	Ol. 1 Spec. 2	Ol. 1 Spec. 3	Ol. 1 Spec. 4	Ol. 1 Avg.
MgO	Oxide	24.91	24.92	24.96	24.80	24.90
Al_2O_3	wt%					
SiO_2		34.65	34.68	34.79	34.74	34.72
CaO		0.13	0.21	0.18	0.22	0.19
MnO		0.52	0.61	0.54	0.54	0.55
FeO		40.39	40.26	40.41	40.41	40.37
NiO		0.18	0.19			0.19
Total		100.79	100.85	100.88	100.72	100.81
Mg	Cations	1.05	1.05	1.05	1.05	1.05
Al	Norm.					
Si	to	0.98	0.98	0.99	0.99	0.98
Ca	4 oxygens	0.00	0.01	0.01	0.01	0.01
Mn		0.01	0.01	0.01	0.01	0.01
Fe		0.96	0.95	0.96	0.96	0.96
Ni		0.00	0.00			0.00
Total		3.02	3.02	3.01	3.01	3.02
Fo		52.37	52.46	52.41	52.24	52.37

CLG-18		Ol. 2 Spec. 1	Ol. 2 Spec. 2	Ol. 2 Spec. 3	Ol. 2 Spec. 4	Ol. 2 Avg.
MgO	Oxide	25.40	25.67	25.65	25.35	25.52
Al_2O_3	wt%					
SiO_2		34.88	35.07	34.80	35.01	34.94
CaO		0.18	0.20	0.18	0.14	0.18
MnO		0.57	0.57	0.58	0.56	0.57
FeO		39.15	39.08	39.60	39.09	39.23

NiO						
Total		100.18	100.60	100.81	100.15	100.44
Mg	Cations	1.07	1.08	1.08	1.07	1.08
Al	Norm.					
Si	to	0.99	0.99	0.98	0.99	0.99
Ca	4 oxygens	0.01	0.01	0.01	0.00	0.01
Mn		0.01	0.01	0.01	0.01	0.01
Fe		0.93	0.92	0.94	0.93	0.93
Ni						
Total		3.01	3.01	3.02	3.01	3.01
Fo		53.63	53.94	53.59	53.62	53.69

CLG-18		Ol. 3 Spec. 1	Ol. 3 Spec. 2	Ol. 3 Spec. 3	Ol. 3 Spec. 4	Ol. 3 Avg.
MgO	Oxide	24.76	24.84	24.81	25.00	24.85
Al_2O_3	wt%					
SiO_2		34.71	34.54	34.49	34.54	34.57
CaO		0.19	0.14	0.20	0.17	0.18
MnO		0.64	0.53	0.51	0.55	0.56
FeO		40.08	40.17	40.51	40.29	40.26
NiO		0.21	0.27	0.15	0.13	0.19
Total		100.58	100.49	100.67	100.68	100.61
Mg	Cations	1.05	1.05	1.05	1.06	1.05
Al	Norm.					
Si	to	0.99	0.98	0.98	0.98	0.98
Ca	4 oxygens	0.01	0.00	0.01	0.01	0.01
Mn		0.02	0.01	0.01	0.01	0.01
Fe		0.95	0.96	0.96	0.96	0.96
Ni		0.00	0.01	0.00	0.00	0.00
Total		3.01	3.02	3.02	3.02	3.02
Fo		52.41	52.43	52.19	52.52	52.39

CLG-20		Ol. 1 Spec. 1	Ol. 1 Spec. 2	Ol. 1 Spec. 3	Ol. 1 Spec. 4	Ol. 1 Avg.
MgO	Oxide	26.35	26.52	26.54	26.29	26.43
Al_2O_3	wt%					
SiO_2		34.83	34.59	34.61	34.34	34.59
CaO		0.21	0.18	0.14	0.15	0.17
MnO		0.59	0.53	0.52	0.58	0.56
FeO		38.09	38.32	38.25	38.35	38.25
NiO		0.19		0.15		0.17
Total		100.26	100.14	100.22	99.71	100.08
Mg	Cations	1.11	1.12	1.12	1.12	1.12
Al	Norm.					
Si	to	0.98	0.98	0.98	0.98	0.98
Ca	4 oxygens	0.01	0.01	0.00	0.00	0.01
Mn		0.01	0.01	0.01	0.01	0.01
Fe		0.90	0.91	0.90	0.91	0.91
Ni		0.00		0.00		0.00
Total		3.02	3.02	3.02	3.02	3.02
Fo		55.22	55.23	55.30	55.00	55.19

CLG-20		Ol. 2 Spec. 1	Ol. 2 Spec. 2	Ol. 2 Spec. 3	Ol. 2 Spec. 4	Ol. 2 Avg.
MgO	Oxide	25.95	26.39	25.95	26.10	26.10
Al_2O_3	wt%					
SiO_2		34.53	34.78	34.28	34.33	34.48
CaO		0.17	0.14	0.20	0.18	0.17
MnO		0.46	0.61	0.57	0.60	0.56
FeO		38.43	38.72	38.66	38.29	38.53
NiO		0.21				0.21
Total		99.75	100.63	99.65	99.51	99.89
Mg	Cations	1.10	1.11	1.10	1.11	1.11
Al	Norm.					
Si	to	0.98	0.98	0.98	0.98	0.98
Ca	4 oxygens	0.01	0.00	0.01	0.01	0.01
Mn		0.01	0.01	0.01	0.01	0.01
Fe		0.91	0.91	0.92	0.91	0.92
Ni		0.00				0.00
Total		3.02	3.02	3.02	3.02	3.02
Fo		54.62	54.85	54.47	54.86	54.70

CLG-20		Ol. 3 Spec. 1	Ol. 3 Spec. 2	Ol. 3 Spec. 3	Ol. 3 Spec. 4	Ol. 3 Avg.
MgO	Oxide	27.71	27.44	27.43	27.35	27.48
Al_2O_3	wt%					
SiO_2		34.95	34.78	34.98	34.92	34.91
CaO		0.07	0.15	0.22	0.09	0.13
MnO		0.69	0.59	0.62	0.65	0.64
FeO		37.00	37.34	37.01	36.68	37.01
NiO		0.16			0.00	0.08
Total		100.59	100.30	100.26	99.70	100.21
Mg	Cations	1.16	1.15	1.15	1.15	1.15
Al	Norm.					
Si	to	0.98	0.98	0.98	0.98	0.98
Ca	4 oxygens	0.00	0.00	0.01	0.00	0.00
Mn		0.02	0.01	0.01	0.02	0.02
Fe		0.87	0.88	0.87	0.86	0.87
Ni		0.00			0.00	0.00
Total		3.02	3.02	3.02	3.02	3.02
Fo		57.17	56.71	56.92	57.07	56.97

CLG-23		Ol. 1 Spec. 1	Ol. 1 Spec. 2	Ol. 1 Spec. 3	Ol. 1 Spec. 4	Ol. 1 Avg.
MgO	Oxide	27.26	27.64	27.56	27.51	27.49
Al_2O_3	wt%					
SiO_2		35.16	35.16	35.25	35.26	35.21
CaO		0.17	0.17	0.14	0.15	0.16
MnO		0.42	0.55	0.55	0.56	0.52
FeO		37.52	37.21	37.43	37.15	37.33
NiO		0.12				0.12
Total		100.65	100.73	100.93	100.63	100.74
Mg	Cations	1.14	1.15	1.15	1.15	1.14
Al	Norm.					
Si	to	0.98	0.98	0.98	0.98	0.98

Ca	4 oxygens	0.01	0.01	0.00	0.00	0.00
Mn		0.01	0.01	0.01	0.01	0.01
Fe		0.88	0.87	0.87	0.87	0.87
Ni		0.00				0.00
Total		3.02	3.02	3.02	3.02	3.02
Fo		56.43	56.97	56.76	56.90	56.76

CLG-23		Ol. 2 Spec. 1	Ol. 2 Spec. 2	Ol. 2 Spec. 3	Ol. 2 Spec. 4	Ol. 2 Avg.
MgO	Oxide	25.94	26.05	25.89	25.86	25.94
Al_2O_3	wt%					
SiO_2		35.11	34.51	35.10	34.91	34.91
CaO		0.20	0.12	0.11	0.11	0.14
MnO		0.52	0.54	0.57	0.61	0.56
FeO		38.97	38.85	39.00	38.90	38.93
NiO		0.14	0.23	0.30		0.22
Total		100.89	100.30	100.96	100.39	100.64
Mg	Cations	1.09	1.10	1.09	1.09	1.09
Al	Norm.					
Si	to	0.99	0.98	0.99	0.99	0.98
Ca	4 oxygens	0.01	0.00	0.00	0.00	0.00
Mn		0.01	0.01	0.01	0.01	0.01
Fe		0.92	0.92	0.92	0.92	0.92
Ni		0.00	0.01	0.01		0.00
Total		3.01	3.02	3.01	3.01	3.02
Fo		54.27	54.45	54.20	54.23	54.29

CLG-23		Ol. 3 Spec. 1	Ol. 3 Spec. 2	Ol. 3 Spec. 3	Ol. 3 Spec. 4	Ol. 3 Avg.
MgO	Oxide	26.04	26.03	26.04	26.00	26.03
Al_2O_3	wt%					
SiO_2		34.39	34.25	34.75	34.59	34.50
CaO		0.17	0.11	0.14	0.08	0.13
MnO		0.64	0.51	0.51	0.46	0.53
FeO		38.17	38.64	38.65	38.70	38.54
NiO		0.23			0.25	0.24
Total		99.63	99.54	100.10	100.08	99.84
Mg	Cations	1.11	1.11	1.10	1.10	1.10
Al	Norm.					
Si	to	0.98	0.98	0.98	0.98	0.98
Ca	4 oxygens	0.01	0.00	0.00	0.00	0.00
Mn		0.02	0.01	0.01	0.01	0.01
Fe		0.91	0.92	0.92	0.92	0.92
Ni		0.01			0.01	0.00
Total		3.02	3.02	3.02	3.02	3.02
Fo		54.88	54.56	54.57	54.50	54.63

CLG-25		Ol. 1 Spec. 1	Ol. 1 Spec. 2	Ol. 1 Spec. 3	Ol. 1 Spec. 4	Ol. 1 Avg.
MgO	Oxide	38.83	38.65	38.42	38.39	38.57
Al_2O_3	wt%					
SiO_2		37.50	37.77	37.94	37.51	37.68

CaO		0.16	0.11	0.06	0.13	0.12
MnO		0.39	0.28	0.32	0.25	0.31
FeO		23.00	23.04	23.44	22.81	23.07
NiO		0.44	0.25	0.30	0.28	0.32
Total		100.31	100.10	100.48	99.36	100.06
Mg	Cations	1.51	1.51	1.49	1.51	1.51
Al	Norm.					
Si	to	0.98	0.99	0.99	0.99	0.99
Ca	4 oxygens	0.00	0.00	0.00	0.00	0.00
Mn		0.01	0.01	0.01	0.01	0.01
Fe		0.50	0.50	0.51	0.50	0.51
Ni		0.01	0.01	0.01	0.01	0.01
Total		3.02	3.01	3.01	3.01	3.01
Fo		75.06	74.94	74.50	75.00	74.88

CLG-25		Ol. 2 Spec. 1	Ol. 2 Spec. 2	Ol. 2 Spec. 3	Ol. 2 Spec. 4	Ol. 2 Avg.
MgO	Oxide	38.09	38.74	38.31	38.53	38.42
Al_2O_3	wt%					
SiO_2		37.38	37.10	37.42	37.61	37.38
CaO		0.09	0.09	0.16	0.17	0.13
MnO		0.28	0.34	0.31	0.36	0.32
FeO		23.10	23.22	23.21	23.46	23.25
NiO		0.29	0.39	0.34	0.26	0.32
Total		99.23	99.87	99.75	100.39	99.81
Mg	Cations	1.50	1.52	1.50	1.50	1.51
Al	Norm.					
Si	to	0.99	0.98	0.98	0.98	0.98
Ca	4 oxygens	0.00	0.00	0.00	0.00	0.00
Mn		0.01	0.01	0.01	0.01	0.01
Fe		0.51	0.51	0.51	0.51	0.51
Ni		0.01	0.01	0.01	0.01	0.01
Total		3.01	3.02	3.02	3.02	3.02
Fo		74.62	74.84	74.63	74.54	74.66

CLG-25		Ol. 3 Spec. 1	Ol. 3 Spec. 2	Ol. 3 Spec. 3	Ol. 3 Spec. 4	Ol. 3 Avg.
MgO	Oxide	39.38	39.16	39.23	39.38	39.29
Al_2O_3	wt%					
SiO_2		37.44	37.72	37.85	37.54	37.64
CaO		0.06	0.13	0.11	0.14	0.11
MnO		0.34	0.31	0.26	0.34	0.31
FeO		22.96	22.84	22.69	22.73	22.81
NiO		0.18	0.37	0.22		0.26
Total		100.35	100.53	100.36	100.12	100.34
Mg	Cations	1.53	1.52	1.52	1.53	1.53
Al	Norm.					
Si	to	0.98	0.98	0.99	0.98	0.98
Ca	4 oxygens	0.00	0.00	0.00	0.00	0.00
Mn		0.01	0.01	0.01	0.01	0.01
Fe		0.50	0.50	0.49	0.50	0.50
Ni		0.00	0.01	0.00		0.00
Total		3.02	3.02	3.01	3.02	3.02

Fo		75.35	75.35	75.50	75.54	75.44

CLG-28		Ol. 1 Spec. 1	Ol. 1 Spec. 2	Ol. 1 Spec. 3	Ol. 1 Spec. 4	Ol. 1 Avg.
MgO	Oxide	27.45	27.17	27.09	27.06	27.19
Al_2O_3	wt%					
SiO_2		35.01	35.29	34.92	35.00	35.06
CaO		0.08	0.11	0.07	0.12	0.10
MnO		0.61	0.59	0.46	0.46	0.53
FeO		37.63	37.80	37.42	37.66	37.63
NiO		0.14		0.25		0.20
Total		100.91	100.96	100.22	100.30	100.60
Mg	Cations	1.14	1.13	1.14	1.13	1.14
Al	Norm.					
Si	to	0.98	0.98	0.98	0.98	0.98
Ca	4 oxygens	0.00	0.00	0.00	0.00	0.00
Mn		0.01	0.01	0.01	0.01	0.01
Fe		0.88	0.88	0.88	0.88	0.88
Ni		0.00		0.01		0.00
Total		3.02	3.02	3.02	3.02	3.02
Fo		56.53	56.17	56.34	56.16	56.30

CLG-28		Ol. 2 Spec. 1	Ol. 2 Spec. 2	Ol. 2 Spec. 3	Ol. 2 Spec. 4	Ol. 2 Avg.
MgO	Oxide	25.84	25.78	25.58	25.55	25.69
Al_2O_3	wt%					
SiO_2		34.74	34.80	34.49	34.62	34.66
CaO		0.13	0.15	0.16	0.14	0.15
MnO		0.65	0.51	0.45	0.64	0.56
FeO		39.20	39.60	39.21	39.28	39.32
NiO		0.15		0.23		0.19
Total		100.73	100.84	100.12	100.23	100.48
Mg	Cations	1.09	1.08	1.08	1.08	1.08
Al	Norm.					
Si	to	0.98	0.98	0.98	0.98	0.98
Ca	4 oxygens	0.00	0.00	0.00	0.00	0.00
Mn		0.02	0.01	0.01	0.02	0.01
Fe		0.93	0.93	0.93	0.93	0.93
Ni		0.00		0.01		0.00
Total		3.02	3.02	3.02	3.02	3.02
Fo		54.02	53.71	53.77	53.69	53.80

CLG-28		Ol. 3 Spec. 1	Ol. 3 Spec. 2	Ol. 3 Spec. 3	Ol. 3 Spec. 4	Ol. 3 Avg.
MgO	Oxide	25.62	25.62	25.89	25.80	25.73
Al_2O_3	wt%					
SiO_2		34.60	34.68	34.45	34.43	34.54
CaO		0.06	0.12	0.07	0.16	0.10
MnO		0.53	0.51	0.48	0.51	0.51
FeO		38.87	38.86	39.20	39.17	39.03
NiO		0.13	0.27	0.20	0.26	0.22
Total		99.82	100.06	100.29	100.33	100.13

Mg	Cations	1.09	1.08	1.10	1.09	1.09
Al	Norm.					
Si	to	0.98	0.99	0.98	0.98	0.98
Ca	4 oxygens	0.00	0.00	0.00	0.00	0.00
Mn		0.01	0.01	0.01	0.01	0.01
Fe		0.93	0.92	0.93	0.93	0.93
Ni		0.00	0.01	0.00	0.01	0.00
Total		3.02	3.01	3.02	3.02	3.02
Fo		54.02	54.03	54.07	54.01	54.03

CLG-39		Ol. 1 Spec. 1	Ol. 1 Spec. 2	Ol. 1 Spec. 3	Ol. 1 Spec. 4	Ol. 1 Avg.
MgO	Oxide	30.35	30.54	30.61	30.37	30.47
Al_2O_3	wt%			0.11		0.11
SiO_2		35.60	35.44	35.67	35.73	35.61
CaO		0.25	0.20	0.26	0.25	0.24
MnO		0.48	0.51	0.53	0.53	0.51
FeO		32.82	32.53	32.63	32.95	32.73
NiO		0.18	0.16	0.22		0.19
Total		99.68	99.38	100.03	99.83	99.73
Mg	Cations	1.25	1.26	1.26	1.25	1.25
Al	Norm.			0.00		0.00
Si	to	0.98	0.98	0.98	0.99	0.98
Ca	4 oxygens	0.01	0.01	0.01	0.01	0.01
Mn		0.01	0.01	0.01	0.01	0.01
Fe		0.76	0.75	0.75	0.76	0.76
Ni		0.00	0.00	0.00		0.00
Total		3.02	3.02	3.02	3.01	3.02
Fo		62.24	62.60	62.58	62.16	62.40

CLG-39		Ol. 2 Spec. 1	Ol. 2 Spec. 2	Ol. 2 Spec. 3	Ol. 2 Spec. 4	Ol. 2 Avg.
MgO	Oxide	29.42	29.17	29.21	28.77	29.14
Al_2O_3	wt%	0.10			0.17	0.14
SiO_2		35.50	35.25	35.22	35.21	35.30
CaO		0.11	0.17	0.19	0.23	0.18
MnO		0.52	0.52	0.54	0.44	0.51
FeO		34.19	34.53	34.03	34.21	34.24
NiO		0.33	0.18	0.21		0.24
Total		100.16	99.83	99.40	99.04	99.61
Mg	Cations	1.21	1.21	1.22	1.20	1.21
Al	Norm.	0.00			0.01	0.00
Si	to	0.98	0.98	0.98	0.99	0.98
Ca	4 oxygens	0.00	0.01	0.01	0.01	0.01
Mn		0.01	0.01	0.01	0.01	0.01
Fe		0.79	0.80	0.79	0.80	0.80
Ni		0.01	0.00	0.00		0.00
Total		3.02	3.02	3.02	3.01	3.02
Fo		60.54	60.09	60.48	59.99	60.27

CLG-39		Ol. 3	Ol. 3	Ol. 3	Ol. 3	Ol. 3

		Spec. 1	Spec. 2	Spec. 3	Spec. 4	Avg.
MgO	Oxide	29.80	29.29	29.87	29.31	29.57
Al_2O_3	wt%					
SiO_2		35.94	35.39	35.46	35.96	35.69
CaO		0.20	0.16	0.24	0.16	0.19
MnO		0.52	0.51	0.55	0.47	0.51
FeO		34.26	34.13	34.66	34.14	34.30
NiO						
Total		100.73	99.47	100.78	100.04	100.26
Mg	Cations	1.22	1.22	1.23	1.21	1.22
Al	Norm.					
Si	to	0.99	0.99	0.98	0.99	0.99
Ca	4 oxygens	0.01	0.00	0.01	0.00	0.01
Mn		0.01	0.01	0.01	0.01	0.01
Fe		0.79	0.80	0.80	0.79	0.79
Ni						
Total		3.01	3.01	3.02	3.01	3.01
Fo		60.79	60.47	60.57	60.48	60.58

CLG-41		Ol. 1 Spec. 1	Ol. 1 Spec. 2	Ol. 1 Spec. 3	Ol. 1 Spec. 4	Ol. 1 Avg.
MgO	Oxide	31.69	31.79	31.47	31.66	31.65
Al_2O_3	wt%					
SiO_2		35.88	35.97	35.65	35.52	35.76
CaO		0.13	0.13	0.07	0.08	0.10
MnO		0.44	0.58	0.51	0.50	0.51
FeO		31.15	31.28	31.13	31.20	31.19
NiO		0.33	0.34	0.22	0.25	0.29
Total		99.61	100.09	99.06	99.21	99.49
Mg	Cations	1.30	1.29	1.29	1.30	1.30
Al	Norm.					
Si	to	0.98	0.98	0.98	0.98	0.98
Ca	4 oxygens	0.00	0.00	0.00	0.00	0.00
Mn		0.01	0.01	0.01	0.01	0.01
Fe		0.71	0.71	0.72	0.72	0.72
Ni		0.01	0.01	0.00	0.01	0.01
Total		3.02	3.02	3.02	3.02	3.02
Fo		64.46	64.43	64.31	64.40	64.40

CLG-41		Ol. 2 Spec. 1	Ol. 2 Spec. 2	Ol. 2 Spec. 3	Ol. 2 Spec. 4	Ol. 2 Avg.
MgO	Oxide	32.08	32.02	32.53	31.88	32.13
Al_2O_3	wt%					
SiO_2		36.82	36.43	36.57	36.21	36.51
CaO		0.22	0.15	0.17	0.17	0.18
MnO		0.34	0.47	0.41	0.40	0.41
FeO		31.35	31.67	31.00	31.37	31.35
NiO		0.16	0.22	0.26	0.19	0.21
Total		100.96	100.96	100.94	100.22	100.77
Mg	Cations	1.29	1.29	1.31	1.29	1.30
Al	Norm.					
Si	to	0.99	0.99	0.99	0.99	0.99
Ca	4 oxygens	0.01	0.00	0.00	0.00	0.01

Mn		0.01	0.01	0.01	0.01	0.01
Fe		0.71	0.72	0.70	0.71	0.71
Ni		0.00	0.00	0.01	0.00	0.00
Total		3.01	3.01	3.01	3.01	3.01
Fo		64.59	64.32	65.16	64.43	64.63

CLG-41		Ol. 3 Spec. 1	Ol. 3 Spec. 2	Ol. 3 Spec. 3	Ol. 3 Spec. 4	Ol. 3 Avg.
MgO	Oxide	31.72	31.55	31.87	31.47	31.65
Al_2O_3	wt%					
SiO_2		35.81	35.96	35.55	35.78	35.78
CaO		0.14		0.06	0.11	0.10
MnO		0.50	0.44	0.51	0.50	0.49
FeO		31.17	31.11	31.16	31.13	31.14
NiO		0.16	0.22	0.38	0.27	0.26
Total		99.50	99.28	99.52	99.25	99.39
Mg	Cations	1.30	1.29	1.31	1.29	1.30
Al	Norm.					
Si	to	0.98	0.99	0.98	0.99	0.98
Ca	4 oxygens	0.00		0.00	0.00	0.00
Mn		0.01	0.01	0.01	0.01	0.01
Fe		0.72	0.72	0.72	0.72	0.72
Ni		0.00	0.00	0.01	0.01	0.01
Total		3.02	3.01	3.02	3.01	3.02
Fo		64.46	64.39	64.58	64.31	64.44

CLG-42		Ol. 1 Spec. 1	Ol. 1 Spec. 2	Ol. 1 Spec. 3	Ol. 1 Spec. 4	Ol. 1 Spec. 5	Ol. 1 Spec. 6	Ol. 1 Avg.
MgO	Oxide	36.21	36.49	36.50	36.43	36.39	36.87	36.48
Al_2O_3	wt%	0.04	0.12	0.12	0.18	0.10		0.11
SiO_2		37.03	36.93	37.16	36.84	36.90	36.88	36.96
CaO								
MnO		0.34	0.37	0.40	0.39	0.41	0.48	0.40
FeO		25.71	25.75	25.57	25.65	25.77	25.86	25.72
NiO		0.31	0.09	0.21	0.22	0.15	0.50	0.25
Total		99.64	99.74	99.95	99.71	99.73	100.59	99.89
Mg	Cations	1.44	1.45	1.44	1.45	1.44	1.45	1.45
Al	Norm.	0.00	0.00	0.00	0.01	0.00	0.00	0.00
Si	to	0.99	0.98	0.99	0.98	0.98	0.98	0.98
Ca	4 oxygens							
Mn		0.01	0.01	0.01	0.01	0.01	0.01	0.01
Fe		0.57	0.57	0.57	0.57	0.57	0.57	0.57
Ni		0.01	0.00	0.00	0.00	0.00	0.01	0.01
Total		3.01	3.02	3.01	3.02	3.02	3.02	3.02
Fo		71.52	71.64	71.79	71.69	71.57	71.76	71.66

CLG-42		Ol. 2 Spec. 1	Ol. 2 Spec. 2	Ol. 2 Spec. 3	Ol. 2 Spec. 4	Ol. 2 Spec. 5	Ol. 2 Spec. 6	Ol. 2 Avg.
MgO	Oxide	37.25	37.04	37.53	36.99	37.01	37.19	37.17
Al_2O_3	wt%	0.09	0.16	0.16	0.05	0.18	0.04	0.11
SiO_2		36.70	36.93	37.07	36.98	37.06	37.15	36.98
CaO		0.10	0.14	0.02	0.04	0.12	0.08	0.08

MnO		0.41	0.38	0.31	0.31	0.41	0.43	0.38
FeO		24.69	25.17	25.21	24.87	24.76	24.89	24.93
NiO		0.21	0.23	0.26	0.14	0.22	0.11	0.20
Total		99.45	100.05	100.56	99.38	99.77	99.89	99.85
Mg	Cations	1.48	1.46	1.47	1.47	1.46	1.47	1.47
Al	Norm.	0.00	0.00	0.00	0.00	0.01	0.00	0.00
Si	to	0.98	0.98	0.98	0.98	0.98	0.98	0.98
Ca	4 oxygens	0.00	0.00	0.00	0.00	0.00	0.00	0.00
Mn		0.01	0.01	0.01	0.01	0.01	0.01	0.01
Fe		0.55	0.56	0.56	0.55	0.55	0.55	0.55
Ni		0.00	0.00	0.01	0.00	0.00	0.00	0.00
Total		3.02	3.02	3.02	3.02	3.02	3.02	3.02
Fo		72.90	72.40	72.63	72.61	72.71	72.70	72.66

CLG-42		Ol. 3 Spec. 1	Ol. 3 Spec. 2	Ol. 3 Spec. 3	Ol. 3 Spec. 4	Ol. 3 Spec. 5	Ol. 3 Avg.
MgO	Oxide	36.03	35.96	36.11	36.30	36.24	36.13
Al_2O_3	wt%						
SiO_2		37.05	36.99	36.91	36.68	36.64	36.85
CaO		0.06	0.10	0.13	0.10	0.15	0.11
MnO		0.38	0.43	0.38	0.43	0.48	0.42
FeO		25.81	25.85	26.14	25.77	25.76	25.87
NiO		0.11	0.12	0.38	0.33	0.28	0.24
Total		99.44	99.46	100.06	99.60	99.55	99.62
Mg	Cations	1.43	1.43	1.43	1.45	1.44	1.44
Al	Norm.						
Si	to	0.99	0.99	0.98	0.98	0.98	0.98
Ca	4 oxygens	0.00	0.00	0.00	0.00	0.00	0.00
Mn		0.01	0.01	0.01	0.01	0.01	0.01
Fe		0.58	0.58	0.58	0.58	0.58	0.58
Ni		0.00	0.00	0.01	0.01	0.01	0.01
Total		3.01	3.01	3.02	3.02	3.02	3.02
Fo		71.33	71.26	71.12	71.52	71.49	71.35

CRYSTAL LAKE GABBRO SPINEL

CLG-25		Spinel 1 Spec. 1	Spinel 1 Spec. 2	Spinel 1 Spec. 3	Spinel 1 Spec. 4	Spinel 1 Avg.
Na_2O	Oxide	0.32	0.16	0.21	0.24	0.23
MgO	wt%	4.94	5.03	4.98	5.17	5.03
Al_2O_3		9.42	9.05	9.16	9.09	9.18
SiO_2		0.28	0.39	0.41	0.24	0.33
CaO		0.09	0.12	0.16	0.13	0.13
TiO_2		6.56	6.65	6.68	6.65	6.64
V_2O_5		0.74	0.55	0.65	0.65	0.65
Cr_2O_3		33.42	33.70	33.18	33.08	33.35
FeO		31.63	32.05	32.02	31.39	31.77
Fe_2O_3		12.83	12.61	12.59	13.29	12.83
NiO		0.33	0.31	0.29	0.20	0.28
Total		100.57	100.61	100.33	100.13	
Na	Cations	0.02	0.01	0.01	0.02	0.02
Mg	Norm.	0.25	0.26	0.25	0.26	0.26
Al	to	0.38	0.37	0.37	0.37	0.37
Si	4 oxygens	0.01	0.01	0.01	0.01	0.01
Ca		0.00	0.00	0.01	0.00	0.00
Ti		0.17	0.17	0.17	0.17	0.17
V		0.02	0.01	0.01	0.01	0.01
Cr		0.90	0.91	0.90	0.90	0.90
Fe2+		0.91	0.92	0.92	0.90	0.91
Fe3+		0.33	0.33	0.33	0.34	0.33
Ni		0.01	0.01	0.01	0.01	0.01
Total		3.00	3.00	3.00	3.00	3.00

CLG-25		Spinel 2 Spec. 1	Spinel 2 Spec. 2	Spinel 2 Spec. 3	Spinel 2 Spec. 4	Spinel 2 Avg.
Na_2O	Oxide	0.12	0.18	0.18	0.00	0.12
MgO	wt%	7.85	7.61	7.38	7.63	7.62
Al_2O_3		13.22	13.14	13.15	13.12	13.16
SiO_2		0.38	0.30	0.35	0.35	0.35
CaO		0.00	0.09	0.10	0.05	0.06
TiO_2		7.12	7.13	7.05	7.06	7.09
V_2O_5		0.60	0.58	0.53	0.69	0.60
Cr_2O_3		29.84	29.54	29.82	29.87	29.77
FeO		29.54	29.13	29.45	30.13	29.56
Fe_2O_3		12.49	13.16	12.96	11.66	12.57
NiO		0.19	0.45	0.41	0.27	0.33
Total		101.35	101.32	101.38	100.83	
Na	Cations	0.01	0.01	0.01	0.00	0.01
Mg	Norm.	0.38	0.37	0.36	0.38	0.37
Al	to	0.51	0.51	0.51	0.51	0.51
Si	4 oxygens	0.01	0.01	0.01	0.01	0.01
Ca		0.00	0.00	0.00	0.00	0.00
Ti		0.18	0.18	0.17	0.18	0.18
V		0.01	0.01	0.01	0.02	0.01
Cr		0.77	0.77	0.78	0.78	0.77
Fe2+		0.81	0.80	0.81	0.83	0.81
Fe3+		0.31	0.33	0.32	0.29	0.31
Ni		0.01	0.01	0.01	0.01	0.01
Total		3.00	3.00	3.00	3.00	3.00

CLG-25		Spinel 3 Spec. 1	Spinel 3 Spec. 2	Spinel 3 Spec. 3	Spinel 3 Spec. 4	Spinel 3 Avg.
Na_2O	Oxide	0.00	0.00	0.19	0.12	0.08
MgO	wt%	7.74	7.25	7.58	7.62	7.55
Al_2O_3		12.54	12.34	12.81	12.69	12.60
SiO_2		0.00	0.32	0.00	0.32	0.16
CaO		0.05	0.11	0.08	0.00	0.06
TiO_2		7.37	7.60	7.43	7.32	7.43
V_2O_5		0.57	0.63	0.60	0.57	0.59
Cr_2O_3		29.39	29.53	29.57	29.60	29.52
FeO		29.28	30.88	29.08	29.83	29.77
Fe_2O_3		13.28	11.78	13.52	13.00	12.90
NiO		0.41	0.20	0.33	0.19	0.28
Total		100.63	100.64	101.18	101.26	
Na	Cations	0.00	0.00	0.01	0.01	0.00
Mg	Norm.	0.38	0.36	0.37	0.37	0.37
Al	to	0.49	0.48	0.50	0.49	0.49
Si	4 oxygens	0.00	0.01	0.00	0.01	0.01
Ca		0.00	0.00	0.00	0.00	0.00
Ti		0.18	0.19	0.18	0.18	0.19
V		0.01	0.01	0.01	0.01	0.01
Cr		0.77	0.78	0.77	0.77	0.77
Fe2+		0.81	0.86	0.80	0.82	0.82
Fe3+		0.33	0.30	0.34	0.32	0.32
Ni		0.01	0.01	0.01	0.01	0.01
Total		3.00	3.00	3.00	3.00	3.00

CLG-42		Spinel 1 Spec. 1	Spinel 1 Spec. 2	Spinel 1 Spec. 3	Spinel 1 Spec. 4	Spinel 1 Spec. 5	Spinel 1 Spec. 6	Spinel 1 Avg.
MgO	Oxide	4.83	4.92	4.97	4.86	4.76	4.90	4.87
Al_2O_3	wt%	9.06	9.31	9.25	9.24	9.15	9.10	9.19
SiO_2		0.29	0.28	0.21	0.28	0.32	0.20	0.26
TiO_2		8.32	8.52	8.38	8.40	8.47	8.37	8.41
V_2O_5		0.84	0.78	0.79	0.77	0.89	1.00	0.85
Cr_2O_3		29.33	29.23	29.67	29.32	29.44	28.64	29.27
FeO		34.98	35.00	34.86	34.85	35.24	34.86	34.97
Fe_2O_3		13.11	12.90	13.08	13.19	12.23	13.22	12.95
MnO		0.53	0.55	0.46	0.69	0.59	0.59	0.57
Total		101.29	101.49	101.67	101.60	101.09	100.88	
Mg	Cations	0.25	0.25	0.25	0.25	0.24	0.25	0.25
Al	Norm.	0.37	0.37	0.37	0.37	0.37	0.37	0.37
Si	to	0.01	0.01	0.01	0.01	0.01	0.01	0.01
Ti	4 oxygens	0.21	0.22	0.21	0.22	0.22	0.22	0.22
V		0.02	0.02	0.02	0.02	0.02	0.02	0.02
Cr		0.79	0.79	0.80	0.79	0.80	0.78	0.79
Fe2+		1.00	1.00	0.99	0.99	1.01	1.00	1.00
Fe3+		0.34	0.33	0.33	0.34	0.32	0.34	0.33
Mn		0.02	0.02	0.01	0.02	0.02	0.02	0.02
Total		3.00	3.00	3.00	3.00	3.00	3.00	3.00

CLG-42		Spinel 2 Spec. 1	Spinel 2 Spec. 2	Spinel 2 Spec. 3	Spinel 2 Spec. 4	Spinel 2 Spec. 5	Spinel 2 Spec. 6	Spinel 2 Avg.
MgO	Oxide	3.77	3.72	3.70	3.92	3.93	3.88	3.82
Al_2O_3	wt%	7.43	7.44	7.54	7.37	7.56	7.24	7.43
SiO_2		0.17	0.30	0.18	0.16	0.19	0.19	0.20
TiO_2		9.44	9.21	9.27	9.24	9.25	9.20	9.27

V_2O_5		1.03	0.93	0.94	0.98	1.00	0.90	0.96
Cr_2O_3		25.55	25.70	25.78	26.16	25.90	26.03	25.85
FeO		37.51	37.46	37.26	37.14	37.18	36.97	37.25
Fe_2O_3		16.21	16.52	16.11	16.65	16.40	16.92	16.47
MnO		0.60	0.58	0.59	0.63	0.61	0.62	0.61
Total		101.71	101.86	101.37	102.25	102.02	101.94	
Mg	Cations	0.20	0.19	0.19	0.20	0.20	0.20	0.20
Al	Norm.	0.30	0.30	0.31	0.30	0.31	0.29	0.30
Si	to	0.01	0.01	0.01	0.01	0.01	0.01	0.01
Ti	4 oxygens	0.25	0.24	0.24	0.24	0.24	0.24	0.24
V		0.02	0.02	0.02	0.02	0.02	0.02	0.02
Cr		0.70	0.70	0.71	0.71	0.71	0.71	0.71
Fe2+		1.09	1.08	1.08	1.07	1.07	1.07	1.08
Fe3+		0.42	0.43	0.42	0.43	0.43	0.44	0.43
Mn		0.02	0.02	0.02	0.02	0.02	0.02	0.02
Total		3.00	3.00	3.00	3.00	3.00	3.00	3.00

CLG-42		Spinel 3 Spec. 1	Spinel 3 Spec. 2	Spinel 3 Spec. 3	Spinel 3 Spec. 4	Spinel 3 Spec. 5	Spinel 3 Spec. 6	Spinel 3 Avg.
MgO	Oxide	3.00	3.19	3.14	3.14	3.21	2.91	3.10
Al_2O_3	wt%	6.50	6.48	6.35	6.42	6.43	6.36	6.42
SiO_2		0.22	0.29	0.34	0.14	0.24	0.26	0.25
TiO_2		9.10	9.23	9.28	9.22	9.25	8.95	9.17
V_2O_5		0.87	0.73	0.92	0.93	0.89	0.99	0.89
Cr_2O_3		23.82	23.66	23.32	23.33	23.77	24.14	23.67
FeO		38.31	37.87	38.32	37.91	38.25	38.71	38.23
Fe_2O_3		19.92	20.32	19.88	20.25	20.05	19.00	19.91
MnO		0.44	0.64	0.57	0.64	0.48	0.00	0.46
Total		102.19	102.42	102.12	101.98	102.58	101.32	
Mg	Cations	0.16	0.17	0.17	0.17	0.17	0.16	0.17
Al	Norm.	0.27	0.27	0.26	0.26	0.26	0.26	0.26
Si	to	0.01	0.01	0.01	0.00	0.01	0.01	0.01
Ti	4 oxygens	0.24	0.24	0.24	0.24	0.24	0.24	0.24
V		0.02	0.02	0.02	0.02	0.02	0.02	0.02
Cr		0.66	0.65	0.64	0.64	0.65	0.67	0.65
Fe2+		1.12	1.10	1.12	1.11	1.11	1.14	1.12
Fe3+		0.52	0.53	0.52	0.53	0.52	0.50	0.52
Mn		0.01	0.02	0.02	0.02	0.01	0.00	0.01
Total		3.00	3.00	3.00	3.00	3.00	3.00	3.00

CLG-42		Spinel 4 Spec. 1	Spinel 4 Spec. 2	Spinel 4 Spec. 3	Spinel 4 Spec. 4	Spinel 4 Spec. 5	Spinel 4 Spec. 6	Spinel 4 Avg.
MgO	Oxide	3.68	3.50	3.70	3.63	3.53	3.80	3.64
Al_2O_3	wt%	6.75	7.03	7.02	6.86	6.92	6.96	6.92
SiO_2		0.16	0.27	0.09	0.24	0.37	0.28	0.24
TiO_2		10.21	10.48	10.57	10.43	10.36	10.35	10.40
V_2O_5		1.14	0.82	0.83	1.08	1.10	0.95	0.99
Cr_2O_3		23.97	24.28	24.13	23.90	23.90	24.00	24.03
FeO		39.00	39.17	38.80	39.42	39.53	38.79	39.12
Fe_2O_3		16.83	16.04	16.71	16.54	15.76	16.45	16.39
	0.00	0.00	0.00	0.00	0.00	0.00	0.00	0.00
Total		101.74	101.60	101.85	102.11	101.47	101.58	
Mg	Cations	0.19	0.18	0.19	0.19	0.19	0.20	0.19
Al	Norm.	0.28	0.29	0.29	0.28	0.28	0.28	0.28
Si	to	0.01	0.01	0.00	0.01	0.01	0.01	0.01

Ti		4 oxygens	0.27	0.27	0.28	0.27	0.27	0.27	0.27
V			0.03	0.02	0.02	0.02	0.03	0.02	0.02
Cr			0.66	0.67	0.66	0.65	0.66	0.66	0.66
Fe2+			1.13	1.14	1.13	1.14	1.15	1.13	1.14
Fe3+			0.44	0.42	0.44	0.43	0.41	0.43	0.43
Mn			0.00	0.00	0.00	0.00	0.00	0.00	0.00
Total			3.00	3.00	3.00	3.00	3.00	3.00	3.00

CLG-42			Spinel 5 Spec. 1	Spinel 5 Spec. 2	Spinel 5 Spec. 3	Spinel 5 Spec. 4	Spinel 5 Spec. 5	Spinel 5 Spec. 6	Spinel 5 Avg.
MgO		Oxide	10.57	10.46	10.74	10.50	10.30	10.40	10.50
Al_2O_3		wt%	25.74	25.53	25.63	25.69	25.54	25.71	25.64
SiO_2			0.28	0.40	0.27	0.37	0.31	0.42	0.34
TiO_2			2.73	2.80	2.62	2.64	2.74	2.66	2.70
V_2O_5			0.48	0.41	0.52	0.55	0.41	0.41	0.46
Cr_2O_3			27.69	27.42	27.51	27.74	27.72	27.53	27.60
FeO			23.71	23.76	23.20	23.89	23.70	23.74	23.67
Fe_2O_3			9.83	9.62	9.98	9.43	9.25	9.39	9.59
	0.00		0.00	0.00	0.00	0.00	0.00	0.00	0.00
Total			101.03	100.40	100.47	100.81	99.98	100.26	
Mg		Cations	0.48	0.47	0.49	0.47	0.47	0.47	0.47
Al		Norm.	0.93	0.93	0.93	0.93	0.93	0.94	0.93
Si		to	0.01	0.01	0.01	0.01	0.01	0.01	0.01
Ti		4 oxygens	0.06	0.06	0.06	0.06	0.06	0.06	0.06
V			0.01	0.01	0.01	0.01	0.01	0.01	0.01
Cr			0.67	0.67	0.67	0.67	0.68	0.67	0.67
Fe2+			0.61	0.61	0.60	0.61	0.61	0.61	0.61
Fe3+			0.23	0.22	0.23	0.22	0.22	0.22	0.22
Mn			0.00	0.00	0.00	0.00	0.00	0.00	0.00
Total			2.99	2.99	2.99	2.99	2.99	2.99	2.99

Mount Mollie Dyke Plagioclase

Sample 12		Plag 1 Spec. 1	Plag 1 Spec. 2	Plag 1 Spec. 3	Plag 1 Spec. 4	Plag 1 Spec. 5	Plag 1 Spec. 6	Avg.
Na_2O	Oxide	4.86	4.94	4.83	4.90	5.03	4.78	4.89
MgO	wt%							
Al_2O_3		28.11	28.38	28.25	28.27	28.11	27.89	28.17
SiO_2		54.01	53.57	53.33	53.74	53.36	53.76	53.63
CaO		11.93	11.86	11.88	11.88	11.88	11.77	11.87
FeO		0.46	0.42	0.52	0.42	0.41	0.41	0.44
K_2O		0.33	0.39	0.38	0.36	0.36	0.36	0.36
TiO_2								
Total		99.70	99.56	99.19	99.58	99.16	98.97	
Na	Cations	0.43	0.44	0.43	0.43	0.45	0.42	0.43
Mg	Norm.							
Al	to	1.51	1.53	1.52	1.52	1.52	1.51	1.52
Si	8 oxygens	2.46	2.44	2.44	2.45	2.45	2.46	2.45
Ca		0.58	0.58	0.58	0.58	0.58	0.58	0.58
Fe		0.02	0.02	0.02	0.02	0.02	0.02	0.02
K		0.02	0.02	0.02	0.02	0.02	0.02	0.02
Ti								
Total		5.01	5.02	5.02	5.02	5.03	5.01	5.02
An		56.49	55.78	56.38	56.10	55.49	56.45	56.11
Ab		41.65	42.04	41.48	41.87	42.51	41.49	41.84
Or		1.86	2.18	2.15	2.02	2.00	2.06	2.05

Sample 12		Plag 2 Spec. 1	Plag 2 Spec. 2	Plag 2 Spec. 3	Avg.
Na_2O	Oxide	5.08	5.11	5.08	5.09
MgO	wt%				
Al2O_3		27.67	27.66	27.94	27.76
SiO_2		54.29	53.99	54.33	54.20
CaO		11.53	11.30	11.56	11.46
FeO		0.41	0.56	0.40	0.46
K_2O		0.37	0.37	0.40	0.38
TiO_2					
Total		99.34	99.00	99.71	
Na	Cations	0.45	0.45	0.45	0.45
Mg	Norm.				
Al	to	1.49	1.49	1.50	1.49
Si	8 oxygens	2.48	2.47	2.47	2.47
Ca		0.56	0.55	0.56	0.56
Fe		0.02	0.02	0.02	0.02
K		0.02	0.02	0.02	0.02
Ti					
Total		5.01	5.02	5.02	5.02
An		54.48	53.84	54.45	54.26
Ab		43.44	44.06	43.30	43.60
Or		2.08	2.10	2.24	2.14

Sample 12		Plag 3 Spec. 1	Plag 3 Spec. 2	Plag 3 Spec. 3	Plag 3 Spec. 4	Plag 3 Spec. 5	Plag 3 Spec. 6	Avg.
Na_2O	Oxide	4.82	4.81	4.75	5.01	4.91	4.69	4.83
MgO	wt%							

Al_2O_3		28.14	28.12	28.54	28.33	28.12	28.52	28.30
SiO_2		53.61	53.50	53.30	53.78	53.84	52.93	53.49
CaO		11.87	11.98	12.09	11.64	11.80	12.23	11.94
FeO		0.50	0.37	0.39	0.42	0.39	0.42	0.42
K_2O		0.32	0.40	0.30	0.38	0.40	0.34	0.36
TiO_2								
Total		99.25	99.19	99.37	99.56	99.46	99.13	
Na	Cations	0.43	0.43	0.42	0.44	0.43	0.42	0.43
Mg	Norm.							
Al	to	1.52	1.52	1.54	1.52	1.51	1.54	1.52
Si	8 oxygens	2.45	2.45	2.43	2.45	2.46	2.43	2.44
Ca		0.58	0.59	0.59	0.57	0.58	0.60	0.58
Fe		0.02	0.01	0.01	0.02	0.01	0.02	0.02
K		0.02	0.02	0.02	0.02	0.02	0.02	0.02
Ti								
Total		5.01	5.02	5.02	5.02	5.02	5.02	5.02
An		56.60	56.61	57.45	55.01	55.76	57.90	56.56
Ab		41.59	41.13	40.85	42.85	41.99	40.18	41.43
Or		1.82	2.25	1.70	2.14	2.25	1.92	2.01

Sample 12		Plag 4 Spec. 1	Plag 4 Spec. 2	Plag 4 Spec. 3	Plag 4 Spec. 4	Plag 4 Spec. 5	Avg.
Na_2O	Oxide	5.01	4.78	4.91	5.32	5.25	5.05
MgO	wt%						
Al_2O_3		28.42	28.53	27.82	27.67	27.55	28.00
SiO_2		53.48	53.42	54.13	54.44	54.17	53.93
CaO		11.98	11.92	11.74	11.30	11.13	11.61
FeO		0.39	0.46	0.57	0.40	0.56	0.48
K_2O		0.35	0.31	0.35	0.38	0.37	0.35
TiO_2							
Total		99.63	99.43	99.52	99.52	99.03	
Na	Cations	0.44	0.42	0.43	0.47	0.47	0.45
Mg	Norm.						
Al	to	1.53	1.53	1.49	1.49	1.49	1.51
Si	8 oxygens	2.44	2.44	2.47	2.48	2.48	2.46
Ca		0.59	0.58	0.57	0.55	0.55	0.57
Fe		0.01	0.02	0.02	0.02	0.02	0.02
K		0.02	0.02	0.02	0.02	0.02	0.02
Ti							
Total		5.03	5.01	5.01	5.02	5.02	5.02
An		55.82	56.93	55.79	52.85	52.82	54.84
Ab		42.24	41.31	42.23	45.03	45.09	43.18
Or		1.94	1.76	1.98	2.12	2.09	1.98

Sample 12		Plag 5 Spec. 1	Plag 5 Spec. 2	Plag 5 Spec. 3	Plag 5 Spec. 4	Plag 5 Spec. 5	Plag 5 Spec. 6	Avg.
Na_2O	Oxide	4.80	4.68	4.58	4.72	4.69	4.55	4.67
MgO	wt%							
Al_2O_3		28.66	28.80	28.76	28.48	28.78	28.27	28.63
SiO_2		53.14	53.18	52.74	53.18	53.38	52.42	53.01
CaO		12.41	12.38	12.47	12.28	12.44	12.21	12.37
FeO		0.48	0.45	0.44	0.38	0.42	0.44	0.44
K_2O		0.32	0.35	0.33	0.38	0.36	0.32	0.34
TiO_2								

Total		99.82	99.84	99.32	99.41	100.06	98.21	
Na	Cations	0.42	0.41	0.41	0.42	0.41	0.41	0.41
Mg	Norm.							
Al	to	1.54	1.55	1.55	1.53	1.54	1.54	1.54
Si	8 oxygens	2.42	2.42	2.42	2.43	2.43	2.43	2.42
Ca		0.61	0.60	0.61	0.60	0.61	0.61	0.61
Fe		0.02	0.02	0.02	0.01	0.02	0.02	0.02
K		0.02	0.02	0.02	0.02	0.02	0.02	0.02
Ti								
Total		5.03	5.02	5.02	5.02	5.02	5.02	5.02
An		57.78	58.22	58.96	57.72	58.25	58.63	58.26
Ab		40.44	39.82	39.19	40.15	39.74	39.54	39.82
Or		1.77	1.96	1.86	2.13	2.01	1.83	1.93

Sample 18		Plag 1 Spec. 1	Plag 1 Spec. 2	Plag 1 Spec. 3	Plag 1 Spec. 4	Plag 1 Spec. 5	Avg.
Na_2O	Oxide	4.96	4.93	5.03	5.02	5.01	4.99
MgO	wt%						
Al_2O_3		28.01	28.03	28.04	27.96	27.84	27.98
SiO_2		54.52	53.97	54.07	54.36	54.39	54.26
CaO		11.42	11.37	11.76	11.40	11.64	11.52
FeO		0.47	0.43	0.41	0.39	0.52	0.44
K_2O		0.39	0.40	0.44	0.53	0.41	0.43
TiO_2							
Total		99.77	99.13	99.75	99.67	99.82	
Na	Cations	0.44	0.44	0.44	0.44	0.44	0.44
Mg	Norm.						
Al	to	1.50	1.51	1.50	1.50	1.49	1.50
Si	8 oxygens	2.47	2.47	2.46	2.47	2.47	2.47
Ca		0.56	0.56	0.57	0.56	0.57	0.56
Fe		0.02	0.02	0.02	0.01	0.02	0.02
K		0.02	0.02	0.03	0.03	0.02	0.03
Ti							
Total		5.01	5.01	5.02	5.01	5.01	5.01
An		54.75	54.75	54.99	53.99	54.92	54.68
Ab		43.03	42.96	42.56	43.02	42.78	42.87
Or		2.23	2.29	2.45	2.99	2.30	2.45

Sample 18		Plag 2 Spec. 1	Plag 2 Spec. 2	Plag 2 Spec. 3	Plag 2 Spec. 4	Avg.
Na_2O	Oxide	4.95	5.03	5.06	5.08	5.03
MgO	wt%					
Al_2O_3		28.14	28.02	27.79	28.05	28.00
SiO2		53.71	53.81	54.12	54.12	53.94
CaO		11.49	11.40	11.59	11.52	11.50
FeO		0.47	0.42	0.47	0.37	0.43
K_2O		0.44	0.46	0.39	0.43	0.43
TiO_2						
Total		99.21	99.15	99.41	99.57	
Na	Cations	0.44	0.45	0.45	0.45	0.45
Mg	Norm.					
Al	to	1.52	1.51	1.49	1.51	1.51
Si	8 oxygens	2.46	2.46	2.47	2.46	2.46

Ca		0.56	0.56	0.57	0.56	0.56
Fe		0.02	0.02	0.02	0.01	0.02
K		0.03	0.03	0.02	0.02	0.03
Ti						
Total		5.02	5.02	5.02	5.02	5.02
An		54.79	54.16	54.64	54.28	54.47
Ab		42.71	43.24	43.17	43.31	43.11
Or		2.50	2.60	2.19	2.41	2.42

Sample 18		Plag 3 Spec. 1	Plag 3 Spec. 2	Plag 3 Spec. 3	Plag 3 Spec. 4	Plag 3 Spec. 5	Avg.
Na_2O	Oxide	4.89	4.83	4.93	4.84	4.64	4.83
MgO	wt%						
Al_2O_3		28.76	28.71	28.62	28.41	28.64	28.63
SiO_2		54.14	54.17	54.09	54.17	53.77	54.07
CaO		12.19	12.15	12.02	12.02	12.26	12.13
FeO		0.40	0.35	0.31	0.34	0.48	0.38
K_2O		0.41	0.40	0.41	0.38	0.33	0.39
TiO_2							
Total		100.79	100.61	100.40	100.16	100.12	
Na	Cations	0.43	0.42	0.43	0.42	0.41	0.42
Mg	Norm.						
Al	to	1.53	1.53	1.52	1.52	1.53	1.53
Si	8 oxygens	2.44	2.44	2.45	2.45	2.44	2.44
Ca		0.59	0.59	0.58	0.58	0.60	0.59
Fe		0.02	0.01	0.01	0.01	0.02	0.01
K		0.02	0.02	0.02	0.02	0.02	0.02
Ti							
Total		5.02	5.02	5.02	5.01	5.01	5.02
An		56.63	56.86	56.09	56.62	58.24	56.88
Ab		41.11	40.91	41.63	41.25	39.89	40.96
Or		2.27	2.23	2.28	2.13	1.87	2.16

Sample 18		Plag 4 Spec. 1	Plag 4 Spec. 2	Plag 4 Spec. 3	Plag 4 Spec. 4	Avg.
Na_2O	Oxide	4.48	4.44	4.40	4.27	4.40
MgO	wt%					
Al_2O_3		28.69	29.04	28.76	28.42	28.73
SiO_2		53.11	52.92	52.61	52.74	52.85
CaO		12.50	12.69	12.48	12.85	12.63
FeO		0.46	0.42	0.48	0.50	0.47
K_2O		0.39	0.31	0.31	0.36	0.34
TiO_2						
Total		99.62	99.82	99.03	99.14	
Na	Cations	0.40	0.39	0.39	0.38	0.39
Mg	Norm.					
Al	to	1.54	1.56	1.56	1.54	1.55
Si	8 oxygens	2.42	2.41	2.41	2.42	2.42
Ca		0.61	0.62	0.61	0.63	0.62
Fe		0.02	0.02	0.02	0.02	0.02
K		0.02	0.02	0.02	0.02	0.02
Ti						
Total		5.01	5.01	5.01	5.01	5.01

An		59.32	60.16	59.97	61.17	60.16
Ab		38.47	38.09	38.26	36.79	37.90
Or		2.20	1.75	1.77	2.04	1.94

Sample 18		Plag 5 Spec. 1	Plag 5 Spec. 2	Plag 5 Spec. 3	Plag 5 Spec. 4	Avg.
Na_2O	Oxide	4.55	4.61	4.77	4.54	4.62
MgO	wt%					
Al_2O_3		28.67	28.57	28.54	29.03	28.70
SiO_2		52.74	53.08	53.37	52.71	52.98
CaO		12.54	12.28	11.81	12.59	12.31
FeO		0.31	0.32	0.46	0.41	0.38
K_2O		0.32	0.41	0.45	0.40	0.40
TiO_2						
Total		99.13	99.27	99.39	99.68	
Na	Cations	0.40	0.41	0.42	0.40	0.41
Mg	Norm.					
Al	to	1.55	1.54	1.54	1.56	1.55
Si	8 oxygens	2.42	2.43	2.44	2.41	2.42
Ca		0.62	0.60	0.58	0.62	0.60
Fe		0.01	0.01	0.02	0.02	0.01
K		0.02	0.02	0.03	0.02	0.02
Ti						
		5.02	5.02	5.02	5.03	5.02
An		59.28	58.17	56.30	59.16	58.23
Ab		38.92	39.52	41.15	38.60	39.54
Or		1.80	2.31	2.55	2.24	2.23

Sample 18		Plag 6 Spec. 1	Plag 6 Spec. 2	Plag 6 Spec. 3	Plag 6 Spec. 4	Plag 6 Spec. 5	Plag 6 Spec. 6	Avg.
Na_2O	Oxide	4.16	4.18	4.25	4.12	4.25	4.75	4.29
MgO	wt%							
Al_2O_3		29.54	29.40	29.28	29.57	29.28	28.43	29.25
SiO_2		52.13	52.06	52.47	51.94	52.47	53.19	52.38
CaO		13.11	13.46	13.03	13.16	13.03	11.90	12.95
FeO		0.33	0.23	0.38	0.37	0.38	0.35	0.34
K_2O		0.28	0.26	0.29	0.27	0.29	0.40	0.30
TiO_2								
Total		99.56	99.59	99.70	99.44	99.70	99.01	
Na	Cations	0.37	0.37	0.38	0.37	0.38	0.42	0.38
Mg	Norm.							
Al	to	1.59	1.58	1.57	1.60	1.57	1.54	1.58
Si	8 oxygens	2.38	2.38	2.39	2.38	2.39	2.44	2.39
Ca		0.64	0.66	0.64	0.65	0.64	0.58	0.63
Fe		0.01	0.01	0.01	0.01	0.01	0.01	0.01
K		0.02	0.02	0.02	0.02	0.02	0.02	0.02
Ti								0.00
Total		5.01	5.02	5.01	5.01	5.01	5.02	5.02
An		62.51	63.09	61.85	62.85	61.85	56.74	61.49
Ab		35.90	35.46	36.51	35.61	36.51	40.99	36.83
Or		1.59	1.45	1.64	1.54	1.64	2.27	1.69

Sample 23		Plag 1	Plag 1	Plag 1	Plag 1	Plag 1

		Spec. 1	Spec. 2	Spec. 3	Spec. 4	Spec. 5	Avg.
Na_2O	Oxide	4.88	4.77	4.67	4.83	4.89	4.81
MgO	wt%						
Al_2O_3		28.37	28.27	27.99	28.33	28.38	28.27
SiO_2		54.58	54.38	54.13	54.53	54.41	54.41
CaO		11.84	11.97	12.03	11.98	12.05	11.97
FeO		0.36	0.45	0.46	0.43	0.38	0.42
K_2O		0.44	0.42	0.46	0.50	0.44	0.45
TiO_2		0.13	0.13	0.14	0.17	0.18	0.15
Total		100.61	100.38	99.89	100.77	100.72	
Na	Cations	0.43	0.42	0.41	0.42	0.43	0.42
Mg	Norm.						
Al	to	1.51	1.51	1.50	1.50	1.51	1.50
Si	8 oxygens	2.46	2.46	2.46	2.46	2.45	2.46
Ca		0.57	0.58	0.59	0.58	0.58	0.58
Fe		0.01	0.02	0.02	0.02	0.01	0.02
K		0.03	0.02	0.03	0.03	0.03	0.03
Ti		0.00	0.00	0.00	0.01	0.01	0.01
Total		5.01	5.01	5.00	5.01	5.01	5.01
An		55.86	56.72	57.21	56.20	56.25	56.45
Ab		41.67	40.91	40.19	41.00	41.31	41.01
Or		2.47	2.37	2.60	2.79	2.45	2.54

Sample 23		Plag 2 Spec. 1	Plag 2 Spec. 2	Plag 2 Spec. 3	Plag 2 Spec. 4	Plag 2 Spec. 5	Avg.
Na_2O	Oxide	4.29	4.34	4.23	4.39	4.30	4.31
MgO	wt%						
Al_2O_3		29.22	29.28	29.20	29.29	28.98	29.19
SiO_2		52.89	52.42	52.92	52.88	52.56	52.73
CaO		12.88	12.82	13.01	12.97	13.07	12.95
FeO		0.47	0.41	0.59	0.54	0.45	0.49
K_2O		0.39	0.38	0.39	0.39	0.34	0.38
TiO_2		0.08	0.07	0.04	0.17	0.06	0.08
Total		100.22	99.72	100.36	100.63	99.75	
Na	Cations	0.38	0.38	0.37	0.39	0.38	0.38
Mg	Norm.						
Al	to	1.56	1.58	1.56	1.56	1.56	1.56
Si	8 oxygens	2.40	2.39	2.40	2.39	2.40	2.40
Ca		0.63	0.63	0.63	0.63	0.64	0.63
Fe		0.02	0.02	0.02	0.02	0.02	0.02
K		0.02	0.02	0.02	0.02	0.02	0.02
Ti		0.00	0.00	0.00	0.01	0.00	0.00
Total		5.01	5.02	5.01	5.02	5.02	5.02
An		61.02	60.68	61.57	60.67	61.49	61.09
Ab		36.78	37.18	36.23	37.16	36.61	36.79
Or		2.20	2.14	2.20	2.17	1.90	2.12

Sample 23		Plag 3 Spec. 1	Plag 3 Spec. 2	Plag 3 Spec. 3	Plag 3 Spec. 4	Plag 3 Spec. 5	Avg.
Na_2O	Oxide	3.83	3.74	3.55	3.71	3.98	3.76
MgO	wt%						
Al_2O_3		29.52	29.61	29.96	30.10	29.62	29.76
SiO_2		51.57	51.32	50.51	50.84	51.67	51.18
CaO		13.65	13.76	14.39	14.10	13.56	13.89

FeO		0.48	0.36	0.43	0.38	0.44	0.42
K_2O		0.37	0.29	0.24	0.29	0.30	0.30
TiO_2		0.08	0.10	0.08	0.07	0.08	0.08
Total		99.50	99.19	99.16	99.47	99.65	
Na	Cations	0.34	0.33	0.32	0.33	0.35	0.33
Mg	Norm.						
Al	to	1.60	1.60	1.63	1.63	1.60	1.61
Si	8 oxygens	2.37	2.36	2.33	2.33	2.37	2.35
Ca		0.67	0.68	0.71	0.69	0.66	0.68
Fe		0.02	0.01	0.02	0.01	0.02	0.02
K		0.02	0.02	0.01	0.02	0.02	0.02
Ti		0.00	0.00	0.00	0.00	0.00	0.00
Total		5.02	5.01	5.02	5.02	5.02	5.02
An		64.93	65.92	68.20	66.64	64.21	65.98
Ab		32.97	32.42	30.45	31.73	34.10	32.33
Or		2.10	1.65	1.35	1.63	1.69	1.68

Sample 29		Plag 1 Spec. 1	Plag 1 Spec. 2	Plag 1 Spec. 3	Plag 1 Spec. 4	Plag 1 Spec. 5	Plag 1 Spec. 6	Avg.
Na_2O	Oxide	4.79	4.79	4.88	5.03	4.83	4.90	4.87
MgO	wt%							
Al_2O_3		28.29	28.27	28.15	28.04	27.86	28.02	28.11
SiO_2		54.07	53.53	53.61	54.05	54.14	54.66	54.01
CaO		11.74	11.81	11.92	11.83	11.84	11.80	11.82
FeO		0.41	0.43	0.45	0.51	0.47	0.41	0.45
K_2O		0.44	0.49	0.52	0.47	0.50	0.51	0.49
TiO_2		0.08	0.16	0.07	0.19	0.04	0.18	0.12
		99.81	99.49	99.60	100.13	99.68	100.48	
Na	Cations	0.42	0.42	0.43	0.44	0.43	0.43	0.43
Mg	Norm.							
Al	to	1.51	1.52	1.51	1.50	1.50	1.49	1.51
Si	8 oxygens	2.46	2.44	2.45	2.45	2.47	2.47	2.46
Ca		0.57	0.58	0.58	0.58	0.58	0.57	0.58
Fe		0.02	0.02	0.02	0.02	0.02	0.02	0.02
K		0.03	0.03	0.03	0.03	0.03	0.03	0.03
Ti		0.00	0.01	0.00	0.01	0.00	0.01	0.00
Total		5.01	5.02	5.03	5.02	5.01	5.01	5.02
An		56.09	56.07	55.78	55.04	55.91	55.47	55.72
Ab		41.41	41.16	41.32	42.35	41.28	41.68	41.53
Or		2.50	2.77	2.90	2.60	2.81	2.85	2.74

Sample 29		Plag 2 Spec. 1	Plag 2 Spec. 2	Plag 2 Spec. 3	Plag 2 Spec. 4	Plag 2 Spec. 5	Avg.
Na_2O	Oxide	4.34	4.17	4.33	4.19	4.23	4.25
MgO	wt%						
Al_2O_3		28.69	29.02	29.13	29.16	29.38	29.08
SiO_2		52.36	52.67	52.49	52.44	52.09	52.41
CaO		12.74	12.93	12.81	13.13	13.33	12.99
FeO		0.47	0.51	0.41	0.53	0.54	0.49
K_2O		0.39	0.41	0.47	0.41	0.39	0.41
TiO_2		0.09	0.06	0.05	0.09	0.11	0.08
		99.08	99.77	99.68	99.95	100.07	
Na	Cations	0.39	0.37	0.38	0.37	0.37	0.38

Mg	Norm.						
Al	to	1.55	1.56	1.57	1.57	1.58	1.57
Si	8 oxygens	2.41	2.40	2.40	2.39	2.38	2.40
Ca		0.63	0.63	0.63	0.64	0.65	0.64
Fe		0.02	0.02	0.02	0.02	0.02	0.02
K		0.02	0.02	0.03	0.02	0.02	0.02
Ti		0.00	0.00	0.00	0.00	0.00	0.00
Total		5.02	5.01	5.02	5.02	5.03	5.02
An		60.50	61.68	60.41	61.93	62.15	61.33
Ab		37.30	36.00	36.95	35.76	35.69	36.34
Or		2.21	2.33	2.64	2.30	2.16	2.33

Sample 29		Plag 3 Spec. 1	Plag 3 Spec. 2	Plag 3 Spec. 3	Plag 3 Spec. 4	Plag 3 Spec. 5	Plag 3 Spec. 6	Avg.
Na_2O	Oxide	4.19	4.31	4.36	4.12	4.41	4.32	4.29
MgO	wt%							
Al_2O_3		29.11	28.96	28.93	28.53	29.17	28.63	28.89
SiO_2		52.51	52.01	52.24	52.51	52.28	52.52	52.35
CaO		13.16	12.96	12.71	13.04	12.71	12.82	12.90
FeO		0.40	0.40	0.43	0.46	0.53	0.45	0.45
K_2O		0.35	0.35	0.40	0.34	0.30	0.38	0.35
TiO_2		0.08	0.09	0.15	0.13	0.14	0.08	0.11
		99.81	99.07	99.22	99.13	99.55	99.20	
Na	Cations	0.37	0.38	0.39	0.37	0.39	0.38	0.38
Mg	Norm.							
Al	to	1.57	1.57	1.56	1.54	1.57	1.55	1.56
Si	8 oxygens	2.40	2.39	2.40	2.41	2.39	2.41	2.40
Ca		0.64	0.64	0.62	0.64	0.62	0.63	0.63
Fe		0.02	0.02	0.02	0.02	0.02	0.02	0.02
K		0.02	0.02	0.02	0.02	0.02	0.02	0.02
Ti		0.00	0.00	0.01	0.00	0.00	0.00	0.00
Total		5.01	5.02	5.02	5.01	5.02	5.02	5.02
An		62.20	61.20	60.31	62.39	60.39	60.79	61.21
Ab		35.83	36.83	37.44	35.67	37.92	37.07	36.79
Or		1.97	1.97	2.26	1.94	1.70	2.15	2.00

Sample 35		Plag 1 Spec. 1	Plag 1 Spec. 2	Plag 1 Spec. 3	Plag 1 Spec. 4	Plag 1 Spec. 5	Avg.
Na_2O	Oxide	5.16	4.92	4.62	4.92	5.11	4.95
MgO	wt%						
Al_2O_3		27.40	27.98	27.79	27.77	27.79	27.75
SiO_2		54.67	54.23	54.54	54.53	54.03	54.40
CaO		11.25	11.24	11.24	11.32	11.30	11.27
FeO		0.34	0.45	0.44	0.37	0.42	0.40
K_2O		0.49	0.47	0.47	0.50	0.47	0.48
TiO_2			0.05		0.12	0.12	0.10
Total		99.31	99.34	99.12	99.53	99.24	
Na	Cations	0.46	0.43	0.41	0.43	0.45	0.44
Mg	Norm.						
Al	to	1.47	1.50	1.49	1.49	1.50	1.49
Si	8 oxygens	2.49	2.47	2.49	2.48	2.47	2.48
Ca		0.55	0.55	0.55	0.55	0.55	0.55
Fe		0.01	0.02	0.02	0.01	0.02	0.02
K		0.03	0.03	0.03	0.03	0.03	0.03

Ti		0.00	0.00	0.00	0.00	0.00
Total	5.01	5.01	4.98	5.00	5.02	5.00
An	53.14	54.29	55.75	54.37	53.54	54.20
Ab	44.11	43.01	41.47	42.77	43.81	43.05
Or	2.76	2.70	2.78	2.86	2.65	2.75

Sample 35		Plag 2 Spec. 1	Plag 2 Spec. 2	Plag 2 Spec. 3	Plag 2 Spec. 4	Plag 2 Spec. 5	Plag 2 Spec. 6	Avg.
Na_2O	Oxide	4.57	4.66	4.44	4.62	4.52	4.40	4.54
MgO	wt%							
Al_2O_3		28.73	28.93	28.32	28.79	28.63	28.66	28.68
SiO_2		53.18	52.99	53.29	53.13	53.26	53.09	53.16
CaO		12.51	12.59	12.16	12.46	12.31	12.48	12.42
FeO		0.42	0.47	0.48	0.41	0.39	0.41	0.43
K_2O		0.45	0.41	0.44	0.45	0.47	0.45	0.45
TiO_2		0.17	0.11	0.07	0.15	0.17	0.14	0.14
Total		100.03	100.16	99.19	100.01	99.75	99.62	
Na	Cations	0.40	0.41	0.39	0.41	0.40	0.39	0.40
Mg	Norm.							
Al	to	1.54	1.55	1.53	1.54	1.54	1.54	1.54
Si	8 oxygens	2.42	2.41	2.44	2.42	2.43	2.42	2.42
Ca		0.61	0.61	0.60	0.61	0.60	0.61	0.61
Fe		0.02	0.02	0.02	0.02	0.01	0.02	0.02
K		0.03	0.02	0.03	0.03	0.03	0.03	0.03
Ti		0.01	0.00	0.00	0.01	0.01	0.00	0.00
Total		5.02	5.03	5.00	5.02	5.01	5.01	5.02
An		58.69	58.53	58.69	58.34	58.48	59.49	58.70
Ab		38.80	39.20	38.78	39.15	38.86	37.96	38.79
Or		2.51	2.27	2.53	2.51	2.66	2.55	2.50

Sample 35		Plag 3 Spec. 1	Plag 3 Spec. 2	Plag 3 Spec. 3	Plag 3 Spec. 4	Plag 3 Spec. 5	Plag 3 Spec. 6	Avg.
Na_2O	Oxide	4.75	4.71	4.80	4.54	4.68	4.81	4.72
MgO	wt%							
Al_2O_3		28.51	28.41	28.15	28.33	28.18	28.48	28.34
SiO_2		53.64	53.62	53.38	53.43	53.37	53.74	53.53
CaO		11.99	12.10	11.99	11.98	12.01	12.01	12.01
FeO		0.46	0.45	0.35	0.53	0.49	0.50	0.46
K_2O		0.51	0.47	0.51	0.43	0.48	0.50	0.48
TiO_2		0.07	0.17	0.17	0.18	0.06	0.11	0.13
Total		99.93	99.93	99.36	99.41	99.27	100.16	
Na	Cations	0.42	0.42	0.43	0.40	0.42	0.42	0.42
Mg	Norm.							
Al	to	1.53	1.52	1.52	1.52	1.52	1.52	1.52
Si	8 oxygens	2.44	2.44	2.44	2.44	2.44	2.44	2.44
Ca		0.58	0.59	0.59	0.59	0.59	0.58	0.59
Fe		0.02	0.02	0.01	0.02	0.02	0.02	0.02
K		0.03	0.03	0.03	0.03	0.03	0.03	0.03
Ti		0.00	0.01	0.01	0.01	0.00	0.00	0.00
Total		5.02	5.02	5.02	5.00	5.02	5.02	5.02
An		56.58	57.12	56.34	57.85	57.05	56.36	56.88
Ab		40.56	40.24	40.81	39.67	40.23	40.85	40.40
Or		2.87	2.64	2.85	2.47	2.71	2.79	2.72

Sample 37		Plag 1 Spec. 1	Plag 1 Spec. 2	Plag 1 Spec. 3	Plag 1 Spec. 4	Plag 1 Spec. 5	Plag 1 Spec. 6	Avg.
Na_2O	Oxide	5.13	5.21	5.12	5.13	5.12	5.16	5.15
MgO	wt%	0.17	0.12	0.16	0.18	0.18	0.17	0.16
Al_2O_3		27.67	27.14	27.28	27.29	27.27	27.25	27.32
SiO_2		54.31	54.53	54.47	54.57	54.71	54.23	54.47
CaO		11.17	11.18	11.32	11.32	11.30	11.25	11.26
FeO		0.47	0.49	0.65	0.57	0.49	0.58	0.54
K_2O		0.36	0.39	0.35	0.40	0.35	0.45	0.38
TiO_2		0.12	0.14	0.15	0.07	0.15	0.15	0.13
Total		99.39	99.20	99.49	99.54	99.58	99.23	
Na	Cations	0.45	0.46	0.45	0.45	0.45	0.46	0.45
Mg	Norm.	0.01	0.01	0.01	0.01	0.01	0.01	0.01
Al	to	1.49	1.46	1.47	1.47	1.46	1.47	1.47
Si	8 oxygens	2.48	2.49	2.48	2.49	2.49	2.48	2.48
Ca		0.55	0.55	0.55	0.55	0.55	0.55	0.55
Fe		0.02	0.02	0.02	0.02	0.02	0.02	0.02
K		0.02	0.02	0.02	0.02	0.02	0.03	0.02
Ti		0.00	0.00	0.01	0.00	0.01	0.01	0.00
Total		5.01	5.02	5.02	5.02	5.01	5.02	5.02
An		53.49	53.06	53.90	53.70	53.86	53.26	53.54
Ab		44.46	44.74	44.12	44.04	44.16	44.21	44.29
Or		2.05	2.20	1.98	2.26	1.99	2.54	2.17

Sample 37		Plag 2 Spec. 1	Plag 2 Spec. 2	Plag 2 Spec. 3	Plag 2 Spec. 4	Plag 2 Spec. 5	Plag 2 Spec. 6	Avg.
Na_2O	Oxide	5.19	5.19	5.20	5.09	5.15	5.29	5.19
MgO	wt%	0.06	0.09	0.11	0.16	0.12	0.15	0.12
Al_2O_3		27.62	27.54	27.59	27.81	27.67	27.69	27.65
SiO_2		54.61	54.23	54.39	54.12	55.01	54.67	54.51
CaO		11.54	11.41	11.47	11.57	11.59	11.36	11.49
FeO		0.62	0.69	0.62	0.54	0.59	0.57	0.61
K_2O		0.36	0.36	0.36	0.35	0.34	0.39	0.36
TiO_2		0.09	0.08	0.14	0.10	0.13	0.11	0.11
Total		100.08	99.61	99.88	99.73	100.58	100.23	
Na	Cations	0.46	0.46	0.46	0.45	0.45	0.46	0.46
Mg	Norm.	0.00	0.01	0.01	0.01	0.01	0.01	0.01
Al	to	1.48	1.48	1.48	1.49	1.47	1.48	1.48
Si	8 oxygens	2.48	2.47	2.47	2.46	2.48	2.48	2.47
Ca		0.56	0.56	0.56	0.56	0.56	0.55	0.56
Fe		0.02	0.03	0.02	0.02	0.02	0.02	0.02
K		0.02	0.02	0.02	0.02	0.02	0.02	0.02
Ti		0.00	0.00	0.00	0.00	0.00	0.00	0.00
Total		5.02	5.02	5.02	5.02	5.01	5.03	5.02
An		54.02	53.74	53.83	54.58	54.38	53.09	53.94
Ab		43.97	44.24	44.16	43.45	43.72	44.74	44.05
Or		2.01	2.02	2.01	1.97	1.90	2.17	2.01

Sample 39		Plag 1 Spec. 1	Plag 1 Spec. 2	Plag 1 Spec. 3	Plag 1 Spec. 4	Plag 1 Spec. 5	Plag 1 Spec. 6	Avg.
Na_2O	Oxide	2.47	2.45	2.33	2.35	2.35	2.39	2.39
MgO	wt%	0.05	0.02	0.07	0.09	0.10	0.02	0.06

Al_2O_3		31.77	31.90	31.74	32.30	32.22	31.66	31.93
SiO_2		48.08	47.88	47.91	48.10	47.80	47.85	47.94
CaO		16.34	16.37	16.34	16.46	16.66	16.55	16.45
FeO		0.47	0.42	0.58	0.55	0.54	0.44	0.50
K_2O		0.23	0.13	0.19	0.18	0.15	0.16	0.17
TiO_2		0.02	0.03	0.04	0.10	0.02	0.08	0.05
Total		99.42	99.22	99.19	100.14	99.83	99.14	
Na	Cations	0.22	0.22	0.21	0.21	0.21	0.22	0.21
Mg	Norm.	0.00	0.00	0.00	0.01	0.01	0.00	0.00
Al	to	1.73	1.74	1.74	1.75	1.75	1.73	1.74
Si	8 oxygens	2.23	2.22	2.22	2.21	2.21	2.22	2.22
Ca		0.81	0.81	0.81	0.81	0.82	0.82	0.82
Fe		0.02	0.02	0.02	0.02	0.02	0.02	0.02
K		0.01	0.01	0.01	0.01	0.01	0.01	0.01
Ti		0.00	0.00	0.00	0.00	0.00	0.00	0.00
Total		5.03	5.02	5.02	5.02	5.03	5.02	5.02
An		77.50	78.11	78.62	78.65	78.99	78.56	78.41
Ab		21.20	21.15	20.29	20.32	20.16	20.53	20.61
Or		1.30	0.74	1.09	1.02	0.85	0.90	0.98

Sample 39		Plag 2 Spec. 1	Plag 2 Spec. 2	Plag 2 Spec. 3	Plag 2 Spec. 4	Plag 2 Spec. 5	Plag 2 Spec. 6	Avg.
Na_2O	Oxide	5.02	5.09	5.13	5.12	5.00	5.11	5.08
MgO	wt%	0.09	0.13	0.04		0.04		0.08
Al_2O_3		27.68	27.49	27.60	27.56	27.80	27.67	27.63
SiO_2		54.08	54.44	54.20	53.97	54.26	54.34	54.22
CaO		11.22	11.25	11.15	11.30	11.23	11.22	11.23
FeO		0.35	0.36	0.41	0.36	0.40	0.40	0.38
K_2O		0.65	0.58	0.61	0.60	0.57	0.62	0.61
TiO_2		0.13	0.03	0.09	0.15	0.11	0.11	0.10
Total		99.22	99.37	99.23	99.06	99.41	99.47	
Na	Cations	0.44	0.45	0.45	0.45	0.44	0.45	0.45
Mg	Norm.	0.01	0.01	0.00		0.00		0.00
Al	to	1.49	1.48	1.49	1.49	1.49	1.49	1.49
Si	8 oxygens	2.47	2.48	2.48	2.47	2.47	2.48	2.48
Ca		0.55	0.55	0.55	0.55	0.55	0.55	0.55
Fe		0.01	0.01	0.02	0.01	0.02	0.02	0.01
K		0.04	0.03	0.04	0.04	0.03	0.04	0.04
Ti		0.00	0.00	0.00	0.01	0.00	0.00	0.00
Total		5.02	5.02	5.02	5.02	5.01	5.02	5.02
An		53.23	53.19	52.69	53.10	53.59	52.91	53.12
Ab		43.10	43.55	43.87	43.54	43.18	43.61	43.47
Or		3.67	3.26	3.43	3.36	3.24	3.48	3.41

Sample 39		Plag 3 Spec. 1	Plag 3 Spec. 2	Plag 3 Spec. 3	Plag 3 Spec. 4	Plag 3 Spec. 5	Plag 3 Spec. 6	Avg.
Na_2O	Oxide	2.70	2.68	2.74	2.79	2.70	2.73	2.72
MgO	wt%		0.06	0.05	0.12	0.08	0.03	0.07
Al_2O_3		31.45	31.16	31.53	31.44	31.31	31.53	31.40
SiO_2		48.51	48.51	48.63	48.85	48.46	48.67	48.61
CaO		15.88	16.01	15.83	15.80	15.84	15.81	15.86
FeO		0.36	0.38	0.39	0.39	0.41	0.33	0.38
K_2O		0.24	0.21	0.30	0.21	0.24	0.22	0.24
TiO_2		0.07	0.08	0.08	0.13	0.05	0.02	0.07

Total		99.22	99.10	99.53	99.72	99.08	99.34	
Na	Cations	0.24	0.24	0.25	0.25	0.24	0.24	0.24
Mg	Norm.		0.00	0.00	0.01	0.01	0.00	0.00
Al	to	1.72	1.70	1.72	1.71	1.71	1.72	1.71
Si	8 oxygens	2.25	2.25	2.24	2.25	2.25	2.25	2.25
Ca		0.79	0.80	0.78	0.78	0.79	0.78	0.79
Fe		0.01	0.01	0.02	0.02	0.02	0.01	0.01
K		0.01	0.01	0.02	0.01	0.01	0.01	0.01
Ti		0.00	0.00	0.00	0.00	0.00	0.00	0.00
Total		5.02	5.02	5.03	5.02	5.02	5.02	5.02
An		75.43	75.84	74.86	74.89	75.39	75.24	75.28
Ab		23.21	22.97	23.45	23.93	23.25	23.51	23.39
Or		1.36	1.18	1.69	1.19	1.36	1.25	1.34

Sample 44		Plag 1 Spec. 1	Plag 1 Spec. 2	Plag 1 Spec. 3	Plag 1 Spec. 4	Plag 1 Spec. 5	Plag 1 Spec. 6	Avg.
Na_2O	Oxide	2.64	2.53	2.57	2.62	2.58	2.59	2.59
MgO	wt%							
Al_2O_3		31.75	31.76	31.54	31.79	31.35	31.76	31.66
SiO_2		48.45	48.16	48.21	48.06	48.14	48.55	48.26
CaO		16.26	16.17	16.02	16.21	16.06	16.20	16.15
FeO		0.46	0.51	0.62	0.52	0.47	0.53	0.52
K_2O		0.16	0.18	0.25	0.19	0.19	0.22	0.20
TiO_2			0.08	0.08		0.03		0.06
Total		99.71	99.38	99.29	99.38	98.83	99.84	
Na	Cations	0.24	0.23	0.23	0.24	0.23	0.23	0.23
Mg	Norm.							
Al	to	1.73	1.73	1.72	1.73	1.72	1.72	1.73
Si	8 oxygens	2.23	2.23	2.23	2.23	2.24	2.24	2.23
Ca		0.80	0.80	0.80	0.80	0.80	0.80	0.80
Fe		0.02	0.02	0.02	0.02	0.02	0.02	0.02
K		0.01	0.01	0.01	0.01	0.01	0.01	0.01
Ti		0.00	0.00	0.00	0.00	0.00	0.00	0.00
Total		5.03	5.02	5.02	5.03	5.02	5.02	5.02
An		76.60	77.14	76.40	76.54	76.64	76.60	76.65
Ab		22.51	21.84	22.18	22.39	22.28	22.16	22.23
Or		0.90	1.02	1.42	1.07	1.08	1.24	1.12

Sample 44		Plag 2 Spec. 1	Plag 2 Spec. 2	Plag 2 Spec. 3	Plag 2 Spec. 4	Plag 2 Spec. 5	Plag 2 Spec. 6	Avg.
Na_2O	Oxide	4.01	4.04	4.03	4.02	4.09	3.98	4.03
MgO	wt%							
Al_2O_3		29.44	29.48	29.36	29.18	29.49	29.39	29.39
SiO_2		51.61	51.87	51.38	51.98	51.94	51.47	51.71
CaO		13.35	13.53	13.43	13.53	13.27	13.43	13.42
FeO		0.60	0.45	0.53	0.61	0.53	0.64	0.56
K_2O		0.38	0.36	0.42	0.42	0.40	0.37	0.39
TiO_2		0.09	0.10	0.02	0.04	0.15	0.10	0.08
Total		99.48	99.83	99.16	99.79	99.87	99.39	
Na	Cations	0.36	0.36	0.36	0.36	0.36	0.35	0.36
Mg	Norm.							
Al	to	1.59	1.59	1.59	1.57	1.59	1.59	1.59
Si	8 oxygens	2.37	2.37	2.37	2.38	2.37	2.37	2.37

Ca		0.66	0.66	0.66	0.66	0.65	0.66	0.66
Fe		0.02	0.02	0.02	0.02	0.02	0.02	0.02
K		0.02	0.02	0.02	0.02	0.02	0.02	0.02
Ti		0.00	0.00	0.00	0.00	0.01	0.00	0.00
Total		5.02	5.02	5.03	5.02	5.02	5.02	5.02
An		63.39	63.61	63.28	63.51	62.75	63.73	63.38
Ab		34.46	34.37	34.36	34.15	35.00	34.18	34.42
Or		2.15	2.02	2.36	2.35	2.25	2.09	2.20

Sample 44		Plag 3 Spec. 1	Plag 3 Spec. 2	Plag 3 Spec. 3	Plag 3 Spec. 4	Plag 3 Spec. 5	Plag 3 Spec. 6	Avg.
Na_2O	Oxide	4.03	3.93	3.94	3.95	3.94	3.94	3.96
MgO	wt%							
Al_2O_3		29.69	29.74	29.56	29.79	29.37	29.38	29.59
SiO_2		51.39	51.29	51.32	51.45	51.49	51.06	51.33
CaO		13.80	13.74	13.84	13.56	13.67	13.82	13.74
FeO		0.60	0.59	0.73	0.51	0.71	0.51	0.61
K_2O		0.33	0.23	0.31	0.32	0.32	0.31	0.30
TiO_2		0.11	0.04	0.12	0.07	0.10	0.09	0.09
Total		99.94	99.55	99.82	99.65	99.58	99.11	
Na	Cations	0.36	0.35	0.35	0.35	0.35	0.35	0.35
Mg	Norm.							
Al	to	1.60	1.61	1.60	1.61	1.59	1.60	1.60
Si	8 oxygens	2.35	2.35	2.35	2.36	2.36	2.36	2.36
Ca		0.68	0.68	0.68	0.67	0.67	0.68	0.68
Fe		0.02	0.02	0.03	0.02	0.03	0.02	0.02
K		0.02	0.01	0.02	0.02	0.02	0.02	0.02
Ti		0.00	0.00	0.00	0.00	0.00	0.00	0.00
Total		5.03	5.02	5.03	5.02	5.02	5.03	5.03
An		64.23	65.04	64.86	64.30	64.54	64.82	64.63
Ab		33.94	33.66	33.41	33.89	33.66	33.44	33.67
Or		1.83	1.30	1.73	1.81	1.80	1.73	1.70

Sample 55		Plag 1 Spec. 1	Plag 1 Spec. 2	Plag 1 Spec. 3	Plag 1 Spec. 4	Plag 1 Spec. 5	Avg.
Na_2O	Oxide	2.35	2.28	2.37	2.37	2.31	2.34
MgO	wt%						
Al_2O_3		32.20	32.40	32.46	32.25	32.36	32.33
SiO_2		48.13	48.37	48.06	48.27	48.02	48.17
CaO		16.47	16.80	16.70	16.57	16.65	16.64
FeO		0.55	0.44	0.56	0.48	0.46	0.50
K_2O		0.18	0.21	0.17	0.19	0.23	0.20
TiO_2		0.07	0.19		0.14		0.13
Total		99.96	100.68	100.32	100.28	100.03	
Na	Cations	0.21	0.20	0.21	0.21	0.21	0.21
Mg	Norm.						
Al	to	1.75	1.75	1.76	1.74	1.75	1.75
Si	8 oxygens	2.22	2.21	2.21	2.22	2.21	2.21
Ca		0.81	0.82	0.82	0.81	0.82	0.82
Fe		0.02	0.02	0.02	0.02	0.02	0.02
K		0.01	0.01	0.01	0.01	0.01	0.01
Ti		0.00	0.01		0.00		0.00
Total		5.02	5.02	5.03	5.02	5.02	5.02

An		78.66	79.34	78.81	78.59	78.89	78.86
Ab		20.31	19.48	20.24	20.34	19.81	20.04
Or		1.02	1.18	0.96	1.07	1.30	1.11

Sample 55		Plag 2 Spec. 1	Plag 2 Spec. 2	Plag 2 Spec. 3	Plag 2 Spec. 4	Avg.
Na_2O	Oxide	2.06	2.05	2.09	2.06	2.07
MgO	wt%					
Al_2O_3		32.36	32.26	32.31	32.35	32.32
SiO_2		47.36	46.84	47.07	47.11	47.10
CaO		17.06	17.12	17.15	17.16	17.12
FeO		0.60	0.60	0.63	0.61	0.61
K_2O		0.16	0.19	0.14	0.13	0.16
TiO_2		0.07		0.09		0.08
Total		99.68	99.07	99.48	99.43	
Na	Cations	0.18	0.19	0.19	0.19	0.19
Mg	Norm.					
Al	to	1.76	1.77	1.77	1.77	1.77
Si	8 oxygens	2.19	2.18	2.18	2.19	2.19
Ca		0.85	0.85	0.85	0.85	0.85
Fe		0.02	0.02	0.02	0.02	0.02
K		0.01	0.01	0.01	0.01	0.01
Ti		0.00		0.00		0.00
Total		5.02	5.03	5.03	5.03	5.03
An		81.32	81.31	81.28	81.55	81.37
Ab		17.77	17.62	17.93	17.72	17.76
Or		0.91	1.07	0.79	0.74	0.88

Sample 55		Plag 3 Spec. 1	Plag 3 Spec. 2	Plag 3 Spec. 3	Plag 3 Spec. 4	Plag 3 Spec. 5	Avg.
Na_2O	Oxide	2.32	2.34	2.37	2.18	2.33	2.31
MgO	wt%						
Al_2O_3		32.33	32.45	32.20	32.21	32.33	32.30
SiO_2		48.33	48.24	48.05	48.62	48.20	48.29
CaO		16.68	16.67	16.52	16.80	16.99	16.73
FeO		0.56	0.64	0.41	0.56	0.63	0.56
K_2O		0.18	0.19	0.17	0.21	0.15	0.18
TiO_2							
Total		100.41	100.53	99.72	100.58	100.63	
Na	Cations	0.21	0.21	0.21	0.19	0.21	0.21
Mg	Norm.						
Al	to	1.75	1.75	1.75	1.74	1.75	1.75
Si	8 oxygens	2.22	2.21	2.22	2.22	2.21	2.21
Ca		0.82	0.82	0.82	0.82	0.83	0.82
Fe		0.02	0.02	0.02	0.02	0.02	0.02
K		0.01	0.01	0.01	0.01	0.01	0.01
Ti							
Total		5.02	5.02	5.02	5.01	5.03	5.02
An		79.08	78.89	78.62	80.02	79.45	79.21
Ab		19.90	20.04	20.41	18.79	19.72	19.77
Or		1.02	1.07	0.96	1.19	0.84	1.01

Sample 67		Plag 1	Plag 1	Plag 1	Plag 1	Plag 1

		Spec. 1	Spec. 2	Spec. 3	Spec. 4	Spec. 5	Avg.
Na_2O	Oxide	2.30	2.41	2.26	2.41	2.27	2.33
MgO	wt%	0.09	0.14	0.13	0.15	0.07	0.12
Al_2O_3		32.02	32.27	32.02	32.34	32.11	32.15
SiO_2		48.04	48.61	48.22	48.04	47.63	48.11
CaO		16.50	16.71	16.57	16.48	16.76	16.60
FeO		0.48	0.49	0.45	0.54	0.58	0.51
K_2O		0.14	0.14	0.18	0.10	0.21	0.15
TiO_2		0.07				0.09	0.08
Total		99.64	100.78	99.83	100.06	99.72	
Na	Cations	0.21	0.21	0.20	0.21	0.20	0.21
Mg	Norm.	0.01	0.01	0.01	0.01	0.00	0.01
Al	to	1.74	1.74	1.74	1.75	1.75	1.74
Si	8 oxygens	2.22	2.22	2.22	2.21	2.20	2.21
Ca		0.82	0.82	0.82	0.81	0.83	0.82
Fe		0.02	0.02	0.02	0.02	0.02	0.02
K		0.01	0.01	0.01	0.01	0.01	0.01
Ti		0.00			0.00	0.00	0.00
Total		5.02	5.02	5.02	5.03	5.03	5.02
An		79.22	78.68	79.38	78.63	79.36	79.05
Ab		19.98	20.53	19.59	20.81	19.45	20.07
Or		0.80	0.78	1.03	0.57	1.18	0.87

Sample 67		Plag 2 Spec. 1	Plag 2 Spec. 2	Plag 2 Spec. 3	Plag 2 Spec. 4	Plag 2 Spec. 5	Avg.
Na_2O	Oxide	2.19	2.29	2.37	2.36	2.37	2.32
MgO	wt%						
Al_2O_3		31.93	32.14	32.14	31.93	32.19	32.07
SiO_2		47.48	47.43	47.81	47.95	47.96	47.73
CaO		16.66	16.52	16.57	16.53	16.83	16.62
FeO		0.59	0.59	0.53	0.59	0.48	0.56
K_2O		0.17	0.18	0.17	0.15	0.19	0.17
TiO_2					0.12		0.12
Total		99.02	99.15	99.59	99.62	100.02	
Na	Cations	0.20	0.21	0.21	0.21	0.21	0.21
Mg	Norm.						
Al	to	1.75	1.76	1.75	1.74	1.75	1.75
Si	8 oxygens	2.21	2.20	2.21	2.22	2.21	2.21
Ca		0.83	0.82	0.82	0.82	0.83	0.82
Fe		0.02	0.02	0.02	0.02	0.02	0.02
K		0.01	0.01	0.01	0.01	0.01	0.01
Ti					0.00		0.00
Total		5.02	5.03	5.03	5.02	5.03	5.02
An		80.00	79.13	78.68	78.79	78.85	79.09
Ab		19.03	19.85	20.36	20.36	20.09	19.94
Or		0.97	1.03	0.96	0.85	1.06	0.97

Sample 67		Plag 3 Spec. 1	Plag 3 Spec. 2	Plag 3 Spec. 3	Plag 3 Spec. 4	Plag 3 Spec. 5	Avg.
Na_2O	Oxide	1.92	2.02	2.00	2.07	1.86	1.97
MgO	wt%	0.13			0.13	0.12	0.13
Al_2O_3		32.49	31.82	32.20	32.18	32.01	32.14
SiO_2		47.11	47.47	46.87	46.85	46.87	47.03
CaO		17.12	17.09	17.26	17.05	16.99	17.10

FeO		0.54	0.64	0.61	0.68	0.52	0.60
K_2O		0.11	0.17	0.12	0.16	0.13	0.14
TiO_2			0.12				0.12
Total		99.42	99.31	99.04	99.11	98.50	
Na	Cations	0.17	0.18	0.18	0.19	0.17	0.18
Mg	Norm.	0.01			0.01	0.01	0.01
Al	to	1.78	1.74	1.77	1.77	1.76	1.76
Si	8 oxygens	2.18	2.20	2.18	2.18	2.19	2.19
Ca		0.85	0.85	0.86	0.85	0.85	0.85
Fe		0.02	0.02	0.02	0.03	0.02	0.02
K		0.01	0.01	0.01	0.01	0.01	0.01
Ti			0.00				0.00
Total		5.02	5.02	5.03	5.03	5.01	5.02
An		82.60	81.58	82.10	81.24	82.83	82.07
Ab		16.76	17.45	17.22	17.85	16.41	17.14
Or		0.63	0.97	0.68	0.91	0.75	0.79

Sample 75		Plag 1 Spec. 1	Plag 1 Spec. 2	Plag 1 Spec. 3	Plag 1 Spec. 4	Plag 1 Spec. 5	Plag 1 Spec. 6	Avg.
Na_2O	Oxide	2.17	1.93	2.10	1.99	1.79	1.81	1.97
MgO	wt%							
Al_2O_3		32.67	32.51	32.66	32.58	32.76	32.83	32.67
SiO_2		47.44	47.69	47.27	47.08	47.34	46.74	47.26
CaO		17.15	17.01	17.25	17.50	17.63	17.68	17.37
FeO		0.56	0.47	0.57	0.52	0.60	0.59	0.55
K_2O		0.14	0.16	0.13	0.12	0.15	0.13	0.14
TiO_2		0.09						0.09
Total		100.22	99.77	99.98	99.78	100.28	99.78	
Na	Cations	0.19	0.17	0.19	0.18	0.16	0.16	0.18
Mg	Norm.							
Al	to	1.77	1.77	1.78	1.78	1.78	1.79	1.78
Si	8 oxygens	2.18	2.20	2.18	2.18	2.18	2.16	2.18
Ca		0.85	0.84	0.85	0.87	0.87	0.88	0.86
Fe		0.02	0.02	0.02	0.02	0.02	0.02	0.02
K		0.01	0.01	0.01	0.01	0.01	0.01	0.01
Ti		0.00						0.00
Total		5.03	5.01	5.03	5.03	5.02	5.03	5.02
An		80.73	82.20	81.35	82.38	83.76	83.75	82.36
Ab		18.48	16.88	17.92	16.95	15.39	15.52	16.86
Or		0.78	0.92	0.73	0.67	0.85	0.73	0.78

Sample 75		Plag 2 Spec. 1	Plag 2 Spec. 2	Plag 2 Spec. 3	Plag 2 Spec. 4	Plag 2 Spec. 5	Plag 2 Spec. 6	Avg.
Na_2O	Oxide	2.49	2.52	2.58	2.58	2.67	2.61	2.58
MgO	wt%							
Al_2O_3		31.72	31.61	31.41	31.41	31.75	31.75	31.61
SiO_2		48.49	48.18	48.93	48.93	48.68	48.73	48.66
CaO		16.21	16.18	16.09	16.09	16.18	16.17	16.15
FeO		0.48	0.53	0.52	0.52	0.61	0.59	0.54
K_2O		0.17	0.20	0.24	0.24	0.19	0.25	0.22
TiO_2		0.10					0.08	0.09
Total		99.65	99.20	99.78	99.78	100.09	100.17	
Na	Cations	0.22	0.23	0.23	0.23	0.24	0.23	0.23

Mg	Norm.							
Al	to	1.72	1.73	1.70	1.70	1.72	1.72	1.72
Si	8 oxygens	2.24	2.23	2.25	2.25	2.24	2.24	2.24
Ca		0.80	0.80	0.79	0.79	0.80	0.80	0.80
Fe		0.02	0.02	0.02	0.02	0.02	0.02	0.02
K		0.01	0.01	0.01	0.01	0.01	0.01	0.01
Ti		0.00					0.00	0.00
Total		5.02	5.02	5.02	5.02	5.03	5.02	5.02
An		77.49	77.13	76.46	76.46	76.18	76.31	76.67
Ab		21.54	21.74	22.19	22.19	22.75	22.29	22.12
Or		0.97	1.14	1.36	1.36	1.07	1.40	1.21

Sample 75		Plag 3 Spec. 1	Plag 3 Spec. 2	Plag 3 Spec. 3	Plag 3 Spec. 4	Plag 3 Spec. 5	Avg.
Na_2O	Oxide	3.74	3.66	3.94	3.87	3.94	3.83
MgO	wt%						
Al_2O_3		29.32	29.16	29.18	29.51	29.49	29.33
SiO_2		51.97	51.17	51.81	51.66	51.99	51.72
CaO		13.69	13.82	13.43	13.45	13.39	13.56
FeO		0.62	0.58	0.43	0.56		0.55
K_2O		0.35	0.49	0.36	0.38	0.36	0.39
TiO_2		0.09	0.10	0.13	0.13	0.51	0.19
Total		99.78	98.99	99.28	99.57	99.67	
Na	Cations	0.33	0.33	0.35	0.34	0.35	0.34
Mg	Norm.						
Al	to	1.58	1.59	1.58	1.59	1.59	1.59
Si	8 oxygens	2.38	2.36	2.38	2.37	2.37	2.37
Ca		0.67	0.68	0.66	0.66	0.65	0.67
Fe		0.02	0.02	0.02	0.02	0.00	0.02
K		0.02	0.03	0.02	0.02	0.02	0.02
Ti		0.00	0.00	0.00	0.00	0.02	0.01
Total		5.01	5.02	5.01	5.01	5.00	5.01
An		65.58	65.73	63.99	64.34	63.92	64.71
Ab		32.42	31.50	33.97	33.50	34.04	33.08
Or		2.00	2.77	2.04	2.16	2.05	2.21

MOUNT MOLLIE DYKE CLINOPYROXENE

Sample 12		CPX 1 Spec. 1	CPX 1 Spec. 2	CPX 1 Spec. 3	CPX 1 Spec. 4	CPX 1 Spec. 5	CPX 1 Spec. 6	Avg.
Na_2O	Oxide	0.35	0.37	0.28	0.30	0.34	0.32	0.33
MgO	wt%	14.60	14.46	14.84	14.50	14.80	14.57	14.63
Al_2O_3		2.32	2.26	2.29	2.13	2.05	2.13	2.20
SiO_2		50.41	50.55	50.47	50.76	51.09	50.92	50.70
CaO		19.00	19.45	18.49	19.59	19.07	19.50	19.18
TiO_2		1.01	1.27	1.15	1.21	1.17	0.90	1.12
V_2O_5		0.14	0.13	0.15	0.10	0.12	0.16	0.13
Cr_2O_3		0.13	0.09	0.14	0.09	0.21	0.10	0.13
MnO		0.23	0.40	0.28	0.21	0.25	0.25	0.27
FeO		12.29	11.95	12.00	11.29	11.85	11.55	11.82
Total		100.47	100.93	100.08	100.19	100.95	100.40	
Na	Cations	0.03	0.03	0.02	0.02	0.02	0.02	0.02
Mg	Norm.	0.82	0.81	0.83	0.81	0.82	0.81	0.82
Al	to	0.10	0.10	0.10	0.09	0.09	0.09	0.10
Si	6 oxygens	1.89	1.89	1.90	1.90	1.90	1.91	1.90
Ca		0.76	0.78	0.74	0.79	0.76	0.78	0.77
Ti		0.03	0.04	0.03	0.03	0.03	0.03	0.03
V		0.00	0.00	0.00	0.00	0.00	0.00	0.00
Cr		0.00	0.00	0.00	0.00	0.01	0.00	0.00
Mn		0.01	0.01	0.01	0.01	0.01	0.01	0.01
Fe		0.39	0.37	0.38	0.35	0.37	0.36	0.37
Total		4.03	4.03	4.02	4.02	4.02	4.02	4.03
Mg#		67.92	68.32	68.79	69.60	69.01	69.22	68.81
%wo		38.85	39.77	38.12	40.32	38.99	39.97	39.34
%en		41.54	41.15	42.57	41.53	42.10	41.55	41.74
%fs		19.62	19.08	19.31	18.14	18.91	18.48	18.92

Sample 12		CPX 2 Spec. 1	CPX 2 Spec. 2	CPX 2 Spec. 3	CPX 2 Spec. 4	Avg.
Na_2O	Oxide	0.31	0.23	0.38	0.39	0.33
MgO	wt%	14.13	14.15	13.84	13.69	13.95
Al_2O_3		1.55	1.70	1.68	1.77	1.68
SiO_2		50.60	50.07	50.14	50.12	50.23
CaO		19.13	19.38	19.60	20.05	19.54
TiO_2		0.92	1.09	1.02	1.13	1.04
V_2O_5		0.04	0.06	0.22	0.19	0.13
Cr_2O_3				0.09		0.09
MnO		0.27	0.33	0.20	0.27	0.27
FeO		12.24	12.28	12.36	11.79	12.17
Total		99.21	99.29	99.54	99.39	
Na	Cations	0.02	0.02	0.03	0.03	0.02
Mg	Norm.	0.80	0.80	0.78	0.78	0.79
Al	to	0.07	0.08	0.08	0.08	0.08
Si	6 oxygens	1.92	1.91	1.91	1.91	1.91
Ca		0.78	0.79	0.80	0.82	0.80
Ti		0.03	0.03	0.03	0.03	0.03
V		0.00	0.00	0.01	0.00	0.00
Cr				0.00		0.00
Mn		0.01	0.01	0.01	0.01	0.01
Fe		0.39	0.39	0.39	0.38	0.39
Total		4.02	4.03	4.03	4.03	4.03

Mg#		67.30	67.26	66.62	67.43	67.15	
%wo		39.57	39.83	40.41	41.51	40.33	
%en		40.67	40.47	39.70	39.44	40.07	
%fs		19.76	19.70	19.89	19.05	19.60	

Sample 12		CPX 3 Spec. 1	CPX 3 Spec. 2	CPX 3 Spec. 3	CPX 3 Spec. 4	CPX 3 Spec. 5	Avg.
Na_2O	Oxide	0.34	0.28	0.24	0.42	0.28	0.31
MgO	wt%	14.98	14.79	14.81	14.22	14.78	14.72
Al_2O_3		1.90	1.83	2.04	2.11	1.79	1.93
SiO_2		50.70	50.88	50.47	50.31	50.63	50.60
CaO		19.16	19.91	19.24	20.06	19.19	19.51
TiO_2		1.08	0.97	0.92	1.09	0.95	1.00
V_2O_5			0.15	0.11		0.08	0.11
Cr_2O_3		0.17	0.04	0.13	0.09	0.12	0.11
MnO		0.27	0.31	0.19	0.26	0.28	0.26
FeO		11.73	10.71	11.08	10.74	11.19	11.09
Total		100.33	99.88	99.24	99.30	99.27	
Na	Cations	0.02	0.02	0.02	0.03	0.02	0.02
Mg	Norm.	0.84	0.83	0.84	0.80	0.83	0.83
Al	to	0.08	0.08	0.09	0.09	0.08	0.09
Si	6 oxygens	1.90	1.91	1.91	1.91	1.92	1.91
Ca		0.77	0.80	0.78	0.81	0.78	0.79
Ti		0.03	0.03	0.03	0.03	0.03	0.03
V			0.00	0.00		0.00	0.00
Cr		0.01	0.00	0.00	0.00	0.00	0.00
Mn		0.01	0.01	0.01	0.01	0.01	0.01
Fe		0.37	0.34	0.35	0.34	0.35	0.35
Total		4.03	4.02	4.02	4.03	4.02	4.03
Mg#		69.48	71.11	70.44	70.24	70.19	70.29
%wo		38.97	40.76	39.67	41.59	39.57	40.11
%en		42.40	42.13	42.49	41.03	42.41	42.09
%fs		18.63	17.11	17.83	17.38	18.01	17.80

Sample 18		CPX 1 Spec. 1	CPX 1 Spec. 2	CPX 1 Spec. 3	CPX 1 Spec. 4	CPX 1 Spec. 5	Avg.
Na_2O	Oxide	0.37	0.18	0.31	0.28	0.23	0.27
MgO	wt%	13.88	14.40	14.07	14.37	14.51	14.25
Al_2O_3		1.66	1.46	1.67	1.63	1.62	1.61
SiO_2		50.37	50.69	50.66	50.82	50.96	50.70
CaO		19.00	17.46	18.84	17.41	18.00	18.14
TiO_2		1.00	0.92	1.03	0.88	0.93	0.95
V_2O_5		0.03	0.06	0.17	0.06	0.15	0.09
Cr_2O_3		0.19	0.02	0.03			0.08
MnO		0.32	0.30	0.40	0.43	0.33	0.36
FeO		12.69	14.14	12.37	14.16	13.70	13.41
Total		99.52	99.63	99.56	100.03	100.43	
Na	Cations	0.03	0.01	0.02	0.02	0.02	0.02
Mg	Norm.	0.79	0.82	0.80	0.81	0.81	0.80
Al	to	0.07	0.07	0.07	0.07	0.07	0.07
Si	6 oxygens	1.92	1.93	1.92	1.92	1.92	1.92
Ca		0.77	0.71	0.77	0.71	0.73	0.74
Ti		0.03	0.03	0.03	0.03	0.03	0.03
V		0.00	0.00	0.00	0.00	0.00	0.00
Cr		0.01	0.00	0.00			0.00

Mn		0.01	0.01	0.01	0.01	0.01	0.01
Fe		0.40	0.45	0.39	0.45	0.43	0.42
Total		4.03	4.02	4.02	4.02	4.02	4.02
Mg#		66.10	64.48	66.97	64.40	65.37	65.44
%wo		39.40	35.97	39.19	35.93	36.82	37.46
%en		40.05	41.29	40.73	41.26	41.30	40.93
%fs		20.54	22.74	20.09	22.81	21.88	21.61

Sample 18		CPX 2 Spec. 1	CPX 2 Spec. 2	CPX 2 Spec. 3	CPX 2 Spec. 4	CPX 2 Spec. 5	Avg.
Na_2O	Oxide	0.31	0.32	0.40	0.36	0.25	0.33
MgO	wt%	14.65	14.91	15.01	14.86	14.67	14.82
Al_2O_3		2.20	2.16	2.07	2.19	2.16	2.16
SiO_2		50.35	50.38	49.90	50.09	50.11	50.17
CaO		19.35	19.26	19.32	19.82	19.95	19.54
TiO_2		1.09	1.13	1.04	1.06	0.86	1.04
V_2O_5		0.11	0.14	0.11	0.22	0.34	0.18
Cr_2O_3		0.14	0.26	0.28	0.21	0.22	0.22
MnO		0.27	0.28	0.32	0.21	0.25	0.27
FeO		10.95	11.15	10.73	10.34	10.56	10.75
Total		99.42	99.99	99.17	99.35	99.38	
Na	Cations	0.02	0.02	0.03	0.03	0.02	0.02
Mg	Norm.	0.83	0.84	0.85	0.84	0.83	0.83
Al	to	0.10	0.10	0.09	0.10	0.10	0.10
Si	6 oxygens	1.90	1.89	1.89	1.89	1.89	1.90
Ca		0.78	0.78	0.78	0.80	0.81	0.79
Ti		0.03	0.03	0.03	0.03	0.02	0.03
V		0.00	0.00	0.00	0.01	0.01	0.00
Cr		0.00	0.01	0.01	0.01	0.01	0.01
Mn		0.01	0.01	0.01	0.01	0.01	0.01
Fe		0.35	0.35	0.34	0.33	0.33	0.34
Total		4.02	4.03	4.04	4.03	4.03	4.03
Mg#		70.46	70.45	71.38	71.92	71.23	71.09
%wo		40.08	39.54	39.77	40.81	41.04	40.25
%en		42.22	42.59	42.99	42.57	42.00	42.48
%fs		17.70	17.87	17.24	16.62	16.96	17.28

Sample 18		CPX 3 Spec. 1	CPX 3 Spec. 2	CPX 3 Spec. 3	CPX 3 Spec. 4	Avg.
Na_2O	Oxide	0.31	0.29	0.38	0.38	0.34
MgO	wt%	14.75	14.98	14.61	14.55	14.72
Al_2O_3		2.30	2.28	2.31	2.33	2.31
SiO_2		50.78	50.82	50.69	50.46	50.69
CaO		19.82	19.57	20.33	20.09	19.95
TiO_2		1.03	1.15	1.13	1.04	1.09
V_2O_5		0.09	0.13	0.24	0.24	0.18
Cr_2O_3		0.22	0.21	0.30	0.27	0.25
MnO		0.20	0.17	0.20	0.24	0.20
FeO		10.45	10.66	10.24	10.56	10.48
Total		99.96	100.26	100.43	100.16	
Na	Cations	0.02	0.02	0.03	0.03	0.02
Mg	Norm.	0.82	0.83	0.81	0.81	0.82
Al	to	0.10	0.10	0.10	0.10	0.10
Si	6 oxygens	1.90	1.90	1.89	1.89	1.90

Ca		0.80	0.78	0.81	0.81	0.80
Ti		0.03	0.03	0.03	0.03	0.03
V		0.00	0.00	0.01	0.01	0.00
Cr		0.01	0.01	0.01	0.01	0.01
Mn		0.01	0.01	0.01	0.01	0.01
Fe		0.33	0.33	0.32	0.33	0.33
Total		4.02	4.02	4.02	4.03	4.02
Mg#		71.56	71.47	71.78	71.07	71.47
%wo		40.86	40.15	41.78	41.35	41.04
%en		42.32	42.77	41.79	41.68	42.14
%fs		16.82	17.07	16.43	16.97	16.82

Sample 23		CPX 1 Spec. 1	CPX 1 Spec. 2	CPX 1 Spec. 3	CPX 1 Spec. 4	CPX 1 Spec. 5	Avg.
Na_2O	Oxide	0.34	0.26	0.36	0.36	0.34	0.33
MgO	wt%	14.37	14.55	14.60	14.54	14.66	14.54
Al_2O_3		1.51	1.44	1.63	1.54	1.49	1.52
SiO_2		51.44	51.62	51.27	51.35	51.56	51.45
CaO		19.82	19.47	19.52	19.54	19.46	19.56
TiO_2		1.02	0.89	0.84	0.89	0.94	0.92
V_2O_5		0.02	0.08	0.15	0.07	0.01	0.07
Cr_2O_3		0.13			0.07	0.01	0.07
MnO		0.27	0.38	0.29	0.24	0.42	0.32
FeO		11.52	11.68	11.48	11.77	11.56	11.60
Total		100.43	100.37	100.12	100.36	100.46	
Na	Cations	0.02	0.02	0.03	0.03	0.02	0.02
Mg	Norm.	0.80	0.81	0.82	0.81	0.82	0.81
Al	to	0.07	0.06	0.07	0.07	0.07	0.07
Si	6 oxygens	1.93	1.93	1.92	1.93	1.93	1.93
Ca		0.80	0.78	0.79	0.79	0.78	0.79
Ti		0.03	0.03	0.02	0.03	0.03	0.03
V		0.00	0.00	0.00	0.00	0.00	0.00
Cr		0.00			0.00	0.00	0.00
Mn		0.01	0.01	0.01	0.01	0.01	0.01
Fe		0.36	0.37	0.36	0.37	0.36	0.36
Total		4.02	4.02	4.02	4.02	4.02	4.02
Mg#		68.98	68.95	69.39	68.77	69.33	69.08
%wo		40.61	39.87	40.00	39.91	39.81	40.04
%en		40.97	41.46	41.63	41.33	41.73	41.42
%fs		18.42	18.67	18.36	18.77	18.46	18.54

Sample 23		CPX 2 Spec. 1	CPX 2 Spec. 2	CPX 2 Spec. 3	CPX 2 Spec. 4	CPX 2 Spec. 5	CPX 2 Spec. 6	Avg.
Na_2O	Oxide	0.29	0.30	0.18	0.30	0.30	0.35	0.29
MgO	wt%	15.06	15.00	14.69	15.14	15.14	15.11	15.02
Al_2O_3		1.83	1.78	1.80	1.75	1.75	1.72	1.77
SiO_2		50.54	50.85	50.65	50.49	50.49	50.88	50.65
CaO		19.07	18.93	19.05	19.06	19.06	19.15	19.05
TiO_2		1.17	1.13	1.08	1.08	1.08	1.15	1.12
V_2O_5		0.03	0.11	0.06	0.09	0.09	0.10	0.08
Cr_2O_3		0.15	0.22	0.15	0.12	0.12	0.04	0.13
MnO		0.33	0.25	0.20	0.32	0.32	0.29	0.29
FeO		11.56	11.17	11.39	11.42	11.42	11.34	11.38
Total		100.00	99.74	99.26	99.78	99.78	100.12	

Na	Cations	0.02	0.02	0.01	0.02	0.02	0.03	0.02
Mg	Norm.	0.85	0.84	0.83	0.85	0.85	0.85	0.84
Al	to	0.08	0.08	0.08	0.08	0.08	0.08	0.08
Si	6 oxygens	1.90	1.91	1.92	1.90	1.90	1.91	1.91
Ca		0.77	0.76	0.77	0.77	0.77	0.77	0.77
Ti		0.03	0.03	0.03	0.03	0.03	0.03	0.03
V		0.00	0.00	0.00	0.00	0.00	0.00	0.00
Cr		0.00	0.01	0.00	0.00	0.00	0.00	0.00
Mn		0.01	0.01	0.01	0.01	0.01	0.01	0.01
Fe		0.36	0.35	0.36	0.36	0.36	0.36	0.36
Total		4.03	4.02	4.01	4.03	4.03	4.03	4.03
Mg#		69.90	70.54	69.69	70.27	70.27	70.37	70.17
%wo		38.88	39.01	39.37	38.86	38.86	39.06	39.01
%en		42.72	43.02	42.25	42.96	42.96	42.89	42.80
%fs		18.40	17.97	18.38	18.18	18.18	18.06	18.19

Sample 23		CPX 3 Spec. 1	CPX 3 Spec. 2	CPX 3 Spec. 3	CPX 3 Spec. 4	CPX 3 Spec. 5	CPX 3 Spec. 6	Avg.
Na_2O	Oxide	0.29	0.34	0.35	0.27	0.34	0.33	0.32
MgO	wt%	13.71	15.02	15.41	13.92	15.18	14.86	14.68
Al_2O_3		1.47	1.69	1.57	1.83	1.56	1.66	1.63
SiO_2		50.72	50.70	50.38	50.92	50.84	50.50	50.68
CaO		21.23	18.38	18.39	21.26	19.09	19.29	19.61
TiO_2		0.95	1.14	1.12	1.00	1.09	1.09	1.07
V_2O_5		0.14	0.01		0.12	0.13	0.03	0.09
Cr_2O_3		0.15	0.12	0.07	0.12	0.19	0.19	0.14
MnO		0.27	0.28	0.41	0.42	0.26	0.29	0.32
FeO		10.42	11.59	11.42	9.77	11.05	11.00	10.88
Total		99.37	99.26	99.12	99.64	99.71	99.24	
Na	Cations	0.02	0.02	0.03	0.02	0.02	0.02	0.02
Mg	Norm.	0.77	0.85	0.87	0.78	0.85	0.84	0.83
Al	to	0.07	0.08	0.07	0.08	0.07	0.07	0.07
Si	6 oxygens	1.92	1.92	1.91	1.92	1.91	1.91	1.92
Ca		0.86	0.74	0.75	0.86	0.77	0.78	0.79
Ti		0.03	0.03	0.03	0.03	0.03	0.03	0.03
V		0.00	0.00		0.00	0.00	0.00	0.00
Cr		0.00	0.00	0.00	0.00	0.01	0.01	0.00
Mn		0.01	0.01	0.01	0.01	0.01	0.01	0.01
Fe		0.33	0.37	0.36	0.31	0.35	0.35	0.34
Total		4.02	4.02	4.03	4.02	4.03	4.03	4.02
Mg#		70.11	69.79	70.64	71.75	71.01	70.66	70.65
%wo		43.83	38.03	37.72	44.06	39.09	39.73	40.40
%en		39.38	43.25	43.99	40.14	43.25	42.59	42.10
%fs		16.79	18.72	18.29	15.80	17.66	17.68	17.49

Sample 29		CPX 1 Spec. 1	CPX 1 Spec. 2	CPX 1 Spec. 3	CPX 1 Spec. 4	CPX 1 Spec. 5	CPX 1 Spec. 6	Avg.
Na_2O	Oxide	0.27	0.41	0.28	0.34	0.42	0.34	0.34
MgO	wt%	15.19	15.18	14.98	15.22	15.12	15.44	15.19
Al_2O_3		2.97	2.98	2.92	2.99	2.92	2.98	2.96
SiO_2		49.73	49.89	50.28	50.20	50.46	49.82	50.06
CaO		20.18	20.01	21.08	20.63	20.81	19.72	20.41
TiO_2		1.27	1.24	1.11	1.17	1.18	1.12	1.18
V_2O_5		0.11		0.15	0.24	0.10	0.11	0.14
Cr_2O_3		0.58	0.69	0.57	0.59	0.73	0.72	0.65

MnO		0.31	0.25	0.19	0.27	0.11	0.19	0.22
FeO		8.71	8.64	8.38	8.46	8.39	9.20	8.63
Total		99.32	99.28	99.94	100.10	100.23	99.63	
Na	Cations	0.02	0.03	0.02	0.02	0.03	0.02	0.02
Mg	Norm.	0.85	0.85	0.83	0.85	0.84	0.86	0.85
Al	to	0.13	0.13	0.13	0.13	0.13	0.13	0.13
Si	6 oxygens	1.87	1.88	1.88	1.87	1.88	1.87	1.87
Ca		0.81	0.81	0.84	0.82	0.83	0.79	0.82
Ti		0.04	0.04	0.03	0.03	0.03	0.03	0.03
V		0.00		0.00	0.01	0.00	0.00	0.00
Cr		0.02	0.02	0.02	0.02	0.02	0.02	0.02
Mn		0.01	0.01	0.01	0.01	0.00	0.01	0.01
Fe		0.27	0.27	0.26	0.26	0.26	0.29	0.27
Total		4.03	4.03	4.02	4.03	4.03	4.03	4.03
Mg#		75.66	75.80	76.11	76.23	76.26	74.95	75.84
%wo		41.94	41.79	43.49	42.61	43.00	40.75	42.26
%en		43.93	44.12	43.01	43.75	43.47	44.40	43.78
%fs		14.13	14.09	13.50	13.64	13.53	14.84	13.95

Sample 29		CPX 2 Spec. 1	CPX 2 Spec. 2	CPX 2 Spec. 3	CPX 2 Spec. 4	CPX 2 Spec. 5	CPX 2 Spec. 6	Avg.
Na_2O	Oxide	0.33	0.37	0.38	0.46	0.36	0.28	0.36
MgO	wt%	15.73	15.87	15.77	15.48	15.86	15.89	15.77
Al_2O_3		2.14	2.04	2.00	2.09	2.05	2.27	2.10
SiO_2		50.94	51.18	51.08	51.04	51.66	51.38	51.21
CaO		20.10	20.33	20.34	20.96	20.46	20.44	20.44
TiO_2		0.92	0.94	0.90	0.83	0.88	0.88	0.89
V_2O_5		0.18	0.18	0.12	0.04	0.08	0.13	0.12
Cr_2O_3		0.51	0.41	0.68	0.54	0.58	0.65	0.56
MnO		0.23	0.26	0.22	0.15	0.22	0.20	0.21
FeO		8.51	8.72	8.58	8.48	8.40	8.70	8.57
Total		99.59	100.31	100.06	100.07	100.56	100.82	
Na	Cations	0.02	0.03	0.03	0.03	0.03	0.02	0.03
Mg	Norm.	0.88	0.88	0.88	0.86	0.87	0.88	0.87
Al	to	0.09	0.09	0.09	0.09	0.09	0.10	0.09
Si	6 oxygens	1.90	1.90	1.90	1.90	1.91	1.90	1.90
Ca		0.80	0.81	0.81	0.84	0.81	0.81	0.81
Ti		0.03	0.03	0.03	0.02	0.02	0.02	0.02
V		0.00	0.00	0.00	0.00	0.00	0.00	0.00
Cr		0.02	0.01	0.02	0.02	0.02	0.02	0.02
Mn		0.01	0.01	0.01	0.00	0.01	0.01	0.01
Fe		0.27	0.27	0.27	0.26	0.26	0.27	0.27
Total		4.02	4.03	4.03	4.04	4.02	4.02	4.03
Mg#		76.72	76.44	76.62	76.49	77.09	76.50	76.64
%wo		41.33	41.30	41.52	42.67	41.68	41.42	41.66
%en		45.01	44.87	44.80	43.85	44.96	44.81	44.72
%fs		13.66	13.83	13.67	13.48	13.36	13.76	13.63

Sample29		CPX 3 Spec. 1	CPX 3 Spec. 2	CPX 3 Spec. 3	CPX 3 Spec. 4	CPX 3 Spec. 5	CPX 3 Spec. 6	Avg.
Na_2O	Oxide	0.35	0.42	0.27	0.40	0.29	0.31	0.34
MgO	wt%	15.78	15.56	15.81	15.82	15.93	15.54	15.74
Al_2O_3		2.25	2.14	2.02	2.07	2.10	2.17	2.13
SiO_2		51.04	51.00	51.40	50.97	51.10	51.03	51.09

CaO		19.91	19.87	20.14	20.02	20.08	20.14	20.03
TiO_2		0.83	0.86	0.79	0.87	0.84	0.81	0.83
V_2O_5		0.12	0.12		0.08	0.10	0.04	0.09
Cr_2O_3		0.54	0.51	0.59	0.63	0.58	0.63	0.58
MnO		0.19	0.27	0.27	0.22	0.25	0.27	0.25
FeO		8.67	8.77	8.52	8.67	8.78	8.80	8.70
Total		99.68	99.52	99.80	99.75	100.05	99.73	
Na	Cations	0.03	0.03	0.02	0.03	0.02	0.02	0.02
Mg	Norm.	0.88	0.87	0.88	0.88	0.88	0.87	0.88
Al	to	0.10	0.09	0.09	0.09	0.09	0.10	0.09
Si	6 oxygens	1.91	1.91	1.92	1.90	1.90	1.91	1.91
Ca		0.80	0.80	0.80	0.80	0.80	0.81	0.80
Ti		0.02	0.02	0.02	0.02	0.02	0.02	0.02
V		0.00	0.00		0.00	0.00	0.00	0.00
Cr		0.02	0.02	0.02	0.02	0.02	0.02	0.02
Mn		0.01	0.01	0.01	0.01	0.01	0.01	0.01
Fe		0.27	0.27	0.27	0.27	0.27	0.28	0.27
Total		4.02	4.02	4.02	4.03	4.03	4.02	4.02
Mg#		76.44	75.98	76.79	76.49	76.38	75.89	76.33
%wo		40.94	41.08	41.28	41.02	40.89	41.41	41.10
%en		45.15	44.77	45.09	45.11	45.15	44.46	44.95
%fs		13.92	14.15	13.63	13.87	13.96	14.12	13.94

Sample 35		CPX 1 Spec. 1	CPX 1 Spec. 2	CPX 1 Spec. 3	CPX 1 Spec. 4	CPX 1 Spec. 5	Avg.
Na_2O	Oxide	0.40	0.38	0.36	0.22		0.34
MgO	wt%	14.45	14.41	14.51	14.26	14.57	14.44
Al_2O_3		1.19	1.32	1.29	1.32	1.22	1.27
SiO_2		51.83	51.48	51.67	51.71	51.64	51.67
CaO		20.14	19.87	19.62	20.39	19.61	19.93
TiO_2		0.59	0.63	0.70	0.62	0.57	0.62
V_2O_5							
Cr_2O_3		0.05	0.05	0.05	0.01		0.04
MnO		0.33	0.27	0.30	0.33	0.35	0.32
FeO		11.56	11.68	11.94	11.58	12.32	11.82
Total		100.53	100.08	100.46	100.44	100.28	
Na	Cations	0.03	0.03	0.03	0.02	0.00	0.02
Mg	Norm.	0.81	0.81	0.81	0.80	0.82	0.81
Al	to	0.05	0.06	0.06	0.06	0.05	0.06
Si	6 oxygens	1.94	1.94	1.94	1.94	1.94	1.94
Ca		0.81	0.80	0.79	0.82	0.79	0.80
Ti		0.02	0.02	0.02	0.02	0.02	0.02
V							
Cr		0.00	0.00	0.00	0.00		0.00
Mn		0.01	0.01	0.01	0.01	0.01	0.01
Fe		0.36	0.37	0.37	0.36	0.39	0.37
Total		4.03	4.03	4.03	4.02	4.02	4.02
Mg#		69.02	68.74	68.42	68.70	67.83	68.54
%wo		40.88	40.52	39.93	41.38	39.61	40.46
%en		40.81	40.89	41.10	40.27	40.96	40.81
%fs		18.31	18.59	18.97	18.35	19.43	18.73

Sample 35	CPX 2 Spec. 1	CPX 2 Spec. 2	CPX 2 Spec. 3	CPX 2 Spec. 4	CPX 2 Spec. 5	CPX 2 Spec. 6	Avg.

Na_2O	Oxide	0.42	0.28	0.38	0.40	0.29	0.40	0.36
MgO	wt%	14.18	14.44	14.26	14.16	14.12	14.45	14.27
Al_2O_3		1.59	1.66	1.62	1.78	1.52	1.51	1.61
SiO_2		50.95	51.15	51.23	51.24	50.82	51.12	51.09
CaO		19.77	19.82	19.84	20.10	20.19	20.34	20.01
TiO_2		0.71	0.84	0.81	0.83	0.83	0.80	0.80
V_2O_5		0.10	0.30	0.11	0.16	0.14	0.20	0.17
Cr_2O_3					0.06			0.06
MnO		0.25	0.30	0.33	0.31	0.19	0.23	0.27
FeO		11.41	11.46	11.36	10.97	11.16	11.05	11.24
Total		99.38	100.25	99.93	100.00	99.26	100.10	
Na	Cations	0.03	0.02	0.03	0.03	0.02	0.03	0.03
Mg	Norm.	0.80	0.81	0.80	0.79	0.80	0.81	0.80
Al	to	0.07	0.07	0.07	0.08	0.07	0.07	0.07
Si	6 oxygens	1.93	1.92	1.93	1.93	1.93	1.92	1.93
Ca		0.80	0.80	0.80	0.81	0.82	0.82	0.81
Ti		0.02	0.02	0.02	0.02	0.02	0.02	0.02
V		0.00	0.01	0.00	0.00	0.00	0.00	0.00
Cr					0.00			0.00
Mn		0.01	0.01	0.01	0.01	0.01	0.01	0.01
Fe		0.36	0.36	0.36	0.34	0.35	0.35	0.35
Total		4.03	4.02	4.02	4.02	4.02	4.03	4.02
Mg#		68.90	69.19	69.11	69.71	69.28	69.98	69.36
%wo		40.84	40.56	40.86	41.56	41.59	41.45	41.14
%en		40.76	41.13	40.87	40.74	40.47	40.98	40.82
%fs		18.40	18.31	18.26	17.70	17.94	17.58	18.03

Sample 35		CPX 3 Spec. 1	CPX 3 Spec. 2	CPX 3 Spec. 3	CPX 3 Spec. 4	CPX 3 Spec. 5	CPX 3 Spec. 6	Avg.
Na_2O	Oxide	0.28	0.47	0.31	0.43	0.37	0.31	0.36
MgO	wt%	14.17	14.25	14.40	14.47	14.51	14.30	14.35
Al_2O_3		2.42	2.41	2.39	2.30	2.42	2.44	2.40
SiO_2		50.17	49.86	50.35	50.21	50.36	50.02	50.16
CaO		20.35	20.41	20.32	20.26	20.16	20.31	20.30
TiO_2		1.42	1.39	1.37	1.27	1.33	1.38	1.36
V_2O_5			0.28	0.22	0.22	0.16	0.20	0.22
Cr_2O_3		0.25	0.14	0.09	0.08	0.18	0.05	0.13
MnO		0.29	0.34	0.35	0.23	0.38	0.27	0.31
FeO		10.42	10.60	10.60	10.59	10.59	10.49	10.55
Total		99.76	100.16	100.40	100.06	100.46	99.78	
Na	Cations	0.02	0.03	0.02	0.03	0.03	0.02	0.03
Mg	Norm.	0.80	0.80	0.80	0.81	0.81	0.80	0.80
Al	to	0.11	0.11	0.11	0.10	0.11	0.11	0.11
Si	6 oxygens	1.89	1.88	1.89	1.89	1.89	1.89	1.89
Ca		0.82	0.82	0.82	0.82	0.81	0.82	0.82
Ti		0.04	0.04	0.04	0.04	0.04	0.04	0.04
V			0.01	0.01	0.01	0.00	0.00	0.00
Cr		0.01	0.00	0.00	0.00	0.01	0.00	0.00
Mn		0.01	0.01	0.01	0.01	0.01	0.01	0.01
Fe		0.33	0.33	0.33	0.33	0.33	0.33	0.33
Total		4.02	4.04	4.02	4.03	4.03	4.02	4.03
Mg#		70.80	70.56	70.77	70.89	70.95	70.85	70.80
%wo		42.22	42.07	41.78	41.63	41.47	41.96	41.86
%en		40.91	40.87	41.20	41.38	41.53	41.12	41.17
%fs		16.87	17.06	17.01	16.99	17.00	16.92	16.98

Sample 37		CPX 1 Spec. 1	CPX 1 Spec. 2	CPX 1 Spec. 3	CPX 1 Spec. 4	CPX 1 Spec. 5	CPX 1 Spec. 6	Avg.
Na_2O	Oxide	0.31	0.30	0.18	0.33	0.29	0.26	0.28
MgO	wt%	14.28	14.96	14.98	13.76	14.22	14.64	14.47
Al_2O_3		1.75	1.53	1.62	1.70	1.74	1.51	1.64
SiO_2		50.08	50.15	50.61	49.89	50.32	50.31	50.23
CaO		17.48	16.46	15.80	19.02	17.75	17.45	17.33
TiO_2		1.05	1.02	0.85	1.16	1.16	1.08	1.05
V_2O_5		0.12	0.14	0.04	0.09	0.13	0.03	0.09
Cr_2O_3		0.03	0.04					0.04
MnO		0.39	0.39	0.44	0.35	0.31	0.43	0.39
FeO		14.15	14.64	15.40	12.78	13.67	14.22	14.14
Total		99.63	99.63	99.95	99.07	99.59	99.93	
Na	Cations	0.02	0.02	0.01	0.02	0.02	0.02	0.02
Mg	Norm.	0.81	0.85	0.85	0.78	0.81	0.83	0.82
Al	to	0.08	0.07	0.07	0.08	0.08	0.07	0.07
Si	6 oxygens	1.91	1.91	1.92	1.91	1.91	1.91	1.91
Ca		0.71	0.67	0.64	0.78	0.72	0.71	0.71
Ti		0.03	0.03	0.02	0.03	0.03	0.03	0.03
V		0.00	0.00	0.00	0.00	0.00	0.00	0.00
Cr		0.00	0.00					0.00
Mn		0.01	0.01	0.01	0.01	0.01	0.01	0.01
Fe		0.45	0.47	0.49	0.41	0.43	0.45	0.45
Total		4.03	4.03	4.02	4.03	4.02	4.03	4.03
Mg#		64.27	64.56	63.42	65.75	64.97	64.73	64.66
%wo		36.12	33.79	32.47	39.51	36.82	35.67	35.65
%en		41.06	42.74	42.83	39.77	41.05	41.64	41.61
%fs		22.82	23.46	24.70	20.72	22.14	22.69	22.75

Sample 37		CPX 2 Spec. 1	CPX 2 Spec. 2	CPX 2 Spec. 3	CPX 2 Spec. 4	CPX 2 Spec. 5	Avg.
Na_2O	Oxide	0.26	0.30	0.33	0.40	0.32	0.32
MgO	wt%	15.09	14.51	15.07	15.09	14.43	14.84
Al_2O_3		2.06	2.06	1.81	2.14	2.09	2.03
SiO_2		50.06	50.02	50.06	50.24	49.60	50.00
CaO		17.12	17.60	17.10	17.05	18.01	17.38
TiO_2		1.22	1.31	1.18	1.14	1.31	1.23
V_2O_5		0.18	0.14	0.13	0.19	0.17	0.16
Cr_2O_3		0.12					0.12
MnO		0.31	0.30	0.28	0.32	0.30	0.30
FeO		13.06	13.45	13.71	13.48	12.78	13.30
Total		99.48	99.69	99.66	100.06	99.02	
Na	Cations	0.02	0.02	0.02	0.03	0.02	0.02
Mg	Norm.	0.85	0.82	0.85	0.85	0.82	0.84
Al	to	0.09	0.09	0.08	0.10	0.09	0.09
Si	6 oxygens	1.90	1.90	1.90	1.90	1.89	1.90
Ca		0.70	0.72	0.70	0.69	0.74	0.71
Ti		0.03	0.04	0.03	0.03	0.04	0.04
V		0.00	0.00	0.00	0.00	0.00	0.00
Cr		0.00					0.00
Mn		0.01	0.01	0.01	0.01	0.01	0.01
Fe		0.41	0.43	0.44	0.43	0.41	0.42
Total		4.02	4.02	4.03	4.03	4.03	4.03

Mg#	67.32	65.79	66.21	66.62	66.81	66.55
%wo	35.44	36.45	35.06	35.10	37.47	35.90
%en	43.46	41.81	43.00	43.23	41.78	42.66
%fs	21.10	21.74	21.94	21.66	20.76	21.44

Sample 37		CPX 3 Spec. 1	CPX 3 Spec. 2	CPX 3 Spec. 3	CPX 3 Spec. 4	CPX 3 Spec. 5	CPX 3 Spec. 6	Avg.
Na_2O	Oxide	0.31	0.38	0.33	0.33	0.30	0.46	0.35
MgO	wt%	14.20	14.18	14.05	14.05	14.16	13.80	14.07
Al_2O_3		1.26	1.20	1.38	1.36	1.37	1.34	1.32
SiO_2		50.84	51.07	50.78	51.07	50.77	50.78	50.89
CaO		18.93	19.28	19.41	19.42	19.35	19.87	19.38
TiO_2		0.82	0.86	0.81	0.86	0.79	0.68	0.80
V_2O_5		0.25	0.05	0.14		0.08	0.12	0.13
Cr_2O_3		0.01	0.07	0.06	0.08	0.09		0.06
MnO		0.25	0.31	0.19	0.39	0.20	0.18	0.25
FeO		12.73	12.23	12.33	12.48	12.30	11.92	12.33
Total		99.60	99.62	99.46	100.04	99.40	99.15	
Na	Cations	0.02	0.03	0.02	0.02	0.02	0.03	0.03
Mg	Norm.	0.80	0.80	0.80	0.79	0.80	0.78	0.80
Al	to	0.06	0.05	0.06	0.06	0.06	0.06	0.06
Si	6 oxygens	1.93	1.93	1.93	1.93	1.93	1.93	1.93
Ca		0.77	0.78	0.79	0.79	0.79	0.81	0.79
Ti		0.02	0.02	0.02	0.02	0.02	0.02	0.02
V		0.01	0.00	0.00		0.00	0.00	0.00
Cr		0.00	0.00	0.00	0.00	0.00		0.00
Mn		0.01	0.01	0.01	0.01	0.01	0.01	0.01
Fe		0.40	0.39	0.39	0.39	0.39	0.38	0.39
Total		4.02	4.02	4.02	4.03	4.03	4.03	4.03
Mg#		66.54	67.39	67.01	66.74	67.24	67.36	67.04
%wo		38.93	39.70	39.95	39.87	39.77	41.07	39.88
%en		40.64	40.64	40.24	40.14	40.50	39.69	40.31
%fs		20.44	19.66	19.81	20.00	19.73	19.23	19.81

Sample 39		CPX 1 Spec. 1	CPX 1 Spec. 2	CPX 1 Spec. 3	CPX 1 Spec. 4	CPX 1 Spec. 5	CPX 1 Spec. 6	Avg.
Na_2O	Oxide	0.31	0.29	0.35	0.36	0.38	0.33	0.34
MgO	wt%	15.06	15.10	15.01	14.96	14.96	14.89	15.00
Al_2O_3		1.78	1.69	1.76	1.81	1.81	1.81	1.78
SiO_2		50.76	50.62	50.61	50.70	50.79	50.62	50.68
CaO		19.02	19.10	19.21	19.19	19.21	19.10	19.14
TiO_2		1.02	1.21	1.15	1.17	1.10	1.08	1.12
V_2O_5		0.15	0.11	0.12	0.15	0.30	0.14	0.16
Cr_2O_3		0.15			0.07	0.02	0.08	0.08
MnO		0.30	0.19	0.34	0.30	0.27	0.25	0.28
FeO		11.20	11.16	11.31	11.29	11.18	11.01	11.19
Total		99.75	99.47	99.86	100.02	100.01	99.31	
Na	Cations	0.02	0.02	0.03	0.03	0.03	0.02	0.02
Mg	Norm.	0.85	0.85	0.84	0.84	0.84	0.84	0.84
Al	to	0.08	0.08	0.08	0.08	0.08	0.08	0.08
Si	6 oxygens	1.91	1.91	1.91	1.91	1.91	1.91	1.91
Ca		0.77	0.77	0.78	0.77	0.77	0.77	0.77
Ti		0.03	0.03	0.03	0.03	0.03	0.03	0.03
V		0.00	0.00	0.00	0.00	0.01	0.00	0.00
Cr		0.00			0.00	0.00	0.00	0.00

Mn		0.01	0.01	0.01	0.01	0.01	0.01	0.01
Fe		0.35	0.35	0.36	0.35	0.35	0.35	0.35
Total		4.02	4.02	4.03	4.03	4.02	4.02	4.03
Mg#		70.56	70.69	70.29	70.26	70.46	70.68	70.49
%wo		39.04	39.12	39.26	39.31	39.40	39.45	39.26
%en		43.02	43.04	42.69	42.64	42.70	42.80	42.81
%fs		17.95	17.84	18.05	18.05	17.90	17.75	17.92

Sample 39		CPX 2 Spec. 1	CPX 2 Spec. 2	CPX 2 Spec. 3	CPX 2 Spec. 4	CPX 2 Spec. 5	CPX 2 Spec. 6	Avg.
Na_2O	Oxide	0.24	0.39	0.29	0.34	0.39	0.32	0.33
MgO	wt%	14.55	14.58	14.36	14.60	14.43	14.47	14.50
Al_2O_3		1.28	1.36	1.53	1.44	1.33	1.21	1.36
SiO_2		51.80	51.59	51.55	51.57	51.60	51.67	51.63
CaO		21.28	21.27	21.21	21.63	21.27	21.36	21.34
TiO_2		0.47	0.46	0.48	0.50	0.36	0.44	0.45
V_2O_5		0.07	0.02	0.24	0.00	0.08	0.20	0.10
Cr_2O_3		0.12	0.19	0.05	0.26	0.16	0.13	0.15
MnO		0.24	0.30	0.32	0.34	0.16	0.31	0.28
FeO		9.38	9.35	9.42	9.35	9.34	9.54	9.40
Total		99.41	99.52	99.46	100.03	99.13	99.64	
Na	Cations	0.02	0.03	0.02	0.02	0.03	0.02	0.02
Mg	Norm.	0.82	0.82	0.81	0.82	0.81	0.81	0.81
Al	to	0.06	0.06	0.07	0.06	0.06	0.05	0.06
Si	6 oxygens	1.95	1.94	1.94	1.93	1.95	1.94	1.94
Ca		0.86	0.86	0.85	0.87	0.86	0.86	0.86
Ti		0.01	0.01	0.01	0.01	0.01	0.01	0.01
V		0.00	0.00	0.01	0.00	0.00	0.00	0.00
Cr		0.00	0.01	0.00	0.01	0.00	0.00	0.00
Mn		0.01	0.01	0.01	0.01	0.01	0.01	0.01
Fe		0.29	0.29	0.30	0.29	0.29	0.30	0.30
Total		4.02	4.03	4.01	4.03	4.02	4.02	4.02
Mg#		73.44	73.54	73.10	73.57	73.36	73.00	73.34
%wo		43.56	43.53	43.69	43.92	43.73	43.64	43.68
%en		41.45	41.53	41.16	41.26	41.28	41.14	41.30
%fs		14.99	14.94	15.15	14.82	14.99	15.22	15.02

Sample 39		CPX 3 Spec. 1	CPX 3 Spec. 2	CPX 3 Spec. 3	CPX 3 Spec. 4	CPX 3 Spec. 5	CPX 3 Spec. 6	Avg.
Na_2O	Oxide	0.24	0.26	0.37	0.33	0.37	0.30	0.31
MgO	wt%	15.21	15.13	15.20	15.18	15.31	15.22	15.21
Al_2O_3		1.62	1.67	1.61	1.73	1.64	1.71	1.66
SiO_2		50.84	50.61	50.67	50.89	50.98	50.79	50.80
CaO		19.19	19.12	19.04	19.05	19.16	19.19	19.13
TiO_2		1.06	1.06	1.11	0.97	0.95	1.10	1.04
V_2O_5		0.17	0.13	0.11		0.32	0.11	0.17
Cr_2O_3		0.05						0.05
MnO		0.24	0.20	0.29	0.38	0.25	0.29	0.28
FeO		11.65	11.60	11.46	11.38	11.31	11.55	11.49
Total		100.25	99.78	99.86	99.91	100.29	100.25	
Na	Cations	0.02	0.02	0.03	0.02	0.03	0.02	0.02
Mg	Norm.	0.85	0.85	0.85	0.85	0.85	0.85	0.85
Al	to	0.07	0.07	0.07	0.08	0.07	0.08	0.07
Si	6 oxygens	1.91	1.91	1.91	1.91	1.91	1.91	1.91

Ca		0.77	0.77	0.77	0.77	0.77	0.77	0.77
Ti		0.03	0.03	0.03	0.03	0.03	0.03	0.03
V		0.00	0.00	0.00		0.01	0.00	0.00
Cr		0.00						0.00
Mn		0.01	0.01	0.01	0.01	0.01	0.01	0.01
Fe		0.37	0.37	0.36	0.36	0.35	0.36	0.36
Total		4.03	4.03	4.03	4.03	4.03	4.03	4.03
Mg#		69.95	69.93	70.28	70.40	70.70	70.14	70.23
%wo		38.81	38.84	38.75	38.83	38.87	38.86	38.83
%en		42.80	42.77	43.05	43.06	43.22	42.89	42.96
%fs		18.39	18.39	18.21	18.11	17.91	18.26	18.21

Sample 44		CPX 1 Spec. 1	CPX 1 Spec. 2	CPX 1 Spec. 3	CPX 1 Spec. 4	CPX 1 Spec. 5	CPX 1 Spec. 6	Avg.
Na_2O	Oxide	0.36	0.35	0.41	0.45	0.34	0.37	0.38
MgO	wt%	15.61	15.59	15.79	15.64	15.56	15.72	15.65
Al_2O_3		2.77	2.61	2.70	2.78	2.65	2.78	2.72
SiO_2		50.72	50.55	50.14	50.88	49.92	50.70	50.49
CaO		20.74	20.44	20.19	19.85	20.51	20.44	20.36
TiO_2		0.94	0.97	1.06	1.06	1.03	0.98	1.01
V_2O_5		0.21	0.15	0.23	0.77	0.08	0.07	0.25
Cr_2O_3		0.80	0.73	0.63		0.76	0.64	0.71
MnO		0.21	0.17	0.21	0.21	0.25	0.10	0.19
FeO		8.12	8.10	8.64	8.55	8.10	8.15	8.28
Total		100.46	99.66	100.01	100.19	99.20	99.95	
Na	Cations	0.03	0.03	0.03	0.03	0.02	0.03	0.03
Mg	Norm.	0.86	0.87	0.88	0.86	0.87	0.87	0.87
Al	to	0.12	0.11	0.12	0.12	0.12	0.12	0.12
Si	6 oxygens	1.88	1.89	1.87	1.89	1.88	1.89	1.88
Ca		0.82	0.82	0.81	0.79	0.83	0.81	0.81
Ti		0.03	0.03	0.03	0.03	0.03	0.03	0.03
V		0.01	0.00	0.01	0.02	0.00	0.00	0.01
Cr		0.02	0.02	0.02		0.02	0.02	0.02
Mn		0.01	0.01	0.01	0.01	0.01	0.00	0.01
Fe		0.25	0.25	0.27	0.27	0.25	0.25	0.26
Total		4.03	4.02	4.04	4.01	4.03	4.03	4.03
Mg#		77.41	77.43	76.51	76.53	77.40	77.47	77.12
%wo		42.50	42.18	41.28	41.11	42.30	41.99	41.89
%en		44.51	44.77	44.93	45.07	44.66	44.94	44.81
%fs		12.99	13.05	13.79	13.82	13.04	13.07	13.29

Sample 44		CPX 2 Spec. 1	CPX 2 Spec. 2	CPX 2 Spec. 3	CPX 2 Spec. 4	CPX 2 Spec. 5	CPX 2 Spec. 6	Avg.
Na_2O	Oxide	0.44	0.34	0.46	0.41	0.41	0.35	0.40
MgO	wt%	15.48	15.82	15.67	15.87	15.63	15.54	15.67
Al_2O_3		2.45	2.39	2.32	2.33	2.35	2.23	2.35
SiO_2		50.22	50.50	50.21	50.23	50.42	50.80	50.40
CaO		19.87	19.51	19.65	18.97	19.84	19.16	19.50
TiO_2		1.44	1.48	1.39	1.40	1.27	1.39	1.40
V_2O_5		0.11	0.07	0.14	0.02	0.07	0.23	0.11
Cr_2O_3		0.15	0.21	0.18	0.15	0.22	0.22	0.19
MnO		0.16	0.20	0.27	0.20	0.30	0.28	0.24
FeO		9.52	9.70	9.62	10.07	9.46	9.75	9.69
Total		99.83	100.21	99.91	99.66	99.97	99.93	

Na	Cations	0.03	0.02	0.03	0.03	0.03	0.03	0.03
Mg	Norm.	0.86	0.88	0.88	0.89	0.87	0.86	0.87
Al	to	0.11	0.11	0.10	0.10	0.10	0.10	0.10
Si	6 oxygens	1.88	1.88	1.88	1.89	1.89	1.90	1.89
Ca		0.80	0.78	0.79	0.76	0.80	0.77	0.78
Ti		0.04	0.04	0.04	0.04	0.04	0.04	0.04
V		0.00	0.00	0.00	0.00	0.00	0.01	0.00
Cr		0.00	0.01	0.01	0.00	0.01	0.01	0.01
Mn		0.01	0.01	0.01	0.01	0.01	0.01	0.01
Fe		0.30	0.30	0.30	0.32	0.30	0.30	0.30
Total		4.03	4.03	4.04	4.04	4.04	4.02	4.03
Mg#		74.35	74.41	74.38	73.75	74.65	73.97	74.25
%wo		40.68	39.74	40.13	38.78	40.51	39.59	39.91
%en		44.10	44.84	44.53	45.15	44.41	44.68	44.62
%fs		15.22	15.42	15.34	16.07	15.08	15.73	15.47

Sample 44		CPX 3 Spec. 1	CPX 3 Spec. 2	CPX 3 Spec. 3	CPX 3 Spec. 4	CPX 3 Spec. 5	CPX 3 Spec. 6	Avg.
Na_2O	Oxide	0.31	0.41	0.44	0.34	0.44	0.30	0.37
MgO	wt%	15.52	15.07	15.46	15.32	15.19	15.99	15.43
Al_2O_3		2.39	2.28	2.27	2.12	2.34	2.39	2.30
SiO_2		50.40	49.95	50.34	49.75	50.32	50.45	50.20
CaO		19.69	20.19	19.04	19.94	19.82	17.81	19.42
TiO_2		1.25	1.24	1.40	1.43	1.28	1.29	1.32
V_2O_5		0.20	0.05	0.06	0.11	0.11		0.11
Cr_2O_3		0.11	0.12	0.18	0.09	0.17	0.17	0.14
MnO		0.24	0.25	0.20	0.25	0.26	0.24	0.24
FeO		9.71	9.38	9.73	9.76	9.59	10.47	9.77
Total		99.81	98.94	99.12	99.12	99.52	99.10	
Na	Cations	0.02	0.03	0.03	0.02	0.03	0.02	0.03
Mg	Norm.	0.87	0.85	0.87	0.86	0.85	0.90	0.87
Al	to	0.11	0.10	0.10	0.09	0.10	0.11	0.10
Si	6 oxygens	1.89	1.89	1.90	1.88	1.89	1.90	1.89
Ca		0.79	0.82	0.77	0.81	0.80	0.72	0.78
Ti		0.04	0.04	0.04	0.04	0.04	0.04	0.04
V		0.00	0.00	0.00	0.00	0.00		0.00
Cr		0.00	0.00	0.01	0.00	0.01	0.01	0.00
Mn		0.01	0.01	0.01	0.01	0.01	0.01	0.01
Fe		0.30	0.30	0.31	0.31	0.30	0.33	0.31
Total		4.03	4.04	4.02	4.04	4.03	4.02	4.03
Mg#		74.02	74.12	73.91	73.67	73.85	73.14	73.78
%wo		40.29	41.64	39.54	40.80	40.91	36.92	40.03
%en		44.20	43.25	44.68	43.62	43.63	46.13	44.25
%fs		15.51	15.10	15.77	15.59	15.45	16.94	15.73

Sample 55		CPX 1 Spec. 1	CPX 1 Spec. 2	CPX 1 Spec. 3	CPX 1 Spec. 4	CPX 1 Spec. 5	Avg.
Na_2O	Oxide	0.33	0.33	0.29	0.30	0.35	0.32
MgO	wt%	15.44	15.16	15.19	14.94	15.01	15.15
Al_2O_3		2.78	2.58	2.64	2.56	2.64	2.64
SiO_2		50.13	50.41	50.28	50.27	50.40	50.30
CaO		19.99	20.66	20.56	20.77	20.35	20.47
TiO_2		1.17	1.39	1.45	1.30	1.41	1.34
V_2O_5		0.22	0.18	0.13	0.20	0.11	0.17
Cr_2O_3					0.18	0.18	0.18

MnO		0.32	0.23	0.21	0.21	0.28	0.25
FeO		9.52	9.50	9.40	8.99	9.27	9.34
Total		99.89	100.44	100.15	99.71	99.99	
Na	Cations	0.02	0.02	0.02	0.02	0.03	0.02
Mg	Norm.	0.86	0.84	0.85	0.83	0.84	0.84
Al	to	0.12	0.11	0.12	0.11	0.12	0.12
Si	6 oxygens	1.88	1.88	1.88	1.88	1.88	1.88
Ca		0.80	0.83	0.82	0.83	0.82	0.82
Ti		0.03	0.04	0.04	0.04	0.04	0.04
V		0.01	0.00	0.00	0.00	0.00	0.00
Cr					0.01	0.01	0.00
Mn		0.01	0.01	0.01	0.01	0.01	0.01
Fe		0.30	0.30	0.29	0.28	0.29	0.29
Total		4.03	4.03	4.03	4.02	4.02	4.03
Mg#		74.30	73.99	74.23	74.76	74.27	74.31
%wo		40.87	42.02	41.93	42.76	41.98	41.91
%en		43.93	42.90	43.11	42.80	43.09	43.17
%fs		15.20	15.08	14.96	14.45	14.93	14.92

Sample 55		CPX 2 Spec. 1	CPX 2 Spec. 2	CPX 2 Spec. 3	CPX 2 Spec. 4	CPX 2 Spec. 5	CPX 2 Spec. 6	Avg.
Na_2O	Oxide	0.31	0.33	0.33	0.42	0.32	0.27	0.33
MgO	wt%	14.64	14.83	14.81	14.89	14.96	15.12	14.88
Al_2O_3		2.10	2.18	1.97	1.93	2.02	2.12	2.05
SiO_2		50.58	51.09	50.82	50.88	50.75	50.66	50.80
CaO		21.45	21.06	21.46	21.25	21.22	20.98	21.24
TiO_2		0.91	0.95	0.93	1.00	0.90	1.03	0.95
V_2O_5		0.14	0.11	0.12		0.18	0.14	0.14
Cr_2O_3				0.16	0.09	0.13	0.00	0.10
MnO		0.30	0.35	0.20	0.29	0.32	0.27	0.29
FeO		9.37	9.23	8.65	8.64	8.83	8.76	8.91
Total		99.80	100.15	99.46	99.39	99.63	99.34	
Na	Cations	0.02	0.02	0.02	0.03	0.02	0.02	0.02
Mg	Norm.	0.82	0.83	0.83	0.83	0.84	0.85	0.83
Al	to	0.09	0.10	0.09	0.09	0.09	0.09	0.09
Si	6 oxygens	1.90	1.91	1.91	1.91	1.90	1.90	1.91
Ca		0.86	0.84	0.86	0.86	0.85	0.84	0.85
Ti		0.03	0.03	0.03	0.03	0.03	0.03	0.03
V		0.00	0.00	0.00		0.00	0.00	0.00
Cr				0.00	0.00	0.00	0.00	0.00
Mn		0.01	0.01	0.01	0.01	0.01	0.01	0.01
Fe		0.29	0.29	0.27	0.27	0.28	0.28	0.28
Total		4.03	4.03	4.03	4.03	4.03	4.03	4.03
Mg#		73.58	74.12	75.32	75.44	75.13	75.47	74.84
%wo		43.65	43.07	43.96	43.62	43.37	42.94	43.43
%en		41.46	42.20	42.21	42.53	42.55	43.06	42.34
%fs		14.89	14.73	13.83	13.85	14.09	14.00	14.23

Sample 55		CPX 3 Spec. 1	CPX 3 Spec. 2	CPX 3 Spec. 3	CPX 3 Spec. 4	CPX 3 Spec. 5	Avg.
Na_2O	Oxide	0.28	0.35	0.44	0.33	0.48	0.38
MgO	wt%	14.49	14.60	14.95	15.25	15.47	14.95
Al_2O_3		3.08	3.09	2.85	2.76	2.72	2.90
SiO_2		49.85	50.03	49.84	50.37	49.10	49.84

CaO		20.05	20.02	19.30	18.37	17.09	18.97
TiO_2		1.54	1.45	1.46	1.26	3.07	1.76
V_2O_5		0.21		0.17	0.13	0.16	0.17
Cr_2O_3		0.18	0.25	0.13	0.20	0.24	0.20
MnO		0.26	0.33	0.17	0.22	0.37	0.27
FeO		9.45	9.40	9.98	10.22	11.53	10.12
Total		99.40	99.52	99.30	99.10	100.24	
Na	Cations	0.02	0.03	0.03	0.02	0.03	0.03
Mg	Norm.	0.81	0.82	0.84	0.86	0.87	0.84
Al	to	0.14	0.14	0.13	0.12	0.12	0.13
Si	6 oxygens	1.88	1.88	1.88	1.90	1.84	1.87
Ca		0.81	0.81	0.78	0.74	0.69	0.76
Ti		0.04	0.04	0.04	0.04	0.09	0.05
V		0.01		0.00	0.00	0.00	0.00
Cr		0.01	0.01	0.00	0.01	0.01	0.01
Mn		0.01	0.01	0.01	0.01	0.01	0.01
Fe		0.30	0.30	0.31	0.32	0.36	0.32
Total		4.01	4.02	4.03	4.01	4.02	4.02
Mg#		73.21	73.47	72.75	72.68	70.52	72.49
%wo		42.13	41.99	40.30	38.62	35.89	39.79
%en		42.37	42.62	43.44	44.61	45.21	43.65
%fs		15.50	15.39	16.27	16.77	18.90	16.56

Sample 67		CPX 1 Spec. 1	CPX 1 Spec. 2	CPX 1 Spec. 3	CPX 1 Spec. 4	CPX 1 Spec. 5	Avg.
Na_2O	Oxide	0.31	0.39	0.31	0.36	0.30	0.33
MgO	wt%	15.96	16.10	15.88	15.88	16.14	15.99
Al_2O_3		2.57	2.59	2.47	2.63	2.75	2.60
SiO_2		50.14	50.14	50.11	50.18	50.28	50.17
CaO		20.25	20.14	20.05	20.08	19.93	20.09
TiO_2		1.62	1.42	1.59	1.55	1.42	1.52
V_2O_5			0.17	0.15	0.23	0.22	0.19
Cr_2O_3		0.11					0.11
MnO		0.27	0.29	0.31	0.12	0.15	0.23
FeO		8.16	8.15	8.22	7.94	8.20	8.13
Total		99.39	99.40	99.08	98.98	99.39	
Na	Cations	0.02	0.03	0.02	0.03	0.02	0.02
Mg	Norm.	0.89	0.90	0.89	0.89	0.90	0.89
Al	to	0.11	0.11	0.11	0.12	0.12	0.11
Si	6 oxygens	1.88	1.88	1.88	1.88	1.88	1.88
Ca		0.81	0.81	0.81	0.81	0.80	0.81
Ti		0.05	0.04	0.04	0.04	0.04	0.04
V			0.00	0.00	0.01	0.01	0.00
Cr		0.00					0.00
Mn		0.01	0.01	0.01	0.00	0.00	0.01
Fe		0.26	0.26	0.26	0.25	0.26	0.25
Total		4.03	4.03	4.02	4.02	4.02	4.03
Mg#		77.71	77.88	77.50	78.10	77.82	77.80
%wo		41.47	41.18	41.29	41.51	40.85	41.26
%en		45.48	45.81	45.50	45.68	46.03	45.70
%fs		13.05	13.01	13.21	12.81	13.12	13.04

Sample 67		CPX 2 Spec. 1	CPX 2 Spec. 2	CPX 2 Spec. 3	CPX 2 Spec. 4	CPX 2 Spec. 5	Avg.

Na_2O	Oxide	0.32	0.30	0.36	0.34	0.37	0.34
MgO	wt%	17.37	17.08	16.25	15.72	16.28	16.54
Al_2O_3		2.51	2.51	2.48	2.59	2.58	2.53
SiO_2		51.73	51.26	50.67	50.40	51.00	51.01
CaO		18.52	19.05	20.21	21.48	20.59	19.97
TiO_2		1.26	1.25	1.18	1.24	1.21	1.23
V_2O_5		0.00	0.14	0.15	0.12	0.09	0.10
Cr_2O_3		0.44	0.33	0.40	0.39	0.42	0.40
MnO		0.08	0.12	0.12	0.13	0.15	0.12
FeO		8.42	8.33	7.04	6.82	7.49	7.62
Total		100.65	100.37	98.86	99.24	100.17	
Na	Cations	0.02	0.02	0.03	0.02	0.03	0.02
Mg	Norm.	0.95	0.94	0.91	0.88	0.90	0.91
Al	to	0.11	0.11	0.11	0.11	0.11	0.11
Si	6 oxygens	1.90	1.89	1.89	1.88	1.89	1.89
Ca		0.73	0.75	0.81	0.86	0.82	0.79
Ti		0.03	0.03	0.03	0.03	0.03	0.03
V		0.00	0.00	0.00	0.00	0.00	0.00
Cr		0.01	0.01	0.01	0.01	0.01	0.01
Mn		0.00	0.00	0.00	0.00	0.00	0.00
Fe		0.26	0.26	0.22	0.21	0.23	0.24
Total		4.02	4.02	4.02	4.03	4.03	4.02
Mg#		78.62	78.52	80.45	80.43	79.49	79.47
%wo		37.59	38.62	41.83	44.13	41.94	40.83
%en		49.06	48.19	46.80	44.94	46.15	47.03
%fs		13.34	13.18	11.37	10.94	11.91	12.15

Sample 67		CPX 3 Spec. 1	CPX 3 Spec. 2	CPX 3 Spec. 3	CPX 3 Spec. 4	CPX 3 Spec. 5	Average
Na_2O	Oxide	0.42	0.37	0.50	0.37	0.35	0.40
MgO	wt%	14.94	15.05	15.81	15.73	15.20	15.35
Al_2O_3		4.00	3.79	3.25	3.38	3.38	3.56
SiO_2		48.42	48.80	49.79	49.60	49.34	49.19
CaO		20.15	19.99	20.12	20.49	21.18	20.39
TiO_2		1.55	1.65	1.67	1.39	1.65	1.58
V_2O_5		0.15	0.23	0.22	0.13	0.16	0.18
Cr_2O_3		0.57	0.50	0.44	0.55	0.58	0.53
MnO		0.24	0.24	0.16	0.08	0.30	0.20
FeO		9.28	8.50	7.88	7.86	7.32	8.17
Total		99.72	99.12	99.85	99.58	99.47	
Na	Cations	0.03	0.03	0.04	0.03	0.03	0.03
Mg	Norm.	0.84	0.85	0.88	0.88	0.85	0.86
Al	to	0.18	0.17	0.14	0.15	0.15	0.16
Si	6 oxygens	1.82	1.84	1.85	1.85	1.85	1.84
Ca		0.81	0.81	0.80	0.82	0.85	0.82
Ti		0.04	0.05	0.05	0.04	0.05	0.04
V		0.00	0.01	0.01	0.00	0.00	0.00
Cr		0.02	0.01	0.01	0.02	0.02	0.02
Mn		0.01	0.01	0.01	0.00	0.01	0.01
Fe		0.29	0.27	0.25	0.25	0.23	0.26
Total		4.05	4.03	4.03	4.03	4.03	4.03
Mg#		74.16	75.94	78.15	78.11	78.73	77.00
%wo		41.82	42.02	41.68	42.23	44.08	42.37
%en		43.15	44.03	45.58	45.12	44.02	44.38
%fs		15.03	13.95	12.74	12.65	11.89	13.25

Sample 75		CPX 1 Spec. 1	CPX 1 Spec. 2	CPX 1 Spec. 3	CPX 1 Spec. 4	CPX 1 Spec. 5	CPX 1 Spec. 6	Avg.
Na_2O	Oxide	0.41	0.33	0.35	0.41	0.44	0.38	0.39
MgO	wt%	15.76	15.46	16.28	15.47	15.96	15.74	15.78
Al_2O_3		3.29	3.31	3.26	3.35	3.23	3.43	3.31
SiO_2		50.17	50.46	50.33	50.46	50.40	50.10	50.32
CaO		20.98	20.67	20.14	21.06	19.70	20.72	20.55
TiO_2		1.28	1.27	1.16	1.17	1.24	1.27	1.23
V_2O_5		0.00		0.12	0.16		0.00	0.07
Cr_2O_3		0.81	0.84	0.69	0.80	0.81	0.86	0.80
MnO		0.15	0.22	0.15	0.16	0.14	0.12	0.16
FeO		7.56	7.44	7.87	7.41	8.12	7.59	7.67
Total		100.41	100.00	100.35	100.44	100.05	100.21	
Na	Cations	0.03	0.02	0.03	0.03	0.03	0.03	0.03
Mg	Norm.	0.87	0.86	0.90	0.85	0.88	0.87	0.87
Al	to	0.14	0.14	0.14	0.15	0.14	0.15	0.14
Si	6 oxygens	1.86	1.87	1.86	1.87	1.87	1.86	1.87
Ca		0.83	0.82	0.80	0.83	0.78	0.82	0.82
Ti		0.04	0.04	0.03	0.03	0.03	0.04	0.03
V		0.00		0.00	0.00		0.00	0.00
Cr		0.02	0.02	0.02	0.02	0.02	0.03	0.02
Mn		0.00	0.01	0.00	0.01	0.00	0.00	0.00
Fe		0.23	0.23	0.24	0.23	0.25	0.24	0.24
Total		4.04	4.02	4.03	4.02	4.03	4.03	4.03
Mg#		78.80	78.74	78.67	78.82	77.80	78.71	78.58
%wo		42.98	43.07	41.15	43.54	40.83	42.68	42.37
%en		44.93	44.83	46.29	44.50	46.03	45.12	45.29
%fs		12.09	12.10	12.55	11.96	13.14	12.20	12.34

Sample 75		CPX 2 Spec. 1	CPX 2 Spec. 2	CPX 2 Spec. 3	CPX 2 Spec. 4	CPX 2 Spec. 5	CPX 2 Spec. 6	Avg.
Na_2O	Oxide	0.36	0.43		0.41		0.43	0.41
MgO	wt%	14.91	15.20	17.08	15.04	15.95	15.73	15.65
Al_2O_3		3.31	3.26	3.03	3.35	3.34	3.32	3.27
SiO_2		49.93	49.82	50.39	49.76	50.00	50.57	50.08
CaO		21.52	21.36	19.16	21.51	20.45	20.03	20.67
TiO_2		1.23	1.29	1.18	1.23	1.18	1.19	1.22
V_2O_5								
Cr_2O_3		0.75	0.58	0.67	0.67	0.59	0.66	0.65
MnO								
FeO		7.19	7.43	8.74	7.21	7.85	7.89	7.72
Total		99.21	99.36	100.26	99.19	99.36	99.81	
Na	Cations	0.03	0.03		0.03		0.03	0.02
Mg	Norm.	0.83	0.85	0.94	0.84	0.89	0.87	0.87
Al	to	0.15	0.14	0.13	0.15	0.15	0.15	0.14
Si	6 oxygens	1.87	1.87	1.87	1.87	1.87	1.88	1.87
Ca		0.86	0.86	0.76	0.86	0.82	0.80	0.83
Ti		0.03	0.04	0.03	0.03	0.03	0.03	0.03
V								
Cr		0.02	0.02	0.02	0.02	0.02	0.02	0.02
Mn								
Fe		0.23	0.23	0.27	0.23	0.25	0.25	0.24
Total		4.02	4.03	4.02	4.03	4.02	4.02	4.02

Mg#	78.71	78.48	77.70	78.81	78.36	78.04	78.33
%wo	44.94	44.21	38.51	44.75	41.93	41.66	42.65
%en	43.33	43.78	47.77	43.54	45.51	45.53	44.92
%fs	11.72	12.01	13.71	11.71	12.56	12.81	12.43

MOUNT MOLLIE DYKE OLIVINE

Sample 12		Ol 1 Spec. 1	Ol 1 Spec. 2	Ol 1 Spec. 3	Ol 1 Spec. 4	Ol 1 Spec. 5	Ol 1 Spec. 6	Avg.
MgO	Oxide	20.34	20.01	19.87	20.14	19.88	19.84	20.01
Al_2O_3	wt%							
SiO_2		33.36	33.35	33.21	33.67	33.38	32.97	33.32
CaO		0.19	0.25	0.21	0.21	0.23	0.28	0.23
MnO		0.67	0.77	0.67	0.74	0.80	0.70	0.73
FeO		45.99	45.63	45.76	45.91	46.27	45.78	45.89
NiO								
Total		100.54	100.02	99.73	100.67	100.56	99.56	
Mg	Cations	0.89	0.88	0.88	0.88	0.87	0.88	0.88
Al	Norm.							
Si	to	0.98	0.98	0.98	0.99	0.98	0.98	0.98
Ca	4 oxygens	0.01	0.01	0.01	0.01	0.01	0.01	0.01
Mn		0.02	0.02	0.02	0.02	0.02	0.02	0.02
Fe		1.13	1.13	1.13	1.12	1.14	1.14	1.13
Ni								
Total		3.02	3.02	3.02	3.01	3.02	3.02	3.02
Fo		44.08	43.87	43.63	43.88	43.37	43.58	43.74

Sample 12		Ol 2 Spec. 1	Ol 2 Spec. 2	Ol 2 Spec. 3	Ol 2 Spec. 4	Ol 2 Spec. 5	Ol 2 Spec. 6	Avg.
MgO	Oxide	20.76	20.26	20.27	20.07	20.23	20.08	20.28
Al_2O_3	wt%							
SiO_2		33.45	33.26	33.48	34.07	33.46	33.25	33.50
CaO		0.19	0.21	0.24	0.22	0.29	0.23	0.23
MnO		0.73	0.68	0.72	0.69	0.73	0.72	0.71
FeO		45.86	45.45	45.16	45.73	45.65	45.26	45.52
NiO								
Total		100.98	99.85	99.87	100.78	100.36	99.53	
Mg	Cations	0.90	0.89	0.89	0.87	0.89	0.89	0.89
Al	Norm.							
Si	to	0.98	0.98	0.99	0.99	0.98	0.98	0.98
Ca	4 oxygens	0.01	0.01	0.01	0.01	0.01	0.01	0.01
Mn		0.02	0.02	0.02	0.02	0.02	0.02	0.02
Fe		1.12	1.12	1.11	1.12	1.12	1.12	1.12
Ni								
Total		3.02	3.02	3.01	3.01	3.02	3.02	3.02
Fo		44.66	44.28	44.45	43.89	44.13	44.16	44.26

Sample 12		Ol 3 Spec. 1	Ol 3 Spec. 2	Ol 3 Spec. 3	Ol 3 Spec. 4	Avg.
MgO	Oxide	19.95	20.15	19.98	19.82	19.98
Al_2O_3	wt%					
SiO_2		33.42	33.28	33.23	33.38	33.33
CaO		0.21	0.20	0.23	0.22	0.22
MnO		0.66	0.71	0.64	0.83	0.71
FeO		46.52	46.37	45.73	45.71	46.08
NiO						
Total		100.76	100.71	99.80	99.97	
Mg	Cations	0.87	0.88	0.88	0.87	0.88

Al	Norm.					
Si	to	0.98	0.98	0.98	0.99	0.98
Ca	4 oxygens	0.01	0.01	0.01	0.01	0.01
Mn		0.02	0.02	0.02	0.02	0.02
Fe		1.14	1.14	1.13	1.13	1.14
Ni						
Total		3.02	3.02	3.02	3.01	3.02
Fo		43.33	43.65	43.78	43.60	43.59

Sample 18		Ol 1 Spec. 1	Ol 1 Spec. 2	Ol 1 Spec. 3	Ol 1 Spec. 4	Avg.
MgO	Oxide	22.08	21.90	22.12	21.95	22.01
Al_2O_3	wt%					
SiO_2		33.74	33.59	33.74	33.60	33.67
CaO		0.21	0.20	0.19	0.16	0.19
MnO		0.55	0.67	0.62	0.62	0.62
FeO		43.17	43.41	43.25	43.44	43.32
NiO						
Total		99.76	99.77	99.92	99.77	
Mg	Cations	0.96	0.95	0.96	0.96	0.96
Al	Norm.					
Si	to	0.98	0.98	0.98	0.98	0.98
Ca	4 oxygens	0.01	0.01	0.01	0.01	0.01
Mn		0.01	0.02	0.02	0.02	0.02
Fe		1.05	1.06	1.05	1.06	1.06
Ni						
Total		3.02	3.02	3.02	3.02	3.02
Fo		47.69	47.35	47.69	47.39	47.53

Sample 18		Ol 2 Spec. 1	Ol 2 Spec. 2	Ol 2 Spec. 3	Ol 2 Spec. 4	Ol 2 Spec. 5	Ol 2 Spec. 6	Avg.
MgO	Oxide	21.56	21.47	21.55	21.55	21.72	21.34	21.53
Al_2O_3	wt%							
SiO_2		33.20	33.09	33.79	33.17	33.20	33.15	33.27
CaO		0.24	0.30	0.24	0.19	0.22	0.26	0.24
MnO		0.52	0.66	0.58	0.69	0.66	0.71	0.64
FeO		43.87	43.87	43.69	43.86	43.87	43.67	43.81
NiO								
Total		99.39	99.39	99.85	99.46	99.68	99.13	
Mg	Cations	0.95	0.94	0.94	0.95	0.95	0.94	0.94
Al	Norm.							
Si	to	0.98	0.97	0.99	0.98	0.97	0.98	0.98
Ca	4 oxygens	0.01	0.01	0.01	0.01	0.01	0.01	0.01
Mn		0.01	0.02	0.01	0.02	0.02	0.02	0.02
Fe		1.08	1.08	1.07	1.08	1.08	1.08	1.08
Ni								
Total		3.02	3.03	3.01	3.02	3.03	3.02	3.02
Fo		46.70	46.59	46.79	46.69	46.88	46.56	46.70

Sample 18		Ol 3 Spec. 1	Ol 3 Spec. 2	Ol 3 Spec. 3	Ol 3 Spec. 4	Ol 3 Spec. 5	Ol 3 Spec. 6	Avg.
MgO	Oxide	22.06	22.08	22.19	21.92	22.18	22.17	22.10

Al_2O_3	wt%							
SiO_2		33.34	33.80	33.49	33.60	33.66	33.54	33.57
CaO		0.16	0.16	0.19	0.20	0.21	0.19	0.19
MnO		0.55	0.54	0.59	0.57	0.65	0.62	0.59
FeO		43.19	43.05	43.31	42.72	43.27	42.97	43.09
NiO								
Total		99.30	99.64	99.76	99.02	99.98	99.50	
Mg	Cations	0.96	0.96	0.97	0.96	0.96	0.97	0.96
Al	Norm.							
Si	to	0.98	0.99	0.98	0.99	0.98	0.98	0.98
Ca	4 oxygens	0.01	0.00	0.01	0.01	0.01	0.01	0.01
Mn		0.01	0.01	0.01	0.01	0.02	0.02	0.01
Fe		1.06	1.05	1.06	1.05	1.05	1.05	1.05
Ni								
Total		3.02	3.01	3.02	3.01	3.02	3.02	3.02
Fo		47.66	47.76	47.74	47.77	47.75	47.91	47.76

Sample 18		Ol 4 Spec. 1	Ol 4 Spec. 2	Ol 4 Spec. 3	Ol 4 Spec. 4	Avg.
MgO	Oxide	21.74	21.71	21.46	21.25	21.54
Al_2O_3	wt%					
SiO_2		33.34	33.48	33.52	33.21	33.39
CaO		0.18	0.20	0.16	0.19	0.18
MnO		0.50	0.60	0.55	0.59	0.56
FeO		44.20	43.43	43.45	43.88	43.74
NiO						
Total		99.95	99.43	99.13	99.12	
Mg	Cations	0.95	0.95	0.94	0.94	0.94
Al	Norm.					
Si	to	0.98	0.98	0.99	0.98	0.98
Ca	4 oxygens	0.01	0.01	0.01	0.01	0.01
Mn		0.01	0.01	0.01	0.01	0.01
Fe		1.08	1.07	1.07	1.08	1.07
Ni						
Total		3.02	3.02	3.01	3.02	3.02
Fo		46.72	47.12	46.82	46.33	46.75

Sample 18		Ol 5 Spec. 1	Ol 5 Spec. 2	Ol 5 Spec. 3	Ol 5 Spec. 4	Avg.
MgO	Oxide	22.05	22.23	22.02	22.12	22.11
Al_2O_3	wt%					
SiO_2		33.70	33.62	33.86	33.51	33.67
CaO		0.24	0.21	0.17	0.17	0.20
MnO		0.54	0.63	0.54	0.57	0.57
FeO		42.86	43.06	43.26	43.00	43.05
NiO						
Total		99.40	99.75	99.85	99.37	
Mg	Cations	0.96	0.97	0.96	0.97	0.96
Al	Norm.					
Si	to	0.99	0.98	0.99	0.98	0.98
Ca	4 oxygens	0.01	0.01	0.01	0.01	0.01
Mn		0.01	0.02	0.01	0.01	0.01
Fe		1.05	1.05	1.05	1.05	1.05

Ni						
Total		3.01	3.02	3.01	3.02	3.02
Fo		47.84	47.92	47.57	47.84	47.79

Sample 18		Ol 6 Spec. 1	Ol 6 Spec. 2	Ol 6 Spec. 3	Ol 6 Spec. 4	Avg.
MgO	Oxide	22.00	21.73	21.60	21.77	21.78
Al_2O_3	wt%					
SiO_2		33.60	33.37	33.40	33.20	33.39
CaO		0.20	0.21	0.19	0.18	0.20
MnO		0.68	0.52	0.66	0.53	0.60
FeO		43.38	43.27	43.26	43.35	43.32
NiO						
Total		99.86	99.08	99.11	99.03	
Mg	Cations	0.96	0.95	0.95	0.96	0.95
Al	Norm.					
Si	to	0.98	0.98	0.98	0.98	0.98
Ca	4 oxygens	0.01	0.01	0.01	0.01	0.01
Mn		0.02	0.01	0.02	0.01	0.01
Fe		1.06	1.06	1.06	1.07	1.06
Ni						
Total		3.02	3.02	3.02	3.02	3.02
Fo		47.48	47.24	47.09	47.24	47.26

Sample 23		Ol 1 Spec. 1	Ol 1 Spec. 2	Ol 1 Spec. 3	Ol 1 Spec. 4	Ol 1 Spec. 5	Avg.
MgO	Oxide	26.58	26.82	26.85	27.25	27.02	26.90
Al_2O_3	wt%						
SiO_2		34.95	35.07	34.74	34.84	34.99	34.92
CaO		0.18	0.25	0.25	0.22	0.20	0.22
MnO		0.61	0.65	0.54	0.54	0.56	0.58
FeO		37.64	37.59	37.81	37.90	37.97	37.78
NiO							
Total		99.95	100.39	100.18	100.74	100.74	
Mg	Cations	1.12	1.12	1.13	1.14	1.13	1.13
Al	Norm.						
Si	to	0.99	0.99	0.98	0.98	0.98	0.98
Ca	4 oxygens	0.01	0.01	0.01	0.01	0.01	0.01
Mn		0.01	0.02	0.01	0.01	0.01	0.01
Fe		0.89	0.88	0.89	0.89	0.89	0.89
Ni							
Total		3.01	3.01	3.02	3.02	3.02	3.02
Fo		55.73	55.98	55.87	56.17	55.92	55.93

Sample 23		Ol 2 Spec. 1	Ol 2 Spec. 2	Ol 2 Spec. 3	Ol 2 Spec. 4	Ol 2 Spec. 5	Ol 2 Spec. 6	Avg.
MgO	Oxide	25.99	26.24	26.31	26.39	26.10	26.16	26.20
Al_2O_3	wt%							
SiO_2		34.73	34.94	34.51	34.43	34.54	34.46	34.60
CaO		0.13	0.12	0.20	0.12	0.17	0.18	0.15
MnO		0.55	0.64	0.61	0.58	0.66	0.52	0.59
FeO		38.60	38.12	38.06	38.80	38.20	38.39	38.36

NiO								
Total		99.99	100.06	99.69	100.32	99.66	99.71	
Mg	Cations	1.10	1.11	1.11	1.11	1.11	1.11	1.11
Al	Norm.							
Si	to	0.98	0.99	0.98	0.97	0.98	0.98	0.98
Ca	4 oxygens	0.00	0.00	0.01	0.00	0.01	0.01	0.00
Mn		0.01	0.02	0.01	0.01	0.02	0.01	0.01
Fe		0.92	0.90	0.90	0.92	0.91	0.91	0.91
Ni								
Total		3.02	3.01	3.02	3.03	3.02	3.02	3.02
Fo		54.55	55.10	55.20	54.80	54.91	54.85	54.90

Sample 23		Ol 3 Spec. 1	Ol 3 Spec. 2	Ol 3 Spec. 3	Ol 3 Spec. 4	Ol 3 Spec. 5	Ol 3 Spec. 6	Avg.
MgO	Oxide	26.54	26.30	26.35	26.53	26.33	26.54	26.43
Al_2O_3	wt%							
SiO_2		34.77	35.04	34.96	35.04	34.39	34.67	34.81
CaO		0.18	0.15	0.22	0.17	0.18	0.19	0.18
MnO		0.47	0.58	0.58	0.56	0.58	0.48	0.54
FeO		38.02	38.20	38.42	38.04	38.22	38.44	38.22
NiO								
Total		99.97	100.27	100.52	100.35	99.71	100.33	
Mg	Cations	1.12	1.11	1.11	1.11	1.12	1.12	1.11
Al	Norm.							
Si	to	0.98	0.99	0.98	0.99	0.98	0.98	0.98
Ca	4 oxygens	0.01	0.00	0.01	0.01	0.01	0.01	0.01
Mn		0.01	0.01	0.01	0.01	0.01	0.01	0.01
Fe		0.90	0.90	0.90	0.90	0.91	0.91	0.90
Ni								
Total		3.02	3.01	3.02	3.01	3.02	3.02	3.02
Fo		55.44	55.10	55.01	55.42	55.12	55.17	55.21

Sample 29		Ol 1 Spec. 1	Ol 1 Spec. 2	Ol 1 Spec. 3	Ol 1 Spec. 4	Ol 1 Spec. 5	Ol 1 Spec. 6	Avg.
MgO	Oxide	28.33	28.01	28.20	28.07	28.26	28.05	28.15
Al_2O_3	wt%							
SiO_2		34.86	34.77	34.80	34.83	35.00	34.79	34.84
CaO		0.13	0.11	0.09	0.17	0.17	0.16	0.14
MnO		0.53	0.54	0.53	0.61	0.49	0.67	0.56
FeO		35.90	35.97	35.59	35.67	35.52	35.75	35.73
NiO		0.06	0.11	0.15	0.08	0.09	0.02	0.09
Total		99.81	99.50	99.36	99.42	99.53	99.44	
Mg	Cations	1.18	1.18	1.18	1.18	1.18	1.18	1.18
Al	Norm.							
Si	to	0.98	0.98	0.98	0.98	0.98	0.98	0.98
Ca	4 oxygens	0.00	0.00	0.00	0.01	0.01	0.00	0.00
Mn		0.01	0.01	0.01	0.01	0.01	0.02	0.01
Fe		0.84	0.85	0.84	0.84	0.83	0.84	0.84
Ni		0.00	0.00	0.00	0.00	0.00	0.00	0.00
Total		3.02	3.02	3.02	3.02	3.02	3.02	3.02
Fo		58.45	58.13	58.55	58.38	58.65	58.31	58.41

Sample 29		Ol 2 Spec. 1	Ol 2 Spec. 2	Ol 2 Spec. 3	Ol 2 Spec. 4	Ol 2 Spec. 5	Ol 2 Spec. 6	Avg.
MgO	Oxide	28.05	28.09	28.20	28.01	28.02	28.35	28.12
Al_2O_3	wt%							
SiO_2		34.95	34.90	35.14	34.84	34.97	34.90	34.95
CaO		0.11	0.09	0.12	0.20	0.17	0.14	0.14
MnO		0.49	0.55	0.51	0.51	0.63	0.52	0.54
FeO		35.73	35.66	35.76	35.66	36.11	35.39	35.72
NiO		0.09		0.06	0.34		0.12	
Total		99.41	99.31	99.79	99.55	99.91	99.43	
Mg	Cations	1.18	1.18	1.18	1.17	1.17	1.19	1.18
Al	Norm.							
Si	to	0.98	0.98	0.98	0.98	0.98	0.98	0.98
Ca	4 oxygens	0.00	0.00	0.00	0.01	0.01	0.00	0.00
Mn		0.01	0.01	0.01	0.01	0.01	0.01	0.01
Fe		0.84	0.84	0.84	0.84	0.85	0.83	0.84
Ni		0.00		0.00	0.01		0.00	0.00
Total		3.02	3.02	3.02	3.02	3.02	3.02	3.02
Fo		58.32	58.41	58.43	58.34	58.04	58.81	58.39

Sample 29		Ol 3 Spec. 1	Ol 3 Spec. 2	Ol 3 Spec. 3	Ol 3 Spec. 4	Ol 3 Spec. 5	Ol 3 Spec. 6	Avg.
MgO	Oxide	28.27	27.98	28.09	28.00	27.98	27.92	28.04
Al_2O_3	wt%							
SiO_2		34.95	34.78	34.65	34.90	34.85	34.77	34.82
CaO		0.12	0.18	0.14	0.14	0.19	0.18	0.16
MnO		0.57	0.42	0.46	0.46	0.52	0.47	0.48
FeO		35.83	35.86	35.92	35.72	35.74	35.95	35.84
NiO		0.16		0.19	0.03	0.09	0.17	
Total		99.88	99.22	99.45	99.27	99.37	99.46	
Mg	Cations	1.18	1.18	1.18	1.18	1.17	1.17	1.18
Al	Norm.							
Si	to	0.98	0.98	0.98	0.98	0.98	0.98	0.98
Ca	4 oxygens	0.00	0.01	0.00	0.00	0.01	0.01	0.00
Mn		0.01	0.01	0.01	0.01	0.01	0.01	0.01
Fe		0.84	0.85	0.85	0.84	0.84	0.85	0.84
Ni		0.00		0.00	0.00	0.00	0.00	0.00
Total		3.02	3.02	3.02	3.02	3.02	3.02	3.02
Fo		58.45	58.17	58.23	58.29	58.26	58.06	58.24

Sample 35		Ol 1 Spec. 1	Ol 1 Spec. 2	Ol 1 Spec. 3	Ol 1 Spec. 4	Ol 1 Spec. 5	Avg.
MgO	Oxide	26.76	27.06	27.06	27.07	26.77	26.94
Al_2O_3	wt%						
SiO_2		34.71	34.87	34.67	34.92	34.60	34.75
CaO		0.18	0.30	0.24	0.11	0.14	0.19
MnO		0.42	0.58	0.49	0.53	0.57	0.52
FeO		37.45	37.12	37.11	37.02	37.61	37.26
NiO							
Total		99.53	99.93	99.57	99.65	99.69	
Mg	Cations	1.13	1.14	1.14	1.14	1.13	1.14
Al	Norm.						0.00
Si	to	0.98	0.98	0.98	0.99	0.98	0.98

Ca	4 oxygens	0.01	0.01	0.01	0.00	0.00	0.01
Mn		0.01	0.01	0.01	0.01	0.01	0.01
Fe		0.89	0.87	0.88	0.87	0.89	0.88
Ni							
Total		3.02	3.02	3.02	3.01	3.02	3.02
Fo		56.02	56.51	56.52	56.59	55.92	56.31

Sample 35		Ol 2 Spec. 1	Ol 2 Spec. 2	Ol 2 Spec. 3	Ol 2 Spec. 4	Ol 2 Spec. 5	Ol 2 Spec. 6	Avg.
MgO	Oxide	26.82	26.73	26.66	26.92	26.87	26.68	26.78
Al_2O_3	wt%	0.21	0.18	0.12	0.17	0.17	0.16	0.17
SiO_2		34.72	34.63	34.89	34.74	34.51	34.76	34.71
CaO		0.21	0.15	0.13	0.19	0.15	0.15	0.16
MnO		0.52	0.65	0.54	0.55	0.40	0.60	0.54
FeO		36.98	36.76	37.04	37.06	37.07	36.98	36.98
NiO								
Total		99.46	99.10	99.37	99.63	99.18	99.34	
Mg	Cations	1.13	1.13	1.13	1.13	1.14	1.13	1.13
Al	Norm.	0.01	0.01	0.00	0.01	0.01	0.01	0.01
Si	to	0.98	0.98	0.99	0.98	0.98	0.98	0.98
Ca	4 oxygens	0.01	0.00	0.00	0.01	0.00	0.00	0.00
Mn		0.01	0.02	0.01	0.01	0.01	0.01	0.01
Fe		0.87	0.87	0.88	0.88	0.88	0.88	0.88
Ni								
Total		3.01	3.01	3.01	3.02	3.02	3.01	3.01
Fo		56.39	56.45	56.20	56.42	56.37	56.26	56.35

Sample 35		Ol 3 Spec. 1	Ol 3 Spec. 2	Ol 3 Spec. 3	Ol 3 Spec. 4	Ol 3 Spec. 5	Ol 3 Spec. 6	Avg.
MgO	Oxide	26.73	27.07	27.02	26.72	27.27	26.82	26.94
Al_2O_3	wt%	0.13			0.14	0.01	0.07	0.09
SiO_2		34.84	34.58	34.60	34.63	34.74	34.65	34.67
CaO		0.14	0.11	0.16	0.15	0.15	0.17	0.15
MnO		0.52	0.56	0.53	0.48	0.56	0.54	0.53
FeO		37.15	37.11	36.97	36.93	37.32	36.83	37.05
NiO								
Total		99.51	99.43	99.27	99.05	100.05	99.08	
Mg	Cations	1.13	1.14	1.14	1.13	1.15	1.14	1.14
Al	Norm.	0.00			0.00	0.00	0.00	0.00
Si	to	0.99	0.98	0.98	0.98	0.98	0.98	0.98
Ca	4 oxygens	0.00	0.00	0.00	0.00	0.00	0.01	0.00
Mn		0.01	0.01	0.01	0.01	0.01	0.01	0.01
Fe		0.88	0.88	0.88	0.88	0.88	0.87	0.88
Ni								
Total		3.01	3.02	3.02	3.01	3.02	3.01	3.02
Fo		56.19	56.53	56.58	56.33	56.57	56.49	56.45

Sample 37		Ol 1 Spec. 1	Ol 1 Spec. 2	Ol 1 Spec. 3	Ol 1 Spec. 4	Ol 1 Spec. 5	Avg.
MgO	Oxide	24.73	24.53	24.26	24.76	24.56	24.57
Al_2O_3	wt%						
SiO_2		34.23	34.02	34.19	34.19	34.05	34.14

CaO		0.24	0.26	0.34	0.31	0.22	0.27
MnO		0.57	0.49	0.55	0.54	0.53	0.54
FeO		40.18	40.27	40.05	40.26	40.13	40.18
NiO					0.12	0.09	0.11
Total		99.95	99.57	99.39	100.18	99.58	
Mg	Cations	1.06	1.05	1.04	1.06	1.05	1.05
Al	Norm.						
Si	to	0.98	0.98	0.98	0.98	0.98	0.98
Ca	4 oxygens	0.01	0.01	0.01	0.01	0.01	0.01
Mn		0.01	0.01	0.01	0.01	0.01	0.01
Fe		0.96	0.97	0.96	0.96	0.97	0.96
Ni					0.00	0.00	0.00
Total		3.02	3.02	3.02	3.02	3.02	3.02
Fo		52.32	52.06	51.92	52.30	52.18	52.15

Sample 37		Ol 2 Spec. 1	Ol 2 Spec. 2	Ol 2 Spec. 3	Ol 2 Spec. 4	Ol 2 Spec. 5	Ol 2 Spec. 6	Avg.
MgO	Oxide	25.63	25.53	25.46	25.48	25.64	25.41	25.53
Al_2O_3	wt%							
SiO_2		34.25	34.36	34.21	34.32	34.51	34.36	34.34
CaO		0.24	0.27	0.34	0.29	0.26	0.23	0.27
MnO		0.57	0.59	0.55	0.56	0.64	0.52	0.57
FeO		39.22	39.60	39.49	39.45	39.17	39.52	39.41
NiO								
Total		99.91	100.35	100.04	100.10	100.23	100.04	
Mg	Cations	1.09	1.08	1.08	1.08	1.09	1.08	1.08
Al	Norm.							
Si	to	0.98	0.98	0.98	0.98	0.98	0.98	0.98
Ca	4 oxygens	0.01	0.01	0.01	0.01	0.01	0.01	0.01
Mn		0.01	0.01	0.01	0.01	0.02	0.01	0.01
Fe		0.94	0.94	0.94	0.94	0.93	0.94	0.94
Ni								0.00
Total		3.02	3.02	3.02	3.02	3.02	3.02	3.02
Fo		53.81	53.47	53.47	53.52	53.85	53.41	53.59

Sample 37		Ol 3 Spec. 1	Ol 3 Spec. 2	Ol 3 Spec. 3	Ol 3 Spec. 4	Ol 3 Spec. 5	Ol 3 Spec. 6	Avg.
MgO	Oxide	25.29	25.28	25.45	25.40	25.44	25.22	25.35
Al_2O_3	wt%							
SiO_2		34.44	34.13	34.07	34.21	34.15	34.22	34.20
CaO		0.21	0.26	0.32	0.22	0.28	0.33	0.27
MnO		0.55	0.56	0.58	0.55	0.57	0.60	0.57
FeO		38.75	38.86	38.49	38.56	39.00	39.16	38.80
NiO		0.04	0.07	0.08	0.15	0.16		0.10
Total		99.27	99.16	99.00	99.09	99.60	99.53	
Mg	Cations	1.08	1.08	1.09	1.09	1.09	1.08	1.08
Al	Norm.							
Si	to	0.99	0.98	0.98	0.98	0.98	0.98	0.98
Ca	4 oxygens	0.01	0.01	0.01	0.01	0.01	0.01	0.01
Mn		0.01	0.01	0.01	0.01	0.01	0.01	0.01
Fe		0.93	0.93	0.93	0.93	0.93	0.94	0.93
Ni		0.00	0.00	0.00	0.00	0.00		0.00
Total		3.01	3.02	3.02	3.02	3.02	3.02	3.02

Fo		53.78	53.70	54.10	54.01	53.76	53.45	53.80

Sample 39		Ol 1 Spec. 1	Ol 1 Spec. 2	Ol 1 Spec. 3	Ol 1 Spec. 4	Ol 1 Spec. 5	Avg.
MgO	Oxide	28.59	28.81	28.47	28.88	28.71	28.69
Al_2O_3	wt%						
SiO_2		35.02	34.95	34.78	35.40	34.89	35.01
CaO		0.14	0.11	0.19	0.14	0.17	0.15
MnO		0.50	0.56	0.48	0.45	0.48	0.49
FeO		35.48	35.63	35.17	35.54	35.26	35.42
NiO		0.21	0.06	0.22	0.17	0.09	0.15
Total		99.94	100.13	99.31	100.59	99.60	
Mg	Cations	1.19	1.20	1.19	1.19	1.20	1.20
Al	Norm.						
Si	to	0.98	0.98	0.98	0.98	0.98	0.98
Ca	4 oxygens	0.00	0.00	0.01	0.00	0.01	0.00
Mn		0.01	0.01	0.01	0.01	0.01	0.01
Fe		0.83	0.83	0.83	0.82	0.83	0.83
Ni		0.00	0.00	0.00	0.00	0.00	0.00
Total		3.02	3.02	3.02	3.02	3.02	3.02
Fo		58.96	59.04	59.07	59.16	59.21	59.09

Sample 39		Ol 2 Spec. 1	Ol 2 Spec. 2	Ol 2 Spec. 3	Ol 2 Spec. 4	Ol 2 Spec. 5	Ol 2 Spec. 6	Avg.
MgO	Oxide	28.58	28.62	28.88	28.71	28.46	28.62	28.65
Al_2O_3	wt%							
SiO_2		35.21	34.99	34.92	34.78	34.92	35.55	35.06
CaO		0.14	0.14	0.14	0.15	0.14	0.16	0.15
MnO		0.32	0.50	0.50	0.46	0.50	0.47	0.46
FeO		35.60	35.32	35.51	35.71	35.40	35.61	35.53
NiO		0.11		0.20	0.09	0.02	0.15	0.11
Total		99.96	99.57	100.16	99.89	99.45	100.56	
Mg	Cations	1.19	1.20	1.20	1.20	1.19	1.18	1.19
Al	Norm.							
Si	to	0.98	0.98	0.97	0.97	0.98	0.99	0.98
Ca	4 oxygens	0.00	0.00	0.00	0.00	0.00	0.00	0.00
Mn		0.01	0.01	0.01	0.01	0.01	0.01	0.01
Fe		0.83	0.83	0.83	0.84	0.83	0.83	0.83
Ni		0.00		0.00	0.00	0.00	0.00	0.00
Total		3.02	3.02	3.03	3.03	3.02	3.01	3.02
Fo		58.87	59.09	59.18	58.90	58.90	58.89	58.97

Sample 39		Ol 3 Spec. 1	Ol 3 Spec. 2	Ol 3 Spec. 3	Ol 3 Spec. 4	Ol 3 Spec. 5	Ol 3 Spec. 6	Avg.
MgO	Oxide	28.24	28.11	28.19	28.61	28.47	28.23	28.31
Al_2O_3	wt%	0.02	0.15	0.05	0.09	0.04	0.08	0.07
SiO_2		34.75	34.69	34.90	34.96	34.60	34.91	34.80
CaO		0.09	0.18	0.13	0.16	0.14	0.11	0.14
MnO		0.56	0.52	0.45	0.48	0.54	0.51	0.51
FeO		35.35	35.53	35.32	35.67	35.35	35.25	35.41
NiO		0.16	0.12	0.08	0.21	0.15	0.04	0.13
Total		99.17	99.29	99.13	100.17	99.30	99.14	

Mg	Cations	1.19	1.18	1.18	1.19	1.20	1.18	1.19
Al	Norm.	0.00	0.00	0.00	0.00	0.00	0.00	0.00
Si	to	0.98	0.98	0.98	0.98	0.97	0.98	0.98
Ca	4 oxygens	0.00	0.01	0.00	0.00	0.00	0.00	0.00
Mn		0.01	0.01	0.01	0.01	0.01	0.01	0.01
Fe		0.83	0.84	0.83	0.83	0.83	0.83	0.83
Ni		0.00	0.00	0.00	0.00	0.00	0.00	0.00
Total		3.02	3.02	3.02	3.02	3.02	3.02	3.02
Fo		58.75	58.51	58.72	58.84	58.94	58.81	58.77

Sample 44		Ol 1 Spec. 1	Ol 1 Spec. 2	Ol 1 Spec. 3	Ol 1 Spec. 4	Ol 1 Spec. 5	Ol 1 Spec. 6	Avg.
MgO	Oxide	33.29	33.20	33.20	33.08	33.23	33.20	33.20
Al_2O_3	wt%							
SiO_2		36.20	36.03	36.15	36.30	36.25	36.10	36.17
CaO		0.17	0.14	0.11	0.09	0.17	0.09	0.13
MnO		0.46	0.41	0.42	0.46	0.41	0.43	0.43
FeO		28.88	29.26	29.40	29.37	29.21	29.27	29.23
NiO		0.09	0.11	0.19		0.09	0.03	0.10
		99.04	99.14	99.48	99.31	99.37	99.13	
Mg	Cations	1.35	1.35	1.35	1.34	1.35	1.35	1.35
Al	Norm.							
Si	to	0.99	0.98	0.98	0.99	0.99	0.98	0.99
Ca	4 oxygens	0.00	0.00	0.00	0.00	0.00	0.00	0.00
Mn		0.01	0.01	0.01	0.01	0.01	0.01	0.01
Fe		0.66	0.67	0.67	0.67	0.66	0.67	0.67
Ni		0.00	0.00	0.00		0.00	0.00	0.00
Total		3.01	3.02	3.02	3.01	3.01	3.02	3.01
Fo		67.27	66.92	66.81	66.75	66.97	66.91	66.94

Sample 44		Ol 2 Spec. 1	Ol 2 Spec. 2	Ol 2 Spec. 3	Ol 2 Spec. 4	Ol 2 Spec. 5	Ol 2 Spec. 6	Avg.
MgO	Oxide	33.62	33.53	33.47	33.55	33.69	33.73	33.59
Al_2O_3	wt%							
SiO_2		36.37	36.40	36.02	36.23	36.34	35.78	36.15
CaO		0.11	0.07	0.15	0.15	0.06	0.04	0.09
MnO		0.33	0.44	0.40	0.34	0.37	0.45	0.40
FeO		29.12	29.22	29.14	29.14	29.38	29.14	29.20
NiO		0.04	0.13	0.15	0.06	0.16	0.16	0.13
Total		99.59	99.79	99.34	99.48	100.00	99.31	
Mg	Cations	1.36	1.35	1.36	1.36	1.36	1.37	1.36
Al	Norm.							
Si	to	0.99	0.99	0.98	0.98	0.98	0.98	0.98
Ca	4 oxygens	0.00	0.00	0.00	0.00	0.00	0.00	0.00
Mn		0.01	0.01	0.01	0.01	0.01	0.01	0.01
Fe		0.66	0.66	0.66	0.66	0.66	0.66	0.66
Ni		0.00	0.00	0.00	0.00	0.00	0.00	0.00
Total		3.01	3.01	3.02	3.02	3.02	3.02	3.02
Fo		67.30	67.17	67.19	67.24	67.15	67.36	67.23

Sample 44		Ol 3	Ol 3	Ol 3	Ol 3	Ol 3	Ol 3	

		Spec. 1	Spec. 2	Spec. 3	Spec. 4	Spec. 5	Spec. 6	Avg.
MgO	Oxide	33.53	33.25	33.30	33.36	33.30	33.35	33.35
Al_2O_3	wt%							
SiO_2		36.47	36.14	36.38	36.07	35.91	35.92	36.15
CaO		0.13	0.17	0.11	0.11	0.10	0.18	0.13
MnO		0.43	0.36	0.46	0.51	0.38	0.42	0.43
FeO		29.76	29.10	29.24	29.33	29.32	29.59	29.39
NiO		0.30	0.24	0.12	0.13	0.07	0.13	0.17
		100.63	99.25	99.62	99.50	99.08	99.59	
Mg	Cations	1.35	1.35	1.35	1.35	1.36	1.35	1.35
Al	Norm.							
Si	to	0.98	0.98	0.99	0.98	0.98	0.98	0.98
Ca	4 oxygens	0.00	0.00	0.00	0.00	0.00	0.01	0.00
Mn		0.01	0.01	0.01	0.01	0.01	0.01	0.01
Fe		0.67	0.66	0.66	0.67	0.67	0.67	0.67
Ni		0.01	0.01	0.00	0.00	0.00	0.00	0.00
Total		3.02	3.02	3.01	3.02	3.02	3.02	3.02
Fo		66.76	67.07	67.00	66.97	66.94	66.77	66.92

Sample 55		Ol 1 Spec. 1	Ol 1 Spec. 2	Ol 1 Spec. 3	Ol 1 Spec. 4	Ol 1 Spec. 5	Avg.
MgO	Oxide	33.48	33.59	33.14	33.29	33.54	33.41
Al_2O_3	wt%	0.13		0.12	0.13	0.11	0.12
SiO_2		36.15	36.22	36.22	35.76	35.89	36.05
CaO		0.00	0.10	0.09	0.08	0.09	0.07
MnO		0.40	0.42	0.42	0.44	0.41	0.42
FeO		28.95	29.21	28.89	29.10	29.38	29.11
NiO		0.27	0.25	0.21	0.37	0.13	0.25
Total		99.37	99.80	99.10	99.17	99.56	
Mg	Cations	1.36	1.36	1.35	1.36	1.36	1.35
Al	Norm.	0.00		0.00	0.00	0.00	0.00
Si	to	0.98	0.98	0.99	0.98	0.98	0.98
Ca	4 oxygens	0.00	0.00	0.00	0.00	0.00	0.00
Mn		0.01	0.01	0.01	0.01	0.01	0.01
Fe		0.66	0.66	0.66	0.66	0.67	0.66
Ni		0.01	0.01	0.00	0.01	0.00	0.01
Total		3.02	3.02	3.01	3.02	3.02	3.02
Fo		67.34	67.21	67.16	67.10	67.05	67.17

Sample 55		Ol 2 Spec. 1	Ol 2 Spec. 2	Ol 2 Spec. 3	Ol 2 Spec. 4	Ol 2 Spec. 5	Ol 2 Spec. 6	Avg.
MgO	Oxide	33.09	33.16	33.00	33.02	33.08	33.09	33.07
Al_2O_3	wt%		0.14	0.14	0.00	0.00	0.10	0.06
SiO_2		35.91	36.18	35.88	36.29	35.94	35.75	35.99
CaO		0.09	0.11	0.08	0.15	0.17	0.10	0.12
MnO		0.38	0.38	0.47	0.51	0.44	0.33	0.42
FeO		29.62	29.49	29.35	29.33	29.31	29.44	29.42
NiO		0.28		0.19	0.19	0.22	0.33	0.24
Total		99.36	99.45	99.11	99.48	99.16	99.13	
Mg	Cations	1.35	1.34	1.34	1.34	1.35	1.35	1.34
Al	Norm.		0.00	0.00	0.00	0.00	0.00	0.00
Si	to	0.98	0.98	0.98	0.99	0.98	0.98	0.98
Ca	4 oxygens	0.00	0.00	0.00	0.00	0.00	0.00	0.00

Mn	0.01	0.01	0.01	0.01	0.01	0.01	0.01
Fe	0.68	0.67	0.67	0.67	0.67	0.67	0.67
Ni	0.01	0.00	0.00	0.00	0.00	0.01	0.00
Total	3.02	3.01	3.02	3.01	3.02	3.02	3.02
Fo	66.57	66.72	66.71	66.74	66.80	66.71	66.71

Sample 55		Ol 3 Spec. 1	Ol 3 Spec. 2	Ol 3 Spec. 3	Ol 3 Spec. 4	Ol 3 Spec. 5	Avg.
MgO	Oxide	33.64	33.14	33.23	33.46	33.31	33.36
Al_2O_3	wt%		0.09				0.09
SiO_2		35.92	36.03	35.71	35.97	36.05	35.94
CaO		0.12	0.12	0.11	0.10	0.09	0.11
MnO		0.43	0.38	0.50	0.40	0.42	0.43
FeO		29.35	29.52	29.46	29.37	29.34	29.41
NiO		0.27		0.18	0.36	0.32	0.28
Total		99.73	99.28	99.18	99.65	99.53	
Mg	Cations	1.36	1.35	1.35	1.36	1.35	1.35
Al	Norm.		0.00				0.00
Si	to	0.98	0.98	0.98	0.98	0.98	0.98
Ca	4 oxygens	0.00	0.00	0.00	0.00	0.00	0.00
Mn		0.01	0.01	0.01	0.01	0.01	0.01
Fe		0.67	0.67	0.67	0.67	0.67	0.67
Ni		0.01	0.00	0.00	0.01	0.01	0.00
Total		3.02	3.02	3.02	3.02	3.02	3.02
Fo		67.14	66.68	66.79	67.01	66.93	66.91

Sample 67		Ol 1 Spec. 1	Ol 1 Spec. 2	Ol 1 Spec. 3	Ol 1 Spec. 4	Ol 1 Spec. 5	Avg.
MgO	Oxide	37.91	37.66	37.88	37.64	37.82	37.78
Al_2O_3	wt%	0.09	0.13	0.10			0.11
SiO_2		37.08	37.49	37.09	37.08	37.18	37.18
CaO		0.14	0.08	0.08	0.10	0.06	0.09
MnO		0.28	0.30	0.34	0.35	0.35	0.32
FeO		24.67	24.38	24.28	24.07	24.45	24.37
NiO		0.22	0.18	0.30	0.22	0.29	0.24
Total		100.39	100.23	100.08	99.45	100.17	
Mg	Cations	1.49	1.48	1.49	1.49	1.49	1.48
Al	Norm.	0.00	0.00	0.00			0.00
Si	to	0.98	0.99	0.98	0.98	0.98	0.98
Ca	4 oxygens	0.00	0.00	0.00	0.00	0.00	0.00
Mn		0.01	0.01	0.01	0.01	0.01	0.01
Fe		0.54	0.54	0.54	0.53	0.54	0.54
Ni		0.00	0.00	0.01	0.00	0.01	0.01
Total		3.02	3.01	3.02	3.02	3.02	3.02
Fo		73.26	73.36	73.55	73.60	73.39	73.43

Sample 67		Ol 2 Spec. 1	Ol 2 Spec. 2	Ol 2 Spec. 3	Ol 2 Spec. 4	Ol 2 Spec. 5	Ol 2 Spec. 6	Avg.
MgO	Oxide	37.50	37.76	37.46	37.66	37.53	37.40	37.55
Al_2O_3	wt%		0.15	0.13		0.00	0.12	0.10
SiO_2		37.17	36.82	36.91	37.01	37.12	36.88	36.99
CaO		0.12	0.17	0.19	0.06	0.16	0.16	0.14

MnO		0.47	0.28	0.35	0.38	0.34	0.33	0.36
FeO		24.25	24.03	24.26	24.54	24.23	24.46	24.30
NiO		0.22	0.33	0.25	0.31	0.18	0.34	0.27
Total		99.73	99.54	99.55	99.96	99.56	99.70	
Mg	Cations	1.48	1.49	1.48	1.48	1.48	1.48	1.48
Al	Norm.		0.00	0.00		0.00	0.00	0.00
Si	to	0.98	0.98	0.98	0.98	0.98	0.98	0.98
Ca	4 oxygens	0.00	0.00	0.01	0.00	0.00	0.00	0.00
Mn		0.01	0.01	0.01	0.01	0.01	0.01	0.01
Fe		0.54	0.53	0.54	0.54	0.54	0.54	0.54
Ni		0.00	0.01	0.01	0.01	0.00	0.01	0.01
Total		3.02	3.02	3.02	3.02	3.02	3.02	3.02
Fo		73.38	73.69	73.35	73.23	73.41	73.16	73.37

Sample 67		Ol 3 Spec. 1	Ol 3 Spec. 2	Ol 3 Spec. 3	Ol 3 Spec. 4	Ol 3 Spec. 5	Ol 3 Spec. 6	Avg.
MgO	Oxide	37.88	37.90	37.79	37.68	37.90	37.40	37.76
Al_2O_3	wt%	0.11						0.11
SiO_2		37.04	37.32	37.38	37.21	37.16	37.07	37.20
CaO		0.09	0.15	0.07	0.18	0.13	0.07	0.12
MnO		0.32	0.39	0.30	0.35	0.39	0.32	0.35
FeO		24.17	24.23	24.27	23.96	24.05	23.94	24.10
NiO		0.41	0.26	0.33	0.18	0.15	0.29	0.27
Total		100.02	100.25	100.13	99.55	99.77	99.09	
Mg	Cations	1.49	1.49	1.48	1.49	1.49	1.48	1.49
Al	Norm.	0.00						
Si	to	0.98	0.98	0.98	0.98	0.98	0.99	0.98
Ca	4 oxygens	0.00	0.00	0.00	0.01	0.00	0.00	0.00
Mn		0.01	0.01	0.01	0.01	0.01	0.01	0.01
Fe		0.53	0.53	0.53	0.53	0.53	0.53	0.53
Ni		0.01	0.01	0.01	0.00	0.00	0.01	0.01
Total		3.02	3.02	3.02	3.02	3.02	3.01	3.02
Fo		73.64	73.60	73.51	73.71	73.75	73.58	73.63

Sample 75		Ol 1 Spec. 1	Ol 1 Spec. 2	Ol 1 Spec. 3	Ol 1 Spec. 4	Ol 1 Spec. 5	Avg.
MgO	Oxide	35.63	35.26	35.71	35.57	35.39	35.51
Al_2O_3	wt%						
SiO_2		36.56	36.46	36.51	36.53	36.77	36.57
CaO		0.14	0.16	0.15	0.15	0.08	0.14
MnO		0.44	0.41	0.45	0.26	0.32	0.38
FeO		26.76	27.25	27.46	26.96	26.97	27.08
NiO		0.24	0.37	0.28	0.35	0.24	0.30
Total		99.78	99.91	100.55	99.83	99.77	
Mg	Cations	1.42	1.41	1.42	1.42	1.41	1.42
Al	Norm.						
Si	to	0.98	0.98	0.97	0.98	0.98	0.98
Ca	4 oxygens	0.00	0.00	0.00	0.00	0.00	0.00
Mn		0.01	0.01	0.01	0.01	0.01	0.01
Fe		0.60	0.61	0.61	0.60	0.60	0.61
Ni		0.01	0.01	0.01	0.01	0.01	0.01
Total		3.02	3.02	3.03	3.02	3.02	3.02

Fo		70.36	69.76	69.86	70.17	70.05	70.04

Sample 75		Ol 2 Spec. 1	Ol 2 Spec. 2	Ol 2 Spec. 3	Ol 2 Spec. 4	Ol 2 Spec. 5	Avg.
MgO	Oxide	35.37	35.28	35.67	35.57	35.28	35.43
Al_2O_3	wt%						
SiO_2		36.69	36.77	36.91	36.87	36.63	36.77
CaO		0.12	0.15	0.00	0.19	0.14	0.12
MnO		0.43	0.47	0.39	0.43	0.31	0.41
FeO		27.75	27.69	27.46	27.32	27.25	27.49
NiO		0.21		0.30	0.35	0.36	0.31
Total		100.57	100.35	100.73	100.73	99.98	
Mg	Cations	1.41	1.40	1.41	1.41	1.41	1.41
Al	Norm.						
Si	to	0.98	0.98	0.98	0.98	0.98	0.98
Ca	4 oxygens	0.00	0.00	0.00	0.01	0.00	0.00
Mn		0.01	0.01	0.01	0.01	0.01	0.01
Fe		0.62	0.62	0.61	0.61	0.61	0.61
Ni		0.00	0.00	0.01	0.01	0.01	0.01
Total		3.02	3.02	3.02	3.02	3.02	3.02
Fo		69.44	69.43	69.84	69.89	69.77	69.67

Sample 75		Ol 3 Spec. 1	Ol 3 Spec. 2	Ol 3 Spec. 3	Ol 3 Spec. 4	Ol 3 Spec. 5	Ol 3 Spec. 6	Avg.
MgO	Oxide	35.51	35.57	35.63	35.60	35.55	35.39	35.54
Al_2O_3	wt%							
SiO_2		36.74	36.77	36.75	36.56	36.77	37.12	36.79
CaO		0.07	0.09	0.13	0.16	0.15	0.16	0.13
MnO		0.44	0.34	0.44	0.32	0.46	0.37	0.40
FeO		27.24	27.69	27.22	27.23	27.45	27.34	27.36
NiO		0.22	0.34	0.31	0.37	0.15	0.29	0.28
Total		100.22	100.80	100.48	100.25	100.52	100.66	
Mg	Cations	1.41	1.41	1.42	1.42	1.41	1.40	1.41
Al	Norm.							
Si	to	0.98	0.98	0.98	0.98	0.98	0.99	0.98
Ca	4 oxygens	0.00	0.00	0.00	0.00	0.00	0.00	0.00
Mn		0.01	0.01	0.01	0.01	0.01	0.01	0.01
Fe		0.61	0.62	0.61	0.61	0.61	0.61	0.61
Ni		0.00	0.01	0.01	0.01	0.00	0.01	0.01
Total		3.02	3.02	3.02	3.02	3.02	3.01	3.02
Fo		69.91	69.60	70.00	69.98	69.78	69.77	69.84

APPENDIX D – SULPHUR ISOTOPES

CRYSTAL LAKE GABBRO SULPHUR ISOTOPES

Sample Depth (m)	$\delta^{34}S$ ‰
9.5	13.2
573.7	11.1
657.5	21.0, 20.8, 20.9, 21.0, 21.1, 21.1
528.5	6.3
20.5	11.6
753.1	15.6
649.4	15.2
557.1	9.9
541.4	4.0, 4.1
662.1	11.1
567.2	12.6
744.3	9.6